WIND-DRIVEN NATURAL VENTILATION IN COURTYARD AND ATRIUM-TYPE BUILDINGS

Rafik Bensalem

Bsc(Hons) Arch.

Thesis submitted for the degree of

Doctor of Philosophy

at the Building Science Unit

School of Architectural Studies

University of Sheffield

August 1991

To my parents

Acknowledgements

I would like to express my sincere gratitude to my supervisor Dr Steve Sharples for his guidance and assistance throughout every stage of the experimental work and the writing of the thesis.

I must thank also the technical staff of the Building Science Unit, in particular, Mr Lol Wildgoose who constructed the wind tunnel models, and also, Mr Peter Williams and Mr Roy Webster. I owe thankfulness to other members of staff of the School of Architecture, especially Mrs Hazel Hall, Mrs Pat Hodgkinson, Mrs Susan Cresswell, Mr Jules Alexandrou and Mr Melvyn Broady, for their valued assistance, in one form or the other. I am indebted to my friends and colleagues, especially Anissa Tabet, Salima Benhouhou, Gbadamosi Salami Yakubu, Alice and Fernando Pereira, Hans Kula, Maria Mallard and Joongseok Ryu for their useful suggestions towards the making of this thesis.

Finally, I am highly indebted to my parents, family and friends for their encouragements and support throughout the duration of this research.

This research would not have been possible without the financial support of the Algerian Ministry of Education.

Wind-driven natural ventilation in courtyard and atrium-type buildings

(Rafik Bensalem)

Summary

This study investigated the effectiveness of wind-driven natural ventilation in courtyard and atrium-type buildings, particularly in the context of ventilative cooling.

Courtyard and atrium buildings are currently enjoying great popularity. Perhaps a primary reason for their revival comes from the energy and environmental awareness of the current period, in which courtyard and atrium concepts are emerging as very promising.

Wind-driven ventilation is one of the most basic and probably among the most efficient ways to prevent overheating, and provide cooling in the summer season, especially in humid climates. A review of previous works showed that little attention has been given to the wind-driven natural ventilation capability of these structures, and to the means of maximizing this ventilation. This study was thus aimed to fill part of the gap in this subject.

In order to evaluate the wind-driven ventilation effectiveness of these structures, and to examine some of the influential parameters, experimental wind tunnel tests were made. Actual indoor air flows were measured in small replica models of four-storey courtyard and atrium buildings by means of small calibrated orifice plates. A parametric study of the geometry of the courtyard was made in isolation conditions, where the depth and breadth of the courtyard were systematically varied. Several atrium ventilation modes were tested both in isolation and in urban terrains. The tests involved different roof geometries and various roof porosities. The measurements were followed by a discussion on the validity of simple computational methods to predict airflow in atria.

The investigation portrayed the importance of some factors, such as the wind orientation rather than the courtyard geometry, for enhancing the flow in these structures. The superiority of some atrium designs over the courtyard types, particularly in sheltered sites, was underlined.

The study concluded with a discussion of design guide-lines and referred the reader to an application as an example, describing a simple step-by-step method to estimate the cooling benefits of these structures in a particular site, and making use of the measurement data obtained from the study.

Table of contents:

Chapter 1: Introduction 1

Chapter 2: Introduction to courtyards and atria

2.1 Introduction 3

2.2 Definitions 4

2.2.1 Definitions based on historical evolution and spatial characteristics 4

2.2.2 Definitions based on the daylighting function 5

2.2.3 Definition adopted 6

2.3 Historical overview 6

2.4 Role of courtyards and atria in urban design 9

2.5 Climate control 11

2.5.1 The vernacular courtyard: a coordinate system of natural energy flow . . . 12

2.5.2 Thermal principles in contemporary atria 16

2.5.3 Natural ventilation in perspective 22

2.6 Other environmental aspects 22

2.6.1 Daylighting 22

2.6.2 Wind effects 25

2.6.3 Acoustics 26

2.7 Fire safety 27

2.8 Discussion and conclusion 30

Chapter 3: Natural ventilation: theory and practice

3.1 Introduction **31**

3.2 Ventilation requirements **32**

3.2.1 Minimum ventilation rates or permanent ventilation requirements 33

3.2.2 Thermal Comfort or occasional ventilation requirements 34

3.3 The motive forces **36**

3.3.1 Wind pressure induced ventilation 37

3.3.2 Thermal buoyancy 39

3.3.3 Mechanical ventilation 41

3.3.4 Combined effects of several forces 41

3.4 Strategies for natural ventilation **42**

3.4.1 Wind induced versus thermally induced ventilation 43

3.4.2 Appropriate ventilation strategies to use under certain climates 45

3.5 General Characteristics of the wind **46**

3.5.1 The atmospheric boundary layer structure 46

3.5.2 The variation of the mean wind speed with height 48

3.5.3 The turbulent nature of wind 49

3.6 Basic aerodynamics and influential parameters in the ventilation of buildings **50**

3.6.1 Influential factors in ventilation 50

3.6.2 Flow patterns around a building 51

3.6.3 Internal flow mechanisms 52

3.7 Conclusions **56**

Chapter 4: Related background studies

4.1 Introduction **57**

4.2 Flow and pressure forces around simple clusters of buildings **58**

4.2.1 Flow patterns around clusters of buildings or composite buildings 58

4.2.2 Pressure forces in rows of buildings 59

4.2.2 Ventilation potential in partially enclosed courtyard buildings 66

4.2.3 Ventilation potential in spaces enclosing a courtyard 67
4.2.4 Flow patterns in courtyards 72
4.2.5 Influential parameters in the ventilation of courtyard buildings 73
4.3 Flow in extensive arrays of buildings 74
4.3.1 Effects of the array size on the pressure forces 75
4.3.2 Pressure forces in urban conditions 75
4.4 The use of roof-level openings for natural ventilation 81
4.4.1 Historical examples 82
4.4.2 Research related to ventilation through roof vents 86
4.4.3 Summary of the studies on roof induced ventilation 93
4.5 Conclusions 94

Chapter 5: Methods used to assess natural ventilation in buildings

5.1 Introduction 96
5.2 Techniques used for estimating natural ventilation 97
5.3 The wind tunnel analogue and techniques 103
5.3.1 Introduction to wind tunnels 103
5.3.2 Modelling requirements 105
5.3.3 Measuring techniques in wind tunnels 112
5.4 Conclusions 120

Chapter 6: Experimental apparatus and test procedures

6.1 Introduction 122
6.2 Development and calibration of the orifice plate 122
6.2.1 Description of the orifice plate 122
6.2.2 Calibration 124
6.3 Experimental facilities and procedures 133
6.3.1 Introduction to the experimental programme 133
6.3.2. Description of the wind tunnel 135
6.3.3 Model description 137

6.3.4 Measuring apparatus 141
6.3.5 Test procedure 142
6.3.6 Presentation of the results 143
6.3.7 Modelling philosophy 146
6.3.8 Level of accuracy 148
6.3.9 Test programme 149
6.3.10 Limitation of the study 153
6.4 Conclusion 153

Chapter 7: Ventilation conditions of courtyard buildings in isolation

7.1 Introduction 155
7.2 Surface pressure results 156
7.2.1 Pressure magnitudes 157
7.2.2 Vertical pressure distribution 160
7.2.3 Implications for the ventilation 163
7.2.4 Summary of the surface pressure results 165
7.3 Ventilation conditions in the courtyard building models 165
7.3.1 Models orientated normal to the wind 166
7.3.2 Models orientated at an angle to the wind 167
7.3.3 Comparison with other relevant works 168
7.3.4 The vertical flow profiles 170
7.3.5 Comparison with the results obtained from the surface pressure tests . . . 172
7.4 Influence of the courtyard geometry on the ventilation 173
7.4.1 Effect of the depth 173
7.4.2 Effect of the breadth 175
7.4.3 Summary on the effects of the courtyard geometry 177
7.5 Influence of the wind incidence 178
7.6 Ventilative performances of courtyards 179
7.6.1 Evaluation of criteria 179
7.6.2 Ventilative performances at 0° wind angle 180

7.6.3 Ventilative performances at 30° and 45° wind angles 180

7.7 Conclusions 181

Chapter 8: Ventilation conditions of atria in isolation

8.1 Introduction 184

8.2 Atrium ventilation modes 184

8.3 Methodology of the investigation 186

8.4 Surface pressure results 186

8.4.1 Surface pressures on the external walls 186

8.4.2 External surface pressures on the atrium roofs 188

8.4.3 Comparison with other related works 189

8.4.4 Selection of the atrium roof types for internal flow tests 191

8.5 Results of the internal pressure measurements 192

8.6 Results of the internal flow measurements 194

8.6.1 Flow through the roof vents 194

8.6.2 Flow through the atrium rooms 195

8.6.3 Effects of the wind incidence on the indoor flows 199

8.7 Ventilative performances of atria 200

8.7.1 Models orientated normal to the wind 200

8.7.2 Models orientated 30° or 45° to the wind 202

8.8 Conclusions and discussion 204

Chapter 9: Ventilation conditions of courtyard and atrium buildings in congested urban sites

9.1 Introduction 207

9.2 Modelling of the urban site 207

9.2.1 Influence of the array size on the pressure forces: a review 208

9.2.2 Effects of the fetch on the internal flows 210

9.3 The range of variables considered in the investigation 212

9.4 Estimate of the pressures acting on the model external walls 214

9.5 Results of the internal flow measurements 216

9.5.1 The influence of the group layouts 216

9.5.2 Importance of the ventilative strategy 220

9.5.3 Effects of the orientation to the wind 223

9.6 The ventilative performances 224

9.6.1 At 0° wind orientation angle 224

9.6.2 At 45° wind orientation angle 227

9.7 Conclusions 230

Chapter 10: Estimate of the accuracy of analytical methods for predicting indoor flows in atria

10.1 Introduction 233

10.2 Iterative procedure for the calculation of internal pressures and flow rates 234

10.2.1 The algorithm 236

10.2.2 Reformulation of the equation of discharge 236

10.2.3 Input data 238

10.3 Estimate of the inaccuracies in the predicted values 239

10.4 Possible sources of errors 240

10.4.1 Alteration of the discharge characteristics of the openings 240

10.4.2 Influence of the permeability 242

10.4.3 Comparison with other relevant studies 244

10.4.4 Discussion 245

10.5 Suggested corrections to the predictions to account for the effects of permeability 246

10.6 Recommendations for the use of the numerical methods for predicting indoor flows in atria 248

10.7 Conclusions 249

Chapter 11: Conclusions and recommendations

11.1 Introduction 250

11.2 The main results 251

11.2.1 Courtyard-type buildings in unsheltered sites 251

11.2.2 Atrium-type buildings in unsheltered sites 252

11.2.3 Courtyard and atrium-type buildings in congested urban sites (with no dominant buildings) 253

11.2.4 Estimate of the accuracy of the analytical methods in predicting airflow rates in atrium buildings 254

11.2.5 Design guide-lines 256

11.3 Limitations of the study 256

11.4 Other aspects which must be considered concurrently with the design guide-lines 256

11.5 Recommendations for further work 257

11.6 Conclusion 258

***References* 261**

***Appendices* 279**

Chapter 1:

Introduction

This study was inspired by two contemporary trends in architecture: the interest of passive and low energy applications in buildings and the return of courtyards and atria as generic forms of development in the morphology of the city.

After years of demise, courtyard and atrium structures are now being rediscovered for their multiple inherent qualities. Far from being considered as relics from the past, they are being rehabilitated in their role as a generic form of a cohesive urban development. Atria are presently highly used, for their active role in the restoration of old buildings, their catalytic social functions, marketing economic implications and the flexibility it gives to architectural creativity.

The interest given to these forms also stems from the ways in which they can conserve energy. They have been found to have inherent passive features that enable them to temper the indoor climate and to reduce energy costs.

During the summer seasons, buildings in warm humid climates rely on natural ventilation, (especially the wind-driven ventilation), for the prevention of overheating and the provision of cooling by passive means. How efficient courtyard and atrium buildings are in promoting natural ventilation was the question which initially prompted this study. Indeed, the courtyard concept presents an interesting aerodynamic problem in that, only parts of the buildings, (half at most), can face the wind with the rest being under their wind shadow. For the sheltered portion of the building, slow indoor air movement can be anticipated. What are the methods of maximizing the air movement was the obvious question that followed. Pertinently, the atrium may provide a solution to this problem where the roof is used as a powerful breeze-generating device, (as was claimed in some literature). It was envisaged that the study might also verify the speculations that courtyard geometry was the key element to the adaptation of

vernacular prototypes and that the most shallow form was the most logical one in warm-humid climates.

The study was thus mainly aimed to evaluate the wind-driven ventilation of both courtyard and atrium structures, outline the influential parameters in their ventilation effectiveness and suggest the best solution to maximize it. The results should help the designer to account for this parameter in new designs of courtyards and atria and also in the retrofit of courtyards into atria.

The structure of the work is summarized in Figure 1.1. The thesis starts with an introductory chapter (**Chapter 2**) on the attributes of the courtyard and atrium concepts, and on the various aspects of their design which have to be considered concurrently with natural ventilation. **Chapter 3** introduces general aspects of ventilation, the motive forces and the physics of air movement. This is aimed at providing a background to the literature review, from which the analysis of the experimental work undertaken in this study, can be discussed. **Chapter 4** reviews the related background studies. The intention is to study the state-of-the-art of the subject and to select the influential parameters for evaluation. The next step is to select, among the available ventilation evaluation techniques, the most appropriate for the parametric study that is planned. This is discussed in **Chapter 5**. The experimental tests that have been devised and the experimental set-up are presented in **Chapter 6**. The results and analysis of the tests are given in **Chapters 7, 8** and **9** respectively for the courtyard and atrium buildings in isolation and for both courtyard and atrium buildings in urban sites. **Chapter 10** is devoted to estimating how accurate the usual analytical methods are in predicting the airflow rates in atrium-type buildings, and establishing the limits of their use. **Chapter 11** is the concluding chapter outlining the salient results, the limitations of this work and the need for further work. This study is finalised by a series of design guide-lines enclosed in an appendix (**Appendix F**). An example of their application for a particular case is also provided in an appendix (**Appendix G**).

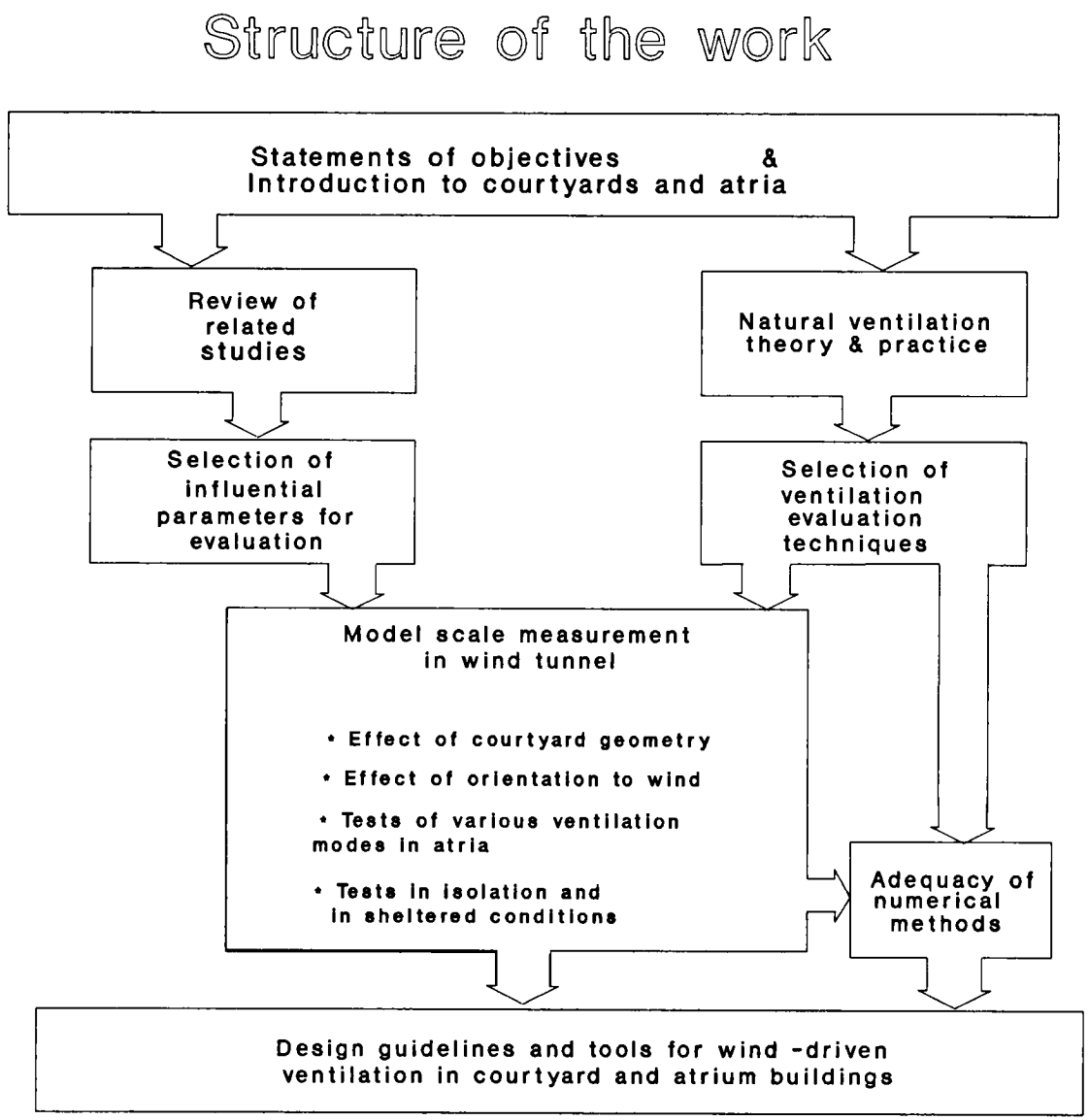

Figure 1.1: Structure of the thesis.

Chapter 2:

Introduction to courtyards and atria

2.1 Introduction

This chapter is intended to draw attention to the inherent qualities of the courtyard and atrium forms which are responsible for their current popularity.

This introduction to courtyards and atria starts with the definition of the terms. An overview of the historical evolution of these structures will follow. This is to further the understanding of the stage of development of these architectural forms in the current period. Also, the so-called "new era of the atrium" will be restored to its historical context.

The role these forms play in the urban design and some of their environmental aspects will be discussed more extensively. The intentions behind the review are two-fold:

i) to outline the urban design qualities of these forms and some of their important environmental assets. This is eventually to justify that these spatial concepts are worth studying.

ii) to outline the design requirements of some environmental aspects which must not be lost in the pursuit of natural ventilation. In particular, the conflicting design requirements for natural ventilation with the need of wind shelter, noise control, and smoke control in the event of a fire are discussed.

2.2 Definitions

Although courtyard and atrium, (plural atria), are words commonly used, it is not often clear which spatial type they refer to, and for a very good reason: no precise definition exist. For the purpose of the present study, a clarification is needed.

2.2.1 Definitions based on historical evolution and spatial characteristics

Courtyard generally refers to an open space in a building surrounded by rooms or walls and whose "primary purpose is to bring light and air to the rooms which surround it. A secondary purpose is to provide a protected or private outdoor room which can be used in conjunction with the building's interior spaces", (Bednar (1986) p. 7). Often the term courtyard is used to designate a `court`, which is "a more general term which relates to many kinds of open-air spaces surrounded or defined by building elements", (Bednar (1986) p. 7). Other alternative words for courtyard exist, such as *cloister, cortile* or *quadrangle*, to designate similar spatial enclosures but usually associated to specific building types, respectively, monasteries, Italian Pallazzo (or medieval houses), and in universities (or schools).

Regarding the *atrium* definition, there is even greater confusion, and this is because the concept has undergone many mutations throughout its evolution. An encyclopedia of Architecture, (Yarwood (1985)), defines the atrium as the *Roman atrium* found in domestic buildings and which is "an open courtyard surrounded by rooms which were covered by roofs sloping towards the centre". Bednar outlined that "the distinction between a Roman atrium and a court is in the degree of the physical and visual relationship between this space and the surrounding rooms", (Bednar (1986) p. 7). The elements surrounding a court have generally exterior walls with windows and few doors which limit the physical and visual access to the court, whereas in the Roman atrium the rooms open directly onto it. The circulation also is generally different in the two cases, taking place in the buildings surrounding a courtyard for the first case, while with the atrium type, the circulation takes place within its perimeter. The distinction between the two models is however not always straightforward.

The hybrids that evolved from the original atrium concept were given sometimes other terms such as galleries, plaza, square, rotunda, to distinguish from the Roman type so as to avoid confusion. Nevertheless the distinction is not always easy and the terms are very often mixed up.

Currently the term atrium refers rather to "a centroidal, interior, daylit space which organizes the space", (Bednar (1986), p. 63), while the ancient form is called Roman atrium. As defined by Bednar, *centroidal* does not mean necessary occupying the geometric centre of a building, but rather a space in which the majority of the spaces relate to it. "An atrium must also be an interior space, that is, a space enclosed and protected from the weather. Otherwise it should be called a courtyard... an atrium must be within a single building. Atria which meet these conditions but spatially relate several different buildings to each other should be termed plaza atria", (Bednar (1986), p. 63).

Bednar describes five main generic forms for the contemporary atrium.

i) the *closed atrium*,
ii) the *open-sided atrium*, where, up to three sides are partially or completely glazed,
iii) the *linear atrium*, are elongated in plan, with ends glazed or defined by building elements.
iv) the *multiple lateral atria*, are several atria within a building, each organising a portion of the building.
v) the *partial atrium*, is an atrium which spatially organizes only a part of a building. An example is the atrium at the base of a tower block.

These spatial organisations are shown in Figure 2.1. Many mutations from these generic forms exist.

2.2.2 Definitions based on the daylighting function

Other distinctive terms for atrium and courtyard concepts are also used according to their functions, even if they share the same general spatial characteristics. Lam (1986) distinguishes *lightcourts, litria* and *lightwells* from *courtyard, atria,* on the basis of their daylighting functions. *Lightcourts* and *litria* are respectively open and covered courtyards which are designed to maximise the potential of using sunlight to light adjacent buildings. They may be designed exclusively for this utilitarian function with fewer other architectural considerations. *Lightwell* is defined as an utilitarian shaft or slot within a building whose primary purpose is to provide natural light and ventilation to adjacent spaces. It may be glazed or open to the sky. *Atria* and *courtyards*

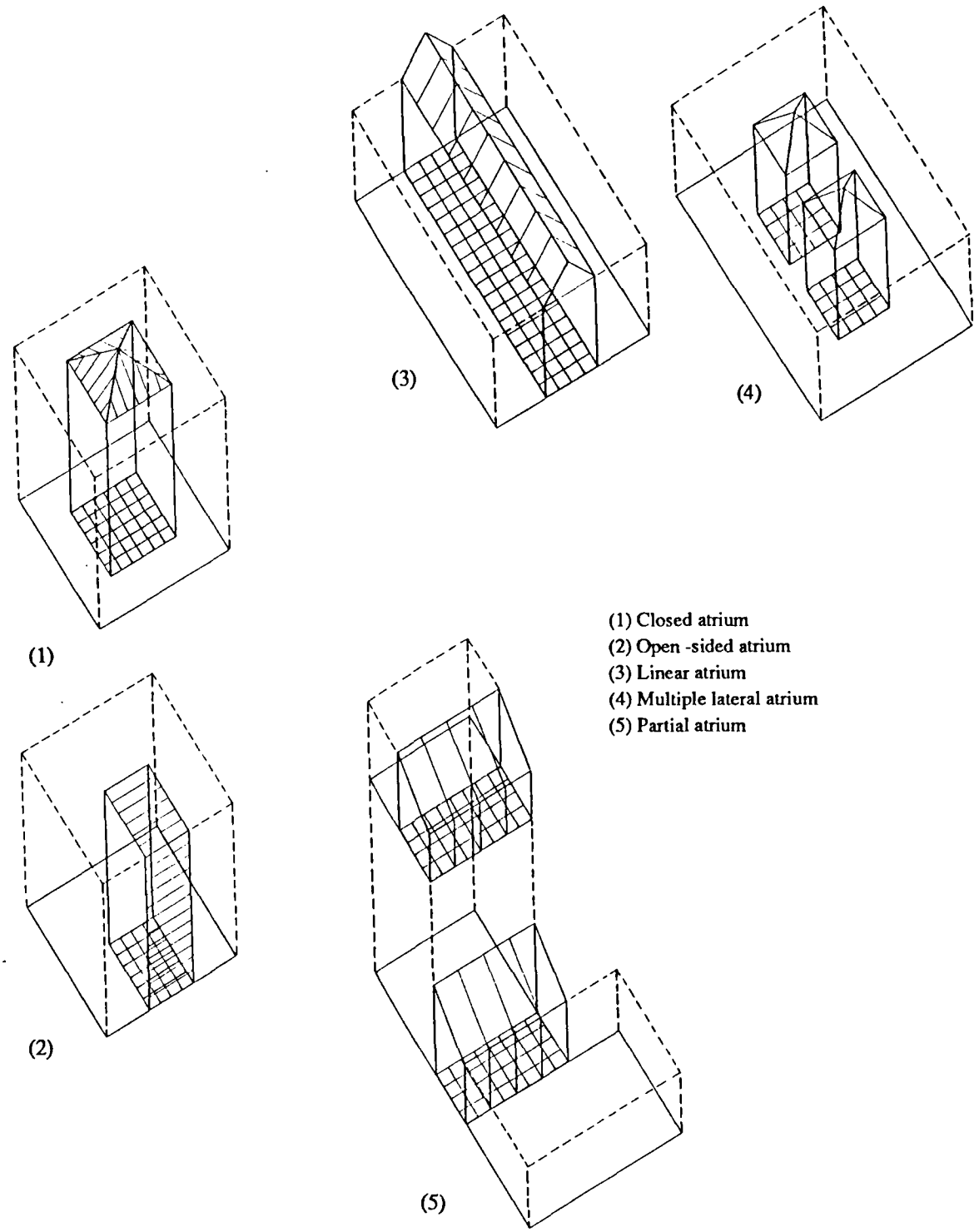

Figure 2.1: Taxonomy of the atrium building types, (After Bednar (1986)).

on the other hand do not attempt to maximise the light delivery to the surrounding space, they are rather designed for the people to enjoy their space.

2.2.3 Definition adopted

For the purpose of this study the definition of atrium given by Bednar is adopted. In wind-driven ventilation, however, the relevant parameters are the geometrical characteristics and not the nature of the building materials, (opaque or transparent), so the study could be addressed also for non-daylit atrium-type buildings, though this solution is hardly encountered. Also, as the atrium is indissociable from the adjacent spaces which are arranged around it, the term may also refer to the building containing the atrium.

2.3 Historical overview

The developments in the atrium design and its hybrids are best understood in the context of a historical perspective.

Contemporary courtyards and atria share the same origins which refer back to Antiquity and the Classical times. Whereas the general spatial characteristics of the courtyard evolved very little, the atrium underwent dramatic mutations. The historical review will be thus more fixed onto the evolution of the atrium concept.

Origins in Antiquity

The earliest examples of courtyard houses that were excavated dated back as far as the third millenium B.C.. They were the typical houses of the cities of Ur in Mesopotamia (2112 B.C.), in the basin of the rivers Tigris and Euphrates, in Assur (1500 B.C.) and Babylon (604 B.C), (see Figure 2.2).

It is believed that the embryonic versions of the courtyard have evolved from some combination of three prehistoric prototypes: a) cave dwellings b) encampments of nomadic people c) fenced compound dwellings of early farmers, (Leung et al (1981)). Nevertheless it is in the early urban settlements that the courtyard appeared as a prevalent form. Therefore, it may well be that the inception of the house was determined by the conditions of urbanism, i.e., the lack of privacy, limited land area. The climatic control of the courtyard forms of development, particularly in hot and dry regions of the globe, is also believed to have been equally a determinant. Amos

Rapoport in his well known book, *House form and culture* (1969), explained also that cultural, religious and social factors may have been also generic parameters of the form.

The classical atrium, Greek and Roman

The courtyard is found in the Greek houses between the fifth and second centuries B.C.. The plan of the house excavated near Thessalonika, shown in Figure 2.3, features a peristyle, (courtyard surrounded by columns), around which the rooms are organised and open onto it.

The classical atrium is sometimes related to the Greek courtyard. Nevertheless, it is with the Roman town house (Domus), that the classical concept of atrium is almost always associated with. The Domus house was based upon the Greek house of which many examples had survived from the Greek colonization of Southern Italy. Most houses had one storey, though some had a second storey added to part of the building. The front hall led directly into an atrium which was open to the sky, and whose primary function was to catch and store rainwater. The surrounding rooms were roofed with their roof surfaces inclined inward down towards the open centre of the atrium, (compluvium), where a basin, (impluvium), was placed . The latter was connected to a rainwater storage cistern beneath the house. Depending on their size, the houses could accommodate one or several garden courts, (the peristyles), located towards the rear of the house. A typical house is shown in Figure 2.4.

Vitrius accredited the invention of the Roman atrium to the Etruscans who used it some 2 or 3 centuries earlier. Vitrius defined five types of atria: Tuscan, Corinthian, Tetrastyle, Displuviate, Testudiate. The Tuscan, Corinthian and Tetrastyle models differed by the construction details of their roofs. The Displuviate, (with roof slopes directed away from the atrium roof opening), and Testudiate atrium (used in two story house and had no roof opening), however, did not have rain harvesting potential and were used as dinning or sitting rooms, (see Bednar (1986)).

Later, the term atrium was borrowed to refer to the enclosure built in front of early Christian basilica and which were surrounded by arcaded walkways. This would rather be called, in the present-day definition, a cloister.

The covered atrium

Despite repeated use of this type of plan intermittently, it was not until the emergence of iron and glass technology in the 19th century that the modern atrium, as

(1) Entrance hall
(2) Staircase
(3) Washroom
(4) Kitchen
(5) Storeroom
(6) Courtyard

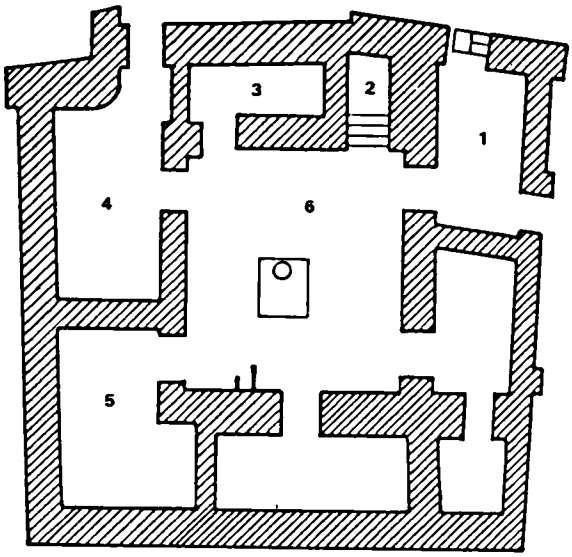

Figure 2.2: Plan of house at Ur. (Source: Bednar (1986), Extracted from E., Camesasca, History of the House, Putnman, New York, 1971, p.32)

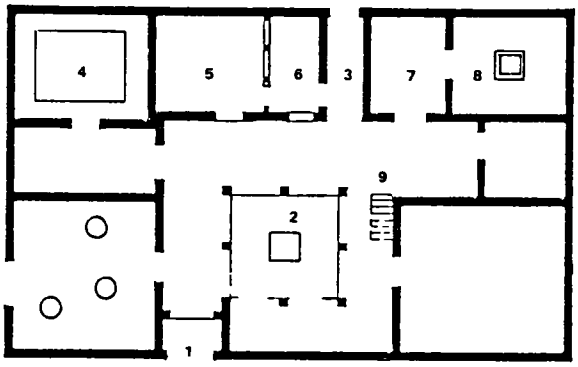

(1) Main hall
(2) Courtyard
(3) Secondary entrance
(4-8) Public rooms
(9) Staircase

Figure 2.3: Ancient Greek house plan. (Source: Bednar (1986), Exctracted from E.,Camesasca, History of the House, Putnman, New York, 1971, p.46).

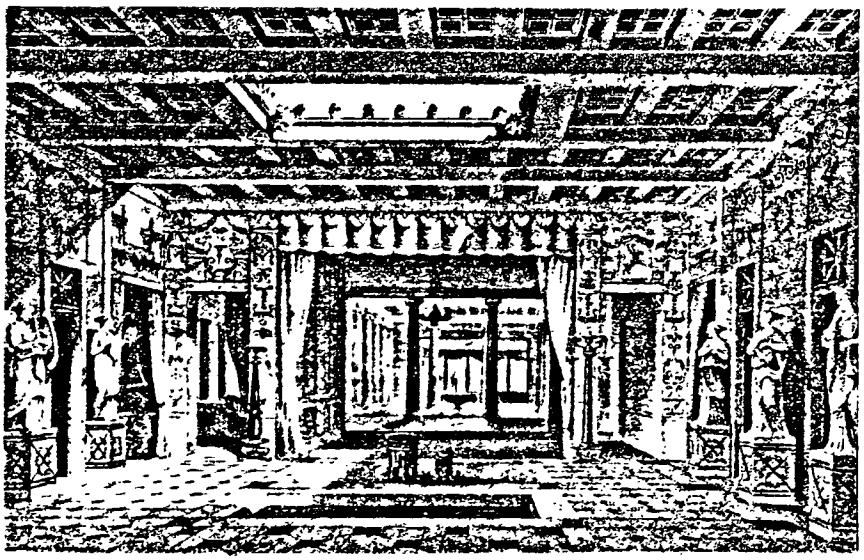

Figure 2.4: The Roman atrium (Source Saxon (1986)).

distinguished from the open-air Roman atrium or the courtyard emerged. A totally new architecture dominated by glass and iron began to blossom in Europe, with the most remarkable examples being probably the Crystal Palace in Hyde Park, London, designed by Joseph Paxton in 1851.

In particular two spatial types emerged and prospered in the course of the nineteenth century: the glazed atrium and the arcade. The arcade was exclusively intended for commercial purposes, whereas the atrium had wider functions. The arcade, a glass covered passageway flanked with shops on their sides, was created to provide a sheltered public space to facilitate sale of luxury goods. The best-known example is probably the Galleries Vittorio Emanuale II in Milan built in 1867.

The Reform Club in London, built in the first half of the nineteenth century is the first known example where the atrium became an interior space. The building borrowed the model of an Italian pallazo, but in which a glazed roof with a metal structure was added to its cortile, (Italian term for courtyard). In France the model was adopted in many large department stores, (called Galleries), to which the "Bon Marche" by Boileau and Eiffel is one of the best-known examples. The model also flourished in many other kinds of buildings, including hotels, museums, apartments and libraries. However, towards the end of the century in Europe, the concept was plagued by the concern for fire safety and waned.

A new era for the atrium took place in the United States at the turn of the nineteenth century. Another demise followed after the First World War, when the contracting world economy and the Modern Movement encouraged more economical building forms. Representative atrium buildings of this era was the Amsterdam Stock Exchange, the Beurs, designed by Berglage, and the Frank Lloyd Wright's Larkin Building in Buffalo, New York.

Current rebirth of the atrium concept

The atrium concept is currently enjoying another rediscovery after a dormancy of two third of the twentieth century, (its third era after Bednar (1986)). Though the revival of the atrium had several precursors, it is often accredited to two major buildings, the Hyatt Regency Hotel in Atlanta by Edwards and Portman in 1967 and the Ford Foundation Headquarters in New York City by Roche and Dinkeloo in 1968, (see Figures 2.5 and 2.6). Both designs were far echos of the ancestors of the beginning of the century.

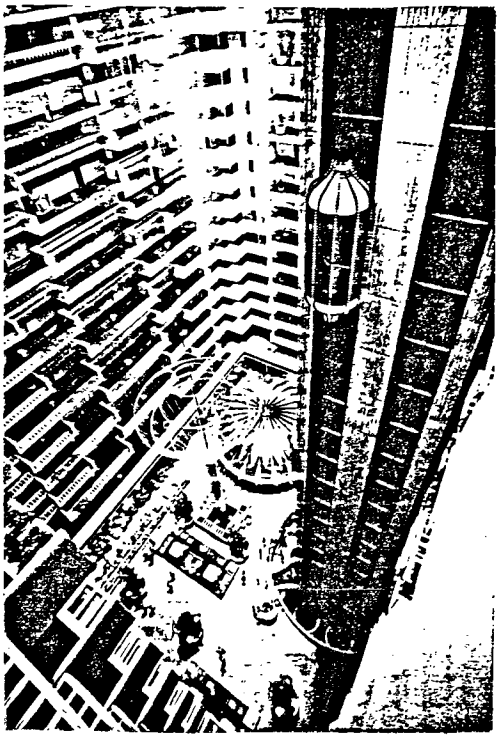

Figure 2.5: The Hyatt Regency Hotel in Atlanta (Architects; Edwards and Portman), (Source Saxon (1986)).

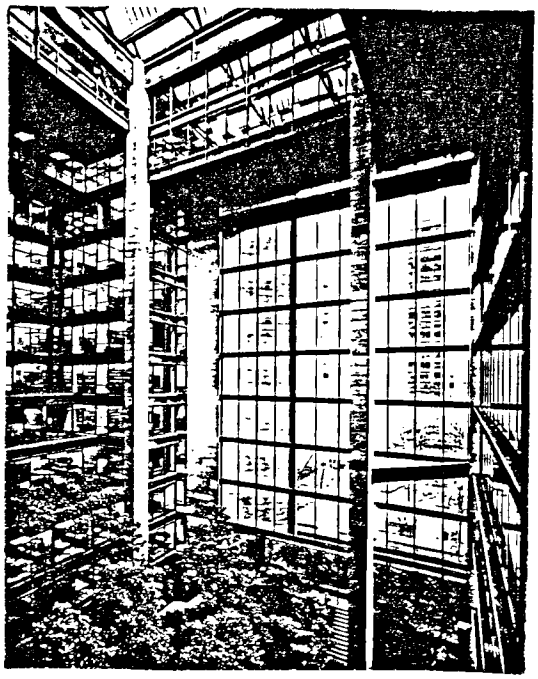

Figure 2.6: The Ford Foundation Headquarters in New York City, (Architects; Roche and Dinkeloo), (Source Bednar (1986)).

> "The Hyatt Regency Hotel in Atlanta was an extravaganza, like no hotel the world had seen before... This grand atrium is surrounded by galleries and balconies, (supporting planters), which serve as a single-loaded corridors for the guest rooms, which also overlooked the city.... The elevators have been pulled out of the walls and placed in the atrium.. and formed a giant kinetic sculpture as they zoom up and down, adding mechanical animation to this grand space.... The atrium became the hallmark of the Hyatt hotel chain", (Bednar (1986) pp. 26-27)

The Ford Foundation Headquarters in New York also had no equivalent precedents, and gave momentum to the concept in office-building design as the Hyatt Regency Hotel for hotel design. The Ford Foundation building was 12 storeys, with the offices disposed in an L-shape plan. The square plan of the building was completed by the atrium glazed walls, enclosing an enormous garden overlooked by the offices. The most innovative aspect of the atrium was its relationship between the city outside and the private inside. It was designed as an indoor park to be used year round by city residents, the general public and the occupants of the office building.

Currently the atrium is enjoying an unprecedented popularity. From the hotel and office prototypes of the sixties, the concept bloomed into buildings of other kinds - hospitals, schools, libraries, specialised housing and in multiuse centres. New concepts have evolved, with an unprecedented variety of spatial qualities and scale, and with extended roles.

Their capability of addressing several issues simultaneously such as marketing economics, aesthetic and energy consciousness of the current period, and their active role in urban design, and in the preservation of historical buildings, are what probably justified this renewal of interest. Some of their urban design and environmental qualities are now reviewed.

2.4 Role of courtyards and atria in urban design

Urban design qualities of the concepts

The call of the Modern Movement for sun, space and greenery had produced the idea of free standing towers. This had disastrous effects on cities which soon became aggregates of disparate elements which disregarded street frontages and the enclosure of space. The streets lost their coherence, and at the building feet the excessive spaces that were left were often channelling strong winds and did not ensure their intended

amenity. The awareness of negative effects associated with the lack of urban cohesion has lead to an ongoing urban renewal in which atria, and to a lesser extent, courtyards, are emerging as among the most versatile and useful urban design elements.

The urban design qualities of these concepts rest in an efficient use of the land, in the maintenance of the streets' continuity and the ability to deal with awkward sites whilst following street frontage. In addition to these practical features, (to which courtyard is probably restricted), the atrium is a new and powerful element in the inventory of public spaces. It has also an inherent capacity for unifying a complex of buildings which gives it an active role in historic preservation strategy.

At the onset of this new atrium era, Martin and March (1966) demonstrated that the courtyard forms of development make more efficient use of land compared to tower and slabs forms. They can deliver the same floor area as the latter forms in lower buildings. They can ensure street continuity, sunlight and greenery, just as well the others with less expense and discomfort. This demonstration had a large contribution in the reaction in Europe against high rise buildings, and allowed courtyard form development to flourish in the field of housing, (see MacCormac (1973)). There has also been an increased awareness in developing countries of the value of high-density courtyard housing for the last 30 years or so. The financial stringencies of various governments has forced designers to look at this type of housing in a realistic manner. Many examples have been built in India, West Asia and North Africa in particular, (see Saini (1984)).

Spatial qualities of the atrium

One of the most exciting urban design values of atria is their contribution towards the richness of pedestrian experience in the city, and which architects and urban designers have explored to a great extent. They owe their large use to the new quality of space they offer, to the multiple characters and functions they can support, as routes, focal space or variants of the two. They can deliver varied and variable moods, depending on programmed social activities, (as private, semi-public, public or variations of these), in their furniture, (fountains, artworks), landscape and in the permanent or occasional activities they accommodate, (exhibitions for example). By being enclosed, sheltered, free from road traffic and noise, their usefulness is extended to many hours of the day, and in all seasons, with advantageous implications for marketing.

Role of atria in the preservation of historical buildings

Preservation of historic buildings has been an important urban design strategy recently. In the preservation schemes, atria have been extensively used to unify old and new structures in order to form a cohesive complex of buildings, and/or to give the old buildings a new interior. In the last application two main processes involving atria were utilised; either covering the courtyards that were contained in the buildings or the streets between buildings, or hollowing out atria in the existing deep planned buildings and producing more useful shallow spaces.

Impacts on the city

Atria have proved to be able to have dramatic effects in revitalizing the city centres in which they were built and change their image. The theatrical atrium Omni International in Atlanta, shown in Figure 2.7, is an example, (Bednar (1986)).

Atria, however, can do more harm than good in the urban environment when they are completely introspective. The threat is that, by turning their back from the street they can engulf most of the activities leaving the streets for service functions rather than human ones.

2.5 Climate control

The interest in energy conservation of recent years was certainly one of the major reasons that contributed towards the rehabilitation of the atrium and courtyard concepts in current architectural practice, as they were revealed to have inherent features to passively temper the indoor climate and reduce purchased energy.

The concepts, (in particular atria), are under the scrutiny of much recent research effort in energy conservation. Studies on the subject are found in the two main trends followed by the passive and low energy architecture research, and which are, i) the rediscovery of the ancestral knowledge behind the adaptation of vernacular buildings to the climate where they were erected, and ii) innovation of passive techniques which make use of the new technology. Reviews in the two fields are presented below.

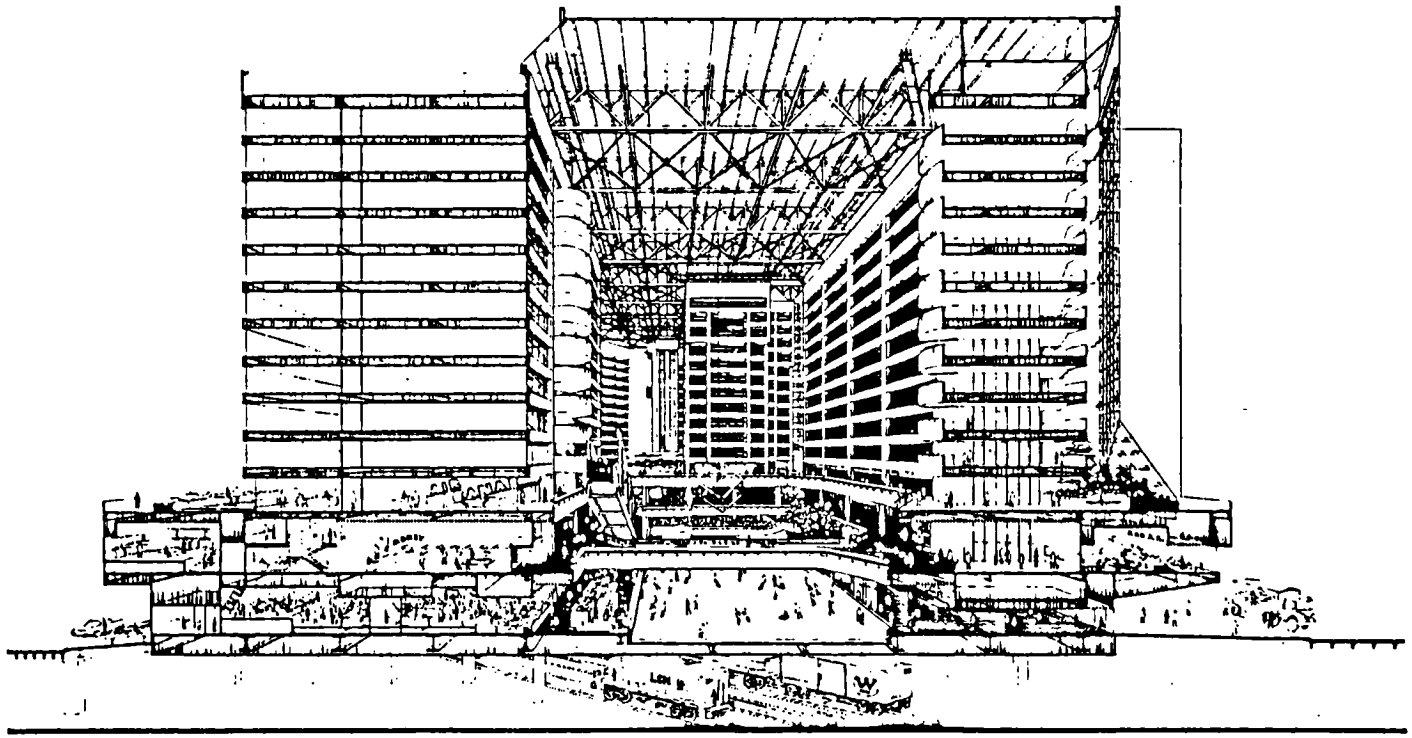

Figure 2.7: The Omni International, Atlanta, Georgia, (Architects; Thompson, Ventulett and Stainback), (Source Bednar (1986)).

2.5.1 The vernacular courtyard: a coordinate system of natural energy flow

2.5.1.1 The courtyard effect

It is recognised that among the primary reasons behind the introspection of the ancient courtyard houses was their ability to enhance the climate. These configurations were, and are, in many parts of the world the traditional building-type, (Hinrichs (1987)). As Dunham (1960) stated,

> "traditional housing all over the world has evolved through a system similar to natural selection: The fittest type survives", (Dunham (1960) p. 663).

Dunham (1960) was the first to explain how the features of the courtyard houses can utilise natural energy flows to compensate for the diurnal climatic variations in hot arid climates, and which is now well known under the "courtyard effect", (Gupta (1984)), (see Figure 2.8).

He explained that the beneficial thermal behaviour of the structure relies upon the radiation to the clear night sky of the heat gained by the structure during the day. The nocturnal temperatures in the vicinity of the surfaces most exposed to the radiant and coldest part of the sky, (the zenith), often drop below the ambient air temperature. The layer of cool air that is formed on the flat roofs is able to sink by gravity into the lowest level, (the courtyard floor and the earth), where it is stored for many hours after sunrise. This pool of cool air and the cool massive building elements are able to reduce the temperatures of the spaces surrounding the courtyard and to absorb internal heat gains during part of the day-time. The courtyard configuration helps also to retain this coldness by protecting the elements from incoming radiant heat, and convective heat from the hot winds. The thermal mass of the walls retards the temperature rise.

There has been hardly any scientific studies to confirm all the thermal mechanisms cited above. In fact, Fardeheb (1987), suggested that there could be some misconceptions about the effect of the down flow of cool air and also on the idea that this could be eased by inward sloped roof. His study was nevertheless inconclusive.

2.5.1.2 The geometrical characteristics of the courtyard: a key parameter

The techniques and tools available to the builders which allow them to achieve this climate regulation are discussed in many publications, for example, Hinrichs (1987) and Gupta (1984)). They were combinations of the following;

i) manipulation of the spatial configuration of the courtyard,
ii) characteristics of the construction materials,
iii) use of plants, water fountain and ponds,
iv) use of programmed ventilation,
v) urban planning.

There is a consensus of opinion that the courtyard proportioning is a determinant in the control of the thermal flows.

Control of solar irradiation

The primary principle to reduce heating and cooling load by passive means lies in the control of the solar irradiation of the building. In the courtyard concept, the manipulation of the court proportions governs the irradiation loads on the courtyard surfaces.

This subject was investigated by Mohsen (1979a) who developed a computer program which determines the amount of irradiation received by the courtyard form. The sets of courtyard proportions that were of relevance for solar loads were described as, i) A ratio indicating the deepness of the form (perimeter/height), ii) A ratio indicating the elongation of its plan (width/length), iii) A ratio indicating its openness to the sky (area of top opening/ground area).

The author undertook a parametric study in the context of the dry climate of Cairo, Egypt, in Mohsen (1979b). The main findings include:

i) For optimum summer conditions, the deepest and/or the most elongated courtyards in the E-W axis were most favourable. In winter the maximum irradiation load favours the shallowest courtyard and/or elongated shape in the E-W direction.

ii) Orientating the courtyard with an angle off its optimum direction (axis E-W) has the effect of increasing the solar radiation load in summer and to decrease it in winter. However courtyards can be orientated as much as 30°, without affecting the

irradiation by more than 10%.

iii) Finally, the irradiation load on the form's surfaces is significantly reduced by introducing a roof projecting over the south wall. The effect is greater than by projecting over any of the other three walls.

Figure 2.9 extracted from Mohsen (1979b) publication indicates that, for a single storey courtyard, the proportions that satisfy the minimum irradiation load in summer differ from the geometry which best satisfies maximum irradiation load in winter. Yet, there is a range of geometries for which the optimum in summer as well as in winter are close.

Control of radiative and convective energy flows

Natural ventilation and night-time radiative cooling are mechanisms that were claimed to have been extensively used in vernacular courtyard buildings to provide cooling. As with solar radiation control these mechanisms are also believed to have been handled through the manipulation of the courtyard geometry, (Leung et al (1981)), though much of the knowledge on this subject is vaguely and qualitatively stated. The review undertaken by Leung et al (1981) revealed very little scientific work on the subject.

Thermally-driven air movement could be set up in courtyards as a result of direct day-time solar radiation or from reradiation of heat stored in the building walls at night. The magnitude of these effects depend on the amount of solar radiation received and thus on the courtyard proportion. Leung et al (1981) suggested that these air currents could be dominant in deep courtyards, where the top and bottom surfaces are under different temperatures.

Wind-driven ventilation is also believed to be greatly influenced by the courtyard size. Leung et al (1981) suggested that the shallowest form is the logical design to enhance wind-driven ventilation. Yet, the authority of the statement is probably based on intuition.

Finally the geometrical characteristics of the courtyard, in particular the sectional aspect ratio (height/width), are likely to affect the radiative cooling performance of the courtyard at night. This component is probably greater for shallow courtyards, since the view angle to the sky vault afforded to the courtyard floor is larger, (Leung et al (1981)).

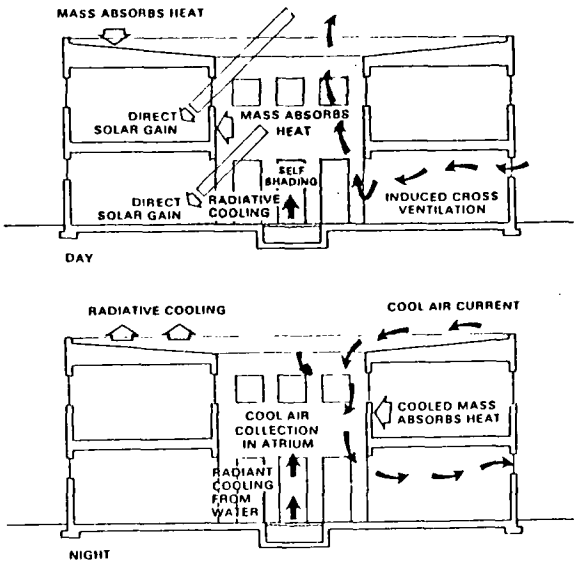

Figure 2.8: The "Courtyard Effect", (Source Bednar (1986)).

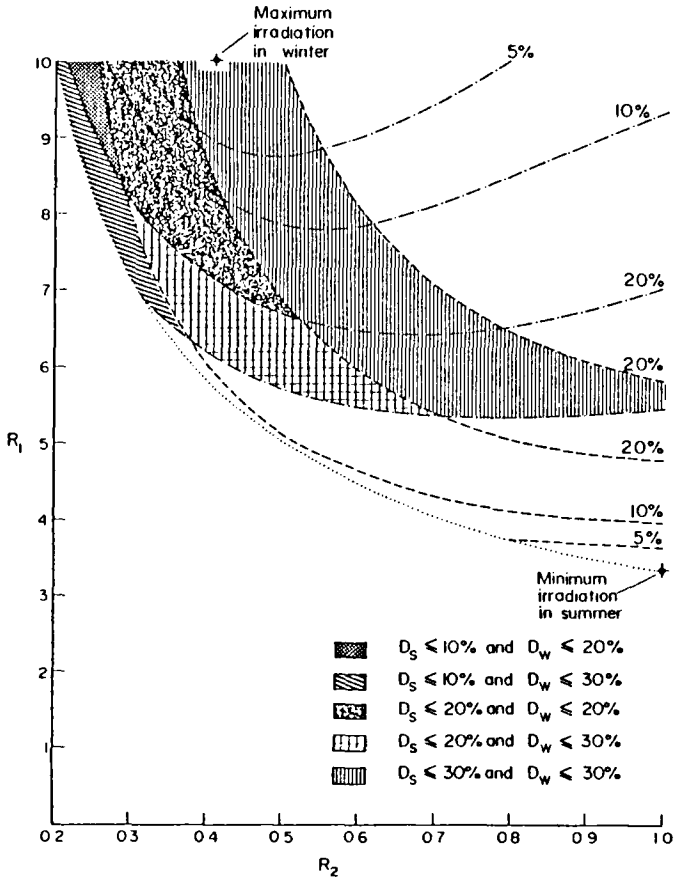

Figure 2.9: Deviations from the optimum irradiation in summer, Ds, and winter, Dw, for a single storey courtyard. *R_1 is the ratio of width to length and R_2, the ratio of perimeter to height,* (After Mohsen (1979b))

2.5.1.3 Vernacular courtyards under various climates

Hinrichs (1987) claimed that courtyard structures are found in most of the climates of the world, but mainly in the Mediterranean and hot arid regions. He believed that fine "adjustments" to "respond to the specific climatic needs" were made through "the proportioning of the courtyard void to the building solid". Leung et al (1981) shared also the same belief. Leung et al (1981) attempted even to prove that this speculation is well grounded by listing the recurrent courtyard geometries, (in particular sectional aspect ratio, (SAR)[1]), which were found under similar climate characteristics. In Figure 2.10, the relative depth of the vernacular examples reviewed by the authors were plotted according to the latitude of their sites. This figure is revealing of the extent of this spatial type under various climates.

Typically, deep courtyards (i.e., SAR > 1.3) are found near 30 degrees north latitude, which corresponds to desert climates, and where the main concern is to avoid solar radiation load. The traditional M'Zab townhouse in Algeria is an illustrative example of such a type, utilising thick walls for thermal mass, and a form of programmed ventilation that consists of opening the lowest courtyard level during summer nights, to allow the collection and storage of the cool night air, and covering it during the day-time. In these latitudes, shallow court (i.e., SAR < 1.3) are also encountered. Yet, in these circumstances the climate of the regions was identified as hot-dry but with relatively modest average summertime temperatures. These courtyards rely then on a diurnal buoyancy-driven process, and for which large view angles of the court floor to the radiant and cold night skies are preferable.

For low latitudes, for which the associated climate is warm and humid, all the courts with one exception were found to be of shallow type. Leung et al (1981) suggested that this is to facilitate wind-driven ventilation for thermal comfort. Vegetal cover were often used as solar protection to compensate for the less efficient self-shading of the court.

As one could expect, the courtyard examples associated with temperate climates had almost always low sectional aspect ratios. In these climates, with moderate to severe winter seasons, the primary need is for maximum solar heat gains in winter, and the court has to be wide enough to receive low angle winter sun. However, at the same time, the courtyard has also to provide some degree of wind shelter to reduce the heat losses. Vernacular examples of temperate climate courtyards were the Greek and

[1] SAR= height of courtyard/narrowest width.

Roman atrium houses, the urban house of Tunis and the compound dwelling of Peking.

2.5.1.4 Thermal performances of traditional courtyards

There is some scientific research behind the opinion that traditional courtyard buildings could present a better thermal environment than designs of much current practice.

Al-Azzawi (1984) for example undertook several measurements of environmental factors in old courtyard houses in Iraq and in more recent domestic buildings. The outcome of the study underlined the fact that better conditions were in general obtained in the old courtyard houses in summer season than with the modern ones. In particular the courtyard building developments were amorphous masses of contiguous buildings which resulted for the buildings of a minimum exposure to the sun. The solar radiation was often minimized in the courtyard by landscaping it. On the other hand, the modern houses were organised in isolated or semi-detached layouts, in which case, there was a maximum exposure of the walls to the sun. Some special devices, such as a wind catcher, and some architectural and construction details in old houses enabled the tempering of the hot and dry internal thermal environment conditions, (see also Al-Azzawi (1969)). The treatment of the old houses in Iraq for thermal comfort included in its equation a seasonal and daily migration of their occupants. In winter time, these vernacular houses were nevertheless suffering less comfortable thermal conditions than the new houses particularly because the rooms were often open directly to the courtyard which was exposed to the full impact of the weather.

As evidenced with the review of Leung et al (1981), very few scientific studies have attempted to unveil the thermal properties of the courtyard form. Many of these aspects still remain obscure and, pertinently, the way in which natural ventilation is induced is not well established, (this will be further discussed in Chapter 4).

2.5.2 Thermal principles in contemporary atria

Thermal performances of atria is the subject of the most up-to-date research in energy conservation. At the time of completing this thesis a whole section of the ISES Solar World Congress 1991, in Denver, will be devoted to atria. The international Energy Agency has also just concluded a seminar in the U.K., in which atria was the main topic, (see IEA (1991)).

In some energy conscious projects, the thermal benefit of the atrium is what

justified its use.

2.5.2.1 Conservation energy approach in atria

The courtyard can provide a kind of thermal regulation to the surrounding spaces while being subjected itself to the full impact of the climate. While the thermal functions of courtyards are clear, those of atria are more controversial, and the reason comes from the confusion in the comfort level to be achieved in the atrium, i.e., should the atrium be heated and cooled or unconditioned?

There seems to be an agreement of opinion that large atria are not a candidate for complete natural energy. The conservation of energy approach should rather attempt to achieve the maximum benefit from the natural flows by exploiting most of the atrium features and complete the task by mechanical means.

Atria should be able to exploit most of the thermal regulation principles of courtyards, at least when the roof is made largely openable. They have, in addition, features that can allow them to provide greater energy savings than courtyards. They are principally efficient in providing buffering effects, better solar gain controls, and the capacity to use the enclosed atrium space as an air plenum.

2.5.2.2 Passive heating and cooling features

Buffering effects

This concept refers to a space that protects the occupied zone from the full impact of the outdoor climate. Although buffering effects are possible in courtyard structures, they are best understood in the case of covered atria. In winter, for example, the temperature in an unheated atrium is greater than the outside due to internal heat gains or solar gains, (see for example the temperature monitored by Baker (1988) in a free-running atrium in Cambridge, U.K.). The elevated temperatures subsequently reduce heat losses from the heated occupied building and consequently save energy. Similarly the buffer concept can be exploited for saving cooling energy in summer.

The buffering effect works best when the glazing of the atrium exposed to the outside is small in comparison with the building wall areas it protects, (see Baker (1983)).

In a courtyard, some buffer effects can exist at least from wind sheltering effects.

Solar gains control

The glazed surface in atria can be located in roofs and walls, as shown in Figure 2.1, without being in conflict with the definition of the term. Top skylight of atria can have a neutral or selective orientation, as with clerestories or a polar roof. Atria can also have glazed side walls. The variety of the options offered allows a great control of the atrium solar irradiation load to suit the climate characteristics and the energy strategy of the building.

Air-handling

The atrium can be exploited to capitalize on infiltration losses. The large contained air volume can be used as a source of preconditioned make-up air for the surrounding buildings, to assist mechanical heating and cooling systems, or can be utilised as a return plenum, in which case the fabric transmission is reduced. The four main air handling principles in atria are;

i) complete separation between occupied space ventilation and the atrium,
ii) use of the atrium as a supply air plenum to occupied spaces,
iii) use of the atrium as a return air plenum,
iv) recirculated air.

2.5.2.2 Heating function

The heating functions of courtyards are restricted to limited thermal buffering, to direct solar gains, and thermal inertia of walls.

For modern atria, the main passive heating principles are, (Watson (1984));

i) maximize the winter solar gains, (heat collection),
ii) provide radiant heat storage, (heat storage),
iii) prevent excessive night-time heat loss,
iv) use the atrium as a supply or return air plenum.

The sensation of warmth can also often be reinforced by the psychological effects provided by the penetration of direct sun into the atrium floor or by the presence of exotic plants and animals, (Baker 1988).

Examples of atria in northern latitudes are numerous. Evidence of atria being

efficient buffer spaces and heat collectors exists. For example, the thermal simulation undertaken by Hawkes and Baker (1987) indicated that the benefits brought by a free-running atrium in the climate of Britain is to produce a "seasonal shift" from January to May. This means that the average temperatures in the atrium in January matches the external average temperatures of May.

Hancock (1987) demonstrated that roofing the courtyard of a hospital with a single glass can reduce the heat losses of the building by 32% under the British climate. If the atrium is used as a supply or return plenum, a further 4 to 5% reduction in heat loss can be achieved. In term of annual reduction of the heating plant this could represent 41% reduction for buffer atrium in comparison with the courtyard case, and a further 9% to 10% with preheating and exhaust ventilation modes.

The contribution of the air-handling could be significant as shown in the above mentioned simulation and that performed by Baker (1988). The latter suggested that the greatest benefits are obtained when the atrium is used as a source of preheated air or when there is a recirculation exchange, which may be obtained simply by opening the windows onto the atrium. In practice however, the technical problems of the exhaust mode are likely to be more solvable than supply mode.

Although the heating function of atria looks promising, it must not be lost from view that the inclusion of an atrium in an otherwise deep plan building is more likely to cause more heat losses than heat gains, owing to the poor levels of insulation of the surfaces of glass, (see Gillette and Treado (1988)).

2.5.2.3 Cooling function

Even in temperate climates, heating savings could represent a relatively small part of the total energy cost for non-domestic buildings, (Baker (1988), Saxon (1986)). Larger savings are often to be made in cooling, and also, summer time conditions are likely to cause more problems than winter in these buildings, (Baker (1983), see also Gillette and Treado (1988)). Also, in many building types incorporating an atrium, in particular commercial buildings, there is a heat surplus year round caused by large internal gains due to occupants, lighting and machines, (Saxon (1986)). Finally, the cost of frigories being higher that of calories[2], it is often the right strategy to reduce the cooling loads to a minimum.

---

[2] This is because artificial cooling consumes larger amounts of energy per degree of temperature change than heating, (Bednar (1986)).

As in any building, the cooling functions of courtyards and atria lie in the prevention of overheating and on the provision of cooling with the use of ambient heat sinks. The passive cooling design principles of covered atria are given in Watson (1984), Lahav et al (1987) and Mills (1990). Watson (1982) recommends to,

i) minimize solar gains, by providing roof shading,
ii) use the atrium as an air plenum,
iii) facilitate natural ventilation,
iv) use thermal mass.

Thermal mass is generally appropriate in climates where there is a large diurnal temperature swing. Nevertheless, it may have also important benefits in other climates either in absorbing solar gains and reducing peak temperatures, (Mills (1990)), or in enhancing stack-driven ventilation during night-time by reradiating the heat accumulated, (Watson (1982)).

There is nevertheless a limit to which cooling can be met by these passive means. Often, the best that can be achieved is internal temperatures slightly higher than ambient, when there is a good combination of shading and ventilation, (Baker 1988). In climates where a large diurnal temperature swing exists, temperatures below ambient can be obtain during a few hours in the mornings following night-time ventilation.

Atrium buildings designed for hot climates and using almost exclusively passive means exist. In the Princeton Professional Park built in 1980, New Jersey, (see Doubilet (1983)), almost the whole battery of the passive cooling techniques was used, including evaporative cooling provided by a roof spray. This was claimed to function in two ways, by rejecting heat by day and by cooling the air that circulates under the metal roof during the night to be stored in the rockbed for day use. State Office Building in Sacramento, California, shown in Figure 2.11, is a highly praised non air-conditioned atrium building. The cooling techniques comprise mainly rockbed storage, destratification fans, motorised louvers, and recirculated atrium air, (see Murphy (1981)).

Performance evaluation of atria for cooling

Evaluations of the thermal performances of atria in passive cooling mode are very scarce. This is probably because the majority of the atrium buildings that are being built

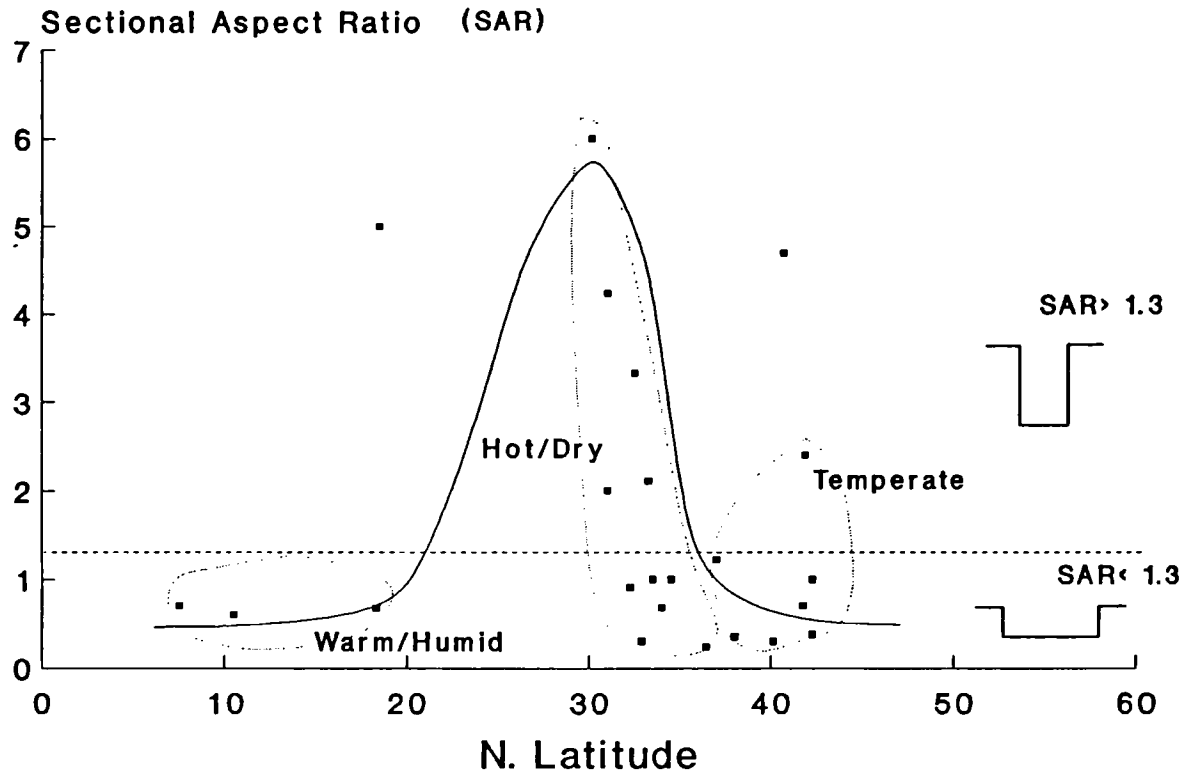

Figure 2.10: Graphic comparison between the proportions of an atrium and the latitude of its site, from 23 examples worldwide, (After Leung et al (1981)).

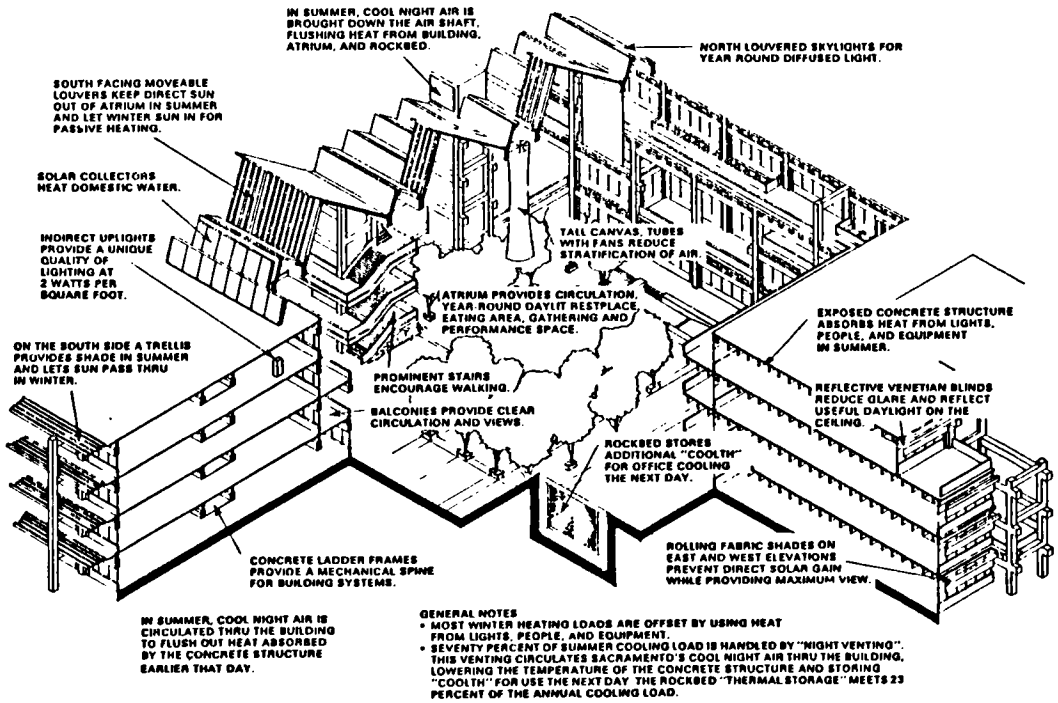

Figure 2.11: State Office Building in Sacramento, California (Architects; Office of the State Architect, Sim Van der Ryn), (Source Bednar (1986)).

in warm and hot climates are full air-conditioned and consequently do not motivate such studies.

Lahav et al (1987) provide the results of computer simulation of a large atrium in the climate of Jerusalem. In the summer season it is claimed that by providing ventilation of 10 air changes per hour, (levels that can be achieved by natural means), and efficient shading, the cooling loads can be virtually eliminated, especially if night ventilation is used, (Lahav et al (1987)).

Hancock (1987) concluded, from a computer simulation of a hospital building incorporating an atrium, that stack effect ventilation would probably be sufficient to vent and cool the atrium and linked building zones to comfortable temperatures in a typical British summer.

The large unconditioned atrium building, "Gateway Two", Basingstoke was claimed to be a successful design relying on natural ventilation during a summer season in Britain, (Hawkes (1984)). A recent monitoring of the building showed that overnight cooling of the structure was the most important factor in keeping the day-time conditions comfortable. The thermal mass and natural ventilation did also contribute to moderate the internal climate of this building which had high levels of internal gains, (see Trollope et al (1991)).

2.5.2.4 Warming, cooling, and convertible atrium

The passive heating and cooling features of the atrium enable the concept to be adaptable to a very wide range of climates, from cold to hot. Its design approach will be generally influenced by the most desired thermal function, i.e., heating or cooling.

Saxon (1986) distinguishes between the **warming atrium**, designed to collect heat, the **cooling atrium**, that normally rejects heat, and the **convertible atrium**, which attempts to do both at different seasons. The choice between each design approach is dictated by;

i) the climate,
ii) the building function. In some cases, offices and shopping centres may have surplus heat year round even in temperate climates,
iii) the degree of comfort required in the atrium.

2.5.3 Natural ventilation in perspective

The use of natural ventilation for cooling has a strategical importance in bioclimatic architecture.

i) As already discussed, passive cooling could be the option which might permit the greatest energy saving, particularly in commercial buildings since they often have surplus heat year round.
ii) The ventilation cooling is vital in a large range of climates, including the hot-dry climate with night-time ventilation, the warm and hot humid areas, such as the equatorial and tropical marine climates, and the Mediterranean climates, (see Givoni (1976)).
iii) Some 85% of the world population live in regions that are hot and humid at least during summer season, (see Meyers and Way (1981)).

There is thus a great importance in examining this aspect in the thermal functions of courtyard and atrium structures. In the next chapter the role of natural ventilation and the way it can be achieved is discussed in more detail.

2.6 Other environmental aspects

Other attributes of the courtyard and atrium concepts lie in the great amenities delivered by the provision of daylight, wind-shelter and protection from noise.

Although the present study is dedicated to natural ventilation the above-mentioned environmental aspects are important assets which preferably must not be lost in the pursuit for natural ventilation.

2.6.1 Daylighting

Daylighting is certainly among the most valuable aspects of an atrium or a courtyard and could not be omitted in this review. Also, requirements for daylighting may encroach upon requirements for natural ventilation, for example in the orientation of the building and in the design of the openings.

The provision of a view, even into a semi-open space, and the ability to have natural light entering the room are important assets. Daylighting in atria has a particular aesthetic role in setting moods and defining space that are very dear to architects.

Besides, there are also important pragmatic aspects such as substantially reducing the energy consumed by artificial light, providing an environment for growing plants and delivering a stimulating environment for work. Gillette and Treado (1988) demonstrated that daylighting was the greatest energy saving component of an atrium building compared to the same building but deep planned. These benefits are somewhat tempered by the increased average peak heating and cooling demand.

The atrium and courtyard configurations are one method of exploiting the natural daylight by allowing light to penetrate deep into the centre of the building and balancing the distribution of natural light within the occupied zone. Although all courtyards and atria have some daylighting implications the daylighting intentions of their designs can be varied. In this respect, Lam (1986), distinguishes atria and courtyard from litria and lightcourts. The latter are intended to maximize light in the adjacent spaces while in the former the daylight is rather intended for the activity held in their space, for growing plants, and most of all to enhance their glamour.

The control of daylighting levels in courtyards, atria, litria and lightcourts lies on the manipulation of three parameters;

1) Admission of light.
2) Distribution of light within the atrium or courtyard space.
3) Distribution of light to the adjacent occupied spaces.

According to their environmental requirements and to the climate characteristics there are different design responses for each of these parameters.

Admission of light

The first design decision on daylighting is about the amount and quality of the daylight to be admitted in the building, and the design response lies in the treatment of the courtyard or atrium apertures. Different design responses exist depending on the nature of the light source and the available levels of illumination.

For temperate climates, skies are expected to be cloudy most of the time. In these circumstances the best design is largely a top-lit unobstructed glazed roof for a covered atrium.

In sunny climates, the atrium and also courtyard apertures should preferably exclude sunlight or convert it into diffuse light, since direct sunlight is too harsh to be useful and is also likely to cause glare problems. Polar roof lights, skylight clerestories,

sawtooth roofs and other roofs types that make use of sunlight reflections are most appropriate. In courtyards, pergolas and trellis can perform this function. In very hot climates, the exclusion of sun is more stringent. A fabric roof can be an effective design solution, transmitting between 5% to 15% sunlight.

Finally, in climates that experience extreme variations in sky conditions, the most appropriate atrium aperture is a combination of sunscoops, to maximize sunlight in winter but minimize it in summer, and lightscoops which always provide diffuse light. In these climates, active shading systems able to respond to changes in sunlight and daylight levels are sometimes used.

Distribution of light

The first governing parameters that controls the rate of decay of light levels in courtyards and atria are their proportions and their orientations. The second parameter is the reflectivity of the walls, furniture, and other elements in the atrium such as plants.

Courtyards and atria, particularly in medium to high rise buildings, rely heavily on the multiple reflections the light undergoes from the various surfaces. In these circumstances wall finishes become important. In covered atria, the fact that the perimeter walls are protected from the atmospheric pollution is an important attribute. Indeed, the building may receive greater reflected light from its atrium than from the external building surfaces dirtied by the urban atmosphere, (Baker (1988)), even if the roof cover causes a loss in daylight admission.

There are several design principles which enable to optimise the distribution of light within atria, and a vertical fenestration hierarchy is an example, (see Saxon (1986)). This consists in increasing the windows progressively from top to bottom in order to avoid glare at the upper floors and bounce the light to the lower floor. Also, a common solution to provide adequate levels of daylight for each floor is to step the building profile vertically. The drawback is that this produces deeper spaces at the base of the atrium when there is less light available.

Distributing light into adjacent spaces

The main design concern for this function is the treatment of the interface between the rooms and the atrium or courtyard. This aspect is crucial with litria and lightcourts. In these structures, the design treatment is based on redirecting the direct or diffuse light into the work area using, for instance, lightshelves, tracking mirror louvres

and on controlling overlighting by local shading devices.

The manipulation of the three aforementioned components, viz-a-viz, admission of light, its distribution in the atrium and in adjacent spaces, is generally tested in physical scale models under natural or simulated skies. This technique is currently the only one available to the designer to simulate the complex behaviour of bounced light in atrium or courtyard surfaces. Calculation methods are nevertheless under development and simplified techniques already exist to deal with conditions of clear and overcast skies, (see Degelman et al (1988), Boyer and Oh (1988), Boyer and Kim (1988) and Kim and Boyer (1988)).

Possible conflicting requirements with natural ventilation

Conflicts in the requirements for daylighting and natural ventilation may arise mainly in the design of windows, since they have to perform both functions. An example of such conflict is when adequate quality of light requires sunscreens and louvres which may be a major obstruction to air flow. Countermeasures exist, however, for example with the segregation of the window functions.

After having opted for a design solution for enhancing natural ventilation, the designer can check with relative ease the daylighting implications in physical scale models or test other alternatives.

2.6.2 Wind effects

Shelter from the wind is uncontestably a valued amenity. Ettouney (1973), who studied the wind environment of courtyards, concluded that they provide a high degree of shelter, (this is true for the courtyard sizes tested, and for which the sides of the plan did not exceed 6 times the height). An order of magnitude for the wind speeds inside the courtyard enclosure is 15% to 45% of the external wind speeds taken both at eye-level. The precise value of shelter is nevertheless a function of the courtyard geometry and the wind characteristics. The best conditions are obtained for the smallest courtyard proportions, and with a wind striking the building at normal incidence.

Being more enclosed, the atrium should logically enjoy even greater sheltering effects from the winds. However, being tall and loosely partitioned, atria are particularly subject to draughts, leading to uncomfortable conditions and excess heat loss, (see Kobayashi and Ohba (1987)). The treatment of entrances are particularly crucial to avoid them becoming wind tunnels.

In the pursuit of offering generous natural ventilation for summer cooling, the wind sheltering qualities of courtyards and atria must not be seriously affected.

2.6.3 Acoustics

Another important quality of the courtyard, which is often forgotten, is its acoustic properties. This subject was investigated by Ettouney (1973). The salient results of the experimental tests showed that the maximum attenuation of the sound was obtained in the courtyard structure when the latter was located close to the noise source. The courtyard configurations could thus have interesting applications in urban planning where they can act as noise shield to other buildings, while enjoying comfortable sound conditions.

The author recommended for the design of courtyards narrow shapes with minimum open links to the spaces external to the buildings. To reduce multiple sound reflections, the surrounding walls of the courtyard should preferably be sound absorbent or have high void to solid ratios, which could be provided by verandas or alcoves. Noise generated within the courtyard could be, on the other hand, problematic owing to the quality of the space and also to the hard finish of the surrounding walls which cause multiple reflections.

Atria could also present a difficult design problem when dealing with internal noise sources, (sources within the internal spaces, from adjacent spaces and noise from HVAC systems). For aesthetic and functional reasons, atria tend to have the quality of outdoor spaces with floors and walls finished in hard materials. These hard finishes cause a long reverberation time which tend to create extremely resonant "ecclesiastical acoustics". Also, the rectangular or square shape with flush internal surfaces, which prevail in atrium design, promote cross reflections between walls, which reinforce certain frequencies and cause an uneven distribution of sound. These acoustical problems can cause concern for the atrium space itself and for the surrounding windows if naturally vented by opening windows.

However, design responses to the noise problem exist. First, the architectural planning for the spaces around the atrium, and the design of the internal shape can help. An internal modelling and layout that serves to break up reflected noise will reduce reverberation time and lower the overall noise levels. Similarly, elements of the design such as walkways, columns and lifts can be positioned so that they can work as acoustic obstructions

Secondly, materials and finishes can be chosen to absorb noise. For aesthetic reasons, however, it is not always possible to introduce large area of these absorptive panels. Nevertheless, placed at strategic locations in the wall cladding, relatively small surfaces of coverage can have dramatic effects. For example, portions of the roof that are opaque can be treated with absorbent materials. Otherwise the absorbent surfaces may be disguised. Sound absorber elements such as banners, drapery hangings and planting can be highly decorative. A large range of features that can be used to assist acoustic design is listed in Mills (1990).

Certainly, there are conflicting requirements between noise control and natural ventilation, since open windows are routes for both air flow and noise. Also winds may cause audible resonances in light elements, such as sunscreens, draperies, or in loosely connected parts. Yet, as discussed above there are responses for these conflicting designs in most of the cases. Examples of designs where natural ventilation and acoustic performances are reported as being both successful exist, such as Gateway Two, Basingstoke U.K., discussed in Hawkes (1983, 1984).

2.7 Fire safety

Fire safety and smoke control in atria is still currently causing some concern. In the past, fire problems was probably a major reason for the atrium decline.

Smoke control has an immediate relevance with natural ventilation of structures and in general with the air-handling systems. Indeed, ventilation used to modify the building environment must not have adverse effects on the smoke extract in the event of a fire. Smoke control strategy is also best dealt with when integrated with the ventilation system.

Fire safety concerns in atria

There have been few atrium fires world-wide from which lessons can be learnt, so the reaction with most fire authorities in dealing with this non-conventional design is extreme caution. This caution is founded as atria present fundamental safety problems: fire and smoke can spread vertically very quickly if openings in the floors are not properly enclosed. This will endanger people on upper floors and impede evacuation and fire fighting. In conventional buildings the spaces are divided by floors which offer greater resistance to the growth of fire and spread of smoke. Despite these problems, atrium buildings are argued by some specialist in the field to be as safe as any

conventional one, provided proper detection, fire and smoke systems exist. In fact, the concept presents many advantages, such as offering superior visibility and clarity of escape routes, as well as facilitating the discovery and access to the fire. The main debate in atrium fire at the moment is on smoke control.

> "The risk of floor to floor fire spread up the inner face of an enclosed atrium is not different to that at the outer face of any building", (Law (1983) p. 15, in MacCormac et al (1983)).

Two incidents that happened in atria in the United States of America reinforce the belief that smoke might be a major problem. It is frequently argued that smoke entering the huge volume of an atrium will be so diluted and so cooled that it will not be a hazard. Unfortunately, this ignores the fact that even a small fire produces vast quantities of smoke in a tall building, and an atrium volume however large can very quickly fill with dense smoke. Certainly smoke entering an atrium will be diluted by the great quantities of cooled air but this is not an advantage since buoyancy forces will be reduced and will inhibit natural venting, (Parnell and Butcher, (1984)).

Smoke extraction concepts

The design of smoke extraction and control in atrium buildings revolves around two main concepts:

i) the atrium is open-sided or enclosed,
ii) the smoke-removal is via the atrium or away from it.

The choice between the options will be largely dictated by the atrium programme, (i.e., activities to be catered and comfort levels to be achieved in the atrium).

Extracting smoke away from the atrium has psychological and physical benefits. The signs of fire being mainly restricted to the fire floor reduce the desire to evacuate other levels. This option is economically feasible when the atrium floor present minimal fire-risk and load. Otherwise, smoke extraction will also be needed for the atrium, which means the systems have to be duplicated. This strategy can be suited for a buffer atrium, (where resistant barriers between atrium and surrounding space exist), or with open-sided atria used exclusively for circulation. This extraction alternative is

appropriate to an atrium used as a supply plenum, (see Figure 2.12, example a).

Extraction via the atrium is mandatory when the atrium presents a fire-risk. Reservoirs and defences against smoke invasion such as screens and suitable edge profiles at the atrium galleries are such countermeasures offered to the designers to tackle the smoke invasion in open floors and open-plans. A reservoir will also be needed in the atrium roof, as very important smoke volumes are generally dealt with, (much greater volume to be extracted than with alternative routes). This reservoir may include upper floor levels if these are screened off. Tall roof reservoirs are advantageous in natural venting strategy as they permit the required area of vent to be reduced, lowering the overall cost of the system. The extraction route via the atrium is compatible with using the atrium as a return or exhaust plenum, (see Figure 2.12, example b).

As with any conventional building of sufficient size, smoke extraction must be complemented by a control of the fire size and by the provision of protected escape routes. Parnell and Butcher, co-authors of the book by Saxon (1986), suggested several possible protected circulation concepts in atria, and which are best protected from smoke invasion by pressurization, (i.e., maintained under positive pressure to ensure that it is kept smoke free). The atrium can also be used as a protected route if the whole atrium is of incombustible construction, contains no fire load, is separated from all accommodation and pressurized. But to the authors knowledge, no such atrium exist. Limiting the fire-size is best achieved by active fire-control methods.

Natural ventilation for smoke control and extraction

Up to atrium heights of about 20 m, smoke should lift itself by its buoyancy forces alone out of roof vents in temperate climates. In taller atria difficulties could arise, as the diluted smoke become cooler and may not lift itself out of the atrium. The natural ascension of smoke may also be inhibited when outside temperatures are higher than smoke temperatures, or when the atrium roof suffers down-draughts from taller building elements surrounding it. In these circumstances, it is necessary to ensure powered extraction delivered by smoke removal fans which are best designed as part of the normal air-handling equipments. Smoke extraction must be accompanied with make-up air. This is generally supplied at the base of the space, at a rate matching the smoke extraction.

Many existing buildings and shopping complexes rely on natural ventilation for

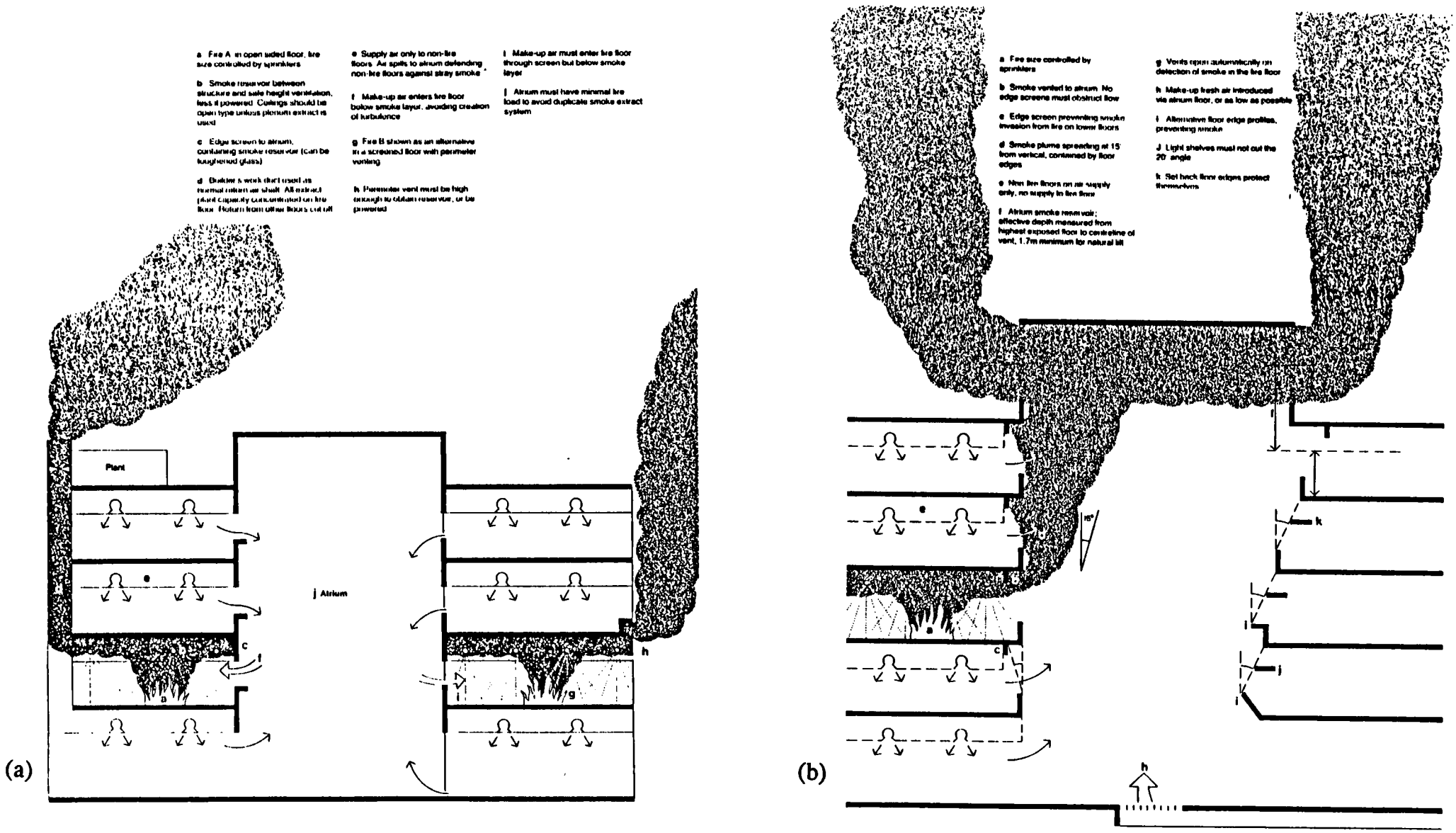

Figure 2.12: Examples of smoke extraction away from the atrium (a) and via the atrium (b), (Source Saxon (1986)).

their smoke extraction and also sometimes for the pressurization of their escape routes. It is particularly advantageous to use natural ventilation when it is also used for environmental control. However, care must be taken to ensure that the way the air movement is handled matches in both cases and that the wind would not have an adverse effect on the discharge of smoke. To rely on natural ventilation for ensuring delicate pressurization of the escape routes is not favoured as the climatic conditions are very changeable. It is also often recommended that permanent openings must be used to ensure continuing cross-ventilation which may well create uncomfortable conditions for the occupants.

Meeting the codes and regulations

Designing for fire safety means meeting the codes and regulations requirements of the local authorities. In the case of atria, problems are often specific for each design, so that every building designs must often be analysed in their own right. The designer must thus preferably involves the authorities at an early stage of the design.

2.8 Discussion and conclusion

This chapter has outlined some of the attributes of courtyards and atria. Among other reasons for the renewal of interest in atria, (and to a lesser extent courtyards), are the role they play in urban design and also the way they temper the indoor climate and save purchased energy.

These concepts, notably the atrium, are currently the focus of interest of research in energy conscious design. Nevertheless, so far its cooling function has been given little attention compared to its heating capability. The lack of knowledge in this field, though of great importance in energy conscious strategy, justifies the theme of the present thesis. Among the different factors involved in the climate regulation function of courtyards and atria, natural ventilation should have an important role to play in cooling.

Designing for natural ventilation must however not segregate the important assets of these configurations, such as daylighting and wind shelter, discussed in this chapter. Acoustical problems and fire safety are also issues to be addressed concurrently in their design.

In the next chapter the natural ventilation requirements, the motive forces and the physics involved in indoor air movement will be discussed.

Chapter 3:

Natural ventilation: theory and practice

3.1 Introduction

In this chapter, the functions of ventilation, the motives forces and the main factors influencing the air motion are reviewed. These background information are necessary before broaching the review of the related studies in the field of ventilation in courtyard and atria.

First of all, some terms must be defined. Ventilation comes from the Latin word *Ventus* and means the movement of air. Three forms of air motion in buildings can be differentiated;

i) natural ventilation,
ii) infiltration,
iii) forced ventilation.

Natural ventilation relates to air movement through purposely designed openings, like open windows, fireplace and open doors. The infiltration is involuntary and is caused by inadvertent leaks through the building envelope, such as cracks and leakage through doors and windows. Finally, forced ventilation is produced by mechanical ventilation systems.

Ventilation can also designate indiscriminately a system providing fresh outdoor air and a circulation of air within a building. In practice the two tend to overlap. However, there are cases where the air is mostly recirculated, (e.g., air conditioning

systems). Depending on the purpose of the ventilation one aspect can be more important than the other. The amount of fresh air and the mixing efficiency are the factors of concern for indoor air quality. For the evaporative cooling of the body, air velocity is of prime importance.

3.2 Ventilation requirements

Ventilation can serve several ends, (see Figures 3.1). These can be conveniently divided into four;

i) health requirement,
ii) thermal comfort,
iii) preservation of the building fabric and furniture.

The first is to provide a sufficient oxygen supply and maintain the quality of the air in the building above a certain minimum level by replacing stale indoor air by fresh outdoor air. This requirement may be termed health ventilation and should be satisfied in all weather conditions.

The second function is to provide thermal comfort. This can be subdivided into two functions. The first relates to the direct effect of the air velocity on the thermal comfort of the occupant, such as increasing the heat loss from the body and preventing discomfort due to moist skin. The second category is often referred to as structural cooling, (or heating), and concerns the removal of excess of heat and storage of coolness by the structure. Both are usually needed during certain weather conditions only.

The third requirement refers to the control of the moisture level necessary to inhibit the development of mould spores, (see for example Brundrett and Onions (1980) and Aberg (1989)) and house mite proliferation, in order to preserve the integrity of the building fabric and furniture.

Finally, the last function of ventilation is to control smoke in the event of a fire. This function was already discussed in Section 2.7, and was seen as being a stringent requirement in the design of atria.

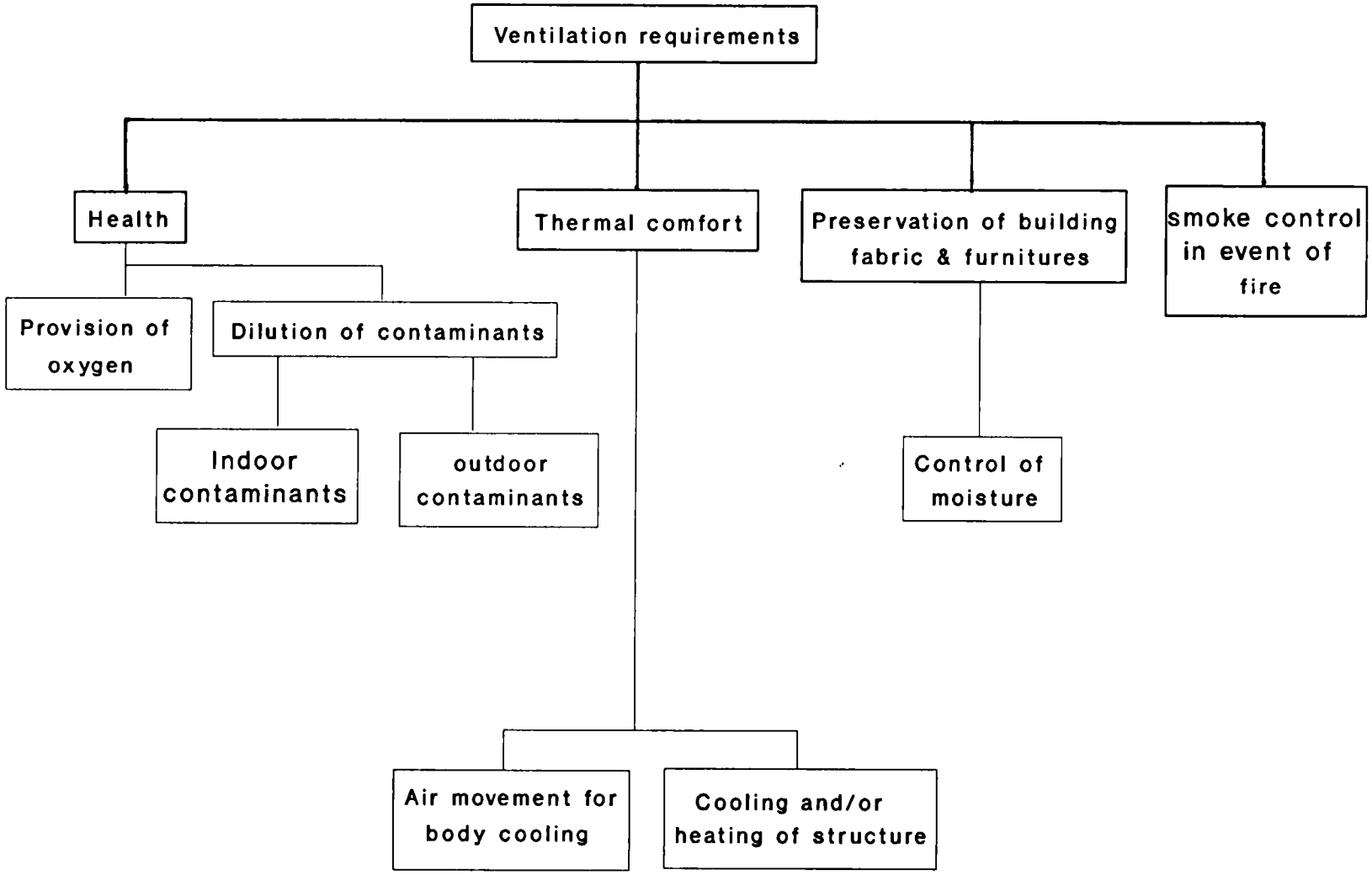

Figure 3.1: The requirements for ventilation

3.2.1 Minimum ventilation rates or permanent ventilation requirements

The minimum ventilation rates which must be ensured in buildings permanently for the occupant health determine generally the ventilation requirements in winter time.

With this ventilation function, not only the rate of fresh air is important, but also the efficiency of the mixing of the new air with the old.

3.2.1.1 Provision of oxygen

The provision of oxygen and the removal of excess CO_2 is hardly the criteria established for minimum ventilation rates. This is because the sufficient flow rates for this function are considerably lower than those for other requirements such as the control of odours or smoke. A design figure for the ventilation needed for CO_2 dilution is 8.5 m^3h^{-1} per person to hold the CO_2 level in a space to 0.25% or below, (CIBSE Guide 1986).

3.2.1.2 Removal of contaminants

The minimum ventilation rates are rather based on the sufficient rates to dilute to acceptable levels contaminants which may be a health hazard to the occupants or which may create an uncomfortable atmosphere. Figure 3.2 lists some of the most common outdoor and indoor contaminants. Further details on indoor contaminants, their generation and their level of toxicity can be found in Meyer (1983).

In most cases, the acceptable levels of body odours and smoke are taken as the minimum ventilation criterion. Several empirically derived ventilation rates of fresh air have been suggested to reduce the body odours to acceptable levels. They were based on the subjective perception of individuals, (see Lehmberg et al (1935) and Yaglou et al (1936, 1937)). The recent minimum air changes suggested by ASHRAE Standard (1981a) required to remove body odours is 5 ft^3min^{-1} per person, (i.e., 2.4 ls^{-1} per person).

Tobacco smoke is objectionable to non-smokers, can cause eye irritation and can interfere with visibility. Because it is persistent and can be absorbed by surfaces for days it is one of the most difficult pollutant to control or eliminate. The air change rates suggested by ASHRAE Standard (1981a) are given in Table 3.1.

The problem of removing other contaminants than tobacco smoke or body odours, when they are in important concentrations, are considered individually. The ventilation

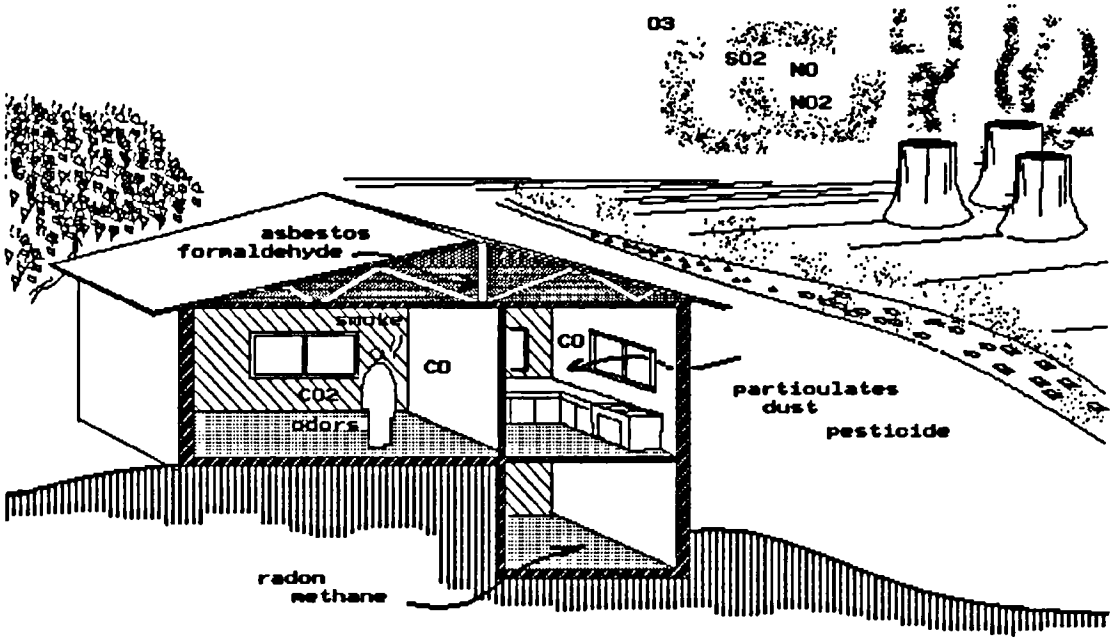

Figure 3.2: Examples of indoor and outdoor air pollutants in residential buildings.

Table 3.1: Recommended minimum ventilation rates for commercial buildings, (Source Meyer (1983)).

Commercial Area	Estimated Persons per 1000 ft² Floor Area	ASHRAE 62-1973 Outdoor Required Ventilation Air per Human Occupant				ASHRAE 62-1981	
		Minimum		Recommended		Smoking	Non-Smoking
		cfm	l/s	cfm	l/s	cfm	cfm
Shoe repair shops (combined work-rooms/trade areas)	10	10	5	15-20	7.5-10	15	10
Garages, auto repair shops, service stations							
Parking garages (enclosed)	—	1.5	7.5	2-3	10-15	1.5	1.5
Auto repair workrooms (general)	—	1.5	7.5	2-3	10-15	1.5	1.5
Theaters							
Auditoriums (no smoking)	150	5	2.5	5-10	2.5-5	35	7
Auditoriums (smoking permitted)	150	10	5	10-20	5-10	35	7
Ballrooms (public)	100	15	7.5	20-25	10-12.5	35	7
Bowling alleys (seating area)	70	15	7.5	20-25	10-12.5	35	7
Gymnasiums and arenas							
Playing floors—minimal or no seating	70	20	10	25-30	12.5-15	—	20
Locker rooms	20	30	15	40-50	20-25	35	15
Spectator areas	150	20	10	25-30	12.5-15	35	7
Amusement parlors and pool rooms	25	20	10	25-30	12.5-15	35	7
Swimming pools	25	15	7.5	20-25	10-12.5	—	0.5
Iceskating, curling, and roller rinks	70	10	5	15-20	7.5-10	—	20
Transportation							
Waiting rooms	50	15	7.5	20-25	10-12.5	35	7
Ticket and baggage areas, corridors, and gate areas	50	15	7.5	20-25	10-12.5	35	7
Concourses	150	10	5	15-20	7.5-10	35	7
Offices							
General office space	10	15	7.5	15-25	7.5-12.5	20	5
Conference rooms	60	25	12.5	30-40	15-20	35	7
Doctors' consultation rooms	—	10	5	10-15	7.5-10	35	7
Waiting rooms	30	10	5	15-20	7.5-10	35	7
Educational Facilities							
Classrooms	—	—	—	—	—	25	5
Laboratories	—	—	—	—	—	—	10
Libraries	—	—	—	—	—	—	5

needed to remove to acceptable levels of concentration of contaminants is generally derived from a knowledge of the generation rate and the decay of the concentration of the pollutant.

3.2.2 Thermal Comfort or occasional ventilation requirements

In summer and hot weather, thermal control is more commonly the determining requirement. In these conditions requirements are related to the thermal characteristics of the building and the pattern of occupancy which determine the thermal loads.

3.2.2.1 Air movement for body cooling

One of the primary conditions for health, well being and comfort is to maintain thermal equilibrium between the human body and its environment. This involves conserving the temperature of the core tissues of the body within a narrow range, regardless of the relatively wide variations in the external environment.

The heat exchange between the human body and its surroundings can be represented as a sum of four major processes:

$$S = M \pm R \pm C - E \qquad (3.1)$$

where S is the change in the heat content of the body, reflecting the variations in the average body temperature, M the rate of metabolism, R, C and E are the radiative, convective and evaporative heat exchanges respectively. Ventilation intervenes in the heat balance in terms of

i) dry heat exchange by convection,
ii) evaporative cooling.

Dry heat exchange by convection

Because the air is a poor heat conductor, the heat exchange between the skin and a layer of air in contact with it relies primarily upon air currents. The convective heat exchange, (heat loss or gain), depends on the difference in temperature between the person's skin and the air, on the velocity of the air and on the clothing. Convection heat exchange is assumed to be proportional to the temperature difference between the air

and the skin and also probably on the power of 0.3 to 0.7 of the air velocity, (ASHRAE Handbook of Fundamentals (1989a), and Givoni and Berner-Nir (1967)).

Evaporative cooling of the skin

The cooling effect of the airflow on the occupants relies also on the evaporation of sweat from the skin. If the surface of the skin is too hot, sweat is secreted from the pores. As it evaporates, this liquid removes the latent heat of evaporation from the surface. This is a highly efficient process because for every gram of water that is evaporated about 0.58 Kcal is consumed, (see Givoni (1976)). The body can lose great quantities of heat even when the ambient air and mean radiant temperatures are above the skin temperatures.

The rate of evaporation is influenced by;

i) the clothing,
ii) the relative humidity,
iii) the air velocity.

The lower the vapour pressure and/or the higher the air velocity, the greater the evaporative potential will be. Clothing reduces the air velocity and increases the humidity over the skin and thus reduces the evaporative cooling potential of the body. Several formulae presenting the computation of the maximum evaporative capacity of the air as a function of the vapour pressure and air velocity can be found in Givoni (1976).

Comfort indices

As a result of the heat loss, the exposure to wind has the same comfort sensation as lowering the temperature of still air. A number of complex indices have been developed combining different comfort parameters such as air temperature, mean radiant temperature, relative humidity and air movement. The methods for the assessment of the human comfort and the computation of the air velocity required for comfort under different conditions are based on these indices. Details and comparisons of the various comfort scales can be found in specialized literature, (ASHRAE Handbook of Fundamentals (1989a), and Givoni (1976)).

In human thermal comfort, the most pertinent ventilation criteria is the local air

speeds in occupied portions of the space rather than the volumetric air change rates or the mixing efficiency used for health requirements.

3.2.2.2 Ventilation for cooling or heating of structures

Another important function of ventilation that is closely related to comfort is to assist in controlling the thermal conditions of buildings, during periods of low or high air temperature, to cool or heat the structure and its contents.

When the building is ventilated the air entering the indoor space has its original outdoor temperature, but in traversing the internal space it mixes with the indoor air and heat is exchanged with the internal surfaces according to the indoor-outdoor temperature difference. This convective air exchanges can be made advantageous in removing the excess of heat caused by casual gains from people, lighting and equipment and from solar gains through the fabric and openings, particularly in summer.

The ventilation can be used similarly to heat massive structural elements in the cold season by introducing warm outdoor air during the day. In these instances, the ventilation air can be preheated before entering the core of the building by solar gains of a greenhouse or an atrium, (see for example Baker (1985)).

The quantity of heat removed from or added by ventilation to the indoor space Qv (W) is the product of the airflow rate Q (m^3s^{-1}), the specific volumetric heat capacity of the air, Cp ($KJ \times kg^{-1} C^{-1}$), the air density, ρ, and the difference between the outdoor and the average indoor temperatures $t_i - t_o$ (°C), (see ASHRAE Handbook of Fundamentals (1989b)).

$$Qv = Q \times \rho \times Cp \times (t_i - t_o) \qquad (3.2)$$

3.3 The motive forces

Whereas in practice there is sufficient infiltration of air through the window cracks to provide the necessary air flow for health requirement in most ordinary buildings, (except when very effective weather stripping is applied), for summer cooling difficulties could arise in attaining the desired air velocities. In particular, the design of the building can be determinant in succeeding or failing to meet the requirements. In the rest of the chapter the discussion will refer to this last function of the ventilation, unless otherwise specified.

The forces driving air exchange are maintained by the natural actions of wind and temperatures and/or by the pressures induced by the operation of mechanical ventilation systems. The mechanisms behind the induction of the flow are now reviewed. A discussion of their aptness to drive ventilation cooling in summer season will follow.

3.3.1 Wind pressure induced ventilation

3.3.1.1 Mean pressure

When wind impinges on a building, some or all of its kinetic energy is transformed into pressure head. The air pressure on the sides facing the wind is elevated above atmospheric pressure, (pressure zone), and on the wake region of leeward sides it is reduced, (suction zone). The pressure differences that are set up across the building determine the potential driving force for ventilation when openings are provided. The static pressures over the building surfaces are almost proportional to the velocity head of the undisturbed airstream. The dynamic wind pressure, Pv, is give by Bernoulli's equation:

$$Pv = \frac{1}{2} \times \rho \times V^2 \qquad (3.3)$$

The pressure difference, ΔP, of the total pressure at any point on the building envelope and the atmospheric pressure is generally expressed as a fraction of the dynamic pressure, (i.e., $\rho \times V^2/2$), and is known as the pressure coefficient, CP, given by the relationship;

$$CP = \frac{\Delta P}{\frac{1}{2} \times \rho \times V^2} \qquad (3.4)$$

Values of CP depend mainly on the building shape, wind direction and neighbouring obstacles.

Flow of air due to mean wind pressures

The most used steady state formulation of the flow induced by mean pressure differences through open windows is that derived from orifice flow theory. It is as follows;

$$Q = Cd \times A \times V_{ref} \times \sqrt{\Delta CP} \qquad (3.5)$$

Where Q is the volume rate of flow (m^3s^{-1}), Cd, the coefficient of discharge, A, the area of opening (m^2), ΔCP, the pressure coefficient difference across the openings and V_{ref}, the velocity at a reference height, (the same for which CP values are referred to).

To achieve maximum airflow through a building, its form, orientation and exposure to wind must be such that the pressure differences between locations of openings are maximised with respect to local wind characteristics. The induction of internal air movement is further discussed in Section 3.6.2.

3.3.1.2 Turbulent fluctuations

The turbulent nature of the atmospheric wind caused by local terrain roughness and eddy shedding results in corresponding fluctuations to the wind induced pressure distribution. These transient departures from the mean pressure distribution are not represented in the steady state formulation of the flow and are generally ignored.

There are, however, instances where the turbulent component of the wind governs the internal flow or contributes an additional component to the rate of air infiltration or ventilation. The effect of fluctuating ventilation is especially significant when the mean pressure difference across an opening is small in comparison with the size of the fluctuating component. The case of two opposite openings orientated parallel to the flow is representative of such a situation, (see Figure 3.3, example a). The pressure fluctuations can result in significant instantaneous pressure differentials that induce air movement through the building alternately from each side. The British Research Establishment, BRE Digest (1978), suggests that the magnitude of the flow can be approximated by giving a value of ΔCP equal to 0.2 in equation (3.5).

Another type of turbulent ventilation to which the single opening enclosure in Figure 3.3, example b, is representative, is the eddy flow, (in opposition to pulsating

flow described before). In this case, air exchange across an opening is due to the penetration of eddies which cause air to enter and exhaust the room through the same opening.

Allowance for turbulence is generally made by considering that the turbulent pressure distribution with respect to time has a Gaussian distribution, (Etheridge and Alexander (1980), and see Liddament (1986) for further details). Nevertheless, there is still insufficient information about these phenomena. This subject is treated by Malinowski (1971) and Haghighat et al (1991). A list of references on the subject is provided in this latter publication and in Allen (1984).

3.3.2 Thermal buoyancy

Whenever there is a difference in temperature, and hence a difference in density between the air indoor and outdoor air, it produces an imbalance in the pressure gradients of the internal and external air masses. This can cause an exchange of air if ventilation openings are located at different levels. The flow of air induced by these pressure differences is similar to the draft associated with a chimney, which is why this process is often referred to as chimney or stack effect.

For a uniform temperature, the pressure of a mass of air at any elevation Z above a convenient datum level Zo, (for example the ground level), is given by;

$$P(z) = P_o - \rho \times g \times Z \qquad (3.6)$$

where P_o is the pressure at the datum level Zo and g the acceleration due to gravity. The vertical pressure gradient equation can be expressed as follows:

$$\frac{dP}{dZ} = -\rho_o \times g \times \frac{273}{T} \qquad (3.7)$$

where ρ_o is the air density at 273 K, (kgm^{-3}), and T the absolute temperature of the air mass (K), (see Liddament (1986)).

A simple case of two openings at h_1 and h_2 levels and vertically separated a distance h apart is illustrated in Figure 3.4, example a. The outdoor temperature is assumed lower than the indoor, (i.e., heating season). The density difference in the air

between the interior and the exterior develops a pressure difference profile across the envelop. The stack induced pressure, Ps, at h_2, with respect to the pressure at h_1, which is represented by the horizontal displacement of the pressure curves at these locations is equal to,

$$Ps = -\rho_o \times g \times 273 \times (h_2 - h_1) \times \left(\frac{1}{T_o} - \frac{1}{T_i} \right) \qquad (3.8)$$

where T_o and T_i are respectively the absolute external and internal temperatures (K), (see Figure 3.4, example a).

The point in the vertical surface where the interior and exterior pressures are equal is called the Neutral Pressure Level (NPL), and corresponds to the transition between inflow and outflow. The level of NPL is a function of the overall distribution and the flow characteristics of openings. For openings uniformly distributed vertically, the NPL will be at mid-height of the building.

In Figure 3.4, example b, the stack effect is illustrated for a building with airtight separations at each floor. In these circumstances, each story acts independently. However, real buildings are neither open inside, (Figure 3.4, example a), nor airtight between stories, (Figure 3.4 example b), but there are vertical passages such as stairways or elevators. Figure 3.4, example c, is more representative of the real case.

Flow of air due to buoyancy alone,(ASHRAE Fundamentals (1989b))

The flow in this case is given by[1];

$$Qs = C_s \times A \times \sqrt{2 \times g \times h_{NPL} \times \frac{T_i - T_o}{T_i}} \qquad (3.9)$$

where Qs is the airflow due to the stack (m^3h^{-1}), A (m^2) is the free area of the inlet or outlet openings (assumed equal), h_{NPL}, the height from lower opening to NPL

[1] The equation given in ASHRAE (1989) contained some inconsistencies (see equation (19) p 23.8 in the book). The corrected form presented here was obtained from ASHRAE Handbook (1990), in the appendix A.7: *Additions and corrections*).

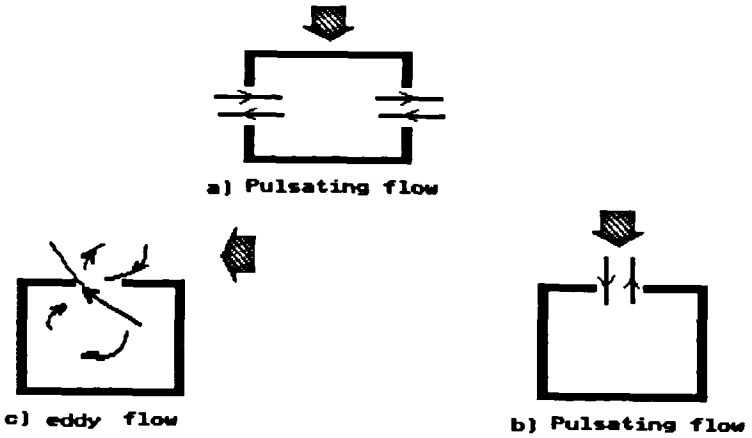

Figure 3.3: Turbulence -driven ventilation, (After Haghighat et al (1991)).

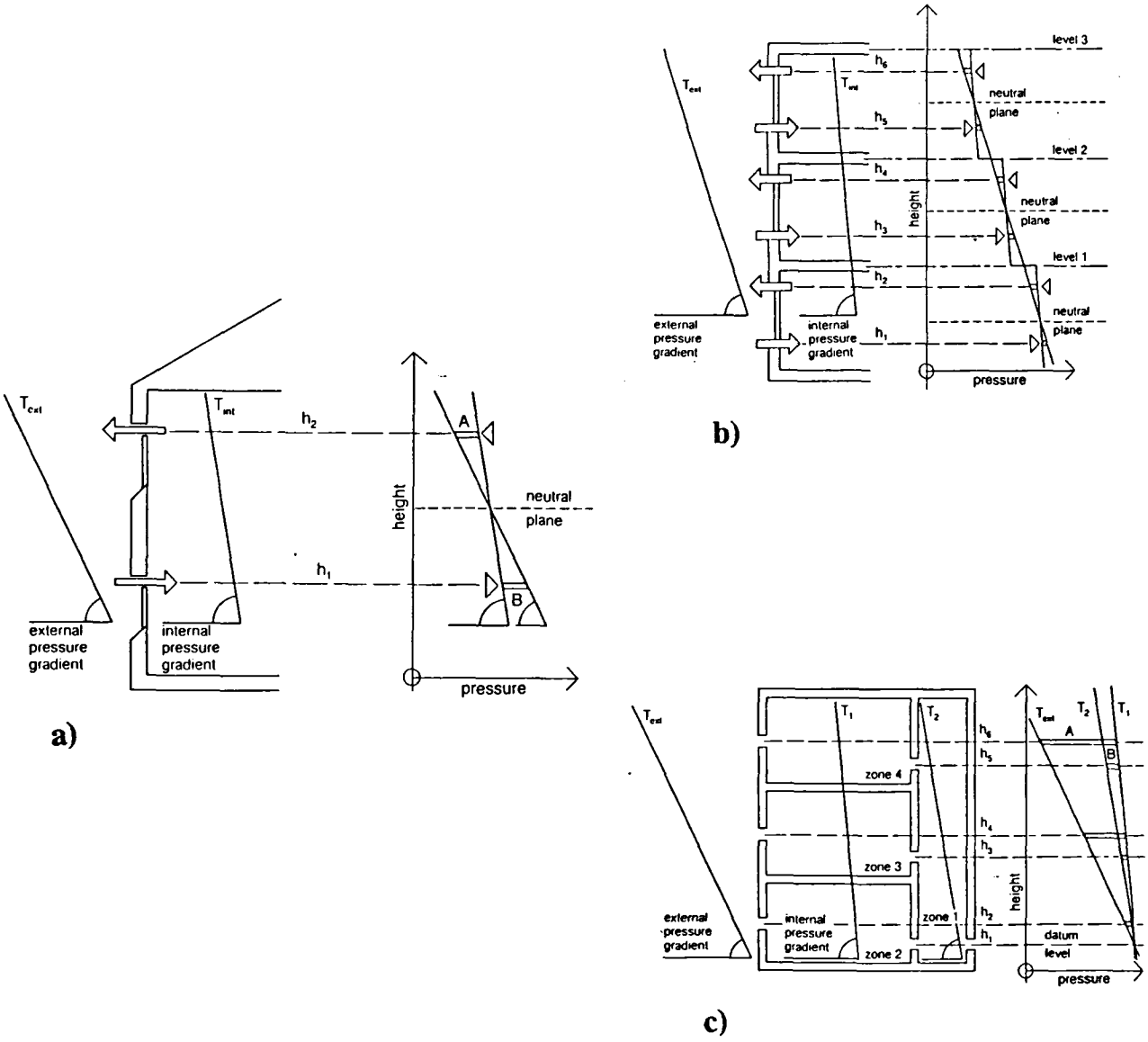

Figure 3.4: Stack induced pressure (Source Liddament (1986)).

(m), T_i, the average temperature of indoor at the height of the NPL, and T_o, the temperature of outdoor air (K), C_s is the discharge coefficient for the openings, (recommended value for C_s is 0.65), and g is the gravitational constant ($\approx 9.81\ ms^{-2}$). This equation applies when $T_i > T_o$, otherwise T_i is replaced in the denominator with T_o and $T_i - T_o$ in the numerator by $T_o - T_i$.

A correction factor must be applied when the inlet and outlet openings are not of the same area, (see ASHRAE Handbook of Fundamentals (1989b)).

Equation (3.9) reveals that the critical parameters in the stack forces are the height between inlet and outlet, the cross section area of inlet and outlet and the difference of temperatures. Application of the stack effect to ventilation is thus limited to situations where these factors are of sufficient magnitude. The most favourable conditions occur in multistory buildings in regions with cold winter climate, where heating of building interiors could create a significant indoor-outdoor temperature difference and which can be used to provide minimum ventilation rates by stack effect.

3.3.3 Mechanical ventilation

Mechanical ventilation causes pressure imbalance across the rooms. The expression of flow rates generated by fans is similar to that of the wind-induced flow;

$$Q_m = K_t (\Delta P_m)^n \qquad (3.10)$$

where K_t, is the total leakage coefficient, ΔP_m, the pressure imbalance created by the fan, and n, is the flow exponent.

3.3.4 Combined effects of several forces

The actual flow rates caused by the combination of various mechanisms is not the sum of the flow generated by each source acting alone. Nonetheless, the pressure differential inducing the actual flow is the algebraic sum of the pressure differences generated by each force separately. The pressure P_i at any opening, i, is given by:

$$P_i = P_{wi} + P_{si} + P_{mi} \qquad (3.11)$$

where the subscripts w, s and m refer to wind, stack and mechanical forces

respectively.

The resulting air flow through the opening is thus proportional to the square root of the combined pressure difference P_i. Therefore, even when the forces are operating in the same direction, the resulting flow can only be slightly higher than what it would be with the greater force alone. Thus, it is a common practice to consider the overall ventilation as that of these highest of the effects when acting alone. In particular the thermal force of ventilation is usually neglected in ventilation cooling in summer as it is usually too small, (refer to the discussion in Section 3.4.1).

When the different motive forces could be of equal magnitudes, and in order to reduce the complexity of the calculation of the flow, the combined effect of the wind and stack could be approximated by adding in quadrature each of the individual effects;

$$Q_{ws} = \sqrt{Q_w^2 + Q_s^2} \qquad (3.12)$$

where Q_{ws} is the combined ventilation rate, Q_w and Q_s respectively the ventilation rate due to wind and density gradient.

The flow due to mechanical systems could be simply added to Q_{ws} when the flow produced is balanced, (i.e., equal supply and exhaust). In this case the interior pressure in the building is not affected. On the other hand, unbalanced flows change the building pressure distribution, and then, the flow caused by mechanical means should be added in quadrature, (see ASHRAE Handbook of Fundamentals (1989b)). Combined effects of various motive forces in the induction of infiltration in buildings can be found in Allard and Herrlin (1989).

3.4 Strategies for natural ventilation

As already discussed in Section 2.5.4, cooling by natural ventilation can be a valuable strategy to use.

Among the three natural motive forces, e.i., turbulence, stack and wind pressure, the last two are viable options to use. However, in warm climates the greatest promises come from wind induction. This is now discussed.

3.4.1 Wind induced versus thermally induced ventilation

It was mentioned in Section 3.3.2 that the thermally-driven ventilation was effective only if the height between inlets and outlets and/or the temperature increment between indoor and outdoor are of sufficient magnitude.

The concept of stack effect for ventilation cooling in summer can work if the average indoor temperatures are greater than the external ambient air temperatures. In particular glazed atria can have a significant potential to drive such air currents.

In temperate climates stack effects may be a viable option to use. Indeed, indoor air temperature higher than ambient can be acceptable under such climate. Also, ventilation is mainly intended to vent away the unwanted heat from solar gains and internal gains, rather than to provide high air velocities for effective evaporative cooling.

The concept was demonstrated from numerous computer simulations to be applicable in atrium configurations under temperate climates. For example, Hancock (1987) concluded from a thermal simulation of a hospital building incorporating a glazed atrium, that stack effect ventilation would probably be sufficient to vent and keep the atrium and linked building zones below 25° C in a typical British summer.

Gateway Two, in Basingstoke, U.K., is an atrium building designed to rely on stack effect during summer season. The design was reported to be successful in inducing air currents, (see Hawkes (1983) and (1984)). Yet, in a recent monitoring of the building, the number of desk fans which were observed evidenced that conditions become uncomfortable on occasions, (see Trollope et al (1991)).

With thermally-driven ventilation, high air speeds generally cannot be obtained, because tolerable indoor temperatures impose a severe constraint on the rate of induced ventilation. In warm to hot climates, in particular, the temperatures may be already too high to welcome greater internal temperatures for stack effects. From equation (3.9) it can be demonstrated that to attain velocities above, say, 1 ms^{-1} for cooling purposes, over a height of 10 m between inlet and outlet, (i.e., approximately a four storey building), indoor air temperatures of 37.5° C would be required for an outdoor temperature of 30° C. This increment in temperature would be even higher for greater outdoor temperatures. Such temperature gradient would probably not be tolerable in an occupied space. However it might be acceptable in part of the building which is deliberately heated by solar radiation and whose main function is to create an exhausting effect, such as a solar chimney.

It is important to stress here the distinction between the stack effect ventilation

due to the building itself and that due to a solar chimney. In the first case, assuming the building to be occupied, good building practice is to keep the increment of the building temperature over the outside temperature as small as possible in the cooling season, with provision for shading or thermal insulation of the building envelope, and courtyard and atrium-type buildings are no exception. In these circumstances, even under poor ventilation conditions, (about 5 ach), the indoor-to-outdoor temperature difference will be less than 5.5°C and usually of the order of 2°C to 3°C, (Chandra (1985) and Aynsley et al (1977)). This will result in a weak stack effect because of the small temperature gradient.

In the second case, however, the chimney is isolated from the occupied spaces of the buildings. Thus, in principle there is no limit to the temperature increment within the chimney and, in fact, maximum solar gains are desirable to maximize the ventilation effects. However, comparable velocities to that attained by the wind, which can be easily of the order of 1 to 2 ms^{-1} for breezes of 3 ms^{-1}, (see velocity ratios given by Givoni (1976)), is difficult to achieve with solar chimneys unless they are of massive proportions, in which case, they may not be cost effective. Furthermore, the thermally-driven ventilation must be induced at all costs to prevent structural heat build-up from the conductive and radiative heat transfer.

The difference between the wind-induced and thermally generated ventilation is not only quantitative but there is also a qualitative difference between the patterns of air flow resulting from the two types of motive forces. The stack induces an air flow by virtue of the pressure difference between the lower and upper openings alone. In general, the inertial force at the inlet is not sufficient in directing the pattern of flow, and thus, causes very little motion of the air mass in the room. On the other hand, the indoor pattern of the air flow induced by wind pressures is largely governed by the inertia of the incoming air mass. This can cause an air flow across the whole room with thus greater cooling benefits than the flow induced by thermal force, (Givoni (1976) p. 288).

Wind-driven ventilation could be therefore most effective for cooling in warm to hot climates and particularly warm-humid. Therefore, the buoyancy forces were not considered further in this work, and the following discussion will be restricted to wind induced ventilation.

3.4.2 Appropriate ventilation strategies to use under certain climates

Two primary strategies can be used for ventilating buildings for thermal comfort control, and the suitability of each is related to the humidity of the regional climate. These can be described as *continual venting* and *night-time venting*, which coincide roughly with the cooling of occupants and the structural cooling, in hot humid and dry climates respectively.

Hot-humid climates

Comfort is attainable by natural means in very humid overheated regions only with a constant movement of air across the skin. The desired air velocities for effective cooling of people is in the range of 0.5 ms^{-1} to 2 ms^{-1}, (Chandra et al (1986)). Nevertheless, ASHRAE Standard (1981b) suggests that, at a velocity above 0.82 ms^{-1}, people may be distracted by loose objets beginning to blow about.

In such regions, the diurnal temperature swing is small, because of the inhibition of the thermal radiation to the sky by a humid atmosphere. For this climate, the most suitable design is lightweight building envelopes, largely open, that cool off quickly at night. During day-time, temperature control is obtained by ventilating as effectively as possible, to dissipate the solar heat absorbed by the building shell as well as for body cooling (see Givoni (1976) and Szokolay (1980)).

It must be emphasized here that since all the ventilation air is drawn from outdoor, it is not possible to reduce the indoor air temperature to below that outdoor, so the best that can be obtained in such cases is to prevent the indoor air from rising more than a few degrees above the outdoor air temperature.

Hot-dry climates

In hot-dry climate the most adequate design is night-time ventilation only. During the day-time, it is desirable to reduce to a minimum the ventilation required for diluting odours generated in the house, owing to the outdoor conditions that usually exceed greatly the comfort zone limits.

A building constructed with massive walls and roofs can maintain relatively moderate temperatures throughout the day-time. In the evenings the heat stored by the structure can be effectively removed by the ventilation because the temperature of the outdoor air in such regions falls sharply in the evenings and nights, owing to the clarity of the atmosphere. In this case, it may be enough to ensure a moderate indoor air

velocity, about 1 ms^{-1} or less, to fulfil this requirement. This is particularly true for buildings that are not occupied at night, since the usual rapid cooling to provide comfortable sleeping conditions does not apply.

The storage of coolness of the previous night can result in lower indoor temperatures during the day when the outdoor air temperature is high. Nevertheless, the depression of temperature may be insufficient to remove entirely the need to rely on evaporative loss. Also, by restricting the day-time ventilation, this approach causes the building to be very sensitive to internal heat gains of any kind during the day. The necessary air motion can however be delivered efficiently by fans, (see Chandra et al (1986), Rohles et al (1983), and Scheatzle et al (1989)).

The assessment of the efficiency of any of the above mentioned strategies must be made at an early stage of the design. This is because if a decision is made to fully air-condition a building, then the ventilation must be reduced to a minimum. With significant air temperature differences between inside and outside, the insulation of the envelope may become critical. Walls, roofs, floors and openings may have to be insulated and the glazing reduced. Such fundamental differences will lead to a very different architectural and constructional design than for the naturally ventilated structure.

Whatever the strategy adopted, (i.e., constant ventilation or night-time-only venting), great care must be taken to the building design and the building layouts in order to maximize the air motion. In the following sections the factors influencing the wind-driven ventilation are discussed.

3.5 General Characteristics of the wind

Building aerodynamics is so closely related to the characteristics of the wind that a review of the former must include, at least, brief comments on the latter. The discussion that follows on the structure of the atmospheric boundary layer will also help to draw the analogy between the real wind structure and that generated by the wind tunnel on which the experimental work will be based, and to sight the limitations of the wind tunnel modelling.

3.5.1 The atmospheric boundary layer structure

In the lower atmosphere, (first few thousand metres or so), there are many local

influences that complicate the weather scale flow pattern of the wind which arises from the differential heating of the Earth. The friction of the Earth's surface with the atmosphere, and the buoyancy forces, produce a boundary layer in which turbulent mixing takes place. This promotes a vertical exchange of heat, mass and momentum. As a result of these transfers, many properties of the mean flow are changed, in particular the velocity, which varies with altitude.

The atmospheric boundary layer (ABL), or the planetary boundary layer as it is commonly referred to, is this lowest part of the atmosphere in which the interactions between the atmosphere and the underlying surface, and the turbulent mixing are significant. As shown in Figure 3.5, the ABL can be divided into;

i) the surface layer occupying the lowest 10% of the ABL, with a typical height of 50 m, but may vary over a wide range, (i.e., 5 to 200 m), as does the ABL height,

ii) the canopy layer or roughness layer which extends well above the tops of roughness elements. The part of the ABL above the surface layer is called the outer layer, (see Arya (1982)).

Depending on the strength of the turbulent mixing and the amplitude of the various forces, (drag or buoyancy forces) involved in the convective activity, the structure of the ABL will be different. On sunny days for example, the warming of the earth surface produces a vertical thermal gradient that promotes strong upward thermal convective movements. A state of instability exists in this ABL, which is characterised by a stretched boundary layer, (BL), and a reduced wind speed gradient. Conversely, during clear nights, there is a downward flux of heat which inhibits the mixing between layers, resulting in a very shallow BL, (less than 100 m), and a steep wind gradient. The ABL is said to be stable. Finally, in cloudy or windy days, the thermal stratification is considerably reduced, resulting in a neutrally stable ABL. However this is an oversimplified categorisation of ABL which are commonly made up of a number of layers of different stabilities.

Although all these ABL structures could be pertinent in natural ventilation studies, in most cases only wind structures similar to the neutral stability case are considered. The reason is that, with many ventilation studies wind tunnel tests are involved. In these cases the simulated flow can only be of this type, except maybe with very special wind tunnels, (see Section 5.3.2.1).

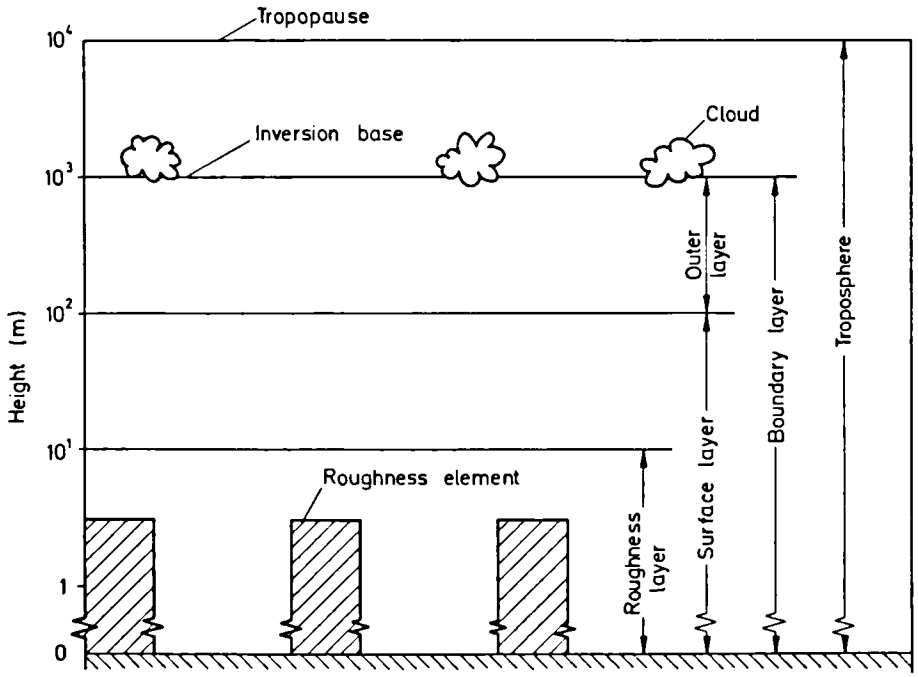

Figure 3.5: Schematic of the vertical structure of the lower atmosphere and its various layers, (After Aray (1982)).

Nonetheless, in wind loading and ventilation studies, to assume that the wind structure is invariant and corresponds to a neutrally stable ABL is believed to give reasonable time averaged results, (Lawson (1980), pp. 10-11). In the following paragraphs, only neutrally stable ABL will be considered.

3.5.2 The variation of the mean wind speed with height

In the neutral ABL, conditions are largely governed by i) the velocity at the upper edge, called free stream velocity, (because the flow is free from the Earth's friction), ii) the roughness of the surface, and iii) the BL depth, called gradient height.

In the surface layer, (the lowest 100 m or so of the atmosphere), the actual form of the wind speed variation with height over a level terrain has been found to be adequately modelled either by the empirically derived power law, equation (3.13), or the logarithmic law, equation (3.14), based more on physical principles of fluid mechanics. The power law is generally expressed as,

$$\frac{U(z_1)}{U(z_2)} = \left[\frac{z_1}{z_2}\right]^{\alpha} \qquad (3.13)$$

where $U(z_1)$ is the mean wind speed at the height z_1 above the ground. z_2 is generally a reference height such as 10 m, suggested by Shellard (1963), (see Torrance (1972)), or the gradient height, z_g, preferred by Davenport (1963). The logarithmic law is given by,

$$\frac{U(z)}{U_*} = \frac{1}{k} \times \ln\left[\frac{z+z_o}{z_o}\right] \qquad (3.14)$$

where U_* is the friction velocity, equivalent to the square root of the ratio between shear stress and air density, (the shear stress depends upon the roughness surface and free wind speed). k is the Von Karman's constant ($k = 0.4$), and z_o the roughness length characterising the terrain, (although not directly related to the size of roughness elements).

Some modified log laws have been suggested, such as the Blackadar log law, (see Harris (1972)), allowing for the variation of the shear stress with height and the effects of the Coriolis forces from the Earth's rotation. One improvement of these laws, of particular importance in very rough terrain has been to measure the height not from the ground level, but some distance above it. The expression of the velocity profile becomes,

$$\frac{U(z)}{U_*} = \frac{1}{k} \times \ln\left[\frac{z+z_o-d}{z_o}\right] \qquad (3.15)$$

or, for the power law,

$$\frac{U(z)}{U_g} = \left[\frac{z-d}{z_g-d}\right]^{\alpha} \qquad (3.16)$$

where d is the zero plane displacement height.

The correction could be very significant in heavily built urban areas, since the effective ground is somewhere near the average roof heights. The early value of power law exponent, $\alpha = 0.4$, given by Davenport (1963), for example, ignored this parameter, and much lower values, e.i., $\alpha = 0.26$ to 0.35, are now adopted as representative of the velocity profile over urban terrains, (Counihan (1972), Lee (1977) and Wardlaw (1972)).

For micro-meteorological problems, the logarithmic law is more frequently used than the power law. Nevertheless, when the surface roughness is significant it becomes difficult to describe the wind profile with the logarithmic law. This can lead to inaccuracies, (see Hanna (1970) and Sadeh et al (1971), reported in Kawatani et al (1971)). In these instances, the power law is preferred owing to its simplicity, (Kawatani et al (1971)).

3.5.3 The turbulent nature of wind

Wind is a stochastic phenomenon to which gusts and lulls are manifestations of turbulence. The wind is generally described as a mean flow and a superimposed motion

which fluctuates both in magnitude and direction. The magnitude of turbulence is either expressed as the root mean square velocity or the standard deviation from the mean. Another feature describing turbulences is their length scales, (i.e., the length of eddies).

The gusty nature of wind is of considerable importance in wind loading studies, which require to know the maximum instantaneous pressures. In ventilation, long time averaged values are generally more pertinent, so the effects of turbulences are secondary.

3.6 Basic aerodynamics and influential parameters in the ventilation of buildings

3.6.1 Influential factors in ventilation

Figure 3.6 lists the main factors influencing the wind-driven cooling ventilation in buildings. The structure of the wind is one of the parameters which affects the efficiency of ventilation but over which the designer has no control. The success or the failure of any design in achieving adequate thermal comfort is generally decided from the frequency of occurrence of wind speeds sufficient to achieve desired indoor air motions, (see an example of application in Appendix G).

On the other hand, the site planning and the building design can be made to maximize the internal flows for a given external wind condition. Designing a building with wind-driven ventilation in mind implies taking decisions at all stages of the design from the overall building envelope and orientation to the detail of the openings.

A list of references of works dealing with some aspects of the design relevant to wind-driven ventilation is provided in the concluding chapter, (Chapter 11). A particularly well reviewed work was that of the window design and internal subdivisions of space, (see Givoni (1976) and Aynsley et al (1977)).

In this thesis only the overall geometry of courtyard and atrium buildings and also the terrain in which the buildings may be found, (i.e., unobstructed or obstructed), will be dealt with.

Before broaching the review of related studies in the field of ventilation in courtyard and atria some revision of the basic aerodynamics and principles of indoor air motion may be helpful to follow the discussion of the subsequent chapters.

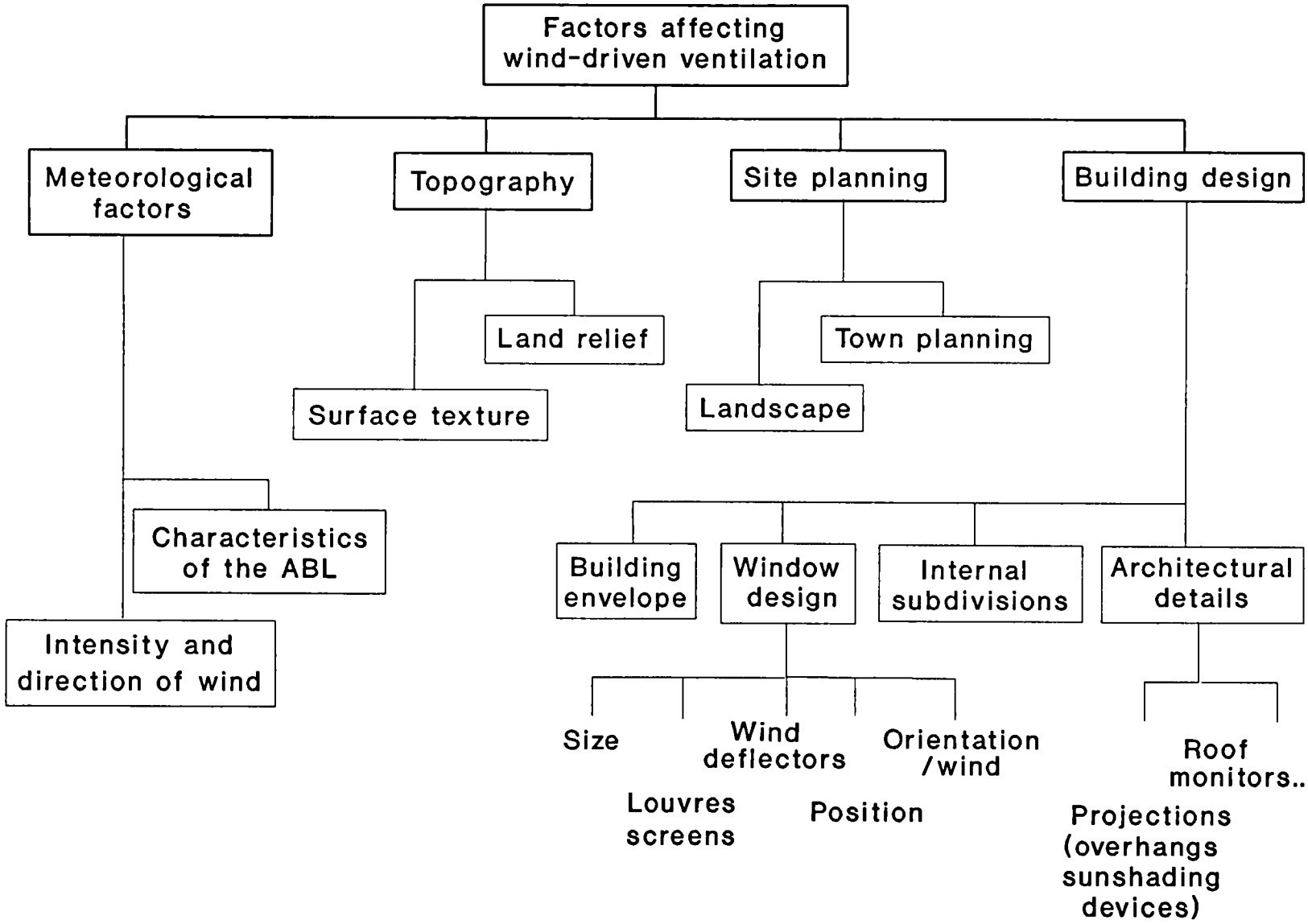

Figure 3.6: Factors affecting wind -driven ventilation in buildings.

3.6.2 Flow patterns around a building

The mean pressure distribution generated on building faces, and on which the internal air motion relies, depends upon the extent to which the airflow is altered by their presence. Streamlines that diverge lead to an increase in pressure, according to the Bernouilli equation, whereas when they converge they result in a decrease in pressure and boundary layer separation with its generation of eddies.

The patterns of the flow around isolated structures are relatively well reviewed, (see Meroney (1982), Fackerell (1982), Beranek (1984), Hosker (1985), Cermak (1976) and Newberry and Eaton (1974) for example). The flow field around a building can typically be divided into;

i) a displacement zone,
ii) a separated flow,
iii) an eventual reattachment,
iv) a cavity zone.

This is shown in Figure 3.7. Upwind to the obstacle there is a displacement zone, where the incident fluid is first influenced by the building. The air is retarded by the windward face and a stagnation point occurs where the flow splits. Air is accelerated around the ends of the building front face and so the side walls and roof are subjected to suction. The flow separates from the exposed surfaces at the sharp edges on the sides and roof, where the flow cannot follow abrupt changes in direction. This causes areas of high local suction. The separated flow generates then a recirculating flow zone that envelops the downwind surfaces of the building. The pressures in the flow cavity zone are low.

The separated flow may reattach to the building sides and the roof when they are long enough, and separates again. The location of the reattachment lines varies with the building proportions and with the fluctuations in the flow field. For a certain range of building geometries, the flow on the roof and sides may randomly oscillate between reattaching and remain fully separated.

At an oblique wind angle, the flow pattern is different from the above mentioned case. The flow is generally attached on the two upstream faces of the building and separates at the outer corners to form a wider recirculating wake region. At the roof, very strong and persistent delta-wing-type vortices are generated along the leading edges on the roof. These trailing vortices generate very high local suction, (see Figure

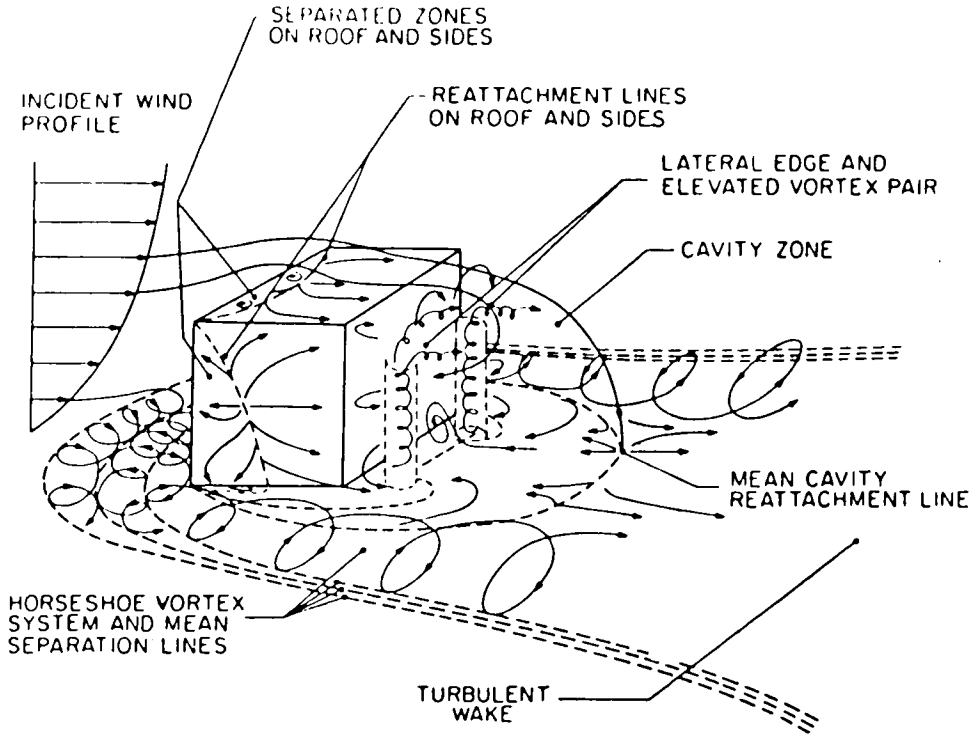

Figure 3.7: Flow around sharp -edged building normal to a deep layer wind, (After Fackrell (1982), source: Hosker (1985)).

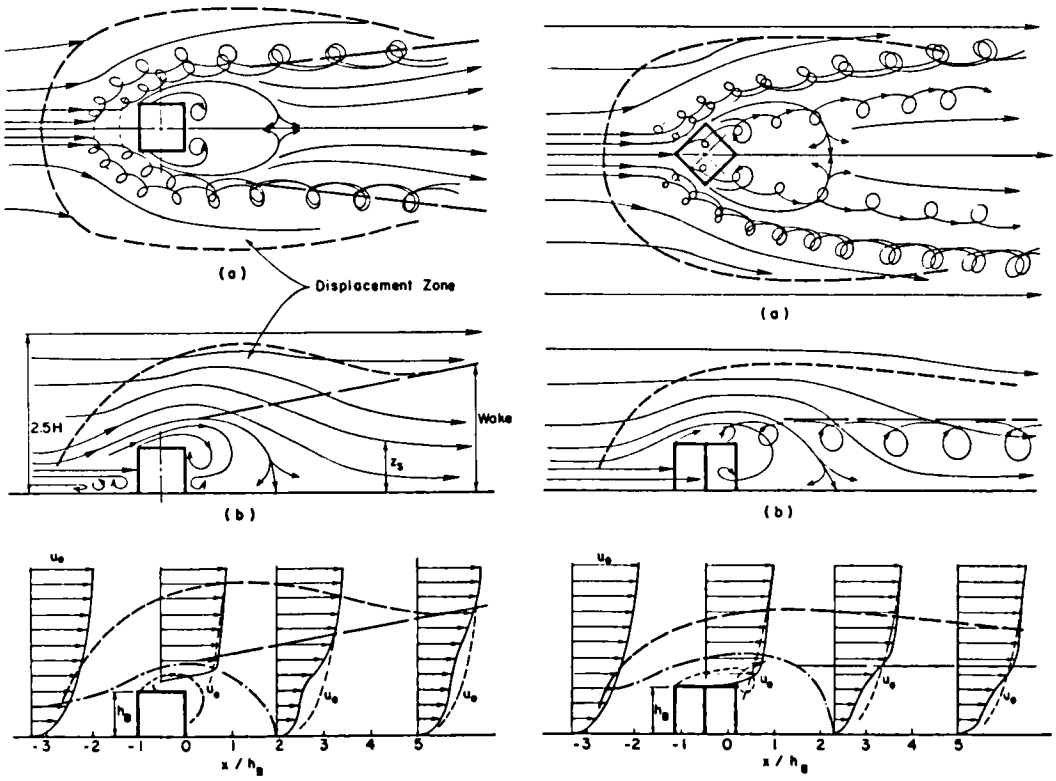

Figure 3.8: Flow around a cubical building at 0° and 45° wind angles, (After Meroney (1982)).

3.8). The flow patterns around an obstruction are largely governed by,

i) the viscosity of the air, which influences the sliding or friction of adjacent layers of the flow;
ii) the inertia of the air, which prevent sudden changes of direction. For low air speeds and/or for small obstructions, the viscous forces are predominant. The flow tends then to be smooth and streamlined. On the other hand, at higher air speeds and/or with larger obstructions, inertial forces become paramount, and the flow tends to become turbulent. The relationship between inertial and viscous forces is expressed by the Reynolds Number, Re, (this is further discused in Section 5.3.2). With sufficiently high Re, the flow patterns are independent of the wind speed and are controlled mainly by the building geometry and the wind characteristics.

Empirical expressions have been given for various parameters which characterise the extent of regions within the flow, (see Fackerel (1982)). However, even with moderately complex shapes, the flow is too complex to allow a generalized description. This precludes also the calculation of the pressure distributions, (except for streamlined bodies for which the flow remains attached to the surface), (see Allen (1984)).

In addition to the flow disturbance generated by any particular building, there are also disturbing effects from neighbouring buildings to be taken into account in assessing the consequential pressure distribution. This will be discussed in detail in the next chapter.

3.6.3 Internal flow mechanisms

3.6.3.1 The flow discharge through an opening

The relationship that exists between the flow rate through an opening and the applied pressure difference depends upon the Reynolds Number and the geometry of the opening. For large openings, such as open windows, the flow is turbulent and the formula given in equation (3.5) applies.

For other types of openings various expressions, empirically derived, are used for different nature of flow, (see Liddament (1986)). For very narrow cracks with relatively long flow paths, the flow is essentially laminar. The flow rate, Q (m^3s^{-1}), can be

approximated by:

$$Q = \frac{\Delta P}{8\mu \times L} \times \pi \times r^4 \qquad (3.17)$$

Where r is the radius of the opening (m), L, the length of flow path (m), and μ, the dynamic viscosity. For small openings such as gaps around closed windows and doors, a power law expression is generally used:

$$Q = C_l (\Delta P)^n \qquad (3.18)$$

Where C_l is the leakage factor, (= $K \times l$ where K= leakage coefficient in m^3s^{-1} per metre of gap length at a ΔP of 1 Pa and l= Total gap length (m)). The flow exponent, n, ranges between 0.5 for fully turbulent flow to 1.0 for laminar flow.

A quadratic formulation of the flow equation is also often adopted to account for a possible mixed nature of flow regimes, (laminar or turbulent), and in which turbulent and laminar flow components are separated.

$$\Delta P = aQ + bQ^2 \qquad (3.19)$$

a and b are empirically derived constants. More complex expressions for flow through cracks which can be more readily justified theoretically have been developed, notably by Etheridge (1977).

3.6.3.2 Internal pressure

The pressure difference responsible for the flow through an aperture is that acting on the outer and inner faces of walls where the opening is located.

When the windows of a building are opened, air will flow into and out of the openings exposed to wind pressure until an equilibrium is reached where the mass of air entering the room equals that leaving, in accordance to the continuity equation:

$$\sum_{1}^{n} Q_i = 0 \qquad (3.20)$$

where Q_i is the flow through each opening. In this steady state condition, the pressures in the buildings reflect a balance between the pressures acting on the external openings. This balance will depend primarily on the distribution of openings in relation to the external pressure distribution, their characteristics, and on the internal resistances of the flow along its path.

A knowledge of the internal pressures is equally as important as the external pressures for ventilation studies since the flow equation depends upon them. In the case of a room with two open windows of equal size in opposite walls, the internal pressure is half way between the minimum and maximum pressure acting on the leeward and windward walls respectively, (see Figure 3.9, example a). This is because the inflow must equal the outflow.

A reduction of the surface of one opening, say the outlet, will cause a diminution of the amount of outflow. The inflow will also be reduced to accommodate the new conditions, which implies that the pressure drop through the windward opening will become smaller than in the previous case. The internal pressure could be found to have shifted towards the external pressure acting on the outer surfaces of the largest opening, (see Figure 3.9, example b). The larger an opening is in comparison with others, the closer the internal pressure will be to that the pressure acting on the external face of the dominant opening. The extreme case would be that of a room with one window, in which case the internal pressure theoretically equals that of the external pressure.

3.6.3.3 Equations of flow networks

For building consisting of a number of interconnected rooms, the estimate of the flow and the internal pressure is complex and is based on the solution of simultaneous non-dimensional flow equations, (see Section 5.2.2.3). For very simple flow paths, where there is either a parallel flow branching or a branching in series, simplified equations can de derived.

The dynamic pressure losses ΔP (Pa) in an airway are proportional to the square of the flow discharge Q (m^3s^{-1}) through the airway, (see Aynsley (1988)).

$$\Delta P = R \times Q^2 \qquad (3.21)$$

Where R ($N \times s^2 m^{-8}$) is the resistance to the airflow. R can be calculated from the discharge coefficient, Cd, as follows:

$$R = \frac{\rho}{2 \times Cd^2 \times A^2} \qquad (3.22)$$

Airflow through openings in series

In this instance, the flow discharge through each airway is the same, (see Figure 3.10). The flow rate Q can be expressed as a function of the pressure differential across the inlet and outlet,

$$Q = \sqrt{\frac{P_1 - P_4}{R1+R2+R3}} \qquad (3.23)$$

The general expression[2] is known as;

$$Q = \sqrt{\frac{CP - CP_{n+1}}{\frac{1}{Cd_1^2 \times A_1^2} + \ldots + \frac{1}{Cd_n^2 \times A_n^2}}} \qquad (3.24)$$

Airflow with parallel branching

In this case, the flow Q is divided into several branches which share the same pressure drop. The equivalent resistance, R_{eq}, in the example of Figure 3.10 is;

$$R_{eq} = \left(\frac{1}{\sqrt{\frac{1}{R2}} + \sqrt{\frac{1}{R3}} + \sqrt{\frac{1}{R4}}} \right)^2 \qquad (3.25)$$

[2] Although additive resistances are generally assumed in the case of an air path where openings are in series, in actual facts, this may only be the case where they are placed far apart. In most cases the first opening (or partition) has the greatest resistance and the subsequent openings have reduced resistances, (see Pitts (1985)).

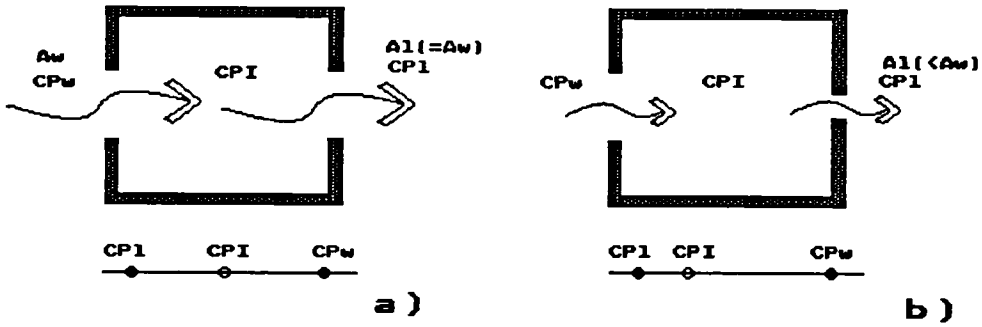

Figure 3.9: Change in the internal pressures associated with change in the internal flows caused by a reduction of the outlet.

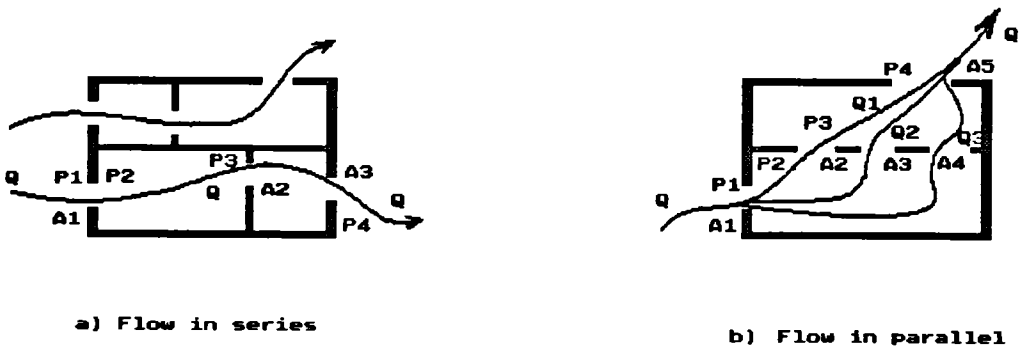

Figure 3.10: Example of flows in series and in parallel.

3.7 Conclusions

In this chapter, the requirements for ventilation have been stated with the ways of achieving them. Natural ventilation driven by wind is probably the most efficient way to achieve high velocity levels in summer for thermal comfort, except maybe in sites with very weak breezes. Yet, in order to achieve the best results the designer must pay attention to several aspects of the design.

The next chapter will focus on the state of knowledge of wind-driven natural ventilation in courtyard and atrium-type buildings and in the city-like terrains, on which this study is more closely related.

Chapter 4:

Related background studies

4.1 Introduction

The problem of ventilation in courtyard buildings differs from most of other types of buildings in that parts of the structure are always under the wind shadow of the upstream wings. This issue addresses thus the more general topic of ventilation in a collection of buildings or in a building complex.

The flow in a cluster of buildings and the mutual flow interference between them has been the subject of many works for several purposes, which could be categorised into;

a) wind loading,
b) wind environment, mainly for dynamic comfort of pedestrians,
c) natural ventilation or infiltration of buildings,
d) dispersal of airborne effluents,
e) wind generated noise.

The review of relevant material in any of these themes of investigation will be made as the findings of any particular study could be useful not only for its original purpose but also to help to understand the phenomena involved in other related categories. In this chapter, three main reviews will be made.

i) The ventilation potential in small clusters of buildings, and the effect of building enclosure will be discussed first, in order to give an insight of what the

ventilative conditions in isolated courtyards could be, and to evaluate the influential parameters which will have to be tested. This will be followed ultimately by the collection of the available knowledge on the flow in courtyard structures.

ii) The sheltering effects in extensive arrays of buildings will follow. This review will give a background for the study on the ventilation of courtyard and atrium building types in urban conditions which will be investigated in Chapter 9.

iii) Finally the last section will be devoted to the use of roof-level ventilation openings in some building types of which the atrium is an example.

Wind shielding could also be caused by vegetal barrier (Mattingly et al (1979)). Generally, because of the large permeability the vegetal barriers offers to the wind, the flow pattern is significantly different from that in a collection of buildings and so the sheltering effect of the vegetation could not be assimilated to the sheltering conditions found in courtyards or with surrounding buildings. For these reasons, this subject was not broached here.

4.2 Flow and pressure forces around simple clusters of buildings

4.2.1 Flow patterns around clusters of buildings or composite buildings

Whereas the flow around an isolated building is relatively well reviewed and unravelled, the flow in an isolated building complex is less well understood. This is because the relative sizes and the distribution of buildings is often so individual as to preclude any generalised description.

Nonetheless, some work has been done in investigating the flow behaviour in simple arrangements of buildings in which variables, such as the element sizes and the spacing between the elements, were systematically changed so as to study their effects and to attempt to draw generalised rules. Most of them were experimental studies undertaken on models in wind tunnels, which offer the possibility to control and to change the variables dealt with.

Gandemer's work

A great deal of experimental work on aerodynamic problems associated with

particular buildings and groups of buildings was made by Gandemer (1976). He published interesting collection of sketches and photographs of the flow patterns of some typical building arrangements. The aerodynamic problems associated with flow channelling, jetting and vortex formation and other effects were identified and related to some typical building types or arrangements like, the "bar"-effect referring to the strong vortex rolling over "bar"-like buildings.

Beranek's study

Beranek (1979) and (1984) introduced the concept of influence area of an isolated building in order to predict the occurrence of mutual interference flow fields that could be responsible for environmental wind discomfort.

The influence area chosen, (equal to the horse-shoe shaped area), could be approximated by a circle joining the upwind flow separation point and downwind flow reattachment, (see Figure 4.1). For very wide or very long buildings the influence area was of an elliptic shape, approximated by two half-circles surrounding each side of the structure and joined by straight lines, (see Figure 4.1).

If the circles of influence overlap then the flow fields of each structure interfere. Beranek suggested that, even after the point of flow interaction has been reached in a cluster of buildings or in composite buildings, there are some cases where the interference is weak, (see Figure 4.2, example a). In these circumstances, the flow patterns, and to some extent the maximum local wind velocities, could be approximately predicted by a kind of superposition of the flow patterns of the individual structures. When strong interaction exists, the flow pattern is made more complex by the effects of flow channelling, jetting between buildings, vortex formation, and other effects which preclude any simple estimates, (see Figure 4.2, example b).

The works of Gandemer and Beranek provide some insights into the flow behaviour in composite buildings or clusters of buildings. However, they were mainly focussing on the level of pedestrian discomfort and the quantitative estimates are of no use for ventilation prediction.

4.2.2 Pressure forces in rows of buildings

Rows of buildings are the elementary arrangements which address the problem of shielding in clusters of buildings. It is thus not surprising that it is the most reviewed

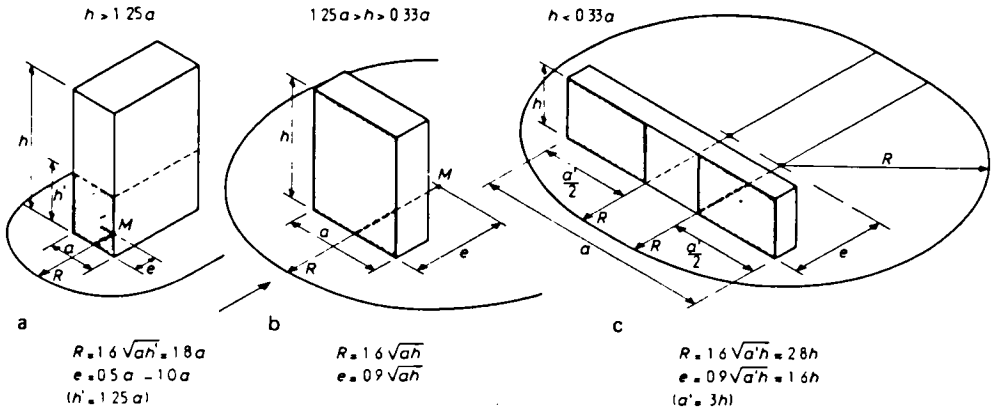

Figure 4.1: Concept of the circular influence area, (After Beranek (1979) and (1984)).

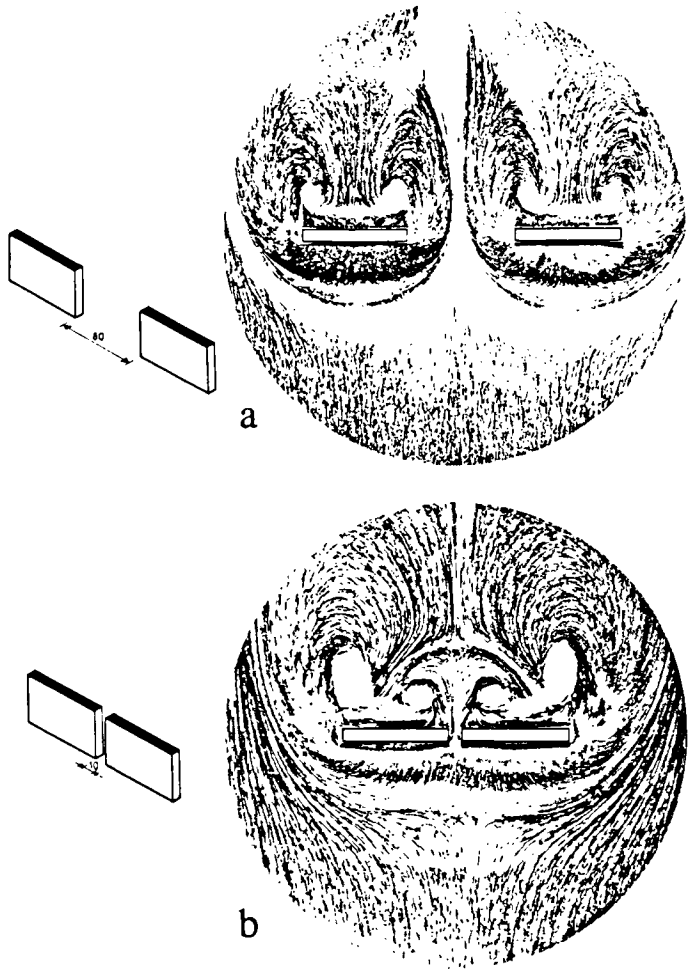

Figure 4.2: Example of a weak, (a), and strong, (b), flow interference between two elements, (After Beranek (1979) and (1984)).

one. Soliman (1976), Hussain (1978) and Hosker (1985) already offer a rich literature in this subject. Some of them are briefly summarised here but most of the review will be concentrated on more recent works.

Wiren's study

Among the most recent and comprehensive studies made on the influence of adjacent buildings on the surface pressure of a test building was that of Wiren (1985) and (1987). The two studies were intended to estimate ultimately the reduction in ventilation heat losses from a wind-exposed condition.

Among a series of building arrangements he tested, was that of one or two building blocks located upwind or adjacent to an instrumented model, (see Table 4.1). The two studies differed only by the shape of the building models used and the spacing between the elements. In the first mentioned report, oblong models were used and represented at a scale of 1/100 five contiguous flat roof two-storey houses while the second study dealt with pitched roof models representing 1 and 1/2 storey single family house common in Sweden. A first arrangement consisted of an element placed upwind to the instrumented model at variable distance. In the second and third arrangement two elements were placed side by side, either upwind to the instrumented model or aligned with it.

The main results of the first arrangement were as follows;

i) the existence of one upstream sheltering element could have large effects in changing both the magnitude and the distribution of the wind pressures, generally, over all the building surfaces;

ii) this effect was greatly dependent on the incidence of the wind and on the separation distance between the elements. It was most marked at low wind angles and at smaller spacings, in which case the pressure magnitudes were substantially reduced, and, on the windward face, the pressures became below atmospheric;

iii) the influence of one block upwind to the model test, and the effect of changing the separation distance between the blocks diminished with the increase of the wind angle, to become negligibly small from a wind incident angle of approximately 60°;

iv) with the wind parallel to the long axis of the models the surface pressures of the instrumented model were not affected at all by the presence of the adjacent model. The interference of the adjacent model on the instrumented model was also negligible

when the former was downwind to the latter.

Table 4.1: Model characteristics and test programme in the work of Wiren (1985) and (1987).

Wiren (1987)	Wiren (1985)
5 contiguous 2 storey houses  Af= L/H= 5.83 As= W/H= 1.49	1 and 1/2 storey house  Af= L/H= 1.76 As= W/H= 1.15 Roof pitch 45°
Test programme	
① 1.2< a/H <7 ② 1.2< a/H <7 & b/H=1.2 ③ 1.2< b/H <3.5	① 1.8< a/H <5.3 ② 1.8< a/H <5.3 & 1.8< b/H <3.5 ③ 1.8< b/H <4.4
simulated open flat terrain boundary layer	
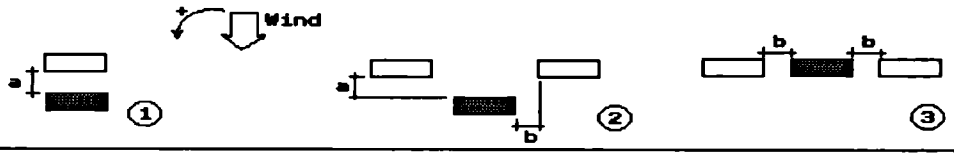	

In the second arrangement the results indicated that;

i) the effects of two elements placed side by side and upwind to the test model were found to be most pronounced with wind angles between 30° and 60° on the upwind model sides, and also at the gable face at 0° wind angle. In these cases, the influence of spacing was important;

ii) with the building models parallel to the wind (90° wind angle), the sheltering effect of the surrounding elements was insignificant.

Finally with the last arrangement, (two elements in line with the test model), it was found that the presence of adjacent elements and also the effect of varying the spacing was most marked at an angle of 90° in which case the test model was aligned in the direction of the wind with the sheltering elements.

From these results it could be drawn that;

i) the sheltering effect of surrounding elements is most felt when they are located in the trajectory of the wind and upstream to the prototype;

ii) the most affected faces would then be those facing the shielding buildings;

iii) in these circumstances, the separation distance between elements becomes

important and has generally the effect to decrease the pressure magnitudes, thus the ventilation driving forces, and to immerse the upwind surfaces into a negative pressure field when the spacing is decreased.

Givoni's work

Few related studies have been undertaken on porous models and where actual indoor air velocities were measured. These works are of a particular interest for the present study because they address the problem of ventilation cooling and they attempt to model more realistic situations where the building windows are largely open. In these circumstances, the large inflows and outflows through the buildings control also the flow pattern and the pressure field around the buildings. The value of these studies lies, as well, in the fact that actual internal flows are measured and not inferred from the flow discharge equation.

Givoni (1968) provides measurements of indoor velocities in a shielded building model downstream to an upstream model or placed between two similar building models in the airstream direction. The details of the tests are summarized in Table 4.2. The tests were made in a uniform flow and, although not clearly specified, the porosity was assumed to be the same as other model studies reported in the article, (i.e., the opening area was equal to 11% the wall area).

The limitations of these tests are numerous. For example, the wind tunnel blockage was significant, and the number of velocity measurements which were made in the models was too small to give a complete picture of the internal flows. Another major limitation was the Reynolds Number problems which were completely ignored in this study.

The author reported that;

i) the range of indoor velocities encountered in the first sheltered model were highly influenced by the element spacing;

ii) the effect of increasing the longitudinal distance of separation between the blocks was to increase the air velocities of the external flows between the blocks. Yet, the indoor air speed reflected first a decrease, up to a spacing equal to 2.75 time the model height, followed by a rapid increase with greater separation distances.

Table 4.2: Model characteristics and test programme in the work of Givoni (1968) related to the effect of shielding on rows of buildings.

Givoni (1968)	
Model characteristics L/H = 1.5 W/H = 0.5 Wall porosity = 11%	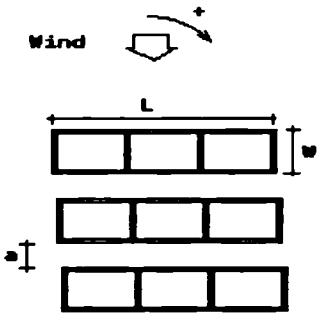
Test programme • Two rows 0.75< a/H <3.25 • Three rows 0.75< a/H <1.25 • Smooth flow	

Weston's study

Weston (1956) also measured internal flows in a porous model representing a simple industrial building with a sawtooth roof at a scale of 1/16. The model was obstructed by other buildings of different forms at various upstream distances. The windows fitted in the model were awning types, open to an angle of 45°, with their projected area representing approximately 8% of the wall surfaces. There were also apertures at the roof level. The results presented in Figure 4.3 showed that;

i) as a general rule, the increase of the separation distance between the building and its obstructions improved the natural ventilation;

ii) there was a separation distance, (for most of the case it was equal to 1.33H), at which the ventilation conditions were at a minimum, and were improved by any increase or decrease of the spacing.

It was suggested that, at small distances of separation, the obstructed building was in the wake of the upwind building and its windward wall was subject to lower pressures than those acting on its leeward wall. In this case the indoor air was flowing in the opposite direction to the main air stream. Decreasing the spacing intensified these conditions and resulted in better ventilation conditions. On the other hand, at larger spacing, the reduced pressure field was no longer affecting the windward wall and, in

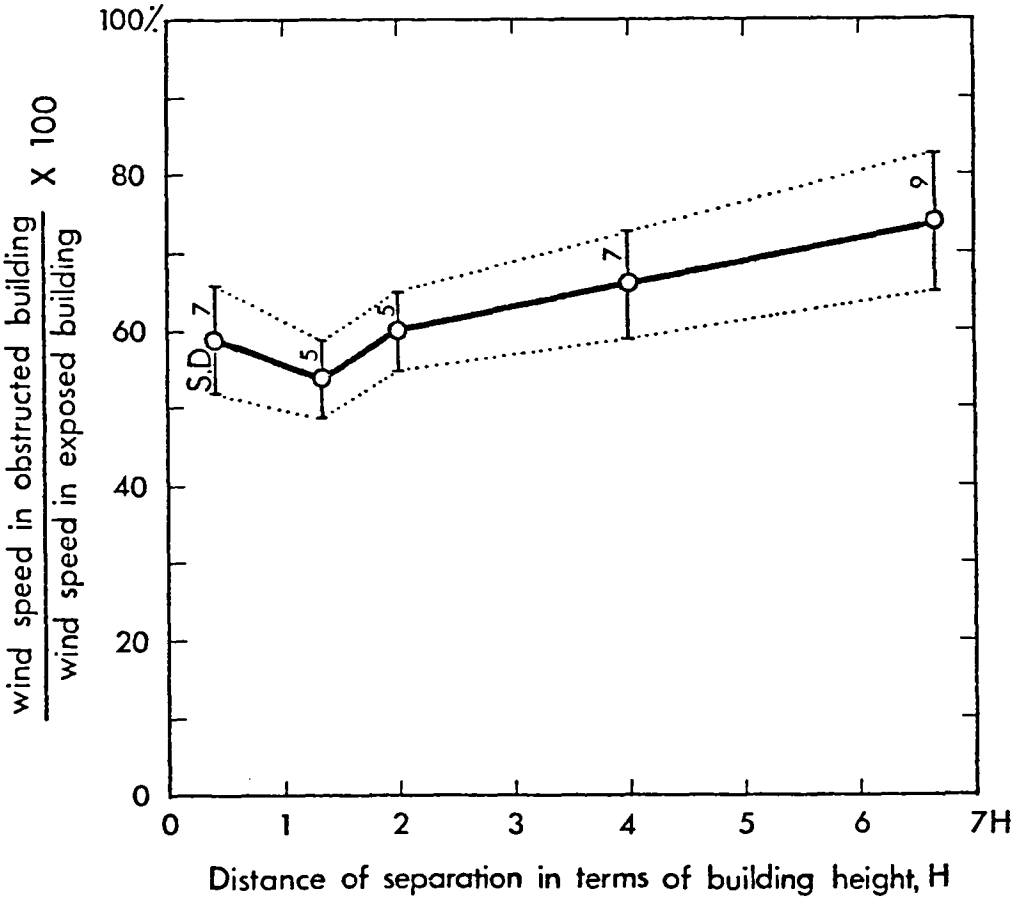

Figure 4.3: Effects of element spacing on the ventilation. A replot of Weston (1956) data, (source: Soliman (1976)).

general, the internal air motion was proportional to the distance of separation;

iii) The suction on the lee of the obstructing building was also found to be amplified by increasing its height or its length normal to the wind. On the other hand, obstructing buildings with elongated shapes in the wind direction or with curved roofs tended to diminish these effects.

Chand's work

A more recent study on similar building arrangement involving porous models was carried out by Chand (1976). Block-like elements representing either semi-detached houses or long row of houses, were placed in parallel rows, facing the wind. The elements were provided with windows, but no indication of the value of the porosity was given. There was no indication either of the nature of the flow, and thus, was assumed to be uniform. The characteristics of the models and the test programme are provided in Table 4.3.

Table 4.3: Model characteristics and test programme in the work of Chand (1976).

Chand (1976)

Model characteristics

(semi-detached type) L/W = 1.5
(long row of houses) L/W = 5

Porous models
(wall porosity not indicated)

Test programme

- Upstream and downstream blocks of equal height

  0.5< a/W <8 Hw = 0.4W
  Hw = 0.6W
  Hw = 1.2W

- Upstream and downstream blocks of different heights

  0.5< a/W <8
  1< Hl/Hw <3

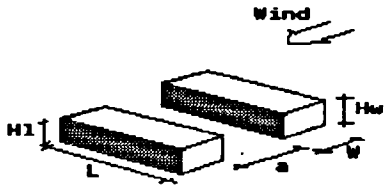

- Windows of the sheilding building were opened or closed
- Smooth flow

The investigation presented several interesting results;

i) the indoor wind speeds in a building model was found to be appreciably lower with the presence of an obstructing building upstream than without, even when the separation from the shielding building was large;

ii) in general, the decrease of the spacing reduced the internal flows. Nonetheless, depending on the proportion of the models placed in rows, the indoor air velocity exhibited different trends with the change of spacing. In Figure 4.4, for example, it can be seen that, with the model numbered 1, the indoor air motion in the shielded building increased, first, rapidly with the increase of the building spacing up to a separation distance of 8H, then the rate of increase became relatively small. However, with the two other models, one or two minimum values of the internal flow was reached at critical spacings. This behaviour were also recorded with other model proportions not shown in the figure. It could remarked that the same trend was recorded in the two aforementioned studies.

Chand explained that, at these critical spacings, (around 3.5 time the model height, H, for model 2, and 0.85H and 5H for model 3), the minimum indoor air speed coincided with the case where the pressures on the opposite walls of the models were almost the same, (see Figure 4.5). A current of air however still existed, mainly driven by turbulences. Any increase or decrease of the element spacing improved the ventilation;

iii) below the critical values of 3.5H and 5H, for the models 2 and 3 respectively, the pressure on the upwind walls of the shielded models became lower than that in the leeward face. In this case, an indoor air current opposite to the main air stream was set;

iv) the ventilation in a shielded element was improved when its height was greater than that of the shielding block. With an obstructing model higher than the instrumented model, a similar trend to that found in models of the same height could be obtained, in that, a minimum value of the flow was found at critical spacings.

An interesting test followed, in which the windows of the shielding model were closed in order to observe the effects of the curtailing of the flow in the upwind model on the ventilation of the instrumented model. The test revealed that the indoor air velocities were then affected. At large distances of separation between blocks, (above 4H), the air motion in the shielded model was in general greater than in the previous arrangement, and sometimes also at very close spacings.

Comparison of the experimental studies involving porous models

Though the experimental details of the three last studies were disparate, a comparison could unveil common behaviours of the indoor air motion in rows of

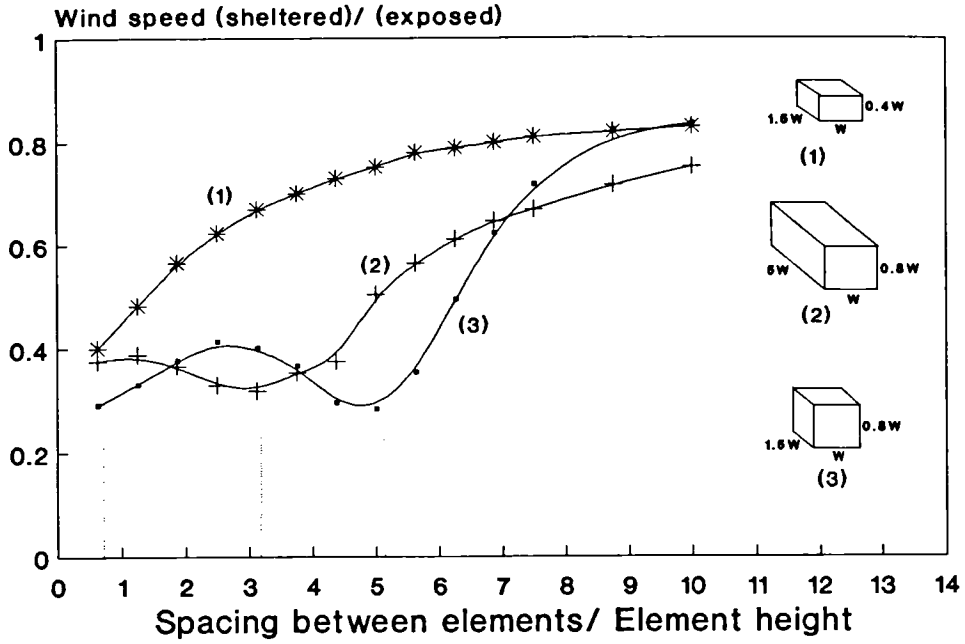

Figure 4.4: Effects of spacing between two elements on the indoor air velocity of the sheltered building model, (After Chand (1976)).

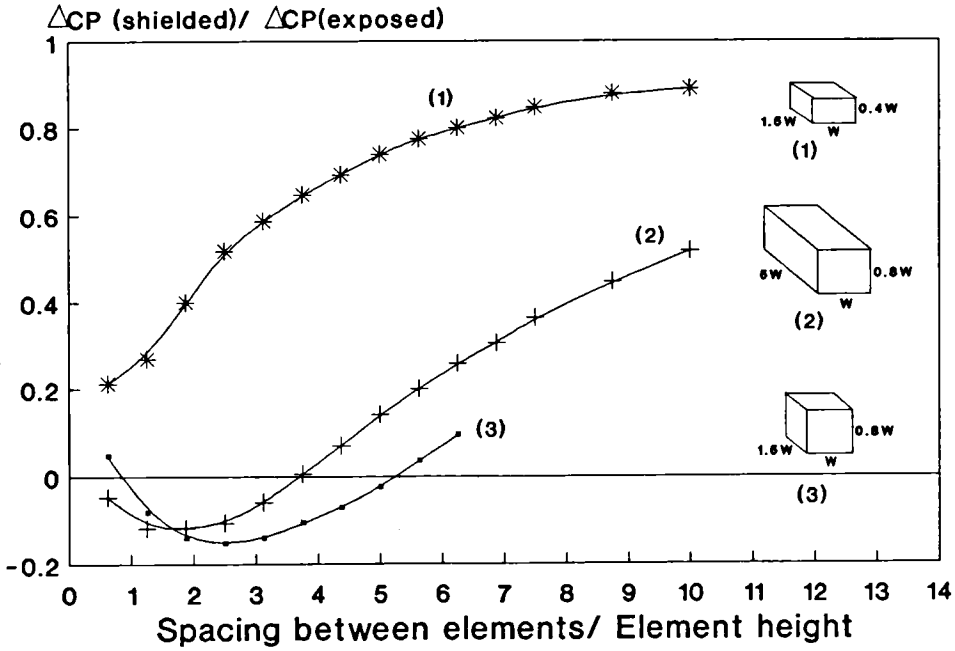

Figure 4.5: Effects of spacing between two elements on the pressure drop across the sheltered building faces, (After Chand (1976)).

elements where the separation distances were changed;

i) the presence of adjacent models restricted substantially the indoor flow of an otherwise isolated block;

ii) as a general rule, the increase of the separation distance between the blocks improved the ventilation;

iii) at particular spacings the internal flow could be reduced to a minimum and any of the increase or decrease of the spacing could improve the flow. The value of this critical spacing could depend on the size of the models and also probably on their porosity and the nature of the incident flow;

iv) the change of the spacing distance from either side of this critical value could occasion reversed flows.

4.2.2 Ventilation potential in partially enclosed courtyard buildings

The presence of a building in the vicinity of another one is not always impairing their ventilation as it may first appear. Weston (1956) for example suggested that the ventilation in a deep building could be improved by locating on its side another narrow building.

Givoni (1968) also examined the effect of restricting the air between two blocks with windows parallel to the wind by adding a third block in-between. This, in the intention to create a pressure gradient around the blocks which could improve the indoor air motion.

The relative indoor air velocities were compared in three different arrangements. One had two facing models, one model unit apart, and with the window parallel to the oncoming wind or oblique. Another arrangement had in addition a third block forming an open court which faced the wind, and finally, the last arrangement had the court at the rear. These arrangements can be seen in Figure 4.6. The main results were;

i) the indoor air motion was higher with the second arrangement than in two separate blocks. Also, the ventilation was more equally distributed between the rooms in the second test;

ii) with the open court at rear, however, no particular improvement was obtained in comparison with separate blocks, particularly for the most downwind rooms.

Other arrangements were tested by the author from which the effect of a progressive enclosure could be followed.

The first layout consisted of three rows of contiguous model blocks. In a second layout, walls were disposed alternatively at one end of each row, (perpendicular to the long block axis), forming two courts half open at alternate sides. Finally another arrangement consisted of two rows of identical blocks and two end walls enclosing a courtyard. A comparison of the ventilation conditions in the first shielded block could be made for the first two layouts. Yet, in the third arrangement, the effect of the enclosure could not be clearly separated from that of the retrenchment of a row of building models. A comparison could indicate that;

i) the ventilation conditions in the first shielded block was better with a partially enclosed courtyard layout than with three rows of blocks with no end walls, when the wind was parallel to the blocks. The restriction of the flow was then creating a pressure gradient between the court open to the air stream and the court that turned its back to the wind;

ii) with the wind facing the blocks, the presence of the side walls in the buildings with partially or fully enclosed courtyards seemed not to cause any substantial effect on the indoor velocities in comparison with the case with no side walls;

iii) at an oblique wind incidence, the upwind walls on the sides tended to restrict the indoor velocities in the rooms located immediately downstream. This was most pronounced in the courtyard case.

4.2.3 Ventilation potential in spaces enclosing a courtyard

Torrance's work

An early study on the wind environment in courtyard structures was made by Torrance (1966) in which the main concern was to investigate the relationship between the courtyard layouts and the shelter they provide, and to test remedies for greater wind shelter. The study involved flow visualization, velocity and surface pressure measurements on models in a wind tunnel.

Fourteen courtyard designs were tested on 1/100 scale models, where the relative depth, breadth and height were changed. The depth and breadth investigated ranged from 0.5H to 6H, (where H is the model height). While in most of these early wind

tunnel studies the atmospheric boundary layer was not simulated, here an attempt was made to generate a shear flow. Nevertheless, the length of the roughness surface was so small that it would have certainly resulted in a poor representation of the atmospheric boundary layer.

The presentation of the pressure coefficient results, which could be of interest for the present study, was solely given in the form of pressure contours, thus, making difficult the exploitation of the results. Nevertheless, some interesting remarks were raised.

i) The pressures found in the courtyard walls were in general below atmospheric.

ii) When the wind was normal to a model face, the suction at the top of the rearmost wall of the courtyard was reduced in comparison with the rest of the wall, and the suction on the roof surfaces immediately behind the courtyard was increased. This was suggested to be due to a portion of the air stream sweeping the top of the court back wall.

iii) In the smallest courtyards these effects were reduced whereas it the largest models, (with sides greater than 3 time the wall height, H), they were amplified to the point that there were pockets of positive pressure in the courtyard back walls.

iv) At an oblique wind angle, larger positive pressure areas were found at the rear walls of the court. This occurred in almost all the models except the smallest ones, (with sides equal to 0.5H). This was imputed to a greater penetration of the vortex sheet issued from the front edge into the courtyard, and so, for two probable reasons. First, it may be because of the increased distance of the rear corner of the courtyard from the front edges. Secondly, two vortices were found to be generated at the leading roof edges of the models and were observed to expand in a downward direction into the courtyard. This is further discussed in Section 4.2.4.

v) The largest pressures and the most extensive areas were found at different wind incidences for different courtyard configurations. At particular wind angles, some courtyard sizes were best for catching the vortex stream in which case the highest pressures in the back walls were recorded. This could be of particular importance for improving the ventilation at these locations.

Givoni's study

Givoni (1968) measured the indoor air velocities in permeable models

representing cruciform courtyard buildings.

The test models were constructed from eight model "units" of 30×30×30 cm each assembled at the corners to form cruciform two-storey buildings with a void at the centre, (see Figure 4.7). Each unit of the upper floor had two square windows of 1/3 of the wall dimensions located in two opposite faces, facing the yard. The opening area represented thus 11% of the external wall. The courtyard at the ground floor was either, i) totally enclosed, with the surrounded rooms sealed, ii) fully open, with columns supporting the first floor, or, iii) open in one side only.

The measurements were taken in 5 locations in the room of the first floor. The results were presented as percentages of "the free wind speed". Since no modelling of the shear flow of the Earth surface was mentioned, it was understood that the tests were made in a uniform flow. The limitations of this study were the same as the previously-mentioned studies of the same author, (i.e., the large wind tunnel blockage, around 20%, and the Reynolds Number implications for internal flow modelling that were completely ignored). The main results that the study revealed were:

i) with the first configuration, which represented a fully enclosed court, and at 0° wind orientation, the air motion in the leeward rooms or in the lateral rooms was very weak in comparison with the windward's. The average relative indoor velocities were found to be 24.4%, 6% and 5.4% for the windward, leeward and side rooms respectively;

ii) at 45° wind angle, the average indoor velocities were higher at both the upwind and downwind rooms. The relative air velocity at the upwind rooms was equal to 33.4% and to 13.9% at the downwind rooms, with particularly high local velocities near the inside room corner facing the oncoming wind;

iii) with the second configuration, (i.e., the ground floor was fully open), better ventilation conditions were obtained at the downwind rooms. The velocity was respectively 8% and 10% of the free wind at the leeward and lateral sides. As with the other configuration, enhanced ventilation was obtained at 45°;

iv) finally with the last configuration, (i.e., courtyard open in one side), the ventilation conditions depended on the orientation of the open side on the ground floor with respect to the oncoming wind. The best case was when the opening of the yard was facing the wind and the worse condition was that of the model with the back of the yard located upstream. With this configuration no particular improvement was obtained at 45° wind incidence.

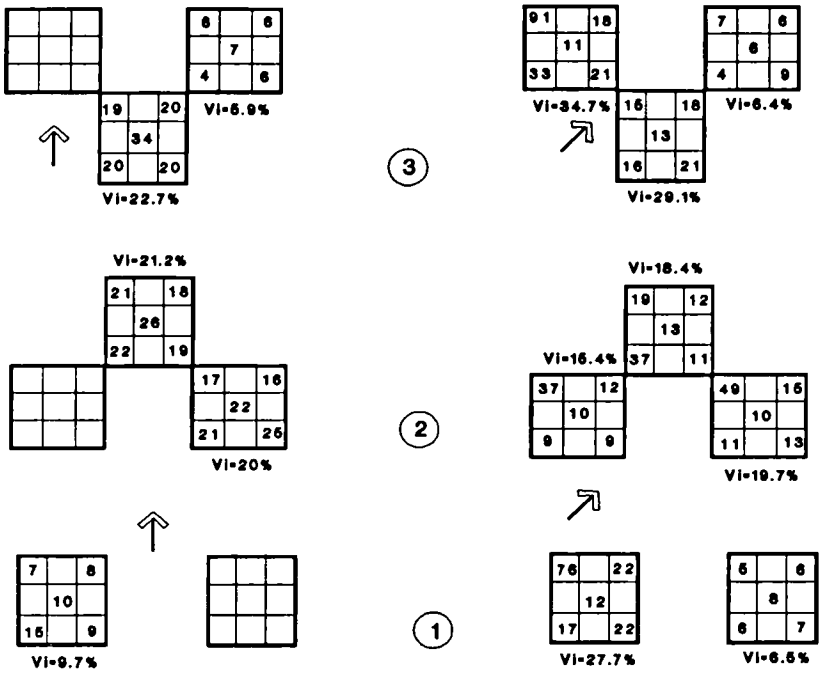

Figure 4.6: Effects of restricting the air between two blocks by adding a third block on the indoor air velocities, (After Givoni (1968)).

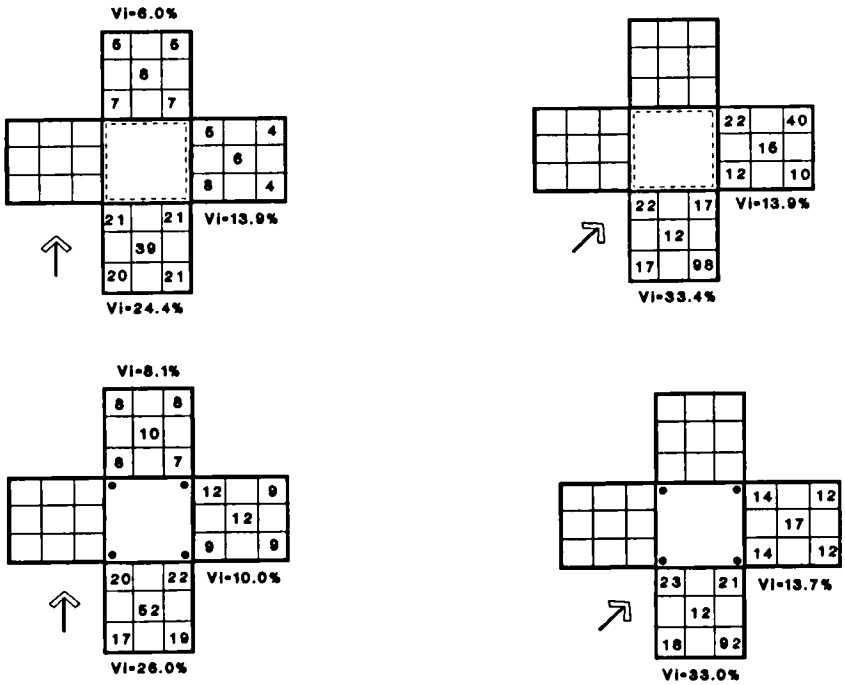

Figure 4.7: Indoor air velocities in a cruciform two -storey building model incorporating a courtyard. *Top drawings: the courtyard is fully enclosed. Bottom: the courtyard is open at ground floor and the first floor is supported by columns*, (After Givoni (1968)).

In the same article, Givoni (1968) reported indoor air velocities in a courtyard model structure constructed from the same basic units. The model represented two-storey buildings facing each other, three units, (i.e., rooms), long and distant by one unit. Two walls in their ends enclosed a rectangular courtyard.

The main results of the test were that, when the wind was normal to the block long axis, the air speed in the leeward rooms was on average 16% of the free wind. This constitutes approximately half the value in the windward rooms. Compared to the courtyard models described earlier, the indoor flows were higher. This indicates thus that the geometry of the courtyard structure may play an important role in the ventilation.

In this test, the author reported that the air in the sheltered rooms was flowing from the outside to the courtyard space at 0° wind angle, 45° or 90°, indicating that the suction in the court was greater than that on the external walls.

Cockroft and Robertson

Cockroft and Robertson (1975) reported some wind tunnel model tests and full-scale measurements of the ventilation in some buildings incorporating lightwells and courtyards, with a particular reference to hospitals.

The proposed design of the United Oxford Hospital, U.K., was a 6 to 8 storey building containing four courtyards which extend to a depth of four floors, (the ratio between one side of the courtyard and its height, or sectional aspect ratio, was estimated to be 1.8 in one direction and 2.3 in the other). An alternative design was examined which includes one-storey high slots at the fourth floor level to allow outside air to ventilate each courtyard base.

Wind tunnel model tests showed that there was a pressure gradient between the four courtyards and that there were significant differences of pressure on the walls within any of the courtyards. The most upstream courtyards were subject to lower pressures and to more variations in pressures than those downstream.

The surface pressures on the courtyard walls were found to be below the atmospheric pressure with the wind direction normal to a face of the building. Yet, once the wind direction was inclined to the walls, pockets of positive pressure began to appear. This was suggested to be due to the air being deflected in the courtyard by the rooftop rooms on the leeward side of the building, or by vortices generated at either the leading corner of the building or the upstream rooftop rooms. The addition of

throughways was found to have only marginal effects on the pressure distribution.

The same authors made a full scale measurement of ventilation rates and external pressures in an occupied hospital in Bellshill, Lanarkshire, U.K. The building was 7 storeys high, and naturally ventilated through four very narrow lightwells, (i.e., the sectional aspect ratio was 0.33).

The results, (although it was not clear how the measurement were made), indicated that the pressure acting on the four faces of the monitored courtyard was fairly uniform. When the wind was facing the rooftop tank room adjacent to the downwind courtyard wall the mean pressures were found to be positive, suggesting that the tank room deflected the flow into the lightwell. Otherwise the pressure were more or less negative. Smoke test indicated that for 65% of the time the courtyard openings served as outlets.

Summary of the findings from the reviewed studies

Despite the disparate nature of the measurements and the very individual characteristics of the courtyards reported here, some broad remarks could be made concerning the ventilation conditions in courtyard buildings.

i) The ventilation conditions in the different wings of a courtyard structure could be very uneven, particularly when the wind faces at right angles, in which case the downwind wings could have very weak internal flows compared to the windward face.

ii) The geometry of the courtyard may be an important parameter in affecting the ventilation. At 0° wind incidence, the penetration of streams of air into the courtyard seemed encouraged in large courtyards, in which case there was a rise of pressure at the rear wall of the courtyard. This may increase the ventilation. Nevertheless, the improvement is likely to be limited in any sizeable courtyard.

iii) The penetration of airstreams into the courtyard seemed to be facilitated at oblique wind angles even in small courtyard sizes. This could lead to better ventilation in the downwind wings of the building.

iv) Protuberances at the roof level could substantially modify the pressure field in the courtyard. It seemed that partial enclosure of the courtyard, in which outside air was allowed into the courtyard through sizeable apertures could have sometimes significant effects.

4.2.4 Flow patterns in courtyards

The flow patterns in courtyards are very complex and a wide variety of flow patterns can occur, changing significantly with the alteration of the building configuration and with architectural features and deviating quickly with small changes in the wind direction, (Cockroft and Robertson (1975)).

Torrance

Torrance (1966) made a series of wind tunnel observations on the external flow in the void of courtyard models of different sizes.

The air in the courtyards was described as having always a rotational nature. In small courtyards, the rotating flow was slow and was occupying only partially the courtyard height, leaving the base with relatively little air movement. It was suggested that the slow rotation motion was in this case induced by the frictional drag between the lower surface of the vortex sheet passing over the courtyard and the upper surface of the trapped air.

In larger courtyards, say from an alongwind dimension equal to the building height, there was a partial or a full penetration of the vortex sheet issued from the front edge into the courtyard. In these cases a continuous rotating flow was filling all the courtyard and the air was escaping at the edges of the patio where there was apparently the least resistance.

At an oblique wind angle, the vortex activity in the courtyard was more vigorous, and was filling the whole courtyard even with the narrowest forms. The flow which entered the court at the rear edges was described as having a general horizontal spiralling motion across the courtyard. This vortex system ended in the diagonally opposite corner where the air stream was able to leave the courtyard without any apparent difficulty.

Cockroft and Robertson

From smoke visualization tests made on models in a wind tunnel, Crokcroft and Robertson (1975) indicated also that a vortex system was occupying the courtyard space. The depth it occupied, the intensity of its activity and the direction of rotation, (clockwise or anti-clockwise), was highly dependent on the wind direction and the geometry of the building. In particular, the depth of the upwind wing and the existence of protuberances at the roof level had marked effects.

Ettouney

In a study on wind climate in courtyards, Ettouney (1973) gave a fine description of the nature of the flow occupying the court. His observations were based on flow visualisation using the surface paint film technique, for flow patterns near the model surfaces, and smoke for a three dimensional view.

Like the above mentioned authors, Ettouney explained that the general flow in the courtyard was governed by a dominant enclosed vortex with its axis horizontal and always perpendicular to the oncoming flow direction as illustrated in Figure 4.8. He explained that a transfer of momentum from the flow which separates at the upstream wall of the building energized the vortex which, from the explanatory drawings, had a clockwise motion. The flow was found to be more complex towards the sides.

The surface paint visualisation unveiled the existence of two secondary vortices in the upstream corners of the courtyard, with their axis perpendicular to the courtyard floor. The side vortices tend to blend into the main vortex system at a short distance above the ground.

At an oblique wind angle, the flow pattern was still governed by the main vortex and the two side vortices with their axis perpendicular to the ground became clearer. Furthermore, two vortices with their axis parallel to the main flow emanated from the upwind corner of the courtyard building and were found to be deflected downwards into the courtyard. Ettouney explained that the rotation of the vortices was such that their interaction produced this downward motion, (see Figure 4.9). These vortices tended to loose their coherence in the main vortex in the courtyard. Meroney (1982) explains that these counter-rotating vortices which are induced at the upwind roof edge of any rectangular building tend to reduce the wake cavity height and increase the centreline velocities as they sweep high velocity fluid downward and could persist far behind in the building wake.

4.2.5 Influential parameters in the ventilation of courtyard buildings

The review made so far on the flow conditions in simple clusters of buildings, in spaces partially enclosed, and ultimately in courtyards, was intended to understand the nature of the flow in courtyard structures and to evaluate the influent parameters. From this review it can be said that:

i) It can be anticipated that the downwind wings of the courtyards will be poorly

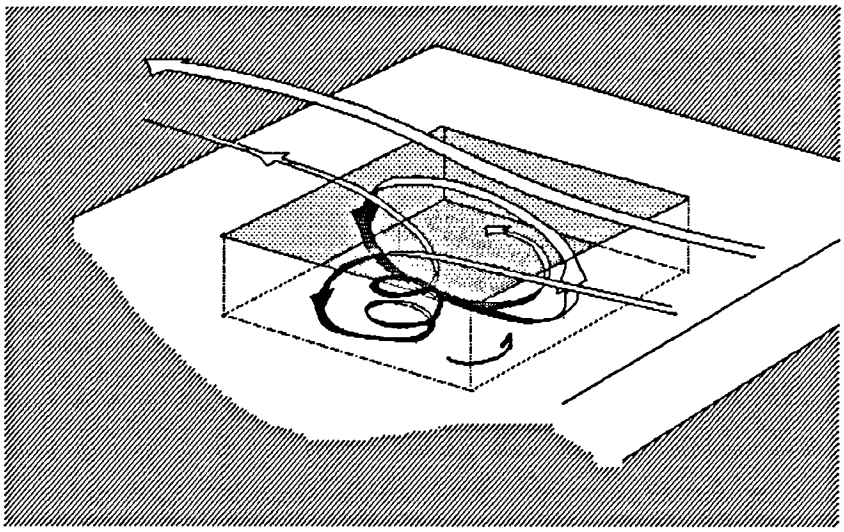

Figure 4.8: Schematic diagrams of air patterns inside the courtyards with the wind striking at right angles, (After Ettouney (1973)).

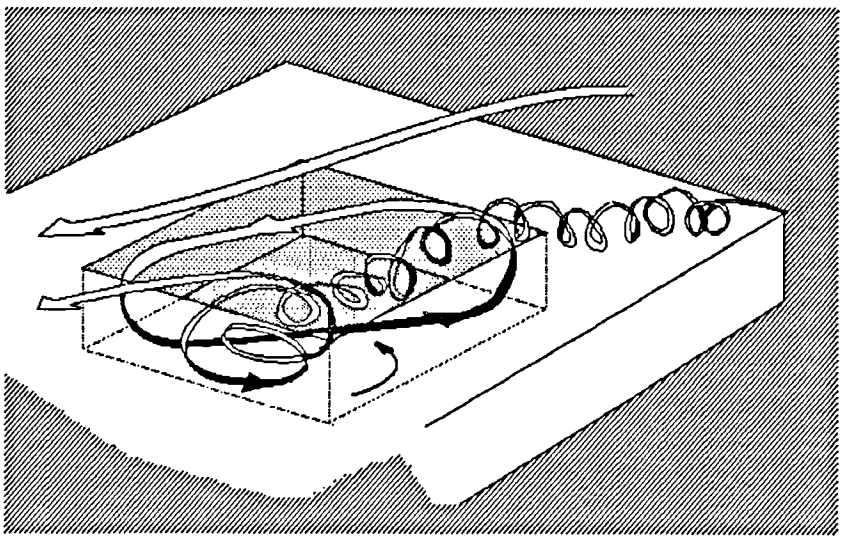

Figure 4.9: Schematic diagrams of air patterns inside the courtyards at an oblique wind incidence angle, (After Ettouney (1973)).

ventilated. This is because they are under the wind shadow of the upwind wings.

ii) Studies made on rows of buildings indicated that, in general, the decrease of the spacing between sheltered and sheltering elements resulted in weaker indoor air flows. However, for particular model proportions, minimum ventilation could be obtained at some critical spacings. In these circumstances almost the same pressure field was found to act on both faces of the sheltered element. Any of the increase or decrease of the spacing could improve the flow. This behaviour may also be possible in courtyards.

iii) The change of separation distances between elements in rows could cause the flow to travel in different directions in the sheltered element. This may also be possible in courtyard configurations.

iv) The limited number of studies on courtyards indicated that, with large sizes, portion of the air stream could penetrate the void, rising locally the pressure on the court back wall. This could increase the cross-ventilation in the downwind walls. This effect was less apparent with smaller courtyards.

v) The wind orientation is anticipated to have important implications on the indoor air movement, particularly at the downwind wings. It was found that at an oblique wind angle the penetration of air into the courtyard was facilitated by vortices generated at the leading roof edge of the building. This could enhance the ventilation.

vi) The curtailment of the flow in a collection of buildings or in composite buildings may under certain circumstances result in better ventilation conditions than without the present of adjacent buildings. This is particularly true for a room orientated parallel to the main air stream in which the presence of a building can create greater pressure gradient around it than without the surrounding building. It can thus be expected that the ventilation in the lateral wings of a courtyard building will not be as weak as in a rectangular shape building in which the rooms are orientated parallel to the wind.

vi) Partial enclosure of a courtyard is anticipated to have some influential effects on the building ventilation.

vii) Protuberances at the roof level and near the courtyard void might also have significant effects on ventilation.

4.3 Flow in extensive arrays of buildings

The flow in an isolated cluster of buildings is generally distinguished from the

large city-like arrays of buildings, though the boundary between the two categories is certainly not definite.

There could be substantial differences between the flow patterns in the two categories. The parameters governing the flow and pressures in a group of two buildings are not even the same than those of more than two, (Vincent and Bailey (1943)).

4.3.1 Effects of the array size on the pressure forces

The effects of the physical progression from isolated structures to more and more extensive arrays have been studied by few authors, for example, Wiren (1985), Soliman (1976) and Hussain (1978).

They indicated that the surface pressure magnitudes decreased progressively with the fetch of the group up to a certain size from which the changes became nominal. This limit could be taken as the required fetch for the group to be representative of more extensive city-like arrays.

The required fetch for the simulation of urban conditions in wind tunnels is discussed elsewhere, (Section 9.2), and, in the following review, only studies which consider extensive array fetches were selected.

4.3.2 Pressure forces in urban conditions

4.3.2.1 Pressure fields

The effect of the layout arrangement on the pressure forces of a building in an array was examined by several authors.

Wiren (1985) and (1987) performed a series of surface pressure tests on models centrally located in regular arrays of identical building models. These represented a 1 and 1/2 storey detached house with a pitched roof in the first study, and five contiguous 2 storey flat roof houses in the second. Both studies were already described in Section 4.2.2. The variables investigated in these works are summarized in Table 4.4 and Table 4.5 respectively.

Bauman et al (1988a) reproduced at a scale of 1/125 a typical setting of contiguous pitched houses commonly found in a Southeast Asian town. The houses were arranged so that their rear was facing a courtyard common to two houses and their front facing an alley. The effects of some architectural features, such as the height of the

walls separating the courtyards and variants of roofs were examined. The variables examined in his work are given in Table 4.6.

Table 4.4: Variables considered in the work of Wiren (1985).

Model proportions	(Af= breadth/height= 1.76, As= depth/height= 1.15)
Longitudinal spacing	1.76H to 3.51H
Transversal spacing	1.76H to 3.51H
Layout pattern	Normal and staggered
Fetch, R	2.9H (with 1 row and smallest spacing) to 14H (with 3 rows and largest spacing)
Incident flow	Simulated open flat terrain flow

Table 4.5: Variables considered in the work of Wiren (1987).

Model proportions	(Af= breadth/height= 5.83, As= depth/height= 1.5)
Longitudinal spacing	1.17H to 2.3H
Transversal spacing	1.17H to 2.3H
Layout pattern	Normal
Fetch, R	2.67H (with 1 row and smallest spacing) to 7.6H (with 2 rows and largest spacing)
Incident flow	Simulated open flat terrain flow

Table 4.6: Variables considered in the work of Bauman et al (1988a).

Longitudinal spacing of the streets	0.5H to 5H
Depth of courtyards attached to houses	0.25H and 1H
Transversal spacing	continuous rows
Layout pattern	Normal
Fetch, R	12.5H
Incident flow	Low density urban wind profile

By far the most comprehensive investigations on the way in which the geometry of a group affects the pressure forces on the elements of the array were that of Soliman (1976) and, later on, Hussain (1978).

The modelling of the group layout was rigourously established in both studies and a fine and exhaustive parametric study was undertaken on the effect of the plan density of a group layout, on the pattern of the layout (normal or staggered) and on the incident flow, (smooth or rough). Hussain, furthermore, extended the study to different geometries of the elements in the group. The variables examined in the study of these works are listed in Table 4.7 and 4.8.

All the above-cited works indicated that the overpressures and underpressures on the surfaces of an element were considerably lower when the element was in an array than in isolated conditions, even with a very low plan density.

The denser the group layout was, the greater the reduction in the pressure gradient became. Hussain (1978), for example, indicated that the presence of neighbouring elements in an array of cubical shaped buildings reduced the element drag by 30% at plan densities around 4%, this becoming approximately half at a density of 9% to 15%. The drag continued to decrease to reach only one third of the values in isolated elements at 17% to 30% layout density before going to zero at 100% density.

As with simple clusters of buildings, the effect of decreasing the separation distance between elements in a large array was to immerse all the surfaces of the

downwind buildings into the wake of the upwind elements, thereby reducing the pressures below atmospheric and creating a uniform pressure field in all the building surfaces.

Table 4.7: The variables considered in Soliman's main investigation, (Soliman (1976)).

Model proportion	cubical, (Af= 1, As= 1)
Plan area density	3.125% to 50%
Layout pattern	Normal staggered
Fetch	R/H = 14
Incident flow	smooth and rough

Table 4.8: The variables considered in Hussain's main investigation, (Hussain (1978)).

Frontal aspect ratio, Af (i.e., breadth/height)	0.5 to 4.0
Side aspect ratio, As (i.e., depth/height)	0.5 to 2.0
Relative height	0.5 to 4.0
Plan area density	2.5 to 60%
Layout pattern	Normal and staggered
Fetch	10< R/H < 25
Incident flow	Atmospheric boundary layer

4.3.2.2 Flow regimes

Soliman (1976) and Hussain (1978) suggested that the cluster problem could be dealt with in terms of three distinct flow regimes which occur at critical separation

distances between the elements of the group. Within each of these flow regimes, the drag coefficient was indicated to decrease with the decrease of the element separation distance in a linear fashion, but the rate of change of the drag was different from one flow regime to another. A similar flow behaviour was also found in studies of pressure forces in two dimensional elements such as grooves, (e.g., Tani et al (1961)), and cut-outs, (e.g., Schofield et al (1974)).

In the following paragraphs, a detailed review of the work of Hussain and Soliman is made. This is to provide a background for the study planned to evaluate the ventilation of courtyard and atrium buildings in congested urban sites. Also, their works have some relevance to the flow phenomena occurring in courtyards owing to the fact that the sectional aspect ratio in one direction are similar in courtyard structures and buildings separated by streets in an urban layout.

Soliman (1976) reported that in a layout of cubical elements, an "**isolated**" flow regime was set when the clear spacing between the elements, Sc, was above 2.4 times the element height, H. There was then no interference between the individual flow fields which were identical to those around isolated elements.

The first change in the flow regime occurred at a relative distance $Sc/H \approx 2.4$ and was revealed from a sudden change in the rate of decrease of the surface pressures on the windward surfaces. The flow regime was called the "**wake interference**" flow regime[1] in which the flow fields began to interact, (see Figure 4.10 and 4.11).

From $Sc/H \approx 1.5$, the rate of change of the leeward wall pressures was in turn modified. The new flow regime that was set was called "**skimming**" roughness flow[2]. In this flow regime stable vortices occupied the gaps between the elements and the main flow no longer entered the spacing but skimmed over the top of the array, (see Figure 4.11).

The wake interference flow roughness was suggested to take place when the space between the elements was approximately equal to the sum of the lengths of the frontal separation and the downstream recirculating region of an isolated element[3], (see Figure

---

[1] Referred to as flow in shallow grooves by Tani et al (1961), or 'k' type roughness flow by Schofield et al (1969).

[2] Referred to as flow in deep grooves by Tani et al (1961), or 'd' type roughness flow by Schofield et al (1969).

[3] Soliman found these distances respectively equal to 1.53H and 0.83H, so the sum was 2.36H, which coincides to the distance separation, 2.4H, where the transition between the flow regimes occurred.

4.11).

The presence of a particular flow regime was manifest in the distinct shapes adopted by the vertical pressure distributions on the walls of the elements, (see Figure 4.12). The pressure profiles on the windward walls took the form of an " S " shape in the isolated roughness flow and tended towards the shape of a reversed " C " in the wake interference flow or the skimming flow. Two distinct families of profile shapes were also found on the leeward walls, one coinciding with the isolated and wake interference flow regimes and the other with the skimming flow regime. The differences between the two was in the vertical location of the maximum suction.

Hussain (1978) extended the work of Soliman (1976) onto various geometries of group elements and on the effect of the group layout on the lift coefficient. The influence the frontal and side aspect ratios of the elements had on the pressure forces were examined, as well as the height of the test model relative to the surrounding elements, (see Table 4.8). The salient results of his work were as follows;

i) The flow behaviour around the rectangular models was found to present similarities with that of cubical shapes, although the change from one flow regime to another was found to take place at different values of spacing between the elements.

ii) The variation of the lift coefficient with the element spacing presented a single break point at the initiation of the skimming flow regime, at $Sc/H \approx 2.4$, after which the lift tended to level out.

iii) Both the frontal aspect ratio, Af, and the side aspect ratio, As, were found to be dominant factors that could alter the flow from the isolated regime to the wake interference flow. However, when the model was long enough for the flow to reattach on the roof and side walls, the increase of the side aspect ratio had no effect on the change of the pressure fields with the change of the element spacing. Also, the transition from one flow regime to another then occurred at the same spacing;

iv) On the other hand, Af or As had lesser effects on the transition between the wake interference and skimming flow regimes, (see results in Table 4.9).

v) The reasons for having the transition between the isolated and the wake interference occurring at various spacing for different model proportions could be explained from the fact that these flow regimes are controlled by the distances of the frontal separation and the downstream reattachment of the flow around the models. Since these dimensions are dependent on the frontal and/or the side aspect ratios, the distance at which a model element began to interfere was variable. On the other hand,

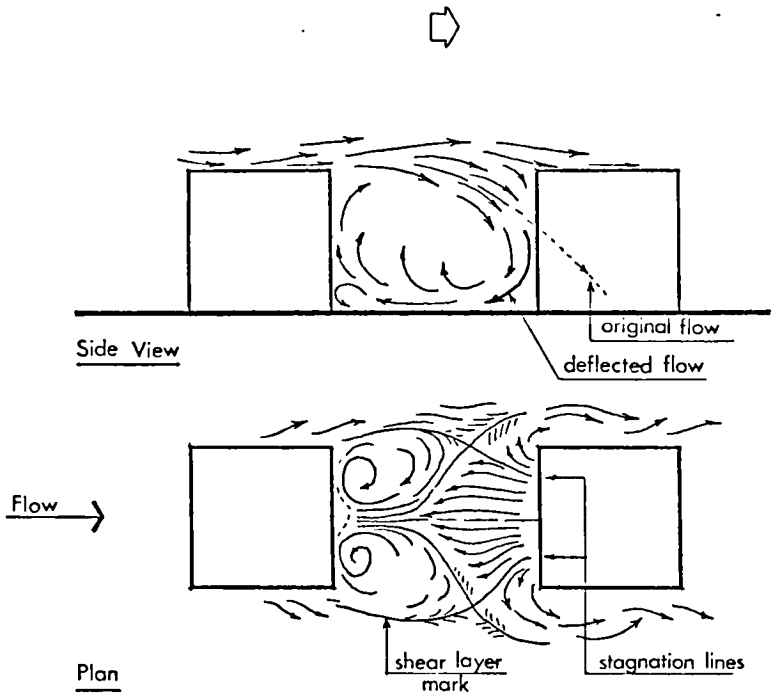

Figure 4.10: Flow pattern in the wake interference flow regime, (After Soliman(1976)).

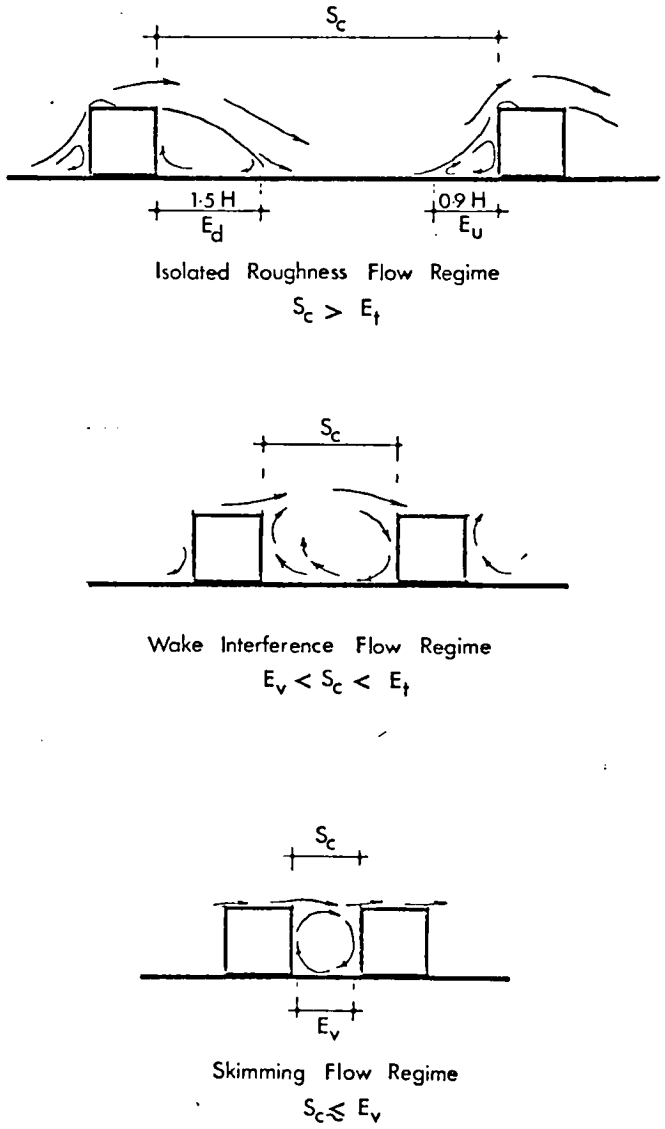

Figure 4.11: Flow patterns and governing conditions for the three flow regimes, (After Soliman(1976)).

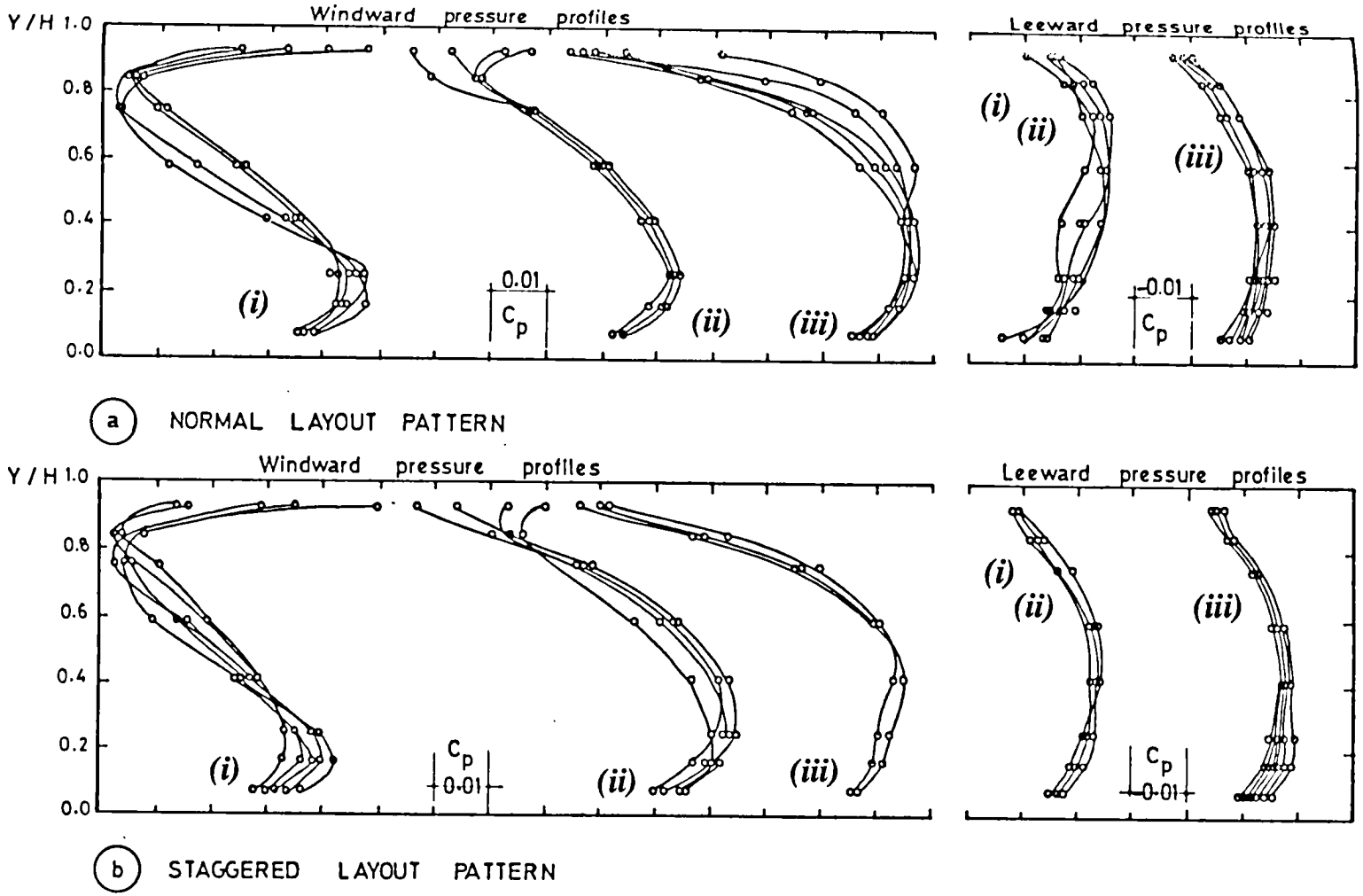

Figure 4.12: Vertical pressure distribution on the windward and leeward walls of elements in an array and grouped according to the flow regimes; *(i) isolated, (ii) wake interference, (iii) skimming flow regimes*, (After Soliman (1976)).

Table 4.8: Element spacings where the flow transitions occurred. *S is the spacing between the elements from axis to axis, Sc is the clear spacing, H is the element height. (W), (S), indicated the onset of wake interference and skimming flows respectively,* (After Hussain (1978)).

Frontal Aspect Ratio Af	Spacing between elements,		Side Aspect Ratio As	Clear spacing between elements,	
	S/H	Sc/H		S/H	Sc/H
Af=0.5	(w)3.25 (S)2.3	2.25 1.3	As=0.5	2.6 1.8	2.1 1.3
Af=1.0	3.4 1.1	2.4 1.4	As=1.0	3.4 1.11	2.4 1.4
Af=1.5	3.6 2.5	2.6 1.5	As=1.5	4.0 2.9	2.5 1.4
Af=2.0	3.7 2.53	2.7 1.53	As=2.0	4.1 2.9	2.1 1.9
Af=4.0	4.0 2.55	3.0 1.55			

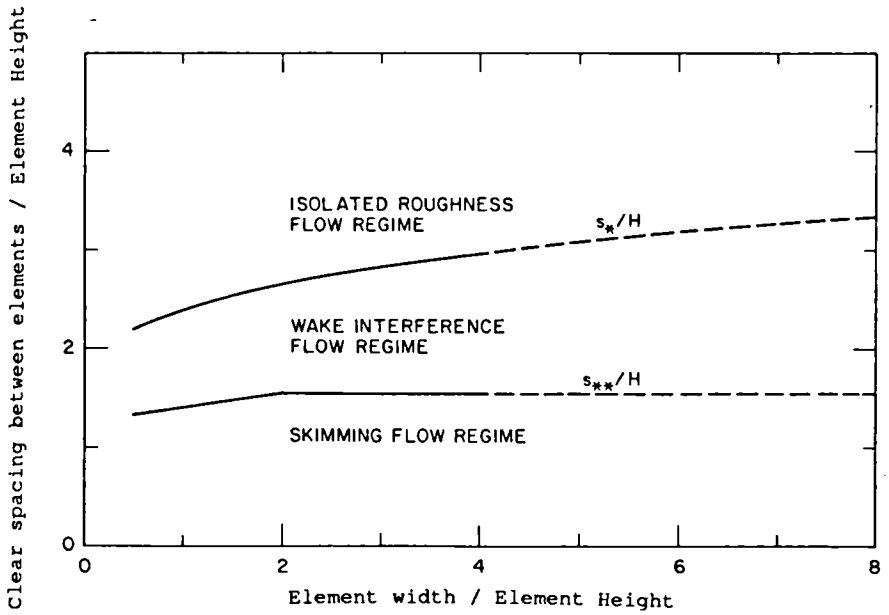

Figure 4.13: Relationship between the flow transition and the relative width of the elements in a regular array. Data obtained from Hussain's work (1978), (After Hosker (1985)).

the change from the wake interference flow regime to the skimming flow was suggested to coincide with the initiation of a stable vortex in the space between the elements and which was argued to depend solely on the depression height.

From Hussain's data, Hosker (1985) suggested a relationship between the flow transition and the relative width of block-like elements in a regular array, and which is graphically represented in Figure 4.13.

vi) The height of the test model relative to the height of the surrounding elements in the array was also found to have dominant effects. The rate of change was different below and above a relative height of 1.3H to 1.6H, which was suggested to correspond to the physical thickness of the inner layer growing over the model layout. The value of the drag was found to be large for a building with a height smaller than that of the elements surrounding it. As the height increased, the drag decreased and when the height of the model reached the outer layer, (in which case the building was considered as high rise), the rate of change of the wall pressures was invariable for different densities. It was suggested that the rate of change was then depending on the velocity profile corresponding to the atmospheric boundary layer simulated upstream to the group layout.

Soliman and Hussain generalised their results with an infiltration prediction procedure for low rise buildings based on the chart of IHVE Guide (1970) applicable to high rise buildings, and in which all the above mentioned parameters were taking into account.

4.4 The use of roof-level openings for natural ventilation

The evaluation of ventilative conditions in atria addresses the more general case of structures incorporating vents at the roof level.

The provision of natural ventilation is generally a function that is endorsed by the windows. However, roof-vents may be used when these requirements cannot be performed by the window. These circumstances might occur when no window can be located on the walls of a room, for example, when the external walls are party walls or are sunk underground.

The need for roof vents might also arise when the windows on the facades have to be reduced for some reasons, such as, to prevent the penetration of solar radiations, sand, dust and hot air, and also for privacy, security and/or for noise control.

Finally, the roof vents might be used to assist the cross-ventilation in deep plan buildings and especially in industrial buildings. In this latter type of buildings, the necessity to expel the contaminated air liberated by the processes immediately above the plants makes the roof vents more suitable than windows.

The value of roof level openings resides first, in the fact that they are more likely to be located in an unobstructed region of the flow than windows which are often under the wind shadow of obstacles nearby. Secondly, even when the wind strikes directly the windows, the air velocities at this level are generally less than that at the roof level as a result of the wind velocity gradient. Finally, the air at higher level is more likely to be cleaner than near the ground.

In the following paragraphs some historical precedents of use of roof-level openings and scientific research carried out in this subject are reviewed. Only examples in which the roof vents were designed to perform a whole-house ventilation have been considered, and no allowance has been made for common roof ventilator types incorporated in domestic or industrial buildings.

4.4.1 Historical examples

4.4.1.1 The wind towers

One of the oldest and most remarkable roof ventilator is certainly the wind tower. Its origins dates back as far as 900 A.D., (Bahadori(1981)). A typical wind tower or *Baad Geer*, as it is called in Iran, resembles a chimney with one end at the bottom of the building and running through to above the roof, overtaking it by 2 m to 20 m, (Bahadori (1978, 1979)). From Persia where they are believed to originate, wind towers spread to Arabia, Pakistan Egypt and North Africa in the 13^{th} Century through the trading routes exiting at that time, (see Figure 4.14).

Wind towers could be very varied in their forms but they all work in the same basic principle to intercept the prevailing summer winds, to cool the air and circulate it through the attached building. In having their intakes as high above ground as possible the towers can catch the winds of higher speed with air which is cooler and cleaner than near the ground. Their use was particularly important in dense urban areas where breezes at the ground level are restricted and where the air is hot and dusty, (Cain et al (1975), and Fathy (1986)).

The upper part of the tower can be divided into several vertical air ducts that end

in openings in the sides of the tower and which function is to divert multidirectional winds into the tower. This kind of tower is found usually on the coast where sea-land breezes are present, (Cain et al (1975)). They could also be designed to catch the wind blowing in a specific direction. In this case, they are often refer as wind scoops or wind catchers.

The wind tower operation does not count solely on the wind's ability to force its way through the rooms but also on the thermal action, (Bahadori (1979, 1981), Cain et al (1975), and Karaman and Egli (1981)), and their operation depends on the wind conditions and the time of day. The towers were of course intended only for summer use and were often coupled with evaporative cooling devices. In winter they were closed otherwise they could greatly increase infiltration heat losses.

Wind towers are still in service and are included in some new buildings to which the University near Doha, in Qatar, designed by EL Kafrawi, is famous, (see Figure 4.15).

4.4.1.2 The wind scoops or wind catchers

Also called *Malqaf* or *Malkaaf hawah* in Egypt and Iraq, the wind scoops appear like chimneys which incorporate at their tops defectors consisting of planes inclined at 45°, (see Figure 4.16). They are believed to be originated from Egypt where they have been found drawn on manuscripts from the pharaonic period, (see Lezine (1971) and Fathy (1986)). They also exist in Iraq, Pakistan and Afghanistan.

Unlike the *Baad Geer*, the *Malqaf* is designed to face one direction the dominant winds, and generally does not extend as high as the wind tower above the roof level. The wind scoops of the old quarter of Cairo, for example, faced north to catch the breeze off the Nile from the Mediterranean. The winds blowing from other directions are from the desert and were avoided. In the coastal region of Sind, Pakistan, the wind scoops were designed to catch the trade winds off the Indian Ocean which are some 7° C to 15° C cooler than the ambient air in summer season, (Bowen (1984)).

Other wind scoops were made moveable to intercept favourable winds coming from multiple directions. In some settlements in Iraq, for example, they incorporate an ingenious system consisting of a fin-like projection into a pivot-mounted scoop, to keep them facing the wind all the time, (Cain et al (1975)).

Like the wind tower, the *Malqaf* does not operate only with the wind pressure forces. Tests made in Cairo throughout a daily cycle, has revealed that there was a

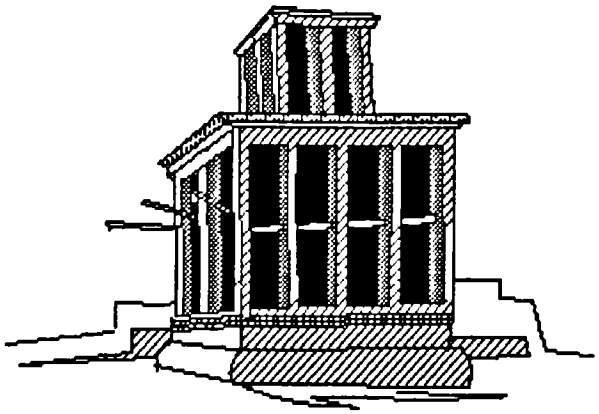

Figure 4.14: Example of double wind tower system in Kerman, Iran.

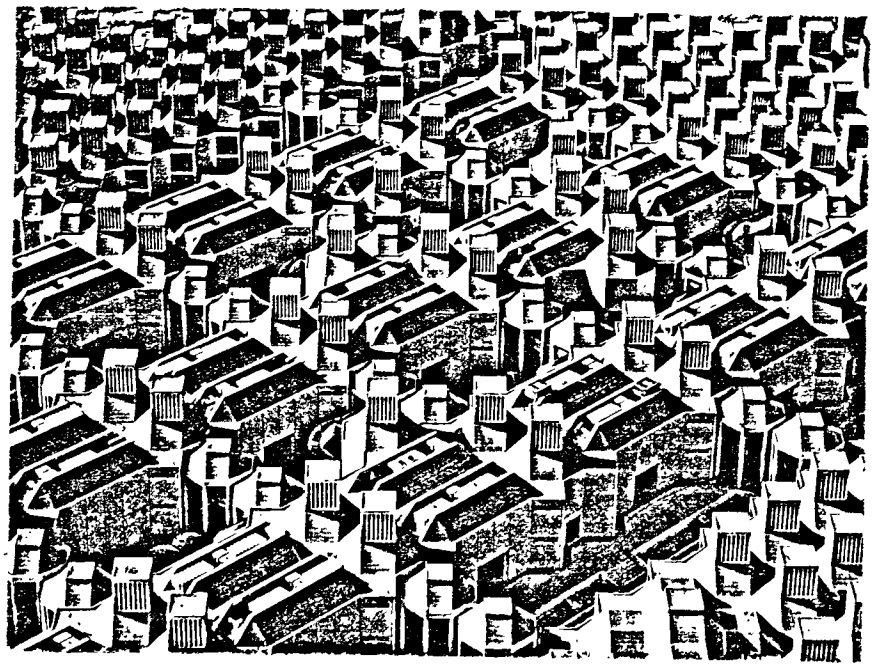

Figure 4.15: Recently built University in Qatar employing wind towers (Architect Kamal El Kafrawi, source: Mimar (1985)).

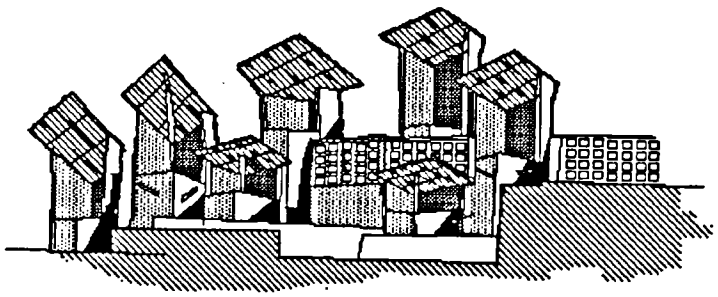

Figure 4.16: Use of wind scoops in a village in the Sind province of Pakistan.

thermosiphonic current of air in the shafts, (Cain et al (1975)).

These sensible cooling systems are sometimes coupled with evaporative cooling devices. Traditionally, a porous water-filled jar was disposed at the lower end of the shaft that permitted to cool the air. Fathy (1986), in the design of a wind catcher for a school in the Gourna village, used beds of wet charcoal for the air to pass over before entering the rooms. He claimed to have measured a drop of 10° C in air temperature.

4.4.1.3 The curved roofs

Curved roofs are often used in hot climates for their structural and thermal advantages, (Cain et al (1975)). Furthermore the aerodynamic properties of these roofs make them suitable ventilators. It is a well-known fact that the velocity of the air flowing over cylindrical or spherical objects increases at the apex, and consequently, produces a large suction which can be exploited if air vents are located there.

In areas where there are dominant winds, cylindrical roofs were built with their axis normal to the wind direction. In areas where the wind blows in all directions, domed roofs were generally employed, (Bahadori (1978).

Curved roofs in conjunction with wind towers were used by the ancient Iranians as part of cooling systems for the seasonal storing of cold water in underground cisterns. The most famous example is that situated in Yazd, Iran, which has 6 wind towers of more than 12 m height, (Bahadori (1978)).

4.4.1.4 The Dymaxian house of Buckminster Fuller

This house, shown in Figure 4.17, was designed by Buckminster Fuller. It incorporated a very elaborated and massive 5.5 m diameter ventilator streamline shaped on its top and coupled with an equally ingenious crossflow heat exchanger, (Sieden (1989), and Fuller and Marks (1973)). This suction-only ventilator was intended to rotate so that the openings were always positioned at the lee, whatever the wind direction. Its sophistication lied in the minimum drag it offered for the maximum exhaust effectiveness. The final version, shown in Figure 4.17, was selected from many types of ventilators that were tested.

Few prototypes of the Dymaxian house were built in the mid-forties. However, lacking of funds the experiment had to be ended. Two prototypes were ultimately acquired by a private owner who modified them.

4.4.1.5 "La Sucka"

La Sucka is a roof-mounted system designed by Fairey and Bettencourt (1981), (see Figure 4.18, example a). Its name derives from the fact that it was designed to always provide a suction at the rooftop outlet and perform a natural whole-house ventilation. Precedent examples of such system exist with maybe a lesser degree of sophistication. This particular example was enclosed in the review because of the attention it was given to assess its performances. The system was reported in several publications, such as Cermak et al (1981, 1982), Chandra (1985), and Chandra et al (1985).

As shown in Figure 4.18, example a, La Sucka was incorporating very simple backdraft dampers mounted on a screen frame to allow one-way flow direction, i.e., air suction in this case. Another design alternative was suggested by Chandra (1985) and shown in Figure 4.18, example b. It worked on the principal of a wind scoop. The major problem of the design was the rainproofing and night-only operation since in day-time the undesired hot air adjacent to the roof could enter the house. Noise created by the flutter could be a severe drawback for these designs.

A prototype of "La Sucka", was installed in a house in Central Florida, U.S.A, and was monitored during August and September 1981. An experimental Passive Cooling Laboratory, (PCL), incorporating such device was also built at Cape Canaveral, Florida. The results of tunnel tests of the PCL will be discussed in Section 4.4.2.2.

4.4.1.6 Roof vents in industrial buildings

Simple roof openings and roof ventilators are commonly used in industrial buildings to assist the ventilation of the whole building or to extract contaminated air above the plant that generates it. The control of natural ventilation plays an important role in these buildings because of the enormous quantities of air that have to be dealt with and because the natural motive forces are often more important than the mechanical forces. The mechanical means are most effectively used as a corrective to natural ventilation in the form of air curtain and local air supply or extract, (Baturin (1972)).

In industrial buildings where hot or contaminated air is the prime problem, the air has to be extracted immediately above the plant through the roof. The simplest and yet effective design is based on the principal that roof vents must always act as suction devices and so whatever the wind direction, to prevent reversal of the rising hot and

Figure 4.17: The Dymaxion house of Buckminster Fuller.

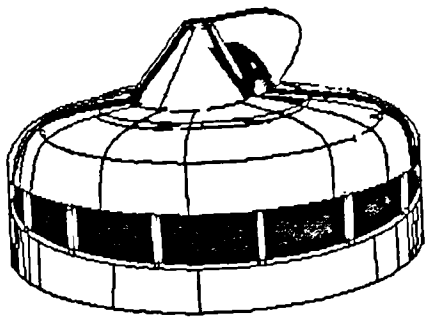

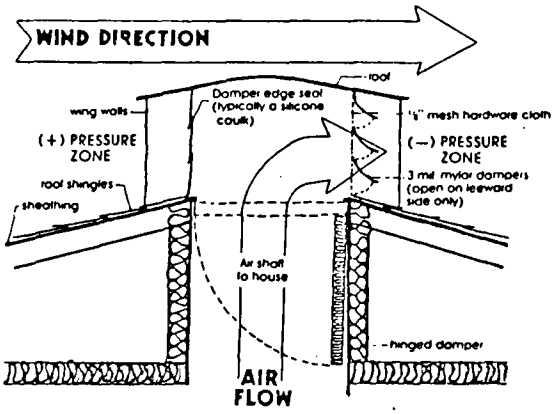

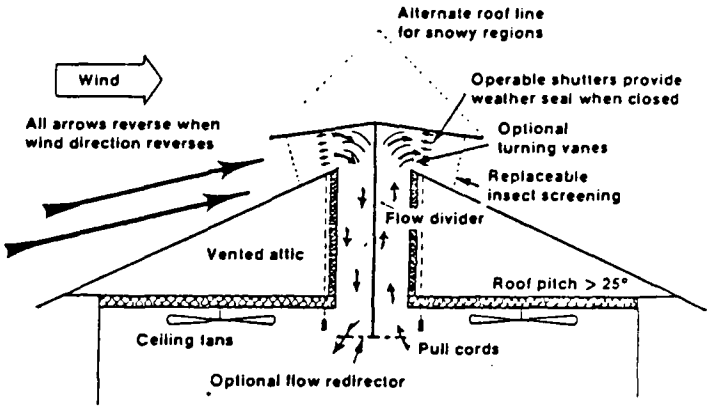

Figure 4.18: (a) "La Sucka", a whole -house roof suction device, devised by Fairey and Bettencourt (1981). (b) Alternative ventilative mode for "La - Sucka", (source: Chandra (1985)).

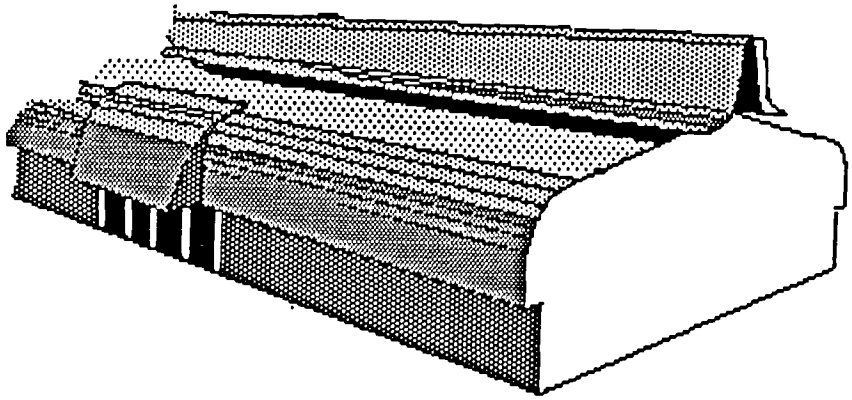

Figure 4.19: Aerodynamically -designed roof induction "sail" incorporated in a recent design of a laboratory of the Agricultural and Food Research Council in U.K. (source: Storllery (1986)).

polluted air currents. For this purpose the apertures of the monitors have to be located in the region of a wind shadow, protected if necessary from the wind by a screen placed transverse to the air flow ahead of the roof. Several designs of such protected monitors are suggested by Baturin (1972). The publication incorporates interesting photographs of the flow associated with some these roof designs, obtained from two dimensional models in a water channel.

A recent example of industrial building incorporating a sophisticated roof which is capable of inducing air suction is shown in Figure 4.19.

4.4.2 Research related to ventilation through roof vents

4.4.2.1 Wind towers and wind catchers

The sensible cooling potential of the old wind towers has attracted the interest of some researchers. Bahadori (1981), for example, examined the operating principles of the Baad-Geer under the wind pressure forces. Wind tunnel tests were conducted on a model of a house incorporating a 10 m tower, and with or without surrounding obstacles. The airflow rates were inferred from the knowledge of the wind pressure coefficients using a calculation techniques that estimates the internal flow balance by iteration.

The major results are depicted in Figure 4.20. They indicated that the Baad-Geer could admit the wind into the house or act as a suction device depending on the wind pressure distribution on the house envelope, which in turn, could be influenced greatly by the presence of courtyard walls or other obstructions and by the wind direction. When the openings of the house were well shielded from the wind, then the wind tower was acting as a wind-scoop in most of the cases, deflecting the air into the house. On the other hand, when the wind was blowing directly onto the house openings, then the flow was generally leaving the tower, except when the tower was upstream to the house.

A significant portion of the air which entered the Baad-Geer from the windward openings was found to leave the tower from its leeward and side openings and never entered the house. This constitutes a loss of the inflow that could contribute to greater air movements in the rooms, (see Karakatsanis et al (1986)). A remedy for this is to provide the tower openings with automatic dampers or use a swivelling head, (Bahadori (1985)). The estimates of the indoor air velocity showed that the design incorporating dampers was more effective than without the dampers, (see Figure 4.21).

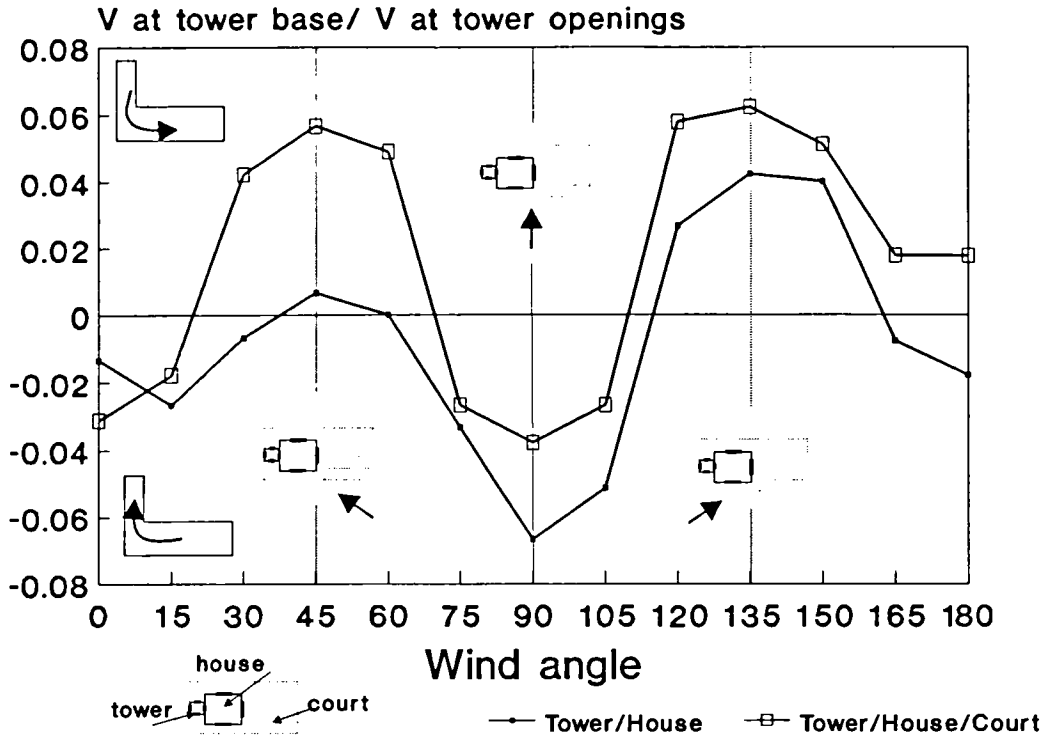

Figure 4.20: Ventilative performance of a wind tower. Replot of data from Karakatsanis et al (1986).

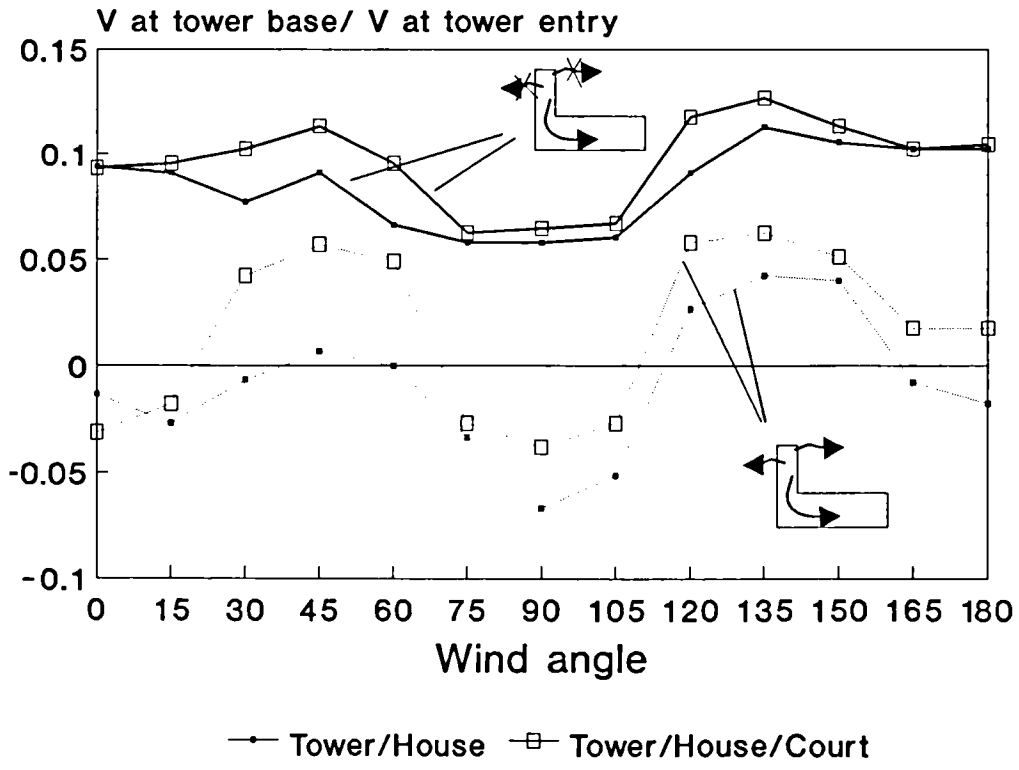

Figure 4.21: Ventilative performance of a wind tower incorporating some kind of dampers. Replot of data from Karakatsanis et al (1986).

Chand et al (1990) studied in a wind tunnel some of the influential ventilation design parameters of wind catchers. The details that were examined on a simple structure were, i) the facade of the catcher, ii) the size and shape of the roof opening, iii) the wind catcher overhang, and, iv) the location of the air supply openings.

The study revealed that the facade size of the catcher were contributing only to a small degree in changing the indoor air velocity at the sill height, (about 5%). On the other hand, the increase of the area of the roof vent from 40% to 60% of the window resulted in 12% to 20% higher indoor flows.

A comparison in the performances of two alternative designs is shown in Figure 4.22, where one is a cross-ventilation through opposite windows, and the other, through a window and the catcher. As an outlet, the wind catcher gave better results than with two windows, but was not performing as good when it was an inlet. It can be suggested that this was because the air entering the catcher was subjected to several successive changes of direction and thus to greater resistance than when it entered the upwind window. This was, however, less critical when the air left through such an airway, because most of its inertia, that prevents abrupt changes of direction, died down at the end of the path.

4.4.2.2 La Sucka

Model wind tunnel tests of a house incorporating this suction ventilator, (see Section 4.4.1.5), was conducted by Cermak and published in Cermak et al (1981, 1982). The test house with its immediate surrounding, and the details of the cupola were modelled at a scale of 1/25. The prototype was located in an open country.

The results of wind tunnel tests are shown in Figure 4.23. The device was particularly effective in inducing air currents when the building windows were facing the wind at an oblique angle, (SE and SW in the figure). On the other hand, the performances were much lower when the window was located in the building wake, (particularly NE). The conclusion that could be inferred is that the cupola was effective in inducing suction, in which case, the most favourable situation was with the room windows located in the high pressure field.

The authors indicated that, in comparison with other ventilation schemes tested, "La Sucka" was the best all-round, (expect for the fully open ground floor, i.e., configuration (I)). This is because it was reasonably well ventilated for all the wind directions in contrast with the other strategies which were very sensitive to the wind

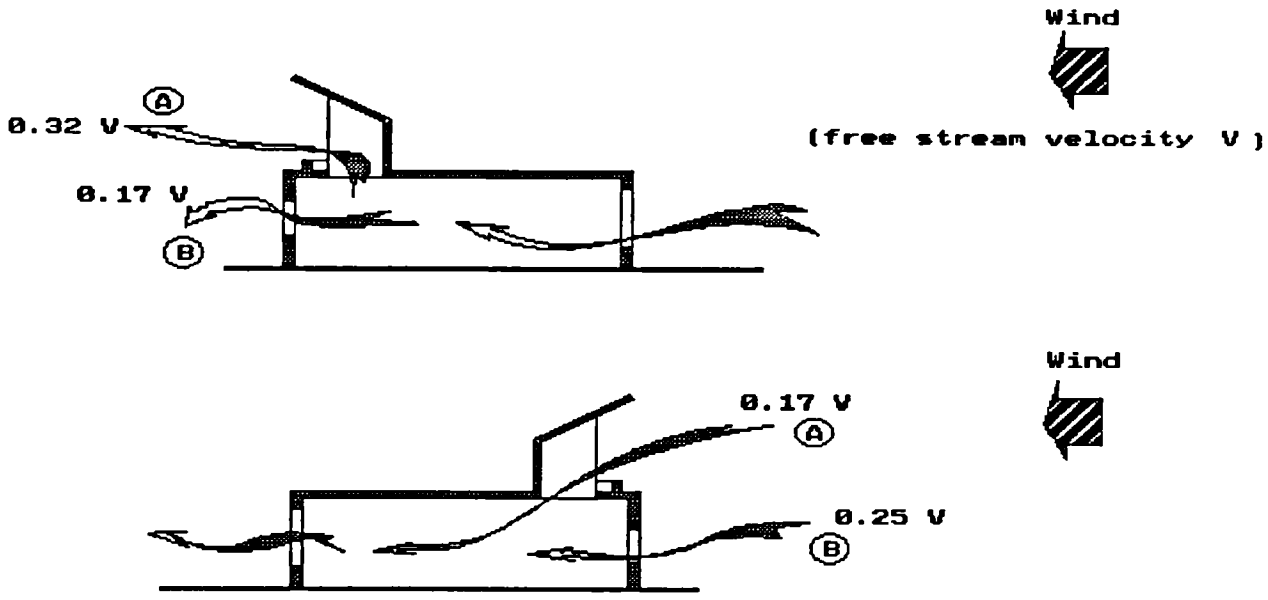

Figure 4.22: Assessment of ventilation in a house fitted with a wind catcher, (From Chand et al (1990)).

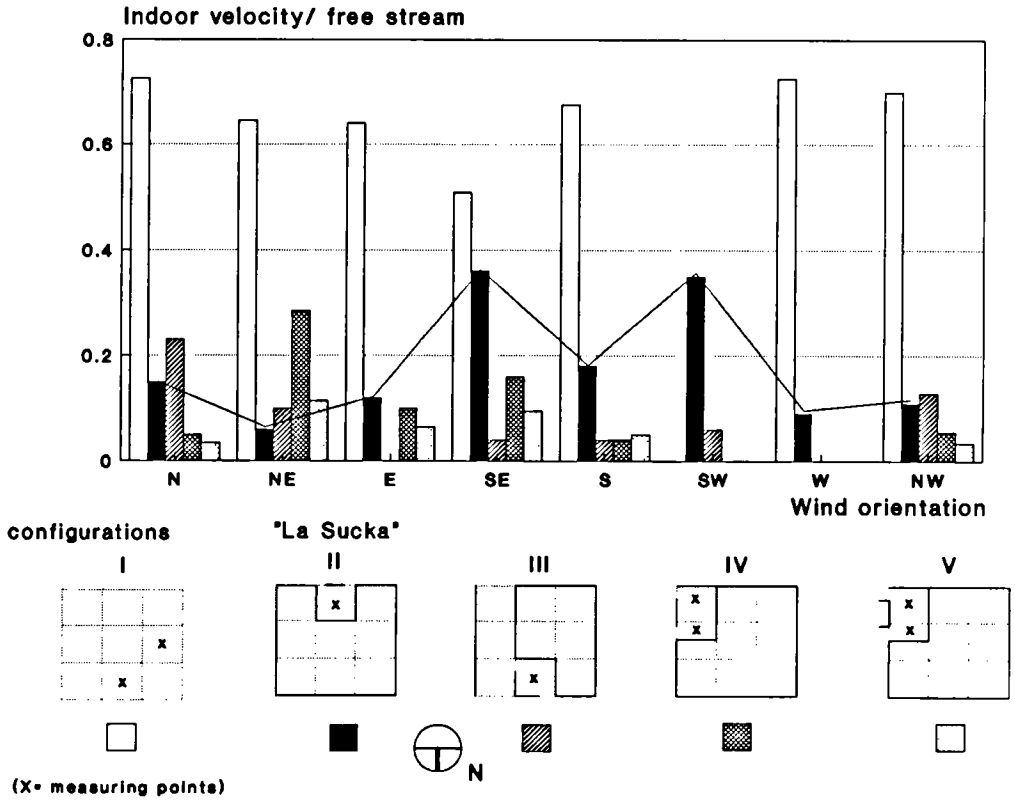

Figure 4.23: Results of wind tunnel tests of "La Sucka". Replot of data from Cermak et al (1981).

orientation.

4.4.2.2 Weston's work

In a wind tunnel experimental test, Weston (1954) examined the value of roof vents in maximizing air movement in industrial building to maintain satisfactory working conditions during summer in Australia.

Roof vents in industrial buildings may be used to satisfy two functions that are, the removal of contaminated air and the provision of air movement for comfortable conditions. The two functions, however, could be combined only with difficulty. This is because the extraction of fumes and smoke generated by the processes are best removed through openings in the roof directly above. however, such upward flow would not contribute in providing cooling effects for the workers.

The objective of Weston's study was thus addressed to industrial buildings in which the problem of contaminated air, and heat liberated by processes, did not arise or was restricted to sections that could be isolated from the rest of the building.

The value of roof openings in inducing air movement at the working level was found to depend primarily on the orientation of the roof apertures in relation to the dominant winds. The most effective utilization of the wind was obtained when openings were located in the region of high pressures at the windward end of the roof.

Next in importance was the openings in the zone of low pressure at the leeward end. These apertures were found to assist in maintaining the increase rate of air movement throughout the length of the building which otherwise tended to die down as the air traversed the building. The combination of apertures at both extreme ends achieved the best results particularly when the wind was blowing at right angle to the plane of the openings.

An interesting remark was that the intermediate roof-light openings did not influence greatly the air movement, and when they were located in areas of reduced pressure, they even seriously impaired the ventilation. This was because the air entering the building was quickly lost through these lights and prejudiced the air movement in the building as a whole. This demonstrated that the instinctive practice to open all available openings to their maximum extent in hot weather could in fact impair the ventilation more often than it improves it.

It has to be mentioned here that the conclusions drawn were based on particular roof geometries and windows, (i.e., awning window type). It is possible that other

designs may not assist the flow at the working level in the same manner.

In another publication, Weston (1956) examined the wind shadow effects of other building's on one of the buildings studied in the previous work. Some of the results are enclosed in Section 4.2.2, reviewing the wind shadowing effects in building clusters.

Even in an obstructed site, the additional openings at the roof level on the windward and leeward ends of the building appeared to be beneficial. In many cases, where there was reasonable separation between the buildings, the air movement in the obstructed building was even higher than the unobstructed building in which all the roof openings were closed.

As in the exposed conditions, the provision of openings in all the roof-lights did not facilitate the air movement in the obstructed building. On the contrary, this could reduce the air currents when the roof openings faced in the opposite direction to the wind. Thus, the roof openings may better be restricted to the extreme ends. It was suggested that the location of the openings at the highest level, and the addition of overhangs acting as downward deflectors were advantageous.

4.4.2.4 Bauman's study

Bauman et al (1988a and 1988b) reported a wind tunnel investigation on the effectiveness of using a roof-level ventilation device, he called "jack roof", to promote ventilation in densely built housing, typical of Southeast Asian cities. The experimental arrangements and some results were already given in Section 4.3.2. The surface pressures were taken on the walls and roofs of a model amidst an array of contiguous houses.

The jack roof can be operated in different modes;

i) as a Venturi system, when both windward and leeward openings of the roof are opened. In this case, it will act as a suction device;
ii) it can deflect the air down into the house, in which case, the windward openings of the roof are open and used as inlets;
iii) it can promote suction of air when the leeward faces of the roof are opened, (see Figure 4.24).

The ventilation potential was estimated from the pressure differential between openings located at different surfaces.

In very densely built conditions, i.e., when the spacing between the rows were less than the average building height, the sheltering effect of the adjacent building models was found to be so great that the ventilation potential through the wall openings alone was reduced to a negligible value. The roof surfaces, on the other hand, exposed to stronger wind conditions had the largest pressure magnitudes of all the building surfaces. Consequently, the jack roof vents could be effective for inducing air movement, (see Figure 4.25). If the front of the jack roof was used as a ventilation inlet, then, both the upwind and downwind walls could serve as outlets. Similarly, with the roof suction mode, the air could be introduced in both facades. The performances of each of the modes depended on the building layout spacing and the wind direction.

At large building spacings, on the other hand, the most appropriate pressure differential to drive ventilation was probably between the wall apertures and without ventilation openings at the roof.

The way the ventilation was estimated in this work, based on the pressure gradient across two surfaces of the building models, could be strongly criticised for the following reasons:

i) The techniques cannot predict accurately the flow rates in structures with large windows as found in warm climates, (Cermak et al (1982)). In particular, this practice was found to appreciably overestimate the flow rates when roof vents were involved, (Vickery et al (1983)). This is further discussed in Chapter 10. This limitation was nevertheless acknowledged by the author.

ii) The flow rates cannot be obtained unless the flow path and the internal pressures are known, (except in the simplest cases). Hence, the above-mentioned predictions could be relevant at most when there is no flow branching, (such as a single room ventilated through identical openings located in two different faces of the envelope).

iii) The ventilation predictions from the pressure coefficient data are anticipated to be poor in the case of low wind speeds and fluctuating flows, (Chandra (1985)), which are expected in urban conditions.

Nevertheless, this does not discard the potential that roof vents could present in dense urban terrains by having the greatest pressure magnitudes. The author concluded on the need to develop design tools to predict internal ventilation rates for configurations using roof-level openings and guide-lines for their natural ventilation

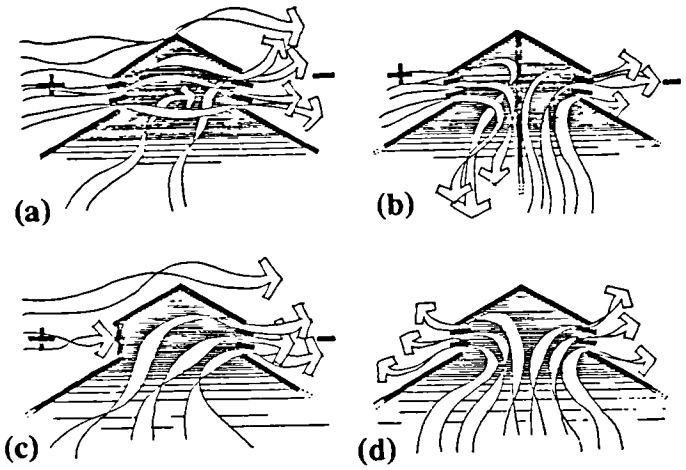

(a) Through-flow (induction effect)

(b) Diverted through-flow

(c) Suction effect

(d) Stack effect

Figure 4.24: The "Jack roof" under various ventilation operating modes, (After Bauman et al (1988)).

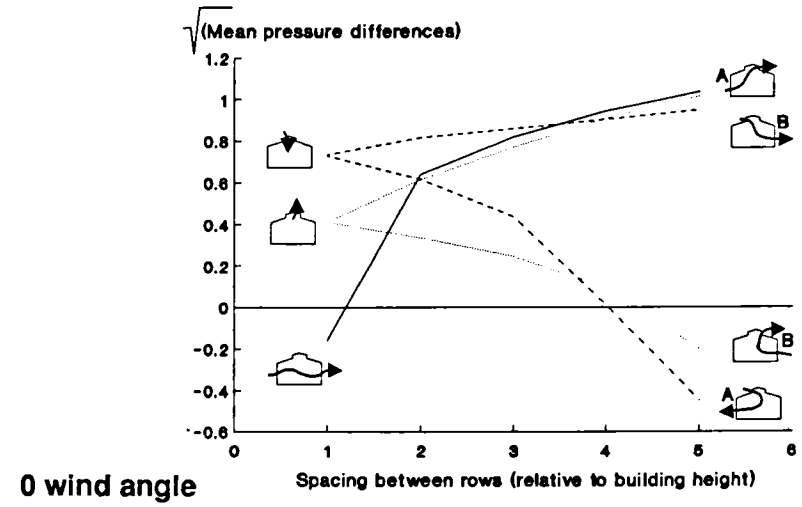

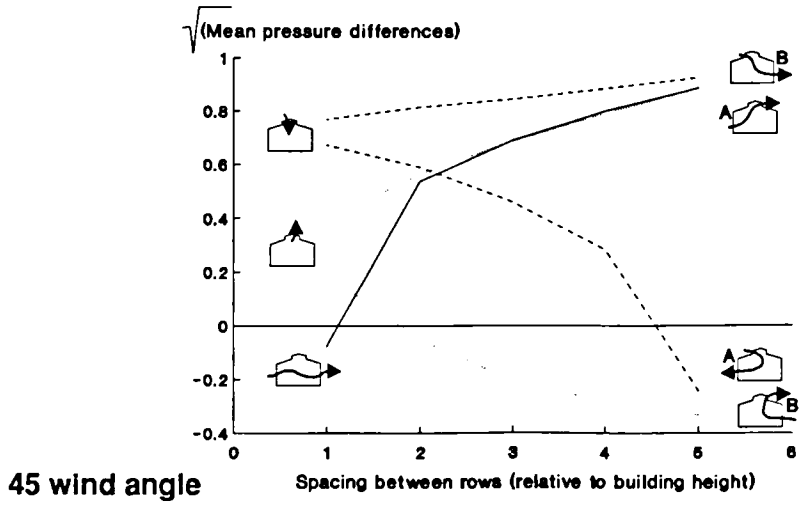

Figure 4.25: Ventilation performances of houses incorporating "Jack roofs" in an urban setting. Replot of Bauman 's data, (Bauman et al (1988)).

design.

4.4.2.5 Vickery's work

Vickery et al (1983) measured in small replica of low rise domestic structures actual airflow rates induced by roof vents. The principal aim of the study was to examine the accuracy of prediction methods based on the flow equations and the knowledge of pressure coefficients measured on sealed models.

The induction of indoor air movement by the roof vents is shown in Figure 4.26. It can be seen to be dependent on the relative porosity of the roof and the incidence of the wind.

For a roof aperture which had a total area smaller than that of the window, the internal flow induced by the roof suction were less than through two identical windows in opposite walls, and so, despite the fact that the deficit of pressure at the roof level was more than twice that of the leeward wall. Only when the roof vent surface was greater than the window area that the value of the roof vents became clear. In this case, the greatest benefit of the roof suction was obtained for an incident wind of 90°. This is because, in these instances, the pressure gradient between the lateral walls and the roof was much larger than between the two lateral walls, which probably had almost the same pressure.

The authors emphasised the poor level of agreement between the predicted and the measured values of the flow when the structures involved roof vents.

4.4.2.6 Atria

Most of the information related to the subject of wind-induced ventilation in atria are sketches of guessed air patterns. The sketches of Bowen (1984) reproduced in Figure 4.27, show an atrium inducing flows of air under two different modes; i) intercepting the air stream at the roof level, (positive pressure mode), as in ancient wind catchers, and, ii) extracting the air through the roof vents, (negative pressure mode).

Scientific studies of wind-driven natural ventilation in covered atria are almost non-existent. Three papers only were found which deal with the indoor air movement in these structures and are related to very specific projects.

Daniels (1983) reported the results of aerodynamic tests made on a large office building in Germany which incorporated a long glass covered passageway and winter gardens, in a study concerned primarily with the thermal performance of the building.

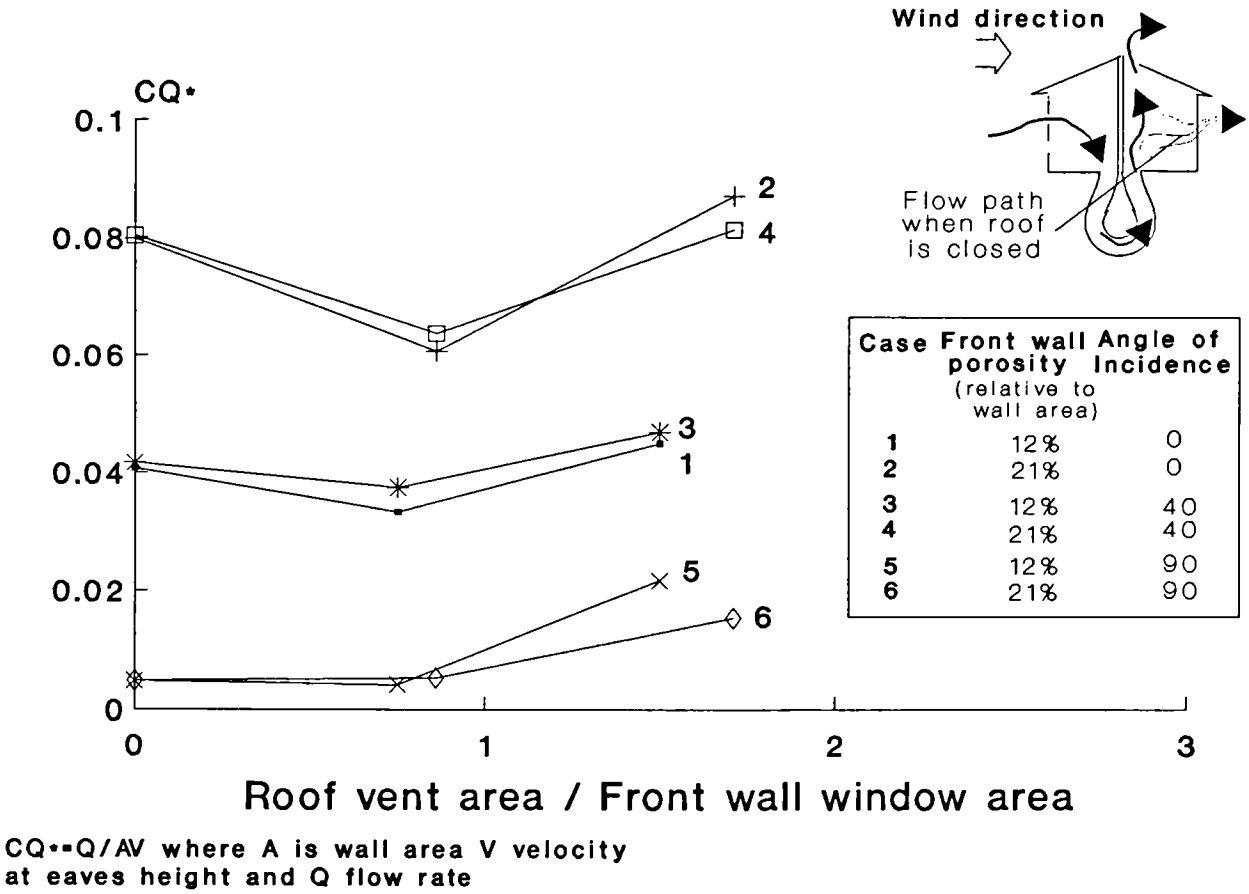

Figure 4.26: Relative indoor air velocities measured on small models incorporating roof vents. Replot of Vickery's data, (Vickery et al (1983)).

Smoke visualisation tests were made on a hollow model to examine the indoor flow patterns. The tests showed that there was an intense air current filling the whole inner passageway when the roof was opened at 30% of its surface, and that no location was left with no circulating air. Although it was concluded that the building could rely on natural cooling ventilation, even in summer time, no quantitative estimate could have been made from the wind tunnel model test.

Kobayashi and Ohba (1987) were interested in the wind effects on human comfort and on their implications on air conditioning system in two atria. They reported the results of full scale measurements of indoor temperatures, air change rates and inner velocity in a 37 storey city hotel incorporating a very large atria. The emphasis was put on the significant draft caused by the outside air flowing through the open entrance doors linked directly to the atrium.

They also undertook wind tunnel measurement on a test model of a 8 storey resort hotel which had a full height atria with a movable roof. It was observed that when the movable roof of the atrium was opened, the airflow rates and the velocities in the windward facade openings increased in comparison with the situation where the roof was close. At the same time, it was remarked that the air extracted at the leeward wall openings were reduced. It was inferred that these changes were caused by the roof vents acting as a suction device.

Qualitative and quantitative estimates of natural ventilation in a real atrium building have been published very recently, (see Trollope et al (1991)). The "Gateway Two" atrium building in U.K., have been praised in several publications as been a successful unconditioned atrium design, intended to rely on natural ventilation in summer season by stack effect, (see Hawkes (1983, 1984)). The monitoring of the building was made to check whether the building was performing as intended. Visualization tests involving helium filled neutrally buoyant balloons, and measurement of the air velocities were made for short period of time. Long term tests, (approximately two months), involving tracer gas measurements were also performed.

The tests allowed to observe that air movement was predominantly from the offices into the atrium. Some high air speeds were locally recorded. In particular, inward air speeds as high as 4 ms^{-1} were measured at the windward side of the building, (see Figure 4.28).

It was implied from the upward movement of air in the atrium that the major motive forces were the stack effects. Nevertheless, there was not enough evidence on which these assumptions could be based, (in particular they could not justify why the

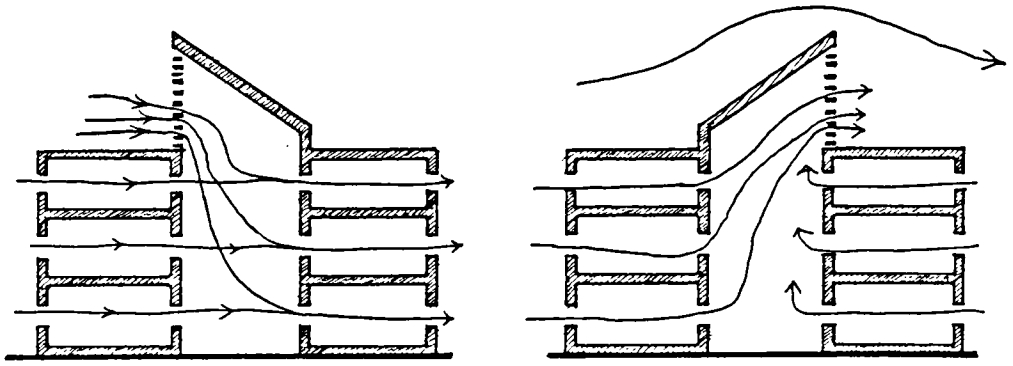

Atrium under positive pressure ventilation

Atrium under negative pressure ventilation

Figure 4.27: Suggested ventilative modes which can be used in atria, (After Bowen (1984)).

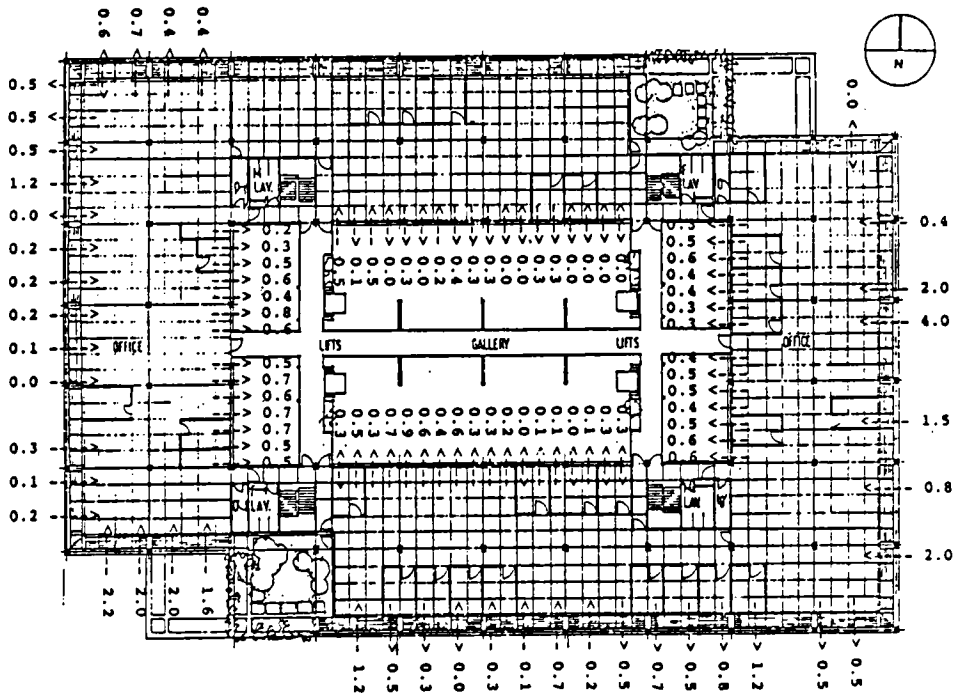

Figure 4.28: Full scale measurements of air speeds in an atrium building, (After Trollope et al (1991)).

highest indoor air velocities were recorded at the windward offices), and suction effects of the atrium may well be caused by wind pressures.

4.4.3 Summary of the studies on roof induced ventilation

It is very difficult to draw from such diversified designs and so specific examples of use of roof vents any general rules. Nevertheless it seems that the main influential parameters in the performances of these configurations are;

i) the relative area of the vents,
ii) the distribution of the openings on the envelope with respect to the wind pressure fields,
iii) the presence of neighbouring obstacles.

Depending on these parameters, roof vents can be used under different operative modes. They could be used as inlets, outlets or both.

The value of the roof level openings seems evident in the case of heavily built-up conditions, where the surrounding buildings are about the same size or lower than the test structure. The roof being less sheltered than the walls, it could be more effective in inducing the ventilation, either by suction or by positive pressure, than the windows alone. Also, in cases where windows cannot be located anywhere expect parallel to the wind, then it is more rewarding to use roof openings in conjunction with one window than two windows in opposite walls, and so, even if the building is unobstructed.

Nevertheless, except the last above-mentioned case, the benefit of the roof apertures in an isolated structure becomes less apparent than with sheltered walls.

As with ventilation through windows, the best arrangement of inlets and outlets on the building envelope is in pressure fields above and below the atmospheric pressures to allow cross-ventilation. If the roof vents are used as inlets, they may not be as effective as windows in an isolated building. This is because, in the first case, (e.g., in the case of traditional wind scoops), the air entering the space has to change direction several times, unlike with windows. On the other hand, in most of the works reviewed it appears that roof vents are best used as outlets, owing to the fact that the greatest suction is obtained at the roof surfaces.

The effectiveness of the roof vents however is dependent to a large degree on their sizes. Even if the deficit of pressure at the roof is much larger than that in the

leeward walls, greater induction of flow is guaranteed only if the roof vent area is large, (i.e., about the same surface or greater than the window's).

The air induction generated by suction or positive pressures from the roof could be partly lost by locating the roof vents in different pressure regions. In this case, the air entering the roof might leave through the vents located downwind and never contribute to the air motion in the space where it is needed. It seems thus an advantage to make the roof work in one mode only, (either suction or positive pressure), which can be realised by incorporating dampers or other designs working as diodes for the flow.

The literature review outlined the absence of studies on the wind-driven ventilation of atria and the lack of a parametric approach to the effects of the influential factors cited above. The techniques used to estimate indoor air flows where sometimes inadequate. Finally, almost all the above-mentioned studies performing wind tunnel tests where dealing with uni-cell examples. It is very difficult to extrapolate the findings to multi-cell cases, most common in reality.

4.5 Conclusions

This literature review of works related to flow in building clusters and courts allowed one to determine what are the most influential parameters in the ventilation of courtyards and which need to be tested. These are :

i) the courtyard geometry,
ii) the orientation to the wind,
iii) some architectural details such as protuberances at the roof levels and major openings into the courtyard.

It was decided that only the two first parameters would be considered in this study since there is an infinity of details which could feature in a courtyard building, and thus, it is unlikely that generalised rules may be drawn from few examples.

The review of structures using roof vents indicated that there could be different modes of inducting ventilation in buildings by means of roof pressure forces. Following the example of the ancient wind catchers, the atrium roof can be used as a wind deflector, as a suction device, or perform both simultaneously. The efficiency of driving air movement in any of these modes is not known and needs to be investigated.

It was shown that the wind climate in an urban site differs significantly from an

open site. The conditions for ventilation need thus to be considered in both types of terrain.

Finally, it was chosen to examine all these parameters in multistory courtyard and atrium buildings with moderate height, (i.e., four floors), which are probably the most representative of their category.

Chapter 5:

Methods used to assess natural ventilation in buildings

5.1 Introduction

In this chapter the available measuring techniques used in ventilation studies are reviewed with the intention of selecting the most appropriate one to investigate the factors which may influence the ventilation in multistory courtyard and atrium buildings.

From the conclusions drawn from the previous chapter, concerning the need for a systematic approach to the effect of courtyard geometry, the orientation to the wind, and the influence of different ventilation modes in atria, a set of requirements for the appropriate technique was defined:

i) ability to investigate several parameters and undertake systematic studies of the effect of the courtyard geometry and atrium roof geometry under different wind environments, (different terrain and incident winds),
ii) owing to the large programme of tests, the technique must offer relatively fast data acquisition,
iii) accuracy of the prediction of the internal flows,
iv) available at not a great cost.

Several publications offer detailed reviews of the main techniques used to study natural ventilation. In this chapter only the measuring techniques that meet most of the above-mentioned criteria are reviewed in detail, otherwise frequent references to other

works are made.

5.2 Techniques used for estimating natural ventilation

A critical appraisal of the conventional techniques used for the investigation of natural ventilation can be found in Hitchin and Wilson (1967), Bilsborrow (1972), and Pitts and Ward (1983).

The available measuring techniques are commonly divided into three categories:

i) full-scale measurements,
ii) analogue methods, (use of digital computer or electrical and hydraulic simulations),
iii) physical models in wind tunnels.

5.2.1 Full scale measurements

There are two main measuring techniques used in full scale:

i) pressurisation tests,
ii) tracer gas measurements.

5.2.1.1 The pressurisation test

Pressurisation tests are generally intended for infiltration and leakage measurements of buildings. The method consists of admitting or extracting a known volume of air to or from rooms or whole buildings with high enough rate to produce measurable pressure differentials. By recording the pressure differential for various rates of flow, a relationship between flow and pressure differences can be obtained which is characteristic of the room or the building and their air flow paths, (See Hopkins and Hanford (1974), Hunt (1978), Shaw et al (1973). Other references are found in Pitts and Ward (1983)).

5.2.1.2 The tracer gas technique

The tracer gas technique is probably the most widely used in full-scale investigations. The principle behind it is that, if a known amount of a gas with some easily identifiable properties is released in a space, then measurement of its dilution can

be used to determine the rate of air in or out of that space.

This technique has been reviewed in several publications, notably Hitchin and Wilson (1967), Sherman et al (1980), and Alexander et al (1980). The difficulties associated with the technique are briefly, the assessment of the time required for the tracer gas to mix with the air in the space, how well the air entering the space is mixed with the air already present, and/or what is the "effective volume" of the space that plays a part in the infiltration process.

5.2.1.3 Other techniques

Other full-scale techniques involves;

i) pressure measurements, mainly used in wind-loading studies, (see Eaton and Mayne (1969, 1974), Eaton et al (1976), Tamura and Wilson (1967)),
ii) velocity measurements, with the use of rotating anemometers in particular,
iii) flow visualisation.

Hitchin and Wilson (1967) and Ower and Pankhurst (1977) described a wide variety of anemometers that can be used in full scale.

5.2.1.4 Discussion

Although the full-scale measurements deliver realistic results, and are the ultimate reference data for the validation of other techniques, they have numerous practical limitations. The main set-backs are that;

i) they are affected by the variability of the weather to which the observer has no control,
ii) meaningful parametric studies are not possible since, the orientation, the geometry and the surroundings of an existing building are generally fixed and can hardly be altered[1],
iii) the techniques are expensive and time consuming.

For the parametric study which was planned, it was evident that full-scale

[1] There are nevertheless studies where the geometry of the building was altered, for example, in the work of Eaton et al (1976) the pitch of a test house was varied.

methods were inadequate.

5.2.2 Analogue models of air movement

5.2.2.1 Water analogues

Water analogues are, in general, more useful for instructive information of general effects and flow patterns than to obtain quantitative estimates for flow parameters.

Nevertheless, the water analogue allows with relative ease the simulation of very complex situations, for example when buoyancy is involved. Rydberg, as reported by Hitchin and Wilson (1967), for instance, modelled the flow behaviour in the case of openable windows where there was a temperature gradient. He used brine as a fluid and by changing the concentration of salt he simulated air densities. A recent application of this principle for the simulation of buoyancy forces in buildings can be found in Linden and Lane-Serff (1989).

Owing to the kinematic viscosity of water, higher Reynolds Number are attainable than with air motion, (of the order of 10 times for the same velocity). Another attractive feature of the technique is its ease to handle visual tests and concentration measurements. However, there are serious difficulties in measuring velocities in water, (Plate (1982)). Water channels are also expensive to build and to maintain.

5.2.2.2 Electrical analogues

Such technique have been developed from the analogy that exists between the equation of the flow of air and that of electrical current, (Kirchoff's laws developed in electrical theory can apply for fluids). The discharge equation of air, equation (3.18), is similar to:

$$U = K \times I^{z} \qquad (5.1)$$

Where U is the voltage, K the resistance (constant), I, the current flow and z the current exponent (constant). The appropriate characteristics of the flow have been successfully reproduced using tungsten lamps, (Scott (1961)).

Although the technique gave good results for the estimate of flow in ducts and pipes, the simulation of natural ventilation is much more difficult, especially if the

system comprises interconnected rooms and corridors, when large openings are involved, and/or when there are low airspeeds. The method is also costly.

Examples of use of the method for predicting flows in pipes and ducts can be found in Scott (1961). Comparative estimates obtained from analytical methods and an electrical analogue applied to infiltration prediction in medium to high-rise buildings can be found in Jackman (1970). No examples of such method applied to ventilation through large openings were found.

5.2.2.3 Mathematical models and digital computer analogues

Indoor flow rates in buildings can be calculated from the equations of flow through openings under appropriate flow regimes and from the continuity equation, (see Sections 3.6.2 and 10.2).

These equations generally show a non-linear relationship between flow rates and pressure differences, thus with numerous flows out and in a space, a complex set of simultaneous non-linear equations must be created and solved. The usual method is to use some form of iterative methods in which the flows are balanced so that the net air flow into the building is equal to that leaving it. This is achieved by varying the absolute pressure in each space of the complex being considered.

Descriptions of computation methods and mathematical models of the airflow can be found for ventilation through large openings in Vickery (1981), Vickery et al (1983, 1987) and infiltration models in Liddament and Thompson (1982), Walton (1984, 1989), Etheridge and Alexander (1980) and Bilsborrow (1973). Other sources of references can be found in Hitchin and Wilson (1967), Pitts and Ward (1983), Allard and Herrlin (1989) and ASHRAE Handbook of Fundamentals (1989b). In Chapter 10, the flow equations and the algorithm of the computation used by Vickery et al (1983, 1987) are described.

The main advantages of the method are the great freedom to carry out systematic studies and the ability to combine wind pressure forces with stack forces in the computation of the ventilation rates. The fast acquisition of the results and the relatively low cost involved make this technique one of the most attractive and the most promising.

In general, the computation of the flows requires beforehand information describing the airflow characteristics. Essential data, such as, the wind pressure distribution and the characteristics of the openings are generally obtained from wind

tunnel model tests. However, some efforts, although still small, are currently made to estimate wind pressures without having to resort to wind tunnels, (see Shaw (1980), Allen (1984), Swami and Chandra (1988), and Kula and Feustel (1988), for example).

The accuracy of digital computer analogues is limited by the accuracy with which air movement can be described by mathematical equations. For airflow through large open windows, (which is of particular interest for the present study), some limitations in the assumptions made in the computation of the flows were pointed out by Vickery et al (1983). The common method to obtain wind pressure data from solid models could lead to substantial errors when the openings represent a large portion of the walls. This is because the flow though the apertures can disturb the pressure field that is measured on solid surfaces and from which the flow rates are derived. In particular, this effect may be very large in the case of roof vents, even of very small surfaces.

The other difficulty is to determine the appropriate discharge characteristics of the openings under consideration. Bilsborrow (1973) and Vickery et al (1983) pointed out that the effective discharge characteristics of the openings are dependent on the air velocities in the vicinities of the apertures, and not only on the geometry as it is generally assumed in the calculation. Allowance for these effects are still not well established. This is further discussed in Chapter 10. Another limitation of the mathematical model is often the small allowance for turbulence-driven ventilation[2] and pulsating flows which may be significant in the case of weak flows.

The foregoing suggestions, that the ventilation prediction could be substantially in error when roof vents are used, was a deterrent to building the conclusions on the effectiveness of ventilation in atria.

However, because of its numerous advantages, the method is very attractive and large efforts are being made to refine the modelling of flows and to create a data-base of pressure coefficients, (see the work of the Air Infiltration Centre, (Allen (1984)). Hence, it was decided to examine its accuracy in predicting internal flows in atrium configurations by comparing the predicted values of flows with values obtained with other means. This is discussed in Chapter 10.

---

[2] The fluctuations are sometimes modelled assuming a Gaussian distribution about the mean value, (Etheridge and Alexander (1980)).

5.2.3 Physical models in wind tunnels

> "...the lower part of the atmospheric boundary layer presents an exact analogue of the lower part of the wind tunnel boundary layer..." (Plate (1982) p. 578).

It is therefore possible to produce a replica of the atmospheric boundary layer and of the site in a wind tunnel to study the wind climate and natural ventilation of buildings.

The advantages of the method are numerous:

i) Contrary to the full scale methods, the wind tunnel techniques allow the geometry of the models to be altered easily and also to change or control better the wind orientation and other environmental parameters.

ii) The tests are independent of the vagaries of the weather. They can be repeated for a given condition which enables different designs to be compared under the same conditions.

iii) The technique, which is suitable for systematic studies is well established now, and is undoubtedly the most popular in wind engineering. Examples of studies comparing full-scale with wind tunnel measurements, and where both were in agreement, can be found in Tieleman et al (1980) and Holdo (1982).

The wind tunnel analogue fulfilled the requirements that have been established for the present study and was thus chosen. Yet, some limitations exist also, which concern the difficulties to reproduce all the aspects of the natural wind and to achieve the dynamic similarities with the full scale. This, however, must not be a deterrent because certain degrees of compromise are possible without causing significant departures in the ventilation estimates from the full-scale.

In the following sections the wind tunnel analogue is described in more detail. The modelling criteria are reviewed extensively to provide a background for the discussion on the modelling philosophy adopted in the experimental tests. Among the ventilation measuring techniques used in wind tunnels, the most adequate for the present study is selected.

5.3 The wind tunnel analogue and techniques

5.3.1 Introduction to wind tunnels

Evolution of the wind tunnel

A history of the development of wind tunnels and wind tunnel techniques can be found in several publications, such as Lawson (1980), Aynsley et al (1977) and Surry and Isyumov (1975).

Wind tunnels were developed in the early days of aeronautics. Over the years the wind tunnels became more sophisticated and were intended to investigate, almost exclusively, aeronautic problems. They were designed to offer more and more smoother air streams. When wind loads were first considered, a few investigations were conducted in the aeronautic wind tunnels, and the results were found to agree poorly with the full scale results available. It soon became evident that the reason for the discrepancies was the lack of adequate simulation of the turbulent shear flow in the model studies, as was recognised in a number of studies in the early 1930's, such as Bailey (1933). However it was not until 1958 that Jensen (1958) introduced the model law which formally state the need to model wind shear in order to obtain realistic estimates of pressure coefficients. Franck (1963) made it clear that the only way to produce an equilibrium boundary layer was to use ground roughness on the wind tunnel. Davenport and Isyumov (1967) were among the pioneers of the boundary layer wind tunnel.

The next step in the history of wind tunnel development was to reduce the excessive length of the wind tunnel roughness by artificially accelerating the growth of the boundary layer. Counihan (1969) pioneered the techniques for accelerated flow growth with the use of turbulence generators and a step upwind of the roughness elements. Several attempts were made to artificially accelerate the growth of the wind tunnel boundary layer. They are described in Lawson (1980)).

Types of wind tunnels

The wind tunnels used nowadays are conventionally divided into two classes- the *low-speed* and the *high-speed* tunnels. In the low-speed tunnels the predominant parameters are inertia and viscosity and the influence of compressibility is negligible.

The high speed tunnels, on the other hand, are intended for the investigation of flows in which the forces due to inertia and compressibility are of major importance, (Pankhurst and Holder (1952)). For architectural aerodynamic studies, low-speed wind tunnels are used.

Among the low-speed wind tunnels, it can be distinguished between the *straight-through* or *open-return* type and the *closed-return* or *return* type wind tunnels. The first resemble an open duct whilst the second is a continuous duct. The other difference that separates wind tunnels is the characteristics of the working section. The *closed working* section is bounded by solid walls and the *open working* section has no wall. The closed working section is preferred for most industrial applications.

Simulation of the natural wind in wind tunnels

The currently accepted methods to simulate the atmospheric boundary layer can be separated into two major categories, (see Plate (1982));

i) The first is to model the natural wind with a turbulent boundary layer grown naturally over a long fetch of appropriate tunnel floor roughness. The method has the advantage that the flow remains in equilibrium[3] over a large portion of the working section. This is particularly suited for "far-field modelling", such as model diffusion studies. This approach lends also greater confidence in the duplication of the flow over a terrain owing to the fundamental dependence of the properties of the flow field on the terrain roughness. One such tunnel is the Colorado State University with a 25 m working section, (Plate and Cermak (1963)).

ii) The second approach for simulating atmospheric flows uses various active and passive devices at the entrance of the test section to artificially create thick turbulent shear flows, and remove thus the need for a long working section. The passive devices in use are varied and could be solid rods, screens, combinations of trips and spires, or vortex generators. The active devices could be counterflowing jets among others, (see Surry and Isyumov (1975), and Plate (1982)). Unlike the other wind tunnel type, the wind tunnels using artificial methods for boundary layer growth are not suitable for generating wind over

[3] The local surface shear stress, the mean velocity profiles and the turbulence intensities and scales remain invariant.

complex terrains for which there are no full scale data. They are also restricted for "near-field modelling", (Plate (1982)).

Ventilation model tests in outdoor natural wind

The use of models to estimate the natural ventilation almost always prerequisites the need of a wind tunnel to generate the flow of air. Chandra et al (1983), however, suggested a new low cost alternative to wind tunnel testing, by studying scale model outdoors in the natural wind. The method has been validated against full-scale measurements of the prototype and scale model measurements in a wind tunnel.

The model used is shown in Figure 5.1 and was built at a scale of 1/25 of the prototype. Most of measurements on the model outdoors were taken under cloudy conditions or at evening and night in a nearly neutral atmosphere where little temperature gradient existed. It was found that the agreement between full scale and model scale tested outdoors was excellent. On the other hand, the wind tunnel values did not agree so well, particularly in turbulence-driven ventilation. The discrepancies between the wind tunnel and the full scale were suggested to be due to Reynolds Number independence in the wind tunnel and also to the wind direction fluctuations in reality, whereas in the wind tunnel the direction of the oncoming wind was fixed.

With this technique, there is no simulation of the ground plane. This, thus, limits the method to low-rise buildings for which the velocity gradient is not important. In the configuration tested the model essentially encounters a uniform speed with a turbulent approach flow.

An earlier example of a model tested in outdoor natural wind was made by Torrance (1972) on a half-scale model of a courtyard building, (see Figure 5.2).

Owing to the uniqueness of the study of Chandra et al (1983), there is not enough evidence on the accuracy of the method. The technique is not adequate for medium to high rise building models. Moreover, the method is still subject to the vagaries of the weather.

5.3.2 Modelling requirements

The simulation requirements in the wind tunnel comprise:

i) the modelling criteria related to the atmospheric boundary layer,
ii) the modelling requirements related to the model and its surroundings.

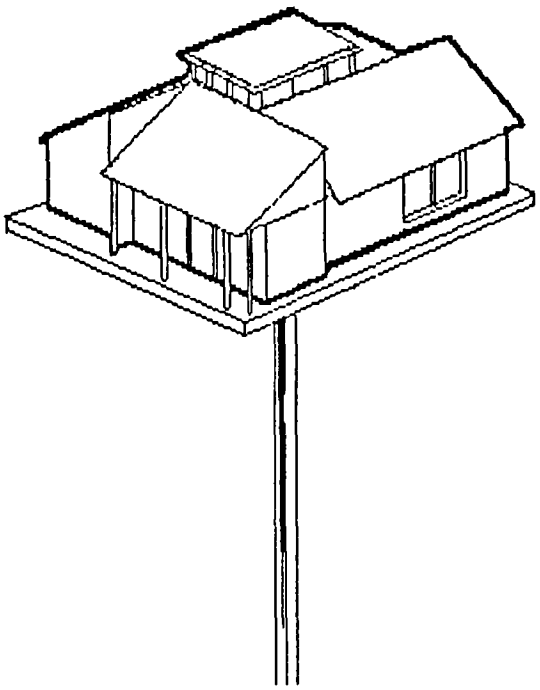

Figure 5.1: Building model tested outdoors in the natural wind for ventilation evaluation, (Chandra et al (1983)).

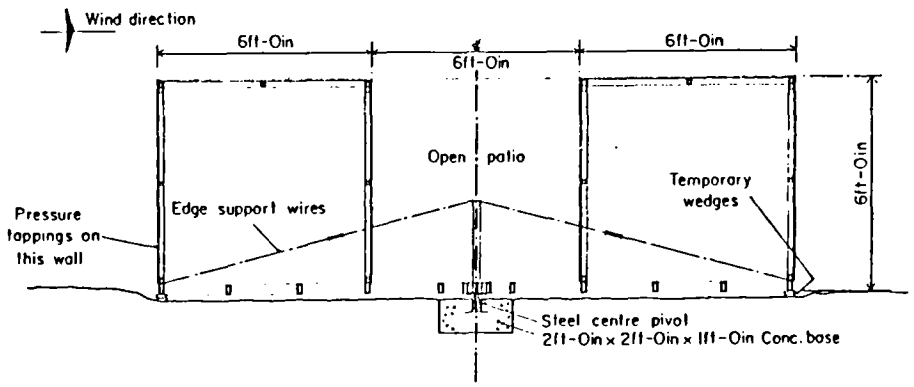

Figure 5.2: Half -full -scale model tested outdoors, (After Torrance (1972)).

5.3.2.1 Modelling requirements for the atmospheric boundary layer

All the characteristics of the atmospheric boundary layer (ABL) described in Section 3.5 are impossible to reproduce in currently available wind tunnels. Nevertheless, the modelling of the ABL is, in most studies feasible, because it is often sufficient to reproduce only the main features of the ABL conditions. Wind loading studies, for example, are concerned with the neutrally stratified boundary layer (BL), and it is sufficient to duplicate the wind profile and turbulence levels. For air pollution and diffusion investigations, the stratified BL has to be reproduced and, although complex, the modelling is also feasible. Ventilation studies generally assume a neutral BL, (see Section 3.5.1).

The requirements for exact similarity and the degree to which some of them can be relaxed for wind tunnel modelling are discussed in Cermak (1971,1974, 1979), Plate (1982), and summarized in Cermak et al (1982) and Allen (1984). These are, in brief, the equality of a series of dimensionless numbers, the modelling of the surface boundary conditions and the reproduction of the approach flow characteristics.

5.3.2.2 Equality of non-dimensional numbers

The non-dimensional numbers, derived from the statement of the conservation of mass, momentum and energy are mainly,

i) the *Rossby number*, describing the Coriolis forces which affect the velocity vector with height,
ii) the *Reynolds Number*, which is the ratio of the inertia forces to the viscous forces and,
ii) the *Richardson number* or *Froude number* used as a measure of the stability of the atmosphere and the state of turbulence.

The effects of the Earth's rotation is very difficult to reproduce. Fortunately, they are believed to be negligible at the building level. Equal Reynolds Numbers generally cannot be obtained. This is not a limiting condition for wind tunnel modelling since the significant flow characteristics are weakly dependent upon the Reynolds Numbers. This is because the flow becomes aerodynamically rough with only Reynolds Numbers $U_* z_0 / \nu > 5$, where U_* is the friction velocity, z_0 the roughness height and ν the kinematic viscosity of the air, (see Plate (1982)). Finally, the Richardson number is a relevant parameter in BL conditions other than the neutrally stratified BL. It is possible

to obtain equal Richardson numbers and the modelling of weak wind BL is feasible, (see Cermak (1974)). However, such modelling requires either a water tunnel with density stratification facilities or a wind tunnel where the temperature of the boundary layer of the test section can be controlled. Because of the complexity and the cost involved, such modelling is generally restricted to air pollution problems which are often critical in stratified BL. The following discussion is restricted to the modelling of the neutral ABL, (i.e., where there is no thermal stratification), which is the one generally considered in ventilation studies, (see Section 3.5.1).

5.3.2.3 Similarities of the surface boundary conditions and the approaching flow

For neutral ABL, the modelling criteria for the approaching flow is mainly, the duplication of the **mean velocity profile** and the **turbulence intensity** and **scale**. Jensen (1958) showed that the primary condition required to reproduce the characteristics of this ABL is to preserve the ratio H/z_0 in the model and the prototype, where H is a representative building height and z_0 the roughness length, (see Figure 5.3). This condition is sufficient to simulate the mean and turbulent flow of the inner layer, i.e., approximately the lowest 10% of the ABL, (Plate (1982) and Cook (1972 and 1973)). To simulate the entire BL, the ratio H/δ must also be preserved, where δ is the thickness of the ABL.

Fortunately, it is not necessary to model the entire height of the ABL, at least in most wind loading and ventilation studies. Indeed, Cook (1972, 1973) introduced the idea that it is only necessary to simulate part of the atmospheric boundary layer. Nowadays this approach is almost universally followed. The major advantage is that it allows the linear scale of a model to be increased independently of the scale of the flow when the height of the wind tunnel working section is limited.

The aforementioned remarks concerning the need to model H/z_0 are only applicable if H/z_0 is large. However, this condition is not sufficient when the model height H is comparable with that of other obstructions nearby, such as in a city-like terrain. In these conditions the flow field is dependent on the actual size and disposition of the obstacles nearby rather than the general measure of their size given by the roughness length z_0. This aspect will be further discussed in Chapter 9, where ventilation conditions of courtyards and atria in congested urban sites will be examined.

The need to correctly model turbulences with both their scale and intensity is evident when the gusty nature of the natural wind is important as in the case of wind-

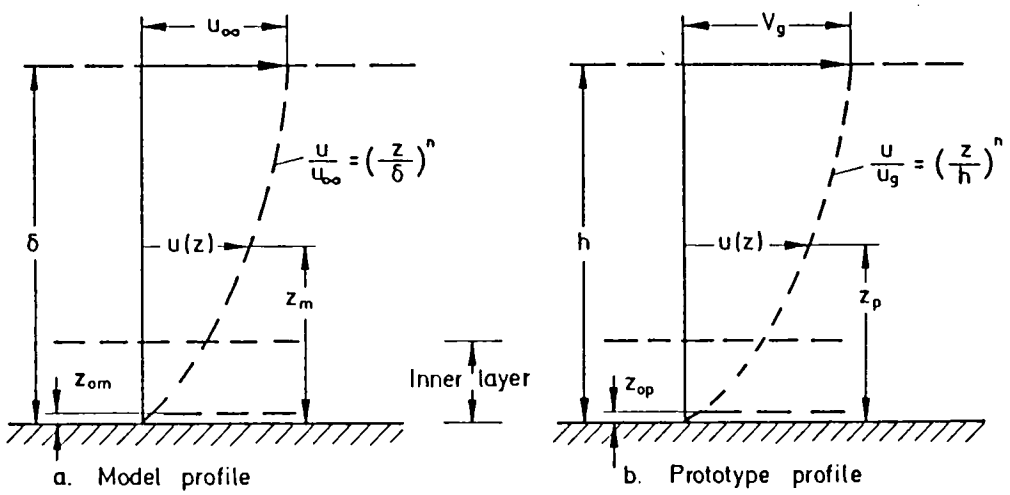

Mean velocity profiles in model and prototype definitions

Figure 5.3: Mean velocity profiles in model (m) and prototype (p). δ *and* h *are the boundary layer thicknesses,* Z_o *is the roughness length,* (After Plate (1982)).

loading studies. In ventilation studies, the main concern is the time averaged flow and correct modelling of the turbulence may not be of significant importance, (Vickery (1981)).

5.3.2.4 Modelling requirements for buildings

A number of scaling recommendations and comments on dynamic similarities can be found in Aynsley (1985b), and are reviewed here under different headings.

As with the modelling considerations of the ABL, the thermal effects in buildings will be disregarded. It was already discussed that during the summer season buoyancy forces are significant only under very weak wind conditions, (see Section 3.4.1). It is also rarely possible to scale thermal effects accurately because different processes obey different scaling laws, (Hitchin and Wilson (1967)). A discussion of the scaling laws involved in the modelling of the combination of wind and thermally induced ventilation in a chemical plant is given in Poreh and Hassid (1982). The authors outlined the limitations of the modelling, particularly the scaling of the temperature rise near the walls and near the heat sources which were impossible to duplicate. Other references on the subject can be found in Hitchin and Wilson (1967).

Wind tunnel blockage

This parameter express the constraint that the boundaries of the wind tunnel may apply upon the flow passing over and around a model, whilst no equivalent constraint exists in the atmosphere. Some corrections must be made to take into account this effect unless the cross sectional area of the model is kept relatively small compared to the working section of the wind tunnel.

The maximum acceptable limit of wind tunnel blockage, (i.e., the cross sectional area ratio), for which no correction is required, is not a definite value. Most workers recommend values less than 3%, although a value of 10% has been suggested to be an acceptable limit, (see Lawson (1980)).

When the blockage in the wind tunnel is above the recommended limits, corrections must be applied to the quantities measured. A review of the blockage corrections relevant to wind engineering studies is found in Melbourne (1982). The writer stressed on the complex interactions that exist between turbulence levels and blockage effects. Because of the turbulence sensitivity of this parameter, the relevant correction coefficients must be determined for each experimental test, for the particular

model and for the specific flow and wind tunnel under consideration.

Scaling considerations

Linear scale

The linear scale of the models are generally determined by the **extent of their blockage**, and by the **lengths scale** related to, both, the mean velocity and turbulence characteristic of the flows. These considerations work against the need to reproduce accurately the architectural details that could influence the surface flow around buildings, (e.g., sun shades, screens).

There are also scaling constraints for the model to match that of the simulated flow. However, this requirement is often relaxed -in particular it is common to reproduce only the lowest part of the ABL enveloping the building model, (see Section 5.3.2.3). Other scaling parameters of the flow concern the scale of turbulence, (see Cook (1973, 1976 and 1978). Here also a mismatch of the scales is often permitted, in ventilation studies at least, in favour of other criteria such as Reynolds Number independence. The reason is that it is not clearly established how they affect the flow patterns. Chandra et al (1983) give a very good example in which a significant mismatch of the model and full-scale parameters of the flow did not lead to inaccurate results. In an innovative ventilation measurement technique a small scale model was tested outdoor in the natural wind (see Section 5.3.1). In this case the agreement of the ventilation measurement with the full scale was found to be excellent.

Velocity scale

The velocity scale can be arbitrary chosen, provided that satisfactory Reynolds Number flows are achieved.

Time scale

The time scale is obtained once these two scales are chosen, and is expressed as follows,

$$\frac{L_m}{L_p} \times \frac{V_p}{V_m} = \frac{T_m}{T_p} \qquad (5.2)$$

where L represents the length, V the speed and where the suffixes m and p refer respectively to the model and the prototype, (see Lawson (1980)).

The time scale is mostly relevant in structural studies where the building is likely to react to gusts of high frequencies.

Reynolds Number considerations

The Reynolds Number Re is the only significant non-dimensional parameter required for dynamic simulations when neglecting internal buoyancy. It is the ratio of the inertia forces, (i.e., mass×acceleration), to the viscous forces and is expressed as follows,

$$Re = \frac{V \times d}{\nu} \qquad (5.3)$$

where V and d are, respectively, representative speed and length appropriate to the situation, and ν the kinematic viscosity.

It is practically impossible to match the Reynolds Number of the prototype ($Re \simeq 10^6$) with the model. Indeed, as ν is generally constant in the model and the full scale, the only means to maintain the same Reynolds Number is to increase the speed by a factor of, say 100, equal to the inverse of the model scale. Fortunately, much lower Reynolds Numbers are often adequate for dynamic similarity of bluff bodies, (i.e., with sharp edges), provided the flow is turbulent. The reason is that, once this flow regime is reached, the flow pattern and the various non-dimensional flow parameters are not altered by further increase in Reynolds Number. Hence, Re can be relaxed up to the minimum value associated with this flow regime.

For different regions of the model flow, (e.g., internal flow, external flow, flow through openings), different values of Re must be considered, (Cermak et al (1981, 1982)).

Smith (1951) was the first to give a Reynolds Number magnitude at which the flow around a model becomes invariant. In a wind tunnel investigation he observed how the flow pattern around models varied with the alteration of the model sizes and the wind speed, thus, Reynolds Number. In particular, he used the reattachment positions of the separated flow on the wake of the model as a criterion for similarity and the following parameter E instead of the Reynolds Number.

$$E = \frac{2 \times A \times V}{P} \qquad (5.4)$$

where A is the cross section area of the model, P its perimeter and V a reference wind speed.

The results showed that below a value of E equal to 0.26 m^2s^{-1}, the reattachment position is very variable, whilst at higher values, it is fairly constant and consistent with some observations at full scale where E was 16 m^2s^{-1}. These results must, however, be taken as an order of magnitude at which Reynolds Number independence of external flow is achieved, since the sample of model sizes was limited, and the conditions of flow was that of a smooth uniform flow. The value of Reynolds Number equal to 2×10^4 has been suggested as the lower limit for flow modelling around models, (Cermak et al (1982)).

A study of Reynolds Number independence for internal flow has been reported by Cermak et al (1981, 1982). The internal to external velocity ratios and the internal turbulence intensities were measured at different locations in a low rise building model and were used as criteria for Reynolds Number independence. Several internal configurations were tested for a range of wind speeds in a wind tunnel.

The main findings were that the flow of air discharging through a small window into a room in the form of a jet became fully turbulent when ,

$$Re_w = \frac{V_w \times d_w}{\nu} \geq 300 \qquad (5.5)$$

Where V_w is the velocity at the window, d_w the dimension of the window and Re_w is the associated Reynolds Number.

For the internal flow modelling, the author suggested the use of a Reynolds Number, Re_r, based on the maximum velocity of the room, which is generally the velocity at the window, V_w, and the smallest dimension of the room L. He suggested that values higher than $Re_r = 2 \times 10^4$ must be obtained for the flow to be turbulent.

$$Re_r = \frac{V_w \times L}{\nu} \geq 2 \times 10^4 \qquad (5.6)$$

5.3.3 Measuring techniques in wind tunnels

In the following paragraphs the main techniques used to assess ventilation are reviewed in the intention to choose the most adequate for the present study. The main techniques used in wind tunnels could be grouped into,

i) pressure measurements,
ii) velocity measurements,
iii) concentration measurements,
iv) flow visualization techniques,
v) flow rate measurement techniques.

5.3.3.1 Pressure measurements

Pressures measured on solid models

This method deduces the ventilation rates from the knowledge of the pressure distribution measured on a solid model, the opening characteristics and the internal flow resistances. Mean flow rates and average air velocities are calculated using the appropriate equations of discharge through openings, (see Section 3.6.2.1).

When the internal path of the flow is simple, from an inlet to an outlet with no internal branching, the flow can be calculated with a manual method, otherwise, under conditions of internal branching of the flow, the estimate of the volumetric flow rates involves the iterative solutions of simultaneous non-linear equations and requires the use of a computer, (see Section 3.6.2, 5.2.2.3 and Chapter 10). In this case the method is equivalent to that reviewed under the heading of digital analogue.

This ventilation prediction method has many advantages, including,

i) the simplicity of acquisition of the pressure data from the models,
ii) the possibility to evaluate the ventilative potential of various flow networks and internal partitioning from one set of data,
iii) there are important collections of data available, gathered also from wind loading studies. This can provide a basis for comparison between different works.

However, the drawbacks are the same as those cited for the digital analogue, (see

Section 5.2.2.3), in that,

i) the mathematical expressions of the flow can be inaccurate in some circumstances,
ii) the method is not applicable when the aperture sizes are relatively large (above 20%), and when the path cannot be clearly predicted, (Cermak et al (1982)),
iii) Estimates of mean internal wind speeds are restricted to locations in the jet close to openings,
iv) Cermak et al (1982) point out the deficiency of the method to predict accurately the flow when inlets and outlets are located in the same wall.

As already mentioned in the discussion on the digital analogue, the pressure distribution measured on solid models may be different from the real case where large windows are open. This can lead to substantial overprediction of the flow. This effect may be particularly significant when roof vents are involved, (see Vickery et al (1983)).

For these reasons this method was judged inadequate for the estimate of internal flows in atria. Nevertheless, the surface pressure technique was suitable to provide information on the pressure field on model surfaces. This method will be used in particular to locate the roof vents of atrium models at particular regions of the external flow, (see Chapter 8). Surface flow visualization techniques are sometimes used for this purpose but do not convey quantitative information.

Pressures measured on hollow models

In order to circumvent the problem of the surface pressure field measured on a solid model being different to that in presence of apertures, the external pressures can be measured on hollow models. The internal pressures can also be monitored instead of being predicted from calculation methods.

However, there are serious difficulties in determining the effective pressure differences responsible for the flow through openings in a model. At the windward face in particular, the pressures vary substantially around the openings and depend on the degree to which the kinetic energy of the oncoming flow is converted into static pressure by the obstruction of the model walls. Aynsley (1976) suggested that a suitable reference of static pressure for the windward openings could be the region of stagnation

usually identified around an opening. For the leeward openings, however, this is not critical because of the uniformity of the pressure field that exist in general.

The location of the pressure difference measurement points must also coincide with that for which the discharge coefficients for building openings were determined, (see Aynsley (1976)). This constrains one to determine in a calibration arrangement the relevant discharge characteristics of the model openings for the particular pressure tapping locations.

Other difficulties are introduced by the significant changes in velocity that occur very close to the perimeter of the openings, making precise measurements difficult with pressure taps. Also, the method may probably be inaccurate due to the additional complexities introduced by pulsations in the flow and turbulence of the wind.

Despite its drawbacks and possible inaccuracies, the technique has been applied in a few works, such as Bilsborrow (1973). He estimated the flow rates through crack-like openings, in which case most of the above-mentioned difficulties were attenuated. An example of use of the method in the case of large openings is provided by Gadi (1987), (see Figure 5.4).

5.3.3.2 Velocity measurements

This technique is probably the most popular among the researchers investigating ventilation through large openings, (see for example Givoni (1968), Chand (1972), Van Straaten (1967), and Aynsley et al (1977)). In particular, this method is ideally suited to study airflow through and around buildings of complex or unusual shapes, when a pressure coefficient approach of such a building would require extensive and detailed measurements, (see Figure 5.5).

A wide range of measuring apparatus are available to measure air velocity in models. Most are listed in Ower and Pankhurst (1977), Hayward (1979), and Clayton (1971) among others.

The thermal anemometers

Thermal anemometers, of which the hot wire anemometers is the most popular, work on the principle that the electric resistance of a piece of wire varies with its temperature. When wind blows over the wire, its temperature, and therefore its resistance, changes. This can be measured and related to the air velocity.

The hot wire is probably the most used because it causes minimum blockage.

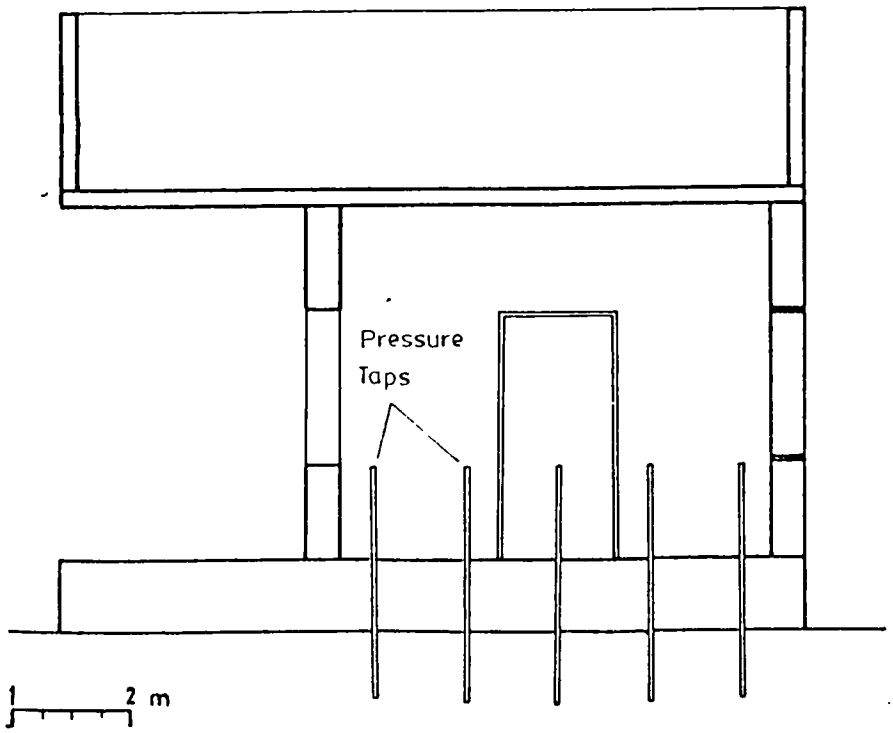

Figure 5.4: An example of pressure measurements on hollow models, (After Gadi (1987)).

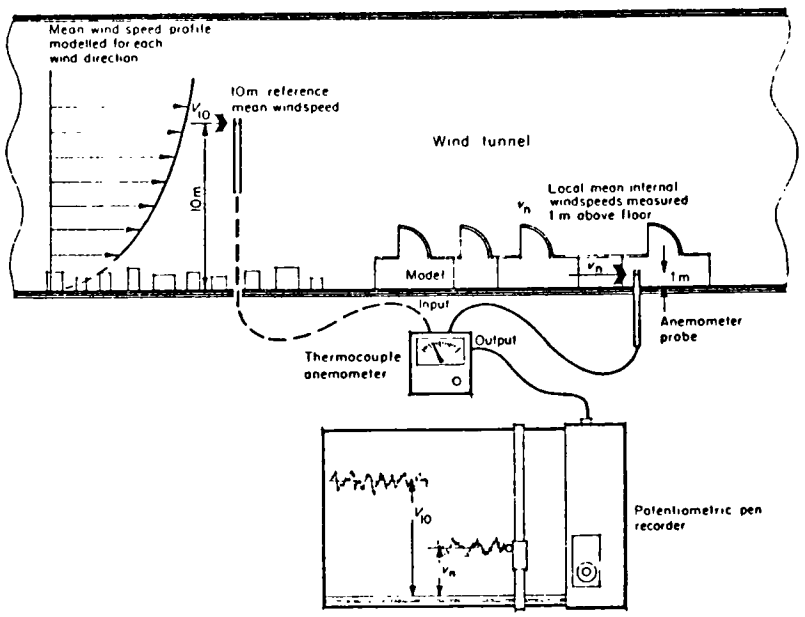

Figure 5.5: An example of use of a hot -wire anemometer for velocity measurements inside wind tunnel models, (After Aynsley et al (1977)).

However, single hot wires respond only to the velocity normal to the wire, and thus, it is necessary to find first the mean flow direction at each point. This could be overcome in ventilation studies with the use of omnidirectional probes such as a heated sphere anemometer or multiple wire anemometers.

The hot wire anemometers are fragile and require frequent calibration.

Rotating anemometers

This class of anemometer includes the vane anemometers and the cup anemometers. They are seldom used in wind tunnel investigations because of their large sizes and are more intended for full-scale measurements. They are prone to errors when there are variations in the flow direction. Aynsley et al (1977) provide an example of use, (see Figure 5.6).

Pitot static tubes

In the measurement of wind speeds around a model, small total pressure tubes are sometimes used. Nevertheless, their low sensitivity greatly restricts their use. As with single hot wire anemometers, Pitot tubes are highly directional. They also present a large obstruction to the flow and corrections for turbulences may have to be applied.

Drag anemometers

These anemometers measure the deflection of a freely hanging plate which can be related to the wind velocity. The range of air speeds which can be measured by these anemometers is often very restricted. These devices are mostly suited for turbulence measurements.

Pros and cons of the velocity measurement technique

The main advantage of the method involving velocity measurements is its ability to give a precise estimate of the natural ventilation or of the local wind climate for any point in or around the model. It is also simple to use and only a reference wind speed and internal mean velocities are required. Cermak et al (1982) gave the most favourable comments for the velocity measurement method with the use of hot-wire anemometers when compared to the pressure measurement technique or the concentration measurement technique applied onto model ventilation studies.

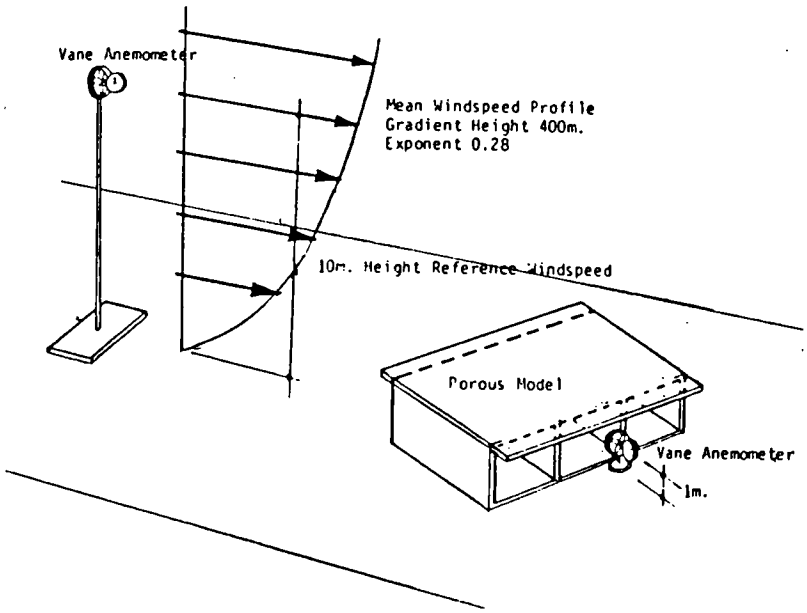

Figure 5.6: An example of use of a vane anemometer in ventilation models, (After Aynsley (1976)).

Nevertheless, there are also a certain number of drawbacks which include,

i) a great care is required to reproduce accurately the prototype and particularly its apertures,
ii) the anemometer may cause significant blockage to the flow through the model. In particular, it is difficult to accommodate an anemometer inside a multistory building model,
iii) the directional anemometers have to face always the main current of air, so that, frequent handling is required,
iv) frequent calibrations of hot wire anemometers are often a necessity,
v) a large number of measurements are required to obtain a complete picture of the internal flow, (Cermak et al (1982)). Nevertheless, this may be circumvented by taking the velocity close to the aperture when only a general idea of the ventilation effectiveness is required. However, in this case, care must be taken to ensure that the flow measured is not a localised turbulent eddy flow.

Because of the above-mentioned drawbacks, in particular the number of measurements involved, other alternatives were looked at.

5.3.3.3 Flow tracing and motion photography method

This technique involves the observation of moving indicators. Beside the instructive applications of the flow visualisation in the understanding of the flow behaviour for which it is often used, quantitative data can be obtained.

There are two main visualisation techniques used in the field of wind climate and ventilation in buildings. The first involves the use of foreign materials in the fluid as visual tracers. The second method makes use of a thin surface coating material with which the fluid flow interacts and develops a certain visible pattern. While the first method can yield quantitative results, the second conveys generally only qualitative information.

The most advance visualisation techniques make use of laser anemometers. The principle behind the method is that, when the light or sound reaches an observer from a moving body, it does so with a frequency that is different from that at which it was emitted. This is called the Doppler effect. The application of this effect has become

practical with the advent of the laser, a light source with the requisite properties of a narrow coherent beam of monochromatic light of very high intensity, (see Merzkirch (1987)).

Examples of use of visualization methods to evaluate the ventilation rates through buildings can be found in Krishnakumar et al (1982) and Chandra et al (1983). The former authors used helium filled soap bubbles to trace the flow though a building. Chandra et al (1983) suggested a relatively low cost flow visualization method for measuring air velocity and usable by building designers. The method involves illumination by lasers with a digitizing video equipment linked to a microcomputer to provide quantitative data from a scale model tested at night, outdoors in the natural wind.

The advantages of flow visualisation techniques are multiple. They provide information about the complete flow field under study and not at discrete points only. Furthermore, in contrast with most of the other techniques, the airflow inside the model is not disturbed by the introduction of any measuring instrument.

However, the stability and smoothness of trajectory of the moving indicators depends to a great part on the degree of the free turbulence in the wind tunnel. The best observation are often obtained at low Reynolds Numbers. This could be a very limiting criterion owing to the necessity to obtain high Reynolds Numbers for full-scale similitude, (see Section 5.3.2.4). It could be argued that free turbulence and high Reynolds Number are not incompatible and this could be obtained if the wind tunnel is appropriately fitted with heavy antiturbulence screening. Yet, in these circumstances the flow would be a poor representation of the ABL. Another important drawback is that the calculation of the ventilation rates is generally based on the assumption that the flow is two dimensional.

It was not attempted to use this method to yield quantitative results of ventilation. The main reasons concern the Reynolds Number independence criterion which works against the method, and also the long learning-time necessary before obtaining adequate observations.

5.3.3.4 Concentration measurements

This technique is generally a full scale technique but occasionally it is used in models, (see Cermak et al (1982) for example). In particular, it could be used effectively in the case of complex building geometries, and/or when small air velocities

have to be measured, and/or when the openings are very small.

The method consists of filling uniformly the model with a tracer gas. The model apertures are then opened and the dilution of the tracer is measured continuously.

Though the method could be praised for being applicable in complex configurations and in inner model rooms where other methods cannot be used, it has many practical difficulties. For example, it is difficult to find a representative sampling position or assessing the quality of the mixing in the model. The rate of the tracer gas released in the model are, in general, very small so that it could not be controlled accurately with ease. Furthermore, it is difficult to realize large decay time constants and at the same time large Reynolds Numbers, (see Cermak et al (1982)).

5.3.3.5 Flow rate measurements

A couple of wind tunnel model scale investigations were found in the literature in which unconventional methods were used to measure airflow rates directly through models by the means of some sort of flowmeters.

Bilsborrow (1973) used an orifice plate placed across the model to measure the flow rate. The orifice plate device works on the principle that a plate with a circular hole constricts the free area through which the air can pass. This causes a local increase in velocity and thus a drop in the pressure which can be measured and related to the flow rate.

Bilsborrow used the device to measure flow rates through perforated models with openings which total an area of the order of 0.6% that of the walls. The orifice plate used was a conical entrance orifice plate suitable for the viscous flow expected in the model tests. Although most of the characteristics of the design of the plate conformed to the BS 1042 recommendations, it was not possible to fully comply with the standards. The lengths of the upstream and downstream pipes, for example, were excessively short. It was thus necessary to calibrate the orifice plate under controlled flow and against a master flowmeter for the range of working flow rates, (see Figure 5.7).

In the case of such small openings, the effect of the orifice plate on the flow was small, i.e, the resistance that the orifice plate opposed to the flow was negligible in comparison with the overall resistance of the model.

The technique is very attractive for several reasons:

i) the orifice plate device is very easy to use,

ii) it does not need to be manipulated once fitted in the model,
iii) it gives direct and accurate readings of the actual flow rates, (of the order of 5% according to Bilsborrow), rather than deduced the flow rates from several velocity measurements at discrete points,
iv) reversed flow can be sensed.

Some drawbacks may arise from the fact that,

i) the ventilation openings may only be located in two opposite walls,
ii) the orifice plate has to be calibrated, though, for accurate measurements of the flow, it is necessary to know the exact characteristics of the openings, in which case, calibration tests are mandatory,
iii) the measured values are mean values of the flow rates, so it is not possible to obtain a reading of the internal flow at local points,
iv) some limitations may arise from the large size of the model required to accommodate the orifice plate and which works against maintaining a low wind tunnel blockage,
v) finally, in the case of large openings, the orifice plate device could oppose excessive resistance to the flow.

Vickery et al (1983) used the model fitted with a flowmeter, shown in Figure 5.8, in a study aimed primarily to estimate the accuracy of internal flows derived from the external pressure distribution measured on sealed models.

A bend in a ducting was used as a flowmeter. The flow passing through the model via the bend was monitored by groups of pressure taps on the inside and the outside of the bend. The flowmeter was calibrated against a master flowmeter commercially available.

The openings on the model facades and on the roof were very large compared to Bilsborrow's test model and were more representative of large open windows found in warm climates. Their total surface in the facades was varied from 3% to 89% of the wall area. The surface of the opening on the roof represented 0% to 36% that of the wall.

The resistance of the flowmeter was significant. It contributed, however, for less than one third of the total losses when the wall porosity was less than 47%, and the authors claimed that this resistance was comparable with the resistance that would be

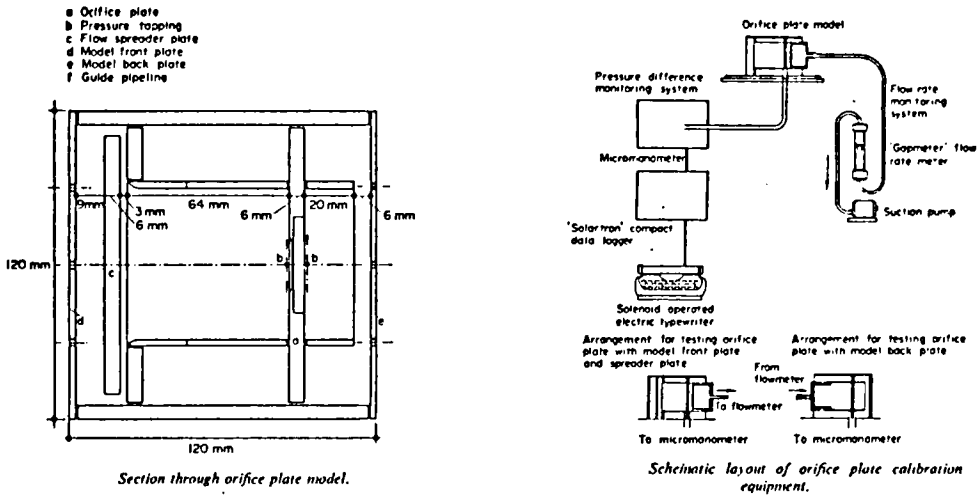

Figure 5.7 Use of an orifice plate for indoor flow measurements in models, (After Bilsborrow et al (1975)).

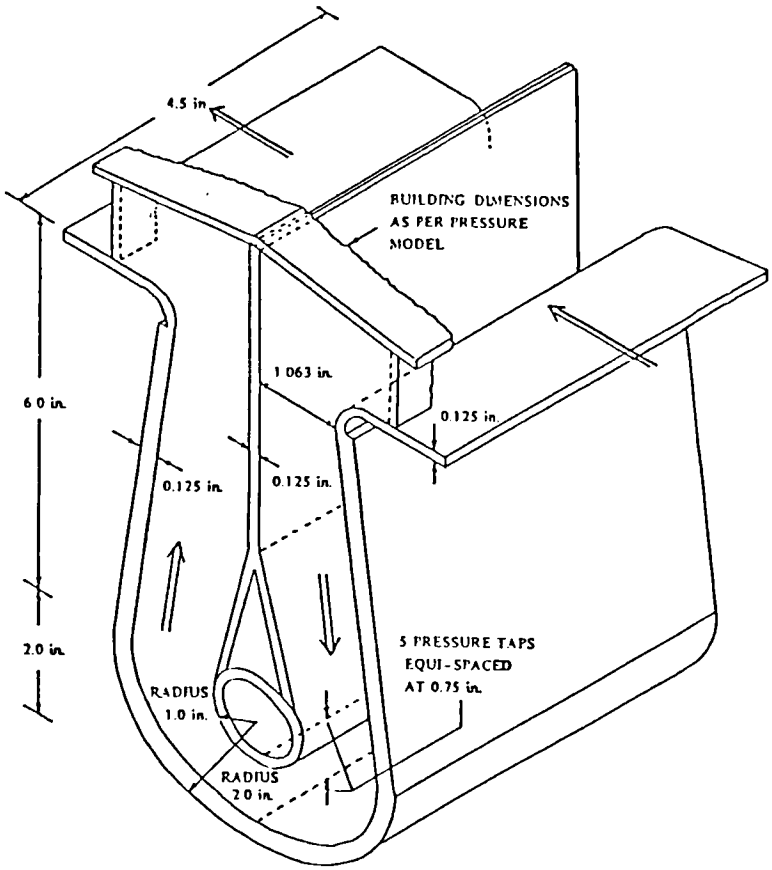

Figure 5.8: Use of a flow -meter for internal flow measurements in ventilation models, (After Vickery et al (1983)).

present in a home with a very open interior floor plan.

The same advantages and drawbacks as the orifice plate can be listed for this flowmeter. However, this latter apparatus cannot be adapted to measure ventilation rates in multistory building models, whereas the other can, provided the model is large enough to accommodate the device in each floor.

For the extensive test programme that was planned, the use of a flowmeter in porous models was highly desirable since the method allows fast data acquisition and very little manipulation. It was thus decided to adopt as technique for measuring the mean ventilation effectiveness an orifice plate device. The preference went to the orifice plate instead of other flowmeters because it is relatively easy to construct and can be fitted in multistory building models.

Nevertheless, it was anticipated that some difficulties may arise in accommodating the device in the models, while keeping the scale low enough to create the least wind tunnel blockage. Also, another stringent limitation may arise from the excessive resistance the flowmeter could oppose to the flow. However, it could be argued here, that, in actual facts, there are almost always internal flow resistances such as partitioning of the space and furniture. Reasonable resistances to internal flows are thus permissible and even desirable for more realistic simulations. The last difficulty that was of concern was the Reynolds Number independence of internal flows. This factor could be checked in a calibration arrangement which is required in any case.

5.4 Conclusions

From the review of the techniques available to assess natural ventilation, the wind tunnel analogue was judged the most suitable for the parametric studies that were planned.

The difficulty of the techniques rests in the modelling of the all the aspects of the external and internal flow at a reduced scale. Fortunately, some relaxation of the modelling can be made. For wind-driven ventilation studies it is enough for the modelling of the external flows to, i) preserve the ratio H/z_0, ii) reproduce the immediate environment in detail, and, iii) ensure that the boundary layer envelopes the model, (Vickery (1981)).

The modelling of the internal flows requires the reproduction of the internal building geometry and Reynolds Number independence of the flow. This makes the simulation difficult, nevertheless, feasible.

Among the ventilation measuring methods used in wind tunnel models, the orifice plate as a flowmeter was adopted to evaluate the ventilation effectiveness of courtyard and atrium buildings. The details of the construction and calibration are presented in the next chapter, as well as, the modelling philosophy and the test programme.

Because of the numerous advantages that the analytical method presents, it was decided to determine how accurate the method is to predict airflow rates in atrium-type buildings and to establish the limits of its use. This will be discussed in Chapter 10.

Chapter 6:

Experimental apparatus and test procedures

6.1 Introduction

This chapter presents the development and calibration of an orifice plate as a flow measuring device in small models.

From the reviewed wind tunnel measuring techniques, the use of a non-conventional flowmeter was found to be the best option to study the ventilation in atrium models. Among the flowmeters, the orifice plate device was chosen because it is well reviewed, relatively cheap to construct, easy to use, and gives an accurate reading. Furthermore, it is not cumbersome and could be fitted in relatively small multistory building models.

6.2 Development and calibration of the orifice plate

6.2.1 Description of the orifice plate

The choice of the type, size and details of the orifice plate was dictated by the need to have the smallest models possible, by the potential of the constriction to measure reverse flows, and the need to present the least resistance to the flow through the model. Following the BS 1042 (1981) and BS 1042 (1984) recommendations, a concentric square edge plate orifice of 17 mm diameter, inserted in a 25 mm diameter pipeline was believed to offer the best compromise to these conflicting requirements .

The square edge orifice plate is generally best suited for flows in which the

Reynolds Numbers exceed 10^4, since at lower values, the tabulated discharge coefficient used in the standard discharge equation, equation (6.1), may not apply. However this limitation was avoided by calibrating the orifice plate at the flow rate range encountered in the model experiment. The calibration was also necessary because of some departures from the BS 1042 specifications for the construction orifice plates; such as the length of the upwind and downwind pipes and the thickness of the plate.

For the need of the experiment, four constriction devices were constructed. Each orifice was cut in a 1.5 mm steel plate and attached to two short brass pipes ending with an aluminium diaphragm. They were fitted with two corner tappings.

The devices were inserted into small perspex boxes, (104×65.5×35 mm) representing a room or a section, (10 m deep at the scale), of the multistory courtyard or atrium building, (the space could be a room, a room with a corridor or two rooms with a corridor). After the calibration test, the boxes, fitted with their orifice plates, were enclosed in the four storey models.

Two of the ends of the boxes were perforated plates, (see Figure 6.1). These represented the facade of the model room. Each facade plate was cut in a 3 mm perspex sheet and had three holes of 10 mm diameter with a total surface of 11.4% of the plate area.

It is convenient in small scale models to reproduce the wall porosity by holes, since it is much easier to drill a hole than cut a rectangular opening. Furthermore, the discharge coefficient of small circular openings becomes constant at lower wind speeds than with rectangular shaped apertures of equivalent area, (see Etheridge and Nolan (1979)). This is a valuable characteristic for internal flow modelling. Also, the change in the characteristics of the model openings is generally not affecting the resulting internal flow, (see Vickery and Karakatsanis (1987)).

Although the calibration of the devices were required, all possible BS 1042 specifications were reproduced in their design and construction.

The diameter of the orifice of the plate was 17 mm, corresponding to a ratio of orifice to pipe diameter of 0.68. The thickness of the plate was 1.5 mm. The brass pipes, upstream and downstream of the plate, had a nominal diameter of 25 mm, a length of 32 mm, corresponding to approximately 1.3 times the pipe diameter, and a thickness of 2 mm. Both pipes ended with two 3 mm -thick aluminium plate diaphragms of the same diameter. Two corner pressure tappings of 1 mm diameter were located on each face of the plate, flush with the surface of the pipe and at the height of its axis centre line. Only the length of the pipes, the thickness of the pipes and the diameter of the pressure

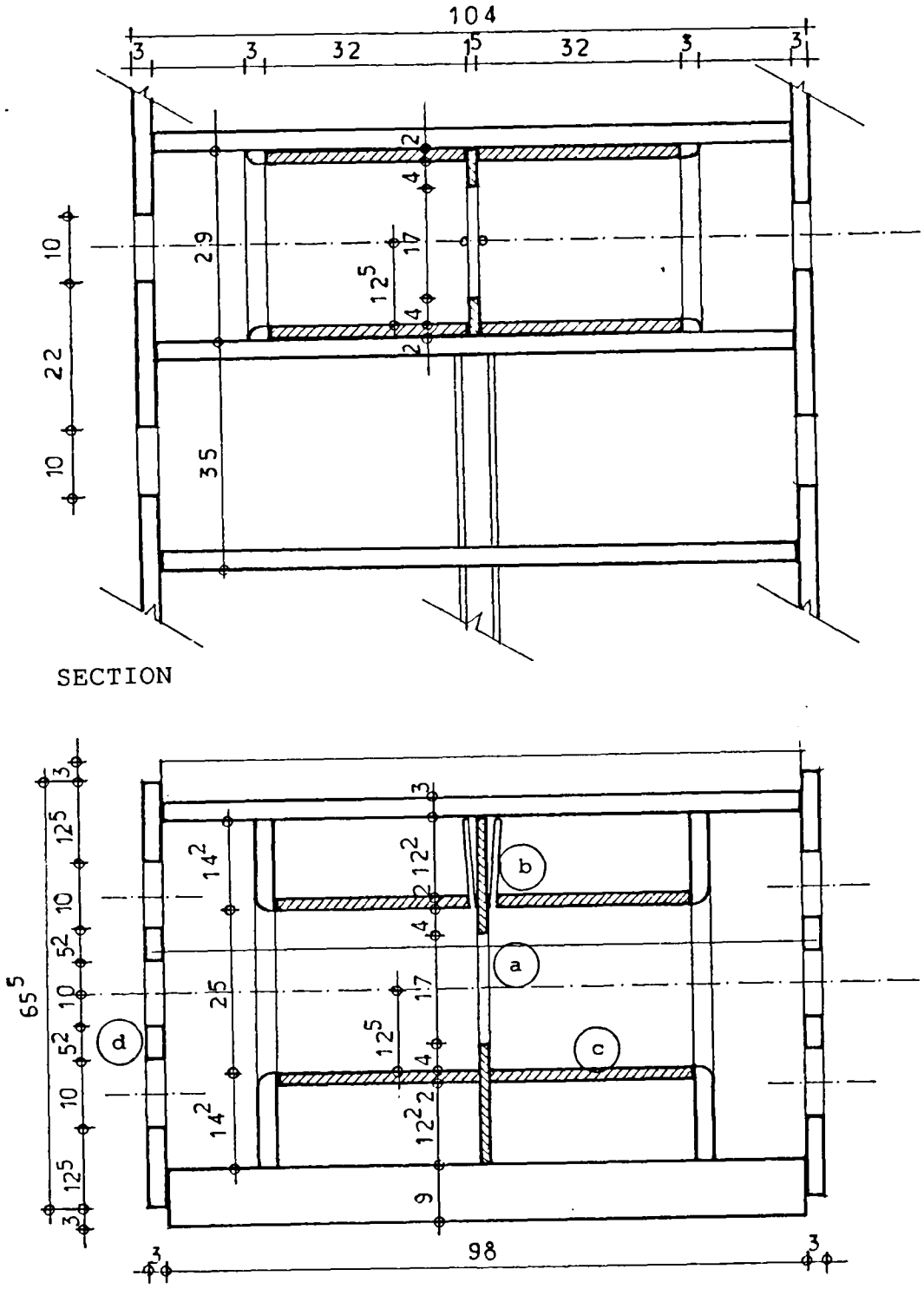

a Orifice plate
b Pressure tapping
c Guide pipeline
d Model facade plate

Figure 6.1: Orifice plate in position in the internal flow test models.

tappings failed to conform to the BS 1042 specifications of the orifice construction.

Each orifice plate was calibrated over a range of flow rates between 0 and 120 lmn^{-1}, which covered the airflow range encountered in the main experiment. The corresponding Reynolds Number range at the throat level was up to 1.3×10^4, which was lower than that recommended by the BS 1042 , (i.e., $Re\geq 5\times10^4$).

6.2.2 Calibration

The standard discharge equation of an orifice plate of this type is as follows,

$$Q= C\times E\times\varepsilon\times\frac{\pi}{4}\times d_o^2\times\sqrt{\frac{2\Delta P_o}{\rho}} \qquad (6.1)$$

where,

Q is the volume rate of flow (m^3s^{-1}),

C is the coefficient of discharge (dimensionless),

E is the velocity of approach factor (dimensionless),

$$E= \left[1-\left[\frac{d_o}{D_o}\right]^4\right]^{-\frac{1}{2}} \qquad (6.2)$$

The product C×E is often referred to as the flow coefficient,

ε is the expansibility factor (dimensionless),

d_o is the diameter of the primary device, (i.e., orifice plate) (m), here equal to 17 mm,

D_o is the upstream internal pipe diameter (m), here equal to 25 mm,

ρ is the mass density of the fluid at the upstream plane of the orifice (kgm^{-3}),

ΔP_o is the differential pressure across the orifice plate (Pa).

The coefficient of discharge, C, is the ratio of the actual discharge to the theoretical and is dependent only on Reynolds Numbers of the fluid. The discharge coefficient values for standard orifice plates with corner tappings can be obtained from

the tables in the BS 1042 (1981), Section 1.1. For values of pipe Reynolds Number of the order of 10^4, the discharge coefficient is found to be 0.636, for a diameter ratio $d_o / D_o = 0.68$ and for $50\,mm \leq D_o \leq 1000\,mm$. For a pipe diameter $25\,mm \leq D_o < 50\,mm$, the discharge coefficient must be multiplied by an appropriate correction factor obtained in nomograms in BS 1042 (1984), Section 1.2. Ultimately, the corresponding value of the discharge coefficient for a standard orifice plate of this size is 0.643, with 3% uncertainty, and for a Reynolds Number working range above 5×10^4.

The expansibility, (or compressibility), factor, ε, is also a coefficient determined experimentally. It is dependent on the diameter ratio d_o / D_o and on the static pressure ratio on the two planes of the orifice. Relevant values for the expansibility coefficient can be found in the publications mentioned above. Provided the ratio P2/ P1 is greater than 0.98, ε can be neglected in the discharge equation, (i.e., $\varepsilon = 1$), (Ower and Pankhurst (1977)). P2 and P1 refer respectively to the pressures measured at the downstream and upstream plane of the constriction.

6.2.2.1 Calibration arrangement and test procedure

Calibration arrangement

The orifice plate devices were calibrated against a T.S.I flowmeter of high accuracy, placed in series downstream to the orifice plate. Along with the calibration of the orifice plate devices, the resistances to the flow by the model and the orifice plate were examined.

Figure 6.2 and 6.3 show the calibration arrangement with the orifice plate mounted in its perspex envelope representing a room of the courtyard or the atrium model. The **pressure drop across the model**, the **differential pressure of the constriction**, the **static pressure** on the upstream plane of the orifice and the **actual airflow rates** were measured simultaneously, as well as, the **temperature in the pipe** and the **barometric pressure** required for the computation of the air density.

The device in position in the model storey was clamped between two rectangular wooden ducts of 35×65.5 mm internal cross-section. The inlet duct had a bell mouth entry and all the internal surfaces of the ducts were treated with a varnish to obtain a smooth flow. Five equidistant static-pressure tappings were located on the top of each duct, upstream and downstream of the model and adjacent to it. They were flush with

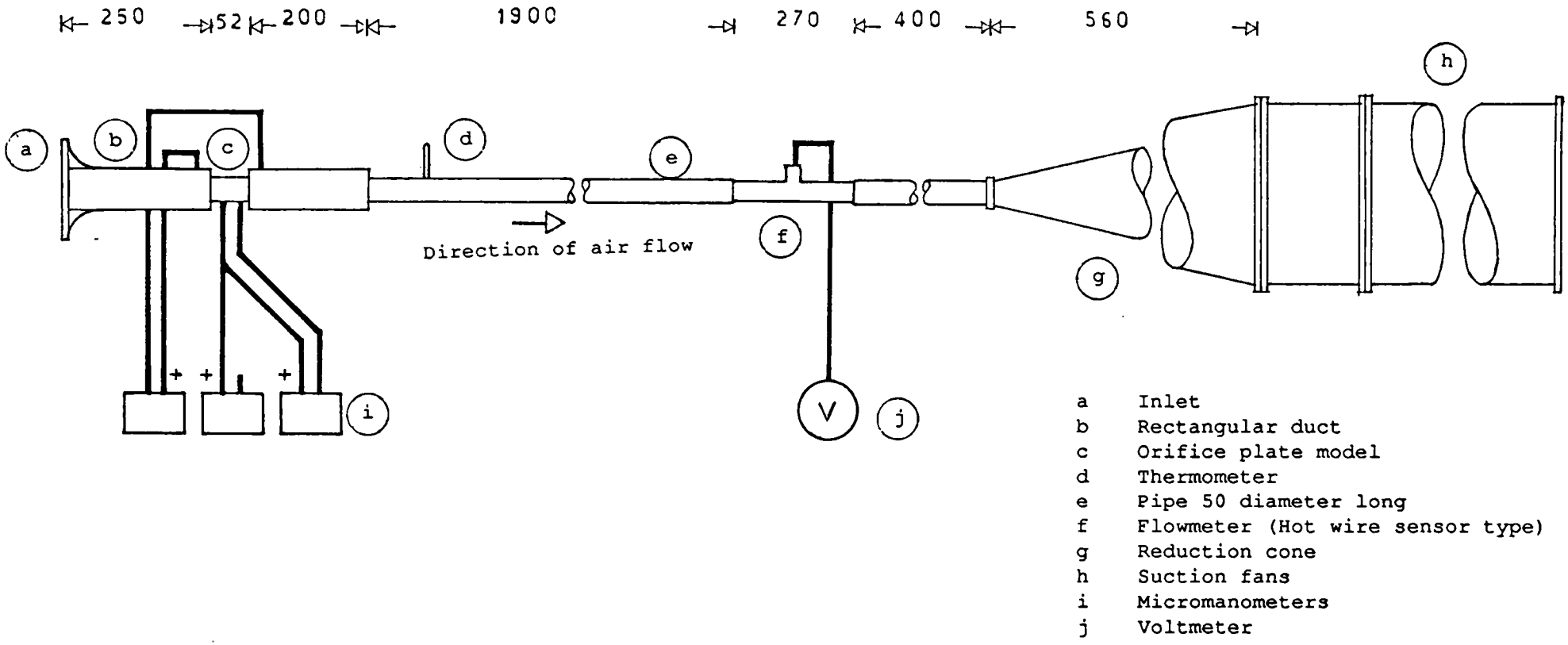

Figure 6.2: Calibration arrangement.

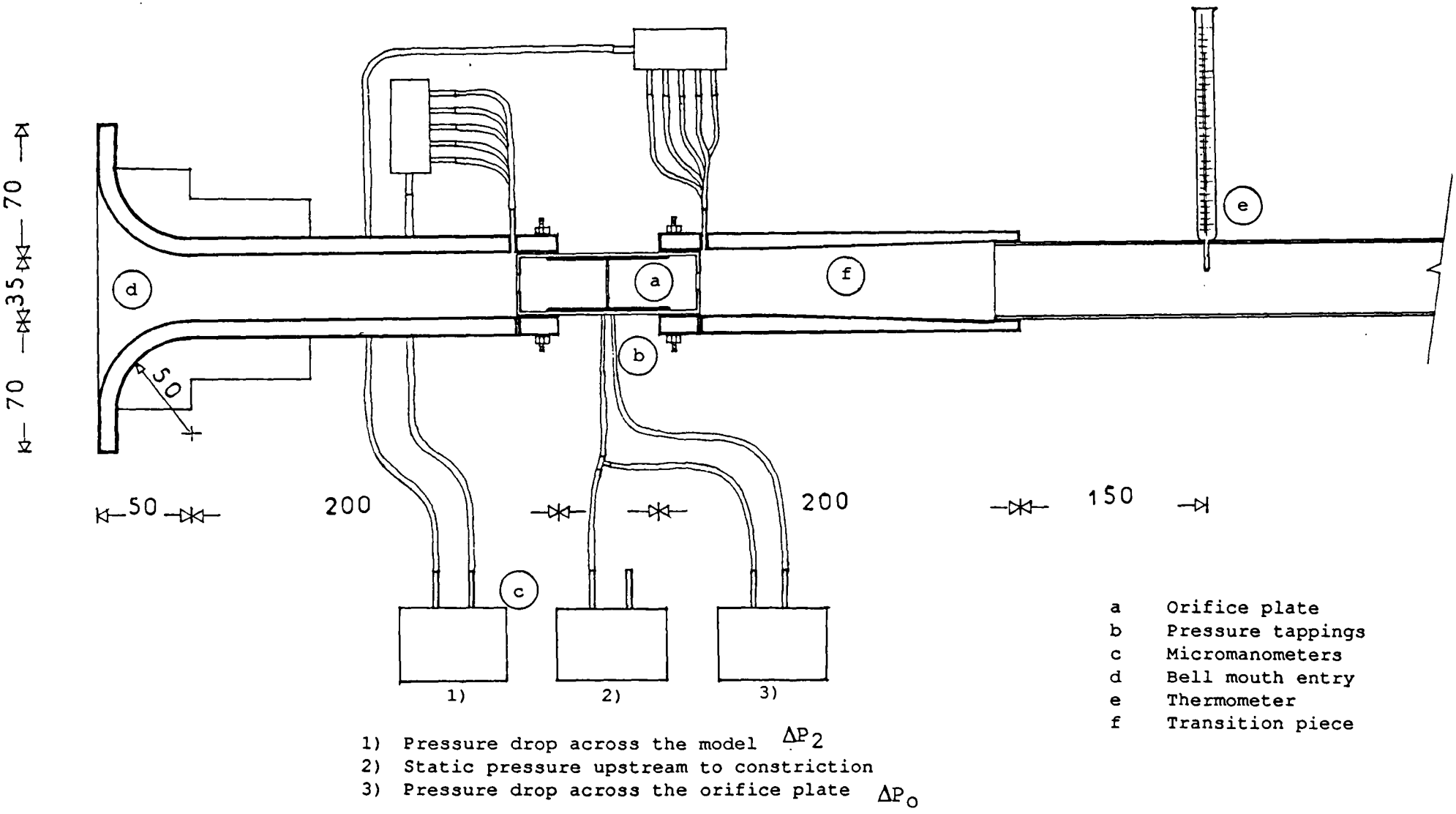

Figure 6.3: Details of the calibration arrangement.

the inner duct surfaces and were linked together to read an average static pressure drop across the opposite facades of the models.

Downstream to the device was a sensitive flowmeter of the hot wire sensor type. It was a T.S.I model 2014 manufactured in S^t Paul, Minnesota, and was capable of measuring airflows in the range of 6 to 600 lmn^{-1}. A recommended 50 diameter, (i.e., 1.9 m), length of straight pipe was inserted between the flowmeter and the rectangular duct and joined to the later by a transition piece.

A small mercury thermometer was located at the top of the pipe, with the bulb entirely inside the duct, at 15 cm of its upstream end.

A short pipe and a reduction cone connected the flowmeter to four 12 inches-diameter suction fans in series, each one with an electric fan controller. All the joints were carefully sealed with plasticine.

The pressure tappings of the rectangular duct and of the orifice plate device were connected to three sensitive digital differential pressure micromanometers. They were manufactured by Furness Controls Limited, type FC 012. Two of them were capable of reading pressure differential up to 19.99 mmH_2O and the third could measure pressure drop up to 199.9 mmH_2O. The upstream pressure tapping of the orifice plate was linked to two of the micromanometers with a double connection as shown in Figure 6.3. One reading was the differential pressure across the constriction. The other reading was the relative static pressure directly upstream of the constriction and which was needed to calculate the mass density at this location, as recommended by the BS 1042 (1981). The value of the density for particular conditions of pressure and temperature were obtained from Tables of Physical and Chemical Constants by Kaye and Laby (1973).

Test procedure

The measurements of the different quantities were taken at fairly steady flow for the required range of speeds. The voltage output of the T.S.I flowmeter was converted into volumetric airflow rates by means of the calibration curve provided by the manufacturer.

The values of the volumetric flow rates were corrected to the actual air density in the calibration duct by a multiplication factor, ρ_0/ρ_1, where ρ_0 is the density at the time of the T.S.I calibration and ρ_1, the actual density. This multiplication factor was suggested by the flowmeter manufacturer and is also discussed by Ower and Pankhurst (1977).

From the first set of measurements, it was found that the static pressure gauge at the upstream plane of the orifice plate was almost the same as the atmospheric pressure, and the temperature in the pipe was fairly close to that of the room, (i.e., ∓0.2 °C). The density of the ambient air was used, instead of the density at the throat level. Also, the expansibility factor, ε, could be neglected in equation (6.1).

The calibration of the orifice was made with and without the front and back facade plates fixed to the perspex box.

6.2.2.2 Results of the calibration

Several sets of measurement were made on one representative orifice plate to check its repeatability and to examine the influence of the perforated facade plates on the calibration. A final set of measurements was made to check that the other orifices had the same characteristics.

Calibration equation without the facades plates

The calibration of the orifice plates without the facade plates in position was best expressed by the following equation,

$$Q = 41.653\ \Delta P_o^{0.457} \qquad (6.3)$$

Where Q is expressed in lmn^{-1} and ΔP_o in mmH_2O. Under the same conditions of temperature and barometric pressure, the standard calibration of such an orifice is of a similar form,

$$Q = 48.179\ \Delta P_o^{0.5} \qquad (6.4)$$

However, the values of the flow calculated with the standard equation differ at some working parts by up to 22% of those measured . The main reasons for these discrepancies could probably be attributed to the fact that some of the BS 1042 specifications were not met in the design of the orifice, as already mentioned. Particularly, the recommended working Reynolds Numbers should be above 5×10^4, for the standard discharge equation, equation (6.1), to be valid, because the discharge

coefficient is then constant. Below this value, and for the low airflow rates encountered in the calibration, this condition could be expected not to be satisfied. Indeed, at certain critical values of Reynolds Numbers, (i.e., approximately 2000), as the flow changes from streamline to turbulent, the discharge coefficient varies considerably. This is shown in Figure 6.4, based on the results of an earlier experiment done on orifice plates at low Reynolds Numbers by Johansen (1930).

A similar trend on the variation of the discharge coefficient with the Reynolds Number was found in the present test, but with smaller discrepancies. This is shown in Figure 6.5. The discharge coefficient was essentially constant and equal to 0.636 for Reynolds Numbers $Re(o) \geq 5\times10^3$, where $Re(o)$ is the Reynolds Number at the throat level.

The discharge coefficient was obtained from the theoretical discharge equation, equation (6.1), as follows,

$$C = \frac{Q}{E\times\varepsilon\times\frac{\pi}{4}\times d_o^2\times\sqrt{\frac{2\Delta P_o}{\rho}}} \qquad (6.5)$$

which leads to,

$$C = \frac{2762.26\times Q\times\sqrt{\rho}}{\sqrt{\Delta P_o}} \qquad (6.6)$$

The Reynolds Number at the throat level was,

$$Re(o) = \frac{Vo\times d_o}{\nu} \qquad (6.7)$$

where,

Vo is the mean axis velocity at the throat (ms^{-1}),

ν is the kinetic viscosity of the air (= 1.4607×10^{-5} m^2s^{-1}).

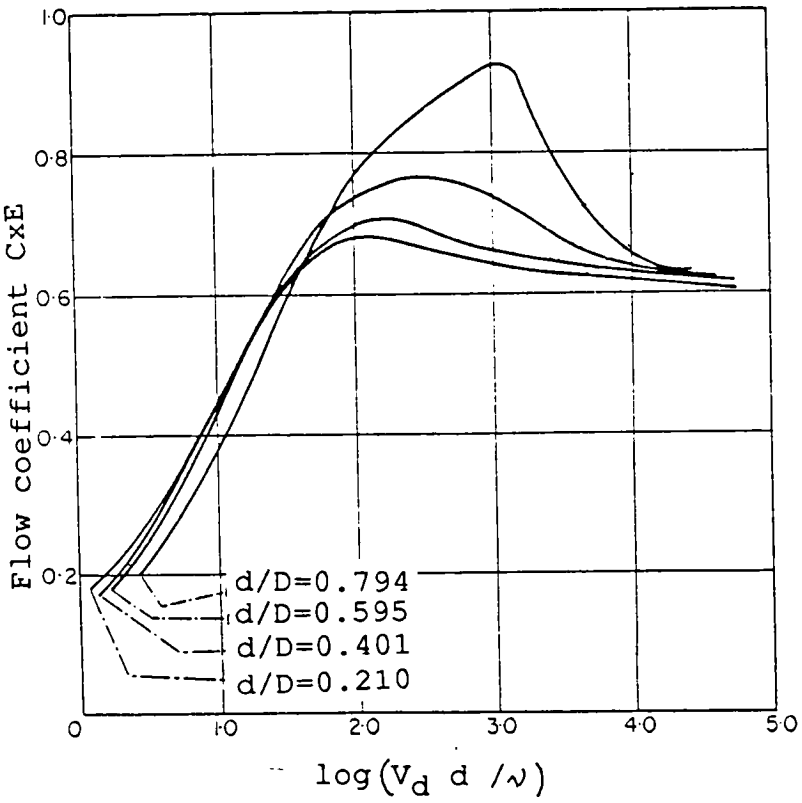

Figure 6.4: Orifice plate discharge coefficient at low Reynolds numbers (After Johansen (1930)).

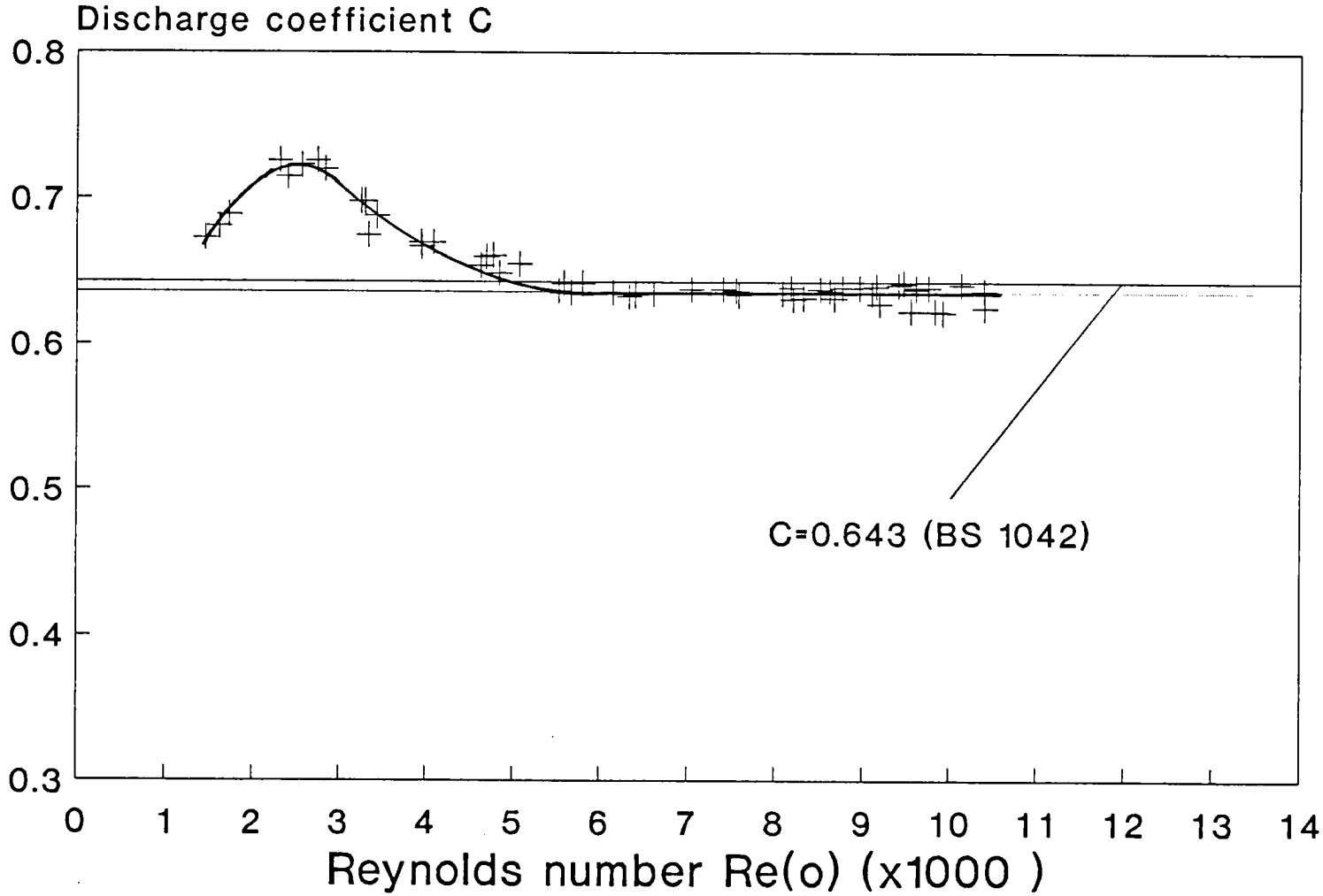

Figure 6.5: Variation of the orifice plate discharge coefficient with Reynolds numbers.

Since,

$$Vo = \frac{4Q}{\pi \times d_o^{\,2}} \qquad (6.8)$$

then,

$$Re(o) = \frac{4Q}{\pi \times d_o \times v} \qquad (6.9)$$

finally,

$$Re(o) = 512.743 \times 10^4 \; Q \qquad (6.10)$$

where Q is expressed in m^3s^{-1}.

It should be made clear, here, that the knowledge of the discharge coefficient was not needed to estimate internal flows, and that the calibration equation (6.3) was the only expression required.

Calibration equation with the facade plates in position

The calibration was repeated with the perforated facade plates mounted in the front and the back of the orifice device. The calibration equation became,

$$Q = 41.526 \; \Delta P_o^{\,0.465} \qquad (6.11)$$

where Q is expressed in lmn^{-1} and ΔP_o, in mmH_2O. Over the working range, the volumetric flow rate calculated from this equation was only ∓1.6% different from that calculated with equation (6.3) where no facade plate was fixed. It was concluded that the effect of the facade plates on the calibration was negligible. The latter equation, equation (6.11), was the one used for the determination of the flow rates in the main experiment. Figure 6.6 shows the calibration curve and the measured data.

The repeatability obtained in the measurements of the internal flows was excellent. The standard deviation of the measured volumetric flows from the calibration equation (6.11) was never more than ∓1.4% when the test was repeated.

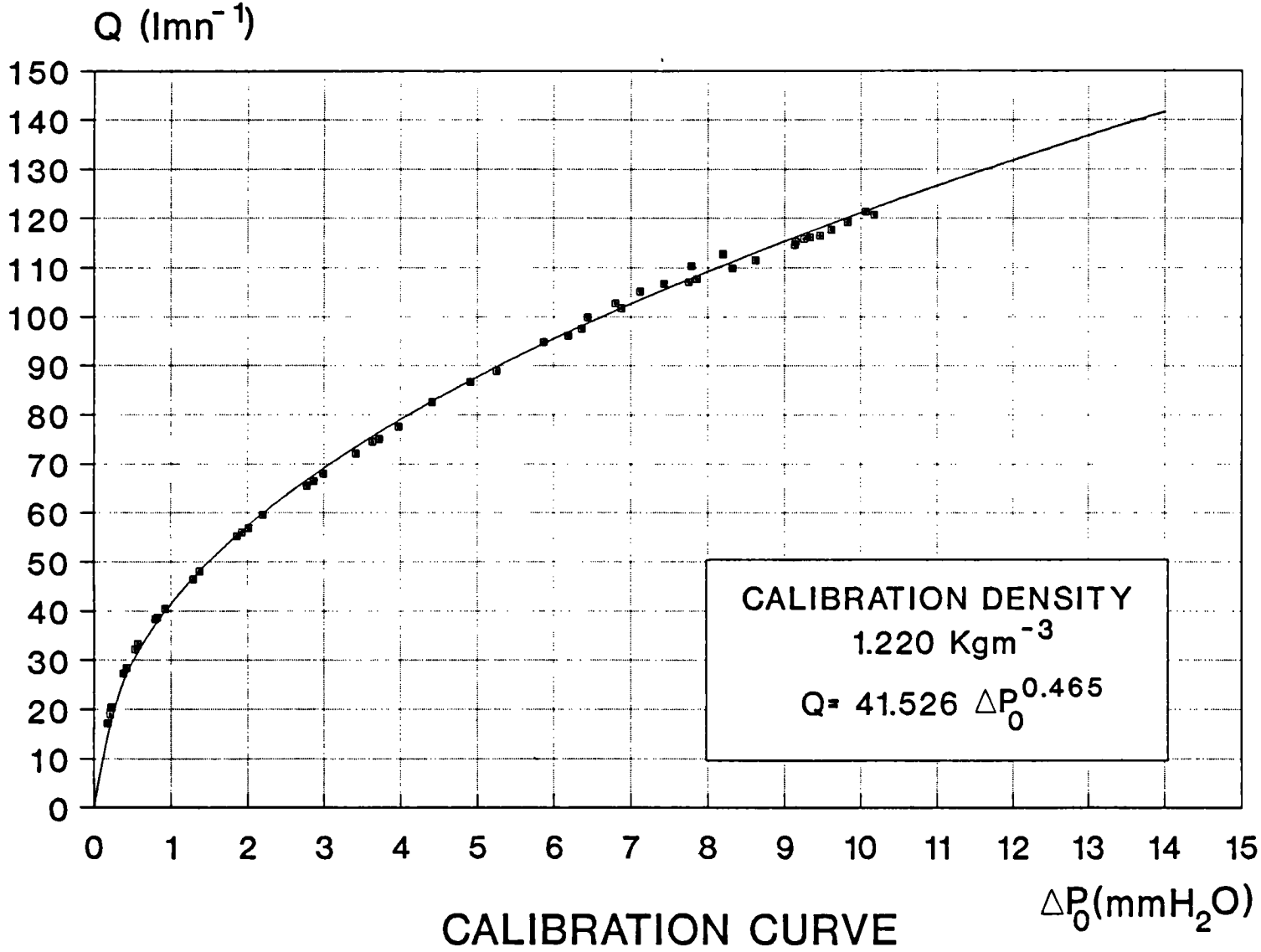

Figure 6.6: Calibration curve of the orifice plate.

6.2.2.3 Flow resistance of the models

The knowledge of the flow resistance of the models was important for the following reasons;

i) to evaluate whether the resistance of the orifice plate to the flow could have its equivalent in the full scale, as series of partitions for example,
ii) to reproduce the resistance of the constriction in the other model storeys. This is in the intention to prevent any possible preferential routes that could be offered to the flow of air instead of through the orifice plate,
iii) to evaluate the range of flow rates where the resistance of the flow is Reynolds Number independent, in which case, it actually represents a full scale situation.

The static pressure at the downstream face of the model in the calibration duct was found to be considerably less than that upstream, particularly when the hollow facade plates were in position. The orifice plate contributed also in generating dynamic pressure losses.

In ducts, the flow resistance caused by obstructions such as bends, tee-junctions, diffusers or orifices is estimated in term of pressure losses, and determined from a local loss coefficient for which data are provided for different types of obstructions (see ASHRAE Handbook of Fundamentals (1989c), for example). The pressure loss coefficient is expressed as,

$$CI = \frac{\Delta P_1}{\rho \times \frac{V_d^2}{2}} \qquad (6.12)$$

where,

CI represents the ratio of the total pressure loss to the dynamic pressure at the referenced cross section (dimensionless),

ΔP_1 is the total pressure loss (Pa), (corresponding here to the pressure drop, ΔP_2, across the room model, see Figure 6.3),

$(\rho V_d^2)/2$ is the dynamic pressure (Pa) at the reference section, here the upstream rectangular duct,

V_d is the mean axial velocity at the referenced section, here the upstream rectangular duct (ms^{-1}),

$V_d = Q / (H_d \times W_d)$,

W_d is the width of the duct (= 65.5×10^{-3} m),

H_d is the height of the duct (= 35×10^{-3} m),

The equation (6.12) can also be written as,

$$CI = \frac{2\ \Delta P_2}{\rho \left[\frac{Q}{H_d \times W_d} \right]^2} \qquad (6.13)$$

thus,

$$CI = \frac{1.051\times10^{-5}\ \Delta P_2}{\rho \times Q^2} \qquad (6.14)$$

Comparison between the resistance to the flow of the orifice plate and that of other internal partitioning

Several obstructions were tested and compared to the resistance of the orifice plate. They consisted of 3 mm perspex plates, disposed vertically, midway, across the model storeys. Two of them were rectangular plates, 53.5 mm wide and 14.5 mm and 19.3 mm high, corresponding respectively to 1/2 and 2/3 of the internal space height of the model rooms. Three others were fitted to flush with the internal perimeter of the model and each had a rectangular opening in the middle. The openings were 49.5×25 mm, 43.5×19 mm and 37.5×13 mm respectively, corresponding to 80%, 53% and 31% of the transverse vertical surface of the model rooms.

The pressure loss coefficient was plotted against the Reynolds Number of the approaching flow in the upstream rectangular duct. The Reynolds Number of the flow in the rectangular duct Re (d) can be expressed as,

$$Re(d) = \frac{V_d \times W_d}{\nu} \qquad (6.15)$$

or,

$$Re(d) = \frac{Q}{H_d \times \nu} \qquad (6.16)$$

which leads to,

$$Re(d) = 195.6 \times 10^4 \; Q \qquad (6.17)$$

where Q is in ms^{-1}. Figure 6.7 shows the cases of the orifice plate model with and without the facade plate at the two ends, the model with the facade plates and without any obstruction inside, and finally, with two different partitions in it. The pressure loss tended to level out at $Re(d) \geq 2000$. Below this value, the pressure loss coefficients showed a decrease, which means that, for the same pressure drop across the opposite facades, the volume of air will be greater in the second case, (e.i., when $Re(d) < 2000$).

The values of CI at $Re(d) < 2000$ represented approximately 0.8 times that at $Re(d) \geq 2000$. For a particular pressure drop across the model, the volumetric flow rate at $Re(d) < 2000$ will only be 12% higher than that with greater $Re(d)$ values, since,

$$\frac{CI(_0)}{CI(_1)} = \left[\frac{Q(_1)}{Q(_0)} \right]^2 \qquad (6.18)$$

The indices $(_0)$ and $(_1)$ refer to the values associated with $Re(d)$, respectively, below and above 2000.

The resistance of the orifice plate contributed only 1/10 of the total pressure losses across the entire model when the facade plates were fitted. The internal partitions with a central void did not add significant resistance to the flow.

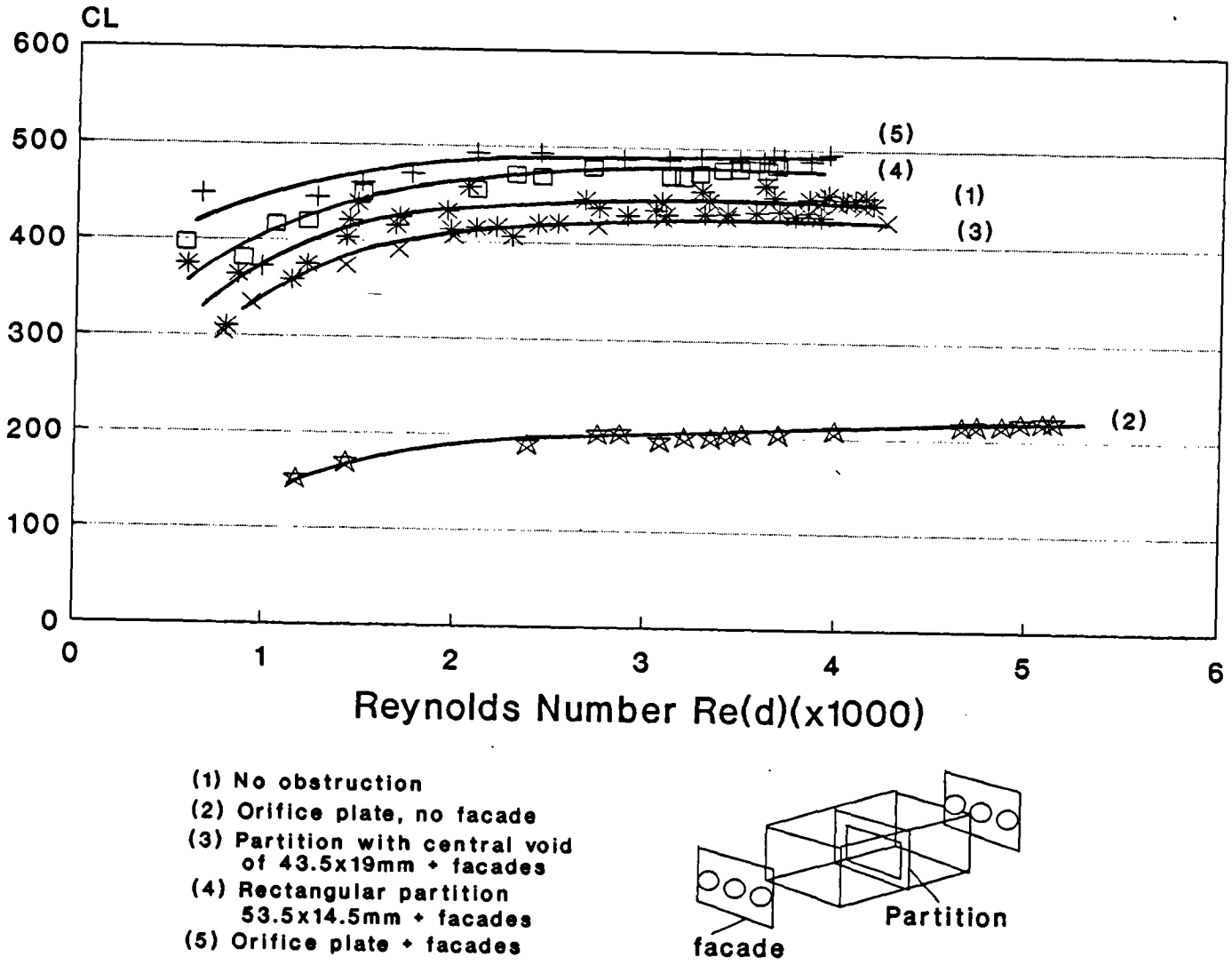

Figure 6.7: Pressure loss coefficient of the test models fitted with various internal partitions versus Reynolds numbers.

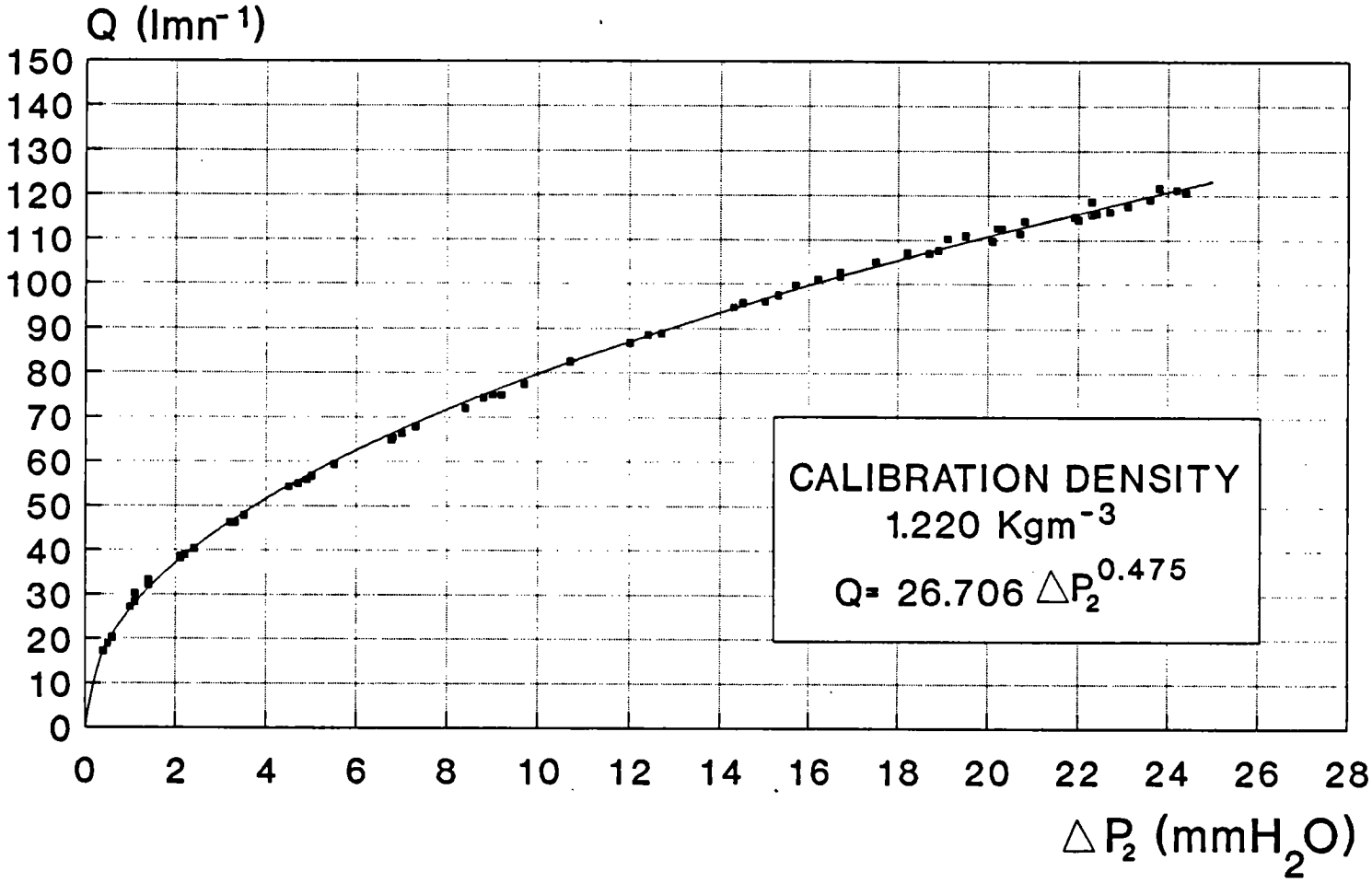

Figure 6.8: Equation of flow discharge through the model rooms.

Over the working flow range, the simple 53.3×14.5 mm rectangular plate had the closest flow resistance to that of the orifice plate. This obstruction was reproduced in all the model rooms except for those forming the corners of the building models and those with an orifice plate.

Discharge equation of the flow through the model rooms

The volumetric flow rates through the model rooms could be related to the pressure differential across their facades by the discharge equation (6.19):

$$Q = 26.706\ \Delta P_2^{0.475} \qquad (6.19)$$

where Q is the volumetric flow rate (lmn^{-1}), ΔP_2, the pressure drop across the model rooms (mmH_2O). The calibration curve is shown in Figure 6.8.

6.3 Experimental facilities and procedures

6.3.1 Introduction to the experimental programme

The experimental programme is shown in Figure 6.9. It involved two type of tests; i) surface pressure measurements and ii) internal flow measurements. The evaluation of the natural ventilation potential of the courtyard and atrium structures involved the internal flow measurement by means of the orifice plate models. The surface pressure tests were generally subsidiary to the internal flow recordings, and were undertaken either, to interpret some of the indoor flow test findings and establish a comparison with other works based on surface pressure measurements, or, were used to select geometries of atrium roofs to be tested in the internal flow experiment.

The experimental programme was divided into three parts, (see Figure 6.9). The results were reported in three different chapters, i.e., Chapters 7, 8, and 9. They involved respectively,

i) the effect of the courtyard geometry and the orientation to the wind under unsheltered conditions;

ii) the ventilation potential of unsheltered atria under different ventilation

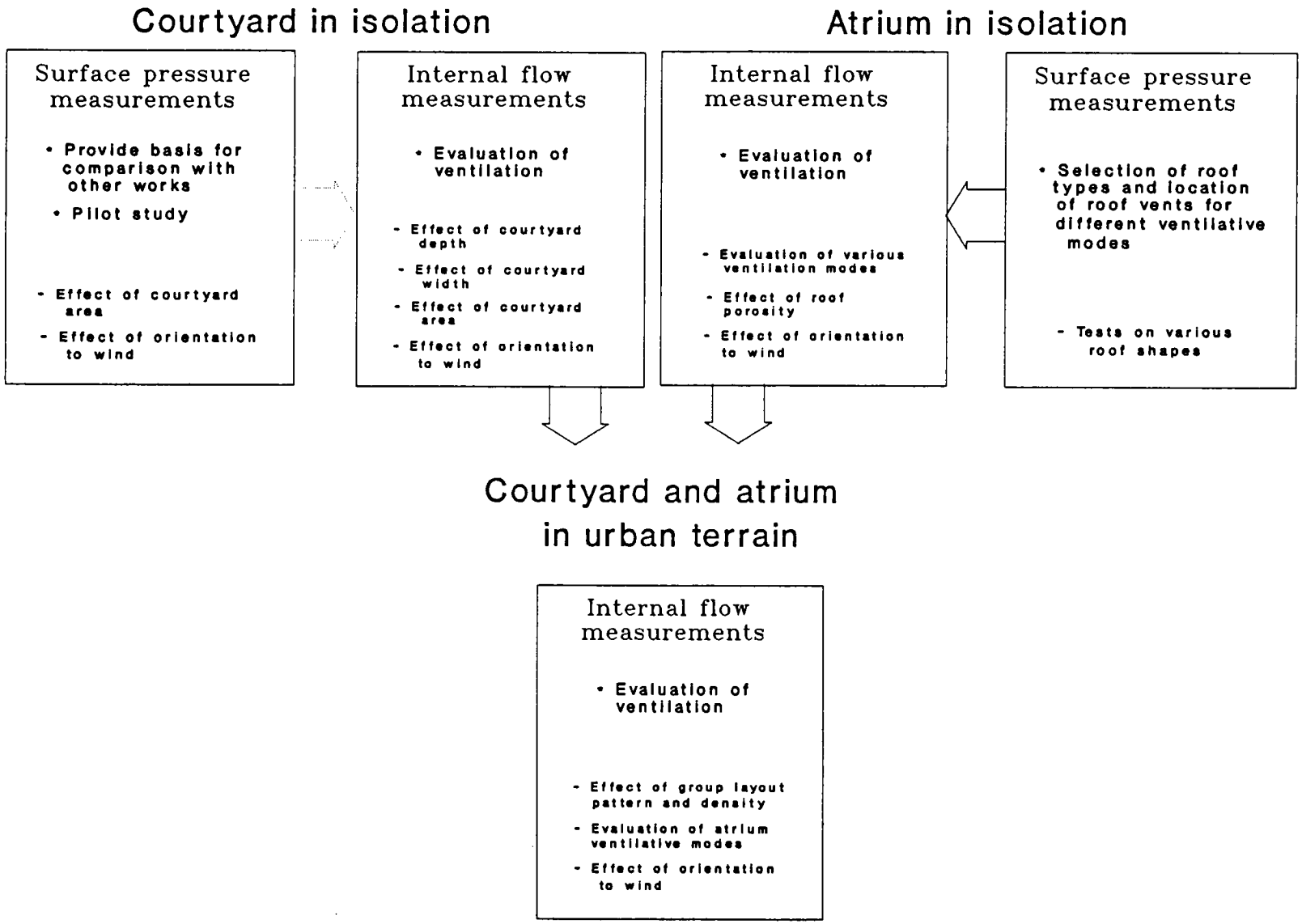

Figure 6.9: Experimental test programme.

modes and the selection of appropriate roof geometries to perform each of these ventilation strategies;

iii) the ventilation potential of both courtyards and atria in sheltered conditions of urban sites.

In the first part of the work, limited numbers of surface pressure measurements were taken in square-shaped courtyard models in which the area was changed. More exhaustive measurements and a more systematic change of the dimensions, i.e., depth and breadth, of the courtyard was made on the internal flow models.

For the second part of the experimental programme, four atrium ventilation modes were identified and tested, (refer to Chapter 9 for more details). They were differentiated by the way in which the air passing over the roof induced currents of air in the atria. The air through the roof apertures can either,

i) induce a suction effect in the atrium,

ii) be deflected in the atrium,

iii) enter and leave the atrium via the roof openings,

iv) the option in which the roof apertures were closed was also considered.

Obviously the design of the roof, its porosity and the location of its openings were crucial in establishing any of these ventilation modes and in offering the best performances. Thus, prior to the internal flow measurements, surface pressure tests were made on several roof shapes to choose the most promising types in each mode. These tests also provided pressure coefficient data which were almost non-existent in the literature for such structures, and which were used later as data inputs for a computer simulation described in Chapter 10.

In the last experimental investigation, internal flows were monitored on selected models used in the two previous internal flow tests, (i.e., courtyard and atrium models in isolation). The presence of surrounding model elements provided a more realistic context in which these building types are generally found. Nevertheless, the isolation condition in which these configurations were first tested was a compulsory passage to grasp some of the phenomena involved before broaching the more complex nature of flow in the shielded conditions.

6.3.2. Description of the wind tunnel

The ventilation experiments were undertaken in the Sheffield University 1.2×1.2m atmospheric boundary layer (ABL) wind tunnel, which has been exhaustively described by Lee (1977), (see Figure 6.10). It is a 7.2 m open-return type, (see definition in Section 5.3.1), using passive means to accelerate the growth of the boundary layer in order to reduce the required length of the roughness floor, (accelerated roughness flow technique). This technique uses a castellated fence located at 320 mm downstream from the honeycomb at the inlet, a row of four spires of triangular section, positioned 200 mm downstream of the fence, directly followed by a regular array of roughness elements of a total fetch of 4.55 m.

The honeycomb is used to straighten the flow at the entry. The role of the barrier is to provide an initial deficit of momentum representing the effect of longer fetch of roughness upwind, while the spires are used as mixing devices to distribute this momentum deficit in the upper part of the growing boundary layer. The roughness elements can be altered to reproduce a large variety of terrains from rural to urban.

6.3.2.1 The simulated boundary layer scale factors

The overall linear scale describing the wind structure in this wind tunnel, and to which the model scale should comply for a strict reproduction of the full scale ABL, is 1/350 and 1/500, for a typical urban and rural terrain respectively, (Lee (1977)). The unique scale factor for each terrain is derived from the integral scale of the turbulences and the scale of the mean velocity characteristics of the simulated flow, following the procedure given by Cook (1978).

6.3.2.2 Simulation of the suburban ABL

The models were chosen to be tested under a simulated flow characteristic of a suburban terrain or an urban terrain with buildings of moderate rise.

To model the wind profile appropriate to these terrains the floor of the wind tunnel was fitted with rows of roughness elements, 20 mm high, alternated with rows of 10 mm high elements and disposed in a staggered manner. Each roughness element measured 3.5×3.5 mm in plan. The gap between the elements was 65 mm in the flow direction, and 80 mm in the transverse direction.

Figure 6.10: Sheffield University 1.2x1.2m ABL wind tunnel.

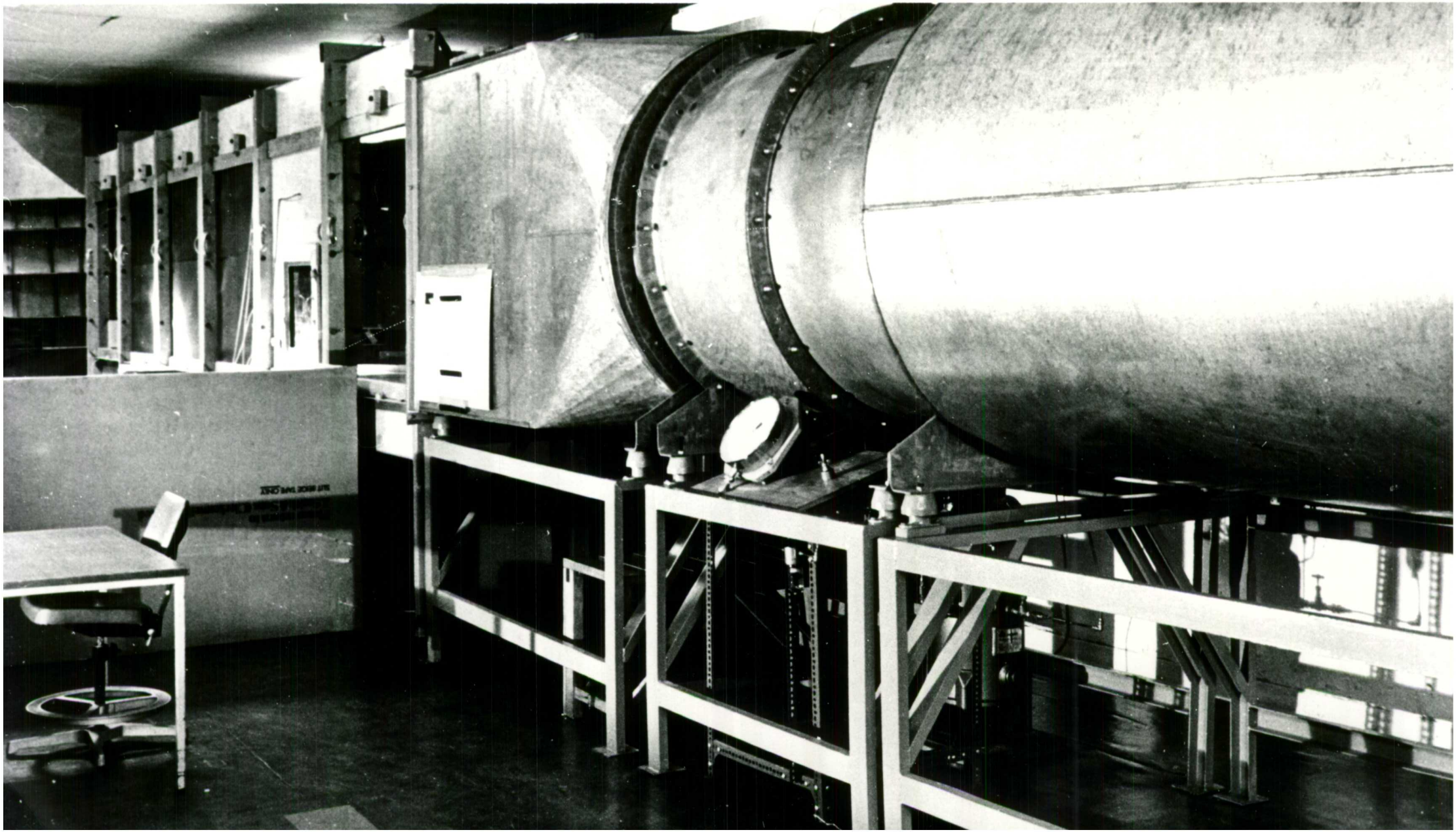

6.3.2.3 The mean wind velocity profile

The mean velocity profile, obtained from this arrangement and measured at the centre of the working section by means of a Pitot static tube, is shown in Figure 6.11. The maximum velocity was reached at a height of approximately 800 mm, which correspond to the physical thickness of the wind tunnel boundary layer. Above this level, the velocity remained fairly constant.

The velocity profile, expressed in the power law form was obtained using a regression fit from the velocity measurement taken at the centre of the turntable and at different heights. The mean velocity profile was best expressed by,

$$\frac{Vh}{V_{800}} = \left[\frac{h}{800} \right]^{0.245} \qquad (6.20)$$

where h is the height above the tunnel floor (mm), and Vh the associated velocity.

Typical power law indices for velocity profiles measured at various urban sites are given in Table 6.1, with the associated sources of data. Comparatively, the exponent $\alpha = 0.245$ obtained in the wind tunnel could be representative of a suburban site or an urban terrain with no imposing high rise buildings.

Table 6.1: Urban power law exponent (source: Lee (1977)).

SITE	α	SOURCES
Liverpool	0.21	Jones et al (1971)
Sheffield	0.22	Caton (1975)
London	0.23	Shellard (1963)
		Caton (1975)
Kokubunji	0.25	Shiotani (1962)
Japanese towns	0.33	Kamei(1955)
City centres	0.40	Davenport (1963)

Some of the highest values of the power law index, given in Table 6.1, and which were measured for heavily built up areas, for instance, the one reported by Davenport,

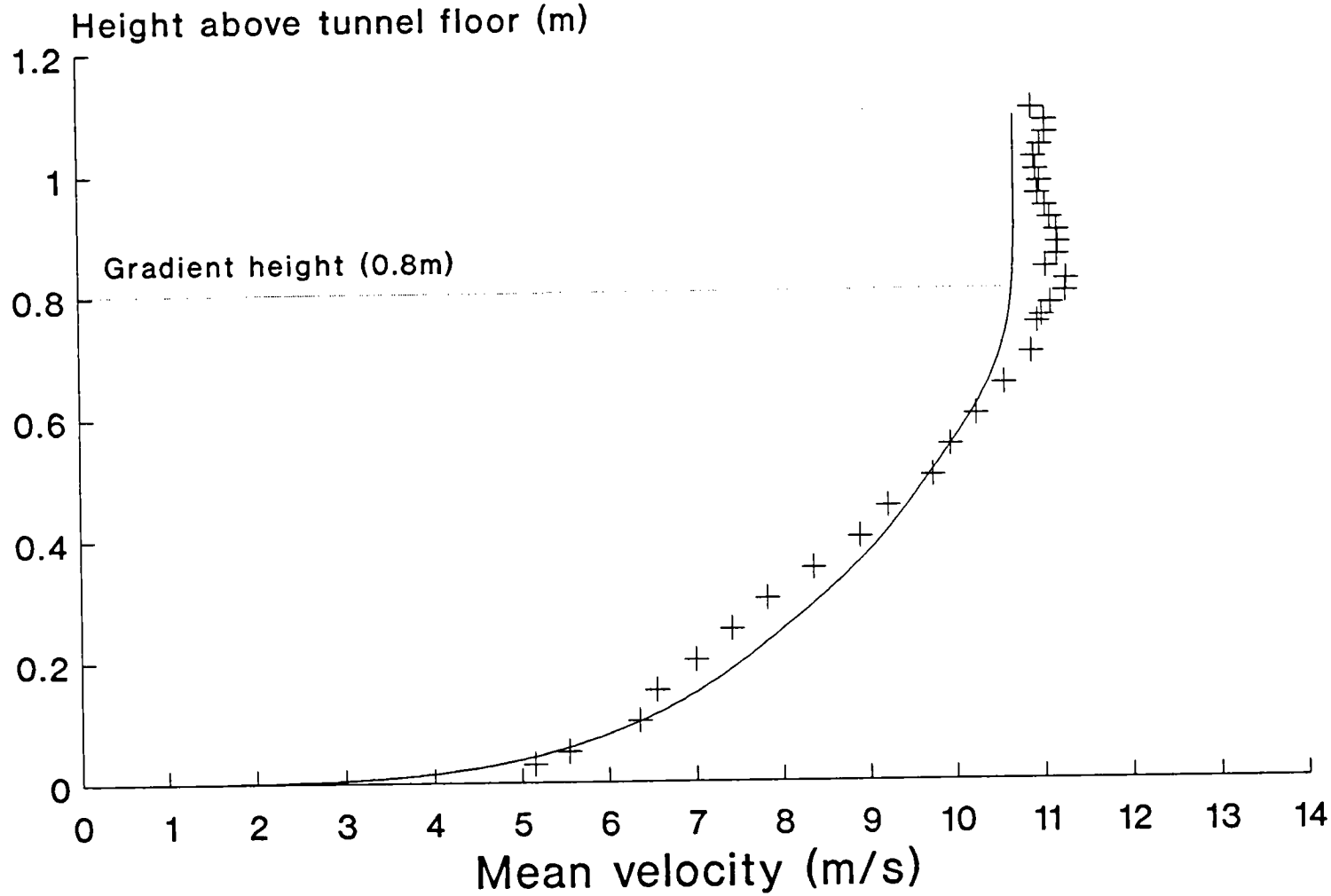

Figure 6.11: The mean velocity profile.

could be in fact reduced if allowance for the zero plane displacement was made, (Lee (1977)). Counihan (1972) indicated that, when the roughness represents a significant proportion of the total boundary layer thickness, then several profiles could be fitted depending on the position at which the profile was measured in relation to a particular roughness element and the height over which the profile was fitted. Some of the high values of the exponents were believed to be associated to non-equilibrium situations. Taking these points into consideration, the exponent representative of an urban terrain was suggested to be 0.3, (Lee (1977)), and 0.28, (Counihan (1973)).

6.3.3 Model description

6.3.3.1 Surface pressure models

Courtyards

Four square shaped non-porous courtyard models were made of wood. At the centre of one of the wings of each model, a void was made to receive a 80×50×100 mm aluminium block fitted on two opposite faces with a total of 10 pressure tappings, (see Figure 6.12). The surfaces of the aluminium block were flush with the surfaces of the wooden models. This guaranteed smooth surfaces in the vicinity of the pressure tappings without having to construct the models entirely with aluminium which would have been very costly.

The models were all of the same height, H, (i.e., 100 mm). The thickness of the wings enclosing the courtyard, was also the same, i.e., 80 mm. Only the area of the patio was changed and was 0.5H×0.5H, H×H, 1.5H×1.5H or 2H×2H.

Atria

The models were made to monitor the surface pressures on the atrium building walls and on the roofs. This test was prior to the internal flow measurements. The main purpose was to select, among common types of roofs, the most promising for each of the possible ventilation modes in atria. Another intention was to determine the pressure zones where the openings could be best located under each ventilation mode.

The models represented four storey atrium buildings at a scale of 1/100. The scale was chosen to match the scale of the internal flow test models, which was in turn

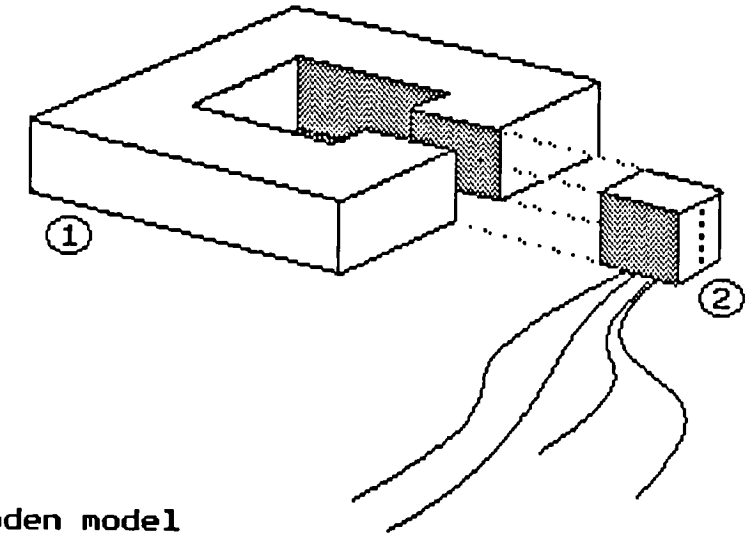

① Wooden model

② aluminium block fitted with pressure tappings

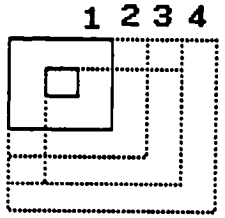

Courtyard sizes tested

Model index :

1) C05x05 (area 0.5Hx0.5H)
2) C10x10 (area HxH)
3) C15x15 (area 1.5Hx1.5H)
4) C20x20 (area 2Hx2H)

Figure 6.12: Courtyard models used for surface pressure tests and test programme.

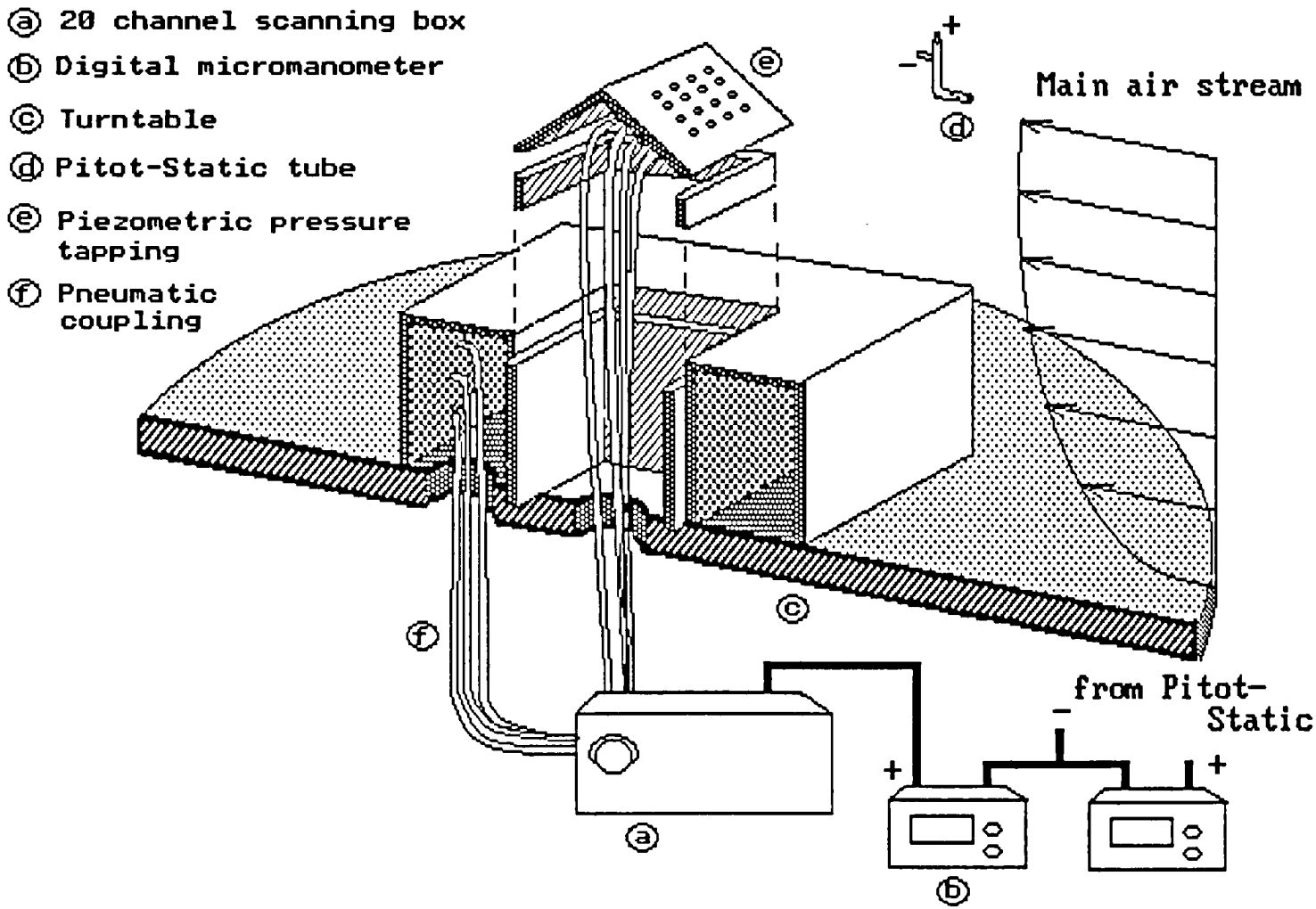

Figure 6.13: Atrium models used for surface pressure tests.

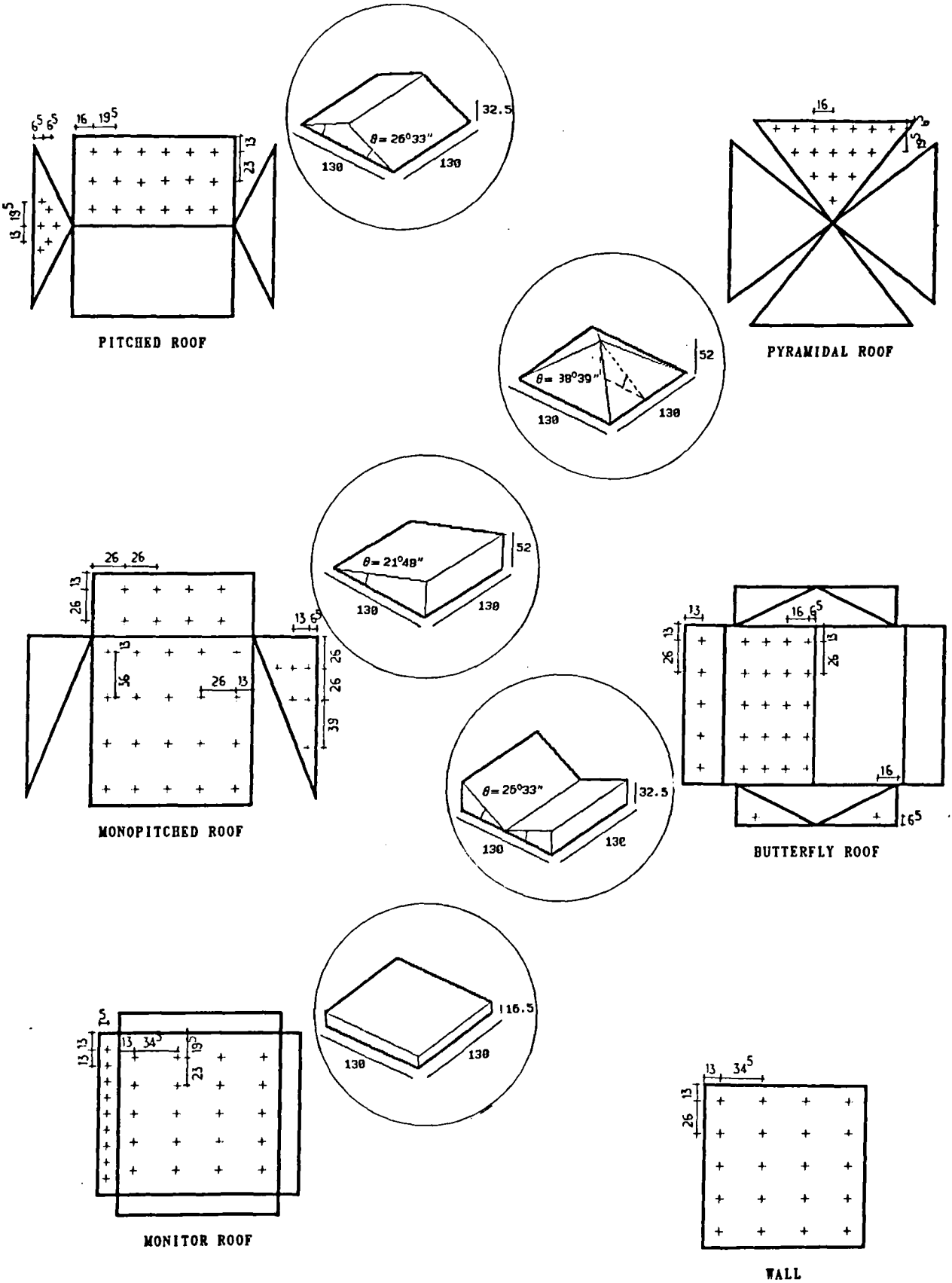

Figure 6.14: Roof types tested for surface pressure measurements.

dictated by the necessity to accommodate the orifice plate device.

Each atrium was mounted from a common aluminium block of 339×339×130 mm high to which was attached a roof at the top, (see Figure 6.13). Five types of atrium roofs were selected, (see Figure 6.14). These were;

a) a roof monitor, (flat surface on the top of vertical contour),
b) a monopitched roof, (sloped face on three vertical surfaces),
c) a pitched roof, (with two sloped surfaces resting on two vertical surfaces),
d) a pyramidal roof,
e) a butterfly roof, (with two surfaces inclined towards the central axis of the atrium).

The roofs and the walls were cut out of 3 mm -thick aluminium sheets. This material ensured that the edges of the models were sharp and the finish of the surface was free of small protuberances that could affect local pressures. For the pyramidal roof type though, it was easier to shape it in one piece from a lump of wood without loosing much the sharpness of the angles. Each piece of the models was screwed together at the edges with hexagonal socket screws with cap heads that were flush with the model surface and avoided any protrusions on the surfaces. All the joints were tapered with sellotape, to avoid any local disturbances of the flow in their vicinity.

The roofs were joined to the aluminium base as illustrated in Figure 6.13. They were screwed to a vertical edge that was used to align them with the contours of the atrium space and were resting on a vertical support inside the atrium. Finally they were fixed with a layer of strong adhesive cloth onto the model.

Some of the model walls and roof surfaces were covered with pressure tappings of 2 mm diameter. These were arranged following a grid pattern which was intended to cover a maximum area. The monitored surface was nevertheless restricted near the edges by the thickness of the adjacent joint surfaces. The pressure distribution on the remaining surfaces were obtained from symmetry and by rotating the model facades and/or the roof. The location of each of the pressure tappings on the wall and roof surfaces is given in Figure 6.14.

The choice of the roof types to be tested was restricted to the most common ones, bearing in mind the concern for simplification and avoidance of Reynolds Number implications introduced by curved shapes. The selection was further reduced to those which could best perform in the various atrium ventilation modes. This led to the

selection of roofs that could present either the largest suction or the greatest positive pressure, or a near-atmospheric pressure field, and also, the most extensive area, so that many openings can be provided for the greatest roof pressure effects, (for more details on the ventilation modes of the atrium buildings see Chapter 8).

6.3.3.2 Models for internal flow measurements

Courtyards

For the test of courtyards in isolation, a total of thirteen perspex models were constructed. They were designed in such a way that they could be assembled to form courtyard building models of various shapes. Four of them were made to form the corners of the model, four others had an orifice plate mounted in, and the five last ones were made to complete the building models.

Each of the model elements consisted of four storey "units" or rooms at the scale of 1/100. They all had hollow facades with the same relative porosity, (i.e., 11.4%), and the same flow resistance, except for the corner ones in which no internal partitioning were inserted.

Each of these model elements had a protuberant perspex plate in one side and an indent in the other side, (see Figure 6.15). They were fitted together by inserting the protuberance into the indent and consolidated by two screws at the top. The joint between two model elements was then tapered with a layer of sellotape.

To change the relative position of an orifice plate model element, the courtyard model had to be dismantled and recomposed with the orifice plate at the new location.

Atria

The rooms of the atria were assembled from the same "lego-like" model elements as the courtyard's, and had the same external size as the sealed atrium models described earlier. The atrium models were actually mounted out of the porous courtyard model C10x10, (for which the courtyard was square in plan , with the sides equal to the height), and to which a roof was added, (see Figure 6.16 and 6.17). The four orifice plates were fitted together in each atrium model.

On the basis of the results of the surface pressure tests, the monopitched roof was selected for the internal flow measurements. It was used for all the ventilation strategies

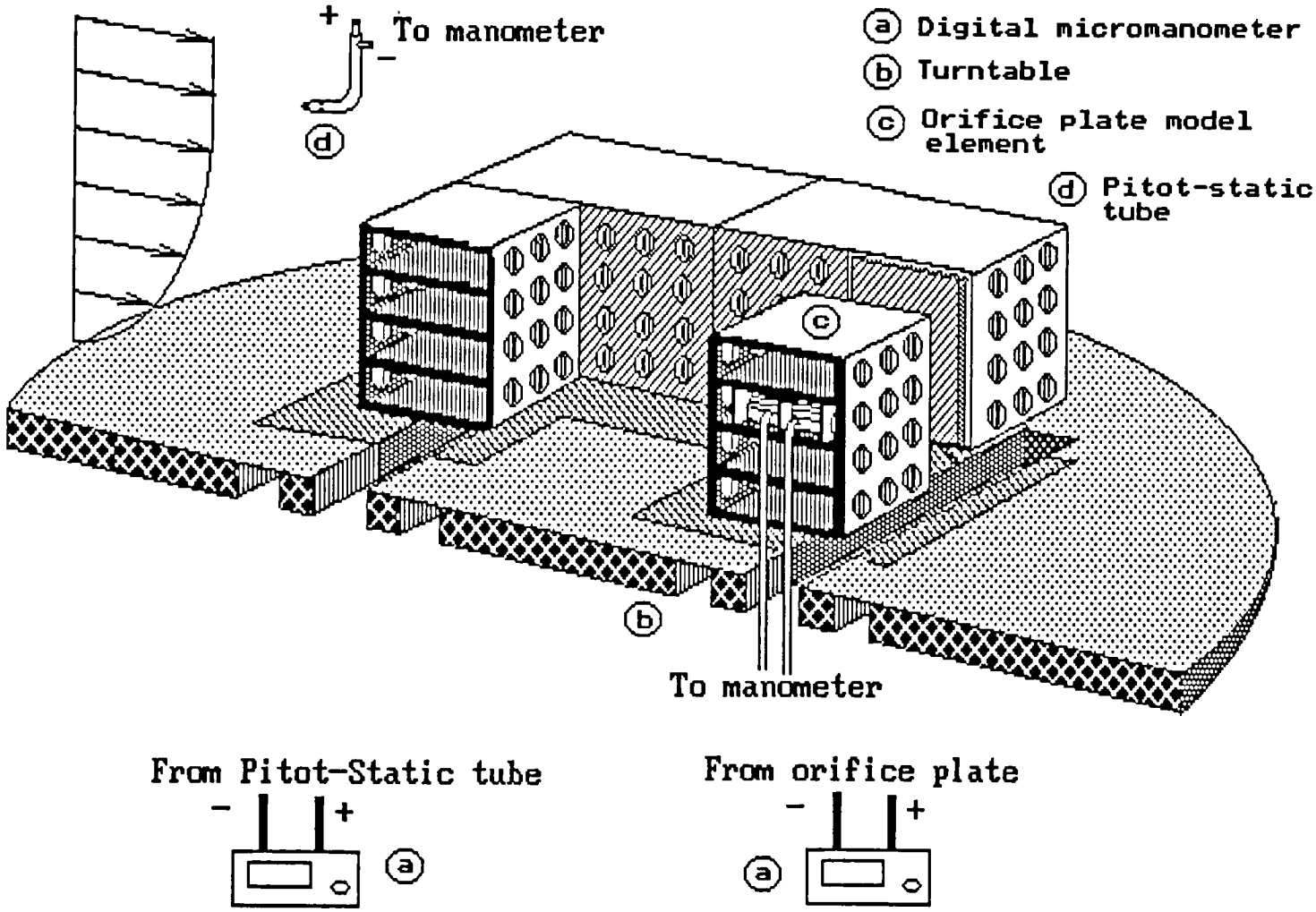

Figure 6.15: courtyard models used for internal flow tests.

Figure 6.16: Photograph of an atrium model used for internal flow measurements in position in the wind tunnel.

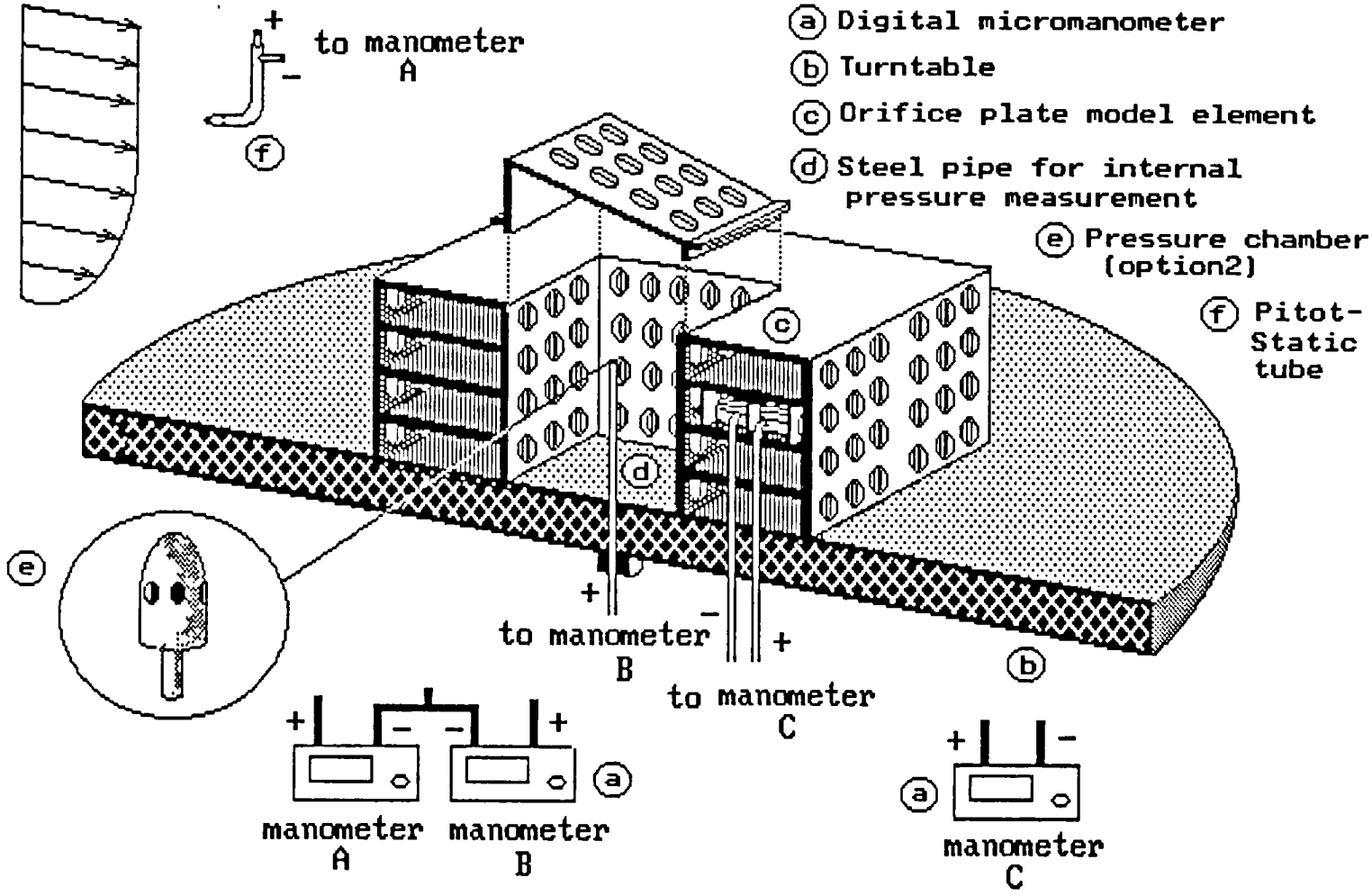

Figure 6.17: Atrium models used for internal flow tests.

defined earlier, but with some modifications. Either its orientation to the wind, its relative porosity or the location of its openings was different from one configuration to another.

Two of this roof-type were constructed. They were made of perspex. One of them had openings located on the vertical surface for which the highest positive pressure could be obtained when facing the wind. In the other roof, the openings were drilled on the sloped surface where suction or near-atmospheric pressure could be found at particular wind incidences. The openings were circular, 10 mm in diameter and identical to the holes on the facades. They were eventually blocked by self adhesive cloth on both inner and outer faces when the porosity of the roof had to be altered. The reason for making two roofs was to reduce the number of vents that would have to be taped when another ventilation mode had to be tested. This would reduce greatly the chances for any undesired leakage.

Instead of dismantling the model to measure the flow at all the measuring locations, the roofs were made removable so that they could face the wind at different angles. They had a base of the same size as the atrium perimeter, with vertical and horizontal edges which allowed the roofs to rest on the top of the atrium and to fit tightly against the inner walls, (see Figure 6.17). This prevented the wind to lift the roofs. A layer of strong adhesive cloth consolidated the attachment. This allowed the roofs to be removed or disposed differently in the various tests. In order to prevent any uncontrolled air leakage, a thin layer of vaseline filled the joints.

Along with the internal flows, the internal pressures in the atria were also measured. A small steel pipe of 2 mm diameter was introduced through the wind tunnel turntable floor in the core of the atrium, (see details in Figure 6.17). The end of the pipe was positioned at the centre of the atrium and at mid-height. Another technique for measuring the ambient pressure in the atrium was to couple the pipe end with a small chamber open to the atrium space by small holes distributed on the horizontal diameter of the chamber. It was thought that the pressure field in the chamber will be more representative of the ambient pressure in the atrium than with the pipe end open directly into the atrium space. Nevertheless, some preliminary tests on an atrium model proved that there was hardly any discrepancy between the two methods. Since the simple open pipe presented less obstruction to the flow, and could be easily removed from the atrium when airflow rates were monitored, this technique was adopted in the subsequent measurements.

6.3.3.3 Fixation to the turntable

When mounted out from their basic elements, the courtyard or the atrium models were then fixed at the centre of the wind tunnel turntable. Each of the elements forming the corners of the models had on their bases a screw bolt which was used to clamp the model to the turntable. A layer of foam sealing strip on the perimeter of the model bases prevented any gap between the turntable floor and the models.

The need to change the size of the courtyard and the location of the orifice plate model elements within the model, while constantly keeping the model at the centre of the wind tunnel, meant that the turntable had to be provided with grooves through which the orifice pressure tappings could emerge and could always be linked to the micromanometers whatever their location.

The ends of the two pipes coming out of the orifice plate were then linked with rubber pipes to a precise micromanometer when the measurements were taken. Otherwise, their leads were blocked with caps fitted in the end of the rubber pipes.

6.3.3.4 Modelling of the urban setting

The last stage of the experimental programme involved internal flow measurements of selected courtyard and atrium models in a large array of buildings. The urban environment was simulated by arranging around the monitored models several rectangular non-porous wooden blocks. The external dimensions, depth (D_b), breadth (B_b) and height (H) were the same as the instrumented models. Nevertheless, to complete the group layout near the wind tunnel walls, other sizes were required. The wooden elements were screwed onto the wind tunnel floor by means of small brackets. The gap between the models and the wind tunnel floor or walls was sealed with adhesive tape.

Upstream to the group layout, the same roughness floor used in the preceding tests was kept. However the fetch of the roughness elements was reduced to accommodate the array of building models. A gap of 120 mm was left between the end of the roughness floor and the beginning of the building group layout.

6.3.4 Measuring apparatus

The pressure differential readings of either the orifice plate or the surface tappings were taken with sensitive digital micromanometers manufactured by Furness Controls Limited. They were FC 012 types of the series, capable of measuring pressure drops up

to 19.99 mmH_2O, with a manufacturer quoted precision of ∓1%. They were fitted with a self calibrating device to ensure compensation from the zero drift but recalibration was recommended before use.

The surface pressure tappings were connected via vinyl tubing to a 20 channel scanning box, type FC 091, from the Furness Controls Limited, that could read up to 20 pressure differential positions without disconnecting the pneumatic couplings.

A Pitot static tube suspended from the ceiling was used to measure the dynamic pressure head at 800 mm above the wind tunnel floor (gradient height) and also the static free stream pressure. The readings were made by another Furness micromanometer, type FC 011, capable of reading a pressure differential up to 199.9 mmH_2O.

6.3.5 Test procedure

6.3.5.1 Internal flows

The models were tested in turn in the wind tunnel. The wind speed at the middle of the turntable and at the gradient height was approximately 25 ms^{-1} when the models were in position. This corresponds to a velocity at the model eaves height of about 16.4 ms^{-1}. Such high air speeds were intended to obtain the highest Reynolds Numbers possible.

To change the size of the courtyard or to cover the internal flow measurements of all the model floors and for all of the measuring locations, the models had to be dismantled and reassembled again. The models were obviously constructed each time with the maximum number of orifice plate elements so as to reduce the number of manipulations. The various atrium models, on the other hand, differed only by the characteristic of their roofs and only the roof had to be manipulated.

To measure the pressure differential across the orifice plates, only one manometer was used. To switch from an orifice plate to another, the pneumatic leads of the first had to be unplugged and their ends blocked, so that the pressure leads of the second could be connected.

The values of the pressures were read directly on the display of the manometer. The maximum, minimum and an estimate of the average pressures were made over approximately 1 minute of almost a continuous reading. Upon switching to a new couple of pressure lines, a delay of approximately 30 seconds was left before starting

the reading to allow the line pressure to stabilize at its new mean value.

The ambient air temperatures and the barometric pressures were taken, along with the internal flow measurements. This was in order to adjust the orifice plate calibration to the change of density which was caused by the heat generated by the wind tunnel motor.

6.3.5.2 Surface pressures

For the measurement of the pressures on the sealed atrium models, the wind tunnel speed was set at 11.3 ms^{-1} at the gradient height, which corresponded to a velocity of 6.8 ms^{-1} at the building wing height. This was enough to ensure Reynolds Number independence of the external flows. The procedure for the reading of the pressure was the same as with the internal flow.

6.3.6 Presentation of the results

The measuring quantities obtained from the orifice plates were pressure drops across the plates. These data were converted into airflow rates using the orifice plate calibration equation (6.11).

The air density during the tests was found to be slightly lower than that when the orifice plate was calibrated (i.e., 1.16 instead of 1.22 kgm^{-3}), as the fan of the wind tunnel generated a large amount of heat. The error introduced by the change of air density was not negligible and was around 1.7%. Therefore the airflow rates had to be corrected to the actual air density.

Since the discharge through an orifice plate is proportional to the inverse of the square root of the density according to equation (6.1), to obtain the flow rates corrected to the actual density, the measured airflow rates were multiplied by the factor $(\rho_0 / \rho_1)^{0.5}$, where ρ_0 is the air density during the calibration and ρ_1 that at the time of the tests. The same correction factor was applied to all the measurements as the conditions of atmospheric pressure and temperature in every tests were similar.

Internal flow coefficients (flow through the facade openings)

The results were then expressed in their final form as a non-dimensional flow coefficient CQ or CQ1 referred respectively to the velocity at the model eaves and at the gradient height and defined as;

$$CQ = \frac{Q}{A \times V_r} \qquad (6.21)$$

or,

$$CQ1 = \frac{Q}{A \times V_{800}} \qquad (6.22)$$

where Q is the measured airflow rates (m^3s^{-1}), A, the area of the openings in one "unit" or room (m^2), (i.e., surface of 3 openings), V_r and V_{800} (ms^{-1}) the reference wind velocities at the model roof eaves and at 800 mm above the wind tunnel floor respectively. Since,

$$\frac{Vr}{V_{800}} = \left(\frac{H}{800} \right)^{0.245} \qquad (6.23)$$

where H is the height to eaves, here 130 mm. It results that;

$$CQ1 = 0.6465 \times CQ \qquad (6.24)$$

The internal flow in a model room, Q, is equal to $A \times V_w$, where V_w is the velocity of the air at the opening level. CQ can also be expressed as,

$$CQ = \frac{V_w}{V_r} \qquad (6.25)$$

and could thus be defined as the ratio of the velocity at the opening level to that at the roof height, and CQ1, to that at the gradient.

The air velocity through each window, or the volume of air passing through a room, can be obtained for other reference wind speeds than that of the present experiment. By multiplying the reference wind speed by the flow coefficient, the air velocity at the building openings is found. The volume of air flowing through each aperture can also be obtained by multiplying the wind speed at the opening level by the aperture surface.

Internal flow coefficients (flow through the atrium roof vents)

The flow coefficient through the roof apertures was defined in a similar manner as the flow through the walls, (see equations (6.21) or (6.22)). However, the flow through the roof was not measured but deduced from the continuity equation;

$$\sum_{1}^{n} Q_i = 0 \qquad (6.26)$$

Where Q_i is the flow through one model opening, assigned with a "+" when the flow enters the building model, and with a "-" when the flow leaves it.

Pressure coefficients

The surface pressures and the internal pressures were presented in the usual dimensionless form, known as pressure coefficients CP:

$$CP = \frac{P - Pst}{\rho \times \frac{V_r^2}{2}} \qquad (6.27)$$

where P is the total pressure at the pressure tapping, Pst the static pressure and V_r the velocity at eaves level.

6.3.7 Modelling philosophy

6.3.7.1 Model scale

The linear scale of the models 1/100 deliberately mismatched the linear scale describing the characteristics of the simulated flow in the wind tunnel, and which was of the order of 1/350, (Lee (1977)). The larger scale used for the models was necessary to accommodate the orifice plate devices and to benefit from larger Reynolds Numbers. The constraints of matching the scale of the model with that of the flow are often relaxed, as it is not known clearly which parameter controls the shape of the flow patterns, (Lee (1977)). In the case of internal flow reproduction, the Reynolds Number independence in the small models is the most critical modelling parameters and for which the greatest attention must be paid.

6.3.7.2 Wind tunnel blockage

The blockage of the models in the wind tunnel did not exceed 4% in the case of courtyards and atria in isolation. However, the blockage was larger when the models were arranged in arrays. It was approximately between 5% and 8% when the wind was normal to the building models, but was up to 11% when the group layout was orientated at 45° to the wind tunnel walls and when it was considered that no gap between the building models could be seen by the oncoming wind. Although this latter value could appear to be above the recommended values, nevertheless, it is believed that the effect on the internal flows would be minor. Indeed, the recommended limits for wind tunnel blockage are based on the effect it has on the pressures forces measured in sealed models. In the present case, the model are porous and small distortion on the pressure field are smeared out. Evidence of this effect was found when the fetch of the group layout was changed and is discussed in Section 9.2.2.

The blockage effect of the pressure surfaces is highly dependent on the characteristics of the wind tunnel, (see Section 5.3.2.4), so that the appropriate correction factor could be known only if the same measurements are made on a representative model arrangement of smaller scale. In the present study it was not possible to reduce the scale without introducing important complications. Because of the above-mentioned reasons, no correction was applied to the internal flow results.

6.3.7.3 Reynolds Number

The most stringent parameter required for the dynamic simulation of the full scale flow is the Reynolds Number independence of the characteristics of the flow, (refer to Section 5.3.2.4). The criteria that could be taken to evaluate the internal flow Reynolds Number independence were the pressure loss coefficient and the discharge coefficient C of the orifice plate.

Cermak et al (1981, 1982) suggested that the flow of air discharging through a window into a room in a form of a jet was fully turbulent when the Reynolds Number referred to the aperture diameter was above 300, (see Section 5.3.2.4). This may be written as;

$$Re_w = \frac{V_w \times d_w}{\nu} \geq 300 \qquad (6.28)$$

since,

$$V_w = CQ \times V_r \qquad (6.29)$$

this leads to,

$$Re_w = 11227.5 \times CQ \geq 300 \qquad (6.30)$$

with $V_r = 16.4\,ms^{-1}$ in the test conditions. Finally, the Reynolds Number independence of the region of the flow at the window level is,

$$CQ \geq 0.03 \qquad (6.31)$$

In almost all the cases, the flow was greater than this critical value.

However, the characteristics of the flow inside model rooms were suggested by Cermak et al (1981, 1982) to be invariable at greater Reynolds Numbers.

From the variation of the discharge coefficient and the pressure loss coefficient shown in Figure 6.5 and Figure 6.7 respectively, it can be observed that the Reynolds Number independence is reached at Re(d) $\geq 2x10^3$ for the pressure loss coefficients,

and Re(o) $\geq 5x10^3$ for the discharge coefficient. Expressing Re(d) and Re(o) in function of CQ, (refer to equations (6.10) and (6.17) for the expression of Re(d) and Re(o) in relation to Q), gives,

$$Re(o) = 19813.2 \times CQ \geq 5 \times 10^3 \qquad (6.32)$$

and,

$$Re(d) = 7558.37 \times CQ \geq 2 \times 10^3 \qquad (6.33)$$

The two expressions lead to almost the same condition: $CQ \geq 0.25$.

Some of the CQ values measured in the tests were below 0.25. In these circumstances, it was expected that these values would be overestimated when compared to a fully turbulent flow, (i.e., full scale conditions). This is because the model resistance to the flow was lower at Reynolds Numbers below the critical values than above, and also, because the discharge coefficient of the orifice plate was higher in the first case than in the second. The decrease of the pressure loss coefficient and the increase of the discharge coefficient at Reynolds Numbers below the critical values would probably lead to an overestimate of the actual flow coefficient of the order of 12%, (refer to Section 6.2.2.3).

6.3.8 Level of accuracy

The accuracy level of the surface pressure measurements depended mainly on the fluctuation from the mean values, which was dependent on the zone of flow where the pressure tappings were located. On the walls, the fluctuation in the pressure coefficient was typically ∓ 0.02 to ∓ 0.05 which corresponded on average to $\mp 3\%$ to $\mp 6\%$ from the mean. On the roof, the mean value of pressure coefficient was within $\mp 7\%$.

The error in the internal flows was estimated to around 10%. The pressure drop across the orifice plate was typically varying within ∓ 0.5 mm of water. For the highest flow coefficient values, which were recorded at 0° wind incidence, this represented an error of only 4% of the mean. At an oblique wind angle, the mean flow coefficient values were lower, and the error was then estimated to be approximately 10%.

A comparison between the values of the internal flows measured at symmetrical locations indicated in general a good agreement, except for the rooms which were

orientated near-parallel to the approaching wind, in which case, there was a very poor coincidence. In these circumstances, the flow was very weak and possibly largely driven by turbulences and pulsating flows. When repeating the experiment, it was found that very small changes in the model orientation could result in very large discrepancies in the readings of the pressure drop through the orifice plate. This was particularly true for the deepest models in the downstream half region. This critical region of the flow could correspond to the point of reattachment of the external flow, and which may be sensitive to small misalignment. Although more care was taken in ensuring that the models were always correctly aligned, the error in the flow was estimated to be of the order 25% of the mean values.

Concerning the atrium tests, the deviation from the mean of the pressure differential through the orifice plate was smaller, in general, (typically 8% of the mean values). Since the flow was proportional to the pressure drop to the exponent of 0.465, it resulted that the accuracy of the flow was of the order of 4%.

6.3.9 Test programme

6.3.9.1 Courtyards in isolation

The range of parameters involved in the problem of ventilation in courtyard buildings is very wide and the need for a systematic approach to cover and analyse the effects of various parameters was imperative. This was lacking in most of the reviewed related literature, in which the cases tested were too individual to draw generalised descriptions.

The variables involved in the ventilation conditions of courtyards could be grouped into three;

a) The physical characteristics of the body which could be subdivided into, i) the shape of the building and its external architectural features, ii) the location, size and shape of the openings and, iii) the configuration of the rooms.
b) The configuration of the site.
c) The characteristics of the incoming wind, which are: i) the velocity characteristics, and ii) the turbulence level.

The ventilation conditions in the models are furthermore dependant on the

dynamic properties of the fluid, particularly, the ratio between the inertial and viscous forces expressed in terms of Reynolds Numbers.

In order to reduce the variables to a sizeable number, the geometry of the courtyard was confined to the rectangular shape. For all that, the variables involved include the courtyard depth, D, the courtyard breadth, B, the courtyard height, H, and the width of the spaces surrounding the courtyard, W_{r1} to W_{r4}, inclusive. The depth and breadth of the models refer respectively to the dimension in the direction of the wind and transverse to the wind, (see Figure 6.18).

The dimensions of the rooms organised around the courtyard were fixed to an average office size at the scale, (i.e., 10 m deep). The porosity and the resistance to the flow were also kept constant and constitute a set of reasonable values. The height of the buildings was the same and represented, to scale, four storeys.

The dimensions that were changed, namely the depth and breadth of the courtyard were selected among the most widespread cases, although it is recognised that the range extends wider. They were changed from 0.5H to H and 1.5H. Larger sizes were not tested for the reason that the courtyard would extend beyond the tunnel turntable borders and would create an excessive wind tunnel blockage.

The incidence of the wind was examined. The models were rotated from $\theta = 0°$ to $\theta = 180°$ by increments of 30° and 45° to cover all the room locations with a wind incidence of 0°, 30° and 45°. Moreover, in order to account for any asymmetry of the flow in the wind tunnel, the models were also rotated at angles $360° - \theta$, and the average of the two measurements was taken. It was found after the analysis of the results that a reasonable symmetry existed.

Table 6.2: Variables examined in the isolated courtyard tests.

Relative courtyard depth	D = 0.5H, 1H, 1.5H
Relative courtyard breadth	B = 0.5H, 1H, 1.5H
Relative courtyard area	$0.25H^2 < \text{Area} < 2.25H^2$
Wind orientation	$0 < \theta < 360°$ by increment of 30° and 45
Incident flow	Atmospheric boundary layer exponent of profile $\alpha = 0.245$

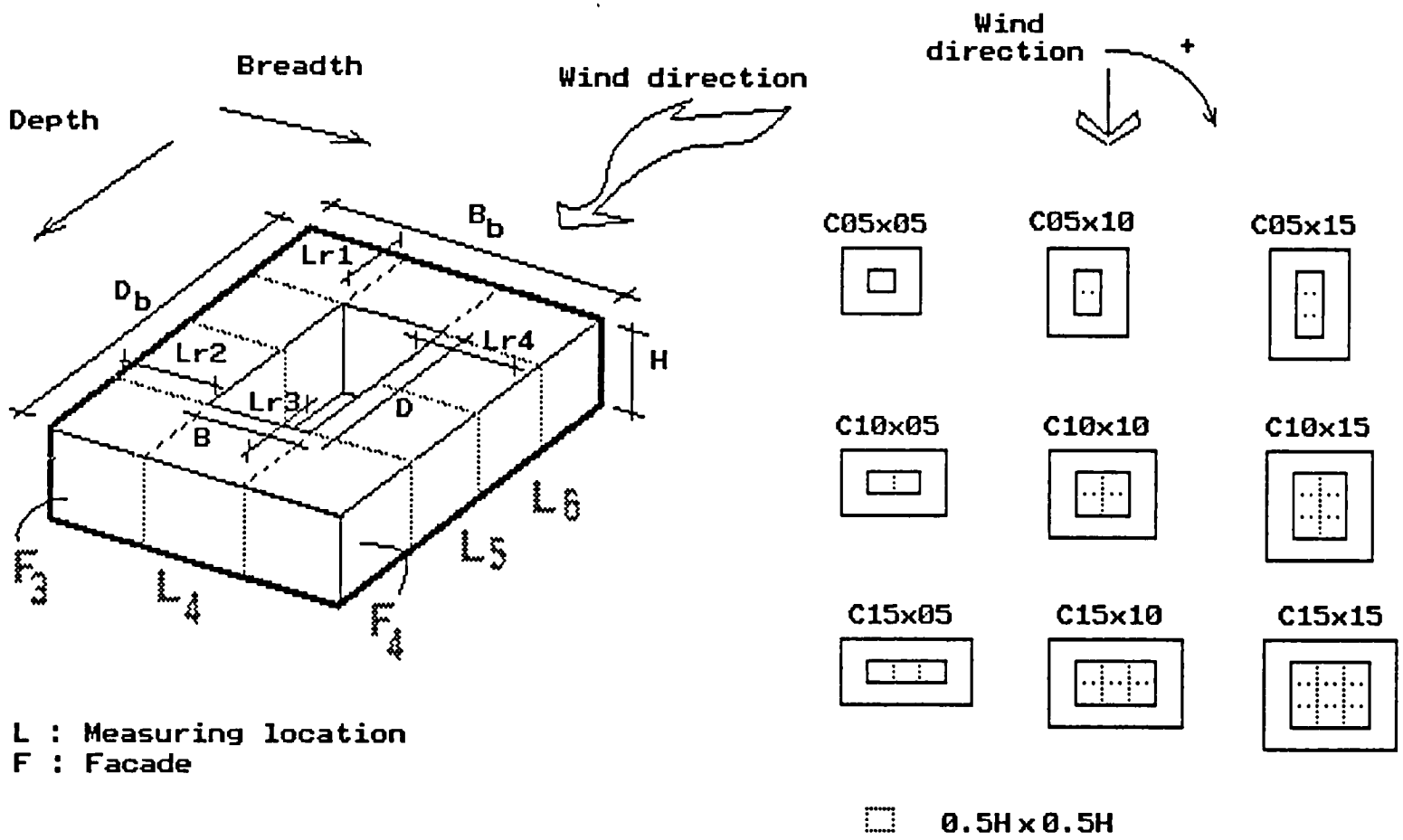

Figure 6.18: Courtyard test programme.

The velocity profile of the wind tunnel boundary layer flow could be considered as appropriate to the site where these building types are commonly found. The range of variables tested is given in Table 6.2.

6.3.9.2 Atria in isolation

The atrium configurations tested differed from one and the other by the number and location of the openings on the roof and the orientation of the roof surfaces to the wind.

The roof porosity is an important parameter that controls the influence of the roof pressure forces. This effect was tested on the model exploiting the roof suction strategy only. The number of open roof apertures was either 8, 16, 24 or 64, which correspond respectively to a porosity of 3.8%, 7.6%, 11.4% and 30.4% relative to an atrium facade area. For the other ventilation modes the roof permeability was fixed. For the near-atmospheric pressure mode, (i.e., when the roof openings were located in a near-atmospheric pressure field, in which case the air at the roof level was expected to enter and leave through the roof openings), the relative roof permeability was 30.4%. In the positive pressure mode, (i.e., the roof openings were located in a positive pressure region, in which case the air at the roof level was expected to be deflected inside the atrium), the relative roof porosity was 11.4%. In the latter case, the relative porosity tested was limited by the available roof surface exposed to positive pressure fields.

In order to cover the measurement of the internal flows for 0°, 30° and 45° wind angles, the models had to be rotated from 0° to ∓30° and ∓45°. Moreover, the roof had to be turned in relation to the orifice plate position, from 0° to 360° by step of 90°. This allowed to cover for half of the measurements. The remaining ones were deduced from the model symmetry. This was possible since, from the courtyard tests, it was learnt that there was a fair symmetry of the flow in the wind tunnel.

Table 6.3: Variables examined in the isolated atrium tests and model indices.

Mode	Suction (-)	Positive (+)	Atmosph (∓)	Closed roof	Without roof
Roof porosity 0% 3.8% 7.6% 11.4% 30.4%	 A2 A3 A4 A5	 A6	 A7	 A1	 C10x10
Wind orientation Incident flow			θ= 0°, ∓30° and ∓45° Atmospheric boundary layer exponent of profile α= 0.245		

6.3.9.3 Courtyards and atria in congested urban sites

The ensemble of the parameters involved in this experiment are shown in Figure 6.19 and are summarized in Table 6.4. They are as follows:

i) The clear spacing between the buildings in the wind direction was either 1.5H or 2.3H.

ii) The building group pattern was either, (a) normal or, (b) staggered.

iii) The building group layout size R, was varied from 4.9H to 14.7H, to test the effect of the fetch on the flow coefficients. It was fixed to 14.7H in the subsequent experiments, (H is the model height).

iv) The incident flow was shear.

v) All the models of the group layout, including the instrumented model, were facing the wind with an angle ϕ equal to 0° or 45°.

vi) The models tested for the shielding effect of the group layout were the courtyard model C10x10, the closed-roof atrium A1, two atria exploiting the roof suction, A4 and A5, with a relative roof porosity P= 11.4% and 30.4% respectively, and the models A6 and A7 exploiting respectively the positive pressure or the near-atmospheric pressure field acting on the roof.

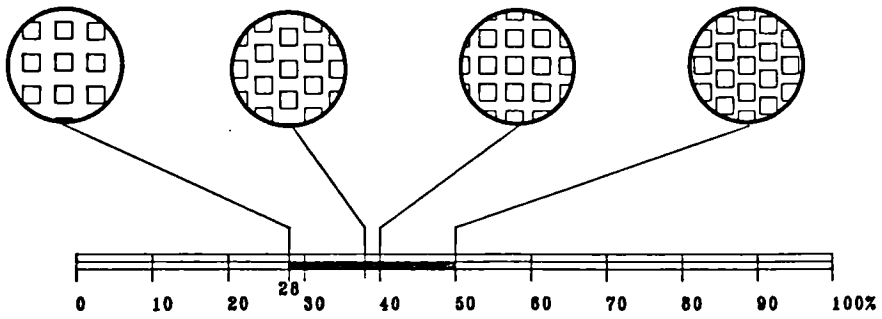

○ Group density

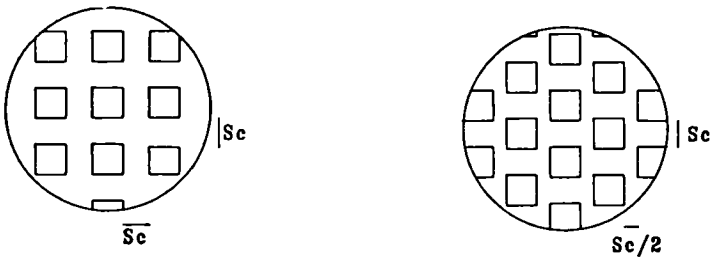

○ Layout pattern

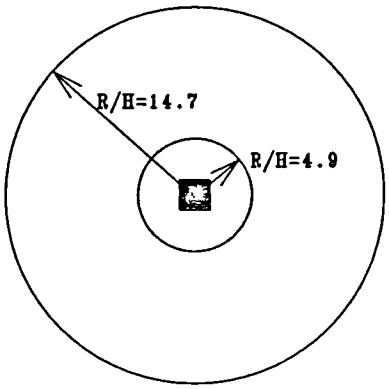

○ Layout size

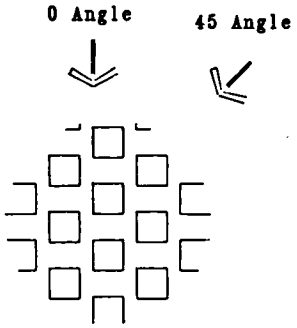

○ Incident flow direction

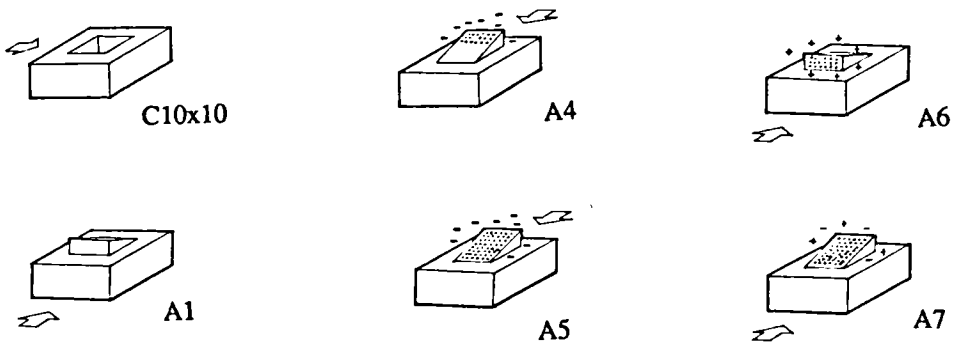

○ Model type

Figure 6.19: Experimental programme for ventilation test of courtyards and atria in urban sites.

Table 6.4: Variables examined in the tests of courtyards and atria in shielded conditions.

Plan area density	PD= 28% to PD= 50%
Clear spacing between elements (upwind)	Sc= 2.3H or Sc= 1.5H
Layout pattern	Normal or staggered
Orientation of the group layout to wind	ϕ= 0° or 45°
Incident flow	Atmospheric boundary layer exponent of profile α= 0.242
Models tested	C10x10, A1, A4, A5, A6, A7

6.3.10 Limitation of the study

The variables involved in the experiment were numerous and a systematic approach was adopted. Nevertheless, the sizeable number of parameters could not cover the range of courtyard and atrium configurations and sites that could affect the ventilation. The geometry of the buildings were kept as simple as possible, and, in particular, no protuberance at the roof were introduced in the courtyard models although it could affect significantly the flow pattern inside the court, (see Section 4.2.5). These limitations obviously narrowed somewhat the field of application of the results and precluded any extended generalisation. As in many studies dealing with architectural aerodynamics, the extrapolation of the results should be made with care as sometimes architectural details can alter significantly the pattern of the flow.

6.4 Conclusion

In the previous chapter, an orifice plate incorporated in a model floor was presented as a very advantageous alternative to other measuring techniques for wind tunnel ventilation tests. In this chapter, the construction of the models and the orifice plate devices were described. The preliminary tests and calibration against a master flowmeter have shown very good accuracy of the device.

As discussed in the previous chapter, the concern was the excessive resistance that

the orifice plate could have on the flow through the models. However, it was found that this was of the order of 1/10 of the overall resistance of the models and was believed to be less than that of the partitioning of rooms and office spaces in reality.

The modelling criteria of the internal flow was based on the Reynolds Number independence of some flow characteristics, such as, the pressure loss coefficient of the models and the discharge coefficient of the orifice plate. For internal flow coefficients, CQ, below 0.25, Reynolds Number independence was not achieved, implying that the flow may not be fully turbulent. In these circumstances, it is possible that CQ would be overestimated by some 12% from the case where the flow was Reynolds Number independent, i.e., the full scale conditions. Nonetheless, the internal flow results presented in the subsequent chapters were not corrected to account for these possible departures.

The analysis of the experimental results are presented in the three subsequent chapters.

Chapter 7:

Ventilation conditions of courtyard buildings in isolation

7.1 Introduction

As evidenced from the literature review in Chapter 4, there is very limited guidance for estimating the likely ventilation in courtyards. The previous related works were found to be often lacking a systematic approach to the problem, which involves numerous parameters, and the cases treated were, most of the time, too individual to draw generalised descriptions.

There were however some common findings between these works. For example it was agreed that the most difficult situations in which to achieve adequate ventilation were that of the downwind wings of the building. The geometry of the courtyard might improve these conditions by increasing the separation between the obstructing and obstructed wings. Also, the penetration of the airstreams in the courtyard which promoted the ventilation seemed to be facilitated when the buildings were orientated obliquely to the wind. Nonetheless, the extent of the improvement of each of these parameters were so far not well established.

As described in the previous chapter, (see Section 6.3.9), the test programme of courtyards in isolation involved the investigation of the effect of the courtyard geometry and the orientation to the dominant winds. Surface pressure measurements and internal flow measurements were carried out.

7.2 Surface pressure results

This test consisted of measuring the pressures on the central axis of the courtyard walls. The pressure coefficient data obtained was envisaged not only to enable comparison with other works, but also, to facilitate the interpretation of some of the internal flow results. This pilot study also enabled familiarisation with the wind tunnel measuring techniques.

Available data

Very few pressure coefficient data are available for courtyard structures. Consequently, pressure coefficients on the external walls are often dealt with as those of a building of the same dimensions but without the courtyard void, (see Newberry and Eaton (1974)). It is nevertheless unlikely that the flow patterns with the separation and reattachment regions, and thus the pressure fields, would remain unchanged with and without the presence of the courtyard.

The pressure data on the courtyard walls are also very reduced and are suggested to be conditioned by the pressures on the roof. One single value is generally adopted for all the inner walls, (see Newberry and Eaton (1974)).

Test programme and terminology

The experimental arrangements of the pressure measurement tests and the test programme were already presented in Chapter 6. In the following discussion some specific terms will be used and are now defined.

i) The depth of the courtyard, D, is the courtyard dimension in the direction of the wind.
ii) The breadth of the courtyard, B, is the courtyard dimension in the transverse direction of the wind.
iii) The sectional aspect ratio, SAR, is the ratio between the courtyard depth, D, and the wall height, H.

The different models are designated with a "C" (for Courtyard), preceded by the product of two numbers, the first referring to the courtyard breadth and the second to the courtyard depth. For example C05x10, is the courtyard having a breadth equal to

0.5H and a depth of 1.0H.

7.2.1 Pressure magnitudes

7.2.1.1 On the outer walls

The pressures were measured on the central axis of the courtyard, on both the external walls and the courtyard faces. The values were converted into pressure coefficients, related to the velocity at the roof height and termed CP. The integration of the values on one face of each model yielded to an average pressure coefficient for this face.

The change of the average pressures on the external walls with the change of the courtyard area, and for different incidences of the wind, is shown in Figure 7.1. The main results are as follows;

Outer upwind walls

As the dimensions of the building were changed, the pressure coefficients on the upwind external walls were found to vary. This could be expected since the dimensions of the model faces presented to the wind were changed, and this have resulted in different external flows and thus dissimilar pressure forces.

The highest pressures on the windward faces were found in the model with a sectional aspect ratio, SAR= 1, (model C10x10), and the lowest values, at the two largest models, (models C15x15 and C20x20). This behaviour may be explained by the fact that, with wider facades, the air may tend to flow over the roofs instead of along the faces creating less stagnation.

Outer downwind walls

On the side wing of the models that made an angle of 90° or 120° with the wind, at 0° and 30° wind incidences respectively, the suction obtained on the central axis tended to decrease with the increase of the model size. One reason could be that, each time the SAR was increased, the measuring point on the face moved away from the upwind edges where separation of the flow is known to occur and at which the suction is maximum.

On the leeward side, the pressures tended to level out at SAR= 1.5. Hussain

(1978) indicated that in simple rectangular building models, once the flow reattaches at the sides and on the roof, the pressures at the leeward face remain constant with the increase of the depth. In the present case, it is possible that the reattachment of the flow at the sides was responsible for the fewer changes on the leeward face for the two largest courtyards.

From this test it was not possible to find out how the presence of the void in the building could affect the surface pressures on the external walls of a building model with no courtyard.

7.2.1.2 On the courtyard walls

Brief recall of the nature of the flow in courtyards

The nature of the flow in courtyards was described in section 4.2.4. This could be briefly touched upon here before broaching the analysis of the surface pressure measurements.

The flow in the courtyard was found to be dominated by a vortex system with its axis horizontal and always parallel to the main air stream. A similar vortex system was also found to govern the flow in two dimensional, (2D), cavities such as grooves, studied by Tani et al (1961), or the 3D flow in streets between buildings in an extensive array, (Soliman (1976) and Hussain (1978)). Soliman and Hussain established an analogy between the two latter flow phenomena. It is likely thus that the analogy could be extended to the courtyard case despite the fact that the courtyard flow is a complex three dimensional system confined between four boundaries, which, in this respect, differs from the 2D flow in grooves or between elements in arrays.

Analysis of the results

In Figure 7.2 the pressure coefficients on the courtyard faces are plotted against the wind angle.

On the face representing the back of the upwind courtyard wing, (i.e., 180° in the graph), a maximum suction was reached when the courtyard depth was equal to the wall height, H. The pressures tended to rise when the model was larger, although the differences were relatively small.

When the face was progressively rotated from the normal wind angle, this trend

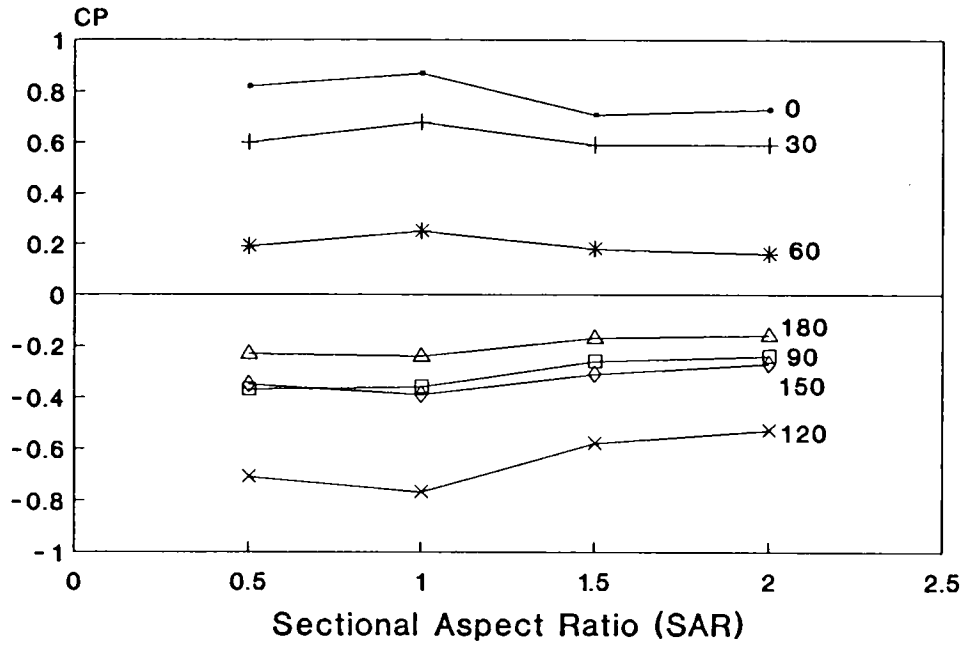

Figure 7.1: Variation of pressure coefficients on the external walls of the courtyard models with changes in SAR, for different wind angles.

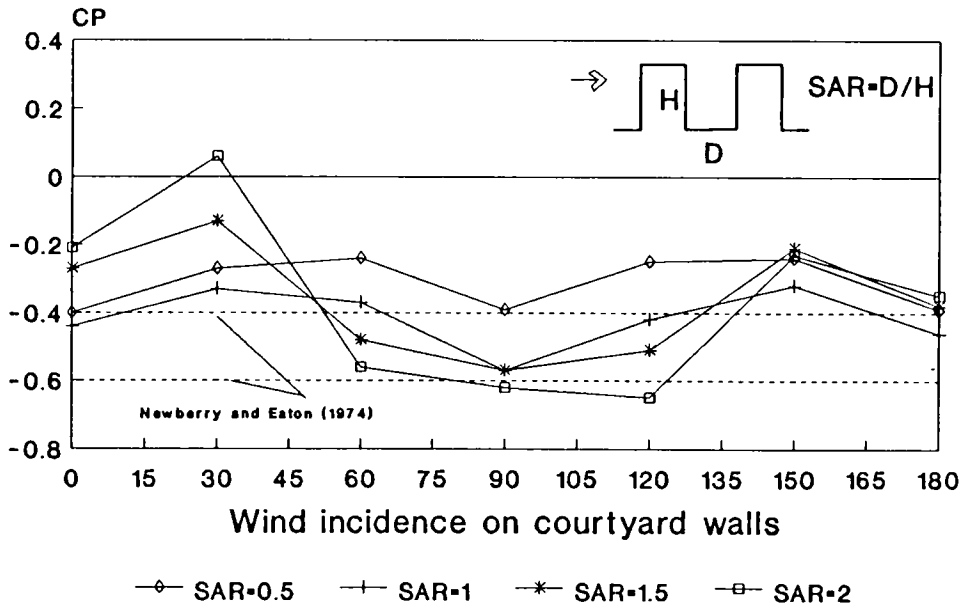

Figure 7.2: Pressure coefficients on the courtyard walls at various wind angles, (measurements taken at the central axis).

was first kept with a rotation angle of 30°, then with a rotation angle of 60° the pressures became generally lower as the model size was increased. At an incident angle of the face of 30° and 0°, (i.e., the wall was then facing the wind), the pressure were found to be the lowest at SAR= 1, and rose significantly with the increase of the courtyard size. At 30° the average pressures were even positive for the largest models.

The rise of pressure on the courtyard wall facing the main air stream with the increase of the courtyard size could be explained by the fact that more air could enter the courtyard and strike the face when the spacing between the courtyard wings was large. In Soliman (1976) and Hussain (1978) studies, the pressures on the upwind walls of elements in an array were also found to rise with the depth of the spacing in a linear fashion within particular flow regimes, (i.e., skimming, wake interference and isolated flow regimes. These were described in Section 4.3.2).

An analogy of the flow with two dimensional grooves (see Tani et al (1961)) could justify why a maximum suction was found on the downwind courtyard wall, (i.e. 180° in the graph), at SAR= 1. Tani explained that at a spacing of 1.4H a stable vortex was initiated in the grooves. When the spacing between the grooves was reduced, the vortex became more vigorous, and at SAR= 0.7H, a maximum suction was obtained on the cavity wall, at the rear of the upwind groove shoulder. The pressures increased again when the spacing was further reduced. Similarly, Hussain (1978) found that the maximum negative values of pressures were found to occur at a critical spacing between elements in a regular array equal to 1H, and Soliman (1976) found the maximum deficit at 1.25H.

The initiation of this stable vortex was indicated to be controlled only by the depth of the cavity, (i.e., groove or streets in an array of building models), and thus it is reasonable to assume that similar phenomena occurred in the courtyard space where the strength of the vortex reached a maximum at SAR= 1.

Two more interesting remarks could be drawn from Figure 7.2. First, the pressures acting on the four faces of the smallest courtyard, at a particular wind angle, were almost the same. As the courtyard area was increased the surface pressures on the four walls diverged. Secondly, the effect of the wind incidence on the pressures of the courtyard walls was most apparent in the largest courtyard models, whereas the pressure fields in the smallest courtyards seemed insensitive to wind angle.

In the courtyard model with the smallest SAR, a slow rotating vortex probably dominated the flow and had little interaction with the flow riding above it. In the larger models, it could be anticipated that some of the flow that separated at the frontal edges

penetrated the court partially, washing down the upwind courtyard wall, and consequently raising the pressures. A more vigorous recirculating vortex was then established, inducing different pressures on the various courtyard walls and also at various measuring levels.

Comparison with available pressure data

From these results a criticism could be made for adopting one pressure coefficient for all the courtyard faces, particularly for large courtyards, as suggested by Newberry et Eaton (1974). Their recommended values of CP for the courtyard walls for wind loading design were -0.4 and -0.6, when H/W $\leq$ 1/2 and H/W > 1/2 respectively, where W is the smaller dimension of the courtyard walls. If there is an asymmetry of the courtyard towards the windward face of the building, then the recommended pressure coefficient could be reduced to -0.7. Finally they suggested that in the case where there is a substantial opening to the exterior, CP should be taken as an intermediate between the closed courtyard values and the CP at the exterior of the throughway.

7.2.2 Vertical pressure distribution

The vertical pressure distributions on both outer and inner walls of the courtyard models are shown in Figure 7.3 for various wind incidences.

On the outer walls

On the outer walls of the models, the pressure distributions exhibited a distinct profile when the walls were facing the wind at normal or 30° angle, and the occurrence of this profile did not depend on the geometry of the model.

This pressure profile had the shape of " S " in which a peak pressure occurred at approximately 2/3 of the model height and the minimum pressures near the roof. At oblique wind angles, however, the shape tended to fade and progressively became a straight vertical line. This profile related the way in which the flow moved vertically along the facades. The maximum pressure corresponded to the stagnation point, where the flow was virtually brought to rest and where all the kinetic energy was converted into pressure head. Above this point, the air was flowing upwards because of the large roof suction. On the lower part a downward flow occurred with increased speed, and thus with a deficit of pressure at approximately the mid-height of the building. This

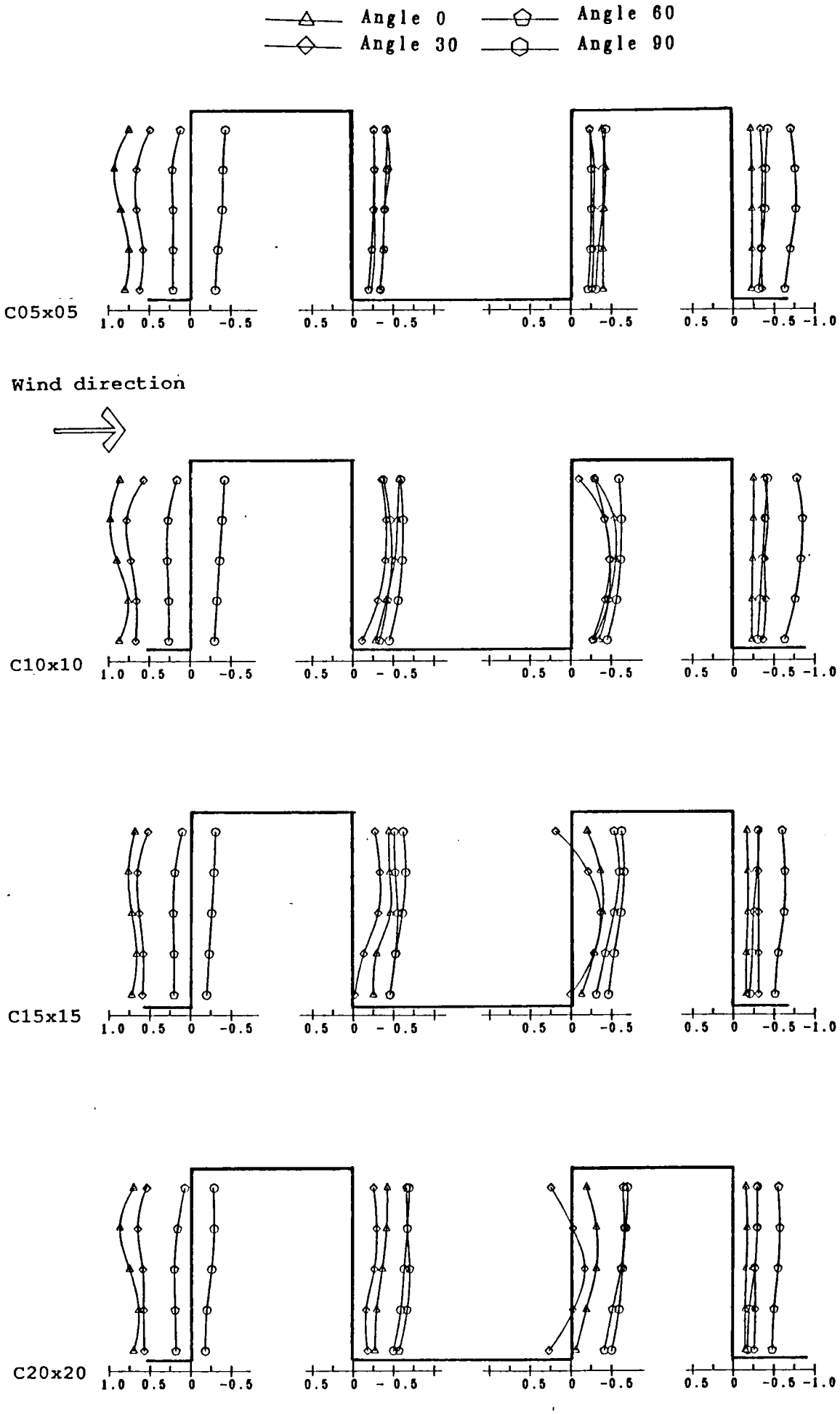

Figure 7.3: Vertical pressure coefficient distribution on inner and outer walls of the courtyard models, (measurements taken at the central axis)

downward movement of air generated some eddy spirals along the face which escaped round the sides. Near the ground, the flow was again retarded with, thus, a recovery in the pressure.

On the external walls located on the lee, the profiles described almost a straight line at any wind angle and irrespective of the model geometry.

On the inner walls

On the inner walls located at the rear of the upwind wing, the profiles could be divided into two sections. The upper halves of the profiles were vertical lines, in almost all the models, while the lower halves were variable. In the courtyard with the smallest SAR, the lower part of the profile was a straight line. With larger SAR, it was rather a concave curve with higher pressures than in the upper sections. The pressure distribution was more uniform when the incidence of the wind on the model was larger than 30°.

On the courtyard wall facing the wind, two distinct profiles appeared as the size of the courtyard was altered. On the smallest model, the vertical pressure distribution was uniform, whereas from SAR= 1, the profile exhibited the shape of a reversed " C ". In the latter case, the pressures at the lowest and the highest measuring locations presented higher pressures than that at mid-height. This profile was most marked at 30°, in which case, pockets of positive pressure were even monitored at the top and bottom of the wall in the two largest courtyards.

Comparison with other related works

An analogy with the nature of flow contained in the spacing between elements, or in grooves, may once again explain the features of the vertical pressure distribution when the courtyard size was altered.

Soliman (1976) and Hussain (1978) obtained similar pressure distributions on the upwind face of an element in a regular array at particular spacing between the elements, (see Section 4.3.2). They explained that, from an element spacing of approximately Sc/H= 2.2 to 3, the flow around the elements started to interact, and a particular flow pattern, called wake interference regime, was established between the elements.

In this flow regime, the pressure profiles exhibited all the same shape of a reverse " C ", at least in the lower 85% of the element heights. This profile was said to relate the way the flow entered the element spacing and washed over the upwind face without any

stagnation point. Near the ground the flow was retarded creating a bubble of high pressure. The shape of the pressure profile could be seen in the work of Soliman and Hussain to blend into a vertical line on the 80% lower section as the spacing was decreased.

Figure 7.4 shows a replot of the pressure profiles of Hussain's work. The ensemble of the profiles obtained with elements of different aspect ratios and for element spacings of approximately 0.5H, 1.0H and 1.5H are presented and grouped according to the element spacing. The resemblance with the present profiles within the same relative height is clear, and this strengthens the hypothesis that the same dominant vortex system was filling the courtyard or the space between buildings in an array, at least, at the central axis of the elements. It should be noticed nevertheless that the variation of pressures along with the vertical wall was more amplified in the present study, and the reason may be that in the case of extensive arrays of building models, the air stream has lost considerable momentum.

As the element spacing was decreased below approximately 1.5H to 1.3H, a different flow, called skimming flow, was identified by Hussain (1978), Soliman (1976) and other authors, (see Section 4.3). In this flow regime the majority of the flow was riding over the top of the buildings causing the trapped air to rotate slowly. On the upwind faces of the elements, the general " C " shaped pressure profile was said to remain, although it could be seen from the graphs found in Soliman's or Hussain's works that the pressure distribution tended to be uniform at the smallest element spacing.

The manifestation of this flow regime, (skimming flow), was spotted by the aforementioned authors from a sudden change in the element drag, as the spacing was decreased. It was suggested also to be detected in the shape of the profile of the rear faces of the elements in the array. Indeed, the shape of the profiles changed from a uniform shape to a shape concave at mid-height. Nevertheless, the initiation of such profiles were not always apparent and could not constitute a criterion to ascertain the change of the flow regimes. Similar trends were obtained in the case of courtyards in the present study. It is thus reasonable to consider that similar changes in the flow pattern may have occurred as the area was diminished. Nevertheless, from the present results there was no indication at which SAR this change occurred from the variation of the profiles in the courtyard downwind faces. But it is likely that with SAR= 0.5, the flow in the courtyard is of a skimming flow type.

At the 30° wind angle, as the courtyard was elongated, more air could be

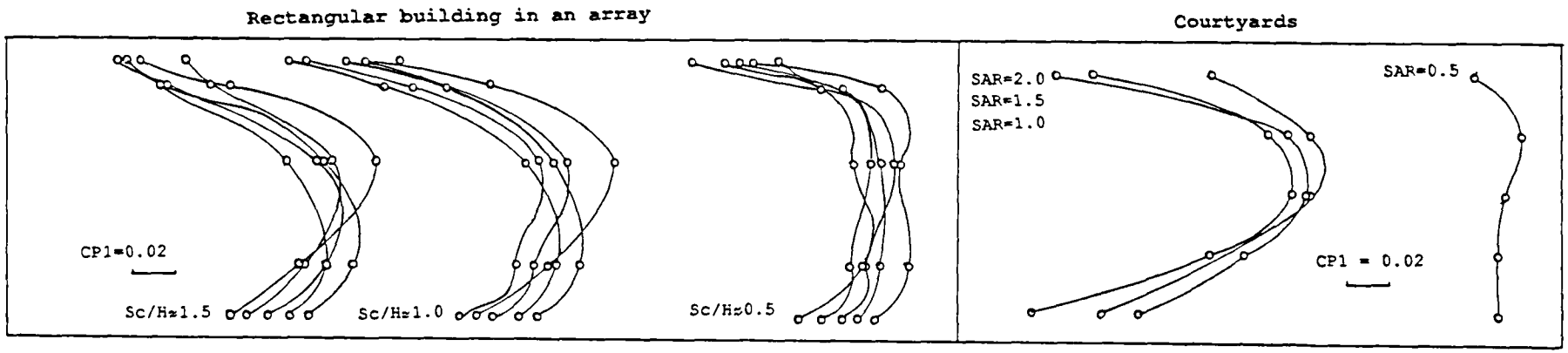

Figure 7.4: Similarities between the vertical pressure coefficient distribution measured on upwind walls of elements in an array and upwind walls of a courtyard.

expected to sink into the courtyard. This could explain why the curvature of the profiles on the courtyard walls facing the wind was more amplified than at 0° wind angle. The description by Ettouney (1973) and Torrance (1966) of the flow pattern in a courtyard space suggested that two horizontal spiral vortices are generated at the upwind edge of the roof and are deflected into the courtyard when the wind incidence is oblique, (see Section 4.2.4). This may be expected to result in a more vigorous vortex activity in the courtyard at oblique wind incidences and could also explain why the vertical pressure gradients were greater in this case than at normal wind angle.

7.2.3 Implications for the ventilation

In Figure 7.5, the overall magnitude of the pressure drop across each wing of the courtyards, and for incident winds of 0° and 30°, is plotted against the courtyard sectional aspect ratio, SAR.

It can be noticed that for a wind angle of 0° or 30°, the magnitude of the pressure drop across the four wings of the models were very dissimilar irrespective of the model geometry. The ventilative driving forces were much larger on the upwind wings than on lateral or leeward wings for which the problem of lack of sufficient air movement could arise. In most of the wings of the building models, the cross ventilation could be altered by both the geometry of the courtyard and the incidence of the wind.

Influence of the wind incidence and the courtyard geometry on the magnitude of the pressure differentials

Upwind wings: It can be noticed that, on the upwind wings, the pressure differential, and thus the driving forces for ventilation, decreased with the increase of the wind angle of attack irrespective of the courtyard geometry. Although the model with SAR= 1 presented larger potential for cross-ventilation than the other models, the effect of changing the courtyard size was generally less than that of changing the wind incidence.

Downwind wings: On the other hand, on the downwind faces, the size of the courtyard played as large role as the wind incidence. In this case, variations of the pressure differential with SAR indicated that the smallest courtyards would be slightly better ventilated than the larger ones at normal wind angle, at least at the central axis where the measurements were made.

When this building wing made an angle of 30° with the wind, the larger the

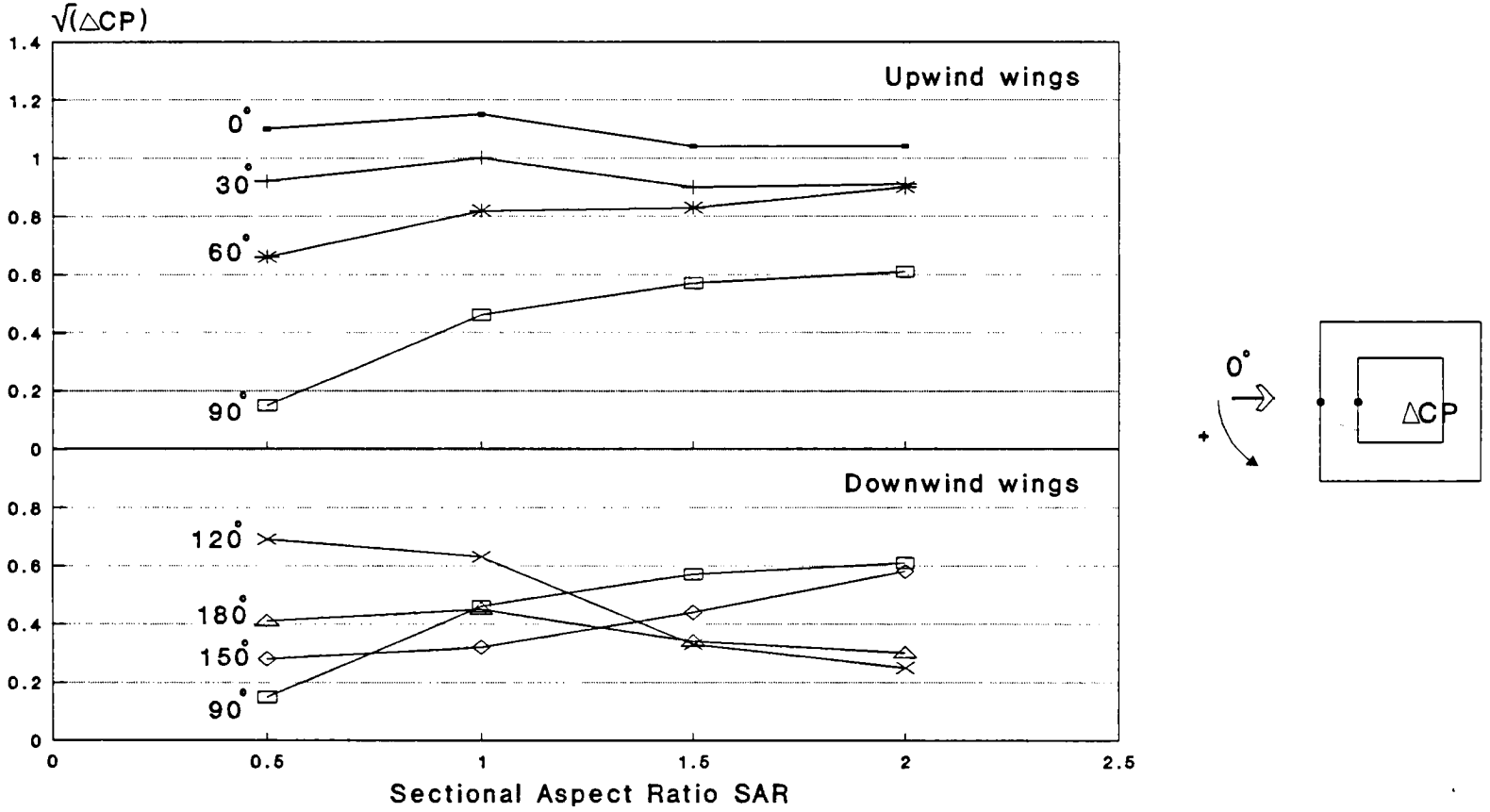

Figure 7.5: Variation in the pressure drop between the inner and outer walls of the courtyard models with changes in SAR.

courtyard the better the ventilation conditions and with a further rotation of 30°, surprisingly, the reversed trend was recorded. Nevertheless, these results were inferred only from the pressure differentials across the central axis of the courtyard wing, and may not reflect the effects of the courtyard size or the wind direction in other locations in the models. In particular, the result may be expected to be very contingent on the position of the measuring pressure tappings with respect to the front of the main vortex which governs the flow in courtyards and which have its plan parallel to the wind direction.

Vertical flow distribution

The vertical distribution of the pressure differential can be seen in Figure 7.6 to be largely dependent on the courtyard geometry at the leeward wings but less at the upwind wings.

The pressure differential profiles on the leeward wings were also affected by the wind incidence, yet, this was very noticeable for courtyards with SAR ≥ 1, but not for lower SAR.

Upwind wings: The profiles can be observed to reflect the pressure profiles shown in Figure 7.3. The " S " shape profile characteristic of wings facing the wind can be seen to fade progressively as the wind incidence diverged from 0° angle, and became slightly curved at 60° wind angle.

The pressure differential which were positive for angles up to 90°, indicated that the air would flow at this location from outside to the courtyard if openings were provided.

Leeward wings: On the leeward wings, the profiles changed progressively from a uniform distribution in models with the smallest courtyard sizes to a " C " shape in bigger courtyards. This latter shape was strongly marked at 30° wind angle. This profile tended to blend into a straight line when the wind angle was beyond 30°.

At 30° wind angle, and for the courtyard models with SAR ≥ 1, the pressure differentials on the downwind wings were negative on the lowest and highest levels, and positive at mid-height. This indicated that the air on the extreme floors would flow from the courtyard to outside, (i.e., in the direction of the main air stream), if apertures were provided and would flow in the opposite direction at the mid-height levels.

At 0° wind angle, the pressure differentials indicated the same opposite flow directions, yet, occurring only at the largest models. Nonetheless, in the smallest

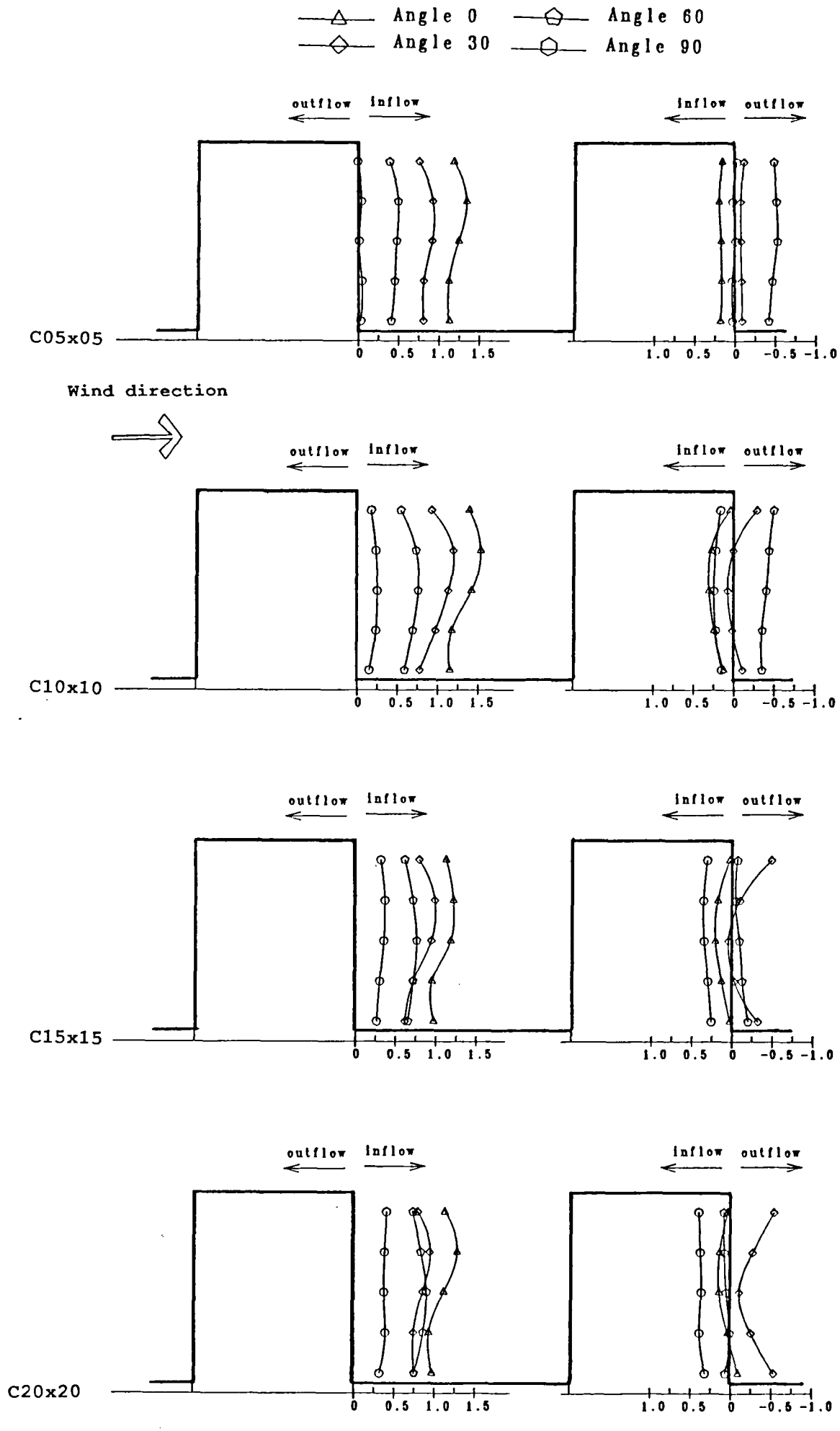

Figure 7.6: Vertical distribution of the pressure differentials across the model wings.

courtyard models, the inflows, (i.e., from outside to courtyard), were very weak on the extreme levels and much stronger at mid-height.

7.2.4 Summary of the surface pressure results

The pressures that acted on the different courtyard walls were far from being uniform except when SAR ≤ 0.5. In particular, at non-normal wind incidence, positive pockets of pressure were obtained at the top and bottom of the upwind courtyard walls, whereas in the remaining walls the pressures were below atmospheric. These high pressures were probably caused by a partial penetration of the flow riding above the courtyard and which was eased by the downward movement of two spiralling vortices generated at the roof leading edges.

A comparison with works made on flow in building layouts or in grooves established an analogy between the nature of the flow in these cavity types and that in courtyards. The works of Soliman (1976) and Hussain (1978), in particular, could provide some explanations to the trend recorded in the average wall pressure coefficients. From these works, it could be inferred that probably the flow pattern in the three largest courtyards was characteristic of the wake interference flow regime, and was of the skimming flow type in the smallest courtyard. In the first case, some of the air flowing over the roof was probably entering the courtyard and was washing over the upwind walls of the courtyards. In the second case, the flow in the courtyard was probably dominated by a slow rotating vortex which had few interactions with the flow riding over the roof. Evidence of these flow patterns were particularly apparent in the vertical pressure profiles.

The analysis of the pressure differentials suggested that both the geometry of the courtyard and its orientation to the dominant winds could alter the internal flows.

The tests so far were conducted on sealed models. These tests were very informative, yet, it was expected that the technique was not accurate to infer the actual ventilation conditions in buildings with largely open windows, and which is the most probable situation encountered in warm and humid summer weather. The ultimate tests were conducted on porous models where actual internal flow measurements were made. This is now discussed.

7.3 Ventilation conditions in the courtyard building models

In Figures 7.7 to 7.9, the detailed results of the flow coefficients, CQ1, obtained at

Figure 7.7: Detailed distribution of flow coefficients within the courtyard models in isolation, (0° wind incidence).

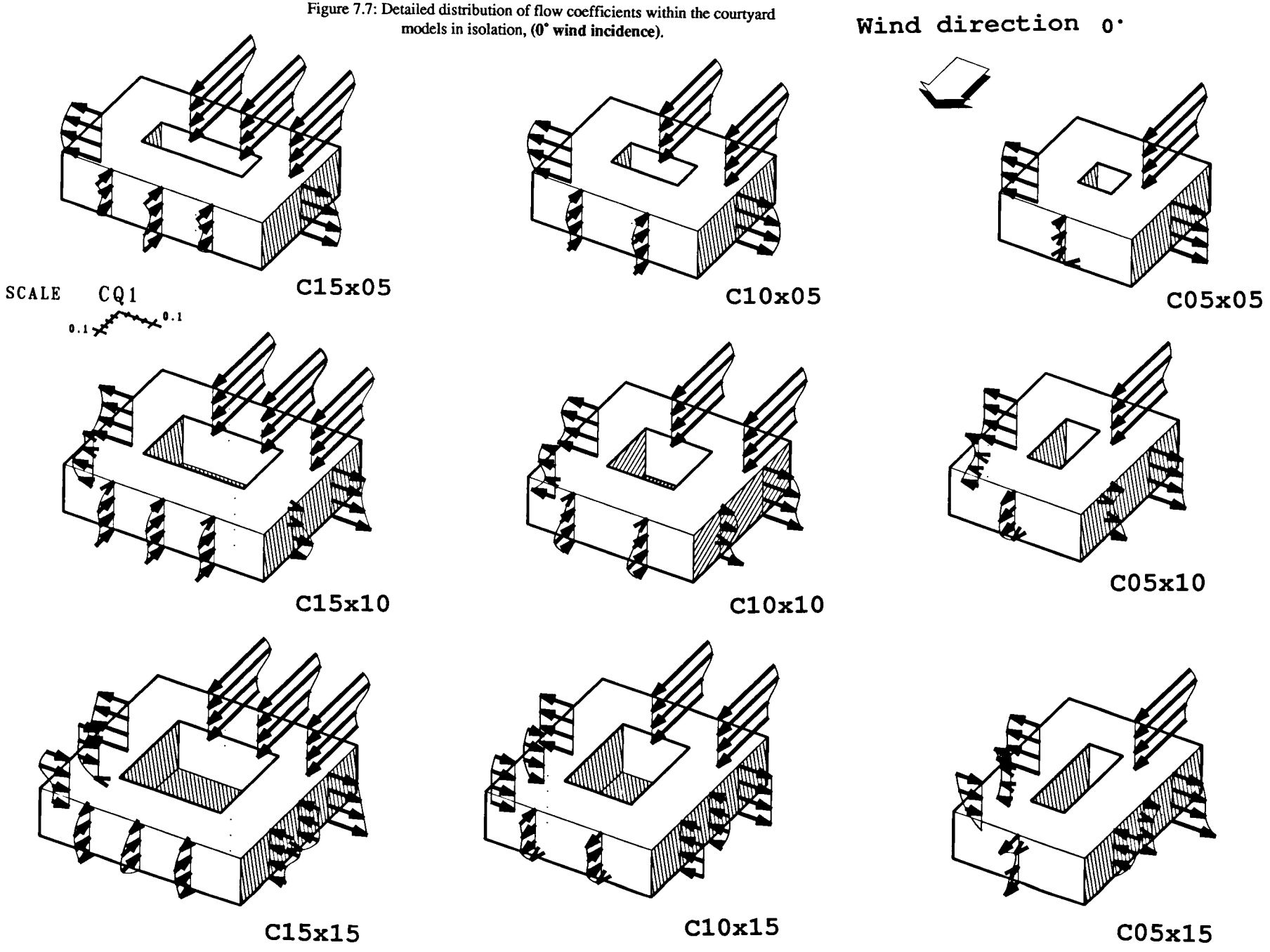

Figure 7.8: Detailed distribution of flow coefficients within the courtyard models in isolation, **(30° wind incidence).**

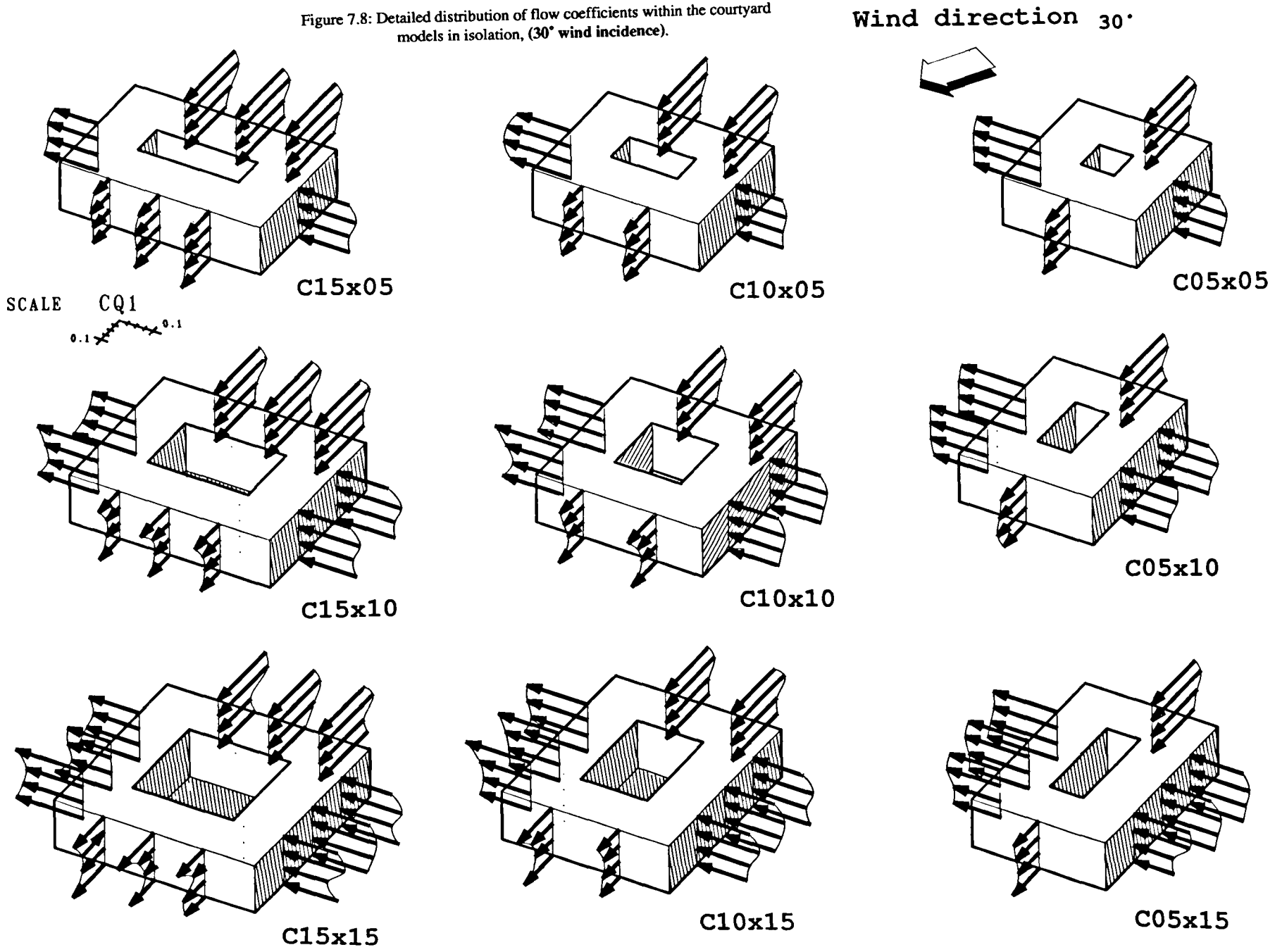

Figure 7.9: Detailed distribution of flow coefficients within the courtyard models in isolation, (45° wind incidence).

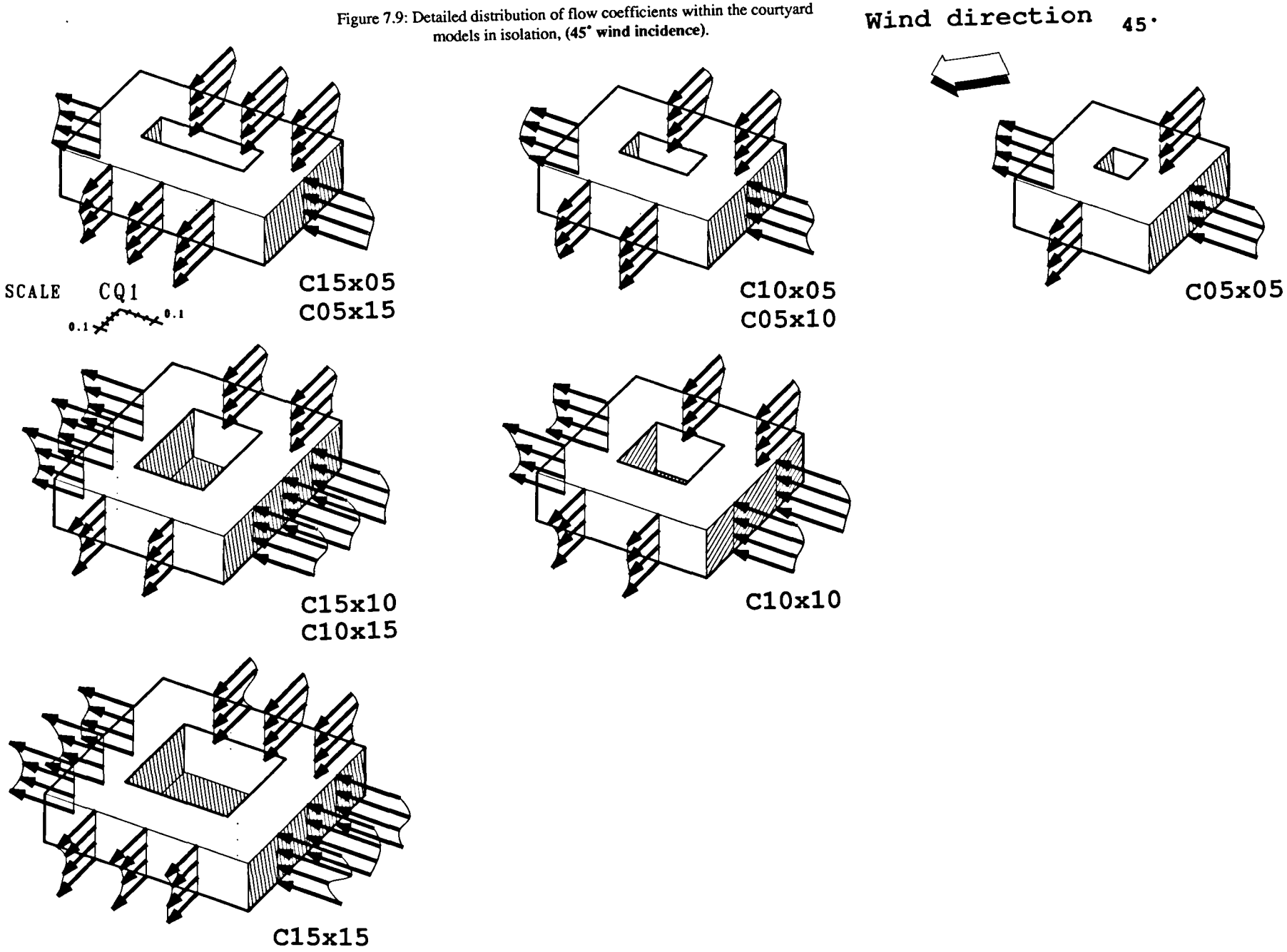

each measuring location and for the whole range of the courtyard structures tested at 0°, 30° and 45° wind incidences are given. The associated data can be found in Appendices B1 to B3. CQ1, and CQ, were already defined in Section 6.3.6 and represent merely the ratio between the air velocity through the model openings, and the wind speed at the gradient height and the model height respectively.

The test programme was already given in Section 6.3.9. The following discussion will refer to Figures 7.7 to 7.9, unless specified otherwise.

7.3.1 Models orientated normal to the wind

The magnitude, the distribution and the direction of the internal flows were diverse from one courtyard model to another, but most of all from one courtyard wing to another. Irrespective of the courtyard sizes, the windward wings were found to be generously ventilated and contrasted greatly with the very weak airflows found in the downwind sides.

Upwind wings

On the upwind rooms, the flow was directed inwards, (from outside to courtyard), and the intensity of the coefficient CQ was between 0.39 and 0.51, depending on the model geometry and the floor level, which means in order words that the velocity of the air at the opening level was 39% to 51% of the stream at the roof height.

Leeward wings

In contrast, on the leeward facades, the flow was found to be very weak with flow coefficients, CQ, never exceeding 0.16. Occasionally CQ was found at some discrete point to be even nil. This does not mean that no air was flowing through the model rooms, but that the instantaneous flows, (positive when an inward flow and negative when an outward flow), averaged over the recording time was nil.

The direction of the flow on the leeward wing was diverse, changing with the courtyard geometry and with the horizontal and vertical measuring location on the facade. In some cases, the indoor flow was found to travel in the opposite direction to the wind.

Lateral wings

On the lateral wings of the courtyard model, the magnitudes of the indoor flows and their directions depended on the measuring location on the facade and also on the courtyard geometry. On the most upstream points of the facades the internal flows were outward irrespective of the courtyard geometry. The intensity of the flow was then moderate, CQ was between 0.13 and 0.20. Further downstream, the flow was significantly weaker, (CQ was between 0.01 and 0.11), and the flow direction was different from one model to another, and sometimes between one floor height and another. Finally, on the most downstream measuring location and on the deepest models, the flow was almost equally weaker than in the latter case. Nevertheless the flow direction was generally inward.

7.3.2 Models orientated at an angle to the wind

When orientated 30° or 45° to the wind, the rooms of the courtyard models were more evenly ventilated than when the wind direction was 0°. In particular, the flow on the downwind sides were much stronger in the first case than in the second.

Although the magnitude of the flow at discrete points differed from one model to another, the discrepancies were smaller than at 0° wind angle and the direction of the flow was always the same.

Upwind wings

In the upwind rooms of the models, the air was entering from the external facade openings and was leaving through the courtyard apertures. The indoor air velocity depended then on the location of the room on the facade and on the angle the face made with the wind.

In general, it could be said that the internal flows in the upwind rooms were greater when the angle between their facade and the wind was closer to the right angle. Also, the ventilation was better in the most upstream rooms than downstream. For instance, when the wind struck the facade at 30° angle, the flow coefficient, CQ, was on average 0.38 on the most upstream measuring location and 0.36 on the most downstream. With a facade orientated 45°, the average CQ value at the most upstream location was reduced to 0.32, and down to only 0.24 at 60° wind incidence.

The flow magnitude gradient that existed between the most upstream and the most downstream points can be explained by the fact that, on a wall which is orientated

obliquely to the wind, the centre of pressure is asymmetric towards the windward edge. Downstream, along the face, the glancing flow accelerates causing less pressure and thus smaller driving forces for the ventilation.

The fact that the more inclined the model face was, with respect to the wind direction, the lower the indoor flows were, can be explained on the basis of a reduction of the external pressure magnitudes and a reduction of the effective aperture area.

It must be said that oblique wind incidences do not always hamper the cross ventilation, and Givoni (1968) found that, in some window arrangements, even higher average indoor air velocities could be obtained at oblique wind angles. This was particularly true for rooms with two windows located in two facing walls. In the present case, the window arrangement was different to that of Givoni's, in that, several windows were located in each wall. In the present case it is very probable that the air that entered the most upstream openings of the upwind model wings left through the downstream ones without ever flowing through the model. This is because there was a considerable pressure gradient across openings in the same facade.

Downwind wings

On the two downwind facades, the flow was directed outwards. Like on the upwind sides, there was a flow coefficient gradient between the most upstream and most downstream measuring locations.

Generally, the indoor air movement was stronger at the locations close to the upwind edges where the external flow separates. The flow separation is known to be accompanied with large suction which could promote the outward movement of air. However, on the larger models, it happened that the most downwind measuring points recorded larger CQ values. A possible reason for this could be that the flow entering the court hit parts of the upwind faces of the courtyard directly and strengthened the outward flow locally. The evidence of the existence of the flow penetration in the courtyard was demonstrated in the surface pressure tests. The most downwind sectors, being the least sheltered by the upwind model wings, were those which benefited the most from this effect.

7.3.3 Comparison with other relevant works

As evidenced in the literature review in Chapter 4, related works are very scarce.

The experimental wind tunnel study carried out by Givoni (1968) gives some

order of magnitude of the indoor air velocity in cruciform shape courtyard models. The geometry of the models, the characteristics of the approaching wind and the quantities measured diverge too much from the present study to expect any closer comparison with the present study other than an overall order of magnitude.

Givoni's study was described in Section 4.2.3. The measured quantities were indoor velocities in cross-ventilated rooms organised around a courtyard, and were presented as a percentage of the free stream velocity. In the present work, the flow coefficient CQ1 is the velocity at the opening level relative to that of the gradient. For a basis of comparison, this should be converted into indoor average velocity, say, at the entrance of the orifice pipe in the orifice plate unit. This relative air speed can be found to be 48% of the value of CQ1.

Table 7.1 gives a comparison of Givoni's results with the current study. The comparison between the first left columns of the table gives much lower values for the present study than Givoni's. A reason for this could be the different characteristics of the flow upstream to the models. In Givoni's test, the approaching wind was uniform so that, from a small distance above the ground, the maximum velocity was reached. In the present tests, however, there was a vertical velocity gradient. In this case, the approaching wind speed at the model height was much lower than that of the gradient height. For example, the velocity of the approaching wind at the roof level was 64% that of the gradient. When the average indoor was referred to the approaching wind at the opening level, (which was assumed to be the free stream velocity in Givoni's tests), in the left column of the table, a better agreement was obtained.

At 45° wind angle, the average indoor velocities at the upwind rooms were lower than that obtained by Givoni. It is believed that, because of the limited number of measuring points, the value that Givoni presented may not be representative of the average air velocity in the room. Also, as already explained in Section 7.3.2, the fact that the rooms of the present models had multiple windows in each face, (unlike in Givoni's models), some air could have entered and left the model rooms through the same facade and never crossed the orifice plate. This can explain the differences in the internal flow velocities between the two studies. Nevertheless, the two studies showed the same order of magnitude for the indoor air velocities.

Table 7.1: Comparison of indoor air velocities measurements in courtyard types models between the present study and Givoni's (1968). *(W), (L), (S) refer to respectively the windward, leeward and side wings of the models.*

Average indoor air velocity (relative to the free stream)		Average indoor air velocity (relative to the approaching wind)	
Givoni's test	Present test (model C10x10)	Givoni's test	Present test
0° wind incidence			
24.4% (W) 6.0% (L) 5.4% (S)	14.0% 3.0% 4.0%	24.4% 6.0% 5.4%	22.0% 5.0% 6.0%
45° wind incidence			
33.4% 13.9%	9.6% 7.7%	33.5% 13.9%	9.6% 12.0%

7.3.4 The vertical flow profiles

In Section 7.2.2, the observation of vertical pressure profiles allowed to infer the way in which the external flow was travelling in the vicinities of the model walls. When the courtyard geometry was altered, the vertical distribution of the pressures indicated that there were families of profiles that were associated with specific patterns of flow in the courtyard. The manifestation of these patterns were found to coincide with those found in the cavity of grooves or in the spacing between buildings in an array. The vertical distribution of the flow coefficient was anticipated to reflect the various pressure profiles.

Upwind wings

At normal wind incidence and on the windward facades, the profile of all the models fell into the same shape of an " S ". The maximum internal flows were measured at the third floor, with, on average, 15% higher values than the first floor. The weakest flows were at the second floor, with 5% lower values than the first floor. This profile

tended to flatten and blend into a straight line as the incidence of the vented facade with the wind diverged from the right angle. This can be observed in Figure 7.10.

Lateral wings

On the lateral sides, the vertical distribution of the flow was fairly uniform at the most upwind points for all the model considered. Further downstream, the profiles tended to adopt a wavy shape.

Leeward wings

At 0° wind incidence and on the leeward wing, the profiles had either a wavy shape or a virtually straight vertical line in the smallest courtyard models. In the deepest models, with D= 1.5H, they adopted a distinct reversed " C " shape. In this case, on the two extreme floors, the air was flowing outwards, (from courtyard to outside), while in the middle floors it was inward, (from outside to courtyard), in general.

At oblique wind angles, this last profile was found at some locations in the two adjacent downwind facades, nevertheless, it was more flattened than at 0° wind incidence. Unlike the conditions at 0° wind angle, the flow in the extreme floors was not directed in the opposite direction to that of the mid-height floors, but the magnitude was much larger at the extreme floors than the mid-height floors. This profile appeared also in courtyards with smaller depths when the wind incidence was oblique than when it was normal, (i.e., from a depth of 1H onwards at 45° wind incidence in comparison with 1.5H at 0° wind incidence).

Comparison with the vertical pressure coefficient profiles

The shape of these profiles coincided with the general form of the pressure drop profiles described in Section 7.2.2, and for which hypotheses were put forward to explain these shapes.

However, there were also major differences between the two types of profiles. For example, at 30° wind incidence, the pressure drop profiles anticipated the indoor flows at the bottom and top floors of the leeward wings to travel in the opposite direction to that in intermediate floors. This was not observed from the internal flow measurements. Also, the curvature of the profiles were more accentuated at 30° wind incidence than at 0° wind angle. No such effect was recorded with the internal flow tests. These

differences should probably be attributed to the influence of the porosity of the models in the latter tests, and which could have distorted the pressure fields measured on the sealed models.

7.3.5 Comparison with the results obtained from the surface pressure tests

A comparison between the results given from surface pressure tests and the internal flow measurements indicated some similar trends but also significant divergences.

In brief, it could be said that the effects of the courtyard geometry were actually lower than those predicted from the surface pressure measurements. Also, the internal flow measurements showed that the influence of the wind incidence was great for all the courtyard geometries, whereas the conclusions drawn from the surface pressures were that it was influencing only certain courtyard sizes. Moreover, the direction of the internal flows did not always match that indicated by the pressure differentials.

It was anticipated that, because of the presence of openings in the internal flow test models, the pressure field was substantially different from that measured on sealed models.

It has been suggested that, if the opening area in models does not exceed 10% to 20% of the wall area, then the pressure field is not significantly disturbed by the flow passing through the apertures, (Aynsley (1976) and Vickery et al (1983)). Nevertheless, Vickery et al (1983) and Holdo et al (1983) indicated that there are regions of flow in which the pressure field could be substantially distorted by the "through-flow" even with small aperture areas. This is further discussed in Chapter 10.

In the case of a confined space as a courtyard it was believed that the flow through the walls could greatly condition the pressure field inside the courtyard. It was probably for these reasons that the ventilation predictions from the surface pressures measured on sealed models were somewhat different from that of the porous models.

Nevertheless, some trends obtained from the pressure measurements correlated with those found from the internal flow tests. For example, the unbalanced distribution of the flow within the courtyard models found at normal wind angle, and the characteristics of the vertical flow profiles for some courtyard forms were common to the two studies.

7.4 Influence of the courtyard geometry on the ventilation

It was implied throughout this discussion and in Section 7.3.4 that the flow pattern in the courtyard could be more sensitive to the alteration of the courtyard dimensions in the wind direction than in the transverse direction. In this section the effects of the depth and breadth are analysed separately.

7.4.1 Effect of the depth

7.4.1.1 On the indoor flow directions and magnitudes

The effect of the courtyard depth on the flow coefficients can be seen in Figure 7.7 to 7.9 to be marked only at some discrete points but the general ventilation conditions remained relatively unaltered.

Windward wing

At the windward wall, the intensity of the flow was hardly changed with the alteration of the courtyard depth even at discrete locations in the face. The comparison of the flow coefficient at each floor level of the windward wing and for all the courtyard models indicated a maximum variation of the flow coefficient of 0.04 which corresponded on average to only 9% of the mean values, for a wind incidence of 0°. At the oblique wind angle, the indoor flow was also relatively undisturbed by the alteration of the depth, and variations of about 7% to 13% of the mean values were recorded at discrete points.

Lateral wings

At 0° wind angle, on the lateral facade and at the most upstream measuring location, the flow coefficient varied at discrete points by up to 0.04, which corresponded, on average, to a difference of 24%.

Further downstream on the faces, the flow magnitudes at discrete points were greatly changed with the alteration of the model depth but was not reflected fully on the variation of the average flow on these wings. The direction of the indoor flow was also affected at this particular region on the lateral wing.

It should be reminded here that at this particular location small errors in

misalignment or orientation were found to have great effects and was suggested to be possibly related to the displacement of the flow reattachment position. Hence, it was difficult to isolate the actual effect of changing the depth to that of small errors of manipulation that could have been made despite the great care taken. Nevertheless, the eventual errors should be meaningless in actual facts since the wind direction is known to fluctuate widely.

Leeward face

At the leeward face, clearly the greatest variation of the flow magnitudes caused by the alteration of the depth was recorded. Although the overall flow on the facade was not greatly affected, the internal flow at discrete points were found to change sometimes by more than twice the mean value of the flow coefficient. The variation in the intensity of the flow coefficient was sometimes accompanied by changes in the flow direction.

At the oblique wind angles, the effect of changing the depth was more significant on the downwind facades than on the upwind ones. The amplitude of the variation of the flow at discrete points could be of the order of 20% to 40% at 30° and 45° wind angles on the downwind facades. However, average values on the faces did not express variations as large as these.

The horizontal gradient of internal flows that existed on the downwind wings when the wind impinged on the building at an angle, was found to be upset by the change of the courtyard depth. In general, on the models with the smallest depth, the strongest flows were located near the upwind edges where the flow separates and where large suction is known to act on the external walls. When the depth was increased the greatest values of flow were moved towards the most downstream measuring locations of the model. This may be due to the fact that the plan of the vortex system in the courtyard, (which is parallel to the wind direction), was displaced and was washing down the courtyard walls at different locations each time the courtyard size was altered. Also, the penetration of the two horizontal spirals generated at the leading roof corner of the models could have also helped to increase the pressures locally and to promote stronger outward indoor flows, (see discussion in Section 7.2.2).

7.4.1.2 On the vertical distribution of the flow

Changing the depth of the courtyard was already shown to have a very marked effect on the pressure distribution on the leeward wing at 0° and on the two downwind

sides at oblique wind angles.

In Figure 7.11, the vertical flow distribution at a particular wing location was grouped for courtyards of the same depth. From the figure, it is clear that it is the change of the depth that affected the internal flow distribution. The profiles could collapse into distinct families of shapes already mentioned in Section 7.2.2. Similarly, the studies of Hussain (1978), Soliman (1976) and Tani et al (1961) indicated that the appearance of such shapes in the pressure distributions was caused by the nature of the flow in the cavities, which in turn, was dictated by the dimensions in the wind direction, i.e., the depth.

7.4.2 Effect of the breadth

7.4.2.1 On the indoor flow directions and magnitudes

Windward wing

On the windward side, the alteration of the breadth caused minor changes in CQ values, with in general slightly higher average values for wider models. The variations recorded at each floor were no more than 0.03, which represent only 5% to 10% of the mean value.

The relative insensitivity of the indoor flow in the windward rooms to the change of the building breadth contrasted with the results on the surface pressure, in which changes of 18% of the average pressures were obtained in some cases. Nevertheless, the differences were expected to be attenuated in the case of internal flows since they are proportional to the square root of the pressure drop. Also, the porosity of the walls in the internal flow tests could have certainly dampened the variations in the surface pressures measured on sealed models by establishing a bridge between the pressure fields on the inner and outer walls of the courtyard models.

Leeward wings

On the leeward face, and at 0° wind angle, the variation of the flow magnitudes caused by the change of the breadth could be very large at discrete points. It was found that, in general, there were higher average flow coefficients in wider building models irrespective of the model depth.

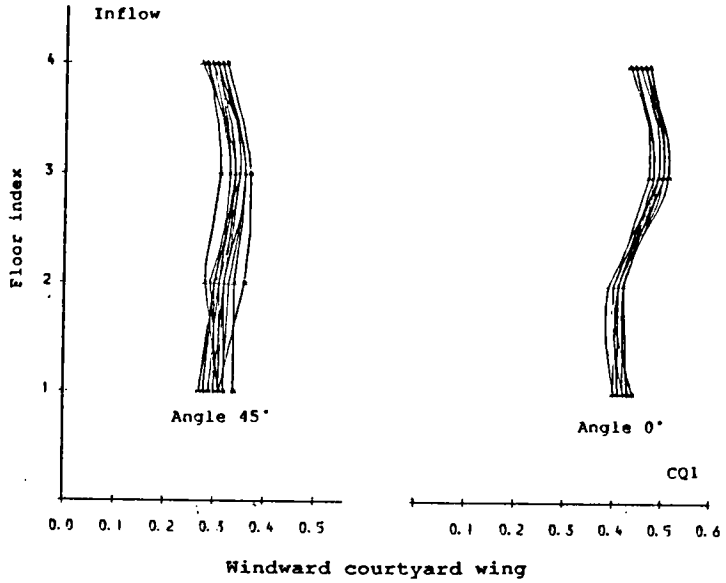

Figure 7.10: Internal flow coefficient profiles on the windward wings of the models for wind incidences of 0° and 45° angle.

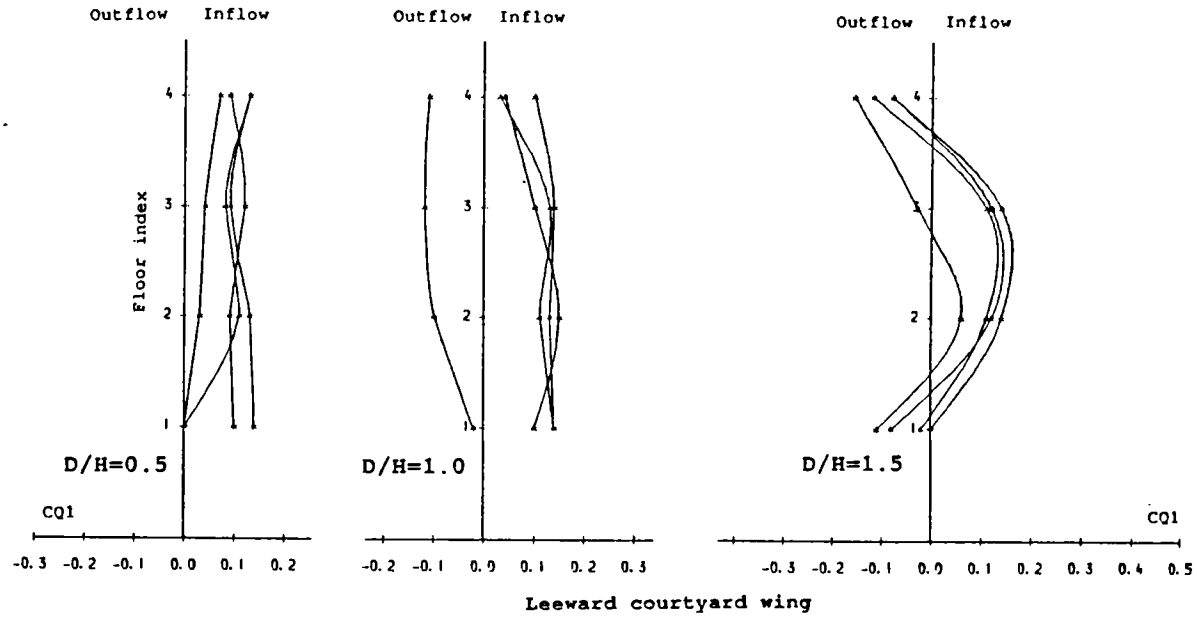

Figure 7.11: Internal flow coefficient profiles on the leeward wings of the models, grouped according to the courtyard depth, (0° wind incidence).

Interesting behaviours of the indoor flow have been recorded in this part of the building models as the breadth was changed. In models in which the courtyard depth was less than 1.5H, the flow was strengthened when the breadth was changed from 0.5H to 1.0H. At the same time, some of the internal flows were reversed to the opposite direction to the main airstream, (see Figure 7.7). This indicated clearly that stronger suction effects were induced from the courtyard walls. In the deepest models, the particular distribution of the flow with a reversed " C " shape, described earlier, was more accentuated as the models became wider. Both behaviours may indicate that the vortex activity in the courtyard was more vigorous in the widest models. The work of Ettouney (1973) on wind climate in courtyards corroborates this assumption.

Further increase of the breadth caused fewer changes in the flow magnitude and no change in the flow direction.

Lateral wings

On the lateral sides and at the most upstream measuring points, the flow was relatively undisturbed when the courtyard breadth was changed. The variations in the flow coefficients were on average 0.02, which corresponds to approximately 13% of the mean values. On the other hand at more downstream points, the discrepancies were larger, of the order of 50% to 70%. In particular, at the second downstream measuring location, (i.e., at 1.55H from the upstream edges), the flow direction changed with the alteration of the breadth from 0.5H to 1.0H, (see Figure 7.7).

Similar to the effect of the depth, when the wind struck the building at an angle, the strongest indoor flows tended to appear in the most downstream locations, in the widest models, instead of near the upwind edges as in narrower courtyards.

7.4.2.2 On the vertical distribution of the flow

The effect of changing the breadth did not have a major influence on the general shape of the vertical distribution of the flow. In particular, at the leeward wing, the distinct forms of the profiles was shown to be governed by the courtyard depth and not the breadth. This could imply that the change of this dimension does not have an effect on the general vortex structure established in the courtyard.

Nevertheless, it was found that in the models with a depth smaller than 1.5H, the increase of the width promoted an inward current of flow, and, in the deepest courtyards, it accentuated the curvature of the reversed " C " shape profiles. This could

lead to the conclusion that the increase of the courtyard breadth amplifies the vortex activity without altering the general pattern of the flow.

7.4.3 Summary on the effects of the courtyard geometry

To sum up, it could be said that the effect of the geometry was more apparent in the change of the flow at discrete locations than on the average values at a particular wing of the building model.

On the upwind wings of the models, the indoor flows were found to be hardly sensitive to the alteration of the courtyard geometry, in particular when the side was facing the wind at normal wind angle. On the other hand, significant changes could occur at the leeward face. At 0° wind incidence, the magnitude and direction of the indoor flows were very variable at this location and at discrete points.

At normal wind angle, a distinct vertical flow distribution was set at the leeward wings of the models when the courtyard depth was greater than 1H. In these circumstances, the indoor air was travelling in the wind direction at the top and bottom floors and in the opposite direction in the intermediate floors. In courtyards with the smaller depths, the air was generally flowing in all the floors in the opposite direction from the wind stream.

The change of the courtyard breadth caused also reversed flows in the leeward rooms, and promoted either large courtyard suction effects, in the models with the smallest depth, or amplified the aforementioned vertical flow distribution in the deepest courtyards.

At the oblique wind angles, the location of the strongest flows at the downwind wings changed when any of the depth or breadth dimensions was changed. In the smallest courtyards, it was at the most upstream sectors that the greatest flows were found, promoted by the large suction resulting from the flow separation at the edges. On the other hand, in the largest models, the strongest flows were located at the most downstream regions. It has been suggested that in these circumstances, the location of these strong local flows coincides with the impact of the front of the plan of the vortex system with the courtyard walls, and probably also with the collision of the strong spiral vortices generated at the upwind roof edge of the models.

The appearance of distinct families of vertical flow profiles, which relate to different ways in which the flows in the courtyard interact with the surface walls, was found to be governed by the courtyard depth. The pattern of the flow that was inferred

presented strong similarities with that in the spacing between elements in arrays studied by Soliman (1976) and Hussain (1978), or in the cavities of grooves related by Tani et al (1961). On the other hand, the increase of the breadth seemed to strengthen the vortex activity in the courtyard without altering the general pattern of the flow in the court.

7.5 Influence of the wind incidence

In contrast with the minor effects the courtyard geometry had on the general ventilation conditions of the building, the influence of the orientation to the wind was remarkable. The oblique orientation had the effects of improving the air motion in most of the courtyard rooms and establishing a more balanced distribution of the flow within the structures.

In Figure 7.12, the average indoor flow in each facade, noted CQF, is indicated for all the courtyard models at wind incidences of 0°, 30° and 45°.

The change of the wind orientation from 0° to 30° or 45° enhanced greatly the airflow in all the building wings that were downwind at normal wind angle, but at the expense of the flow in the windward wing. The reduction of the internal flows at the windward wing was of the order of 15% of the mean value. This was relatively small in comparison with the improvement made in the remaining wings. Indeed, in the facades F2 or F3, for example, the average flow coefficients represented, at 30° wind angle, around 1.5 times to 3 times, and exceptionally almost 6 times the values at 0°. In particular, the improvement was important at the most downstream locations of the elongated models, for which the ventilation was particularly weak when the models were orientated normal to the wind.

The reason for the relatively large outflows in the downwind facades could be due to the combined effect of, first, a larger suction on the external walls which is found generally on any rectangular building model, and secondly, to the more important penetration of some of the airstream into the court and which increased the pressures on the courtyard walls.

The distribution of the flow within the structures was remarkably amended at oblique wind angles. It can be seen in Figure 7.12 that, at 0° wind incidence, the flow coefficients on the windward facade, F1, was often more than 4 times stronger than the values at the leeward face, F3. At 30° wind incidence, the minimum values of CQF were on average half the maximum values. Finally, at 45° wind angle, the distribution of the flow within the structures was the best. The minimum CQF values were on

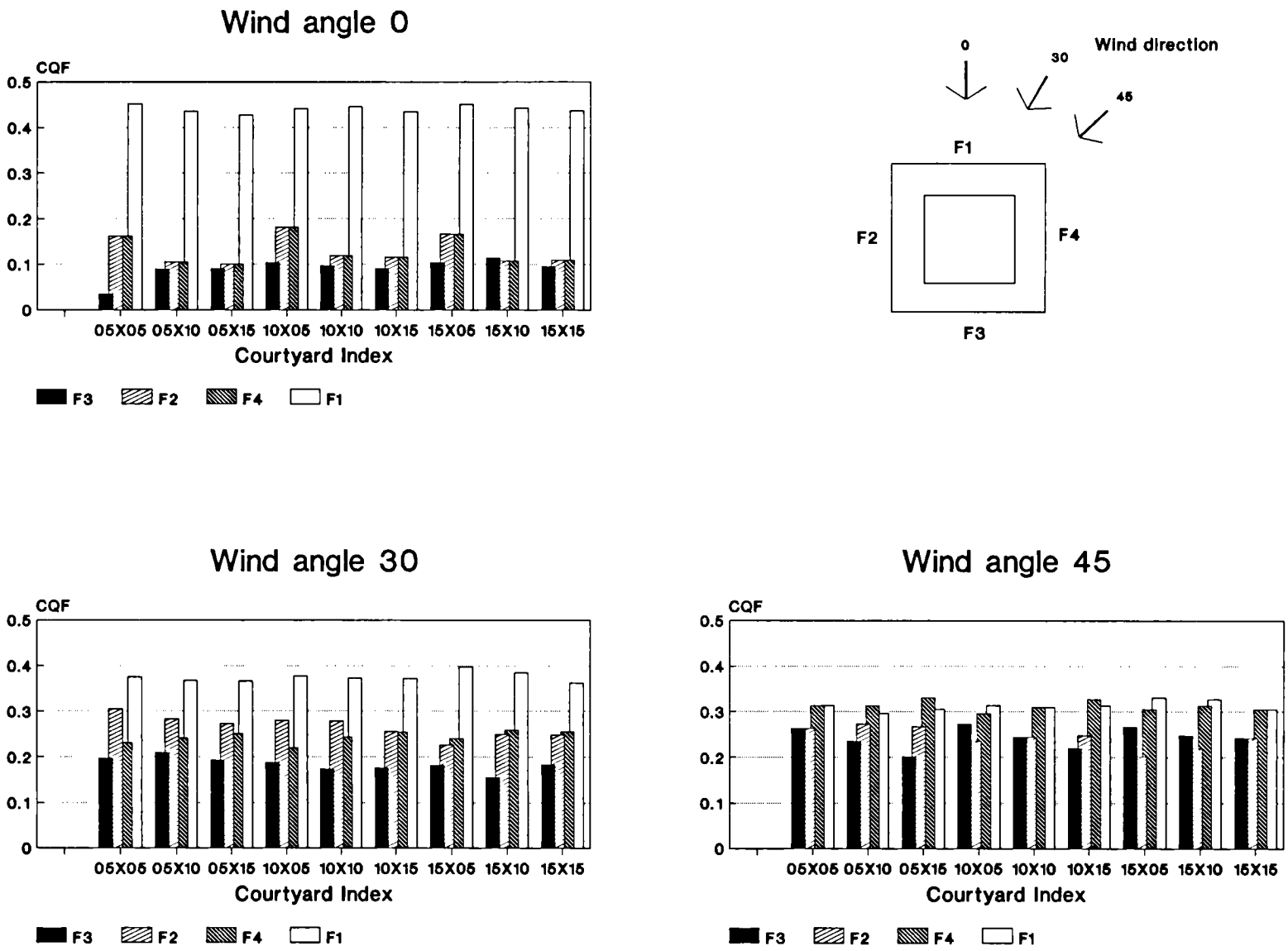

Figure 7.12: Effect of the wind incidence on the distribution of the flow within the model wings.

average equal to 70% of the maximum values.

In real conditions, the orientation of the wind generally fluctuates widely. In these circumstances, the distribution of the flow in the courtyard structures is likely to oscillate between the distributions set at fixed wind angles.

In particular, when reversed flows takes place as a result of the change of the wind incidence, intermediate conditions between the inward and outward indoor air motion could exist. This implies that possibly very weak flows could be encountered. For example, in the case of wind fluctuating from 0° to 30°, there could be small internal flows in the lateral face F4, near the upwind edges, and so, despite the fact that at each of 0° and 30° wind angles the internal flows were relatively strong. This is because the flow direction reverses as the wind angle moves from 0° to 30° or 45° wind incidence.

7.6 Ventilative performances of courtyards

7.6.1 Evaluation of criteria

In order to compare the ventilation performances of the various structures tested, some indices for comparison basis must be chosen.

The overall flow coefficient, CQT, which is the average of the flow magnitude in the entire building, may be an adequate criterion to account for the mean ventilation conditions in the buildings. However this does not indicate how the internal flows are distributed within the building models. It was thus chosen to discuss the ventilation performances in terms of the **percentage of the building falling under certain ranges of flow coefficients.**

To asses the wind-driven ventilation performance of an actual building in its site, however, it is necessary to examine the frequencies of occurrence of ranges of wind speeds and directions, provided by meteorological stations, and establish the frequency of time where comfort levels are achieved.

The spatial distribution of levels of flow coefficients, chosen here as the ventilative performance criterion, could enable the determination of the **fraction of the building** that is under thermal comfort conditions, in conjunction with the **frequency of time** when these conditions are met. An example of application is provided in Appendix G.

7.6.2 Ventilative performances at 0° wind angle

The overall flow coefficient CQT of the different courtyard configurations was ranging between 0.14 and 0.25 and was on average equal to 0.20. This means, in other words, that the mean air velocity through the model apertures was on average 20% of the wind speeds at the roof height, or, 13% of the free stream at the gradient height, (i.e., CQ1 was on average 0.13).

The percentage of building under certain ranges of flow coefficients is shown in Figure 7.13 for the different courtyard configurations. The cumulative percentages are given in Table 7.2.

It can be noticed from this figure that the models recording the larger percentage of building with flow coefficients, CQ1, above 0.25 were the most elongated models in the transverse direction of the wind, (e.g., C10x05, C15x05). On the other hand, the models with the shortest walls facing the wind, (e.g., C05x10 , C05x15), had clearly the smallest percentage of building in the high range of flow coefficients, (CQ1 > 0.25), and also, the most extensive spaces affected by very weak flows, (CQ1 < 0.05).

The explanation for this behaviour is simple. Presenting the longest building face of the model increases the relative proportion of the structures facing directly the wind and reduces the number of rooms orientated parallel to the main air stream, (in particular in rooms located some distance apart from the leading corners) and where ventilation was found to be very weak. This can also be seen in Figure 7.14 to elevate the overall flow coefficients, CQT.

As apparent from Figure 7.13, the largest courtyard sizes did not particularly record the best ventilative performances, in contrast to what is generally believed, (see for example Leung et al (1981) p. 24). The most salient evidence is that model C05x05 recorded clearly better ventilation conditions than models C10x10, C05x10 and C05x15. It had also greater percentage of building under flow coefficients above or equal to 0.10 than any other structures, though, the fraction of building with flow coefficients greater than 0.15 was not as large as with C10x05, C15x05 or C15x10.

7.6.3 Ventilative performances at 30° and 45° wind angles

Although there were some differences in terms of spatial distribution in the flow coefficients between the various models at normal wind incidence, the effect of the geometry was not as dramatic as that of the wind angle.

The overall flow coefficient, CQT, was around 0.27 and 0.28, respectively, at 30°

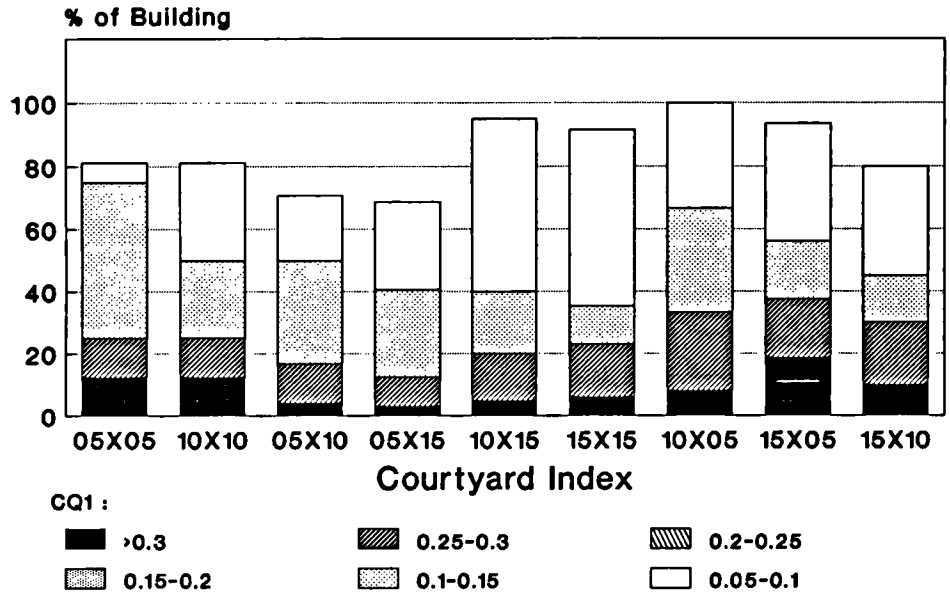

Figure 7.13: Fraction of the courtyard models under ranges of flow coefficients, **(isolation conditions, 0° wind angle).**

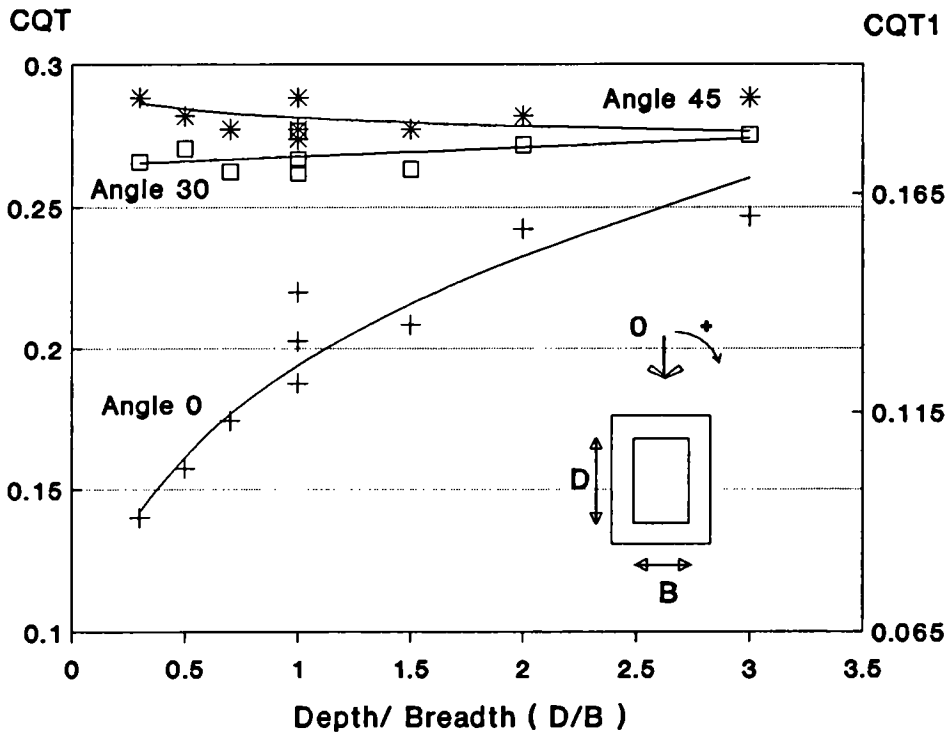

Figure 7.14: Effect of the ratio Depth/Breadth of the courtyard on the overall flow coefficient, CQT, for various wind incidences.

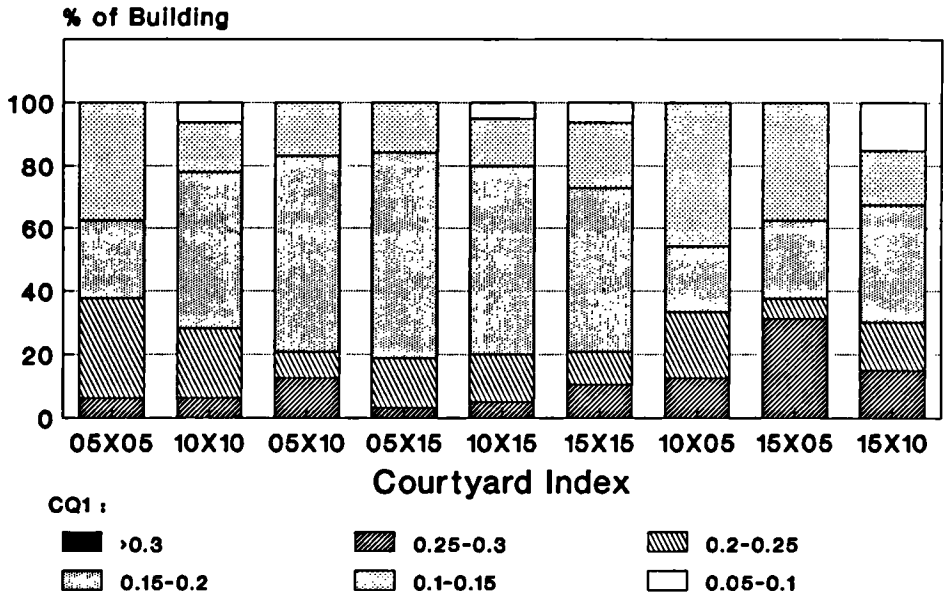

Figure 7.15: Fraction of the courtyard models under ranges of flow coefficients, **(isolation conditions, 30° wind angle).**

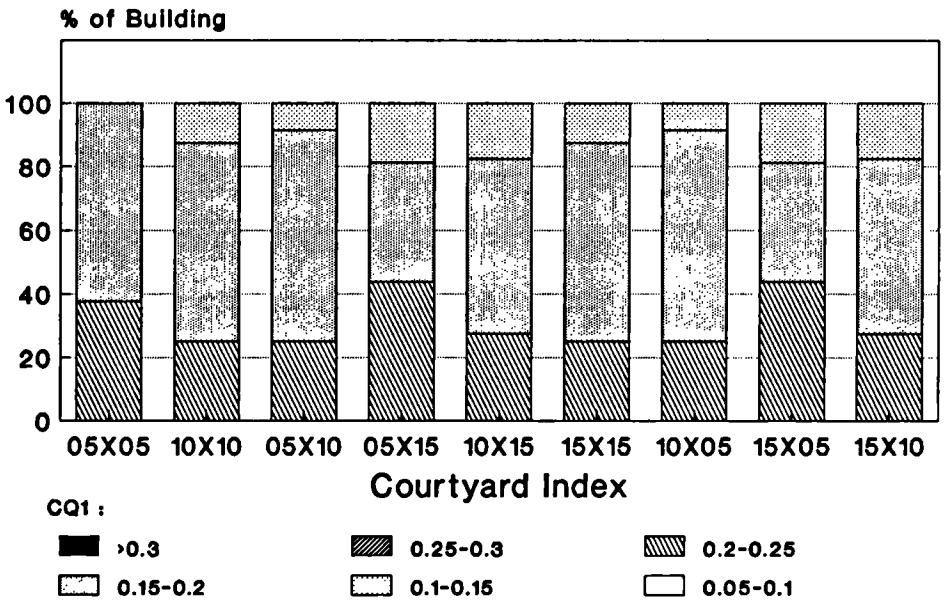

Figure 7.16: Fraction of the courtyard models under ranges of flow coefficients, **(isolation conditions, 45° wind angle).**

Table 7.2: Cumulative percentage (%) of courtyard models under ranges of flow coefficients CQ1, (isolation conditions).

Wind angle 0°						
Model index	CQ1 >0.05	>0.1	>0.15	>0.2	>0.25	>0.3
C05x05	81.2	75	25	25	25	12.5
C10x10	81.2	50	25	25	25	12.5
C05x10	70.8	50	16.6	16.6	16.6	4.16
C05x15	68.7	40.6	12.5	12.5	12.5	3.12
C10x15	95	40	20	20	20	5
C15x15	91.6	35.4	22.9	22.9	22.9	6.25
C10x05	100	66.6	33.3	33.3	33.3	8.33
C15x05	93.7	56.2	37.5	37.5	37.5	18.7
C15x10	80	45	30	30	30	10
Wind angle 30°						
Model index	CQ1 >0.05	>0.1	>0.15	>0.2	>0.25	>0.3
C05x05	100	100	62.5	37.5	6.25	0
C10x10	100	93.7	78.1	28.1	6.25	0
C05x10	100	100	83.3	20.8	12.5	0
C05x15	100	100	84.3	18.7	3.12	0
C10x15	100	95	80	20	5	0
C15x15	100	93.7	72.9	20.8	10.4	0
C10x05	100	100	54.1	33.3	12.5	0
C15x05	100	100	62.5	37.5	31.2	0
C15x10	100	85	67.5	30	15	0
Wind angle 45°						
Model index	CQ1 >0.05	>0.1	>0.15	>0.2	>0.25	>0.3
C05x05	100	100	100	37.5	0	0
C10x10	100	100	87.5	25	0	0
C05x10	100	100	91.6	25	0	0
C05x15	100	100	81.2	43.7	0	0
C10x15	100	100	82.5	27.5	0	0
C15x15	100	100	87.5	25	0	0
C10x05	100	100	91.6	25	0	0
C15x05	100	100	81.2	43.7	0	0
C15x10	100	100	82.5	27.5	0	0

and 45° wind angles. In comparison, CQT was 0.20, on average, at 0° wind angle.

It can be seen in Figure 7.15 and Figure 7.16 that the effect of changing the wind incidence from 0° to 30° resulted in the removal of all flow coefficients, CQ1, below 0.05, and almost all flow coefficients below 0.10. At 45° wind angle, there was no flow coefficient below 0.10, and at least 80% of the building models had flow coefficients above or equal to 0.15. In return, the high flow coefficient ranges were affected. No flow coefficients were equal or above 0.3 at 30° wind incidence, and all CQ1 values were below 0.25 at 45° wind angle. As already discussed, a more evenly distributed flow resulted from the change in the wind orientation from normal to oblique.

As at normal wind angle, there was also some differences in the spatial distribution of ranges of flow coefficients between the various models, though, they tended to wane, particularly at 45° wind angle. Also, the overall flow coefficients shown in Figure 7.14 against the relative courtyard proportion tended to be the same for all the courtyard sizes.

7.7 Conclusions

Firstly, this chapter presented surface pressure measurements and secondly internal flow measurements on building models with courtyards of various sizes in isolation conditions.

Surface pressure measurements

The surface pressure measurements allowed to infer from the comparison with related works on grooves or buildings in array that the nature of the flow in courtyards presents many resemblances with the flow in cavities and streets. In particular, it may be possible that specific and distinct flow regimes were established in the courtyards as their sizes were changed, similar to the phenomena occurring in grooves or streets described by other authors. In the smallest courtyard tested, (C05x05), there were manifestations of the so-called skimming flow regime, and in the three largest courtyard sizes the flow pattern coincided probably with the wake interference flow regime. In the first case, a closed vortex was probably occupying the courtyard space with few interactions with the flow riding over the top. In the second case, a portion of the air stream flowing over the roof was penetrating the courtyard.

At non-normal wind incidences, pockets of positive pressures appeared on the upwind courtyard walls, (i.e., downwind wings). This was suggested to be caused by a

penetration of the flow riding above the courtyard height and which was facilitated by two spiralling vortices generated at the leading roof corner of the building models.

Internal flow measurements

The internal flow tests gave the actual amount of air flowing through each room surrounding the courtyards. A comparison of the results obtained with this test and the previous one indicated similar trends but also substantial divergences. The discrepancies were believed to be due to the fact that in the second test, the models were porous and the pressure fields were anticipated to be different from that acting on sealed model in the first test.

The internal flow tests appraised the ventilation conditions in courtyard structures. The main findings were as follows;

i) At normal wind angle, the windward wings were well ventilated, whereas, in the downwind wings the indoor air movement was very slow. However, on the lateral wing, near the upstream building corners, there was a moderate outward flow which was induced by the suction produced by the external flow separation.

ii) Within the range of courtyard sizes tested, the geometry was found to have minor effects on the internal flows, except at some discrete points. The depth of the court controlled the pattern of the flow in the cavity, whereas, the increase of the breadth seemed to energise the vortex system without affecting the general flow pattern.

iii) On the other hand, changing the orientation of the courtyard with respect to the dominant winds from 0° to 30° or 45° angles caused dramatic effects. The indoor air movement was significantly improved at the downwind wings, yet, at the expense of reducing the indoor air velocities at the windward face. Nevertheless, the distribution of the flow within the model wings was greatly amended at oblique wind angles, and, on average, the velocities of the air passing through the model apertures were 27% to 28% of the wind speeds measured at the roof height in comparison to 20% at normal wind angle.

iv) At normal wind incidence, there was some benefit in orientating the longest facade of the building models to face the wind, in that, a greater portion of the building could be well ventilated, and also, few rooms would be parallel to the wind where cross-ventilation could be very restricted. At oblique wind angles the differences in the courtyard orientations tended to wane.

v) The long-held belief that courtyards with larger sizes facilitate the ventilation

was somewhat demystified in this work, at least with the range of courtyard sizes tested here.

By orientating the courtyard with an angle to the wind, in order to maximize the ventilation in the building, less wind shelter can be anticipated in the courtyard space in comparison with normal wind incidence, (see Section 2.6.3). Nevertheless, there will still be a high degree of wind shelter in the courtyard and an extensive protected area behind the upwind wings for the people to enjoy the courtyard space particularly during winter time, (see Ettouney (1973)).

In the next chapter, the result of the experimental tests on atria are presented and comparisons between their ventilation effectiveness and that of the courtyards are made.

Chapter 8:

Ventilation conditions of atria in isolation

8.1 Introduction

The ventilation conditions in a courtyard-type building were shown in the previous chapter to be problematical for the downwind wings of the building and for normal wind incidence.

By covering the courtyard, in which case it becomes an atrium, and locating openings at the roof level, greater pressure gradients may be obtained and used to improve the ventilation conditions, particularly at the downwind wings. This basic principle of intercepting the unobstructed and faster flows at the roof level have been known about from Antiquity and have produced wind towers and wind catchers.

This chapter reports the results of the tests made on atrium structures in isolation. The possible operating modes that can be used by the atrium concept are explored. Their ventilative performances are given and are compared with that of the courtyard.

8.2 Atrium ventilation modes

It was shown in the literature review of Chapter 4 that various modes of ventilation can be promoted by roof level openings, and were used in some historical examples, such as wind tower and wind catchers. The induction of these ventilation modes depended on the roof geometries of the structures and their orientation to the oncoming wind. In a similar manner, these ventilation modes can be used in atria. Four operating principles can be identified. These are as illustrated in Figure 8.1 and are as

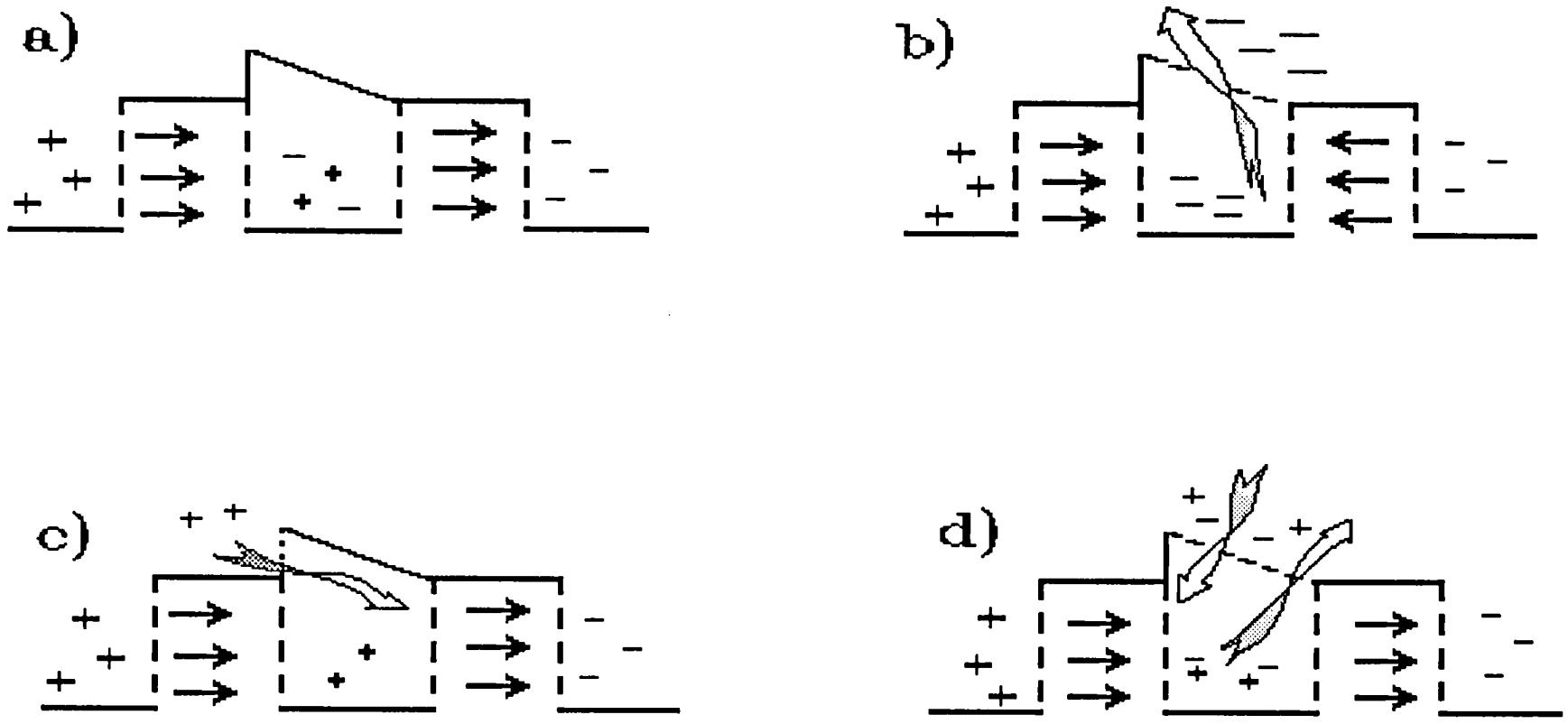

Figure 8.1: The various atrium ventilation modes: **a)** the closed roof atrium, **b)** the roof suction strategy, **c)** the positive pressure strategy and **d)** the near atmospheric pressure mode (b and c used simultaneously)).

follows:

a) Closing the roof, in which case the inflow from the upwind facades will leave through the downwind sides. This mode will be termed in the subsequent paragraphs as "closed-roof".
b) Pumping the air from the external faces out through the roof via the atrium. This strategy could be achieved if the roof is provided with openings at a large suction region. This mode will be termed "suction strategy".
c) Deflecting the air at the roof level into the atrium. This ventilation principle requires openings on a high pressure region of the roof. This mode will be termed "positive pressure strategy".
d) Finally, the roof can be used in both modes b and c by locating the roof opening in a region where the pressures are in-between the upwind and downwind wall pressures. Regions of near-atmospheric pressures should be generally suited. This mode will be termed "near-atmospheric pressure strategy".

How efficient each of these modes is to drive air movement is the subject of this chapter. Nevertheless, independent of these considerations, one strategy may be more suited than another depending on whether it is more appropriate to allow air to enter from the roof or the walls. For instance, if the walls are facing shaded streets with clean air, the suction strategy may be the most suitable. On the other hand, the positive pressure strategy should be more appropriate when the breezes are cleaner and cooler at the roof level, in the example of the wind catcher in the coastal region of Sind, Pakistan, (see Section 4.4.1.2). Also, this latter concept is probably more suited for night-time structural cooling when the lowest temperatures are obtained on surfaces exposed to the clear sky vault, in this case, the roof.

Another consideration intervening in the choice of the ventilation mode is the strategy for smoke control in the event of a fire. As discussed in Section 2.7, smoke can be extracted via the atrium or away from it. In the first case, the principle suits the suction operating mode, while the second is more adequate for the positive pressure strategy. Also, the possible migration of odours, dust and noise must be accounted for in the choice of a ventilation mode.

8.3 Methodology of the investigation

Prior to the internal flow measurements, from which the main results were drawn, an investigation on surface pressures on atria mounted with various roof types had to be done. The main purpose of this work was to determine among a variety of atria the ones that present the greatest potential to drive air currents in each of the above-mentioned modes, and which had to be tested for the internal flow measurements. These tests would also provide pressure coefficient data which are almost non-existent in the literature for such structures, and which are used later, in Chapter 10, to check the adequacy of numerical methods to predict indoor airflows in atria.

Design criteria for the surface pressure test atria

The atrium roof types which were tested were selected from among the roof top lighting concepts enumerated in Robbins (1986). The range of roof types tested can be seen in Figure 8.2. Details of the location of the pressure tappings on the roof surfaces are provided in Figure 6.14.

8.4 Surface pressure results

8.4.1 Surface pressures on the external walls

The full results of the surface pressure measurement are presented in the form of pressure contours on the monitored surfaces and can be found in the Appendices A1 to A15. A concise presentation of the surface pressure results is given in Figures 8.2 and 8.3 with a cross sectional representation.

A mean pressure coefficient was extracted for each surface of the models and was a spatially averaged CP value. Each face was divided into areas for which each pressure tapping was the centre. The mean pressure coefficient was then obtained by integrating the pressure coefficient value at each pressure tapping weighted by its associated area.

Comparison between the models

The surface pressure distributions on the external walls of the atria were found not to be significantly different from one model to another. The pressure coefficient values were, on average, 0.842 on the windward face, -0.329 on the lateral facades, and -0.204

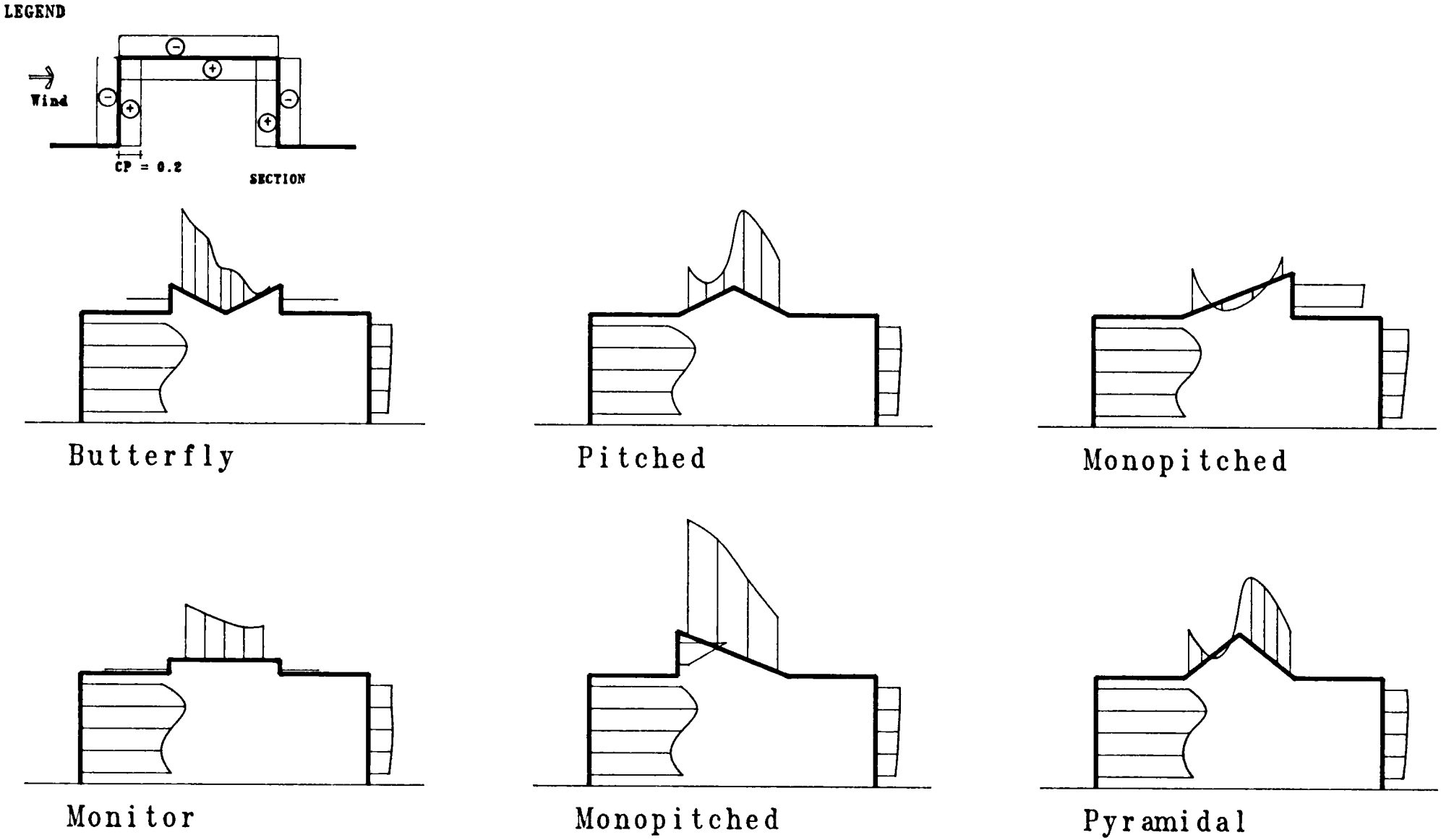

Figure 8.2: Pressure coefficient distribution on the model walls and roofs, with the wind blowing at right angle.

on the leeward faces at normal wind incidence. The standard deviation in pressure recorded at a particular facade of the various models was at most 10% of the mean.

At 45° wind angle, the pressure coefficient was, on average, 0.460, on the two upwind facades, and -0.515 on the downwind facades. The standard deviation was less than 6% of the mean value.

Typical pressure patterns with models normal to the wind

Not only were the average pressures similar for all the configurations but, also, the particular isopressure contours on each facade and at each wind angle were almost undistorted, (refer to Appendices A1 to A15 for details of the pressure contours).

On the windward facade, at normal wind incidence, there was a near-stagnation region at approximately 3/4 of the building height. The pressure decreased towards the top and the bottom. At approximately 1/4 of the building height, there was again an increase of pressure.

On the downwind sides, the pressures were below atmospheric. On the lateral faces the suction was high on the most upstream points, near the separation sector, and decreased steeply downstream. A pressure gradient of CP= 0.30 existed generally between the most upstream and the most downstream measuring points of the face. In contrast, a very uniform pressure field was acting on the leeward face.

Typical pressure patterns with wind incidence of 45°

When the wind was striking the models at 45°, the two upwind facades were under a positive pressure.

There was a significant pressure gradient between the most upstream and the most downstream measuring points on these faces, with pressures decreasing downstream. Closer isopressure lines existed on the 1/4 highest part of the face, (refer to Appendices A1 to A15).

On the two downwind faces, the negative pressures were fairly uniform, with the lowest pressures acting near the edges adjacent to the upwind facades.

8.4.2 External surface pressures on the atrium roofs

Normal wind incidence

At normal wind angle, most of the roofs were totally immersed in a negative pressure field, generated from the flow separation at the frontal wall edge, (see Figure 8.2).

On the most prominent roofs, i.e., the monopitched and the pyramidal roofs, however, pockets of positive pressures were found on the upwind surfaces, with the highest pressures generally located on the upper part of the roof. This implies that these roofs were high enough to reach some of the streamlined flow above the wake cavity created at the breakway point upwind to the atrium roof. The vertical surface of the monopitched roof presented the highest pressures when facing the wind. The same roof, but presenting the sloped surface to the wind, or the pyramidal roof, caused less retardation to the flow, (see Figure 8.2).

On the downwind surfaces of the roofs, the pressures were always below atmospheric. The strongest suction was found to act on the leeward surface of the most dominant roofs.

In general, these large negative pressures were experienced near the roof ridge and were weaker downstream. The suction was highest on the monopitched roof with the vertical surface facing the wind. The minimum average pressure coefficients were as low as -1.10, with some local pressure coefficients below -2.0.

On the lateral surfaces of the roofs the pressure were in general slightly higher than that on the leeward face. There was a large pressure gradient from the most upstream to the most downstream points. The difference in CP was on average 0.20 to 0.40.

Wind incidence of 45°

At 45° wind angle, in all the roofs, positive pressures were experienced on one or several upwind faces, (see Figure 8.3). The average pressure coefficients at the upwind surfaces were higher than when the wind was facing at 0° angle. Nonetheless, a very large pressure gradient existed. The flow was most retarded at the leading edges, where pressure coefficients as high as 0.78 were obtained. The flow accelerated downstream along the edge and caused the pressure to decrease. At this angle of incidence, the wind could even strike the sloped rear surface of the butterfly roof, raising the pressures

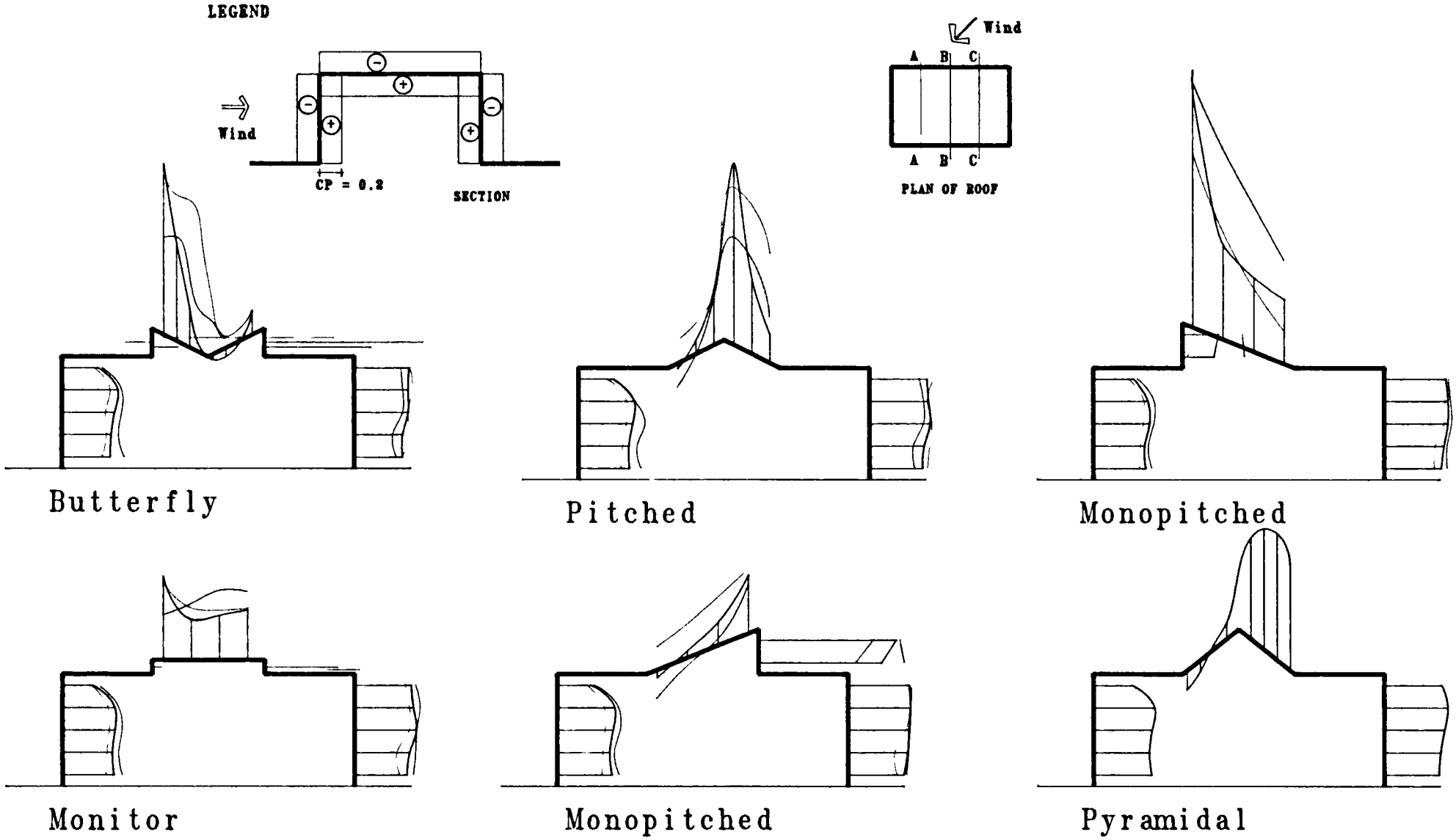

Figure 8.3: Pressure coefficient distribution on the model walls and roofs, with the wind blowing at 45° angle.

above atmospheric on a large part of the surface.

On the downwind surfaces of the roofs and for oblique wind angles, the pressure coefficients were very low. They were in some cases less than -2.0. The minimum pressures occurred near the roof ridge, yet, they increased rapidly downstream, away from the leading edge. Again, the larger pressure magnitudes were found in the most prominent roofs.

Wind incidence of 90°

When the wind struck the lateral surfaces of the roofs, (i.e., 90° wind angle), there were generally lower pressure magnitudes than at 0° wind angle on any of the roof surfaces. There was almost no pressure above atmospheric for any of the roof geometries, except the pyramidal roof.

Summary

As a summary of this section, it could be said that the more prominent the roof appeared, then the higher the pressures on the upwind surfaces, as well as, the larger the suction on the downwind faces. At 45° wind incidence, the pressure magnitudes averaged over these surfaces were greater than at 0°, with very strong peak pressures but with also significant pressure gradients.

The very strong deficits of pressure that were obtained in some roof surfaces may result in significant lift forces. This may cause some concern for the roof structural stability and have to be addressed in the design.

8.4.3 Comparison with other related works

Very few surface pressure measurements were made in structures incorporating a stepped roof, comparable to the types studied here.

Baturin (1972) explained that, in a building with a downstream part higher than the front, the low pressures of the separated region behind the forward roof edge react with the high pressure region that is normally formed upstream of an obstacle. On the roof surface between the front roof edge and the stepped roof downstream, there will be a bounding line between the two zones along which the pressures will be near ambient. The course of this line was suggested to depend on, i) the relative values of the height of the projected roof, ii) on the height of the building, and, iii) the distance between the

forward roof edge and the downstream stepped roof.

The author suggested a nomograph from which the pressures on the windward surface of the stepped roof could be read provided the above mentioned parameters are known. When some of the mean pressure coefficients, measured in the present tests on vertical roof surfaces, (e.g., CP= -0.57, -0.39, 0.26), were compared with the relevant values obtained from this nomograph, (respectively CP= -0.83, -0.4, 0), they were found higher than predicted. This might be attributed to the difference in the nature of the oncoming flow, i.e., shear in the first case and probably smooth in the second. The effect of upwind turbulences in rough flows are known to promote quick reattachment of separated flows, (see Holmes (1983), p.3). In this case, the bubble size of the separated flow at the forward roof edge is likely to be smaller than with smooth flow, and thus would lead to less suction. Another source of discrepancies may be the fact that the pressure coefficients were perhaps not referred to the same dynamic pressure, (not available in the publication of Baturin).

It is interesting to compare the potentialities that the present roofs had to promote suction or positive pressure forces with other roof types. Chien et al (1951) provide many pressure coefficient data for various configurations of buildings, e.g., with cylindrical shapes or block-like forms, with flat or pitched roofs.

The maximum suction pressure obtained at the apex of cylindrical roofs was found at 30° wind angle and was equal to -2.5. On flat roofs the maximum average suctions were around -1.6 to -2.5 with some local peak pressures as high as -7.0. As the pitch increased, the maximum average suction pressure coefficients became -0.7 to -0.9.

Holmes (1983) suggested -1.3 as a maximum average external pressure coefficient for wind loading design of pitched roofs. This author reported works in which minimum local pressures as low as -7.0 were recorded.

Pressure coefficient data for roofs can be found in wind loading codes, though they are generally given to deal with the worse structural cases. Newberry and Eaton (1974) suggested for wind loading design of arched roofs, pressure coefficients up to -1.8. For domes mounted on cylindrical bases, pressure coefficients equal to -1.7 were recommended.

On the basis of the above mentioned data, it can be concluded that the average suction pressures obtained with the present roofs, (in particular the monopitched roof), were among the highest values which can be found in conventional roof types. The design of the roof to induce suction effects could thus be considered as among the most efficient.

The maximum positive pressure which can be obtained on a surface is the dynamic pressure. To achieve pressures approaching these values would require a very tall roof, very costly to build. Thus, although the positive pressures obtained with the present roofs were of moderate magnitudes, it is believed that greater values could be realised only with great difficulty and at a great cost.

8.4.4 Selection of the atrium roof types for internal flow tests

From the observation of the pressure distribution, the choice of the best roof type to perform each of the previously defined ventilation modes had to be made. There was, at this stage of the work, no straightforward ways to infer the internal flows in an atrium model, or to determine whether a configuration could be better ventilated than another one. This is because the flow systems were too complex.

In order to compare the potentialities of each roof, an abstraction of the geometry of the structures was made and the problem was dealt only in terms of pressure fields, associated porosity and opening characteristics. The reasoning was as follows; since the pressure fields acting on the external walls were almost the same for all the atria, it was expected that the same ventilation conditions could be obtained in atria with different roof types, provided the same openings are located in identical pressure fields on the roofs. Following the same logic, it was expected that the greatest roof suction effects would be obtained with the roofs that presented the lowest pressures and also in which a maximum number of openings could be located in this region. The same reasoning applies for the other ventilation strategies. The fact that the same pressure fields were acting on the external walls of all the models reduced greatly the problem of identifying and selecting the most promising models for each of the ventilation modes.

The roofs that present the greatest potential to drive ventilation in each of these modes was thus selected on the basis of adequate pressure field and maximum associated area. The monopitched roof was found to satisfy all the conditions alone and was adopted for all the tests, (see Table 8.1). Indeed, at normal wind incidence, (see Figure 8.2), the roof had the largest suction, and the largest positive pressures on the sloped surface and the vertical windward face respectively. When its sloped surface faced the wind, large regions under near-atmospheric pressures were obtained. The same potentialities were kept at a wind angle of $\mp 45°$.

By changing the porosity of the roof, the roof pressure forces could be altered. It was hoped that many ventilative situations could then be embraced and other cases

Table 8.1: Characteristics of the atrium configurations tested for internal flows, and the pressure coefficients acting on their external surfaces, (pressure data obtained from sealed model pressure tests).

Atrium ventilation mode	Model index	Roof porosity (% facade area)	Average roof pressure coefficeints		Pressure coefficient CP on external walls
			Wind angle		
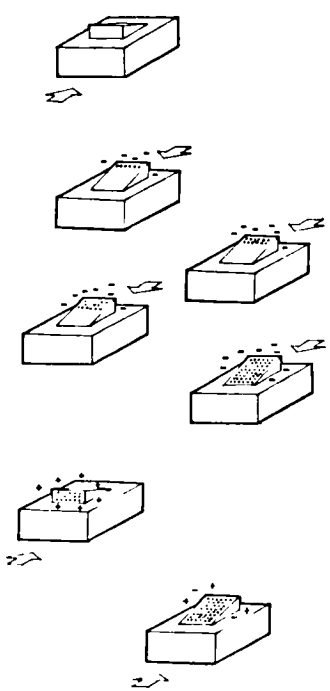	A1	0	0°	45°	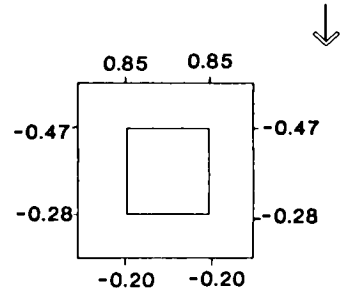
	A2	3.8	-1.08	-2.07	
	A3	7.6	-1.06	-1.91	
	A4	11.4	-1.04	-1.76	
	A5	30.4	-0.83	-1.18	
	A6	11.4	+0.28	+0.29	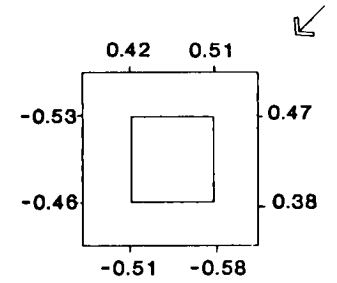
	A7	30.4	-0.09	-0.15	

could be inferred.

The details of the configurations that were selected are given in Section 6.3.3.2. The types are reminded here briefly;

i) One atrium with its roof closed, designated A1.

ii) Four atria exploiting the suction strategy and named A2, A3, A4 and A5. The difference between them lied in the number of apertures on the roof surfaces. The area of the roof vents was varied between 3.8% and 30.4% of the surface of one of the four inner atrium walls, (this will be referred subsequently to relative roof porosity).

iii) One atrium exploiting positive roof pressure mode, named A6,

iv) One atrium with the roof under near-atmospheric pressure, named A7.

Table 8.1 summarizes the main characteristics of these configurations. The average pressure coefficients acting on the locations of the model windows and roof vents, obtained from the surface pressure tests, are given.

The maximum roof porosity tested, (i.e., 30.4%), corresponded, at the scale, to a total vent surface of 50 m^2. This figure represents probably a high value. Nevertheless, if the roof vents have to be used for smoke control in the event of a fire, then the required vent area is expected to be higher than this figure. For example, for an atrium 16 m high, (approximately the size of the present atria), given a fire area of 25 m^2 and a free sight of 12 m, (the height up to the smoke layer), 74 m^2 of roof vents is required for a design time of 15 minutes[1], (see Borresen and Madsen (1990)). If the fire load is great, for example, when the atrium accommodates restaurants, the relevant fire area becomes 60 m^2, in which case, the roof vent area required is around 100 m^2. The large roof area which may be needed to be operable for smoke control may not be economically competitive with mechanical extraction.

8.5 Results of the internal pressure measurements

The indoor flow of air in an atrium can be represented by its equivalent flow system shown in Figure 8.4. The central node of the system represents the internal pressure, and its value will be the result of a balance of the flows through the windows

[1] The design time is the time it takes from when the fire is detected to when poeple have escaped, (Borresen and Madsen (1990)).

and the roof apertures.

It is clear that the parameters which were responsible for the differences in the internal pressures in different models were the porosity of the roofs and the pressure exerted at the roof vents apertures. This is because the flow resistance of the atrium rooms was unchanged, and the pressure field acting on the external walls was known to remain unaffected when the atrium roof shape is changed, (see Section 8.4.1).

The values of the internal pressure coefficients measured on the atrium models for 0°, 30° and 45° wind angle are given in Table 8.2.

Variation of the internal pressure with the roof suction forces

As expected, the internal pressures differed from one atrium configuration to another. It was observed that they tended to be low when the roof suction was exploited and that the deficit was more pronounced when the relative roof porosity was increased. On the other hand, the pressures were generally the highest when the roof openings were located in pressure fields above atmospheric.

With the roof suction strategy, a large range of surface openings were tested. The effects of the roof porosity on the internal pressures are illustrated in Figure 8.5. As expected, the deficit of pressure in the atrium was greater at larger roof porosities. This effect was more pronounced as the wind angle was changed from 0° to 30° and then to 45°. A reason could be that at the oblique wind angles, the suction on the roof surfaces was greater than at normal wind angle so that larger flows were induced out of the roof, thereby reducing the pressure in the atrium core.

The internal pressures tended to level out when the roof became very permeable. One reason could be that the **average suction** acting on the roof apertures was reduced as more openings were accommodated. Indeed, in order to obtain a large porosity some openings had to be located away from the roof ridge and where weaker suction existed. Another reason could be also that, in the case of a dominant opening surface, (in the present case, the roof), the internal pressure tends towards the pressure acting on the outer surface of the opening without ever exceeding it, (see Section 3.6.2.2).

The increase or decrease of the pressure in the atrium went along with the inflow or outflow through the roof. This is because of the interdependent nature of the relationship between the internal flow balance and the internal pressure. The trends are illustrated in Figure 8.6 for the three wind angles tested. The flows were assigned with a positive or negative sign to indicate whether it was an outflow or inflow. Although it

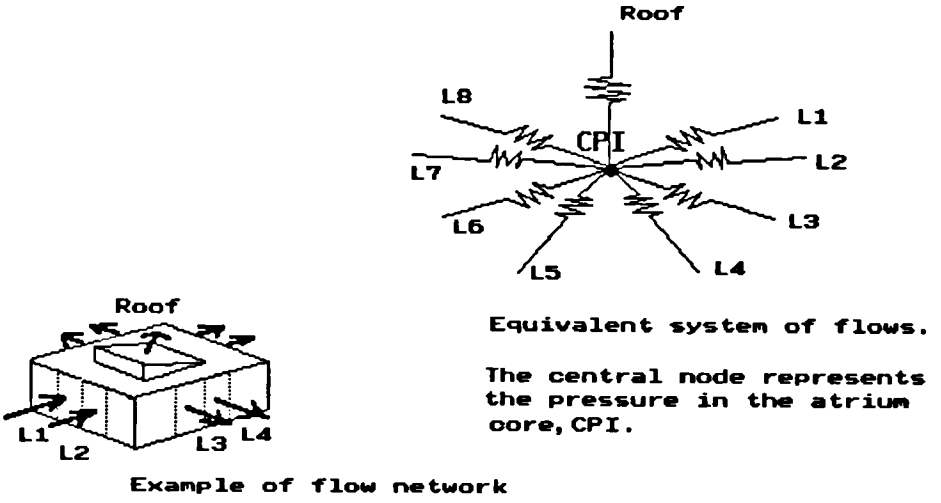

Figure 8.4: Equivalent system of flows in the atrium building models.

Table 8.2: The internal pressure coefficients measured in the core of the atrium models at 0°, 30° and 45° wind incidences.

Atrium index	Internal pressures CPI		
	Wind Angle 0°	30°	45°
A1	-0.17	-0.12	-0.11
A2	-0.26	-0.24	-0.25
A3	-0.29	-0.32	-0.33
A4	-0.33	-0.38	-0.41
A5	-0.44	-0.54	-0.57
A6	-0.11	0.0	0.05
A7	-0.12	-0.12	-0.12

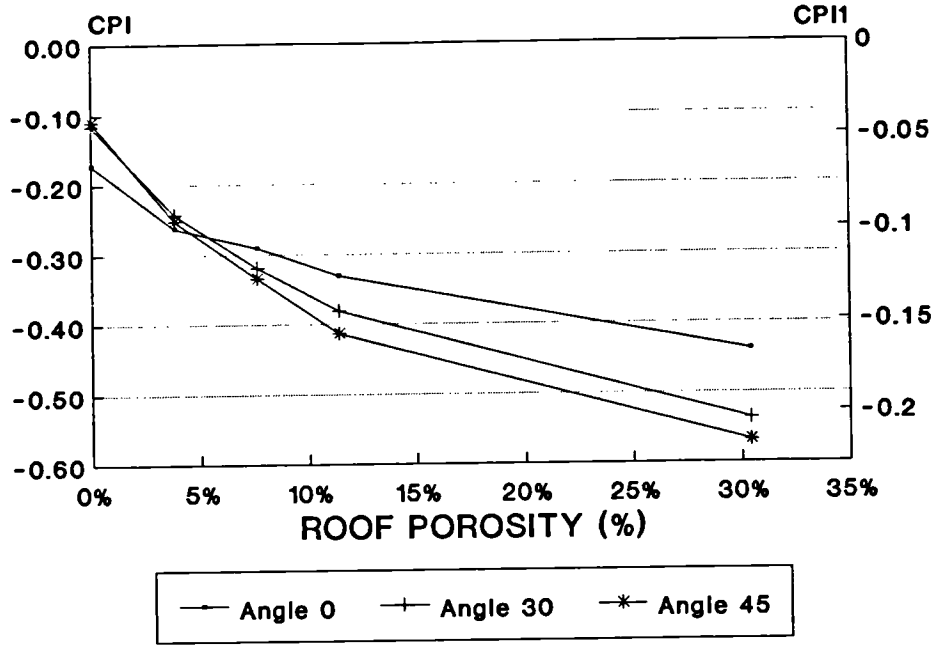

Figure 8.5: Effect of the roof porosity on the pressure in the atrium core with the suction mode, *(CPI is referred to the dynamic wind speed at the roof height, and CPI1 at the gradient height).*

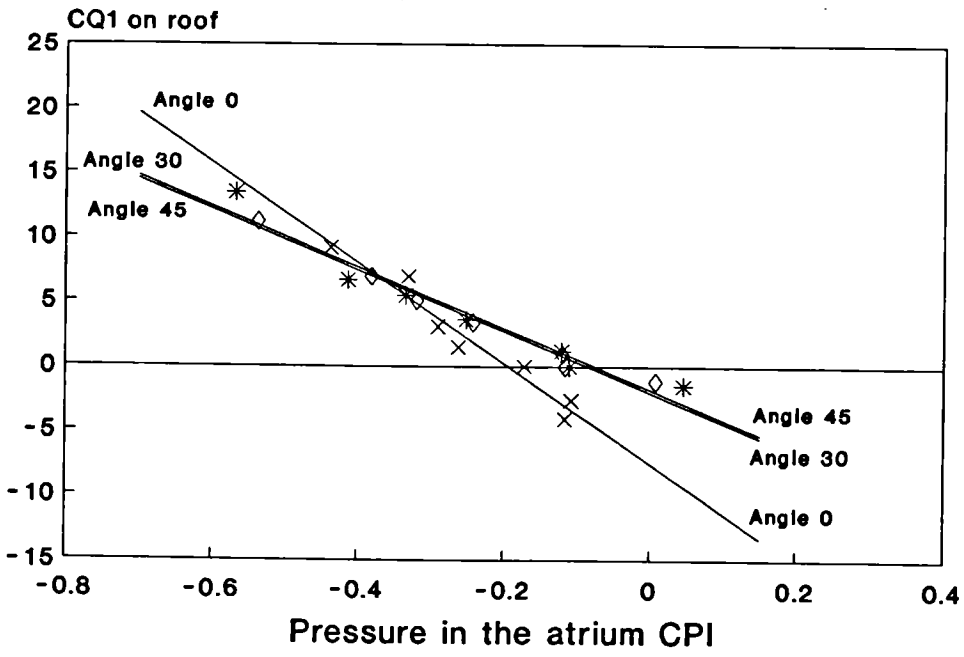

Figure 8.6: Interdependence between the flow through the roof and the pressures in the atrium.

seemed that the best fit between the data was each time a straight line, there was not enough evidence at this stage of the work to suggest a linear relationship due to the limited number of data.

8.6 Results of the internal flow measurements

The detailed measurements of the indoor flows in the atrium models are shown in Figure 8.7 to Figure 8.9, for wind incidences of 0°, 30° and 45° angles. The data can be found in Appendices C1 to C3.

8.6.1 Flow through the roof vents

The volume of air flowing through the model roof vents were not measured but inferred from the continuity equation which states that the mass of air entering a structure must equal that leaving it.

It must be stressed here that the roof openings may permit simultaneously inward and outward currents of air, yet, it is only the algebraic sum of these inflows and outflows that could be known.

Suction strategy

The atrium roofs that were designed to perform roof suction effects worked as intended. The greater the surface of vents located in the suction region were, the larger the volume of air extracted through the roof.

The roof outflows were greater when the models were orientated 30° or 45° to the wind than at 0° wind angle. Though, in the first case, (45° wind angle), the deficit of pressure on the roof was greater, this may not constitute alone a satisfactory reason. This is because each time a complex balance of flows through all the model apertures was achieved, and simple inferences may not be always rightful.

Positive pressure strategy

With this ventilation mode, the flow through the roof was inward as expected. This current of air was found to be substantially reduced at an oblique wind angle. It was believed that this was probably because a portion of the air that was entering the most upstream roof openings was leaving through the most downstream roof vents, owing to the large horizontal pressure gradient in this region, (see Section 8.4.2). This

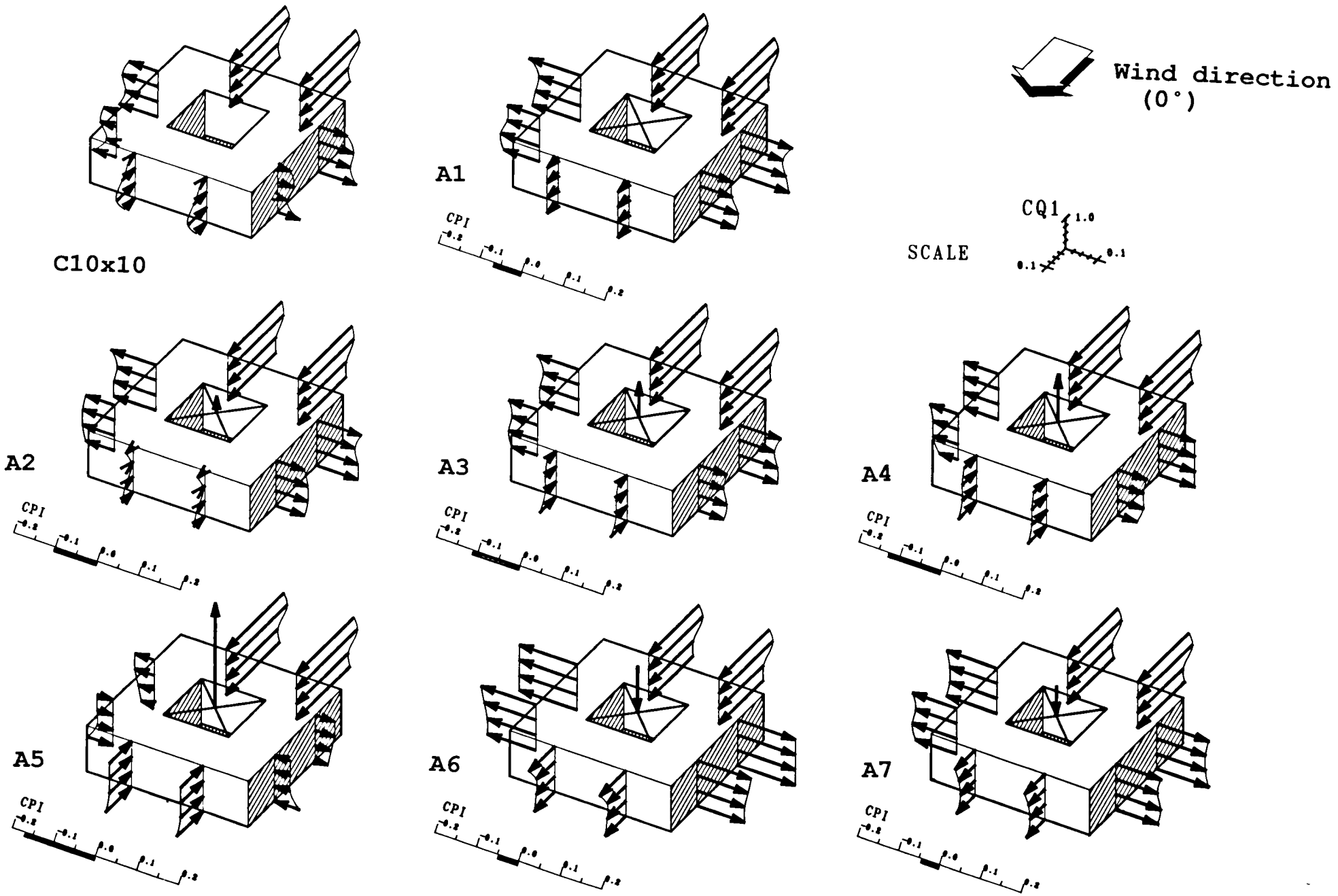

Figure 8.7: Detailed distribution of flow coefficients within the atrium models in isolation, (0° wind incidence).

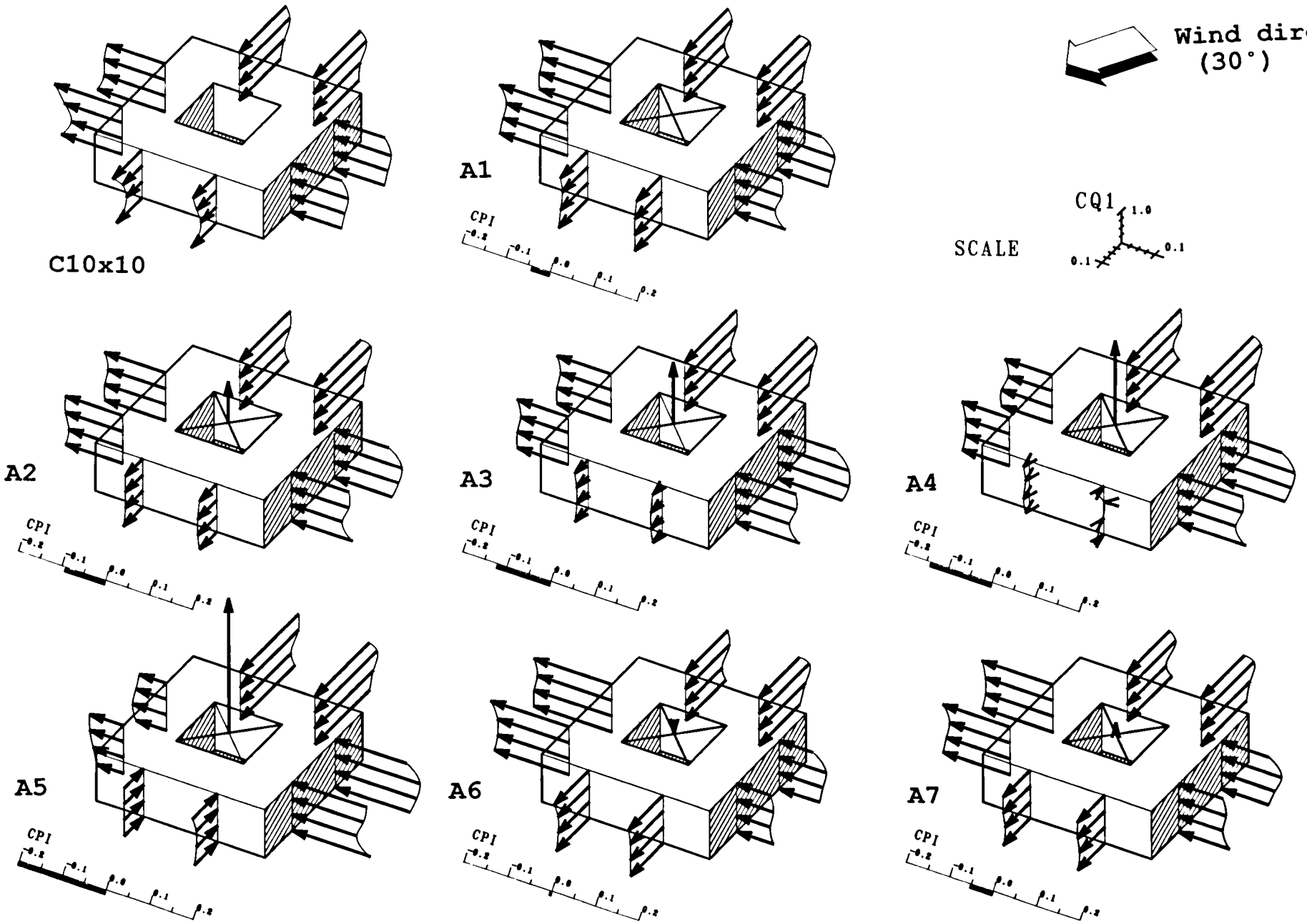

Figure 8.8: Detailed distribution of flow coefficients within the atrium models in isolation, (30° wind incidence).

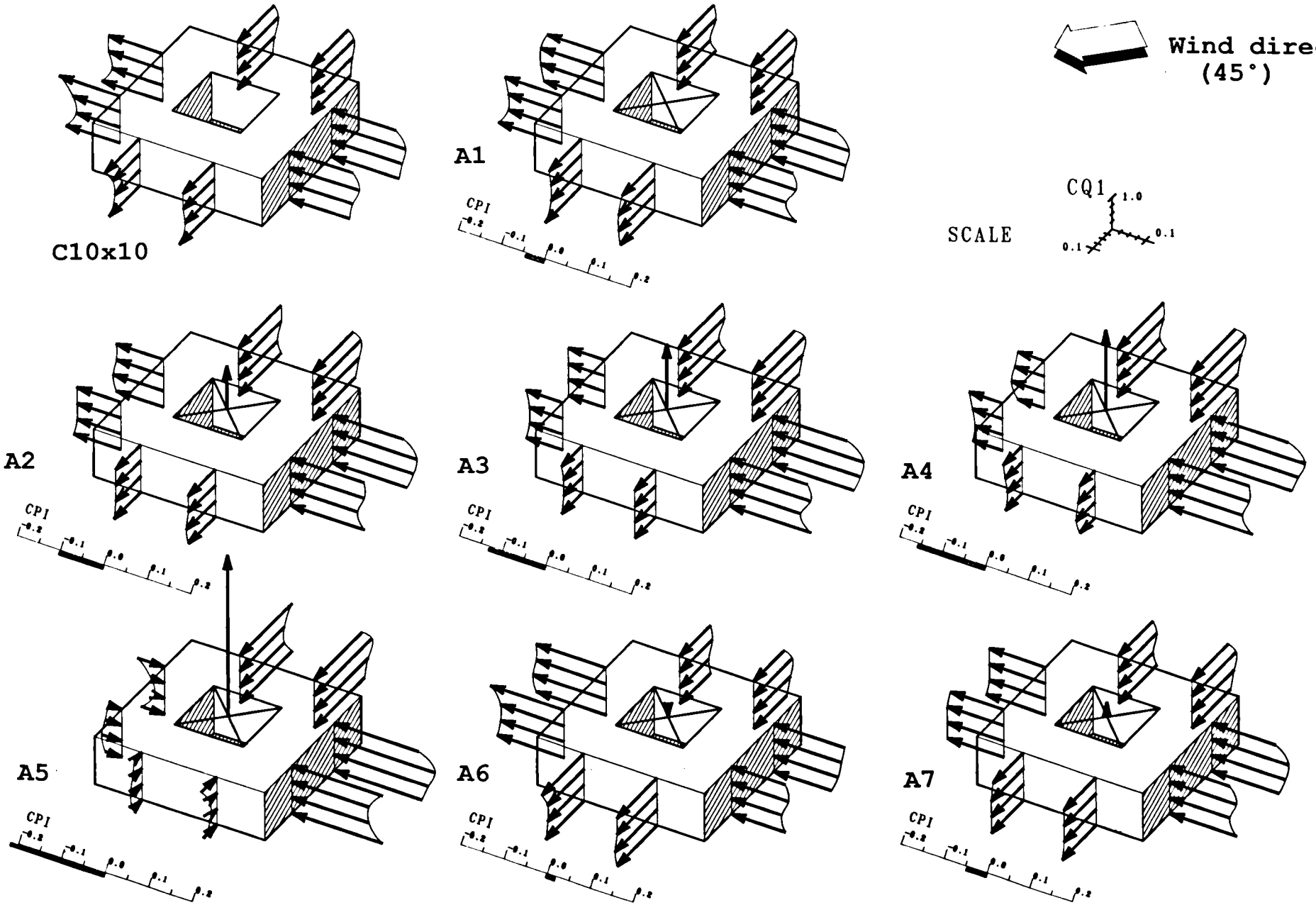

Figure 8.9: Detailed distribution of flow coefficients within the atrium models in isolation, (45° wind incidence).

volume of air never entered the atrium rooms and could not be recorded.

Near-atmospheric pressure strategy

With the roof openings located in a near-atmospheric pressure, it was possible, more than with any other cases, that the roof was used as inlet and outlet at the same time, like in the suggested operating ventilation mode described at the beginning of the chapter. Indeed, there may be sufficient pressure drop between the windward external wall and the roof surfaces to force some of the inflows out through the roof, and also sufficient pressure differential between the roof and the downwind walls for some volume of air to enter the roof openings and leave through the downwind windows. However, this could not be unveiled since the air current through the roof was not monitored. Finally, only the strongest airflow current, (i.e., the algebraic sum of the roof inflows and outflows), was known, so that this ventilation mode could be reduced to one of the other three, depending on the main direction of the flow through the roof and its magnitude.

At normal wind angle, the strategy was working in the same way as the positive pressure mode. At oblique wind incidences, on the other hand, it resembled the suction mode. Nevertheless, the roof of this model was neither used as an efficient suction device nor as a powerful wind deflector.

8.6.2 Flow through the atrium rooms

8.6.2.1 Models orientated normal to the wind

The atrium flow networks

To help to grasp more easily the effects the roof pressure forces had on the indoor air movement, a simplified and schematic flow network was produced and is shown in Figure 8.10. The pressures coefficients acting on the external walls and obtained from surface pressure tests are located on a linear scale. When the internal pressures are superimposed, the relative distance separating the internal pressure and the external pressures can give a rough estimate of the flow through the facades. The direction of flow can also be read. When a point corresponding to an external pressure is located on the right of the internal pressure point, it means that the direction of flow is from

outside into the atrium, (inflow). Reciprocally, when it is on the left, the flow is from the atrium to outside, (outflow).

Different networks of inflows and outflows could be set up in the atrium rooms depending on the way the air is driven through the roof. Five different flow networks could be identified, from the situation where the four facades serve as inlets and the roof as the only air exit, (case E, Figure 8.10), to the situation where all the air enters the roof and leaves through the facades, (case A, Figure 8.10). Out of these five possible networks only three were encountered. These were the flow networks B, C and D in Figure 8.9a. None of the tested configurations were capable of accomplishing a whole-building suction, or of using their roof apertures as the only inlets.

Figure 8.11 shows the values of the average flow coefficients, CQ on several locations of the models, L, and termed CQL. The ventilation conditions in each model can be observed along with the alteration from one model to another. This is now discussed.

Closed-roof atrium, A1

The flow network associated with this model could be identified as the case B in Figure 8.10. With this configuration, the flow entering the windward facade must be equal to the sum of the flows leaving the downwind faces. Consequently, the ventilation was very unbalanced. Approximately 40% of the inflow from the windward facade was leaving through each of the lateral facades and 20% through the leeward facade.

Suction strategy, A2, A3, A4 and A5

The effects of the roof pressure forces can be best followed by considering the closed-roof atrium as a datum. The effect of altering the roof pressure and permeability will be to shift the value of the internal pressure along the scale in Figure 8.10, changing its position in relation to the external pressures. This will be reflected consequently in changes in the amount of flow through each facades.

Forcing air out of the roof had the effect to reduce the outflows and to increase the inflows by lowering the internal pressures. It could be observed in the Figure 8.11 that negative values of CQL, (corresponding to the outflows), tended to diminish and positive values to increase as the roof became more porous, in other word, when the roof suction forces became stronger.

For some of these atria, the sign of some flows changed locally from negative to

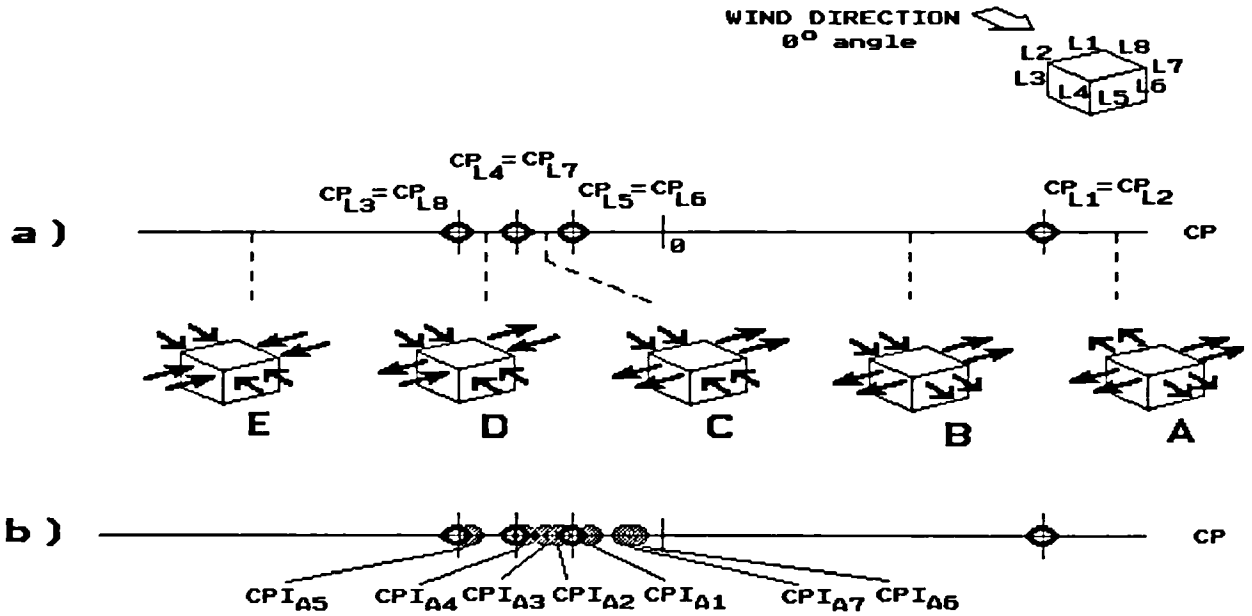

Figure 8.10: a) The different atrium flow networks associated with the distributions of internal pressures in relation with the external wall surface pressures, (at 0° wind incidence).

b) Internal pressures in relation with external pressures.

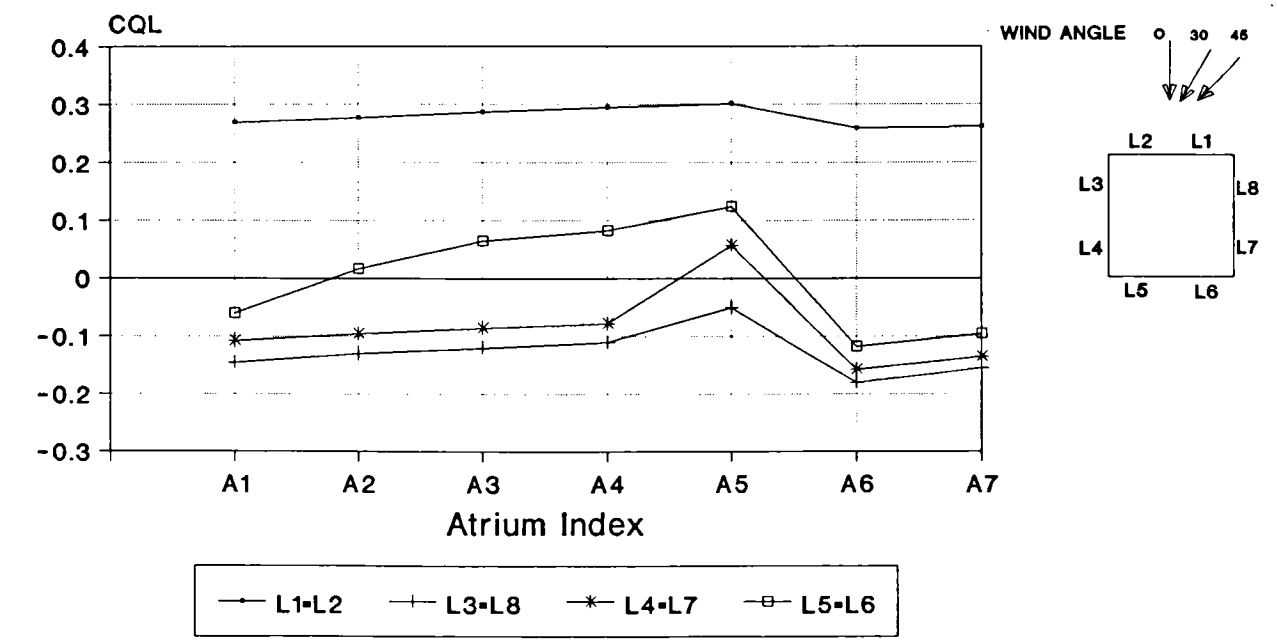

Wind angle 0

Figure 8.11: Variation of the local flow coefficients CQL with the change of the atrium configurations, (0° wind incidence).

positive, indicating that the flow reversed and became inward. This is because the internal pressures were reduced below the pressures acting on the external faces at these locations. In these conditions, the flow network corresponded to C or D in Figure 8.10. On the leeward face, where a relatively weak suction was found to exist, the flow was reversed when the relative roof porosity was 7.6%, (i.e., model A2). On the lateral side, however, it was only at the largest roof permeability, (ie., 30.4%), and only at the most downstream measuring points that the direction of the air current changed. On the locations L3 and L8 on the lateral facades, the very large suction caused by the flow separation at the upwind corners prevented the flow to reverse, even with the largest roof suction forces.

It could be clearly observed in Figure 8.11 that the roof suction strategy promoted large inflows of air. It is obviously implied that these volumes of air were mainly leaving through the roof apertures. For example, with the greatest roof suction effect, (i.e., model A5), 89% of the total inflow was extracted through the roof.

Positive pressure and near-atmospheric pressure strategies, A6, A7

By providing roof apertures in a positive pressure region, in the model A6, a mass of air was deflected from the roof level inside the atrium. This created a build-up of pressure that reduced the amount of inflows through the facades and increased the outflows. This effect was the reverse of what was obtained with the suction strategy.

The near-atmospheric pressure strategy was acting in the same way as the positive pressure mode, though the roof effects were slightly lower.

These ventilation modes could already be seen to be the most obvious strategies to improve the ventilation conditions in the downwind wings of an atrium and which were identified as being the most problematic. This is further discussed in Section 8.7.

8.6.2.2 Models orientated 30° or 45° to the wind

The atrium flow networks

The same schematic representation of the flow networks given in Figure 8.10 may be drawn for the conditions presented at 45° wind incidence, (see Figure 8.12).

The flow networks of all the models, except A5, coincided with the case C in Figure 8.12, in which, the apertures on the upwind facades were used as inlets and the

downwind facades as outlets. This cross-ventilation was encouraged because, when the models were facing the winds with an angle, two of their facades were under pressures above ambient and two in a suction region.

With the configuration A5, (maximum suction effects), however, even the flows in the downwind walls were inward when the model was facing the wind at 45° angle. This corresponded to the flow network E in the figure, in which the totality of the flow was entering the wall openings and was leaving through the roof, (i.e., whole-building suction).

Closed-roof atrium and near-atmospheric pressure strategies, A1, A7

The ventilation conditions of the near-atmospheric pressure mode in A7 was almost indistinguishable from the closed-roof atrium A1, at both 30° and 45° wind incidences. This is because, in A7, the roof flow contributed very little to the ventilation of the model rooms, (see Section 8.6.1). Indeed, only 12% to 14% of the inflows were estimated to leave the roof apertures.

The internal pressures in both models were almost half way between the pressures acting on the downwind and upwind external faces. This constituted an optimal situation in which there was almost equal flow rates in each wing of the atrium models (see Figure 13). The balanced ventilation obtained with these models could be upset whenever strong roof pressure forces were present. This was particularly true for the suction strategy.

Suction strategy, A2, A3, A4, A5

In comparison with the aforementionned configurations, the suction reduced the outflows to the benefit of inflows, (see Figure 8.13). This resulted in a rather unbalanced ventilation within the atrium model wings and could jeopardise seriously the air movement at the downwind wings.

The suction effects were in some models large enough to establish an inward air current at some locations on the downwind facades. However, this occurred for relatively large roof porosities, even though very strong suction was acting at the roof vents, (see Section 8.4.2). The indoor flows on the downwind facades did not start to reverse until the relative roof porosity reached 11.4% (model A4) at 30° wind angle, and 30.4% (model A5) at 45° wind angle. Until this happened, the outward flows decreased with the roof suction forces.

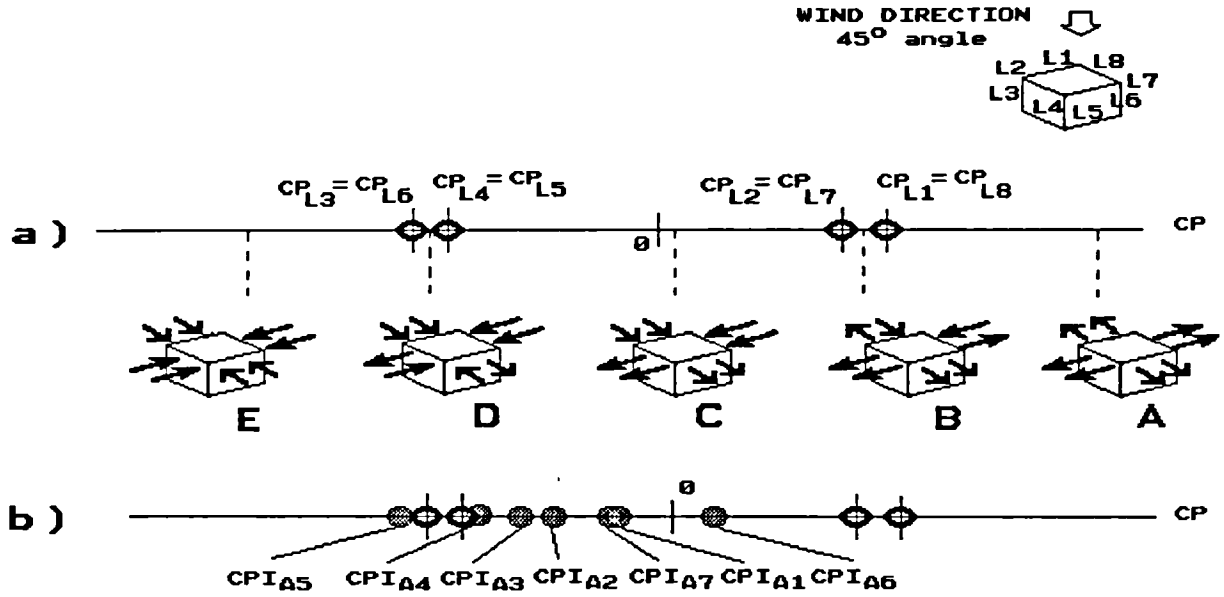

Figure 8.12: a) The different atrium flow networks associated with the distributions of internal pressures in relation with the external wall surface pressures, (at 45° wind incidence).

b) Internal pressures in relation with external pressures.

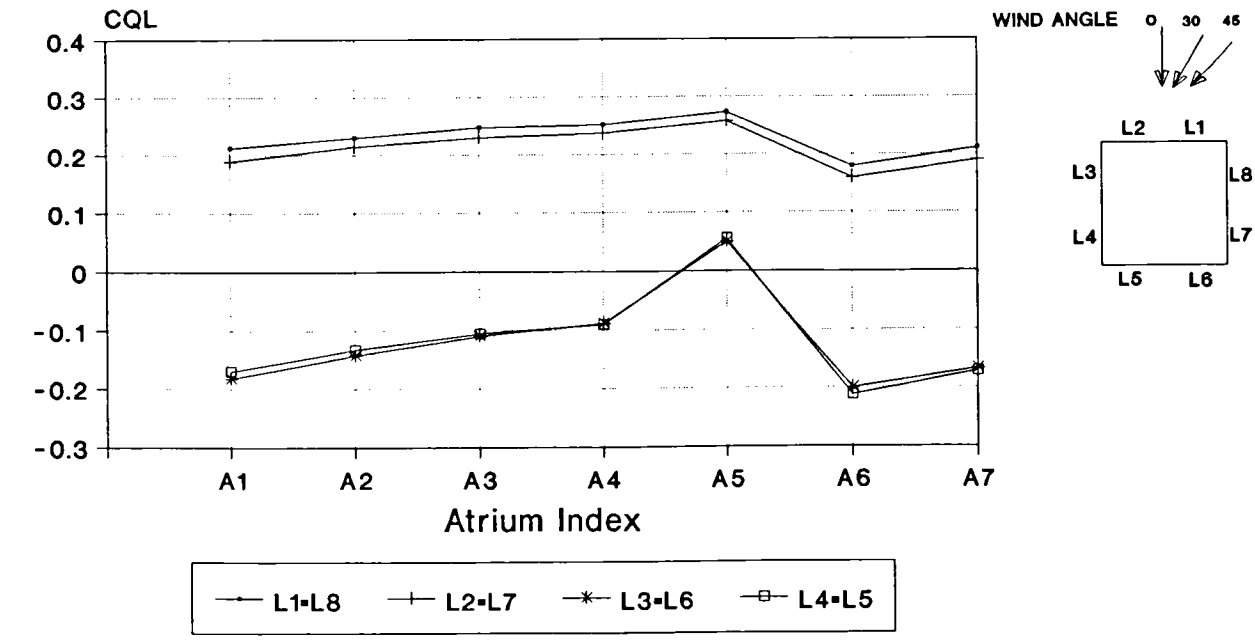

Wind Angle 45

Figure 8.13: Variation of the local flow coefficients CQL with the change of the atrium configurations, (45° wind incidence).

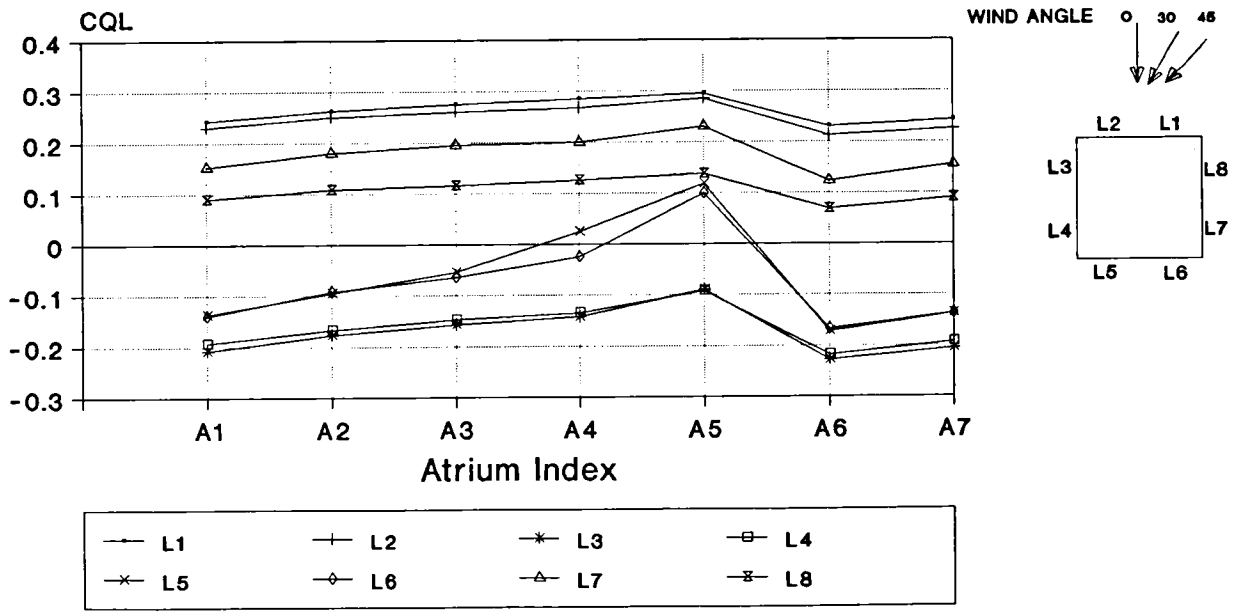

Wind Angle 30

Figure 8.14: Variation of the local flow coefficients CQL with the change of the atrium configurations, (30° wind incidence).

It can be noticed from Figure 8.14 that on the downwind facade that made an angle of 30° with the wind direction, (i.e., L3, L4), the flow did not reverse even with the largest roof suction effects. This testified to a very large suction force on the external walls.

Positive pressure strategy, A6

With the positive pressure strategy, the minimum inflows through the facades and the maximum outflows were obtained. Yet, because the contribution of the roof flows was small, the ventilation conditions in this model were not appreciably different from those in models A1 or A7.

Comparison with other related works

As evidenced in the literature review of Chapter 4, there is hardly any study with which the present results can be compared. This is mainly because the previous works were dealing with uni-cell examples.

The fact that the suction effects of roof vents resulted in higher inflows and lower outflows than the case where the vents were closed was also evidenced in other works, such as, Kobayashi and Ohba (1987) reviewed in Section 4.4.2.6, and also Bahadori and Haghighat (1985). These latter authors tested the influence of a vent at the apex of a dome covering a room. Their data showed clearly this trend on the rates of air flowing through the windows.

8.6.3 Effects of the wind incidence on the indoor flows

The change of the model orientation to the wind caused significant alterations in the indoor flow directions and magnitudes regardless of the atrium configuration.

The most important changes occurred when the orientation to the wind was shifted from 0° to 30°. On the lateral facade, (L7, L8), which was stricken by the wind with an angle of 30°, the flow generally reversed, from an outward to an inward direction. This was accompanied by a dramatic improvement of the flow intensity at this location. There were also significant changes in the flow direction and intensity on the model leeward faces. On the windward walls, (i.e., L1 and L2), the magnitudes of the flow coefficients decreased and on the downwind lateral faces, (i.e., L3 and L4), they increased in general with the change of the wind incidence from 0° to 30°.

The alterations in the indoor flows were generally less important when the wind angle changed from 30° to 45° than when it shifted from 0° to 30° angle. Except with the configuration A4 and A5 at discrete measuring points, the direction of the flows was kept the same in all the model locations. Smaller variations in the magnitude of the flow coefficients were also recorded.

In real situations, the wind direction is far from being steady. The variability of the wind direction is often reported from full scale measurements of being of the order of 30° or more, (see De Gids et al (1987), Chandra et al (1983) and Sherman and Grimsrud (1982)). In actual fact thus, it is most probable that the ventilation conditions in the atrium buildings will oscillate between the distributions set at each wind incidence. In particular, when reversed flow takes place as a result of the change of the wind direction, intermediate conditions between the inward air currents and outward flows can occur, (the reversal of flows occurred in all the models when the wind was changed from 0° to 30°). In this case it is possible that very weak flows may be encountered, driven almost exclusively by wind turbulences.

With the dramatic changes that occurred in the internal flows due to the change of the wind incidence from 0° to 30°, it is very difficult to infer precisely what would be the ventilation conditions in the models at intermediate wind angles. Owing to the interdependent nature of the system of flows, the variation of the air current at one location can cause the entire flow distribution to change. It is most complex to forecast the changes when reversed flows occur.

8.7 Ventilative performances of atria

After having examined the effect of the roof pressure forces on the internal flows in atria, it is of interest to give a verdict on which atrium offers the best ventilative performances, and whether or not atria are superior to courtyards.

As with the courtyard models, the ventilative performances of the atrium structures will be discussed on the basis of the spatial distribution of ranges of flow coefficients. This is given in Figure 8.15 to 8.17, for wind incidences of 0°, 30° and 45°. The cumulative percentages of building models under these ranges of flow coefficients are given in Table 8.3.

8.7.1 Models orientated normal to the wind

The air velocities through the model windows were on average between 21% and

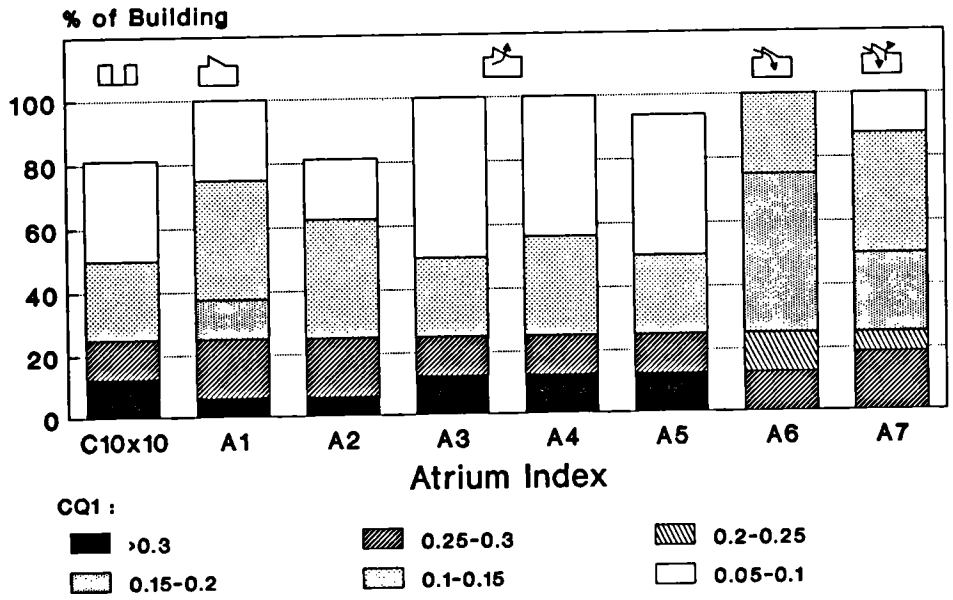

Figure 8.15: Fraction of the atrium models under ranges of flow coefficients, **(isolation conditions, 0° wind angle).**

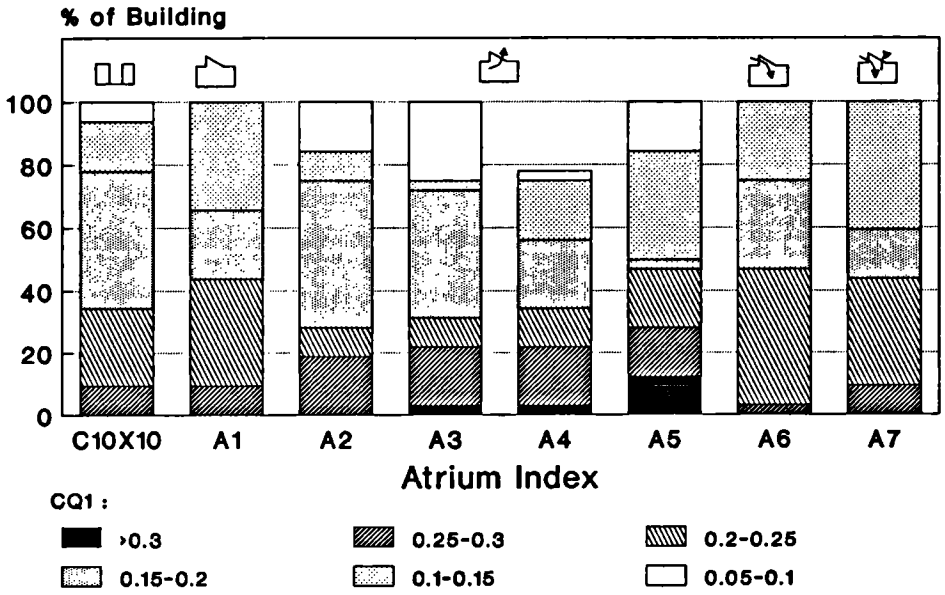

Figure 8.16: Fraction of the atrium models under ranges of flow coefficients, **(isolation conditions, 30° wind angle).**

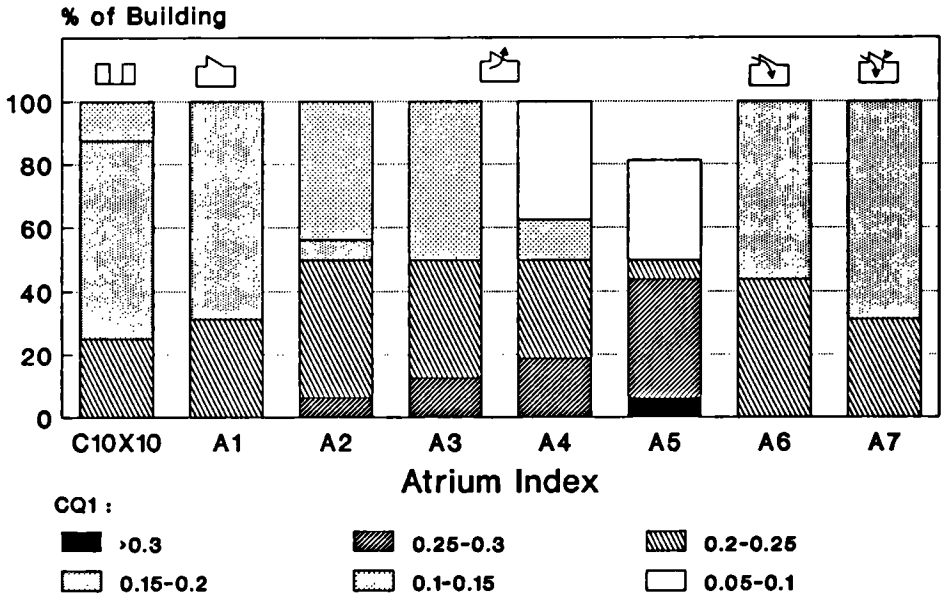

Figure 8.17: Fraction of the atrium models under ranges of flow coefficients, **(isolation conditions, 45° wind angle).**

Table 8.3: Cumulative percentage (%) of building under ranges of flow coefficients CQ1, (isolation conditions).

Angle 0°						
Model index	CQ1 >0.05	>0.1	>0.15	>0.2	>0.25	>0.3
C10x10	81.2	50	25	25	25	12.5
A1	100	75	37.5	25	25	6.25
A2	81.2	62.5	25	25	25	6.25
A3	100	50	25	25	25	12.5
A4	100	56.2	25	25	25	12.5
A5	93.7	50	25	25	25	12.5
A6	100	100	75	25	12.5	0
A7	100	87.5	50	25	18.7	0
Angle 30°						
Model index	CQ1 >0.05	>0.1	>0.15	>0.2	>0.25	>0.3
C10x10	100	93.7	78.1	34.3	9.37	0
A1	100	100	65.6	43.7	9.37	0
A2	81.2	84.3	75	28.1	18.7	0
A3	100	75	71.8	31.2	21.8	3.12
A4	78.1	75	56.2	34.3	21.8	3.12
A5	100	84.3	50	46.8	28.1	12.5
A6	100	100	75	46.8	3.12	0
A7	100	100	59.3	43.7	9.37	0
Angle 45°						
Model index	CQ1 >0.05	>0.1	>0.15	>0.2	>0.25	>0.3
C10x10	100	100	87.5	25	0	0
A1	100	100	100	31.2	0	0
A2	100	100	56.2	50	6.25	0
A3	100	100	50	50	12.5	0
A4	100	62.5	50	50	18.7	0
A5	81.2	50	50	50	43.7	6.25
A6	100	100	100	43.7	0	0
A7	100	100	100	31.2	0	0

28% of the wind speeds measured at the atrium wall heights, (i.e., the flow coefficients averaged over the whole building model, CQT, were between 0.21 and 0.28). These velocities represented 14% to 18% of the wind speeds measured at the gradient height, (i.e., CQT1 were between 0.14 and 0.18). For the courtyard, CQT was equal to 0.19.

Positive pressure and near-atmospheric pressure strategies, A6, A7

It is evident from Figure 8.15 that the configurations A6 and A7, for which the roof apertures were used as inlets, had the largest proportions under flow coefficients, CQ1, above 0.15. In other words, they were those with the least fraction under weak flows and with the most balanced ventilation. It is clear that the advantage of exploiting the roof positive pressure was to improve the ventilation on the downwind wings which presented the most critical conditions.

On the other hand, these structures were lacking of flow coefficients CQ1 above 0.25, when compared with the other structures. There was in no case flow coefficients above 0.30.

These strategies are probably most suitable when the building requires to be entirely ventilated by natural means since these ventilation modes restrict the fraction of the building which may be under poor ventilation conditions. Yet, the success of these strategies will depend on the availability of strong breezes.

Suction strategy, A2, A3, A4, A5

With the roof suction mode, a portion of the building was under strong ventilation. Typically 1/8 of the building models had flow coefficients CQ1 above 0.3, and 1/4 above 0.25. In counter part, weaker flows were also encountered in comparison with the previous models.

The fraction of building which was affected by low range flow coefficients, ($CQ1 < 0.15$), was very variable from one model to another. While a particular configuration could have detrimental effects at a discrete location on the downwind wings, another configuration could improve the ventilation at this same location, but might have adverse effects elsewhere in the model.

Owing to the fact that these structures had an unevenly distributed ventilation, with powerful flows at the windward wing and particularly weak flow at the downwind wings, they should be best suited for conditions where only part of the building is intended to be naturally ventilated, (typically 1/4 of the building), the rest mechanically

cooled. In these circumstances, the breezes should probably not need to be very strong to achieve adequate comfort levels.

Closed-roof atrium, A1

The ventilation conditions of the atrium with a closed roof can be considered as intermediate between those realised by the suction strategy and those of the positive pressure mode.

Comparison with the courtyard, C10x10

In Figure 8.15 the ventilation conditions of a representative courtyard, C10x10, are shown, along with those of the atria, (C10x10 is the same as any of the atria to which the roof was removed).

The distribution of the flow in the courtyard model resembled somewhat that of the suction strategy models. The courtyard configuration had with A2 the largest portion of building under flow below 0.10. At the same time, it had with A3, A4 and A5 the greatest percentage of building with flow coefficients above 0.3.

Depending on whether very good ventilation is sought locally, with few considerations for the rest of the building, or whether the whole building needs to be ventilated naturally, the courtyard could be considered as appropriate or not. However, for both design intentions, there was always some atrium configurations that performed much better than the courtyard.

This result demonstrates clearly that the statements supporting the superiority of the courtyard over atria to drive ventilation are pure speculations, (see for example Leung et al (1981), p. 49).

8.7.2 Models orientated 30° or 45° to the wind

The air velocities through the model windows were on average between 24% and 28% of the wind speeds measured at the atrium wall heights, with a wind incidence of 30°. At 45° wind angle, they were between 25% and 29%. Although it is clear that the overall flow coefficients were higher at an oblique wind angle than at normal wind incidence, this does not indicate always that better ventilation was achieved in all parts of the models.

The spatial distributions of flow coefficients, CQ1, are shown in Figure 8.16 and

Figure 8.17 with the models orientated 30° and 45° to the wind respectively. They can be compared with those at 0° wind angle given in Figure 8.15.

The effect of changing the orientation can be seen to reduce in general the fraction of the building model under the high velocity ranges. At 30° wind angle, only the three most powerful roof suction models had flow coefficients, CQ1, above 0.30. At 45° wind angle, only model A5 reached these levels. In counter part, the change of orientation from normal to oblique angle reduced the fraction of building under weak ventilation. In other words, the oblique wind incidences promoted a more evenly distributed ventilation within the models. Nonetheless, this was not always the case, notably for the models exploiting strong roof suctions. This can be seen clearly in Figures 8.17.

Closed-roof, positive and near-atmospheric pressure strategies, A1, A6, A7

Owing to the fact that the roof flow in model A7 contributed very little to the ventilation of the model rooms, the ventilation condition of this configuration was almost the same as the closed-roof atrium. This was also true for the positive pressure strategy, though, at 30° wind incidence, the roof flow affected somewhat the inflows through the upwind facades.

The flow coefficients, CQ1, of the three models were all above 0.10 and below 0.30, for 30° wind incidence. The interval was narrower at a wind angle of 45°, in which case, all the values were between 0.15 and 0.25. These models had the most evenly distributed ventilation.

Suction strategy, A2, A3, A4, A5

There were large differences in the spatial distribution of ranges of flow rates from one configuration to another. For all the models, however, the ventilation conditions significantly segregated the upwind wings from the downwind wings. There was a strong air movement in the first case and weak ventilation in the second case. At 45° wind angle, these structures had typically half of the building, (upwind wings), with flow coefficients, CQ1, above 0.20.

This ventilation mode is probably most appropriate when the building has to rely partially on natural ventilation, (i.e., only upwind wings). This is particularly true for the configuration A5 having the most powerful roof suction. The same conclusions were reached with the models orientated normal to the wind.

Comparison with the courtyard, C10x10

The spatial distribution of ranges of flow coefficients in the courtyard model resembled that of the closed-roof atrium strategy, the near-atmospheric pressure, or the positive pressure strategies. Nevertheless, compared to these structures, the courtyard presented a penalty, that was, the presence locally of some weaker flows.

8.8 Conclusions and discussion

This chapter presented an appraisal of the ventilation of atrium structures in isolation.

Four possible ventilation modes which can be used by atria were identified: the positive roof pressure strategy, (in the example of the ancient wind catchers), the roof suction mode, the near-atmospheric pressure mode, (which can perform the two aforementionned modes simultaneously), and the atrium with a sealed roof.

Prior to internal flow measurements, surface pressure tests were made to choose among a variety of roof shapes the ones that could best perform under each of these ventilation modes. A tall monopitched roof was selected for all the tests.

The ventilation modes were found to perform as expected. Nevertheless, with the near-atmospheric pressure strategy it was not possible to determine whether the roof vents were used simultaneously as inlets and outlets. This case could be reduced to one of the three others, depending on whether the main air current through the roof was inwards, outwards or nil.

The roof permeability was found to be an important parameter in inducing ventilation under a specific mode. This was tested with the roof suction and showed that maximum roof effects were obtained with the most porous roofs, even though, the average mean suction acting on the openings was lower than with less permeable roofs.

The comparison in the ventilative conditions between the various strategies is as follows:

i) The positive roof pressure mode was found to decrease the inflows in the upwind wings of the atrium and increase the outflows through the downwind walls. This had advantageous implications for the ventilation of atrium buildings since the most critical ventilation conditions were restricted to the downwind walls when the models where normal to the wind. This ventilation mode was also performed by the model intended to be used under the ambient pressure strategy.

ii) With the suction strategy the outflows on the downwind wings were inhibited and the inflows promoted. With the models orientated normal to the wind this often jeopardised seriously the ventilation in the downwind wings. Yet, maximum air movement was achieved in the upwind parts.

iii) At normal wind angle, the ventilation conditions of the atrium with a sealed roof were intermediate between those of atria with roof suction and with positive pressure modes.

iv) Orientated 30° or 45° to the wind direction, the model exploiting the positive pressure mode and the model with the roof located in ambient pressures had almost the same ventilation conditions as the closed-roof atrium. This was because the flow through the roof in the two former cases did not contribute to the ventilation of the atrium rooms. An explanation that was put forward was that, a portion of air which was entering the most upstream roof openings was leaving the most downstream roof vents, owing to the large horizontal pressure gradient in this region. The rooms of these models were evenly ventilated.

v) With the suction mode, however, the ventilation conditions segregated the upwind wings from the downwind sectors. In the first case, there was a powerful air movement, and in the second case, particularly weak flows. The model with the most powerful roof suction effects was capable of establishing a whole-building suction when the model was orientated 45° to the wind.

vi) On the basis of these results, the choice of a strategy was believed to depend mainly on whether the building is intended to be entirely ventilated by natural means or partially, with the rest of the building mechanically cooled. For the first design intention the positive pressure strategy is probably most suitable, since the fraction of the building under weak flow is restricted. Yet, the success of these strategies should depend greatly on the availability of strong breezes. The suction strategy is best suited for the second design strategy, in which case, even weak breezes may be enough to achieve comfort levels for a limited portion of the building.

The location of the cool and clean air can also dictate the position of the air intakes and thus the choice of the ventilation mode. In this respect, the positive pressure strategy is probably best suited for night-time-only venting, since it is expected that at night the cooler air will be located at the roof level. This configuration may also be adequate in sites where cool marine trade winds prevail.

Also, problems of odour and noise migration in the building must be addressed in the choice of the atrium type. Finally, smoke control strategy must be compatible with

the ventilation for environmental control.

vii) When the atrium configurations were compared with the courtyard structure, it was found that for any of the aforementionned design intentions there were always some atrium types which performed much better than the courtyard. This demystifies somewhat the belief that the courtyard is superior to atria for inducing wind-driven natural ventilation.

The results presented here are nevertheless applicable only for structures which are located away from any obstruction. This represents probably very few real cases since courtyards and atria are mostly found in congested urban sites. This topic is discussed in the following chapter.

Chapter 9:

Ventilation conditions of courtyard and atrium buildings in congested urban sites

9.1 Introduction

It was a necessary step to examine, first, the natural ventilation of courtyard and atrium buildings in isolation, before considering the more complex situation of an urban environment. In reality these structures are usually surrounded by other buildings. The courtyard and atrium concepts are then a logical response to the restriction of space, to the need for privacy, view, noise control and daylight. In this chapter, the influence of group layouts is tested on selected models previously used.

In the preceding experiment, only the general roughness of the terrain was modelled and the building model was fully exposed to the wind. In an urban development, however, the close proximity of other buildings is inevitable, and mutual wind shielding exists. In these cases, it is imperative to put the prototype back in its setting where the flow around each individual building may interact. Vickery (1981) stressed that, when the height of the building tested is comparable with that of other obstacles nearby, the flow patterns, and thus the pressure fields near the ground, depend upon the exact size and the arrangement of the obstructions more than the general measure given by the simulated atmospheric boundary layer.

9.2 Modelling of the urban site

The first step of the experiment was to decide on the size of the group layout

which must be modelled accurately in order to obtain representative conditions of an urban site with buildings of moderate heights.

There are advantages in modelling a little of the building surroundings, since it is expensive and time consuming to reproduce in detail an extensive area. However, objections may be raised due to the fact that some characteristics of the actual urban atmospheric boundary layer, which grows generally on very large fetches, may be lost when the group layout size is reduced.

The concern to minimize the extent of a layout which has to be accurately modelled in order to preserve most of the characteristics of the urban flow has motivated few studies. These are now reviewed.

9.2.1 Influence of the array size on the pressure forces: a review

General recommendations

There are several recommendations on how a urban development must be modelled in wind tunnels. Vickery (1981) indicated that the most common practice is to reproduce the urban development around the site for typically 600 m, and to model the general roughness of the terrain beyond this distance.

On the basis of wind tunnel investigations made at Bristol University, U.K., Cook (1972) suggested that the exact reproduction of the surroundings should be made at least to a radius of 5 rows of elements of the same size. Also, any high rise building upstream of the site that could contribute to the flow must be included in the modelling within the general surface roughness.

Wiren's work

Wiren (1985) and (1987) reported two studies on surface pressure measurements made respectively on a detached house and a block of contiguous houses located amidst an array of identical buildings. The size of the array dealt with was small, i.e., one, two or three rows of surrounding elements, representing fetches of approximately 3 to 14 times the building heights. The author indicated that the increase of the surrounding models from one row to two or three had generally minor effects except at an oblique wind angle of approximately 30°, in which case, the additional rows were found to block the air stream which otherwise penetrated the first rows of buildings. The effect

was nevertheless less marked for closely spaced building models.

Soliman's and Hussain's studies

Probably the most comprehensive investigations intended to establish the required size of an array for urban site modelling were those of Soliman (1976) and Hussain (1978). By examining the variation of the drag with the increase of the fetch on cube models in regular arrays, they were able to determine the size of the layout from which changes in the drag would be nominal with further increase of the group size. This was taken as the criterion for modelling.

Soliman (1976) tested array sizes (R) between 3 to 14 times the model height (H), for group plan densities[1] between 3.12% and 50%, with patterns that were either normal, staggered or random. The author indicated that longer fetches were required for larger spacing between the elements in the group, for staggered patterns, and/or for thinner incident boundary layers. He nevertheless suggested that the drag coefficient should stabilise at R/H= 12, irrespective of the group density.

This author also investigated the influence area of the array fetch around a model by removing progressively the surrounding models and examining the limits at which the drag changed by more than ∓5% and ∓10%. The test covered different orientations of the group layout to the wind, but measurements of the model drag were always made with the test model normal to the wind. The boundaries of the influence area on the model drag, plotted for different group layout wind incidences, took the form of a foot print rather than a circular shape. The windward and leeward sectors were emphasised whilst the side regions were found to be less important.

Hussain (1978) repeated Soliman's tests for the establishment of the minimum fetch sizes required for modelling, yet, with more extensive fetches, (R/H extending up to 145 upstream and 25 downstream to the model test). He criticised Soliman's work in that the atmospheric boundary layer was not rigourously established, and claimed that the new experimental arrangement should overcome this weakness.

Hussain indicated that the extent of the array size required for the pressures to stabilize depended on the group density, (the group density tested here was between 5% and 25%), (see Figure 9.1). He suggested that a fetch of 10H to 25H should be sufficient to reproduce the atmospheric boundary layer of an urban site where there is no

[1] The group plan density was defined as the ratio between the building plan area and the building site area.

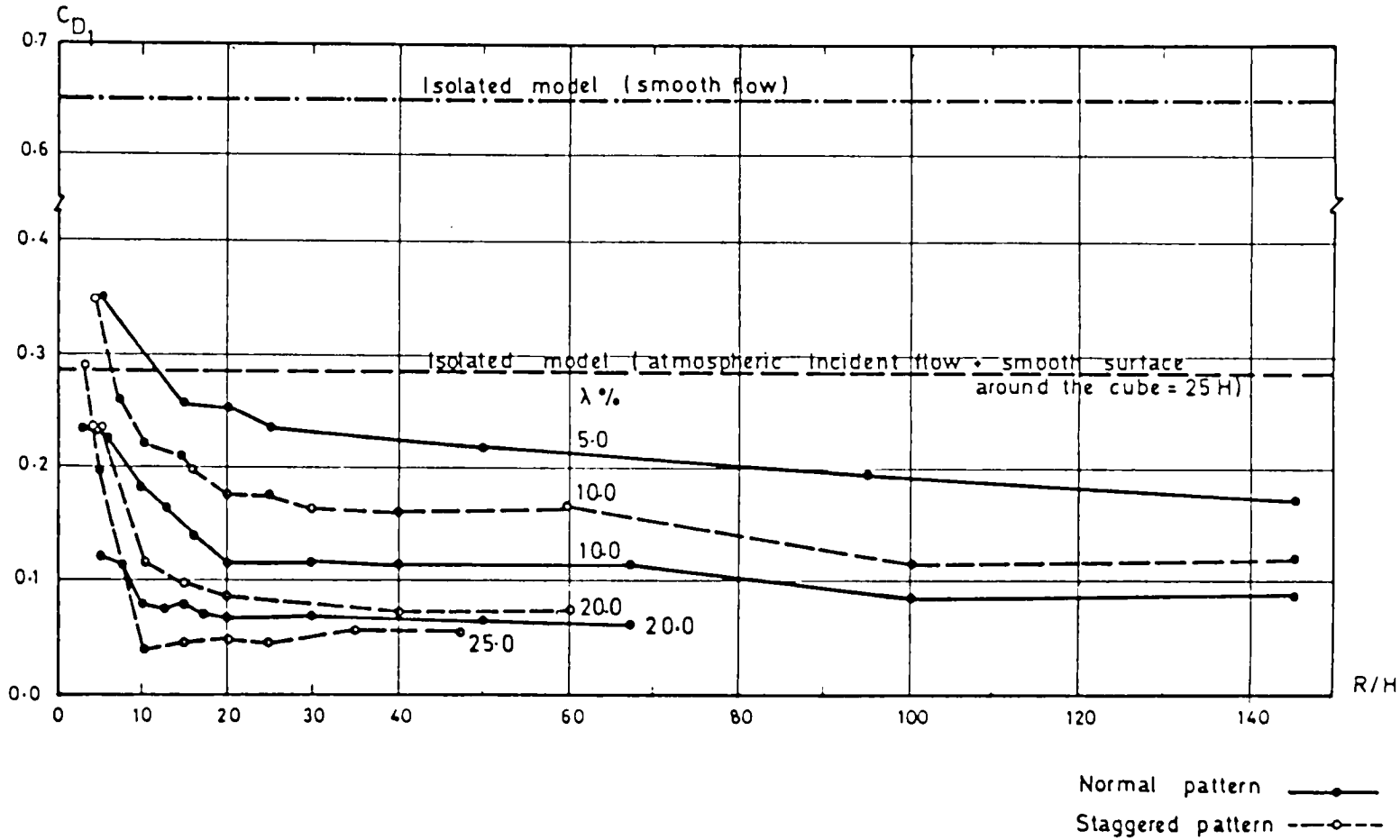

Figure 9.1: Variation of the drag coefficient with the group layout fetch, (After Hussain (1978)). *CD_1 is the drag coefficient referred to the velocity at the gradient height, R is the fetch length, H is the building model height and λ is the group plan density.*

dominant high rise buildings. These distances were expected to be shorter for higher densities. The introduction of the shear flow mechanism upwind to the group layout, with the addition of general roughness elements, was found to reduce further the array size required for the surface pressures to stabilize.

The two aforementioned studies dealt only with the drag or lift and did not consider the pressures on the lateral faces of the building models. For the purposes of this programmed experiment this was unfortunate, since there was no indication on whether the recommended values given for the minimum group layout size would be satisfactory for the region of the flow on the lateral facades. Yet, the test made by Wiren (1987) gave some evidence that the pressure distribution on the lateral facades should not be sensitive to the presence of adjacent obstructions, (see pressure contours provided in the publication).

Necessity to establish the adequate array size for the present tests

The modelling of the upwind and downwind layout fetches to some of the values recommended by Hussain was difficult to realise in the present test because of the large scale used. Not only could the space in the wind tunnel not accommodate such fetches, but also the cost and time to construct the sheltering models would be excessive.

Nevertheless, there were reasons to believe that such large fetches might not be necessary for the present tests. Indeed, it was expected that the differences in the pressure fields, as the size of the array expands, may not be noticeable in terms of flow rates measured by the orifice plate models for two reasons, i) the flow is proportional to the square root of the pressure drop, thus the differences in terms of pressures are reduced when converted into flows, and also, ii) the porosity of the model may dampen the differences in pressures measured on solid models. On the basis of these considerations it was decided to test the effect the fetch has on the internal flow in the present models, and to establish the extent of the array size required for a simulation of the urban setting.

9.2.2 Effects of the fetch on the internal flows

Test arrangements

The influence of the group layout fetch on the internal flows was examined on the

group layout which had the smallest density. The plan area density, PD, was equal to 28%, (PD is the ratio between the building plan area and the site area). On the basis of Hussain's conclusions, it was not necessary to undertake the same test for other programmed layout densities since smaller fetches are required for denser group layouts.

The upwind fetches were changed from one model row, representing a distance equal to 4.9H, to three rows, equivalent to a fetch of 14.7H, (H is the height of the building surrounding the atrium and also the height of the surrounding elements). The downwind fetch was increased by up to two rows owing to the restricted space downstream. On the sides the limited space between the wind tunnel walls allowed only a fetch of 4.6H. This was expected to have minor effects on the windward or leeward wings of the model since, as shown by Soliman (1976), the flow was marginally influenced by the fetch in these regions. From Wiren's (1987) results, which indicated almost no influence of adjacent buildings on the flow on the model lateral faces, it was inferred that the restriction of the layout fetch sideways should not be critical for the modelling of the flow around the test model.

The effects of the fetch was examined with the courtyard model, (i.e., C10x10), and one atrium model, (i.e., A5). Although the test for the atria were restricted to the model A5, the results were believed to apply to any of the other atrium configurations. Indeed, the atria were differentiated by their roof characteristics. Since A5 was the configuration in which the roof effects were the greatest, any distortion of the pressure field at the roof level introduced by changes in the array sizes would be most easily perceivable with this model.

The measurement were first made at the windward and leeward model sides, until the satisfactory array size was obtained. Thereafter, the test was extended to the lateral faces at the largest fetches to make sure that the internal flow did stabilise in all parts of the building models.

Analysis of the results

The results are shown in Figure 9.2. The values of the flow for each location represent an average of the internal flows over the four storeys.

The figure indicates clearly that the group fetch hardly affected the internal flows. The changes between one layout arrangement and another were of the order of 2% to 4% except at the measuring location L4 where it was approximately 15%. It was

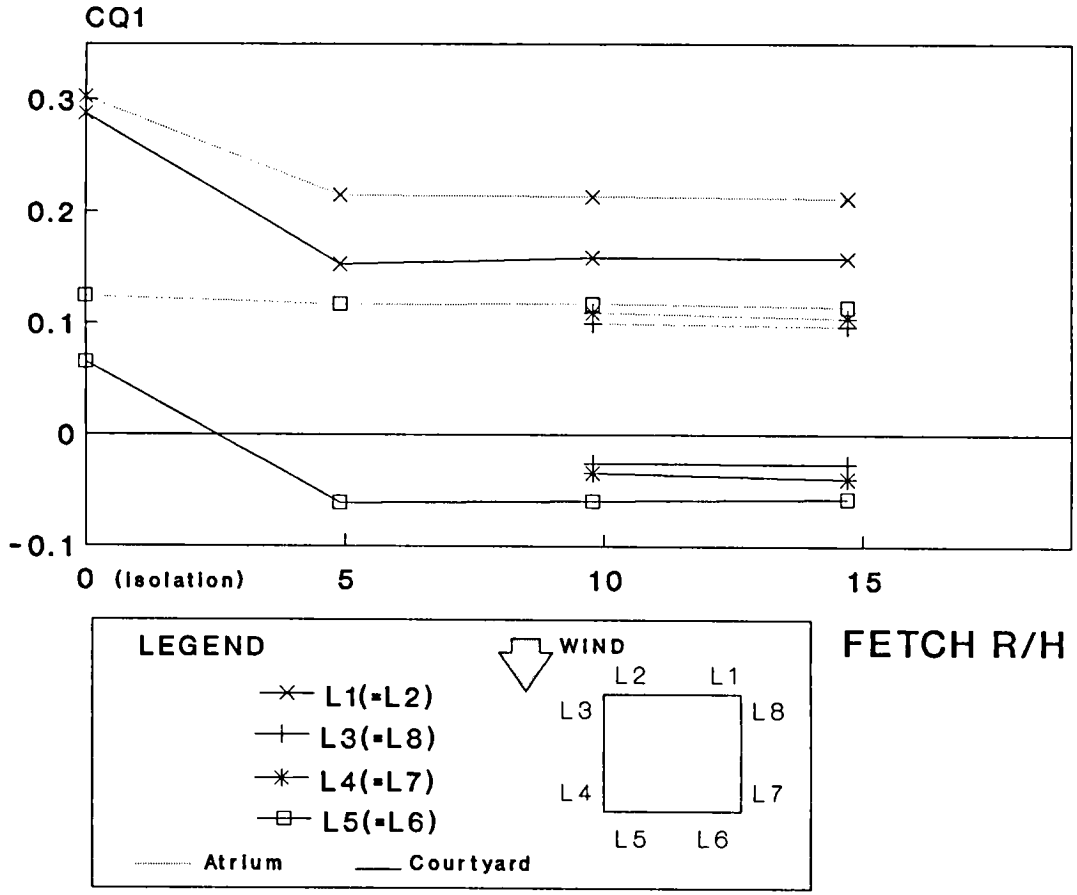

Figure 9.2: Variation of the flow coefficient with the group layout fetch.

already mentioned that the indoor flow at this location was particularly sensitive to small errors of misalignment, (see Section 6.3.8). It was suggested that this could be a result of a displacement of the external flow reattachment position on the walls.

According to Soliman (1976) and Hussain (1978), increasing the fetches beyond the suggested values for modelling would result in nominal changes in the drag. From Hussain's data it can be read that, for fetches varying between 25H and 145H, the differences in the drag were of the order of 20% at a group density equal to 5%, (smallest density). Since the internal flows are proportional to the square root of the drag, such changes in the drag would represent changes in indoor flows of only 6%. Below the suggested fetch limits, on the other hand, the changes in the model drag can be seen in Hussain's data to be important. For example, for a group layout with a density of 20%, the change of the array from 1 surrounding row to 5 rows, that is, a fetch of 3H to 10H, caused the drag to decrease by 80% of its mean value. This should represent approximately a difference of 35% in the internal flows. In the present investigation changing the fetch from 1 to 3 rows had a much smaller effect.

The reason why the internal flows (measured on hollow models) were less sensitive than the drag (measured on sealed models) to the change of fetch could probably be attributed to the effect of the porosity. Soliman's and Hussain 's results showed that there were greater pressures on the windward facade and greater suctions on the leeward surface of a sealed model when the fetches were smaller. If openings were provided, a flow would instantaneously be induced, releasing the high wind pressures on the upwind walls and raising, at the same time, the downwind pressures. The pressure differential between the model faces should thus be subdued in comparison with the sealed model, and the effect could be expected to be greater for larger indoor air currents. Ultimately, the change of the indoor flows could be expected to be even more attenuated since they are proportional to the square root of pressure differentials.

In the subsequent tests, the group layout consisted of three rows of elements upwind to the test model and two rows downwind.

9.3 The range of variables considered in the investigation

The ensemble of the parameters tested were given in Section 6.3.9 and are reminded here:

i) The building clear spacing, Sc, was changed from 1.5H to 2.3H.

ii) The plan area density, PD, was varied between 28% and 50%.

iii) The building group pattern was either, (a) normal, or (b) staggered.

iv) The building group layout size R was fixed to approximately 14.7H upwind and 9.78H downstream. H is the height of the building surrounding the atrium and also the height of the test atrium walls.

v) The group layout was either facing the wind with 0° angle or 45°.

vi) The incident flow was shear. The roughness elements arrangement upstream to the building group layout were the same as in the previous experiments. The boundary layer of the approaching wind was thus characteristic of a suburban to an urban site with buildings of moderate heights.

vii) The models tested were the courtyard model, C10x10, the closed-roof atrium, A1, two atria exploiting the roof suction, A4 and A5, with a relative roof porosity equal to 11.4% and 30.4% respectively, and the models using the positive and near-atmospheric roof pressure modes, A6 and A7 respectively, (see Section 8.2, for definitions of ventilation modes). The two configurations used in the previous experiment, which were omitted here, are A2 and A3, with their roofs made to induce slight suction effects. The ventilation conditions of these structures may be inferred from the conditions found in model A1 and in model A4.

The ample range of group layout densities that was chosen to be tested was motivated by the desire to offer a large range of application to the results. For different group layout densities it can be expected that the external flow would be of a different nature, (see Section 4.3.2). In fact, the distance of separation between the elements were chosen to coincide with the onset of distinct flow regimes -the wake interference flow regime and the skimming roughness flow, which are known to take place approximately at these values of spacing, (see Section 4.3.2). There was, however, little relevance for the present study to determine precisely the nature of the flow. Indeed, the work of Soliman and Hussain showed that the manifestation of different flow regimes is in the difference in the rate of change of the drag with the change of the group layout densities, (see Section 4.3.2). This may eventually translate into differences in rate of change of cross-ventilation in simple structures. In the present case, any trend in ventilation caused by different flow regimes were unlikely to be unveiled. This is

because the network of flows in the structures were very complex and the number of group layout samples that were chosen to be tested was too small. There was, nevertheless, no point in not examining the internal flow conditions in two different flow regimes.

Various sizes of courtyards were not tested in the urban terrain. The courtyard geometry was already found not to be a dominant factor in exposed conditions, and there were strong reasons to believe that it would have even smaller impact in sheltered conditions. Indeed, according to the works reviewed in Section 4.3, the wind-pressure magnitudes on the various wall surfaces of a building are significantly reduced when sheltered by adjacent buildings, in comparison with the exposed conditions. The availability of pressures forces for ventilation through the windows is thus lessened.

Whereas there was little hope in improving the courtyard ventilation by changing its size, the use of roof vents in atria was expected to have some potential, (see the study of Bauman et al (1988a and 1988b), presented in Section 4.4.2.4).

9.4 Estimate of the pressures acting on the model external walls

Before broaching the analysis of the results on the internal flow, and in order to discuss the findings, it is necessary to appreciate the changes that occurred to the surface pressures on the test models in the urban terrain. It must be emphasised that the following pressure data that were obtained and presented here were used solely to substantiate the trend found in the internal flows.

Calculation of the external pressures

The external pressures on the model walls were not measured but estimated using the discharge equation, equation (6.19), of the flow through the model rooms obtained from the calibration tests. This equation can be obtained in S.I. units by multiplying the right term of the equation by 5.635×10^{-6}. The equation becomes;

$$Q = 0.0001505\ \Delta P_2^{0.475} \tag{9.1}$$

where Q is the volumetric flow rate and ΔP_2 the pressure drop across the model rooms. CQ1 can be expressed as a function of ΔCP by replacing Q with $CQ1\times A\times V_{800}$ and ΔP_2 with $\Delta CP\times((\rho/2)\times V_{800}^2)$. The values of V_{800} and ρ were that of the

experimental test, i.e., $V_{800} = 25\ ms^{-1}$ and $\rho = 1.2\ kgm^{-3}$. It follows that,

$$CQ1 = 0.427\ \Delta CP^{0.475} \qquad (9.2)$$

To infer the external pressures acting at the wall openings required the knowledge of the internal pressure, (i.e., the pressure in the atrium core), and the flow coefficient CQ1 at this location.

The pressures derived from this equation may be considered as the pressures responsible for the flow and were not expected to match the pressure measured on sealed models. This is because the presence of openings are known to introduce significant alterations in pressure fields measured on sealed models. This is discussed in detail in Chapter 10.

It was assumed that the estimated pressures acting on the model walls were the same for all the structures at a particular group layout. This assumption seems reasonable in light of the results of pressure tests undertaken on atria having various roof shapes and sizes. These tests showed that there were no substantial differences between one model and another, (see Section 8.4.1). For a particular group layout, the pressures derived for each model and at each facade were averaged. This should damp down the individual pressure distortions that could have been introduced by the flow through the openings in each model. For each group layout, the divergences in the pressures between one model and another was approximately 12% of the mean values. The discrepancies could be higher when the pressures became small.

Analysis of the estimated pressure distribution

The variation of the estimated pressures with the group layouts are shown in Figure 9.3. The effect of wind sheltering on the monitored models was to mitigate appreciably both the overpressures and underpressures.

At normal wind incidence, the passage from isolation to the group layout with the smallest density resulted in a significant drop in the pressure magnitudes on the four facades. Thereafter, further increase in the density did affect mainly the upwind walls. On the lateral wings of the models a great reduction of the suction was recorded once the models were surrounded by other elements. The pressure fields remained unchanged at this location when the lateral clear spacing was lower than 1.5H. In this case, it was found that the pressure along the face was uniform and the horizontal pressure gradient

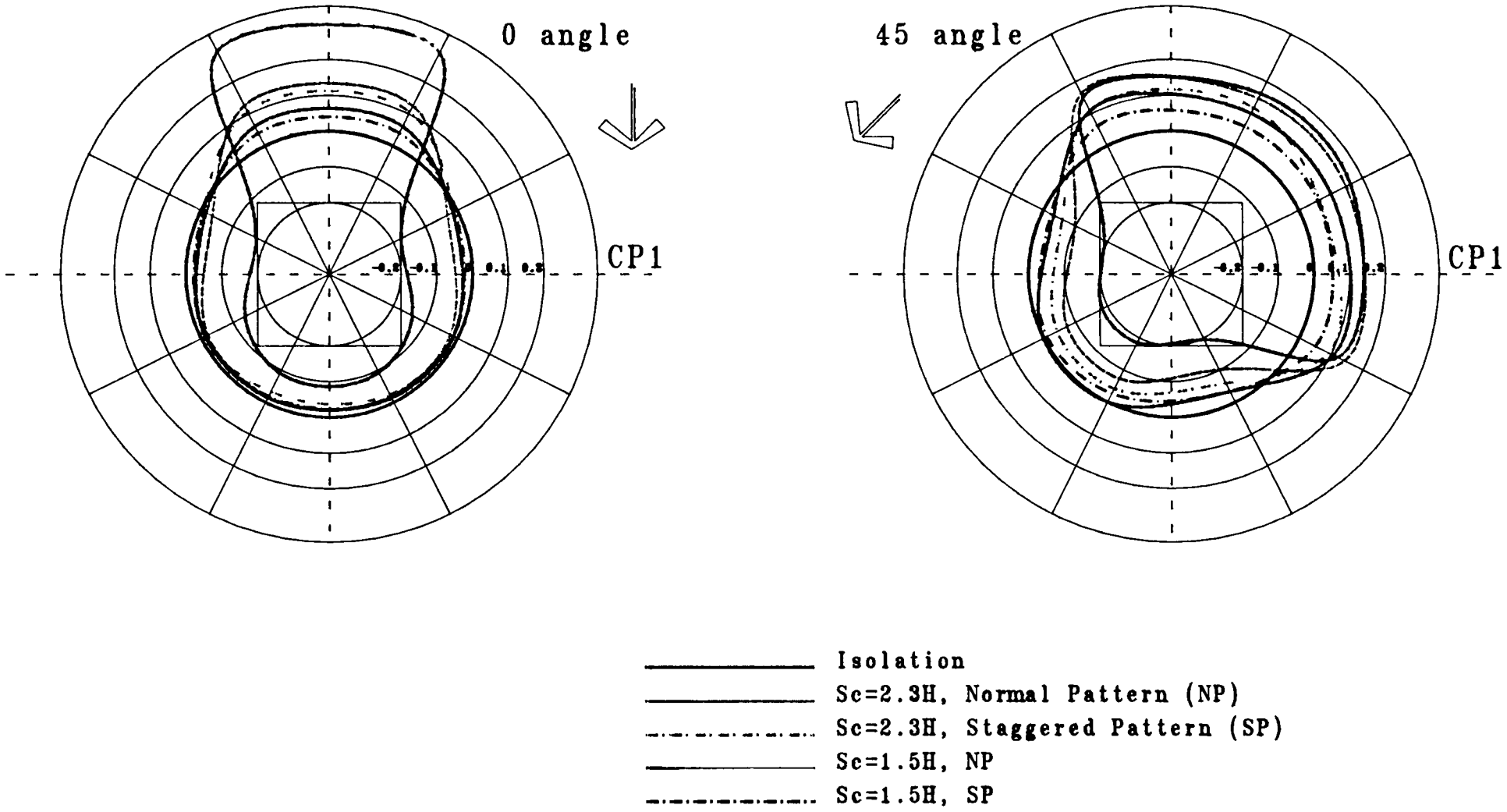

Figure 9.3: Estimated pressures acting on the model external apertures at different group layouts.

that existed in exposed conditions, (see Section 8.4.1), no longer remained.

At 45° wind angle, although the pressure magnitude dropped on all facades when sheltered from the wind, the downwind regions were the most affected. The decrease of the spacing diminished the pressure magnitudes on all the facades. Yet, when the lateral spacing was below 1.5H, almost no changes occurred on the downwind sides.

The pressure magnitudes acting on the external walls of the models in shielding conditions were inferred to be higher at 45° than at 0° wind angle. This was probably because the air could sweep in the street more easily in the first case, resulting in greater pressure gradients across the walls. The same trend can also be found in the pressure measurements taken by Wiren (1985 and 1987).

Having obtained an assessment of the pressures acting on the external walls, it was possible to derive an approximation of the pressures acting on the inner faces of the courtyard. The pressures were found to tend towards the atmospheric pressure as soon as the monitored model was surrounded by shielding models. This was particularly marked at normal wind angle. There were comparatively fewer changes in the pressure fields when the spacing or pattern were changed, and almost the same pressure was acting on the four inner walls. At 45° wind angle, slightly higher pressure magnitudes existed.

9.5 Results of the internal flow measurements

The full results of the indoor flow magnitudes and directions are given in Figures 9.4 to 9. 11. The associated data can be found in Appendices D1 to D8.

The discussion of the results is presented in three parts, each referring to one of the three parameters that were changed, i.e., the group layout, the ventilation strategies and finally the orientation of the group layout to the wind. However, each of the parameters could not be treated totally independently of the others.

9.5.1 The influence of the group layouts

9.5.1.1 Influence on the magnitude of the flow through the walls

The flow coefficients derived from the orifice plate measurements were averaged for each model. The value, CQT1, is shown in Figure 9.12a and Figure 9.12b for each model in each of the group layouts tested.

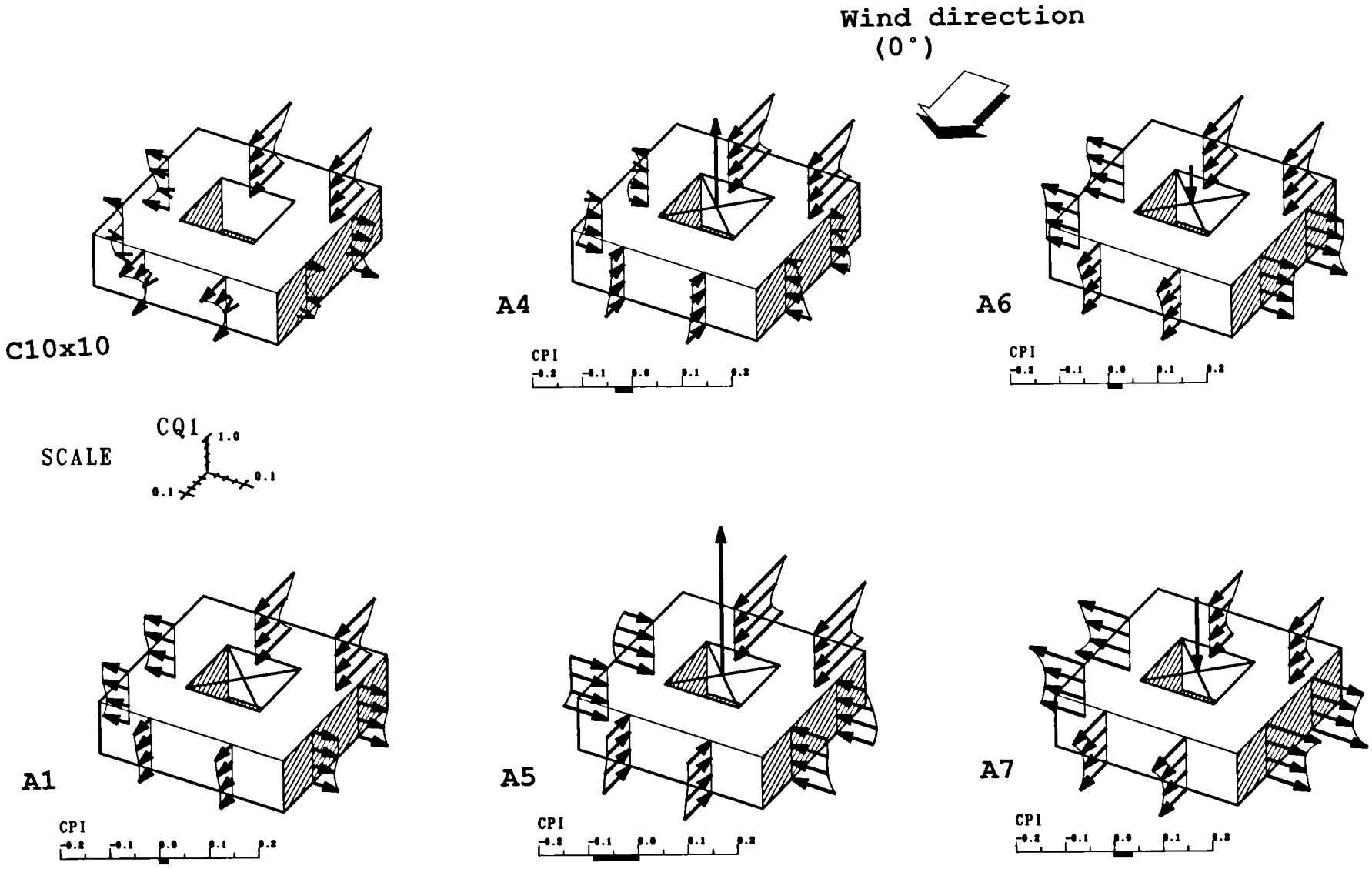

Figure 9.4: Detailed distribution of flow coefficients within the atrium and courtyard models in sheltered sites, **(Group layout density 0.28, 0° wind angle).** CQ1 *through walls were measured,* CQ1 *through roof was inferred.*

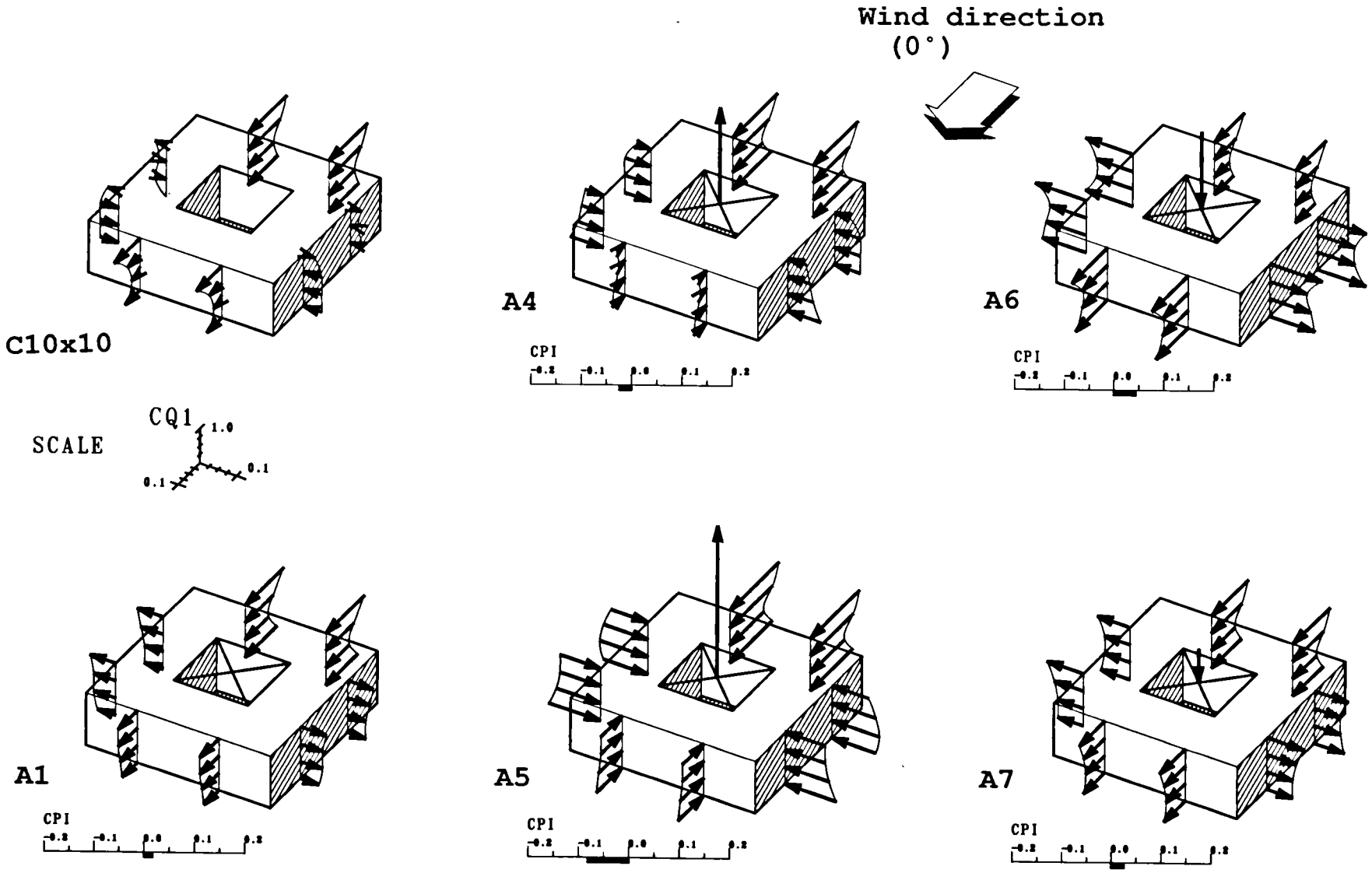

Figure 9.5: Detailed distribution of flow coefficients within the atrium and courtyard models in sheltered sites, **(Group layout density 0.38, 0° wind angle).** CQ1 *through walls were measured,* CQ1 *through roof was inferred.*

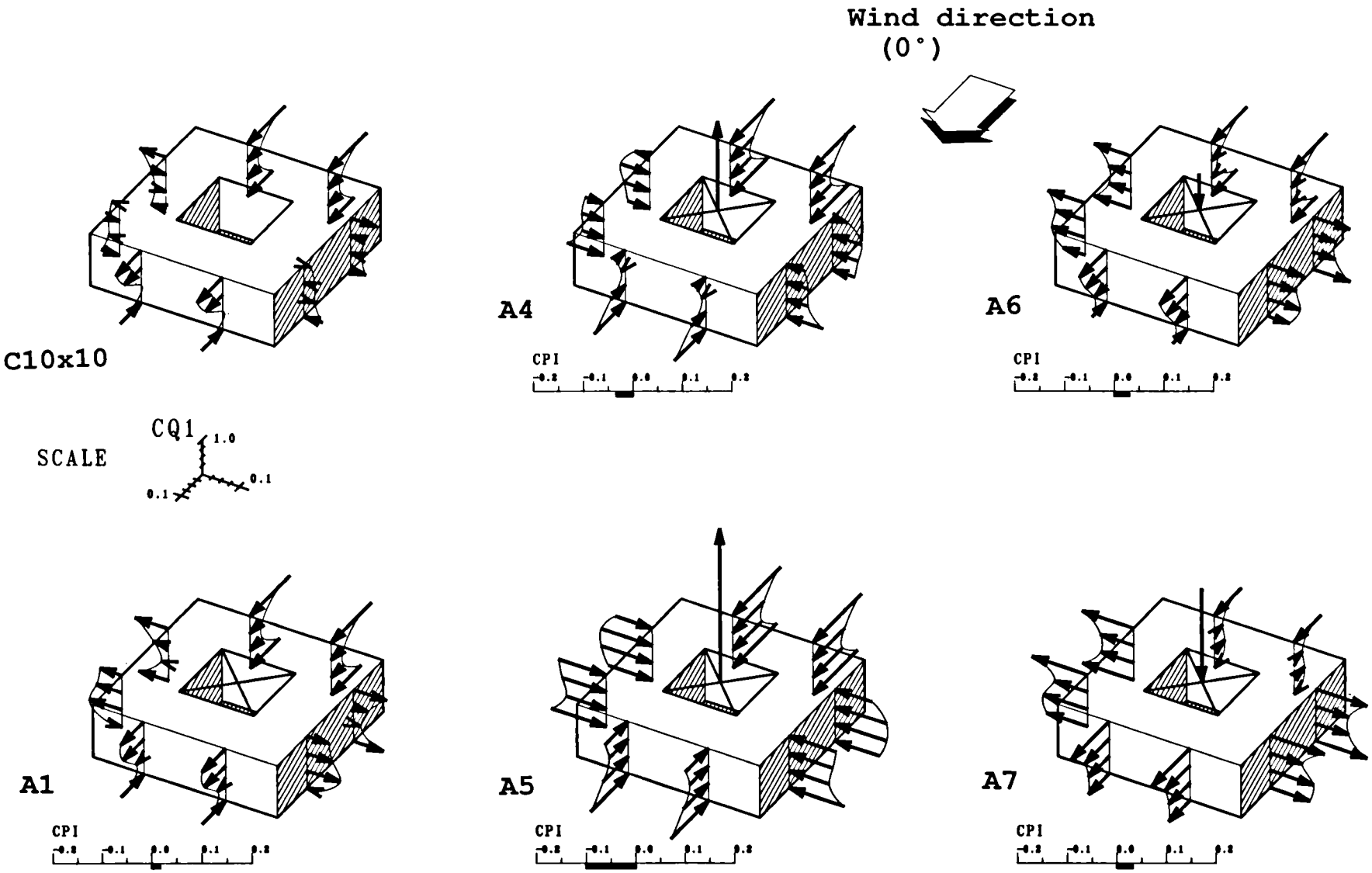

Figure 9.6: Detailed distribution of flow coefficients within the atrium and courtyard models in sheltered sites, **(Group layout density 0.40, 0 wind angle).** CQ1 *through walls were measured,* CQ1 *through roof was inferred.*

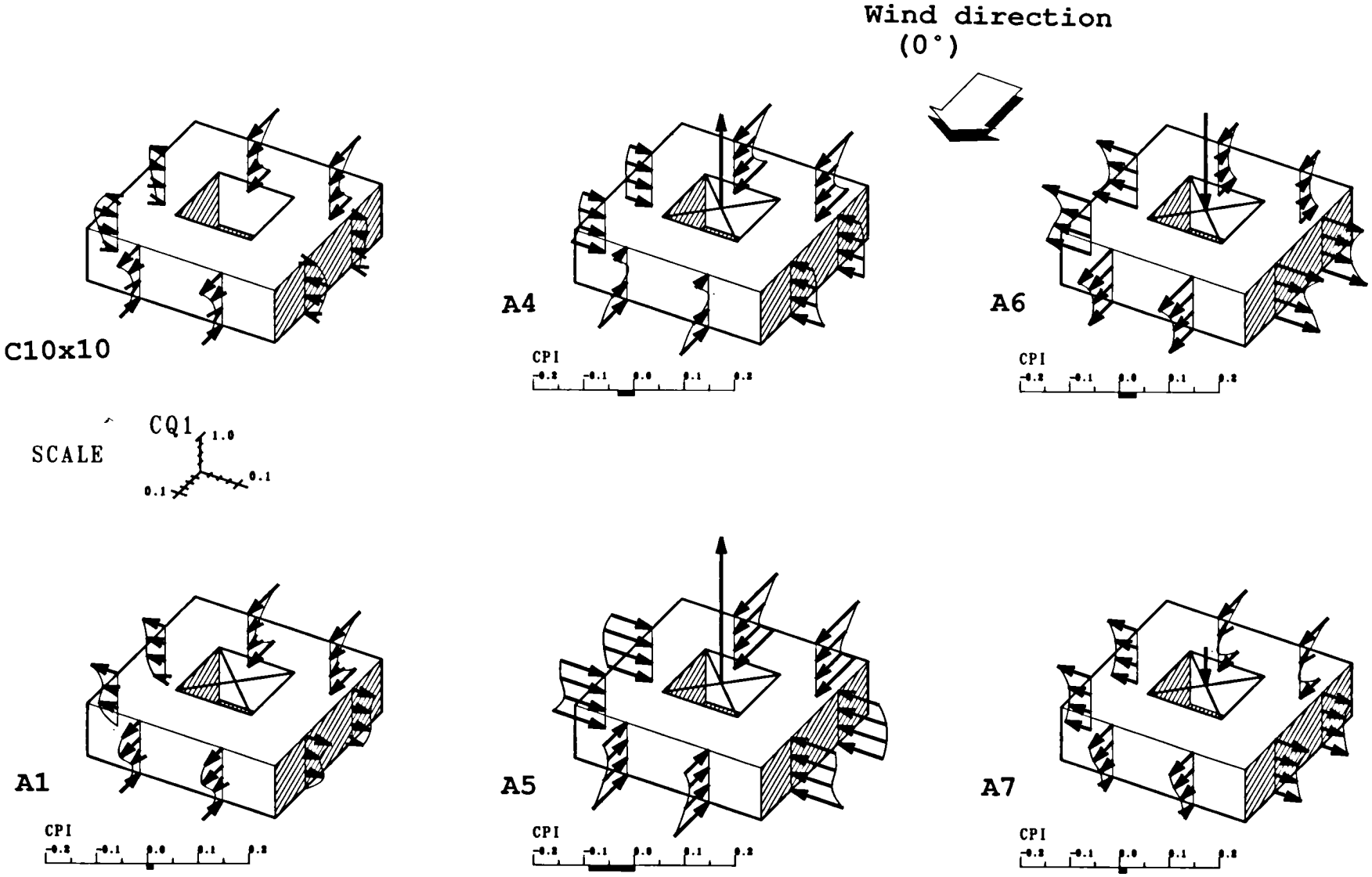

Figure 9.7: Detailed distribution of flow coefficients within the atrium and courtyard models in sheltered sites, **(Group layout density 0.50, 0° wind angle).** CQ1 *through walls were measured,* CQ1 *through roof was inferred.*

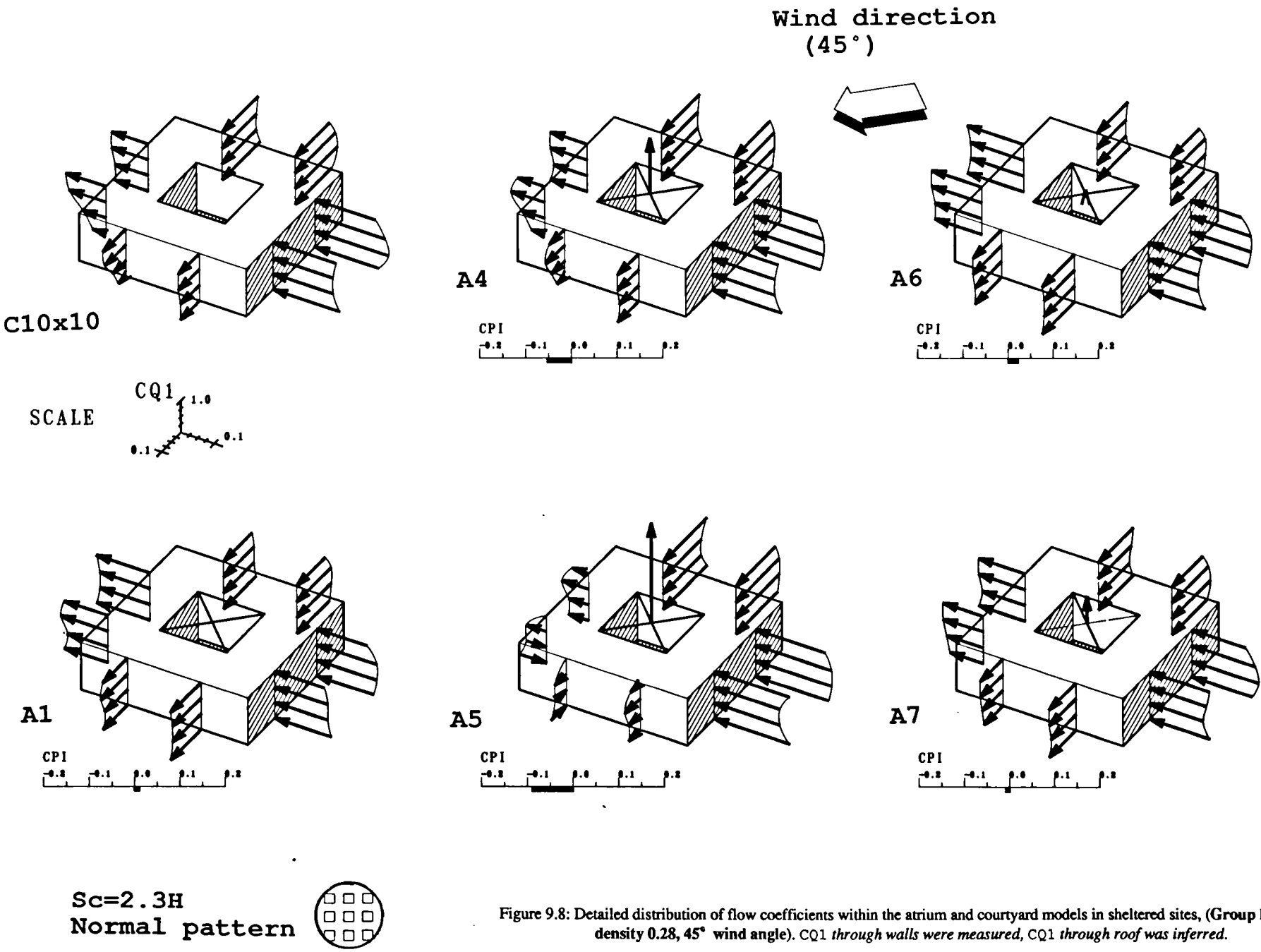

Figure 9.8: Detailed distribution of flow coefficients within the atrium and courtyard models in sheltered sites, **(Group layout density 0.28, 45° wind angle).** CQ1 *through walls were measured,* CQ1 *through roof was inferred.*

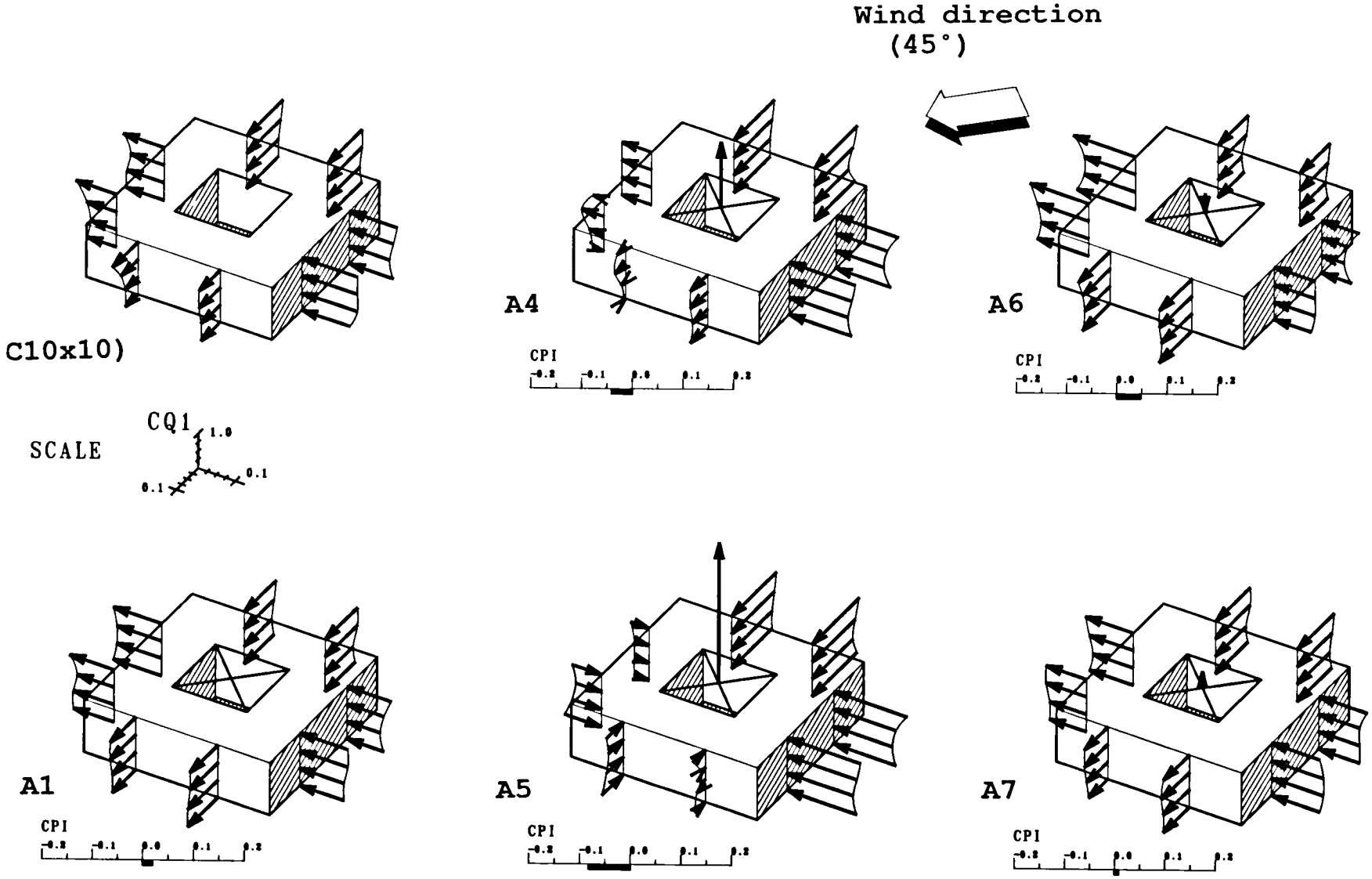

Figure 9.9: Detailed distribution of flow coefficients within the atrium and courtyard models in sheltered sites, **(Group layout density 0.38, 45 wind angle).** CQ1 *through walls were measured,* CQ1 *through roof was inferred.*

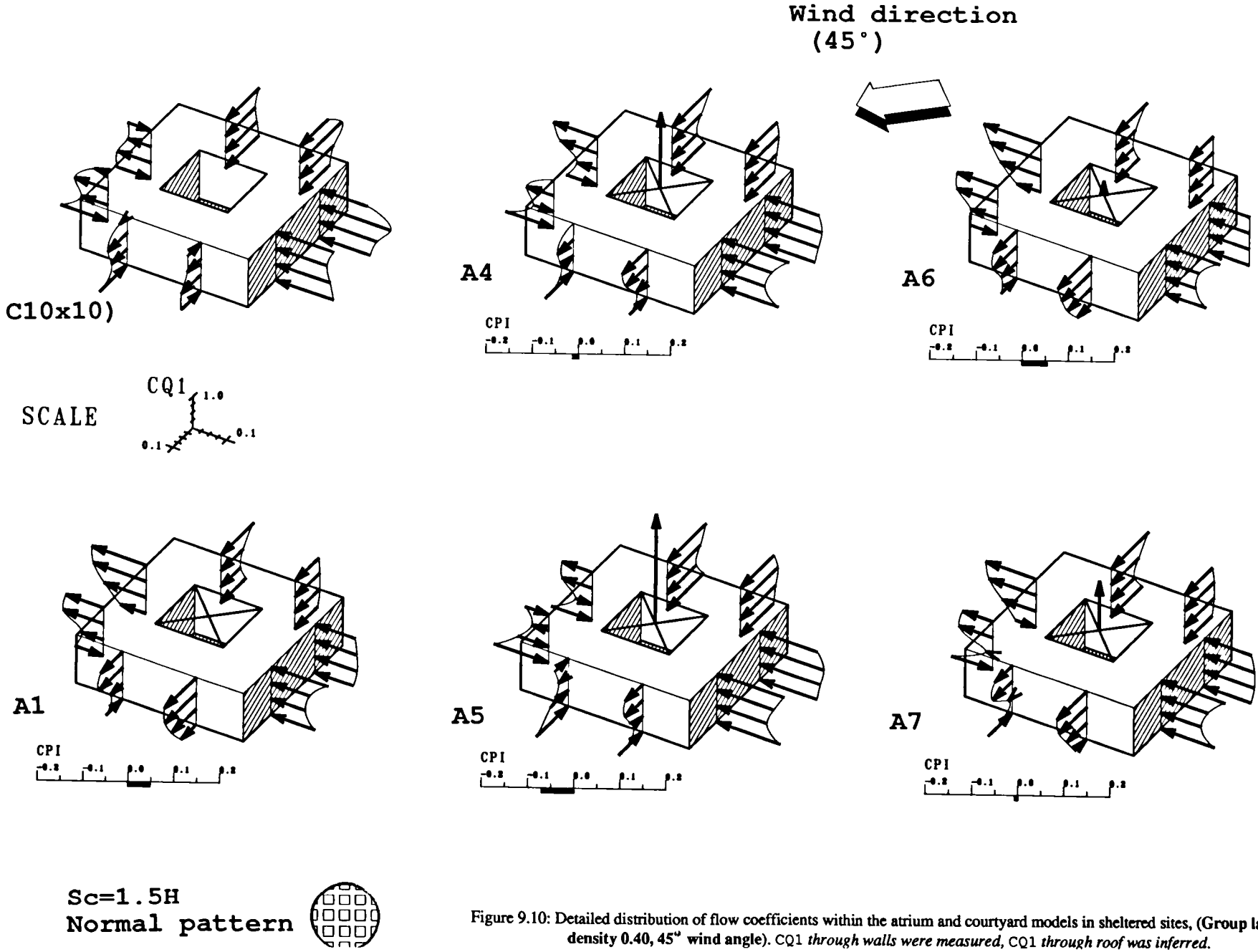

Figure 9.10: Detailed distribution of flow coefficients within the atrium and courtyard models in sheltered sites, **(Group layout density 0.40, 45° wind angle).** CQ1 *through walls were measured,* CQ1 *through roof was inferred.*

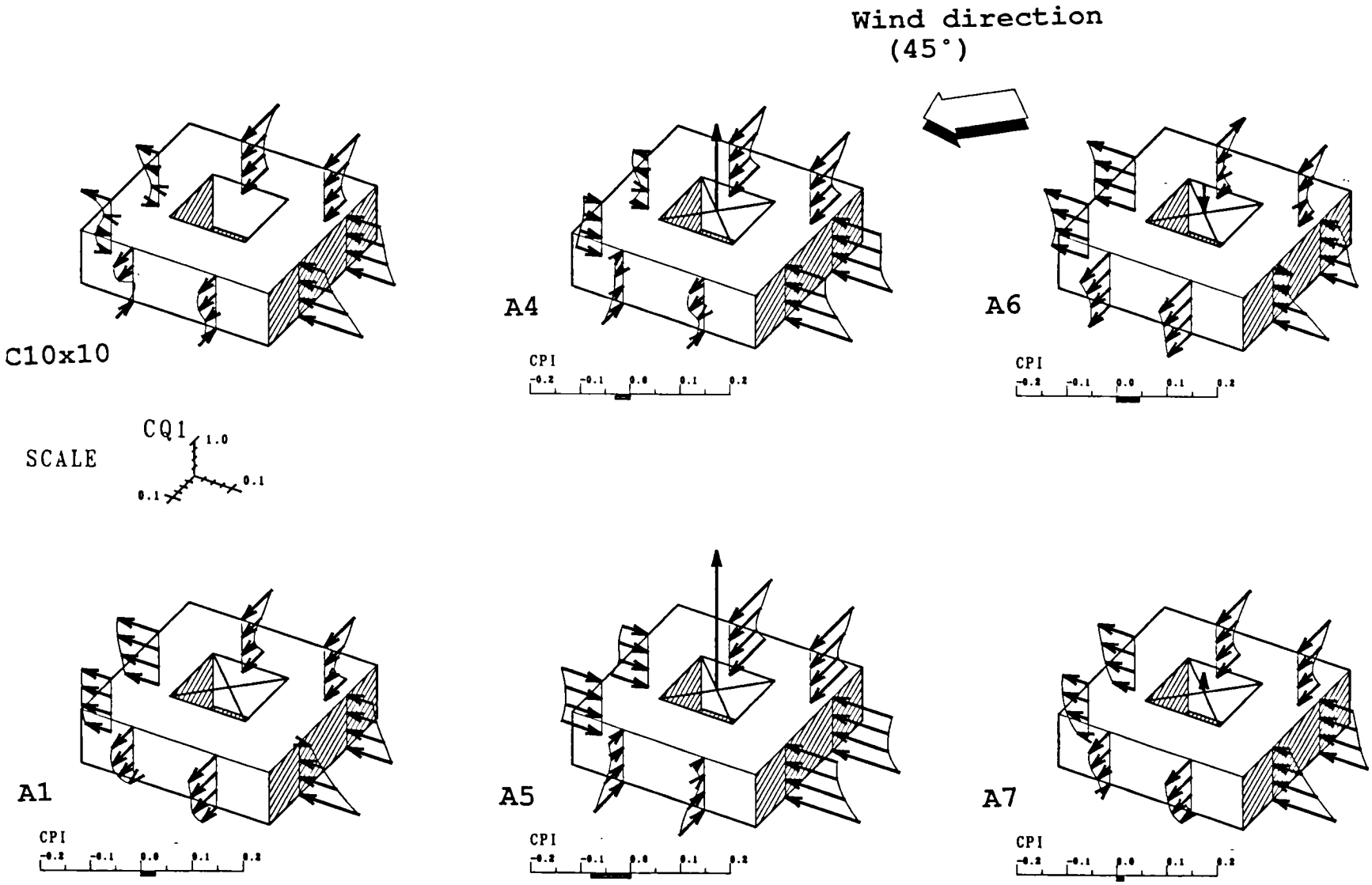

Sc=1.5H
Staggered pattern

Figure 9.11: Detailed distribution of flow coefficients within the atrium and courtyard models in sheltered sites. **(Group layout density 0.50, 45 wind angle).** CQ1 *through walls were measured,* CQ1 *through roof was inferred.*

As expected, almost all the configurations had lower average flow coefficients in the presence of shielding buildings than without, (see also Table 9.1). The main remarks that can be made from the figures are:

i) Excluding model A5, at normal wind incidence, CQT1 was, on average, 62 % of the values measured in isolation when the models were in a group with a density equal to 28%.

ii) At 45° wind angle, CQT1 values in this group layout corresponded on average to 80% of the values in isolation.

iii) All the facades were generally affected. At normal incidence the highest rates of decrease were nevertheless found on the windward wings and on the side wings near the leading edges.

iv) The ventilation was generally reduced further when the spacing between the elements in the group was decreased. At normal wind incidence, the average flow coefficient CQT1 was in most of the cases half the values in isolation when Sc/H= 1.5. At 45° wind angle, they represented 70% and 50% of the values in isolation at group densities equal to PD= 40% and PD= 50% respectively.

The foregoing results are consistent with the existing knowledge of wind pressure distributions around building models in shielded conditions. Indeed, when the models were sheltered, and/or the group layout density increased, the pressure magnitudes on the external walls were reduced. Consequently, the ventilation motive forces were diminished, at least for the structures which relied mostly on the pressure gradients across the walls, and where no extensive use of the roof pressure forces were made. With these configurations, the pressures in the core of the atria were always somewhere between the maximum and minimum pressures acting on the external walls.

Surprisingly, ventilation conditions comparable to that found in exposed situations where encountered in sheltered sites with model A5 when the wind angle was 0°. The overall flow coefficient was also found to be hardly affected by the change of the group layout arrangements. Model A4, which also exploited the roof suction, experienced at normal wind incidence constant flow coefficients with the change of the group layout spacing.

The cases where the overall flow remained constant with changes of the group layout arrangement coincided with situations where the models were performing a whole-building suction, (or almost). In these circumstances, the internal pressures were

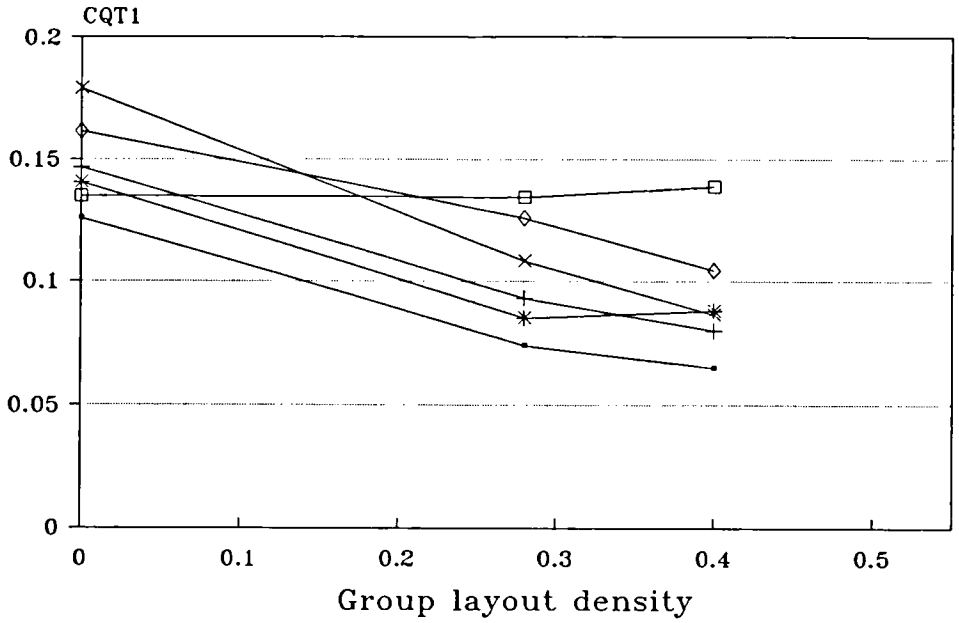

Wind angle 0/ Normal pattern

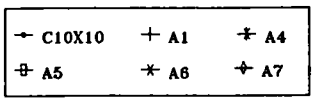

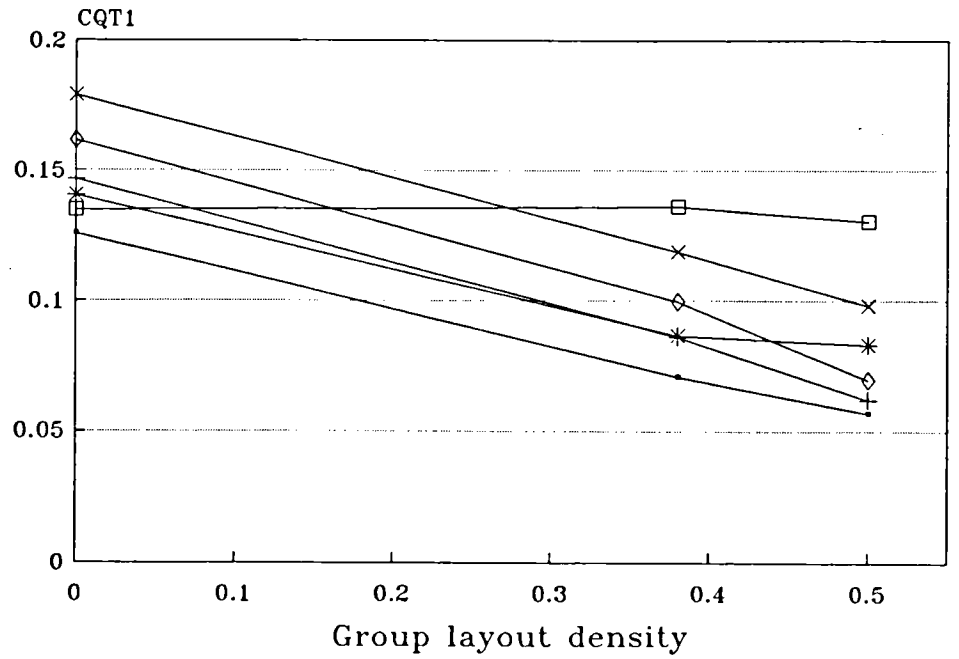

Wind angle 0/ Staggered pattern

Figure 9.12a: Variation of the overall flow coefficients CQT 1 with the change of the group layout, (0° wind angle).

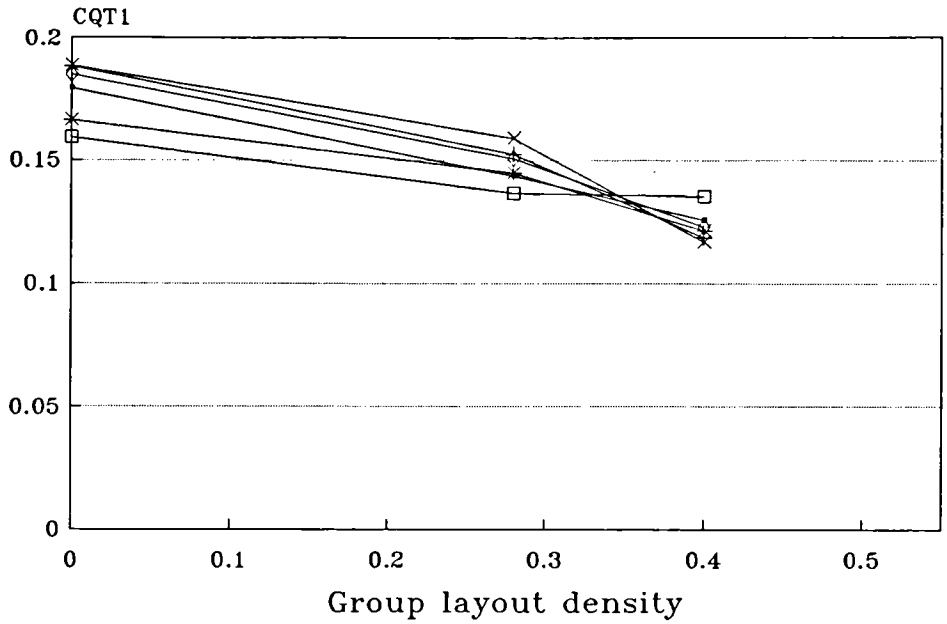

Wind angle 45/ Normal pattern

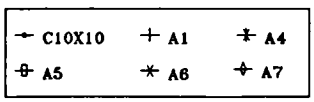

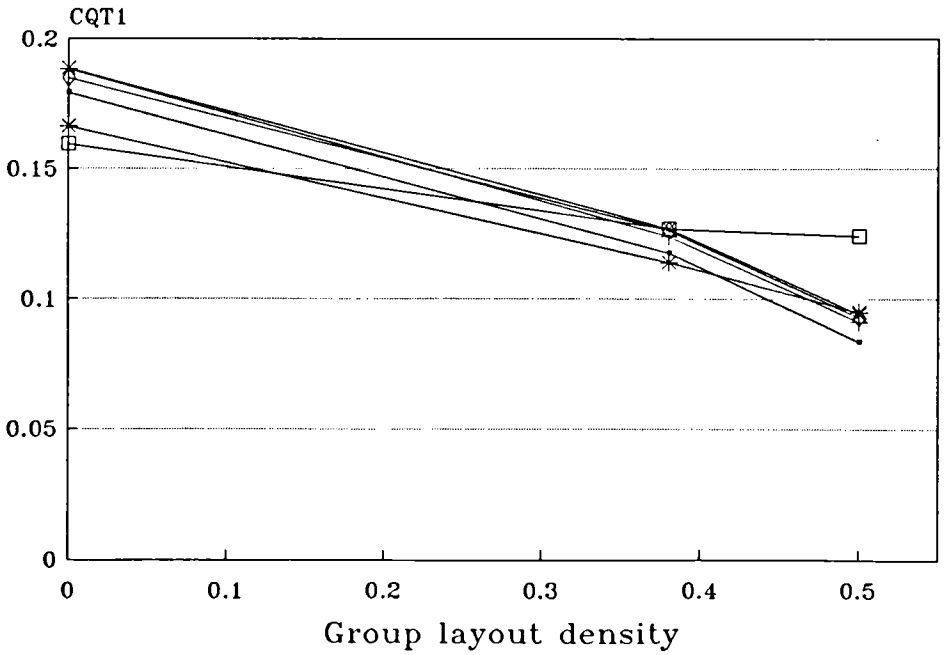

Wind angle 45/ Staggered pattern

Figure 9.12b: Variation of the overall flow coefficients CQT1 with the change of the group layout, (45° wind angle).

Table 9.1: Overall flow coefficient CQT1 of courtyard and atria in shielded conditions and comparison with isolated conditions. *GL is the group layout characterised as follow, GL1(normal pattern (NP), Sc=2.3H), GL2 (Staggered pattern (SP), Sc=2.3H), GL3(NP, Sc=1.5H), GL4(SP, Sc=1.5H).*

	CQT1 (shielded)				CQT1(shielded)/(isolated)			
0° Wind angle								
Model Index	Isolation	GL1	GL2	GL3	GL4	GL1	GL2	GL3	GL4
C10x10	0.126	0.074	0.065	0.071	0.057	58%	52%	56%	45%
A1	0.147	0.093	0.080	0.086	0.062	63%	54%	58%	42%
A4	0.140	0.085	0.088	0.087	0.083	61%	63%	62%	59%
A5	0.135	0.134	0.139	0.136	0.131	99%	103%	101%	97%
A6	0.179	0.108	0.086	0.119	0.098	60%	48%	66%	55%
A7	0.162	0.126	0.104	0.100	0.070	78%	64%	62%	43%
45° Wind angle									
Model Index	Isolation	GL1	GL2	GL3	GL4	GL1	GL2	GL3	GL4
C10x10	0.179	0.144	0.126	0.118	0.084	80%	70%	66%	45%
A1	0.188	0.153	0.119	0.124	0.091	81%	63%	66%	48%
A4	0.166	0.145	0.122	0.114	0.095	87%	73%	69%	57%
A5	0.159	0.137	0.135	0.127	0.124	86%	85%	80%	78%
A6	0.189	0.159	0.117	0.127	0.094	84%	62%	67%	50%
A7	0.162	0.126	0.104	0.100	0.070	78%	64%	62%	43%

beyond the pressures estimated to act on the outer walls of the models. When the group spacing was reduced, the decrease of both the overpressures and the underpressures on the outer walls left the internal pressure relatively unchanged. As shown in Figure 9.13, representing schematically the pressure gradients between the inner and outer walls of the atrium models, the reduced flow in the windward facade was compensated by greater flows in the downwind facades, so that CQT1 remained unchanged.

It must be outlined here that, since the wind shielding have different effects on each of the configurations, it is inappropriate to use for such complex structures a generalized shielding coefficient which depends solely on the site characteristics, such as suggested by Sherman and Grimsrud (1982).

9.5.1.2 Influence on the magnitude of the flow through the roof

The flow through the roof was not measured but was derived from the continuity equation. In general, the roof flows depicted in Figures 9.4 to 9.11 were approximately of the same magnitude as those found in isolation. With the configuration A4 and A5 the flow through the roof apertures were found to be even slightly higher in sheltered conditions.

At 45° wind angle, however, the roof flows of models A4 and A5 were estimated to be appreciably lower than in the case of isolation.

When the group layout arrangement was changed, the general trend was to a constant flow coefficient.

The fact that the roof flow was not noticeably affected by the group layout implied that the sheltering effects in the vicinities of the roof apertures were probably small. This may be attributed to the high location of most of the roof openings, (i.e., approximately 1.3H), well above the roof tops of the surrounding elements. In these circumstances it may be possible that most of the openings were located above the surface layer growing over the group, in which case the pressures at this location were dependent more on the characteristics of the outer boundary layer profile, which was governed by the general roughness surface, than the group layout arrangement.

This assumption could be substantiated by the work of Hussain (1978). This author indicated that when the height of a block-like element amidst a regular group was changed, the rate of change of the roof pressures presented different behaviours above and below heights 1.3 to 1.6 times the height of the surrounding elements. This distance was suggested to correspond to the physical thickness of the inner layer

growing over the group layout. Above these limits, the model that dominated its neighbours tended to act as an isolated high rise element and the roof pressures tended to be unaffected by the group layout. Nevertheless, some degree of deviation in the roof pressure field, (more than 10% deviation), was recorded for elements smaller than 3 times the buildings height, (see Figure 9.14).

A direct comparison of Hussain's work with the present tests was not possible because of the different quantities measured, and also because the features of the models and the characteristics of the simulated atmospheric boundary layer were very different. The flow behaviour in the present tests was complicated by the presence of openings in the models which are known to be the cause of significant distortions in the pressure fields measured on solid models, particularly in roof ridge regions, (see Chapter 10). The way the flow passing through the roof distorts the pressure field is not yet understood and deserves a great research effort.

The fact that the roof openings were still capable of driving significant volumes of air in the shielded conditions gave to some atrium configurations a very promising role, owing to the fact that the wall pressure gradients were weakened. If the collection of buildings had significantly sheltered the roof apertures, which may be expected probably for less prominent roofs, the assistance of the roof pressure forces would have been offset.

9.5.1.3 Influence on the distribution of the flow

The distribution of the flow on the various locations of each building model could be reshaped greatly with the proximity of neighbouring buildings and with the alteration of the group layout. Two illustrative examples are given in Figure 9.15, where the average magnitudes of the flow coefficients are presented for each group layout for models A5 and A7. This reordering of the ventilation distribution on the model face was obviously the result of a redistribution of the pressure fields on the external surfaces of the test models.

It is pertinent to note here that the windward facade, when orientated normal to the wind, did not always record the highest flow rates as it did in the conditions of isolation. In models A6 and A7, for most of the urban sites tested, the ventilation at the windward model wings was weaker than on the downwind faces. In the other cases, the disparity in the flow rates between the windward and the downwind wings of the models was not as considerable as in isolated conditions.

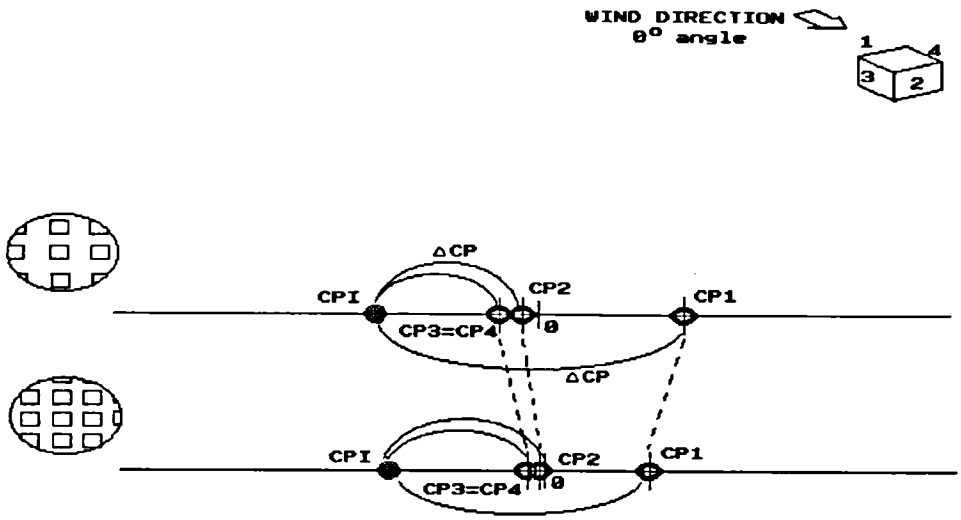

Figure 9.13: Schematic representation of the change in the external pressure gradients on the model A5 with the change of the group layout spacing, (0° wind angle).

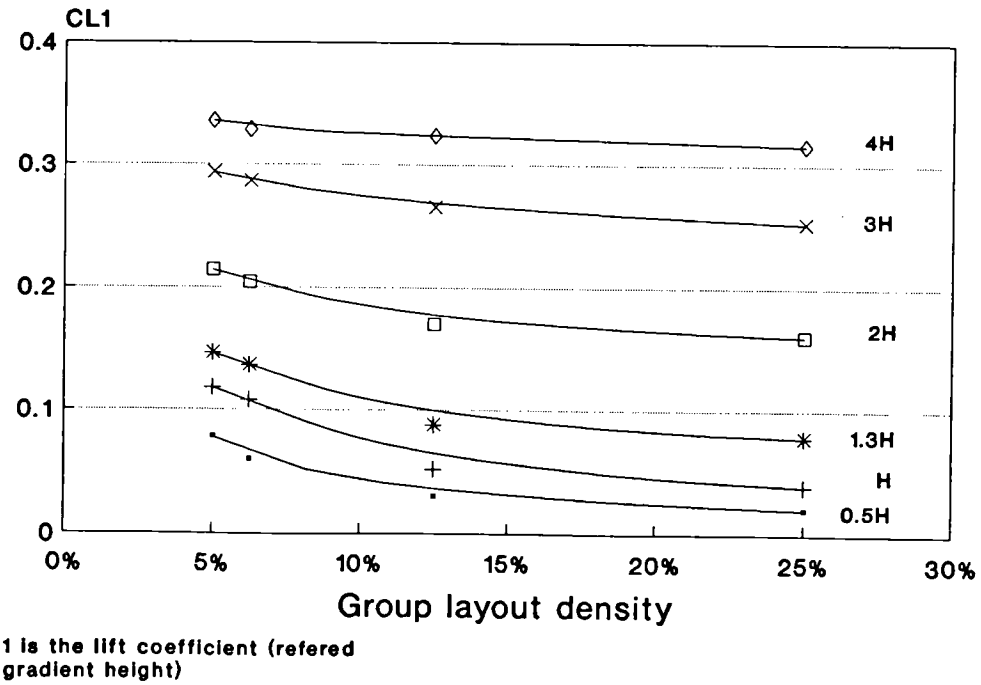

Figure 9.14: Effect of the relative height of a building with respect to surrounding buildings on its lift coefficient. Replot of Hussain's data (1978).

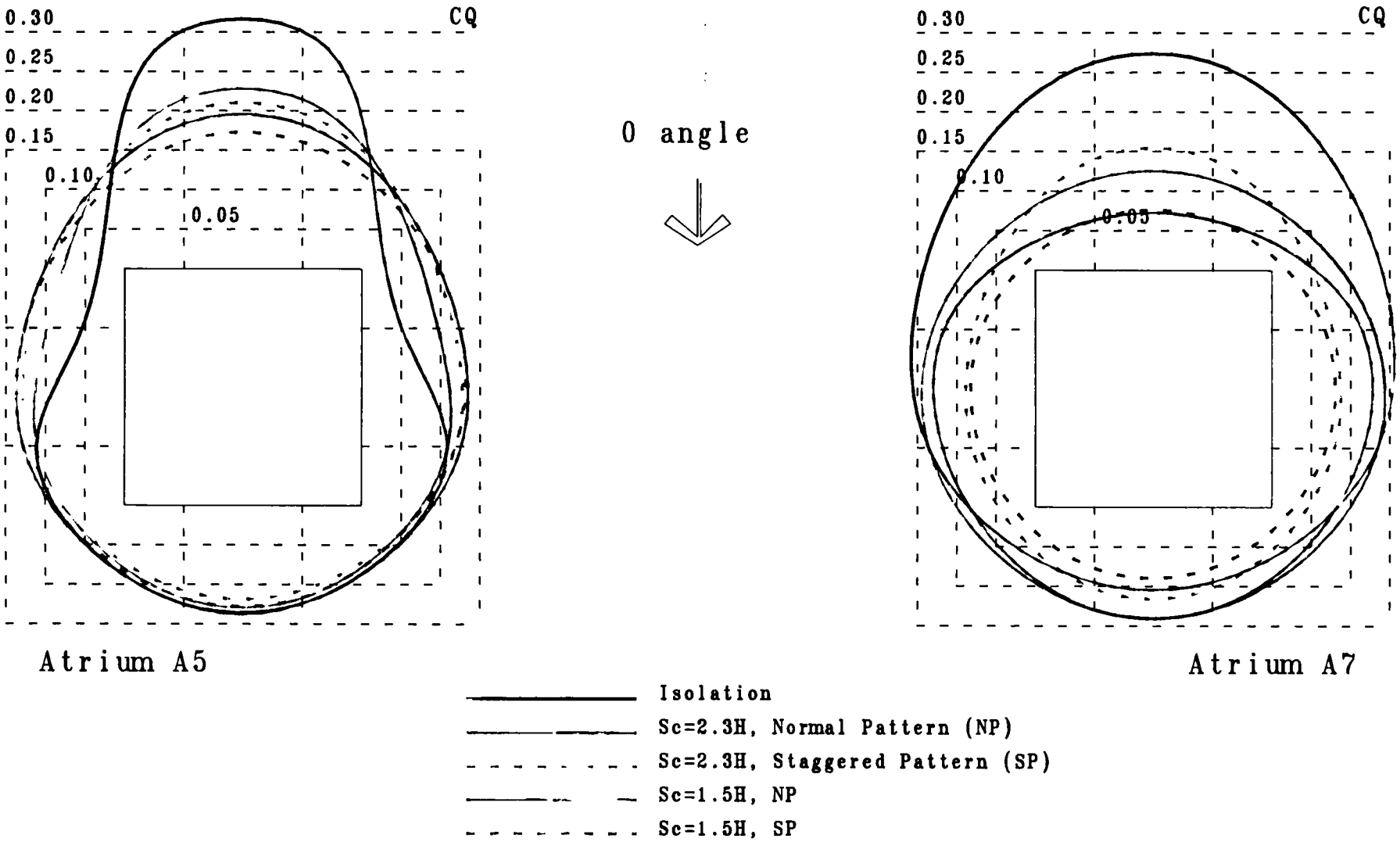

Figure 9.15: Variation in the distribution of the flow magnitudes within the wings of the models A5 and A7 with changes of the group layout, (normal wind incidence).

The vertical distribution of the flow in the sheltered conditions where found to display the shape of a "C" on the windward walls when the wind was striking the building models at right angles. This shape coincides with the profile the pressures exhibit in group layouts where the flow regimes are either the wake interference flow regime or the skimming flow roughness, (see Soliman (1976) and Hussain (1978)). On the leeward side, the distribution of the flow allowed to infer that, as the group element spacing became smaller, the pressures profiles tend to be inclined lines with higher pressures at the base than at the top. This behaviour was also reported in the work of Hussain and Soliman.

9.5.2 Importance of the ventilative strategy

It was already implied that the ventilative conditions of atria in an urban site were largely depend on the roof ventilative strategy used. The effect of the various atrium operating modes could be followed taking the closed-roof atrium, A1, as a datum. If the roof vents were used to expel air, then greater inflow would be driven through the walls openings, and also, lesser outflows when compared to the closed-roof atrium. The reverse is true for roof vents admitting air inside the atrium.

The following discussion refers to Figures 9.4 to 9.11. Although these figures already allow comparative estimates of the model ventilative performances to be made, this is the subject of Section 9.6.

9.5.2.1 At normal wind angle

Flow networks

Compared to the isolation conditions, a wider range of flow networks was encountered in shielded situations, i.e., from the case where all the wall openings were used as inlets and the roof vents as the unique outlets, to the case where almost all the air admitted in the atrium building was through the roof vents and was leaving through the wall apertures, (see Figures 9.4 to 9.7). The emergence of these networks at the extreme end of the spectrum, (non-existent in isolation conditions), was made possible in the urban site because the pressure magnitudes on the walls were very reduced, so the roof pressure forces could dictate the direction of the air currents.

Closed-roof atrium, A1

The ventilation conditions of the closed-roof atrium were generally characterised by strong inflows on the windward facade and weaker outflows on the downwind wings. This was true with all layout densities. Roughly 1/3 of the flow entering the windward openings was leaving through each of the downwind facades. At the smallest spacing Sc= 1.5H, however, the air was also entering the building through the leeward openings in the first floor.

Positive roof pressure and near-ambient roof pressure strategies, A6, A7

Since internal pressure on the closed-roof atrium was close to the downwind external pressures, there was a prospect for obtaining a better distribution of the ventilation by raising the internal pressure in order to reach the same pressure differential on all the atrium wings. The rise of internal pressure could be achieved by admitting air through the roof vents, and was performed by both the atrium A6 and A7. At the largest group layout spacing, Sc= 2.3H, the flow network of these two configurations was the same as A1, (closed-roof), see Figures 9.4 and 9.5.

An optimum situation that consists of almost a parity of the ventilation rates on the four wings of the model lied in-between that realised with these configurations. At Sc= 1.5H, on the other hand, the admission of air through the roof generally prejudiced severely the inward air current on the windward model wing. In the case where there were important roof effects, some of the windward apertures were even used as outlets, (see Figures 9.6 and 9.7).

Roof suction strategy, A4, A5

The provision of a great number of openings in the strong roof suction field of the atrium A5 created a deficit of pressure in the atrium space which was not as great as in the isolation conditions. Nevertheless, this was sufficient to establish a whole-building suction in the urban sites whilst it failed in the isolation conditions. This was made possible because the suction potential of the atrium roof was not significantly affected by the collection of building models, whereas the suction on downwind walls, which was conflicting with this ventilation strategy in isolation conditions, was greatly weakened. It could already be seen in Figure 9.4 to 9.7 that this ventilation amended greatly the ventilation conditions of atria in any group layout but was most remarkable at the smallest spacing.

The atrium A4 accomplished almost in all the model rooms an inward current of air. Yet, because of the lack of sufficient roof opening area, the suction effect was weak and was conflicting with the pressure field on the downwind external walls. In almost all the group layouts, the indoor flow was locally poor in the downwind rooms.

Courtyard C10x10

The courtyard model presented in general very weak and unevenly distributed ventilation. The direction of the flow was very erratic and could differ from one floor level to another, (see Figures 9.4 to 9.7).

9.5.2.2 At 45° wind orientation angle

As revealed in Figures 9.8 to 9.11, the range of flow networks encountered was narrower than at 0°. In general, the apertures on the upwind walls served as inlets while those in the downwind facades served as outlets. This flow network was disturbed very locally at certain group layouts or with the atrium A5. In the sheltered atria as in the exposed ones, the relatively strong gradients between the upwind and downwind wall pressures made it difficult to realise any other flow networks, in particular the whole-building suction which could be achieved at 0° wind angle.

Closed-roof atrium, A1

With atrium A1, the internal pressure in the atrium core was almost half way between the pressures estimated to act on the upwind and downwind walls. This resulted in almost a parity in the ventilation on the different building wings.

Suction strategy, A4, A5

Any extensive use of roof pressure forces could impair the balance found in the ventilation of the closed-roof atrium model, and reduce any of the inflows or outflows. Indeed, models A4 and A5 reduced severely the ventilation in the downwind wings, until a whole-building suction was achieved with A5 only, and for the most dense group layout.

Atrium models A6. and A7

The roof vents of the atrium A6 using the positive pressure strategy was not always admitting air in the building model as it was intended to do in isolation conditions. Also, the roof of model A7 was used in all group layouts as a suction device. Such behaviour could be explained as follows, taking the closed-roof atrium as a datum: it was found that the internal pressure in this model rose with the presence of shielding models, mainly because the underpressures in the downwind walls were diminished. The rise of the internal pressures could thus have caused the pressure gradient between the atrium core and the roof openings in model A6 or A7 to be smaller or even to be reversed.

Generally there was little contribution of the roof pressure forces in these two models and their ventilation conditions resembled very much that of A1.

Courtyard C10x10

In contrast with the courtyard exposed fully to the wind, the sheltered courtyard was weakly ventilated, and it is clear that, for the most congested group layouts, this configuration had among the weakest indoor air movement and the most erratic flow direction.

9.5.3 Effects of the orientation to the wind

The great influence of the orientation of the building to the wind was already outlined for exposed conditions. This was also true for wind sheltered situations.

In the sheltered terrains, the change of the wind direction from 0° to 45° wind angle resulted in greater overall flow coefficients CQT1 and more evenly distributed ventilation, at least for models that did not exploit strong roof pressure forces. The reason for this improvement lies in the fact that greater pressure gradients between upwind and downwind walls existed at 45° wind angle, (see Section 9.4). The same remarks were made in the previous chapter for models exposed to the wind.

The percentage of increase in CQT1 caused by the change of the wind angle depended on the configurations and the characteristics of the group layouts. The values at 45° wind angle were between 0.9 to 2 times that at normal wind angle. The amendment of the ventilation with oblique winds was substantial for the courtyard model, for which the overall flow coefficient was 47% to 94% higher than at normal wind angle. With model A1 the improvement was somewhat lower, between 64% and

44%, whereas with A6 and A7 it was generally between 10% and 35%.

Generally, the largest improvement of the overall flow occurred at the largest spacing and for the normal pattern. But even with the group layout having the greatest sheltering effects, (highest plan area density), the effect of the orientation was still important.

More than with the change of the layout spacing or the pattern, the change of the wind incidence caused some flow to reverse. The way the flow directions were affected was as follows;

i) In general the facade parallel to the wind at 0° wind angle was likely to experience internal flows changing from an outward direction to inward as the wind rotated and struck it at 45°, (see Figures 9.4 to 9.11). This was systematic for models other than A4 and A5, (for the latter the flow was kept inward at this facade when the wind direction changed).

ii) On the other hand, hardly any reversed flow caused by the change of the wind angle occurred for the face that was windward at 0° wind angle. This nevertheless happened locally in model A7, at mid-height, for the smallest layout spacing.

iii) On the downwind facades the flow direction did change generally whenever the air current was inward at 0° wind angle.

In real situations the wind direction is erratic, varying typically within 30°, (see Section 8.6.3). Thus, in actual fact, the ventilation conditions in each face of the models may be intermediate between the conditions measured at fixed wind angles. With winds varying between 0° and 45°, almost all the structures could experience reversed flow locally. It could be expected that during the reversal of the pressure gradient, very weak flow movement could be experienced, driven almost exclusively by wind turbulences. In the case of the atrium A5, the flow network remained however almost the same in group layout density greater than 28%. In the light of the above mentioned assumptions this could be seen as an advantage.

9.6 The ventilative performances

9.6.1 At 0° wind orientation angle

Figures 9.16a to 9.16d present the percentage of building for which the

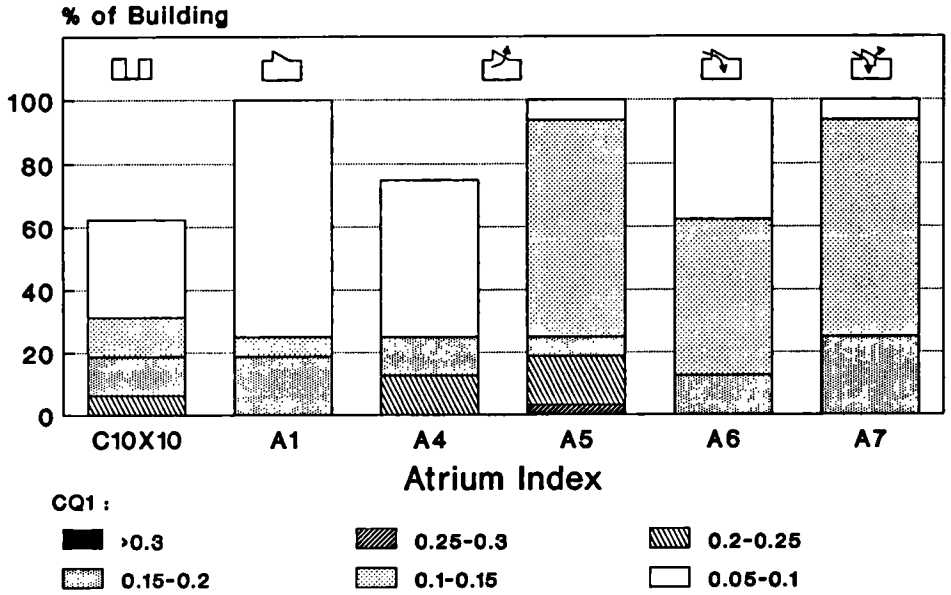

Figure 9.16a: Fraction of the building models under ranges of flow coefficients, **(Group layout density 0.28, 0° wind angle)**

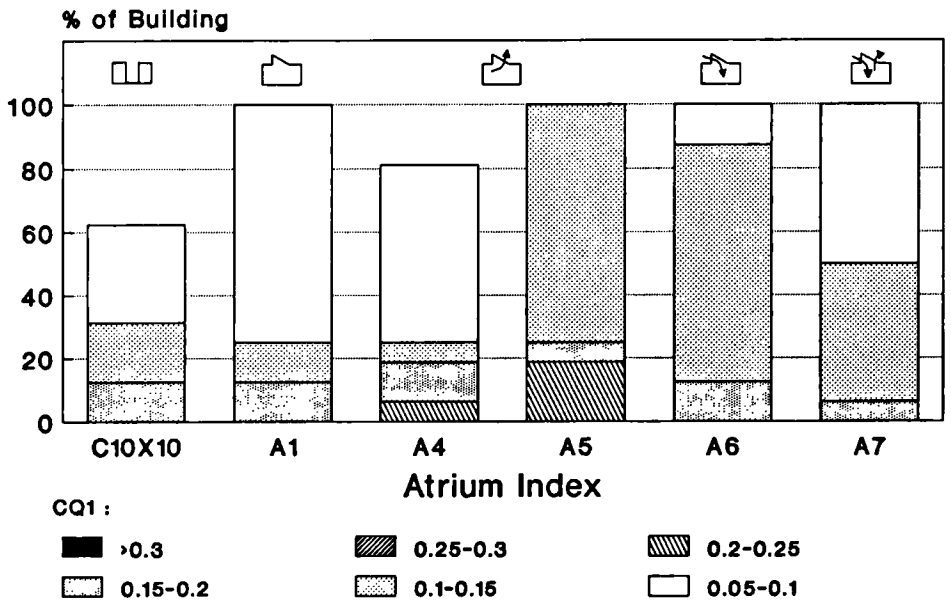

Figure 9.16b: Fraction of the building models under ranges of flow coefficients, **(Group layout density 0.38, 0° wind angle)**

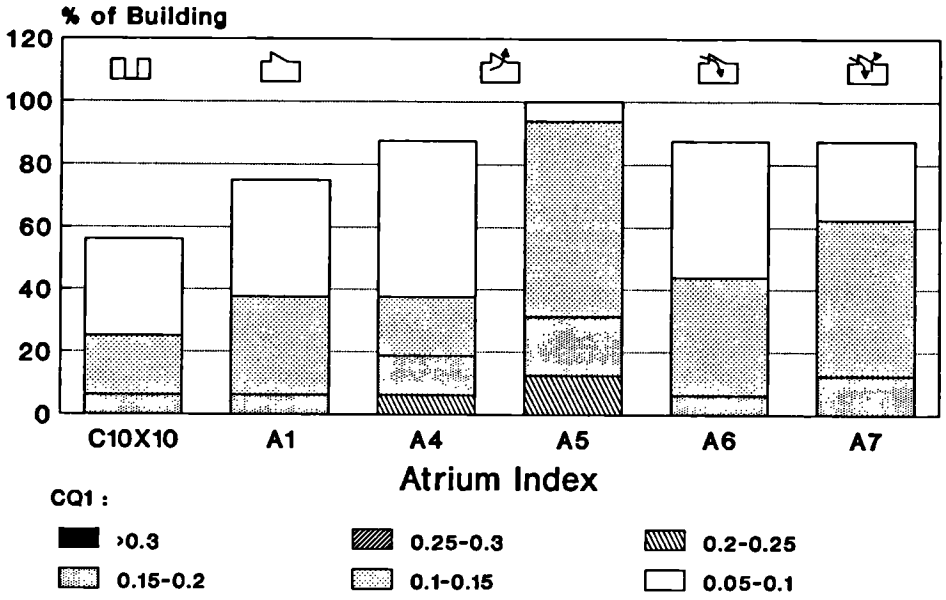

Figure 9.16c: Fraction of the building models under ranges of flow coefficients, **(Group layout density 0.40, 0° wind angle)**

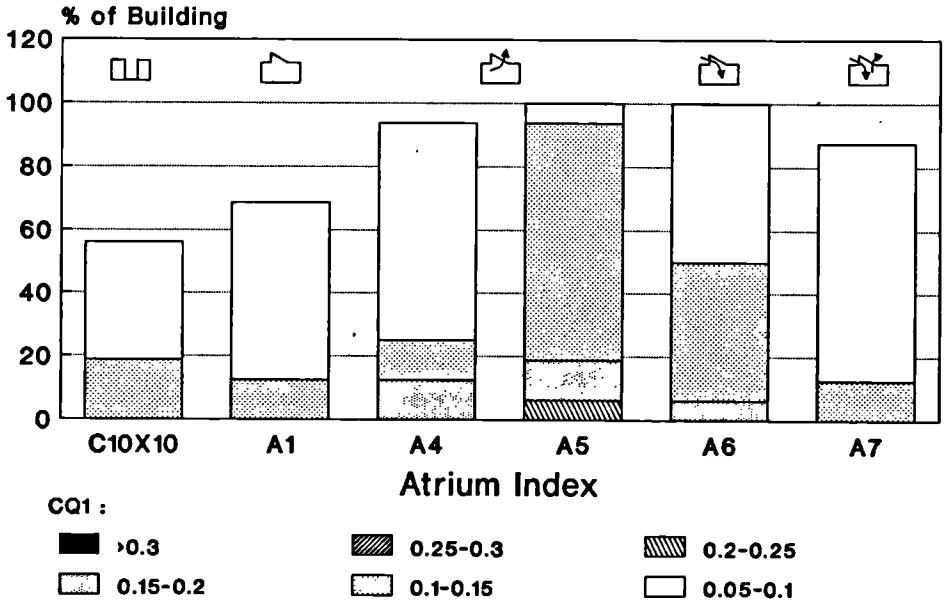

Figure 9.16d: Fraction of the building models under ranges of flow coefficients, **(Group layout density 0.50, 0° wind angle)**

Table 9.2: Cumulative percentage (%) of building under ranges of flow coefficients CQ1.(Shielded conditions, Wind incidence 0° angle)

Group layout (Sc=2.3H, normal pattern)						**Angle 0°**
Model index	CQ1 >0.05	>0.1	>0.15	>0.2	>0.25	>0.3
C10X10	62.5	31.2	18.7	6.25	0	0
A1	100	25	18.7	0	0	0
A4	75	25	25	12.5	0	0
A5	100	93.7	25	18.7	3.12	0
A6	100	62.5	12.5	0	0	0
A7	100	93.7	25	0	0	0
Group layout (Sc=1.5H, normal pattern)						**Angle 0°**
Model index	CQ1 >0.05	>0.1	>0.15	>0.2	>0.25	>0.3
C10X10	56.2	25	6.25	0	0	0
A1	75	37.5	6.25	0	0	0
A4	87.5	37.5	18.7	6.25	0	0
A5	100	93.7	31.2	12.5	0	0
A6	87.5	43.7	6.25	0	0	0
A7	87.5	62.5	12.5	0	0	0
Group layout (Sc=2.3H, staggered pattern)						**Angle 0°**
Model index	CQ1 >0.05	>0.1	>0.15	>0.2	>0.25	>0.3
C10X10	62.5	31.2	12.5	0	0	0
A1	100	25	12.5	0	0	0
A4	81.2	25	18.7	6.25	0	0
A5	100	100	25	18.7	0	0
A6	100	87.5	12.5	0	0	0
A7	100	50	6.25	0	0	0
Group layout (Sc=1.5H, staggered pattern)						**Angle 0°**
Model index	CQ1 >0.05	>0.1	>0.15	>0.2	>0.25	>0.3
C10X10	56.2	18.7	0	0	0	0
A1	68.7	12.5	0	0	0	0
A4	93.7	25	12.5	0	0	0
A5	100	93.7	18.7	6.25	0	0
A6	100	50	6.25	0	0	0
A7	87.5	12.5	0	0	0	0

ventilation rates fall into particular ranges of flow coefficients. The fraction of the building under certain ventilation levels was taken in the previous experiments as the criterion to compare the ventilative performances of the various configurations. Table 9.2 and 9.3, give the cumulative percentage of buildings under ranges of flow coefficients.

The figures show that the proportion of the buildings which were ventilated above certain levels differed largely between the model configurations. The differences were most striking when the group layout density was great. This prompts the conclusion that the choice of the atrium strategy could be very crucial in built-up conditions in order to achieve the best results. In fact, the differences in the performances between the models was more emphasised than in isolation. The average flow coefficients CQT1 of one configuration could be up to 2.3 times that of another in built-up terrains. It was at most 1.4 for the isolation condition.

The most striking feature from the figures is the weak performances of the courtyard and the outstanding superiority of atrium A5, particularly in heavily built-up sites.

Courtyard, C10x10

The average velocities through the windows of the courtyard model were, depending on the group layout, between 6% and 7% of that measured at the gradient height. On average 40% of the structures had flow coefficients below 0.05.

Suction strategy, A5

At the other extreme end of the spectrum, atrium A5, in which the apertures in the roof performed a whole-building suction, recorded clearly the best ventilative performances of all the models and for all the group layouts. The average flow coefficient CQT1 of this structure was found to be between 0.13 and 0.14 depending on the group layout. This value represented an increase over the average value of the courtyard model by approximately 80% to 90% at the largest group spacing, and 110% to 130% at the smallest spacing. Less than 7% of the building had velocities at the window level smaller than 10% that at the gradient height, for the group layouts tested. On average, 1/4 of the building had CQ1 over 0.15.

The increase of the layout density resulted in a decay of the high range velocities but did not affect appreciably the fraction of the building for which CQ1 was

above 0.15.

Positive and near-atmospheric roof pressure modes, A6, A7

Next in the ranking of ventilative performances were generally the atria in which roof vents promoted inward air currents, i.e., A6 and A7. The greatest inflows were reached by A7 at the normal patterns and by A6 at the staggered patterns. Since the roof inflows amended the ventilation in the three downwind faces, the larger the roof inflow was, the greater the proportion of the building that would benefit, even though, the admission of air through the roof reduced severely the inward air currents at the windward wing. The average flow, CQT1, of these models was greater than that of the courtyard by approximately 60% to 70% for A7, and 30% to 45% with A6, at normal patterns. At staggered patterns the improvement over the courtyard was around 60% for A6 and 30% for A7.

Suction strategy, A4

By failing to have vigorous suction forces at the roof level, the atrium of model A4 had a deficit of pressure that was close to the value acting on the downwind external walls, particularly at low group layout densities. This appreciably prejudiced the performances of the structure in which, for the two lowest densities, approximately 20% of the building had flow coefficients weaker than 0.05. In contrast, this structure had, with A5, the largest portion with flow coefficients greater than 0.15 and 0.2. In practical terms, this result means that this configuration may be better suited than A6 or A7 if only a portion of the building has to rely on natural ventilation, but it would not be preferred if the whole building has to be naturally ventilated.

Closed-roof atrium, A1

In general, the closed-roof atrium was among the options with the weakest performances, in particular in the most congested conditions. This is because the model relied entirely on the wall pressure gradients. The portion of the building that fell under flow coefficients weaker than 0.05 was not as great as with the courtyard or model A4 in the two lowest group densities. Nevertheless, the fraction of the building under flows coefficient exceeding 0.10 was clearly the smallest.

Comparison with unsheltered conditions

A comparison between the model ventilative performances in built-up areas and in exposed conditions indicated that they were smaller in the former case, as one could expect. This was particularly manifest with the absence in built-up conditions of flow coefficients exceeding 0.30. Also, the percentage of building space under air currents exceeding a particular value was almost always smaller in the first case. One exception though was model A5.

The portion of this latter model falling in the high range of flow coefficients, (i.e., CQ1 > 0.2), was certainly greater in the exposed conditions, but, also, the percentage of the model under the weakest flow was the largest in these circumstances. For the medium range of flow coefficients, (up to 0.2), the most extensive fraction of building falling in this category was found in urban settings. An interesting implication of this result is that, with this configuration, it would necessitate much weaker winds in isolated conditions to reach adequate air movement in a restricted portion of the building, (around 1/4 of the building), than in sheltered areas. Nevertheless, to ventilate naturally the whole building to certain levels would require much stronger breezes in the isolated case than in the shielded conditions.

Comparison with other related works

The only study from which comparisons may be drawn is that of Bauman et al (1988a and 1988b), (see Section 4.4.2.4), though, only general trends can be compared. This is because the experiment arrangements and measurements are too different.

His remarks, which stated that the use of roof vents were a viable option to improve the flow conditions of houses in densely built-up conditions, corroborate the present findings. However, his experiment showed a superiority of the use of roofs as wind deflector rather than as a suction device, for ranges of layout spacings comparable to those used here. Also, relying on the windows only should give the best overall ventilation for an upwind spacing of 2H according to his results. Neither of these two results were obtained here.

9.6.2 At 45° wind orientation angle

At quartering winds, atria were found in most cases to have the same overall flow coefficients CQT1. Nevertheless, the way in which the flow was distributed within the structures could differ greatly from one building model to another. This is shown in

Figures 9.17a to 9.17d. The casting vote for a preferential configuration would depend on whether the whole building or part of the building had to be naturally ventilated, and also on the strength of the breezes required to restore thermal comfort.

All the structures had, within 10%, the same overall flow coefficient CQT1, except A5 at the most clustered group layout. The average velocities through the windows of these models were between 14% and 16% of the gradient velocity and for a group density PD= 28%. This dropped to 12% to 13% at a density PD= 38% and PD= 40%, to become only 9% at PD= 50%.

Atrium models A1, A6 and A7

The overall flow coefficients of these three models were the same to within 5%. The indoor air movement in these buildings was relying mostly on the pressure gradient on the external walls. Indeed, with models A6 and A7, the roof air currents were found to be minor in most cases, thus the ventilation conditions resembled the closed-roof atrium. Reduced roof induction effects in A6 and A7 were also obtained in isolation conditions (see Section 8.6.1). This was probably due to the fact that some portion of air which was entering the most upwind roof openings was leaving the most downwind roof vents, owing to the large horizontal pressure gradient that existed in this region.

For group layout densities smaller than 50%, the three models presented among the most uniform distributions of ventilation. This was reflected by a large part of the building models falling into a moderate flow coefficient range, and by a relatively small portion of the models with flow coefficients below 0.10.

These structures could be selected for the case when the breezes on the site are strong enough and when the whole building has to be ventilated naturally.

Suction strategy A4 and A5

The configurations exploiting the roof suction on the other hand showed relatively powerful ventilation capabilities, though, restricted to a small portion of the building. In contrast, larger percentages of the building were under weak flow coefficients in comparison with the above mentioned models. With this atrium operating mode, and particularly with model A5, it would be easier to achieve high air velocities than with the aforementionned atria, but for a restricted portion of the building.

At a group density of 50%, the pressure gradient on the model walls was so low that the roof suction mode was proven again to be effective in the case of the atrium A5.

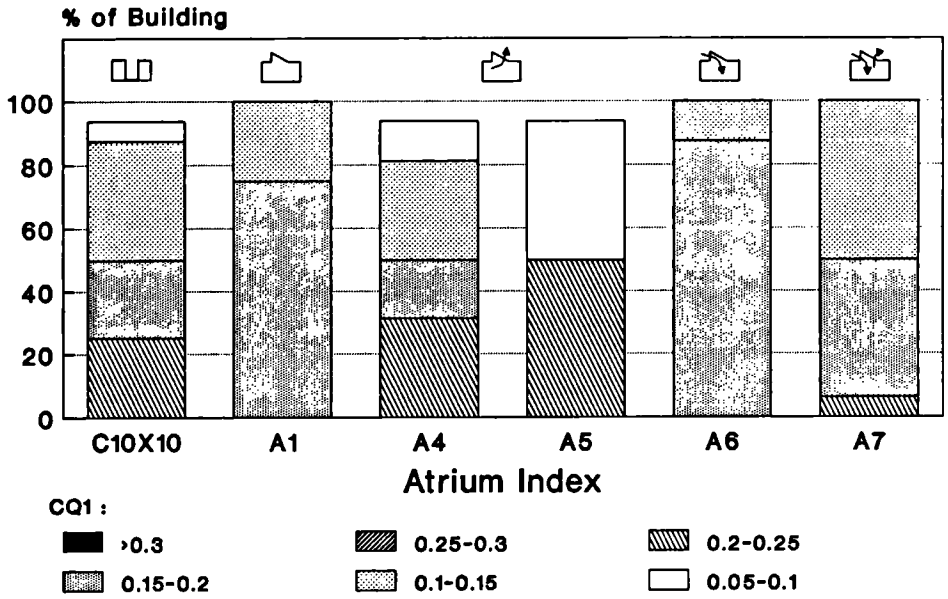

Figure 9.17a: Fraction of the building models under ranges of flow coefficients, **(Group layout density 0.28, 45° wind angle)**

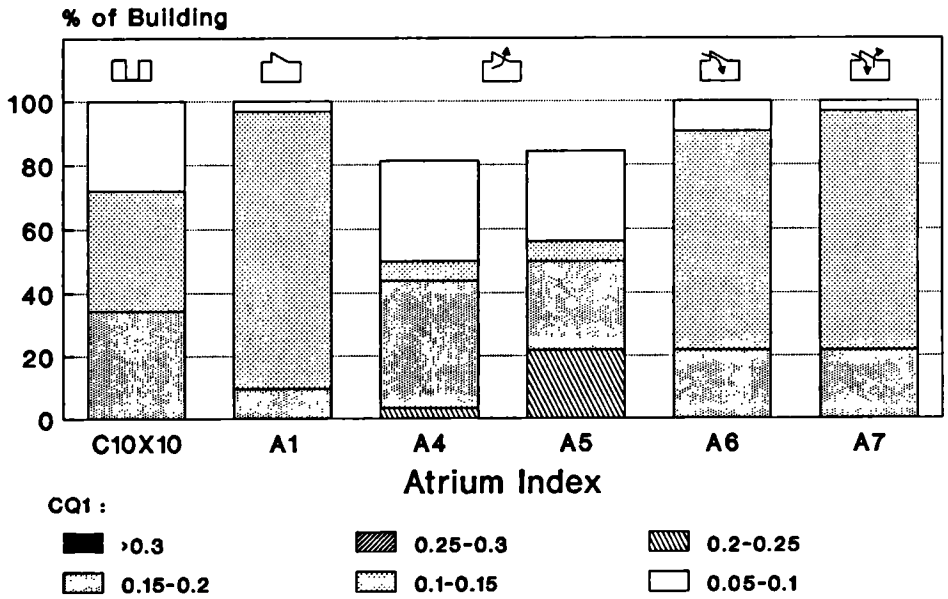

Figure 9.17b: Fraction of the building models under ranges of flow coefficients, **(Group layout density 0.38, 45° wind angle)**

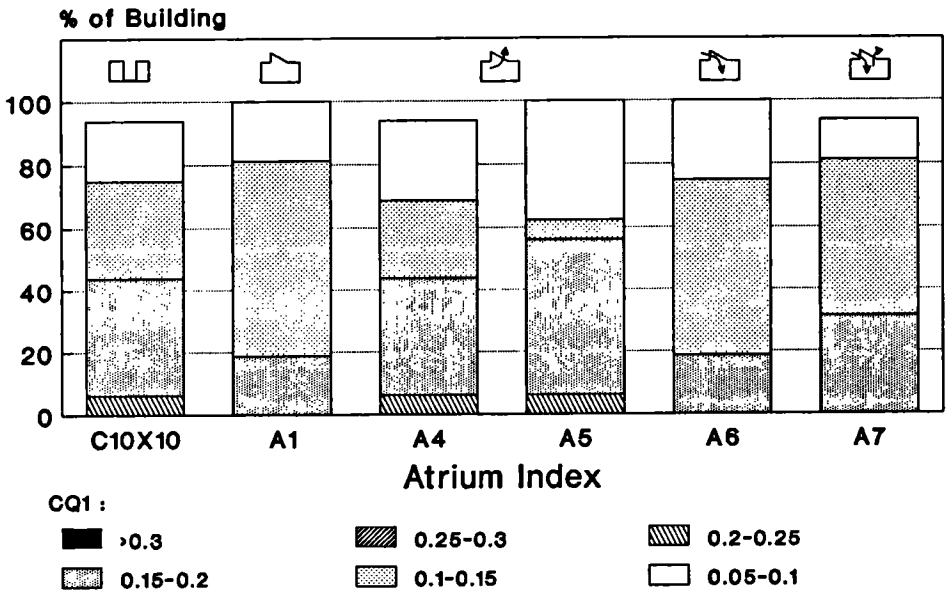

Figure 9.17c: Fraction of the building models under ranges of flow coefficients, **(Group layout density 0.40, 45° wind angle)**

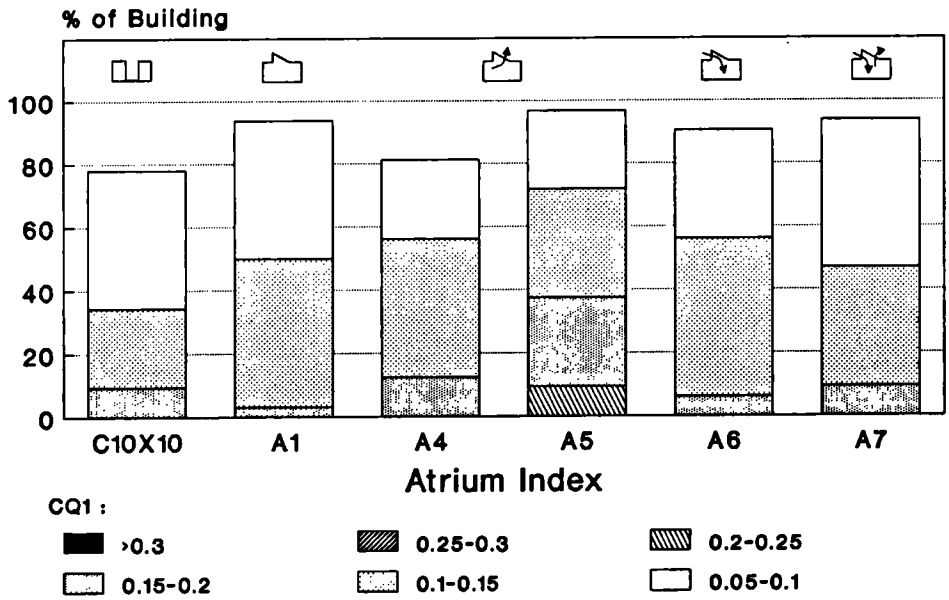

Figure 9.17d: Fraction of the building models under ranges of flow coefficients, **(Group layout density 0.50, 45° wind angle)**

Table 9.3: Cumulative percentage (%) of building under ranges of flow coefficients CQ1.(Shielded conditions, Wind incidence 45° angle)

Group layout (Sc=2.3H, normal pattern)						**Angle 45°**
Model index	CQ1 >0.05	>0.1	>0.15	>0.2	>0.25	>0.3
C10X10	93.7	87.5	50	25	0	0
A1	100	100	75	0	0	0
A4	93.7	81.2	50	31.2	0	0
A5	93.7	50	50	50	0	0
A6	100	100	87.5	0	0	0
A7	100	100	50	6.25	0	0
Group layout (Sc=1.5H, normal pattern)						**Angle 45°**
Model index	CQ1 >0.05	>0.1	>0.15	>0.2	>0.25	>0.3
C10X10	93.7	75	43.7	6.25	0	0
A1	100	81.2	18.7	0	0	0
A4	93.7	68.7	43.7	6.25	0	0
A5	100	62.5	56.2	6.25	0	0
A6	100	75	18.7	0	0	0
A7	93.7	81.2	31.2	0	0	0
Group layout (Sc=2.3H, staggered)						**Angle 45°**
Model index	CQ1 >0.05	>0.1	>0.15	>0.2	>0.25	>0.3
C10X10	100	71.8	34.3	0	0	0
A1	100	96.8	9.37	0	0	0
A4	81.2	50	43.7	3.12	0	0
A5	84.3	56.2	50	21.8	0	0
A6	100	90.6	21.8	0	0	0
A7	100	96.8	21.8	0	0	0
Group layout (Sc=1.5H, staggered pattern)						**Angle 45°**
Model index	CQ1 >0.05	>0.1	>0.15	>0.2	>0.25	>0.3
C10X10	78.1	34.3	9.37	0	0	0
A1	93.7	50	3.12	0	0	0
A4	81.2	56.2	12.5	0	0	0
A5	96.8	71.8	37.5	9.37	0	0
A6	90.6	56.2	6.25	0	0	0
A7	93.7	46.8	9.37	0	0	0

This model had the greatest portion falling into any of the flow coefficient ranges.

Courtyard C10x10

The distribution of the flow in the courtyard resembled that of the roof suction mode in model A4 when the group layout spacing was Sc= 2.3H. With a group density PD= 38%, (Sc= 1.5H, staggered pattern), it was somewhat intermediate between that of model A4 and models A1, A7 or A6. Finally, in the densest group layout, (i.e., plan area density equal to 50%), the courtyard model had clearly the largest percentage of building under low range flow coefficients, (i.e., CQ1 < 0.1).

The courtyard configuration is shown once again, (see case of isolation in Section 8.7), to be inferior to the atrium concept in inducing ventilation, whatever the ventilation design intentions, (i.e., the building to be fully or partially ventilated).

Comparison between conditions at normal and oblique wind incidences

Undoubtedly, the ventilation performances of atria were better at 45° than at 0° wind angle for all the group layouts, except possibly for the configuration A5. Indeed, the ventilation of this building was more evenly distributed at normal wind angle than at 45°. In the latter case a larger portion of the building had flow coefficients over 0.15 or 0.2 than at 0°, yet, at the same time, more of the building was under flows weaker than 0.10. Consequently, unless 15% of the gradient velocity or more is necessary to achieve satisfactory internal air currents and/or unless only a portion of the building is intended to be naturally ventilated, the condition under which the wind impinges on the group layout at right angles is better in the case of this A5 configuration.

Comparison with unsheltered conditions

Comparing the ventilative performances of atrium and courtyard buildings in an urban site with that of the exposed terrain, at 45° wind angle, leads to the same remarks as with 0° wind orientation angle. Better ventilation was achieved in isolation for all the atria, except maybe for A5. For this configuration the fraction of building under the greatest flow coefficients was reduced in built-up conditions, but with the benefit of a larger portion under moderate flow coefficients.

9.7 Conclusions

This chapter has examined ventilation in courtyard and atrium buildings in the context of an urban site, with no dominant buildings in the surroundings. The previously defined atrium ventilative modes were tested, with also one courtyard configuration. Various group layouts of regular elements were examined with dominant winds impinging on the array at 0° or 45°.

In the sheltering conditions of an urban terrain, the pressure magnitudes on the external walls were found to be considerably weakened, particularly at the densest group layouts. Yet, the ventilation induction capabilities of the atrium roofs were, in most of the cases, not significantly affected by the collection of building models.

Almost the full spectrum of flow networks was encountered, from the case where all the air was entering the external walls and was leaving through the roof apertures, to the case where almost all the wall openings served as outlets and the roof apertures as the unique inlets. This could not be obtained in the previous tests on exposed conditions, (except for model A5 at 45° wind incidence). The modifications in the pressure fields resulting from the presence of building elements caused the atrium intended to be used as a positive pressure strategy not to operate under this mode in all circumstances.

The analysis of the internal flow results indicated that almost all the configurations had their ventilation conditions worsened by the presence of surrounding buildings and/or when the plan area density increased, (e.g., CQT 1 was around half the value in isolation for a plan area density of 50%). This was particularly true for models relying mostly on the pressure gradients on the external walls, (e.g., courtyard, closed-roof atrium). However, when strong roof pressure forces were present, as in the configuration A5, (which used the roof as a powerful suction device), ventilation conditions comparable to that in isolation were encountered.

A comparison between the ventilative performances of each model showed clearly the superiority of the atrium A5 when the dominant winds where approaching the array at an angle of 0°. Generally the positive pressure mode and near-atmospheric mode followed in the order of preference. At the other extreme was the courtyard, with indoor air velocities roughly half those in A5. The closed-roof atrium, also relying on the wall pressure gradients, performed very badly. The atrium model A4, which exploited the roof suction to a moderate extent, (because of limited aperture areas), had very strong indoor air movement in some parts, but at the same time, very weak

ventilation locally. This may be suited for buildings relying partly on natural ventilation.

When dominant winds struck the group layout at 45°, the usefulness to resort to the roof pressure forces in urban terrain was less evident than at 0°. The preferential configuration should depend mainly on whether the building has to be partly or fully ventilated by natural means, and also on the availability of strong breezes.

The atrium with small roof effects, (i.e., A1, A6, A7), provided a uniform ventilation distribution for the building model, but of moderate magnitude. These configurations are believed to be suited for buildings relying entirely on natural ventilation. Nevertheless the success of these strategies should depend greatly on the availability of strong breezes.

On the other hand, the models with substantial roof suction effects provided high air velocities locally, but at the same time, part of the building was under very poor ventilation conditions. This strategy is probably more suited for buildings intended to be partly ventilated, with the rest mechanically cooled. In this case, for the limited space to be naturally ventilated, adequate indoor air velocities should be more easily attainable than with the previous types.

In very densely built-up conditions, (plan area densities greater than 40%), the wall pressure gradients became so small that the assistance of roof pressure forces, such as with model A5, becomes the best strategy to use. The courtyard building model was found to have among the weakest indoor air movement, particularly in the most congested areas.

The wind orientation was found to be an important parameter in the ventilation. The wind impinging on the group layout at 45° amended the flow conditions, at least for the models which did not extensively exploit the roof pressure forces. The improvement tended to wane as the density increased.

There may actually be greater benefits in using the roof suction mode in atria than expected solely from the greatest air movements recorded. By having air intakes in the shaded streets, cool air may be introduced into a building's occupied spaces. On the other hand, with the positive pressure strategy, the air could be heated by the roof surfaces before entering the atrium. This may cause more discomfort than relief, unless the air can be cooled by the presence of fountains or plants in the atrium.

The results outlined here are believed to be greatly dependent on the simulated atmospheric boundary layer flow, on the wind incidences chosen, and on the geometry of the models used. In particular, the results are most likely to be contingent upon the

atrium roof shape and its height with respect to the surrounding buildings. This precludes any extrapolation to structures with very different roof shapes and, particularly, to atria with roof heights appreciably lower than the top of the surrounding buildings.

Because of the restricted field of application of these results, it was decided to examine the possibility of using analytical methods to predict internal airflow in atrium buildings. This should enable the designers to appraise the ventilation effectiveness of some specific atrium projects, not covered by the experimental tests. This is discussed in the next chapter.

Chapter 10

Estimate of the accuracy of analytical methods for predicting indoor flows in atria

10.1 Introduction

So far, the research described in this thesis was targeted at discovering the influential parameters involved in the ventilation of courtyard and atrium building types, in giving some estimate of their ventilative performances and to recommend ways of achieving the best results. In this chapter, the appropriateness of using numerical methods for predicting air flow rates in atria is examined. The intention is to provide the designer with a tool for estimating the wind-driven ventilation for cases which were not covered by the experimental tests.

Although the experimental tests produced extensive data that could be used directly to estimate the wind-driven ventilation capabilities of some prototypes in a particular site, the extent to which they can be used may yet be limited. Indeed, the data can strictly apply only to prototypes that do not differ greatly from the tested structures, and only for similar site characteristics and oncoming winds. The velocity ratios CQ are also strongly linked to the porosity of the building model adopted in the tests, (i.e., 11.4% for the walls). This is because the flow through the openings depends on the aperture discharge coefficient, which in turn varies in a non-linear fashion with the size of the aperture. For example, with openings occupying 20% of the wall surfaces, the flow rates are anticipated to be twice that in a building for which the opening area is 10% that of the wall, when assuming a constant pressure differential. However, for a wall porosity of 60%, the internal flows could be more than 7 times higher than in the

case of openings occupying 10% of the wall surface, and not 6 times as expected when a constant discharge coefficient is applied, (see calculation in Appendix E).

A convenient way to evaluate the ventilation potential of atria for cases which deviate greatly from those studied here, would be to use calculation methods based on the knowledge of the pressure coefficient distribution on the building envelope and the equations of flow. As already discussed in Sections 5.2.2.3 and 5.3.3, the method presents many advantages. The calculation of the flow itself is fast and does not require great expertise on the part of the designer unlike the velocity coefficients obtained on porous models. It does require however relevant pressure coefficient data. These can be obtained either from previous ventilation studies but also from wind loading or from wind tunnel tests. When wind tunnel tests are required, it is much easier and cheaper to construct solid models for surface pressure measurements than hollow models for velocity coefficient measurements. Moreover, the collected pressure data can also be used for wind loading calculations.

Nonetheless, as mentioned already in Section 5.2.2.3, the technique may not be accurate in estimating the indoor flows for structures incorporating roof vents.

In this chapter it is attempted to evaluate how reliable the calculation methods are to predict the flow in atrium structures and to establish the conditions under which the technique may or may not be satisfactory. The assessment of the reliability of the conventional calculation methods will be based on a comparison between the calculated values of the internal flows and the measured ones, following the same method as Vickery et al (1983). Also, the computer algorithm used in the present study was identical to that on which their work was based.

10.2 Iterative procedure for the calculation of internal pressures and flow rates

The calculation technique relies essentially on balancing the internal pressures in the building from the knowledge of the external pressures and the opening characteristics so that the net air flow into the building is equal to that leaving it.

Internal pressures CP_i and volumetric flow rates through large openings are generally calculated using the theoretical discharge equation of air through apertures, equation (3.5), in a turbulent flow regime. The discharge through each aperture, Q_i, can be expressed as follows;

$$Q_i = Cd_i \times Ai \times V_{ref} \times \frac{(CP_i - CPI)}{\sqrt{(CP_i - CPI)}} \qquad (10.1)$$

where,

Q_i = flow through the ith aperture

Cd_i = discharge coefficient for the ith aperture

Ai = area of the ith aperture

V_{ref} = reference wind speed at some height

CP_i = external pressure coefficient for the ith aperture

CPI = internal pressure coefficient (unknown)

This equation can be written in a non-dimensional form of flow coefficients, by substitution, using the expression $CQ_i = Q_i / (A_{ref} V_{ref})$.

When all the apertures are identical, A_{ref} can be chosen as the surface of one aperture, Ao. V_{ref} can be taken the same as that for which the CP values are referred to, (e.g., the velocity measured at the roof height or at the gradient). This leads to,

$$CQ_i = Cd_i \times \frac{(CP_i - CPI)}{\sqrt{(CP_i - CPI)}} \qquad (10.2)$$

It can be noticed that the definition of the flow coefficient CQ_i is the same as CQ1 or CQ, used in the previous chapters for the flow of air through the model rooms[1]. However, in the case of the flow through the roof, the coefficient was referred previously to the same reference area as for the rooms, namely the aperture surface of one atrium room. The new definition of CQ for the roof flow is instead associated to the roof aperture area, thus, it is equal to the previous coefficient multiplied by a factor $3/nr$, where nr is the number of opening on the roof, (i.e., $CQ(new) = (3/nr) \times CQ(old)$).

The internal pressure CPI and the flow coefficients CQ_i are given by the solution of the continuity equation, equation (3.20), and obtained by successive iterations.

---

[1] CQ1 is referred to the velocity at the gradient height, CQ is associated with the wind speed at the roof height.

10.2.1 The algorithm

The iterative procedure used to obtain internal pressures and the flow coefficients was that suggested by Vickery et al (1983). It is as follows;

i) Define two starting values of the internal pressure, CPI, as,

$$(CPI)_1 = (\Sigma_1^N CP_i)/N$$

$$(CPI)_2 = (CPI)_1 + 0.01$$

where N = number of apertures.
Compute the corresponding values of the net flow Σ_1, and Σ_2, (algebraic sum of the inflows and outflows),

ii) compute a new estimate, $(CPI)_K$, from the relationship;

$$(CPI)_K = (CPI)_{K-1} + \frac{\Sigma_{K-1}}{\Sigma_{K-2} - \Sigma_{K-1}} \times \left[(CPI)_{K-1} - (CPI)_{K-2}\right]$$

In the above K is the iteration number.
iii) Compute the corresponding value of the net flow,

Σ_K, and test $|\Sigma_K| < 10^{-4}$

If YES : put $CPI = (CPI)_K$ and compute the elemental flow coefficient CQ_i.

If NO : return to (ii).

10.2.2 Reformulation of the equation of discharge

The discharge equation of the flow though the wall openings used in the present case was the equation (6.19), which was derived from the calibration test of the orifice plate models, (see Section 6.2.2.3). This equation takes into account the resistance to the flow of the multiple partitions in the models and the variation of the discharge with Reynolds Numbers. Equation (6.19) can be expressed in terms of difference of pressure coefficients instead of absolute pressures. The final form is as follows;

Discharge equation of the flow though the walls.

$$CQ = 0.4396 \times \frac{(CP_{ex} - CPI)}{(CP_{ex} - CPI)^{0.525}} \qquad (10.3)$$

where CP_{ex} is the pressure coefficient acting on the external walls of an atrium room, and CPI, the pressure coefficient in the atrium core.

For the flow through the atrium roof apertures, however, the theoretical flow equation, equation (10.4), was used in absence of calibration tests. The coefficient of discharge was taken from existing data in Figure 10.1. The discharge coefficient values are dependent on the ratio of the opening area S_O to that of the surface S where the opening are located, and also on the Reynolds Number when the flow is not fully turbulent. For the atrium roof suction strategy, the range of values of S_O/S was between 0.04 and 0.30. The corresponding discharge coefficient, (outflow case in the figure), was between 0.61 and 0.63. The value 0.62 was used as an average. In the case of roof inflow, (positive pressure strategy), S_O/S was equal to 0.30, and the appropriate discharge coefficient was then 0.71.

Discharge equation of the flow though the roof.

$$CQ = Cd \times \frac{(CP_{ex} - CPI)}{\sqrt{(CP_{ex} - CPI)}} \qquad (10.4)$$

The computation of the flow rates using the above-mentioned algorithm is based on the following assumptions:

i) The flow rates can be calculated from equations (10.3) and (10.4).

ii) The internal flow does not disturb the external pressure field measured on the sealed building, (i.e., the pressure field on a porous model is not different from that monitored on a sealed model).

iii) The discharge coefficients of the apertures are dependant only on their geometry and are not affected by the external flow velocities.

iv) The discharge coefficients are constant for the working Reynolds Numbers.

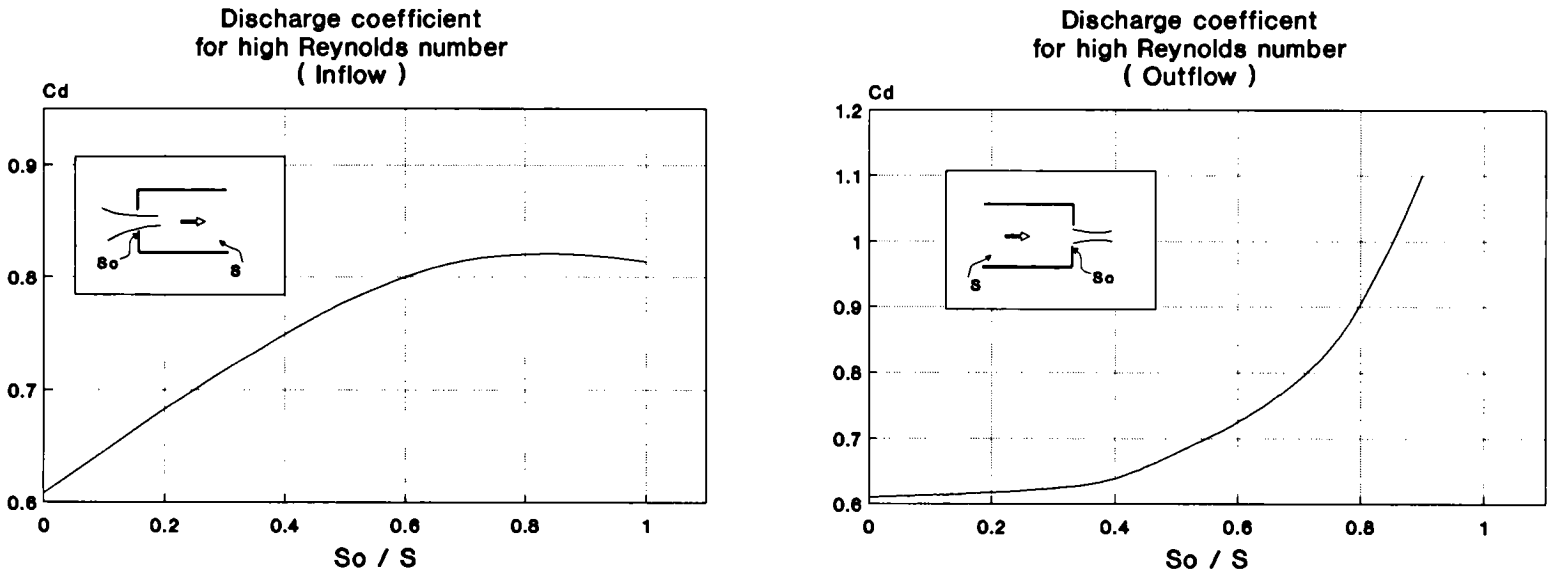

Figure 10.1: Discharge coefficients of inlets and outlets, (Source Vickery et al (1983)).

v) There is a uniform internal pressure.

The algorithm given in Section 10.2.1 was transcribed into GW-Basic and was run on a PC computer.

10.2.3 Input data

The inputs required for the computation of the internal pressures and the flow coefficients are; i) the areas of all the apertures, and, ii) the pressure coefficients acting at the openings.

The internal flows were calculated for the atrium test models in isolation, for which both surface pressure coefficients and internal flows were available, (see Chapter 8), and for which comparisons between predicted and measured values could be made.

Two external pressures were introduced for each of the building model faces. They were the average pressures experienced at one location, L, of the atrium models for which internal flows were available, (see Figure 10.2). One mean pressure coefficient was used for the roof vents and was the averaged value over the region where the openings were located. The system of flow was thus simplified to 9 zones, (i.e., 2 zones for each facade and 1 zone for the roof), for which each zone required 2 inputs, (i.e., the opening area and the pressure coefficient). A schematic representation of the system of flow can be found in Figure 8.4.

To use the mean pressure coefficient values instead of individual pressure coefficients acting on the openings is a logical simplification to make in the case of low-rise buildings. Swami and Chandra (1988) or Wiren (1985) suggested that this practice would not lead to errors greater than 10%. Bilsborrow and Fricke (1975) indicated even lower discrepancies in the case of apertures of the size of cracks. Vickery and Karakatsanis (1987) provide also very strong arguments in favour of the use of mean values. They claimed that there was a good agreement in the flow rate predictions for different input conditions. There was, for example, no significant difference in introducing as inputs the areas of 24 openings assigned with their individual pressure coefficients or a single aperture with one pressure value, equivalent respectively to the total surface of the 24 openings and the average of the 24 pressure coefficients. In high-rise buildings, however, there are large vertical pressure gradients on the windward faces of the buildings so that local pressures must be taken rather than averages for precise estimates of the flow.

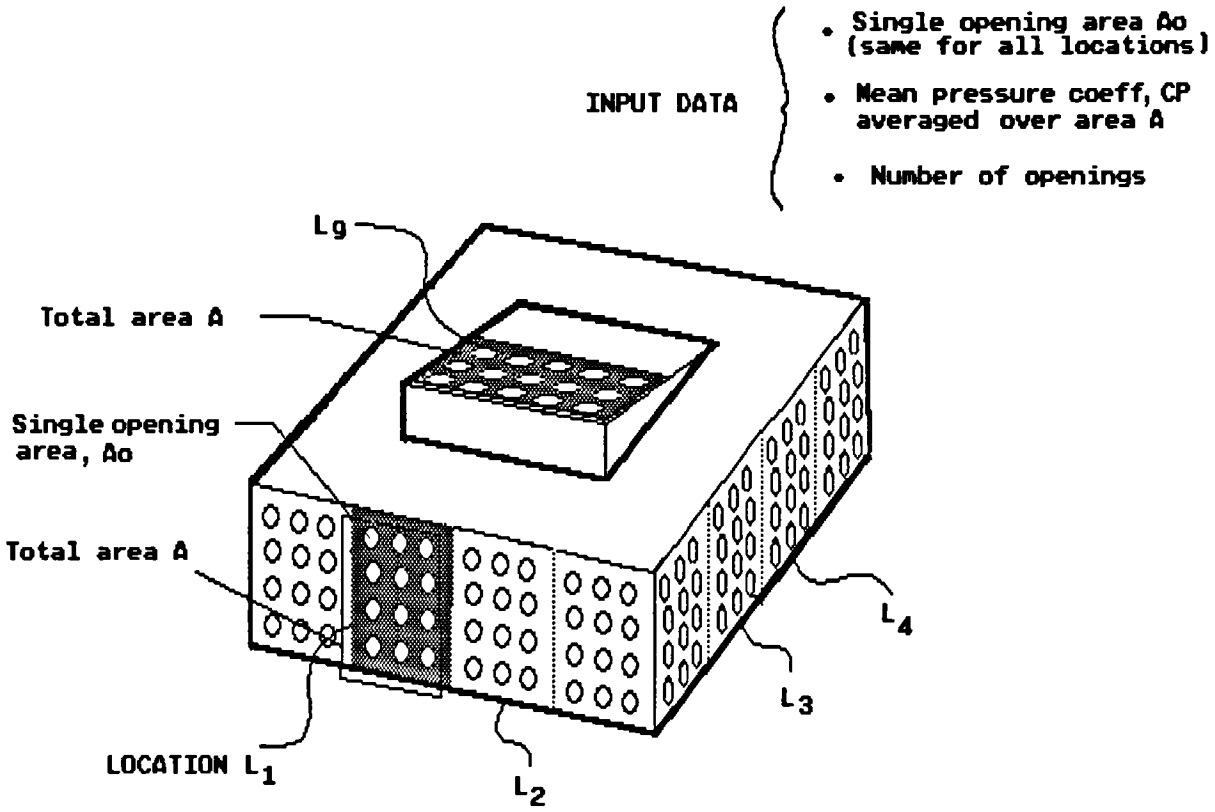

Figure 10.2: Parameters intervening in the computer algorithm.

In the present case, the vertical pressure gradient on the windward walls of the four-storey atrium models was not negligible. However, the concern was to compare the mean values of flow rather than the flows at discrete points, and this justified the use of mean pressure coefficients. It would have been complicated and time-consuming to have considered the detailed network of flows through each hole of the models, for, probably, no more relevance to the overall accuracy of the computational methods than with the simplified network. Furthermore, the pressure at the precise location of each opening was not available.

10.3 Estimate of the inaccuracies in the predicted values

Internal pressures

In Figure 10.3 the calculated internal pressures were compared to the measured ones for all the test atria, at 0° and 45° wind orientation.

The root mean square deviation of the calculated internal pressures from the measured values was 0.059, which corresponded to 23% error on average.

The internal pressures were in most cases closer to the roof pressure values when calculated than when measured. It was as if the effect of the roof pressure forces was overestimated in the calculation.

Flow coefficients

The calculated flows plotted against the measured ones are shown in Figure 10.4. It can be seen that the anticipated values were, in most cases, overestimated.

The root mean square deviation of calculated CQ values from the measured values was 0.052, which represented 21% of the mean value. For low values of CQ, (i.e., between 0.15 and -0.15), the errors were more substantial.

The largest divergences coincide with flows in rooms orientated parallel to the wind, in particular with the atrium A5, (using suction mode with maximum roof area), for which the flow through the roof was the largest.

At 45° wind angle, however, almost all the flow coefficient magnitudes were comprised between 0.15 and 0.40, and, in this case, the agreement between the calculated and measured values was reasonable, (i.e., the root mean square deviation was 0.035, for a mean value of CQ equal to 0.28).

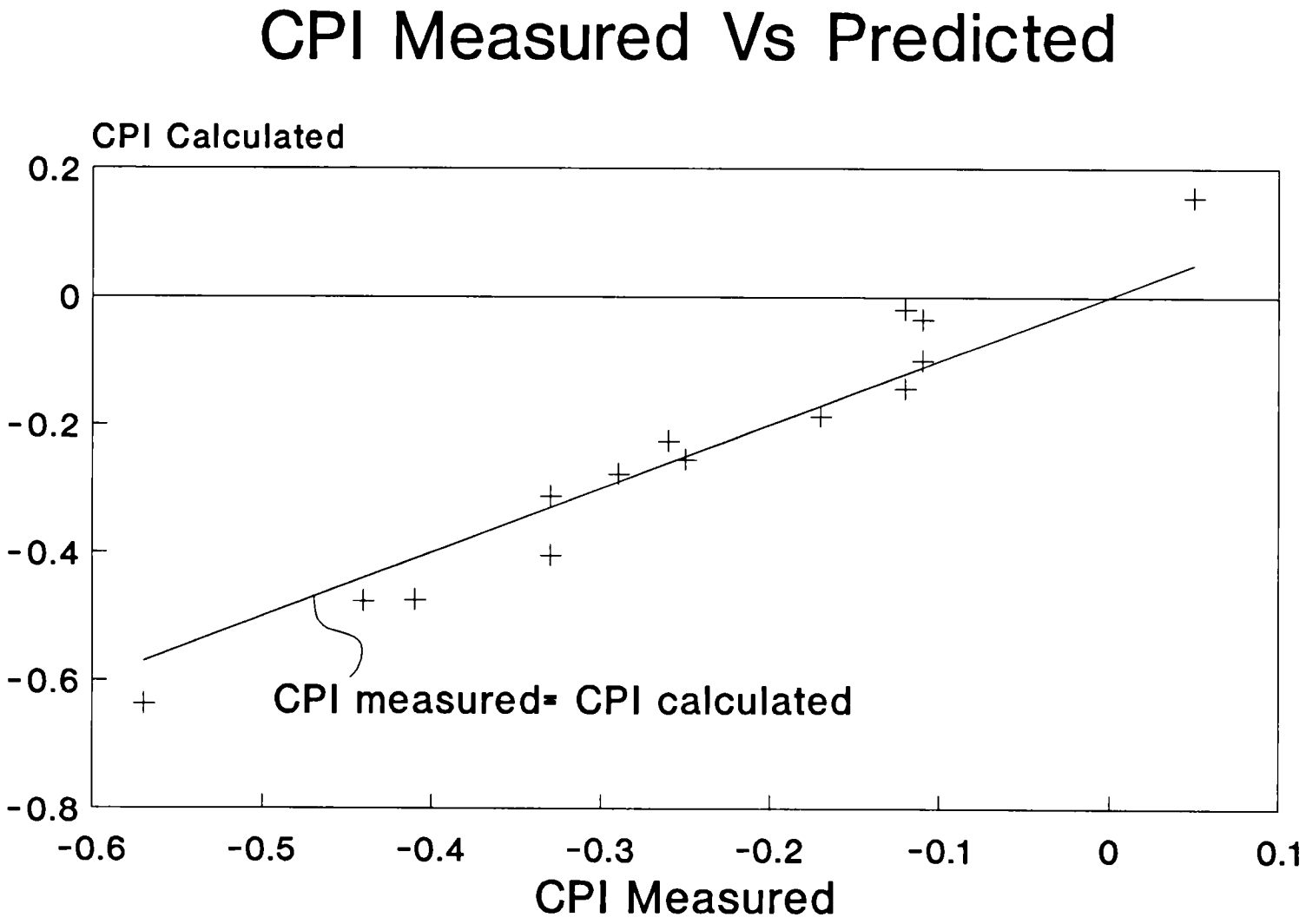

Figure 10.3: Calculated internal pressure coefficients versus measured values.

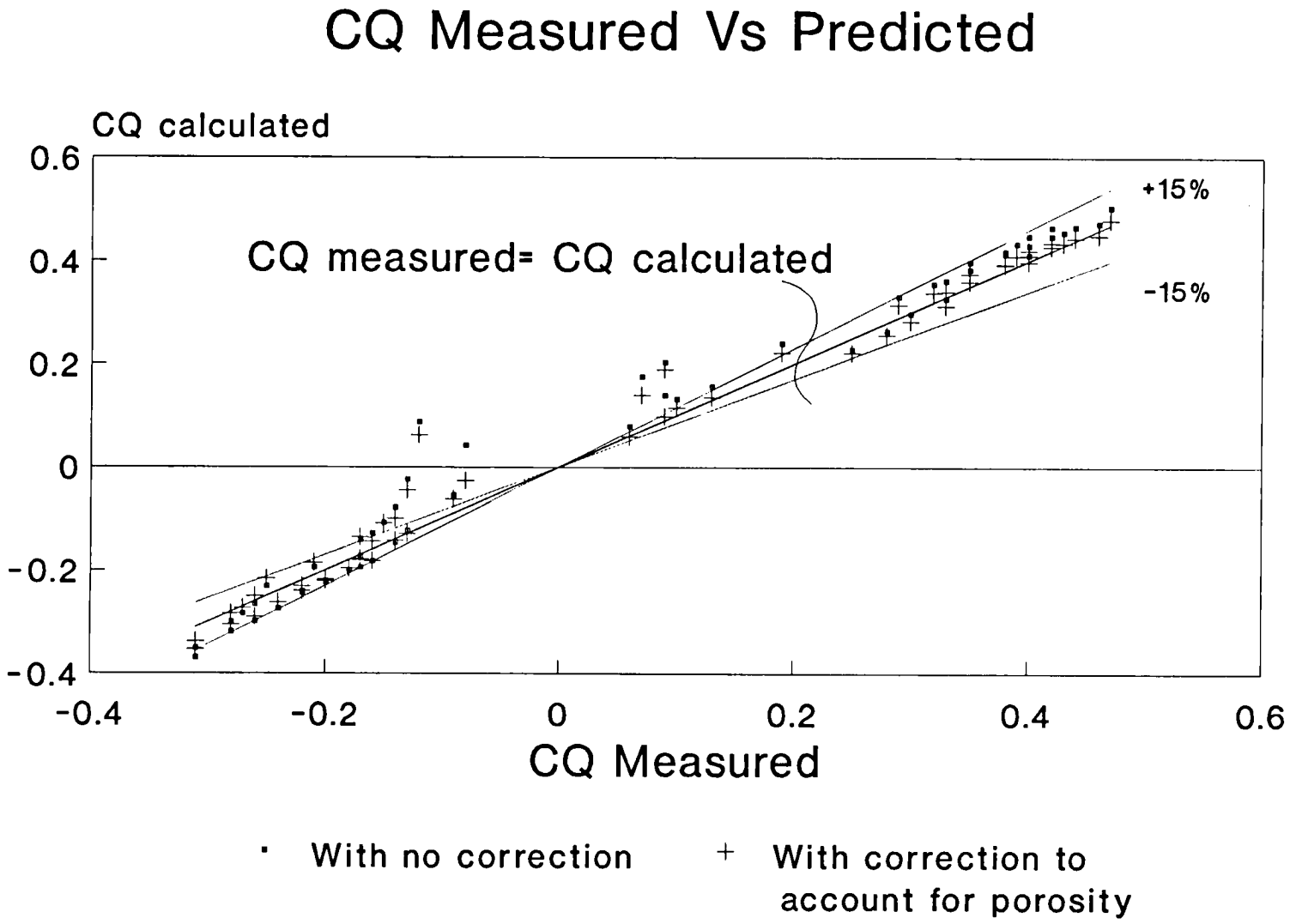

Figure 10.4: Calculated flow coefficients versus measured values.

Two major reasons could be put forward to explain the discrepancies between measured and anticipated values. They refer to the inadequacy of some of the assumptions made in the calculations and are as follows:

i) The calibrated discharge equation may have been different in the conditions of the wind tunnel tests, particularly because of the existence of lateral air movement in the vicinities of the openings. The effects of lateral air velocities are anticipated to be particularly pronounced for apertures which are glanced by the wind.

ii) The external pressure coefficients obtained from solid models, and on which the calculated flows were based, may have been affected by the presence of openings which established a bridge between different pressure fields. This could have in reality reduced the pressure gradient measured across the solid model surfaces.

These arguments are discussed in more details in the following section.

10.4 Possible sources of errors

10.4.1 Alteration of the discharge characteristics of the openings

Contrary to the assumptions that the discharge coefficients of model openings depend solely on the geometry, it was suggested by Vickery et al (1983, 1987), Bilsborrow and Fricke (1975) and Aynsley (1976), that they could also be affected by the external air velocities. The effects could be particularly large at inclined wind angles when fast air glances the facades.

Bilsborrow (1973) compared infiltration rates which were predicted by a analytical methods, with wind tunnel model measurements, and suggested the foregoing effect as a source of error. He interpreted the overestimate of the calculated values as being caused by a reduction of the "operating efficiencies" of some model openings during the wind tunnel tests in comparison to their calibrated characteristics.

He suggested that two major mechanisms may be responsible for the reduction in the performances of the openings. These are;

i) the effect of lateral air flows travelling along the faces of the model interfering with the flow patterns at the air inlet positions,

ii) the effect of fluctuations in the mean pressure differences acting across the

openings.

The author examined experimentally the first effect by determining the discharge coefficients of openings with an air stream of known velocity flowing past the plate which represented the porous facade. The values obtained were compared with the case of no lateral flow. The results indicated that the working efficiencies of the openings acting as air inlets were significantly lower than the calibrated values and decreased as the lateral flow velocity increased. The working efficiencies of the apertures were of the order of 65% to 90% of the calibrated values, depending on the aperture size and the characteristics of the incident flow. On the other hand, the outlet apertures were operating near to their calibrated discharge characteristics measured with no lateral flows, (see Table 10.1). It was suggested that the opening performances could be related to the ratio of the pressure difference acting across the opening to the dynamic pressure of the lateral flow (see Figure 10.5).

The lateral velocities had a lesser effect on the working efficiencies of the smallest openings than the larger ones. Bilsborrow suggested that this could be due to the fact that the air supply for the smallest openings was drawn from the air much nearer to the model surface, where the external velocities were lower due to a boundary layer effect caused by the model surface. On the other hand, for larger openings, the flow was drawn from regions of external flow away from the walls and, hence, having significant velocities which influenced the discharge characteristics of the openings, (see Figure 10.6).

These remarks were made for openings which were representative of building cracks, and where each opening did not exceed 0.18% of the external room walls. These effects could be anticipated to be even more critical in models with apertures representing fully open windows. Indeed, Vickery et al (1983, 1987) suggested that the change of the opening characteristics due to the external flow momentum along the exterior walls could be a major cause for overprediction of the indoor flow rates through well ventilated structures, (although the authors did not mention what the magnitude of these effects might be). The changes in the discharge characteristics of the vents were suggested to increase with the opening size and the air speed outside the wall, and since this latter speed increases with the wind angle, the errors were anticipated to increase with, i) the indoor air velocity, and, ii) the wind incidence. Yet, for openings located in the building wake, where the average velocities are generally small, the distortions should not be excessive.

Table 10.1 : Mean estimated operating efficiencies of inlets and outlets, (After Bilsborrow (1973)).

Angle of incidence	0°	15°	30°	45°	60°
2.5mm diameter openings, simulated open field terrain flow (power exponent, 0.14)					
Windward face	0.86	0.84	0.82	0.74	0.73
Leeward face	1.04	1.02	1.01	1.02	1.01
2.5mm diameter openings, simulated open field terrain flow (power exponent, 0.45)					
Windward face	0.79	0.78	0.73	0.65	0.66
Leeward face	0.96	0.95	0.93	0.88	0.87
1.0mm diameter openings, simulated open field terrain flow (power exponent, 0.14)					
Windward face	0.92	0.92	0.92	0.87	0.88
Leeward face	1.06	1.08	1.07	1.08	1.09
1.0mm diameter openings, simulated open field terrain flow (power exponent, 0.45)					
Windward face	0.86	0.82	0.80	0.81	0.81
Leeward face	0.99	0.96	0.95	0.94	0.94

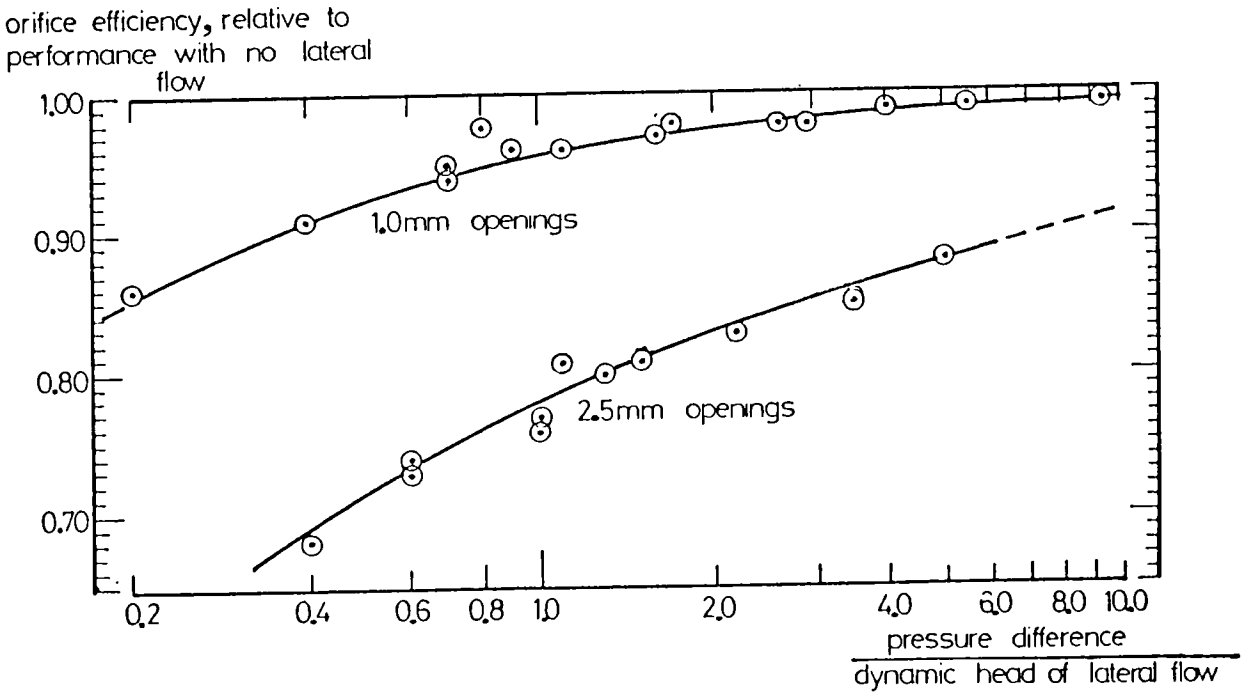

Figure 10.5: Variation of the opening working efficiencies with lateral flow velocity, (After Bilsborrow (1973)).

Aynsley (1976, 1985a, 1988) suggested that the reduction in flow discharge through the inlet openings at an inclined wind incidence could be accounted for by a correction factor equal to the cosine of the angle of incidence, and for wind angles up to 60°. Above 60° incidence, no clear relationship could be obtained, but generally the flow rates were found to continue to decrease.

10.4.2 Influence of the permeability

Another source of error in the predictions is to assume that the indoor flow does not disturb the external pressure field measured on a solid building. Although this could be true for small openings in which the mass flow rate of air introduced by the permeability is not sufficiently large to disturb the flow, for large openings it can be expected that the effects would not be negligible.

The magnitude of the effects due to permeability was examined by several authors who monitored on wind tunnel models the alteration in the flow fields. Nonetheless, the magnitude of the inaccuracies in estimating the flow without accounting for the permeability is still not definite. Also, there is at present no established method of adjusting the external pressures measured on solid models to account for the size and location of openings in buildings.

Both Van Straaten (1967) and Snyckers (1970) suggested that the effect of the permeability on the pressure drop between windward and leeward walls was negligible for wall openings that do not exceed 12% of the wall surfaces. Within these limits the pressure differences measured on solid models can be used to estimate indoor flow rates, (see Aynsley (1976)).

Aynsley (1976) took pressure measurements on the long windward and leeward walls of a model into which slots of increasing width were introduced to examine their effects on the pressure fields. The model was placed amidst two rows of similar porous models which reproduced a typical residential setting.

His results, illustrated in Figure 10.7, indicated that the pressure differential between windward and leeward walls increased with the porosity and reached a peak at a permeability of approximately 20%. With further increase in the opening size, the pressure drop fell until the openings reached 55% of the wall area and then tended to level out with greater porosities. The author indicated that the change in the pressure differential was most severe near the wall ends, in which case, the flow could be underestimated from the pressure drop measured on solid walls by 30%, for a wall

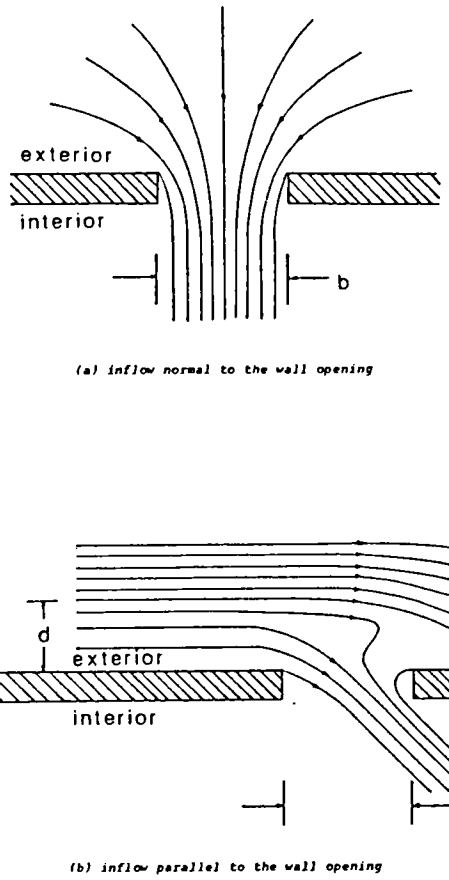

Figure 10.6: Pattern of the flow at the entrance opening for normal and inclined external flows, (After Vickery et al (1987)).

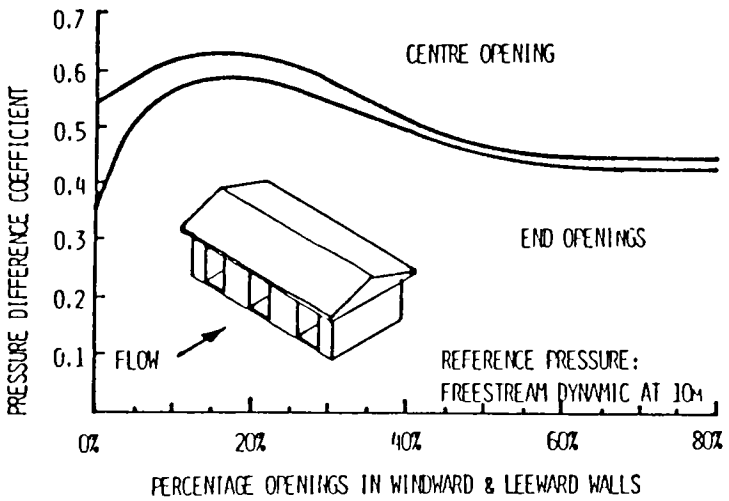

Figure 10.7: Effect of permeability on pressure differential across windward and leeward walls, (After Aynsley (1985)).

porosity of 15% to 20%, (Aynsley (1979, 1985a)). Near the centre of the walls, however, these errors were of the order of ∓10%.

It must be underlined here that, since the test model was surrounded by other elements of variable porosity, the trend recorded on the test model may not be solely the result of its permeability. Another criticism that could be raised here is that the pattern of the flow obtained with the use of slots, to create the desired porosity, is unlikely to be representative of flow patterns obtained with openings in a large room.

Holdo et al (1983) monitored in wind tunnel models the change in the pressure fields caused by small openings which were more representative of cracks than fully open windows. He indicated that substantial changes in the external surface pressures could occur when there were dominant openings, (i.e., with surfaces exceeding 0.75% of the wall). On the other hand, when the openings were uniformly distributed on the model surfaces, and when the aperture surface represented less than 3% of the wall area, then no substantial effects on the external mean pressure distribution were found.

There are some evidences that the magnitude of the distortions in the pressure fields is also related to the location of the openings with respect to different regions of the external flow. Holdo et al (1983) indicated that the divergences were particularly large in surfaces which were glanced by the wind, (near-parallel to the wind), and seemed more critical within regions of separated flows than further downstream. From the figures of the publication, it could be read that in some cases the pressure was only 35% of that measured on the solid model. On the other hand, in the lee or near the stagnation region the effects were much lesser, even though the flow through the apertures was estimated to be almost the same. The authors suggested that while the flow through the openings was not sufficiently large to affect the external flow in the wake of the building, it was sufficient to disturb the separated flow on surfaces parallel to the wind direction.

Holdo et al (1983) concluded from their work that the discharge equation of the flow allows an estimate of the internal pressures within 6% accuracy when the permeability is of the order of 5% in a turbulent flow regime. When effects due to the permeability are observed, particularly when there are dominant openings located in regions of separated flow, the internal pressure could still be predicted with accuracy provided the altered external pressure are used.

Vickery and Karakatsanis (1987) suggested that for permeabilities less than 23% of the walls, the flow rates could be predicted from the knowledge of the external pressure distribution measured on a solid model with an accuracy of about ∓10%. But,

for larger porosities the predicted flow rates could be substantially in error.

In the particular case of openings located in the roof ridge line, the authors explained that even with very small permeabilities the flow injected into the roof wake could have a marked effect on the pressure field. This may well be related to the proximity of the vents to the point of flow separation. In these circumstances, the calculated flow rates were found to be significantly overestimated, (i.e., the measured flows only attained 60% to 70% of the predicted values), and the error tended to increase with the "through-flow".

10.4.3 Comparison with other relevant studies

Vickery et al (1983 and 1987) suggested that the errors in the calculation of flows using the algorithm given in Section 10.2.1 could be of the order of 40% when roof vents are involved. The reasons have been already enumerated. A replot of the calculated and measured flows from their work is shown in Figure 10.8. The magnitude of the inaccuracies can be seen clearly to be much higher than in the present study.

Several reasons could be put forward to explain the relatively low level of inaccuracies in the present case in comparison with the study of Vickery and his colleagues.

i) Contrary to Vickery's model, where the roof vent was a single slot occupying almost the whole width of the roof, in the atrium models the vents were uniformly distributed on the roof surface. The disturbances in the pressure field caused by of a dominant opening was stressed by Holdo et al (1983) to be more severe than in the case of uniformly distributed apertures.

ii) Furthermore, the atrium roof apertures did not exceed 30% of the surface for which the external pressures were integrated, whilst in Vickery's study, this surface was almost all occupied by the opening. It could thus be anticipated that, in the last case, the pressure field in all the perimeter delimited by the opening was subjected to the through-flow, but not in the case of the atrium vents.

iii) The location of the roof openings in relation to regions of external flows was different in the two studies. In the atrium case, the vents were located either on the positive pressure field or in the wake of the roof, a step back from the roof ridge. On the other hand, in Vickery's study, the roof aperture was positioned at the ridge line, probably very close to the separation point, which is believed to be a critical region in

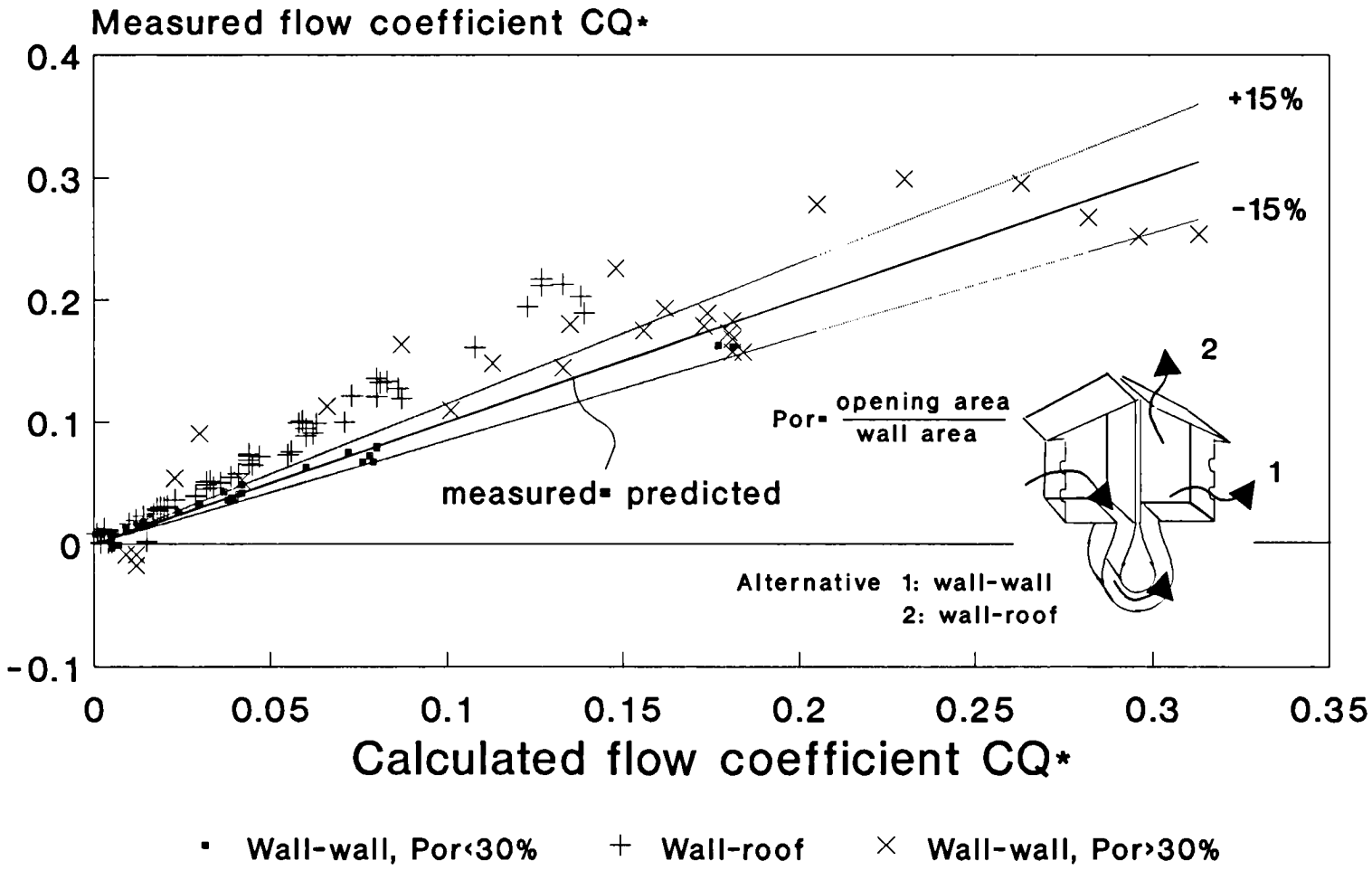

Figure 10.8: Comparison between measured and predicted flows in models using roof vents. *CQ* is the ratio of the indoor flow to the frontal facade area of the model multiplied by the wind speed at eaves height.* Replot of the data from Vickery et al (1983).

which the pressure field could be very severely distorted by the through-flow.

iv) The discharge equation used to predict the flow through the atrium rooms was obtained from the calibration arrangement, (see Section 6.2.2.3). This equation accounted for the resistance to the flow of the internal partitioning of the rooms and of the outer walls. It was also adequate for the working range of Reynolds Numbers[2]. In the experiment of Vickery and his colleagues, the discharge coefficients of the model facade plates were obtained from tabulated values for relevant opening sizes. Yet, there are many additional parameters that could affect the discharge coefficient of an opening than its size. The work of Aynsley (1976), indicated that the arrangement of downwind internal spaces, the thickness of the walls and the sequence of openings in the internal space can affect the jets at the upwind apertures, thereby influencing their discharge characteristics, (see also Aynsley et al (1977)). Another important factor that can influence the discharge characteristics of apertures is the regime of the flow expressed in terms of Reynolds Number. In the work of Vickery et al (1983), the opening discharge coefficients were most probably variable within the working Reynolds Number range. These could be additional sources of errors.

10.4.4 Discussion

It is impossible to indicate in the present study the part each of the two main sources of errors, (i.e., permeability and change in the discharge opening characteristics), plays in the overall discrepancies.

However, it can be seen clearly in Figure 10.4 that for large flow magnitudes, both inflows and outflows were overestimated by the calculation methods, and this could likely be attributed to the effect of the permeability. Indeed, it was implied that the other possible source of error, namely the change of the calibrated discharge characteristics of the openings, was only critical in the case of inlets, and for inclined wind incidences. In these circumstances neither the outflows nor the high values of inflows which were obtained in rooms normal to the approaching wind should be concerned by this latter effect.

An attempt was made to adjust the calculated flows to account for the effect of the permeability. This is now discused.

---

[2] A limitation, though, is that the discharge equation was established for the atrium rooms facing the main air stream at right angle, and not for inclined wind incidences.

10.5 Suggested corrections to the predictions to account for the effects of permeability

Vickery and Karakatsanis (1987) suggested a way of obtaining an approximate estimate of the inaccuracies due to the permeability on the basis of previous work made on the drag of a porous plate, (see Georgiou and Vickery (1979)). These latter authors established that the drag of the plate could be expressed as a function of the porosity, β, as follows:

$$CD_{(\beta)} = CD_{(\beta=0)} \times (1-\beta) \times (1+0.3\beta) \qquad (10.5)$$

Where $CD_{(\beta)}$ is the drag of the perforated plate and $CD_{(\beta=0)}$ the drag of the same plate with no openings. Since the drag is proportional to the pressure drop across the plate, this equation becomes,

$$\Delta CP_{(\beta)} = \Delta CP_{(\beta=0)} \times (1-\beta) \times (1+0.3\beta) \qquad (10.6)$$

Ultimately,

$$Q_{(\beta)} = A \times Cd \times V_{ref} \times \sqrt{\Delta CP_{(\beta=0)}} \times \sqrt{(1-\beta) \times (1+0.3\times\beta)} \qquad (10.7)$$

or,

$$CQ_{(\beta)} = CQ_{(\beta=0)} \times \sqrt{(1-\beta) \times (1+0.3\times\beta)} \qquad (10.8)$$

Where A is the total opening area, Cd, the discharge coefficient of the apertures and V_{ref}, the air velocity at a reference height.

The above mentioned work encouraged the present study to look for similar relationships that would enable adjustments to be made to the flows anticipated from solid model pressures to account for the permeability. The largest values of the measured flows, i.e., $CQ > 0.15$, were best related to the calculated ones with the following expression, obtained from a least square fit;

For the flow through the rooms,

$$CQ_{w(\beta w)} = 0.945 \times CQ_{w(\beta w=0)} - 0.006 \qquad (10.9)$$

(With a correlation coefficient $R^2 = 0.985$)

For the flow through the roof,

$$CQ_{r(\beta r)} = 0.816 \times CQ_{r(\beta r=0)} + 0.023 \qquad (10.10)$$

(with a correlation coefficient $R^2 = 0.953$)

where the indices w and r refer respectively to windows and roof vents.

These equations were in fair agreement with equation (10.8) in which β was equal to 0.11 in the case of the flow through the atrium walls, (equation (10.11)), and equal to 0.30 for the roof, (equation (10.12)), where β represented the ratio of the roof opening area to that of the surface where the pressure were averaged, (see Figure 10.2). These porosities were the same for all the atrium configurations. Using equation (10.8) with the adequate porosity, β, instead of equations (10.9) and (10.10), yielded errors of the order of $\pm 10\%$ of the average flow coefficient.

For the flow through the rooms,

$$CQ_{w(\beta w)} = 0.957 \times CQ_{w(\beta w=0)} \qquad (10.11)$$

For the flow through the roof,

$$CQ_{r(\beta r)} = 0.873 \times CQ_{r(\beta r=0)} \qquad (10.12)$$

The calculated data corrected for the effect of the permeability as suggested by Vickery and Karakatsanis (1987), using equation (10.8), amended the accuracy to $\mp 17\%$ of the average values, (in comparison with $\mp 21\%$ with no correction).

A last attempt to refine the corrections was to use the equation (10.8) with the appropriate porosities for the walls and roof during each iteration of the computation,

with the same inputs as before. The results are shown in Figure 10.4.

In this case, the standard deviation was reduced to 0.04 on average which represented errors of the order of ∓15%. The standard deviation of the flow coefficients was even lower, (i.e., 0.02), in the rooms which were not facing the wind at 90°, (i.e, 0°, 45°, 135°, 180°, 225°, 315°), and represented a deviation of ∓7% from the mean values.

This level of accuracy is believed to be acceptable given the fact that the uncertainties in the site wind data are often much greater, (Aynsley et al (1977)).

10.6 Recommendations for the use of the numerical methods for predicting indoor flows in atria

Vickery et al (1983 and 1987) suggested that the internal flows in a building with no roof vent can be predicted from a knowledge of the external pressure distribution measured on a solid model with an accuracy of about ∓10%, provided, i) the wall porosities are less than 23%, and, ii) with the wind not strongly inclined, (i.e., wind angle with the vented faces not above 45°).

The present study has shown that the limits of use of the conventional prediction procedures could be extended to structures involving roof vents, such as atria, yet, with some limiting conditions which are;

i) the openings must be uniformly distributed within the wall or roof surfaces and there must be no dominant aperture, in particular, in regions close to the flow separation point, (i.e., near the roof ridge line or the wall edges),
ii) the relative porosity should probably not exceed 30%,
iii) the wind incidence to the upwind vented faces must not exceed 45°.

It is also very important to obtain reliable and relevant values of discharge coefficients for the openings. If the indoor flow is not fully turbulent, account for changes of the discharge coefficient with Reynolds Numbers must be made.

Should all these requirements be satisfied, an accuracy of the order of ∓10% to ∓15% could be expected if the empirical corrections for the permeability suggested by Vickery and Karakatsanis (1987) are used in the iteration process.

To examine the potential for natural ventilation of powerful roof suction devices, the numerical computations of flows are anticipated to be inaccurate.

10.7 Conclusions

The adequacy of using numerical methods to predict air flow rates in atria has been examined in this chapter.

A comparison between measured and calculated flow coefficients for the atrium models has shown that the numerical computations of flows, which were suggested to be satisfactory for most buildings vented by windows, can be extended to structures using roof vents, like atria, provided a number of recommendations are followed. These are listed in the above section.

However, the computation techniques based on the knowledge of pressures measured on solid models still need to be refined to account for the effect of the permeability of open windows, and for the change of the working efficiency of the openings caused by lateral external flows. In particular, it would probably be very useful to relate the corrections for the opening working efficiencies to specific regions of external flows around the building envelope. This can be suggested as a theme for further research.

The calculation procedure for wind-driven ventilation, which has been described in this chapter, is simple to program on a computer. The main drawback is the need to obtain the relevant pressure data for the structure which needs to be tested. It has been already mentioned in Chapter 8 that there are little available pressure coefficient data relevant to atria. Hence, it is most probable that before more pressure measurements of such designs are made, the designer would have to resort to wind tunnel tests.

Chapter 11:

Conclusions and recommendations

11.1 Introduction

The potential that courtyards and atria have to promote wind-driven ventilative cooling in multistory buildings has been the subject of this study.

The literature review on the subject revealed that very little work has been done on the subject and very limited guidance was offered to designers to estimate whether or not these buildings can rely on natural ventilation for cooling purposes. Also, there was almost no indication on the most influential parameters which need to be controlled. The present study was aimed at filling some of the lack of information on the subject.

In order to appraise the ventilation capabilities of these structures, experimental tests have been conducted in a wind tunnel where small porous models have been used. The main results were drawn from the measurements of actual airflow rates which were made by means of small orifice plates fitted in the models.

The influential parameters in the ventilation of these building types which have been tested include:

i) the courtyard geometry and the orientation to the wind;

ii) several ventilation modes which can be used by the atrium and which are driven by the atrium roof pressure forces. These modes include the suction, the positive and the near-atmospheric pressure strategies, respectively, in which the atrium roof can act as a suction device, a wind deflector or performs the two actions concurrently;

iii) the atrium and courtyard configurations were tested either in isolation, (unsheltered site), or in various urban layouts.

In this chapter, conclusions drawn from the entire study are used to establish sets of guide-lines for the design of naturally ventilated courtyard and atrium buildings, (see Appendix F). Also, a method is put forward, in Appendix G, upon which some practical application of natural ventilation to thermal control can be evaluated.

The design guide-lines are by no means exhaustive as there is still a lot of work to be done before more comprehensive rules can be established.

11.2 The main results

The salient results of the study are as follows:

11.2.1 Courtyard-type buildings in unsheltered sites

i) The ventilation of courtyard building-type was found to be critical for the leeward part of the building and in most of the rooms which were orientated parallel to the wind.

ii) Changing the geometry of the courtyard had some effects at discrete locations of the building but little influence on the overall conditions. Changing the depth had the effect to affect the flow locally in the leeward wings of the courtyard building, for which, the intensity of the indoor flow and its direction were found to change. The changes of the courtyard width had relatively minor effects on indoor air speeds.

iii) Nevertheless, there was some benefit in controlling the courtyard geometry, in particular, by presenting the largest face of the courtyard building to the wind. In this case, the relative proportion of the structures facing directly the wind was increased and the number of rooms orientated parallel to the main airstream (which were weakly ventilated) reduced.

iv) The largest courtyard sizes did not particularly record the best ventilative performances in contrast to what is generally believed.

v) In contrast with the relatively small influence caused by the alteration of the courtyard geometry, the effect of the wind orientation was more consequential. Changing the orientation to the wind from 0° to 45° had the remarkable effect of amending the ventilation conditions in the downwind wings and venting the whole building more evenly. This was, however, to the detriment of reducing the flow on the

upwind parts of the building. The reason for the improvement of the flow at the downwind locations of the building was explained as being due, in particular, to a greater penetration of part of the airstream inside the courtyard. Strong horizontal vortices which are known to be generated at the upwind edge of building roofs at oblique wind angles were probably responsible for this latter phenomenon.

vi) Comparisons with related works enabled an analogy to be drawn between the flow behaviour in courtyards and that in other cavities, such as, grooves or streets between building blocks. This similarity enabled notably to anticipate that distinct flow regimes could be set up in a courtyard as a result of the change of its geometry. The change of the courtyard depth was believed to govern the variations in the flow patterns. It seemed, on the other hand, that the increase of the breadth had the effect of strengthening the main vortex activity in the courtyard without altering the general flow pattern.

11.2.2 Atrium-type buildings in unsheltered sites

i) The atrium ventilative modes which were conceptualised did perform as expected. Nevertheless, it could not be unveiled whether or not the atrium roof in the near-atmospheric pressure strategy did perform the dual action as a wind deflector and a suction device simultaneously, as was anticipated. The ventilative conditions of this configuration actually resembled one of the three other modes, depending on whether the strongest air current through the roof was inward, outward or nil.

ii) the roof permeability was found to be an important parameter in inducing ventilation under a specific mode. To obtain the greatest roof induction effects, it is not sufficient to locate the roof vents in the appropriate pressure field, say low pressures for suction mode. It is also imperative that an extensive opening area is contained in this region.

iii) Deflecting the air travelling at the roof level inside the atrium caused the inflows through the rooms to decrease in comparison with an atrium with the roof closed, and the outflows to increase. The suction mode resulted in the opposite effect. The positive pressure strategy had thus the advantage of improving the flow in the downwind rooms which were identified as those with the most critical conditions. The suction strategy, on the other hand, amplified the difference in the ventilative conditions which existed between the upwind and downwind wings in all models. The atrium with a sealed roof had intermediate ventilative conditions between the positive and negative

atrium pressure mode.

iv) With the wind blowing at an oblique angle, the atrium building with a roof closed was well and evenly ventilated. In these circumstances, promoting a great roof induction could cause more harm than good. This was particularly true for the suction mode which could impair greatly the outflows in the downwind rooms.

v) The choice of the ventilation mode should depend on whether the building is intended to be entirely ventilated by natural means or partly, with the rest of the building mechanically cooled. For the first design intention, the positive pressure strategy is probably best suited, since the fraction of the building under weak flows is reduced. On the other hand, for the second design intention, the suction strategy is better, and this is because maximum velocity can be obtained, even though it is restricted to part of the building only.

The location of the cool and clean air can also dictate the positioning of the air intakes and thus the choice of the ventilation mode. In this respect, the positive pressure strategy is probably best suited for night-time-only venting. This is because at night the cooler air is generally located at the roof level, but, on the other hand, during the day the air may be heated by the roof surfaces before being introduced in the atrium. This may cause more discomfort than relief. This configuration may be also best suited for sites in which cool marine breezes prevail.

Also, problems of odour migration and noise in the building must be addressed in the choice of the atrium type. Finally the smoke control strategy in the event of a fire must be compatible with the ventilation for environmental control.

vi) For any of the aforementioned design intentions, (whether the building have to rely fully on natural ventilation or partly), there were always some atrium configurations which performed better than the courtyard structure. This demystifies somewhat the belief that the courtyard is superior to atria for inducing wind-driven natural ventilation.

11.2.3 Courtyard and atrium-type buildings in congested urban sites (with no dominant buildings)

i) The pressure magnitudes on the wall of sheltered buildings were found to be considerably lower than unsheltered buildings, in particular, in the most congested group layouts. Nevertheless, the ventilation induction capabilities of the prominent roofs of the atria tested were, in most cases, not significantly affected by the collection of buildings around the prototype.

ii) As anticipated from the pressure fields, the measured flows rates in the models indicated that, in general, the building ventilation was weaker in dense group layouts than in unsheltered sites or in less dense building collection. This was particularly true for buildings in which the roof induction was small. However, with the atrium configuration in which the roof acted as a powerful suction device, ventilation conditions comparable to that in unsheltered sites were recorded.

iii) With the wind impinging on the group layout at right angle, the atrium configuration exploiting strong roof pressure forces had clearly the best ventilative performances. The courtyard was the worst. The atria which had small roof induction effects were also among the worst. This result outlined that the assistance of the roof pressure forces to induce a larger pressure gradient rather than with the walls alone was a concept which worked and which gave the best results. Nevertheless it was imperative to provide an extensive area of roof vents at the appropriate pressure fields.

iv) When the wind impinged on the group layout at 45°, the usefulness to recourse to the roof pressure forces for inducing indoor flows was less evident than at 0° wind incidence, expect in very congested group layouts, (i.e., plan area density of the order of 40% to 50% or more). The preferential configuration should then depend mainly on whether the building has to be fully or partly ventilated by natural means. The atria in which the air flow through the roof is restricted are probably better suited for whole-building ventilation, though the success of the strategy is greatly contingent on the availability of strong breezes. The suction strategy is best suited for buildings intended to be partly ventilated, (typically 1/4 to 1/8 of the building), the rest mechanically cooled, and in this case, the availability of very strong breezes should not be as stringent.

v) There may be actually greater benefits in using the suction roof mode in atria than expected solely from the greatest air movements recorded. By having the air intakes in the shaded streets, the air that is introduced into the building can be cooler than the ambient, with the evident implication of providing greater relief. However, noise and air pollution can be particularly limiting factors for this strategy. These aspects must be addressed in the design options for the atrium.

11.2.4 Estimate of the accuracy of the analytical methods in predicting airflow rates in atrium buildings

In the last part of the study, the estimate of the accuracy of the analytical methods for predicting indoor flows in atria has been studied. These methods are based on the

knowledge of the surface pressure fields measured generally on solid models, (i.e., with no openings), and on the theoretical equations of flow. This study was intended to provide the designer with a tool which would enable him to anticipate the ventilative performances of atrium configurations which were not covered by the present wind tunnel study.

A comparison between measured and calculated flow rates was made. It was found that the air flow rates could be predicted with reasonable accuracy (within ∓10% to ∓15%), provided some conditions are met, and which are;

i) the openings must be evenly distributed within the wall or roof surfaces and there must be no dominant aperture, in particular, in regions close to the flow separation point,
ii) the relative porosity of the walls or roofs should probably not exceed 30%,
iii) the wind incidence to the upwind vented faces must not exceed 45°,
iv) reliable and relevant values of discharge coefficient for the openings and the resistances of internal partitions must be obtained.

The limitations of the computation techniques were identified as being inadequacies of some of the assumptions made in the calculations, and which are as follows;

i) the discharge coefficients are generally assumed to depend solely on the geometry. In actual fact, they could be also affected by the external air velocities. The effects could be particularly large at inclined wind angles, in which case, fast air glances the facades.
ii) It is also assumed that the indoor flow does not disturb the external pressure field measured on a solid building model. In reality, external pressures may be affect by the permeability which establishes a bridge between different pressure fields. This is particularly true for large openings, but also for some critical regions of the flow, such as separation regions, in which case, even small apertures in these sectors can have significant effects.

The analytical methods are believed to be inadequate to predict with enough accuracy the flow in atrium structures for which the roof is used as a very powerful ventilation induction device.

11.2.5 Design guide-lines

The results of the experimental tests are presented in Appendix F under the form of design guide-lines. Appendix G gives an example of the steps to follow in order to evaluate the benefit of natural ventilation in a particular site, and the way in which different design options can be tested.

11.3 Limitations of the study

As with any building aerodynamic study, only sizeable sets of parameters can be investigated. This obviously restrains the range of application of the results. The conclusions presented here are contingent to the range of the geometrical characteristics tested and also to the features of the simulated flow; in particular;

i) the size of the rooms,
ii) the porosity of the walls,
iii) the depth and width of the courtyards and atria,
iv) the shape of the courtyards and atria, (rectangular as opposed to circular, or other forms),
v) the shape of the atrium roofs, in particular their relatively height which can be determinant in urban terrains,
vi) the wind angles chosen,
vii) the simulated atmospheric boundary layer.

Some limitations of the present results are related to the limitations of the wind tunnel analogue. In particular, the wind tunnel technique lacks realism in the fact that wind is considered at fixed angles, whereas in reality the wind direction fluctuates widely with respect to time. Although one way of overcoming this difficulty could be in considering several wind angle increments, nevertheless, it is difficult to extrapolate the conditions at intermediate wind angles in complex cases such as multi-cell models, and also, the time average conditions are difficult to predict.

11.4 Other aspects which must be considered concurrently with the design guide-lines

The design guide-lines presented in Appendix F consider the range of parameters

tested in this study. Nevertheless, there are numerous other factors which might influence the ventilation of buildings, (see Section 3.6.1), from the landscaping and the layout planning to the detail of the openings. An account of these parameters must be made in the building design. A list of relevant references are provided at the end of the chapter (see Table 11.1).

Other considerations which must be made concurrently with natural ventilation are:

i) noise control;
ii) air pollution control;
iii) smoke control in the event of fire;
iv) in the case of atria, where the roof can be used as a powerful suction device, structural implications must be addressed since important lift forces can hamper the stability of the roof, particularly when all its openings are closed during the winter season.

To have extensive moveable roof apertures in an atrium can be costly. Even though they may also be used for smoke control, their cost may not be always justified. It is recommended that a careful analysis of the cost effectiveness of their use for environmental ventilation must be made for each specific project.

11.5 Recommendations for further work

i) Greater ranges of geometries of courtyard and atria are desirable in order to establish with more confidence generalised design rules. In particular, greater courtyard sizes than the range tested here need probably to be tested.

For the atrium structures, tests on oblong shapes and different opening sizes should be a logical extension. For this parametric study, the use of improved computation techniques would probably be the most adequate method to use.

Also, more efficient induction roofs, (or architectural details of some sort which can perform Venturi effects, for example), could also be investigated. It is recommended to study, at the same time, the structural implications due to wind, which were ignored in this study.

ii) For their numerous advantages the computation methods could be invaluable tools for predicting the ventilation performances of buildings, and dealing with

particular cases. Nevertheless, important efforts must be made to improve their accuracy. In particular, they need to be refined to be able to adjust the external pressures measured on solid models to account for the size and location of openings. Also they must account for the change of the working efficiency of the openings caused by lateral external flows.

iii) Full scale measurements of ventilation rates in courtyard and atrium type buildings are very scarce and are strongly recommended as further work. This is because full scale measurements deliver realistic results and are the ultimate reference data for the validation of the predictions with other techniques, such as wind tunnel analogues. In particular, a limitation of the wind tunnel lies in the fact that the wind angle is fixed, whereas, in reality it can fluctuate widely, and the ventilation conditions can be different in the two cases.

iv) Ventilation by stack effect deserves attention, particularly with atria, where it may be a main motive force for ventilation in the case of weak breezes. Stack forces were suggested by some authors to be a viable option for improving thermal comfort by ventilation in atrium buildings during summer seasons in northern latitudes, (see Section 3.4.1). Also, it is interesting to examine the combined effects of wind and stack forces in atria in cases where they are of the same magnitude.

v) There is so far no established criteria on which to judge the potential of natural ventilation as a full climatic/environmental option. In particular, there is no indication of the percentages of time that thermal discomfort is acceptable on a monthly or annual basis, and the limits for which mechanical back-up is required, or for which full air conditioning is indispensable, (see Arens and Watanabe (1986)).

11.6 Conclusion

The subject of this study can be considered in keeping with the topical research effort on bioclimatic architecture as a general theme.

It can be said as a way of concluding this work that it is hoped that this study will contribute in encouraging architects and planners to consider more and more buildings as dynamic envelopes which interact with the local climate, and develop their creativity towards improving low-energy solutions. The recent awareness of global warming, and the fragile politico-economical equilibrium linked with the fossil fuel market, calls more loudly than ever for avoiding energy waste. In this respect, it is hoped that the long-term significance of similar studies will be to reconcile the climate-response

principles in the architectural practice, in an intelligent way, and that bioclimatic architecture will no longer exist a parallel discipline to architecture, as a fashion, or marketing label for projects, as it is often the case nowadays. Instead it will be simply part of basic architectural thinking.

Table 11.1: Relevant references of studies concerned with various aspects of the design involved in wind-driven natural ventilation of buildings.

Site planning	
Town planning	Givoni (1968) Handa (1979) Koenisberger et al (1973)
Landscaping	Olgay (1969) White (1976)
Building design	
Building envelopes	
Wing walls	Aynsley et al (1977)
Pilling	Givoni(1968, 1976)
Window design	
Size, location and orientation to wind	Sobin(1981) Chand (1970), Chand et al (1969) Reed (1953) Givoni (1968, 1976)
Window type	Holleman (1951)
Window accessories (fly-screens, louvres)	Aynsley et al (1977) Givoni (1968, 1976) Koenisberger et al (1974)
Internal partitioning	Givoni (1968,1976) Aynsley et al (1977) Aynsley (1976) Caudill (1952)
Architectural details	
Projections	Caudill et al (1951) Koenisberger et al (1974)
Roof vents	Van Straaten (1967) Yould (1954) Baturin (1972) Fairey et al (1981) Bahadori (1981) Bauman et al (1988) More references in Section 4.4
Roof ventilators	Wannenburg (1957) Yould (1954)

References

Aberg, O., (1989). *Moisture and mould in dwellings in a tropical coastal climate.* Building Issues, Vol. 1, Lund University, Sweden.

Al-Azzawi, S.H., (1969). *Oriental houses in Iraq.* Shelter and Society, edited by P. Oliver , London, Barrie and Rockliff. pp 91-102.

Al-Azzawi, S.H., (1984). *A descriptive, analytical and comparative study of traditional courtyard houses in Baghdad - In the context of urban design in the hot-dry climates of the sub-Tropics.* Ph. D. thesis, Bartlett school of Architecture and Planning, University College, University of London.

Alexander, D.K., Etheridge, D.W., and **Gale, R.,** (1980). *Experimental techniques for ventilation research.* Proceedings 1st AIC Conference Instrumentation and Measuring Techniques, Windsor, Oct. 1980.

Allard, F., and **Herrlin, M.,** (1989). *Wind-induced ventilation.* ASHRAE Transactions Vol. 95, Part 2. pp 722-728

Allen, C., (1984). *Wind pressure data requirements for air infiltration calculations.* Technical Note AIC 13, Air Infiltration Centre, G.B, Jan. 1984.

American Society of Heating, Refrigerating And Air-conditioning Engineers, (1989b). Chapter 23:*Infiltration and ventilation,* ASHRAE Handbook 1989 Fundamentals, Atlanta, GA.

American Society of Heating, Refrigerating And Air-conditioning Engineers, (1989c). Chapter 32: *Duct design.* ASHRAE Handbook 1989 Fundamentals, Atlanta, GA.

American Society of Heating, Refrigerating And Air-conditioning Engineers, (1989a). Chapter 8: *Physiological principles, comfort, and health.* ASHRAE Handbook 1989 Fundamentals, Atlanta, GA.

American Society of Heating, Refrigerating And Air-conditioning Engineers, (1981). *Thermal environmental conditions for human occupancy.* ASHRAE Standard 55-1981, Atlanta, GA.

American Society of Heating, Refrigerating And Air-conditioning Engineers, (1981). *Standard for ventilation required for minimum acceptable indoor air quality.* ASHRAE Standard ANSI-ASHRAE 62-1981, Atlanta, GA.

American Society Of Heating, Refrigerating And Air-conditioning Engineers, (1990). ASHRAE *Handbook 1990 Refrigeration - Systems and Applications,* Atlanta, GA.

Arens, E.A., and **Watanabe, N.S.,** (1986). *A method for designing naturally cooled building using bin climate data.* ASHRAE Transactions, Vol. 92, Part 2B. pp 773-791.

Arens, E.A., Blyholder, A.G., and **Schiller, G.E.,** (1984). *Predicting thermal comfort of people in naturally ventilated buildings.* ASHRAE Transactions, Vol. 90, Part 1B. pp 272-284.

Arya, S.P., (1982). *Atmospheric boundary layers over homogeneous terrain.* Chapter 6 of Engineering Meteorology, Studies in Wind Engineering and Industrial Aerodynamics, Vol. 1, Fundamentals of Meteorology and Their Application to Problems in Environmental and Civil Engineering, Editor E. Plate, Elsevier Scientific Publishing Co..

Aynsley R.M., (1988). *A resistance approach to estimate airflow through buildings with large openings due to wind.* ASHRAE Transactions Vol. 94, Part 2. pp 1661-1669.

Aynsley, R.M, Melbourne, W., and **Vickery, B.J.,** (1977). *Architectural Aerodynamics.* Applied Science Publishers, Architectural Science Series, London.

Aynsley, R.M., (1976). *A study of airflow through and around buildings.* Ph.D. thesis, University of New South Wales, School of Building.

Aynsley, R.M., (1979). *Wind generated natural ventilation of housing for thermal comfort in hot humid climates.* Fifth International Conference on Wind Engineering, Vol. 1, Colorado State University., July 1979. pp 243-254.

Aynsley, R.M., (1985a). *Estimating comfort cooling from natural wind inside buildings using boundary-layer wind tunnels.* ASHRAE Transactions, Vol. 91 Part 2B, Feb. 1985. pp 1748-1760

Aynsley, R.M., (1985b). *Modeling Parameters for Boundary-Layer Wind Tunnel Studies of Natural Ventilation.* Preprint ASHRAE Transactions, Vol. 91, Part 2, HI 85-35.

Bahadori, M.N. and **Haghighat, F.,** (1985). *Passive cooling in hot, arid regions in developing countries by employing domed roofs and reducing the temperature of internal surfaces.* Building and Environment, Vol. 20, No. 2. pp 103-113.

Bahadori, M.N., (1978). *Passive cooling systems in Iranian architecture.* Scientific American, Vol. 238, No. 2, Feb. 1978. pp 144-154.

Bahadori, M.N., (1979). *Natural cooling in hot arid regions.* In Solar Energy Application in Buildings, A.A.M Sayigh (editor), Academic Press.

Bahadori, M.N., (1981). *Pressure coefficients to evaluate air flow pattern in wind towers.* Proceedings of The AS/ISES International Passive and Hybrid Cooling Conference, Miami Beach, Florida, Nov 1981. pp 206-210.

Bahadori, M.N., (1985). *An improved design of wind tower for natural ventilation and passive cooling.* Solar Energy, Vol. 35, No. 2. pp 119-129.

Bailey, A., (1933). *Wind pressure on buildings.* The Institution of Civil Engineers, selected Engineering Papers, No. 139, London.

Baker, N.V., (1983). *Atria and conservatories 3 - Principles of design.* The Architects' Journal, 25 May 1983. pp 67-70.

Baker, N.V., (1984). *The use of passive solar gains for the pre-heating of ventilation air in housing.* Proceedings of The 1st European Solar Energy Conference, Amsterdam, May 1984.

Baker, N.V., (1985). *The use of passive solar gains for the pre-heating of ventilation air.* Report No. ETSU-S-1142, Energy Technology Support Unit, Oxon.

Baker, N.V., (1987). *Passive and low energy building design for tropical island climates.* Commonwealth Secretariat Publications, London.

Baker, N.V., (1988). *The atrium environment.* Building Technical File, No. 21, April 1988. pp 39-48.

Baturin, V.V., (1972). *Fundamentals of Industrial Ventilation.* Pergamon Press.

Bauman, F., Ernest, D., and **Arens, E.,** (1988a). *ASEAN natural ventilation study: Wind pressure distributions on long building rows in urban surroundings.* Centre for Environmental Design Research, University of California, Berkeley, CA.

Bauman, F., Ernest, D., and **Arens, E.,** (1988b). *The effects of surrounding buildings on wind pressure distributions and natural ventilation in long building rows.* ASHRAE Transactions, Vol. 94, Part 2. pp 1670-1695

Bednar, M.J., (1986). *The New Atrium.* Mc Graw-hill, New York, London.

Beranek, W.J., (1979). *General rules for the determination of wind environment.* Proceedings of the fifth International Conference on Wind Engineering, Fort Collins, Co., Vol. 1, edited by J.E., Cermak, Pergamon Press, Oxford, July 1979. pp 225-234.

Beranek, W.J., (1984). *Wind environment around single buildings of rectangular shape and wind environment around building configurations.* Heron Vol. 29, No. 1. pp 2-70.

Bilsborrow, R.E., (1972). *A critical appraisal of previous studies of natural ventilation.* Report No. BS4, Department of Building Science, Faculty of Architectural Studies, University of Sheffield, Dec. 1972.

Bilsborrow, R.E., (1973). *Natural ventilation of buildings.* Ph.D. thesis, Department of Building Science, University of Sheffield, Department of Building Science, Oct. 1973.

Bilsborrow, R.E., and **Fricke F.R.,** (1975). *Model verification of analogue infiltration predictions.* Building Science, Vol. 10. pp 217-230.

Borresen, B.A., and **Madsen, C.N.,** (1990). *Smoke management in large spaces - sizing smoke vents, flow rates and temperatures.* ASHRAE Transactions, Vol. 96, Part 2. pp 701-706.

Bowen, A., (1984). *Design guidelines on vertical airflow in buildings and urban areas.* Passive and Low Energy Ecotechniques, Proceedings of the Third International PLEA Conference, Mexico City, Mexico, 6-11 Aug. 1984, edited by A., Bowen, and S., Yannas, Pergamon Press. pp 178-209.

Boyer L.L., and **Kim, K.S.,** (1988). *Empirically based algorithms for preliminary prediction of daylight performance in toplighted atriums.* ASHRAE Transactions Vol. 94, Part 1. pp 765-782.

Boyer L.L., and **Oh, M.S.,** (1988). *Computer prediction and measurement comparison of daylighting performance in selected atrium buildings using the SERI algorithms.* ASHRAE Transactions Vol. 94, Part 1. pp 799-811.

BRE Digest (1978). *Principles of natural ventilation.* Building Research Establishment Digest No. 210, Garston, Watford, U.K., Feb. 1978.

British Standard, BS 1042: Section 1.1, (1981). *Measurement of Fluid Flow in Closed Circuits.* Part 1 : *Pressure differential devices.* Section 1.1 : *Specification for square-edged orifice plates, nozzles and Venturi tubes inserted in cross-section conduits running full,* BSI 1981, London.

British Standard, BS 1042: Section 1.2, (1984). *Measurement of Fluid Flow in Closed Circuits.* Part 1 : *Pressure differential devices.* Section 1.2 : *Specification for square-edged orifice plates and nozzles (with drain holes, in pipes below 50 mm diameter, as inlet and outlet devices) and other orifice plates and Borda inlets.* BSI 1984, London.

Brundrett, G.W., and **Onions, H.S.,** (1980). *Moulds in the home.* ECRC/M1338, Electricity Council Research Centre, Capenhurst.

Cain, A., Ashfar, F., and **Nortor, J.,** (1975). *Indigenous building and the third world.* Architectural Design, Vol. 45 No. 4, April 1975. pp 207-224.

Caton, P.G.F., (1975). *Standardised maps for hourly mean wind speed over the United Kingdom and some implications regarding wind speed profiles.* Proceedings of The Fourth International Conference on Wind Effects on Buildings and Structures, Heatrow, London, Sept. 1975.

Caudill, W.W, Crites, S.E., and **Smith, E.G.,** (1951). *Some general considerations in the natural ventilation of buildings.* Texas Engineering Experiment Station, College Station, Research Report 22, Feb. 1951.

Caudill, W.W., (1952). *Geometry of classrooms as related to natural lighting and natural ventilation.* Texas Engineering Experiment Station, College Station, Research Report 36, July 1952.

Cermak, E.J., (1971). *Laboratory Simulation of the Atmospheric Boundary Layer.* AIAA Journal, Vol. 9, No. 9 Sept. 1971. pp 1746-1754.

Cermak, E.J., (1974). *Applications of Fluid Mechanics to Wind Engineering.* Presented at the Winter Annual Meeting of the American Society of Mechanical Engineers, ASME, New York, Nov. 1974.

Cermak, E.J., Peterka, J.A., Ayad, S.S., and **Poreh, M.,** (1982). *Wind Tunnel Investigations of Natural Ventilation.* Preprint 82-519 ASCE Convention.

Cermak, E.J., Peterka, J.A., Ayad, S.S., and **Poreh, M.,** (1981). *Passive and Hybrid Cooling Development: Natural Ventilation - A wind Tunnel Study* - FMWEP Report CER81-82JEC24, Oct. 1981.

Cermak, J.E., (1976). *Aerodynamics of buildings.* Annual Review of Fluid Mechanics, Vol. 8. pp 75-105.

Cermak, J.E., (1979). *Applications of wind tunnels to investigation of wind-engineering problems.* AIAA Journal Vol. 17, No. 7, July 1979. pp 679-690.

Chand, I., (1970). *Effect of the distribution of fenestration area on the quantum of natural ventilation of buildings.* Architectural Science Review, Vol. 13 No. 4, Dec. 1970. pp 130-133.

Chand, I., (1972). *prediction of air movement in buildings.* Building Digest No. 100, Central Building Research Institute, Roorkee, India, Sept. 1972.

Chand, I., (1976). *Wind-induced ventilation in shielded buildings.* Ventilation and Air conditioning '76 Conference, Budapest 23-26 March 1976, Paper d19-d38.

Chand, I., and **Krishak, N.,** (1969). *Effect of window size, location and orientation on indoor air motion.* Journal of the Institution of Engineers, India, Vol. 49, No. 9, May 1969. pp 375-378.

Chand, I., Sharma, V.K., and **Krishak, N.L.V.,** (1990). *Studies on the design and performance of wind catchers.* Architectural Science Review, Vol. 33, No. 4, Dec. 1990. pp 93-96.

Chandra, S., (1985). *Passive cooling for residences in hot humid climates. A review of recent research.* FSEC-PF-84/85 - Proceedings US, India Binational Symposium on Solar Energy Research and Applications, Roorkee, India, Hemisphere Press. pp 183-207.

Chandra, S., Fairey, P.W., and **Bowen, A.,** (1982). *Passive cooling by natural ventilation. A literature review.* Report No. FSEC-CR-34-82 (EA), Florida Solar Energy Centre, Cape Canaveral, Florida.

Chandra, S., Fairey, P.W., Kerestecioglu, A.A, and **Kamel, A.A.,** (1986). *Wind tunnel and full-scale data on airflow from natural ventilation and ceiling fans.* ASHRAE Transactions, Vol. 92, Part 2B. pp 804-814.

Chandra, s., Ruberg, K., and **Kerestecioglu, A.,** (1983). *Outdoor testing of small scale naturally ventilated models.* Building and Environment, Vol. 18 No. 1/2. pp 45-53.

Chien, N., Feng, Y., Wang, H.J. and **Siao T.T.,** (1951). *Wind-tunnel studies of pressure distribution on element building forms.* Iowa Institute of Hydraulic research, State University of Iowa, Iowa City.

CIBSE Guide (1986). *Installation and equipment data.* Vol. B, The Chartered Institution of Building Services Engineers, England.

Clayton, C.G., (editor) (1971). *Modern developments in Flow Measurement.* PPL Conference publication 10, Proceedings of the International Conference held at Harwell, 21-23 Sept. 1971, edited by Clayton C.G., Atomic Energy Research Establishment, Harwell, Berks., England, Peter Peregrinus Ltd.

Cockroft, J.P. and **Robertson, P.,** (1975). *The ventilation of deep-plan buildings using lightwells and courtyards.* Report, Building Services Research Unit, University of Glasgow, U.K.

Cook, N.J., (1972). *Wind tunnel simulation of the atmospheric boundary layer methods in current use at Bristol.* Symposium on the external flows, University of Bristol, 4-6th July 1972. pp f1-f5.

Cook, N.J., (1973). *On simulating the lower third of the urban adiabatic boundary layer in a wind tunnel.* Atmospheric Environment. pp 691-705.

Cook, N.J., (1976). *Data for the wind tunnel simulation of the adiabatic atmospheric boundary layer.* Part C, Building Research Establishment Note, N 135/76.

Cook, N.J., (1978). *Determination of the Model Scale Factor in Wind Tunnel Simulations of Adiabatic Atmospheric Boundary Layer.* Journal of Industrial Aerodynamics, Vol. 2, No. 4. pp 311-321.

Counihan, J., (1969). *An improved method of simulating an atmospheric boundary layer in a wind tunnel.* Atmospheric Environment, Vol. 3. pp 197-214.

Counihan, J., (1972). *The structure and the wind tunnel simulation of rural and urban adiabatic boundary layers.* Proceedings of the Symposium on External Flows, Department of Aerodynamic Engineering, University of Bristol.

Counihan, J., (1973). *Simulation of an adiabatic urban boundary layer in a wind tunnel.* Atmospheric Environment, Vol. 7. pp 673-689

Daniels, K., (1983). *Ventilation and air conditioning for atrium buildings. (Luftechnick bei hallenbauten und wintergaten).* In Technick am bau, Nov. 1983. pp 869-874.

Davenport, A.G., (1963). *The relationship of wind structure to wind loading.* Proceedings of the Symposium on Wind Effects on Buildings and Structures, NPL, Paper 2, June 1963.

Davenport, A.G., and **Isyumov, N.**, (1967). *The application of the boundary layer wind tunnel to the prediction of wind loading.* Proceedings of the 2nd International Seminar on Wind Effects on Buildings and Structures, Ottawa 1967, University of Toronto Press.

De Gids, W.F., Phaff, J.C., and **Crommelin, R.D.**, (1987). *The effect of surrounding buildings and fluctuations in wind pressure differences on the ventilation of dwellings.* Report Eur 10877EN. Commission of the European Communities, Energy, Luxembourg.

Degelman, L.O., Molinelli, J.F., and **Kim, K.S.**, (1988). *Integrated daylighting, heating, and cooling model for atriums.* ASHRAE Transactions Vol. 94, Part 1. pp 812-825.

Doubilet, S., (1983). *The decorated climate filtering shed,* Progressive Architecture, April 1983. pp 94-97.

Dunham, D., (1960). *The courtyard house as a temperature regulator.* The New Scientist, 8 Sept. 1960. pp 663-666.

Eaton, K.J., and **Mayne, J.R.**, (1969). *Instrumentation of full-scale wind pressure measurements.* Building Research Station, Current Paper CP 1/69, Feb. 1969.

Eaton, K.J., and **Mayne, J.R.**, (1974). *The measurement of wind pressures on two storey houses at Aylesbury.* Building Research Establishment, Current Paper, CP 70/74, July 1974.

Eaton, K.J., Mayne, J.R., and **Cook, N.J.,** (1976). *Wind loads on low-rise buildings. Effect of the roof geometry.* Building Research Establishment, Current paper CP 1/76, Jan. 1976.

Etheridge, D.W. and **Nolan, J.A.,** (1979). *Ventilation measurements at model scale in a turbulent flow.* Building and Environment, Vol. 14. pp 53-64.

Etheridge, D.W., (1977). *Crack flow equations and scale effect.* Building and Environment, Vol. 12. pp 181-189.

Etheridge, D.W., and **Alexander, D.K.,** (1980). *The British Gas multi-cell model for calculating ventilation.* ASHRAE Transactions, Vol. 86, Part 2. pp 808-821.

Ettouney, S.M., (1973). *Courtyard acoustics and aerodynamics: An investigation of the acoustic and wind environments of courtyard housing.* Ph.D. thesis, University of Sheffield, Department of Building Science, Sept. 1973.

Fackrell, J.E., (1982). *Flow behaviour near isolated rectangular buildings.* Central Electric Generating Board Report TPRD/M/254/N82, available at CEGB, Marchwood Engineering Labs., Marchwood, Southampton U.K.

Fairey, P.W., and **Bettencourt, W.,** (1981). *"La Sucka" - A wind driven augmentation and control device.* Proceedings of The AS/ISES International Conference on Passive and Hybrid Cooling Proceedings, Miami Beach, Florida, Nov. 1981. pp 196-200.

Fardeheb, F., (1987). *Effect of a sloped roof on the radiant cooling capacity of a courtyard house.* Proceedings of the 12th National Passive Solar Conference of the ASES, 12-16 July, Portland, Oregon, USA.

Fathy, H., (1986). *Natural Energy and Vernacular Architecture. Principles and Examples with Reference to Hot Arid Climates.* The University of Chicago Press.

Franck, N., (1963). *Model Law and experimental technique for determination of wind loads on buildings.* Proceedings of The First International Conference on Wind Effects on Buildings and Structures, Teddington, London 1963, HMSO.

Fuller, R., Buckminster, and **Marks, R.,** (1973). *The Dymaxian World of Buckminster Fuller.* Anchor Press, Doubleday, New York.

Gadi, M.B., (1987). *An investigation into the ventilation and thermal performance of contemporary housing in North Africa with special reference to Libya.* M. Phil. thesis, Department of Building Science, University of Sheffield, U.K., April 1987.

Gandemer, J., (1976). *Integration du phenomene vent dans la conception du milieu bati. Guide methodologique et conseils pratiques.* Etude realisee par J. Gandemer et A. Guyot. Paris, Ministere de l'Equipement, Direction de l'Amenagement Foncier et de l'Urbanisme, Direction de la Documentation Francaise, Dec. 1976.

Georgiou, P.N., and **Vickery, B.J.,** (1979). *Wind loads on building frames.* Wind Engineering, Proceeding of Fifth International Conference. pp 421-434.

Gillette, G.L., and **Treado, S.,** (1988). *The daylighting and thermal performance of roof glazing in atrium spaces.* ASHRAE Transactions, Vol. 94, Part 1. pp 826-836.

Givoni, B., (1968). *Ventilation problems in hot countries.* Research Report to the Ford Foundation Building Research Station, Technion, Haifa.

Givoni, B., (1976). *Man , Climate and Architecture.* 2nd Edition (1st ed. 1969, 2nd ed. 1976, Reprint 1981), Architectural science series, Applied Science Publishers Ltd., London.

Givoni, B., and **Berner-Nir, E.,** (1967). *Effect of solar radiation on physiological heat strain in relation to work and clothing.* Research Report to US Public Health Service, Building Research Station, Technion, Haifa.

Gupta, V.K., (1984). *Indigenous architecture and natural cooling.* In energy and Habitat, edited by V., Gupta, John Wiley, New York. pp 41-58.

Haghighat, F., Rao, J., and **Fazio, P.,** (1991). *The influence of turbulent wind on air change rates - a modelling approach.* Building and Environment, Vol. 26 No. 2. pp 95-109

Hancock C.J., (1987). *Lightwell to atrium conversions: A simulated of the thermal effects at the John Radcliffe Hospital.* Proceedings of The ISES Conference (C49), 10 Sept. 1987. UK-ISES, London, pp 6:1-6:16.

Handa, K., (1979). *Wind induced natural ventilation.* Swedish Council of Building Research, Document D10:1979, Stockholm, Sweden.

Hanna, S.R., (1970). *Turbulence and diffusion in the atmospheric boundary layer over urban areas.* Seminar presented at Syracuse University.

Harris, R.I., (1972). *Measurement of wind structure.* Symposium on external flows, Bristol, PPH1, July 1972.

Hawkes, D., (1983). *Air apparent.* The Architects' Journal, 3 Aug. 1983. pp 26-34.

Hawkes, D., (1984). *Energy revisit Gateway Two.* The Architects' Journal, 14 Nov. 1984. pp 72-73.

Hayward, Alan T.J., (1979). *Flowmeters. A Basic Guide and Source Book for Users.* Macmillan, London.

Hinrichs, C.L., (1987). *The courtyard housing form as a traditional dwelling in the Mediterranean region.* Energy and Buildings for Temperate Climates - A Mediterranean Regional Approach. Proceedings of the 6th International PLEA Conference, Porto, Portugal, 27-31 July 1988, edited by E. de Oliveira, Fernandes and S., Yannas, Pergamon Press. pp 53-59.

Hitchin, E. R., and **Wilson, C.B.,** (1967). *A review of experimental techniques for the investigation of natural ventilation in buildings.* Building Science Vol. 2. pp 59-82.

Holdo, A.E., (1982). *Some measurements of the surface pressure fluctuations on wind-tunnel models of a low-rise building.* Journal of Wind Engineering and Industrial Aerodynamics, Vol. 10. pp 361-372.

Holdo, A.E., Houghton, E.L., and **Bhinder, F.E.,** (1983). *Effects of permeability on wind loads on pitched-roof buildings.* Journal of Wind Engineering and Industrial Aerodynamics, Vol. 12. pp 255-279.

Holleman, T.R., (1951). *Airflow through conventional window openings.* Texas Engineering Station, Research Report No 33, Texas A&M College System, College Station, Texas USA.

Holmes, J.D., (1983). *Wind loads on low rise buildings - A review.* Commonwealth Scientific and Industrial Research Organisation, Division of Building Research, Victoria, Australia.

Hopkins, L.P., and **Hansford, B.,** (1974). *Airflow through cracks.* Building Services Engineer, Vol. 42, Sept. 1974.

Hosker, R.P. Jr, (1985). *Flow around isolated structures and building clusters: A review.* ASHRAE Transactions, Vol. 91, Part. 2B. pp 1671-1692.

Humphreys, M.A., (1976). *Desirable temperatures in dwellings.* BRE current paper 75/76, Garston, U.K.

Hunt, C.M., (1978). *Air infiltration : A review of some existing measurement techniques and data.* American Society for testing Machinery, Proceedings of the Symposium on Air Infiltration and Air Change Measurements, Washington DC.

Hussain, M., (1978). *A study of the wind forces on low rise building arrays and their application to natural ventilation design methods.* Ph.D. thesis, University of Sheffield, Department of Building Science, Nov. 1978.

IHVE Guide (1970). *Air infiltration, section A4.* Institution of Heating and Ventilating Engineers, Book A, Design Data, London, 1971.

International Energy Agency, IEA, (1991). *Passive and hybrid solar commercial buildings.* Published by the Renewable Energy Promotion Group, Energy Technology Support Unit, Harwell Laboratory, Oxfordshire, U.K.

Jackman, P.J., (1970). *A study of the natural ventilation of tall office buildings.* Heating and Ventilating Engineer and Journal of Air Conditioning No. 519. pp 183-195.

Jensen, M., (1958). *The Model Law for Phenomena in the Natural Wind.* Ingenioren, Int. Edition, Vol.2, No. 4.

Johansen, F.C., (1930). *Flow Through Pipe Orifices at Low Reynolds Numbers.* Proceedings of the Royal Society of London, A. 126. pp 231-245.

Jones, P.M., Larrinaga, M.A.B., and Wilson, C.B., (1971). *The urban wind velocity profile.* Atmospheric Environment, Vol. 5. pp 89-102.

Kamei, I., (1955). *Studies on natural wind pressure on buildings and other structures.* Report No. 1, Building Research Institute, Ministry of Construction, Japan.

Karakatsanis, C., Bahadori, M.N., and **Vickery, B.J.,** (1986). *Evaluation of pressure coefficients and estimation of air flow rates in buildings employing wind towers,* Solar Energy, Vol. 37, No. 5. pp 363-374.

Karaman, A., and **Egli, H.G.,** (1981). *Vernacular approaches to passive cooling in hot dry climates.* Proceedings of The AS-ISES International Passive and Hybrid Cooling Conference, Miami Beach, Florida, Nov. 1981. pp 3-7.

Kawatani, T., Cermak, J.E., and **Meroney, R.N.,** (1971). *Characteristics of the mean flow over a simulated urban area.* Proceedings of Third International Conference on Wind Effects on Buildings and Structures, Tokyo 1971, Saikon, Co. Ltd., Tokyo. pp 115-124.

Kaye, G.W.C., and **Laby, T.H.,** (1973). *Tables of Physical and Chemical Constants and Some Mathematical Functions.* 14th Edition, (First published in 1911), Longman Group Ltd.

Kim, K.S., and **Boyer L.L.,** (1988). *Daylight prediction and measurement for three-sided multistory atriums under overcast and clear skies.* ASHRAE Transactions Vol. 94, Part 1. pp 783-789.

Kobayashi, N., and **Ohba, M.,** (1987). *Wind effects designing ventilation flow rate of large spaces with many openings.* Journal of Wind Engineering and Industrial Aerodynamics. Vol. 29. pp 283-292.

Koenigsberger, O.H., Ingersoll, T.G., Mayhew, A., and **Szokolay, S.V.,** (1973). *Manual of Tropical Housing and Building. Part 1: Climatic Design.* Longman Group Ltd., London.

Krishnakumar, C.K., Fields, S.F., Henninger, R.H., and **Bettge, D.A.,** (1982). *Evaluating wind ventilation in buildings by wind tunnel tests.* ASHRAE Transactions Vol. 88, Part. 1. pp 227-230.

Kula, H.G., and **Feustel, H.E.,** (1988). *Review of the wind pressure distribution as input data for infiltration models.* LBL-23886, Lawrence Berkeley Laboratories, University of California, Dec. 1988.

Lahav, R., Rigg, T., and **Warshaw, L.,** (1987). *Passive design for a large commercial building: Luz Industries Headquarters, Jerusalem.* Proceedings of the European Conference on Architecture, 6-10 April 1987, Munich. pp 204-209.

Lam, W.M.C., (1986) *Sunlighting As Formgiver For Architecture.* Van Nostrand Reinhold Company, New York.

Lawson, T.V., (1980). *Wind Effects on Buildings. Vol. 1: Design Applications.* Applied Science Publishers Ltd, London.

Lee, B.E., (1977). *The simulation of atmospheric boundary layers in the Sheffield University 1.2x1.2m boundary layer wind tunnel.* BS 38 Report, Department of Building Science, Faculty of Architectural Studies, University of Sheffield, July 1977.

Lehmberg, W.H., Brandt, A.D., and **Morse, K.,** (1935). *A laboratory study of minimum ventilation requirements: Ventilation box experiments.* ASHVE Transactions, Vol. 41. pp 157-164.

Leung S.K. et al (1981). *Thermally induced ventilation applications in atria - State-of-the art report.* California, Eureka Labs. Inc., Sacramento, CA.

Lezine, A., (1971). *La protection contre la chaleur dans l'architecture musulmane d'Egypte.* Bulletin d'Etudes Orientales, Vol. 124, Damascus, Syria.

Liddament, M., and **Thompson, C.,** (1982). *Mathematical models of air infiltration. A brief review and bibliography.* Technical Note AIC 9, The Air Infiltration Centre, Bracknell, England.

Liddament, M.W., (1986). *Air infiltration calculation Techniques. An application guide.* Air Infiltration and Ventilation Centre, England, June 1986.

Linden, P.F., and **Lane-Serff, G.F.,** (1989). *Simulation of natural ventilation in buildings by means of fluid flows applied to the case of Crown and County Courts.* Proceedings of the 2nd European Conference on Architecture, 4-8 Dec. 1989, Paris. pp 138-142.

MacCormac, R., (1973). *Housing form and land use: New research.* RIBA Journal, Nov. 1973. pp 549-551.

MacCormac, R., Van der Ryn, S., and **Law, M.,** (1983). *Daylit delight.* The Architects' Journal, 3 Aug. 1983. pp 13-15.

Malinowski, H.K., (1971). *Wind effect on the air movement inside buildings.* Proceedings of Third International Conference on Wind Effects on Buildings and Structures, Tokyo 1971, Saikon, Co., Ltd., Tokyo. pp 115-124.

Martin, L., and **March, L.,** (1966). *Land use and built forms.* Cambridge Research.

Mattingly, G.E, Harrje, D.T., and **Heisler, G.M.,** (1979). *The effectiveness of an evergreen windbreak for reducing residential energy consumption.* ASHRAE Transactions Vol. 85, Part 2. pp 428-444.

Melbourne, W.H., (1982). *Wind Tunnel Blockage Effects and Corrections.* Wind Tunnel Modelling for Civil Engineering Applications, Proceedings of the International Workshop on Wind Tunnel Modelling Criteria and Techniques in Civil Engineering Applications, Gaithersburg, Maryland, USA. Edited by T.A., Reinhold, Cambridge, April 1982.

Meroney, R.N., (1982). *Turbulent diffusion near buildings.* Chapt. 11 of Engineering Meteorology, Studies in Wind Engineering and Industrial Aerodynamics, Vol. 1, Fundamentals of Meteorology and Their Application to Problems in Environmental and Civil Engineering, edited by E., Plate, Elsevier Scientific Publishing Co.

Merzkirch, W., (1987). *Flow visualization.* 2nd Edition. Academic Press, Inc., London.

Meyer, B., (1983). *Indoor air quality.* Addison-Wesley Publishing Company, Inc.

Meyers, A.C., and **Way, G.E.,** (1981). *Passive solar cooling in hot humid climates: A review of applications.* Proceedings of The AS/ISES International Conference on Passive and Hybrid Cooling, Miami Beach, Florida, Nov. 1981. pp 61-65.

Mills, F., (1990). *Environmental design of atrium buildings in the U.K.* ASHRAE Transactions, Vol. 96, Part 1. pp 14-22.

Mimar (1985). Mimar, Vol. 16, Apr-June 1985. pp 20-27.

Mohsen, M.A., (1979a). *Solar radiation and courtyard house forms-I: a mathematical model.* Building and Environment, Vol. 14. pp 89-106.

Mohsen, M.A., (1979b). *Solar radiation and courtyard house forms-II: application of the model.* Building and Environment, Vol. 14. pp 185-201.

Murphy, J., (1981). *State intentions.* Progressive Architecture Aug. 1981. pp 76-81.

Newberry, C.W., and **Eaton, K.J.,** (1974). *Wind loading handbook.* Building Research Establishment Report.

Olgay, V., (1969). *Design With Climate. Bioclimatic Approach To Architectural Regionalism.* Princeton University Press, Princeton, New Jersey, USA.

Ower, E., and **Pankhurst, R.C.,** (1977). *The Measurement of Air Flow.* 5th edition, (1st Edition 1927), Pergamon, Oxford.

Pankhurst, R.C., and **Holder, D.W.,** (1952). *Wind-tunnel Technique. An Account of Experimental Methods in Low- and High-speed Wind Tunnels.* Pitman Publishing Co.

Parnell, A., and **Butcher, G.,** (1984). *Smoke control.* Building Services Vol. 6, No. 6. pp 65-70.

Pitts, A. C., and **Ward, I. C.,** (1983). *A review of the prediction and investigation of air movement in buildings.* Internal Report BS 69, Department of Building Science, University of Sheffield, U.K., March 1983.

Pitts, A., (1985). *Air movement and energy flows in an air-conditioned and partitioned industrial environment.* Ph.D. thesis, University of Sheffield, Department of Building Science, May 1985.

Plate, E.J., (1982). *Wind tunnel modelling of wind effects in engineering.* Chapter 13, Engineering Meteorology, Fundamentals of Meteorology and their Application to Problems in Environmental and Civil Engineering, edited by E.J., Plate, Elsevier Scientific Publishing Co. pp 573-639.

Plate, E.J., and **Cermak, J.E.,** (1963). *Micro-meteorological wind-tunnel facility.* Technical Report CER63EJP-JEC9, Fluid Dynamics and Diffusion Laboratories, Colorado State University, Fort Collins, Colorado.

Poreh, M., and **Hassid, S.,** (1982). *Simulation of Buoyancy and Wind Induced Ventilation.* Wind Tunnel Modelling for Civil Engineering Applications, Proceedings of the International Workshop on Wind Tunnel Modelling Criteria and Techniques in Civil Engineering Applications, Gaithersburg, Maryland, USA, edited by T.A., Reinhold, Cambridge. April 1982.

Rapoport, A., (1969). *House form and culture.* Prentice Hall, Englewood Cliff, New Jersey.

Reed, R.H., (1953). *Design for natural ventilation in hot humid weather.* Reprint from housing and building in hot-humid and hot-dry climates, Building Research Institute, National Research Council, Washington DC.

Robbins, C.L., (1986). *Daylighting Design and Analysis.* Van Nostrand Company, New York.

Rohles, F.H., Konzs, S.A., and **Jones, B.W.,** (1983). *Ceiling fans as extenders of the summer comfort envelope.* ASHRAE Transactions Vol. 89, Part 1. pp 245-263.

Rydberg, J., (unknown). Building Research Station Library communication 401.

Sadeh, W.Z., Cermak, J.E., and **Kawatani, T.,** (1971). *Flow over high roughness elements.* Boundary-Layer Meteorology, Vol. 1. pp 321-344.

Saini, B.S., (1984). *Climate shelter and settlement.* Passive and Low Energy Ecotechniques. Proceedings of the Third International PLEA Conference, Mexico City, Mexico, 6-11 Aug. 1984, edited by A., Bowen and S., Yannas, Pergamon Press. pp 29-44.

Saxon, R., (1986). *Atrium Buildings - Development and Design.* 2nd edition (1st edition 1983). The Architectural Press, London.

Scheatzle, D.G., Wu, H., and **Yellott, J.,** (1989). *Extending the summer comfort envelope with ceiling fans in hot, arid climates.* ASHRAE Transactions Vol. 95, Part 1. pp 269-280.

Schofield, W.H., Perry, A.E., and **Joubert, P.N.,** (1974). *Pressure distributions in slot type rough walls under turbulent boundary layers.* Australian Department of Supply Report, ARL/M.E.-TN 345.

Scott, D.R., (1961). *Simulation of ventilation problems.* Journal Institute Heating Ventilation Engineers Vol. 29, June 1961. pp 95-101.

Shaw, C.Y., (1980). *Wind and temperature induced pressure differentials and an equivalent pressure difference model for predicting air infiltration in schools.* ASHRAE Transactions, Vol. 86, Part 1. pp 268-279.

Shaw, C.Y., Sander, D.M., and Tamura, G.T., (1973). *Air leakage measurements of the exterior walls of tall buildings.* ASHRAE transactions, Vol. 79, Pt 2.

Shellard, H.C., (1963). *The estimation of design wind speeds.* Proceedings of the Symposium on Wind Effects on Buildings and Structures, NPL, Paper 1, June 1963.

Sherman, M., Grimsrud, D.T., Condon, P.E., and **Smith, B.V.,** (1980). *Air infiltration measurement techniques.* Proceedings of 1st AIC Conference, Air Infiltration Instrumentation and Measurement Techniques. Windsor, U.K.

Sherman, M.H., and **Grimsrud, D.T.,** (1982). *Wind and infiltration interaction for small buildings.* Report LBL 13949, Lawrence Berkeley Laboratory, California, USA, Oct. 1982.

Shiotani, M., (1962). *The relation between wind profiles and the stability of the air layer in the outskirts of the city*. Journal of Meteorological Society of Japan, Series II, Vol. 40 Part. 6. pp 315.

Sieden, F.S., (1989). *Buckminster Fuller's Universe - An Appreciation*. Plenum Press.

Smith, E.G., (1951). *The Feasibility of Using Models for Predicting Natural Ventilation*. Research Report No. 26, Texas Engineering Experiment Station, June 1951.

Snyckers, W.A., (1970). *Wind tunnel studies of the flow of air through rectangular openings with application to natural ventilation of buildings*. Msc thesis in Engineering, University of Pretoria, Dec. 1970.

Sobin, H.J., (1981). *Window design for passive ventilative cooling: An experimental model-scale study*. Proceedings of The AS/ISES International Passive/Hybrid Cooling Conference, Miami Beach, Florida, Nov. 1981. pp 191-195.

Soliman, B.F., (1976). *A study of the wind pressure forces acting on groups of buildings*. Ph.D. thesis, University of Sheffield, Department of Building Science, Oct. 1976.

Storllery, R., (1986). *Design in isolation*. Building supplement, 2 May 1986. pp 4-5.

Surry, D., and **Isyumov, N.,** (1975). *Model studies of wind effects. A perspective on the problems of experimental technique and instrumentation*. Proceedings of the 6th International Congress on Instrumentation in Aerospace Simulation Facilities, Ottawa, Canada, Sept. 1975.

Swami, M.V., and **Chandra, S.,** (1988). *Correlations for pressure distribution on buildings and calculation of natural ventilation airflow*. ASHRAE Transactions, Vol. 94, Part 1. pp 243-266

Szokolay, S.V., (1980). *Environmental Science Handbook for Architects and Builders*. The Construction Press Ltd., England.

Tamura, G.T., and **Wilson, A.G.,** (1967). *Pressure differences caused by chimney effect in three high buildings*. ASHRAE Transactions, Vol. 73, Part 2. (Paper 2046).

Tani, I., Iuchi, M., and **Komoda, H.,** (1961). *Experimental investigation of flow associated with a step or a groove*. Report No. 364, Aeronautical Research Institute, Vol. 27, No. 4, University of Tokyo.

Tieleman, H.W., Akins, R.E., and **Sparks, P.R.,** (1980). *A comparison of wind-tunnel and full-scale wind pressure measurements on low-rise structures*. Proceedings of The 4th Colloquium on Industrial Aerodynamics, Aachen, 19-20 June .

Torrance, V.B., (1966). *A critical investigation of shelter and wind effects on building with patios.* Msc thesis, Heriot Watt University.

Torrance, V.B., (1972). *Wind profiles over a suburban site, and wind effects on half full-scale model building.* Building Science, Vol. 7. pp 1-12.

Trollope, M., Seager, A., Palmer, J., Watkins, R., and **Shaw, P.,** (1991). *IEA XI advanced case study: Gateway 2.* Passive and Hybrid solar commercial buildings, advanced case studies seminar, International Energy Agency Solar Heating and Cooling - Task XI, published by The Renewable Energy Promotion Department, Harwell Laboratory, U.K, April 1991. pp 213-236.

Van Straaten, J.F., (1967). *Thermal Performance of Buildings.* Elsevier publishing Co., Amsterdam.

Vickery, B.J., (1981). *The use of wind tunnel in the analysis of naturally ventilated structures.* Proceedings of The AS/ISES International Conference on Passive and Hybrid Cooling, Miami Beach, Florida, Nov. 1981. pp 728-742.

Vickery, B.J., and **Karakatsanis, C.,** (1987). *External wind pressure distributions and induced internal ventilation flow in low-rise industrial and domestic structures.* ASHRAE Transactions Vol. 93, Part 2. pp 2198-2211.

Vickery, B.J., Baddour, R.E., and **Karakatsanis C.A.,** (1983). *A study of the external wind pressure distributions and induced internal ventilation flow in low-rise industrial and domestic structures.* Boundary layer Wind Tunnel Laboratory, The University of Western Ontario, Faculty of Engineering Science, London, Ontario, Canada, BLWT-SS2-1983.

Vincent, N.D.G., and **Bailey, A.,** (1943). *Wind pressure on buildings including effects of adjacent buildings.* Journal of the Institution of Civil Engineers, Vol. 20 No. 8, Paper No. 5367. pp 243-275.

Walton, G.N., (1984). *A computer algorithm for predicting infiltration and interroom airflows.* ASHRAE Transactions, Vol. 90, Part 1. pp 601-610

Walton, G.N., (1989). *Airflow network models for element-based building airflow modeling.* ASHRAE Transactions, Vol. 95, Part 2. pp 611-620

Wannenburg, J.J., (1957). *Performance testing of roof ventilators.* South African Council for Scientific and Industrial Research, Pretoria, Republic of South Africa, Transactions of the American Society of Heating and Air Conditioning Engineers, Annual Meeting, Quebec, Canada, June 1957.

Wardlaw, R.I., (1972). *Wind tunnel investigations in industrial aerodynamics.* Canadian Aeronautic and Space Journal, Vol. 18. pp 53-59.

Watson, D., (1982). *The energy within the space within.* Progressive Architecture, July 1982. pp 97-102.

Watson, D., (1984). *Energy-efficient atrium design.* Passive and Low Energy Ecotechniques, Proceedings of the 3rd International PLEA Conference, Mexico City, Mexico 6-11 August 1984, edited by Bowen and Yannas, Pergamon Press. pp 172-177.

Weston, E.T, (1954). *Natural ventilation in industrial-type buildings.* Special report No. 14, Commonwealth Experimental Building Station, Sydney, Feb 1954.

Weston, E.T, (1956). *Air movement in industrial buildings: Effect of nearby buildings.* Special report No. 19, Commonwealth Experimental Building Station, Sydney.

White, R.F., (1976). *Effects of landscape development on the natural ventilation of buildings and their adjacent areas.* Texas Engineering Experiment Station, College Station, Research Report 45, (first published in March. 1954).

Wiren, B.G., (1985). *Effect of surrounding buildings on wind pressure distribution and ventilation heat losses for single-family houses. Part 1: 1 1/2-storey detached houses.* The National Swedish Institute for Building Research, Gavle, Sweden, Report No. M85:19.

Wiren, B.G., (1987). *Effects of surrounding buildings on wind pressure distribution and ventilation heat losses for single-family houses. Part 2: 2-storey terrace houses.* The National Swedish Institute for Building Research, Gavle, Sweden, March 1987.

Yaglou, C.P., (1955). *Ventilation requirements for cigarette smoke* . ASHVE Transactions, Vol. 61. pp 25-32.

Yaglou, C.P., and **Witheridge, W.N.,** (1937). *Ventilation requirements.* ASHVE Transactions, Vol. 43, Part 2. pp 432-436

Yaglou, C.P., Riley, E.C., and **Coggins, D.I.,** (1936). *Ventilation requirements.* ASHVE Transactions Vol. 42. pp 133-162

Yarwood, D., (185). *Encyclopaedia of Architecture.* B.T., Batsford Ltd., London.

Yould, E., (1954). *Natural ventilation.* IHVE Journal, Jan. 1954.

Appendices

A1-A15: Surface pressure contours on walls and roofs of atrium models.

B1-B3: Internal flow coefficients for unsheltered courtyard buildings.

C1-C3: Internal flow coefficients for unsheltered atrium buildings.

D1-D8: Internal flow coefficients for courtyard and atrium buildings in congested urban sites.

E1-E2: Estimate of the change of flow rates with change of the room aperture area.

F1-F5: Design-guidelines for wind-driven natural ventilation in courtyard and atrium buildings.

G1-G9: A stepwise method for estimating the natural ventilation cooling potential of courtyard and atrium buildings in a particular site.

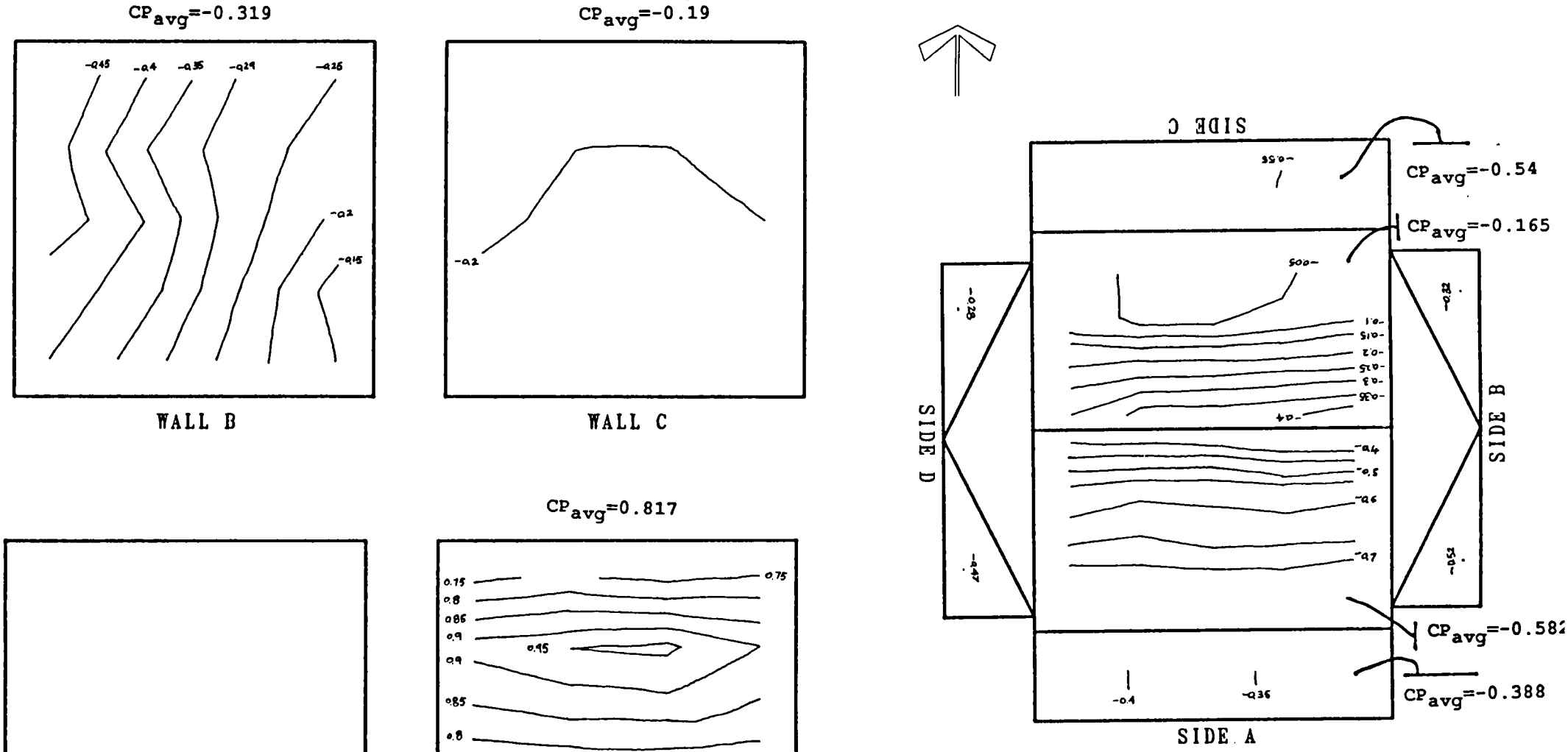

Surface pressure contours on atrium model surfaces.

A 1- **Butterfly roof** (0° wind incidence)

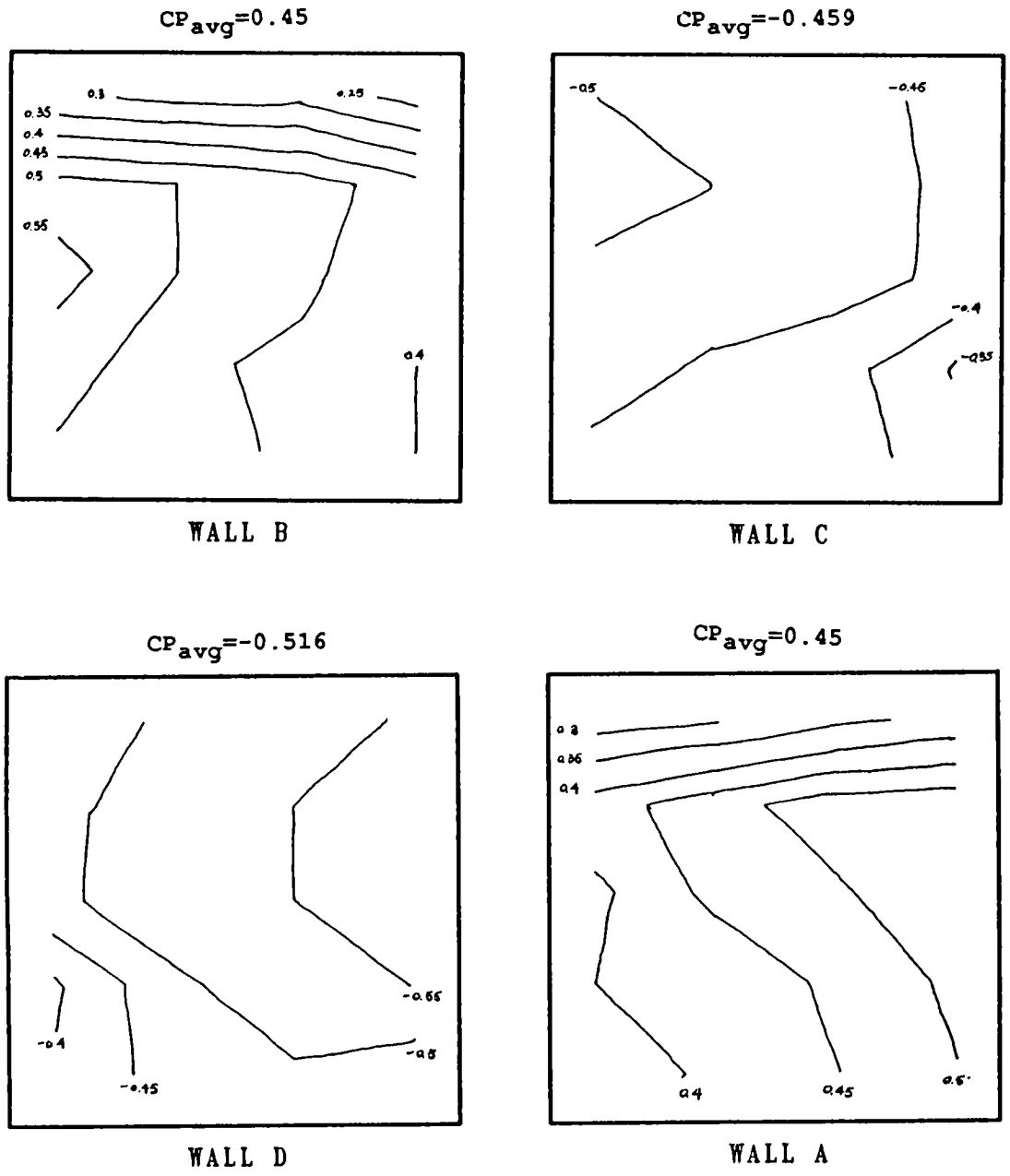

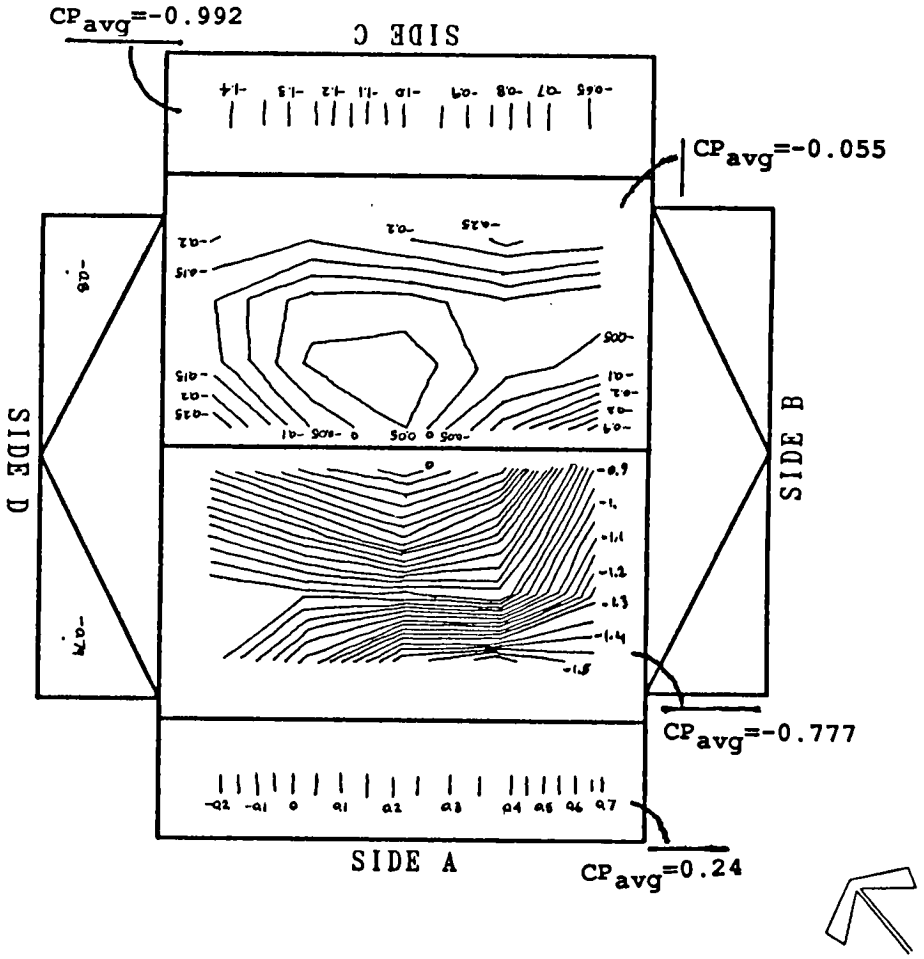

Surface pressure contours on atrium model surfaces.

A 2- **Butterfly roof** (45° wind incidence)

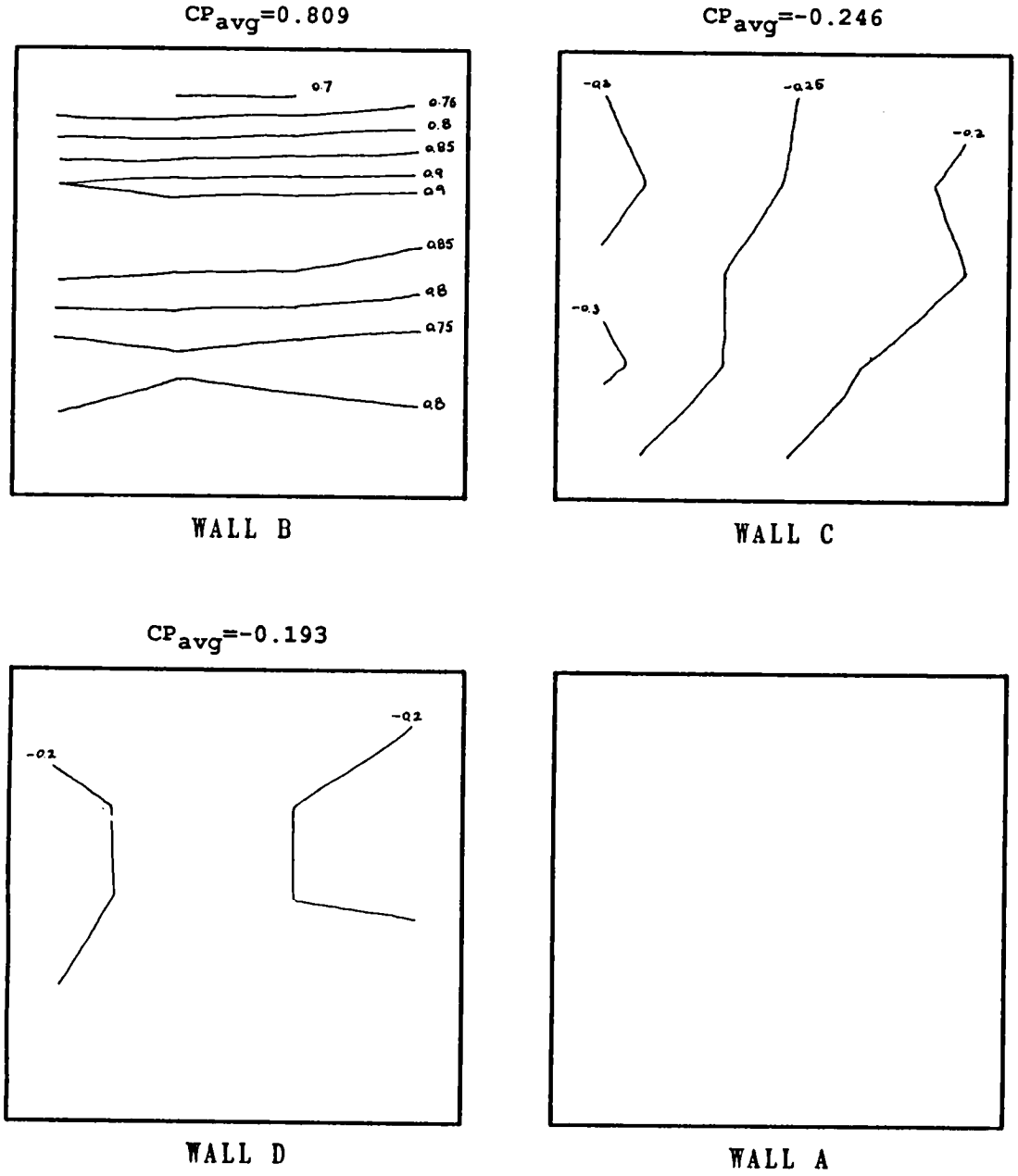

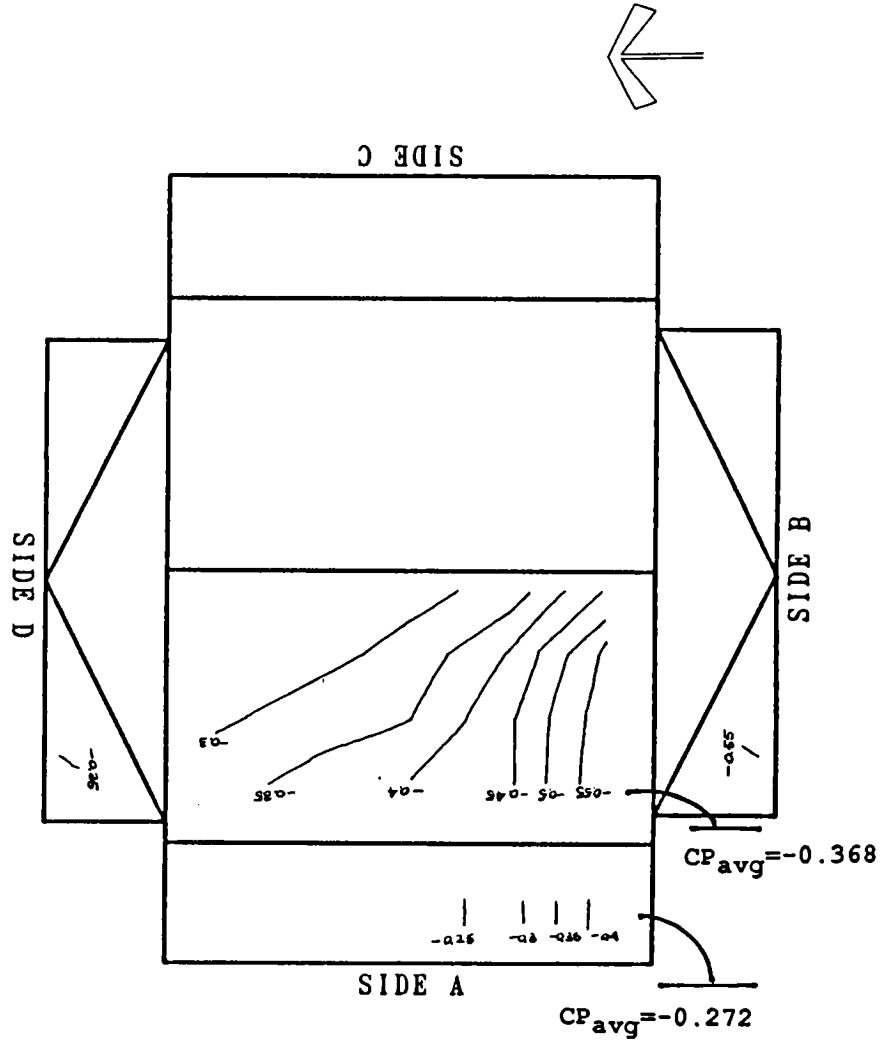

Surface pressure contours on atrium model surfaces.

A 3- **Butterfly roof** (90° wind incidence)

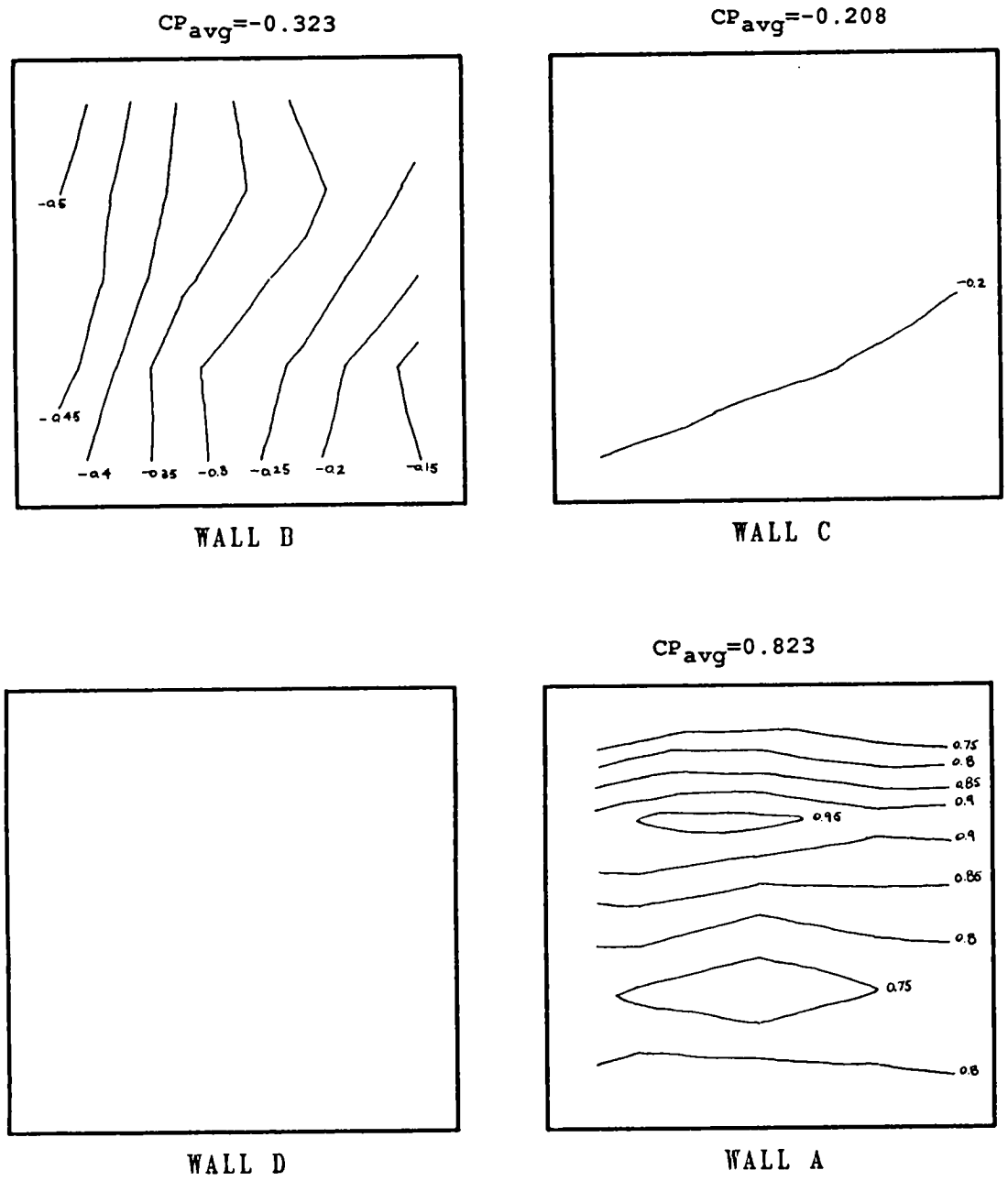

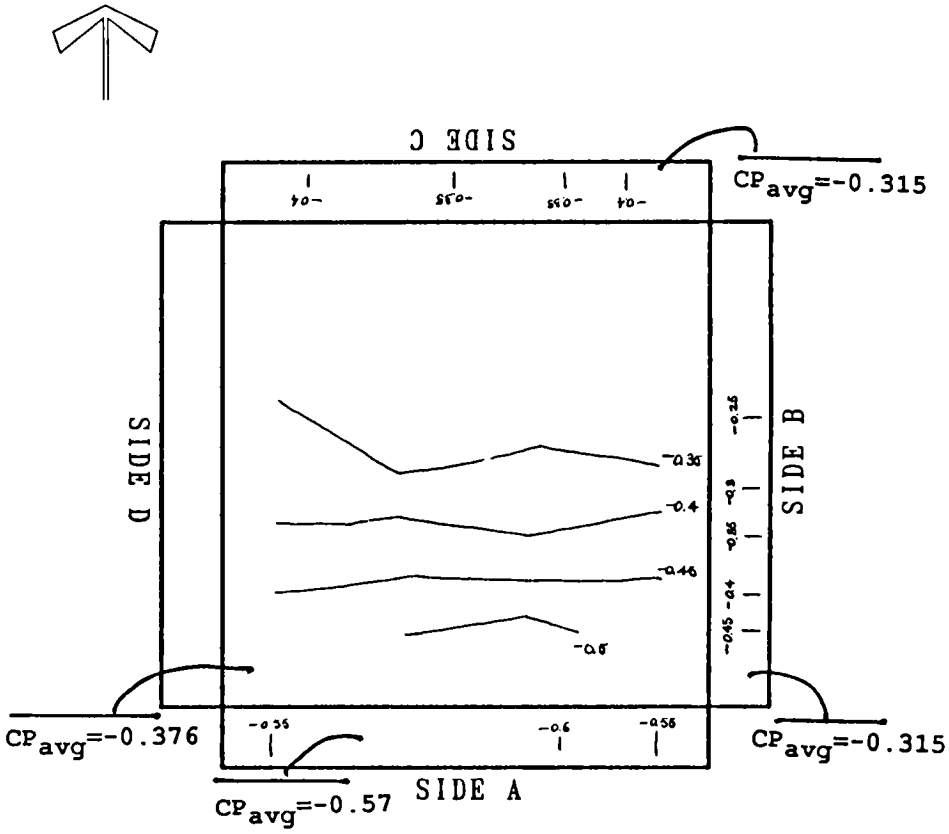

Surface pressure contours on atrium model surfaces.

A 4- **Monitor roof** (0° wind incidence)

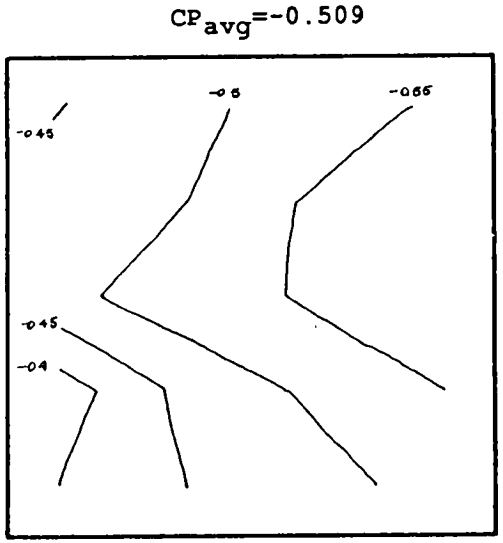

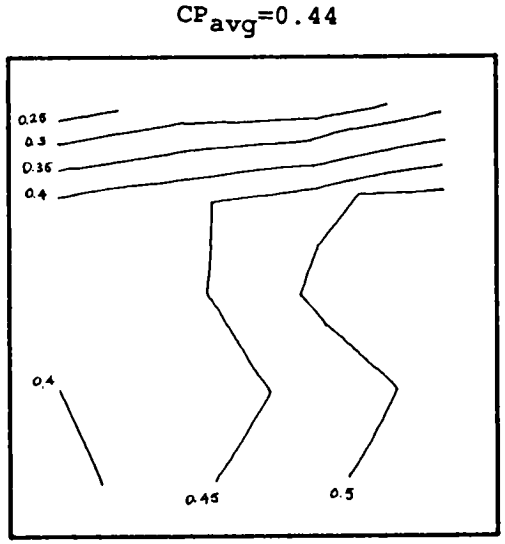

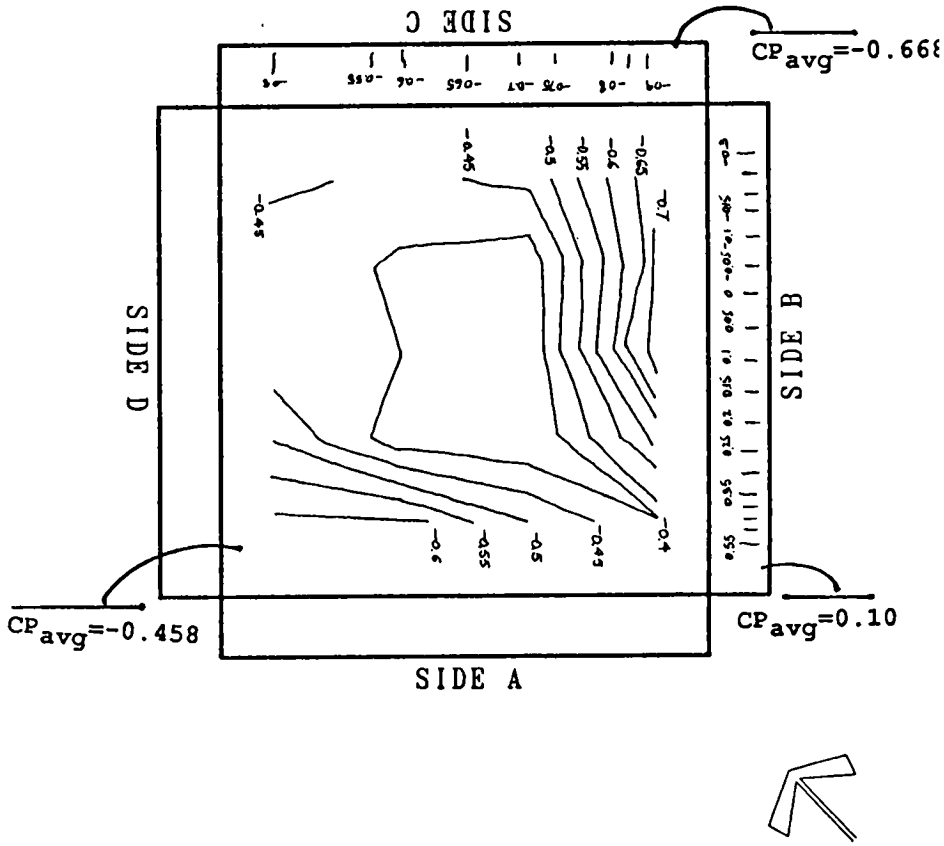

Surface pressure contours on atrium model surfaces.

A 5- **Monitor roof** (45° wind incidence)

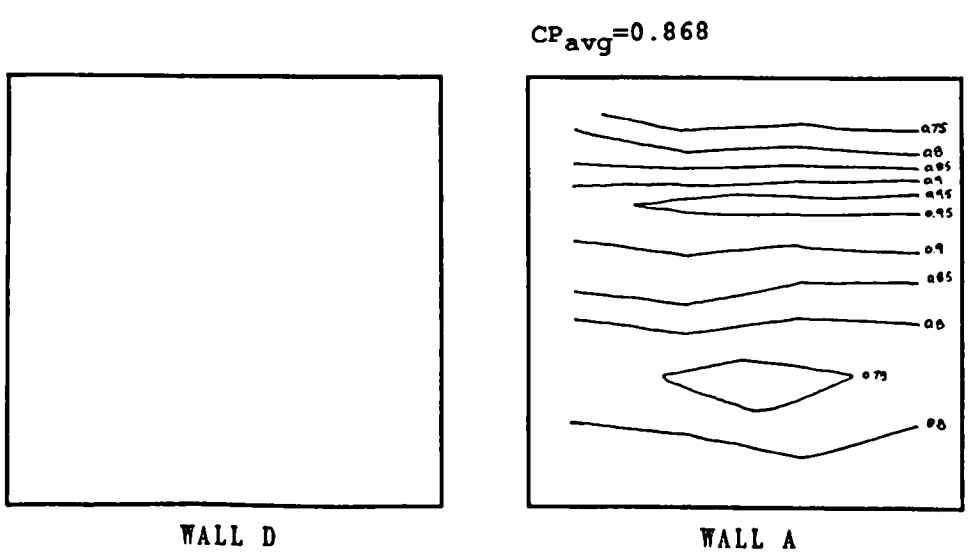

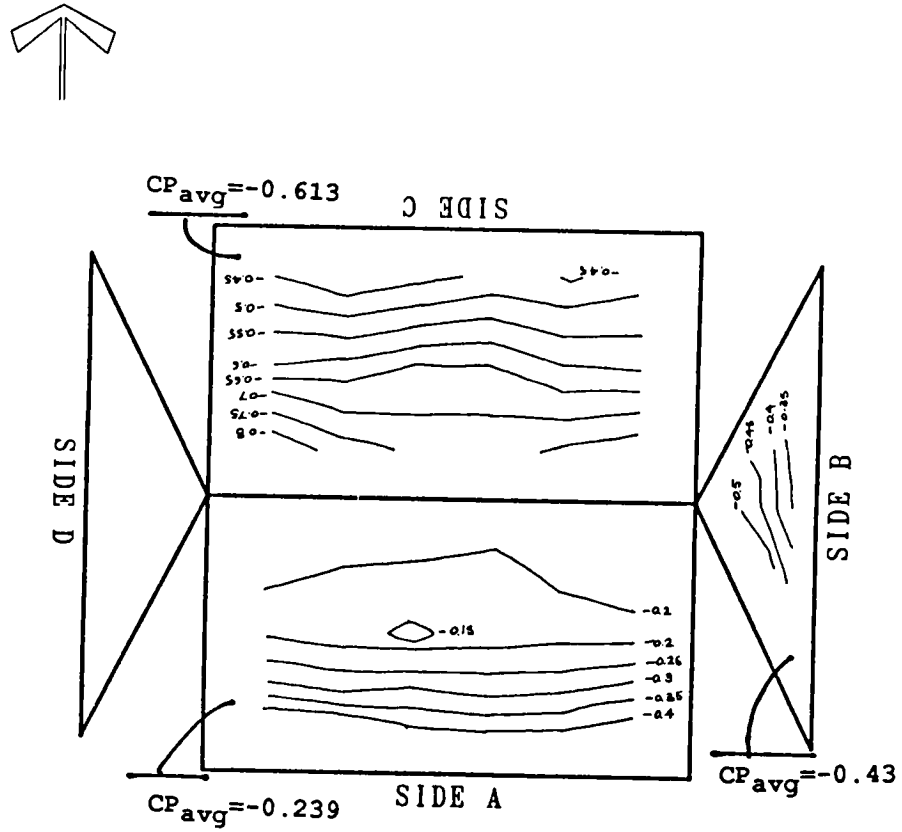

Surface pressure contours on atrium model surfaces.

A 6- **Pitched roof** (0° wind incidence)

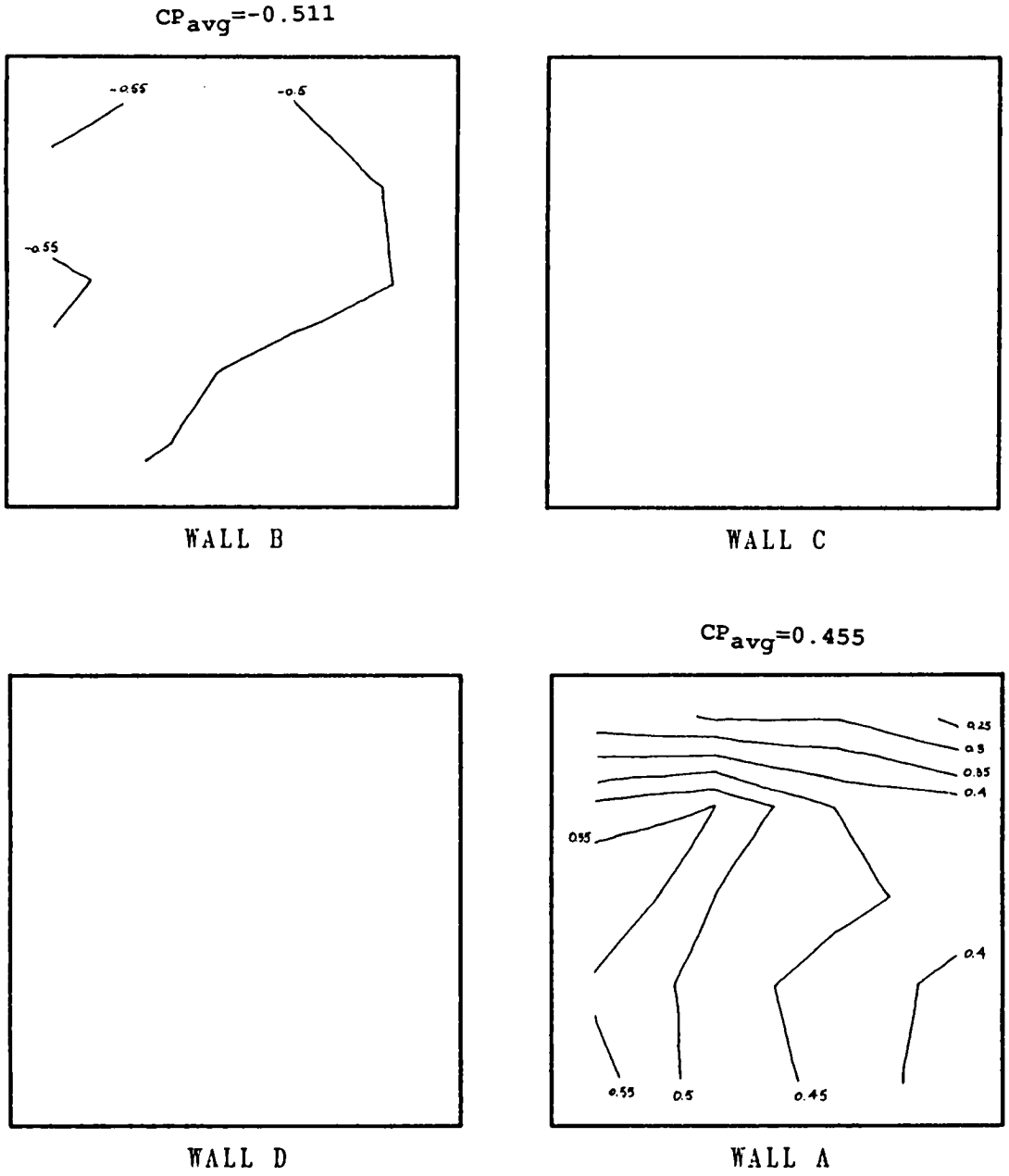

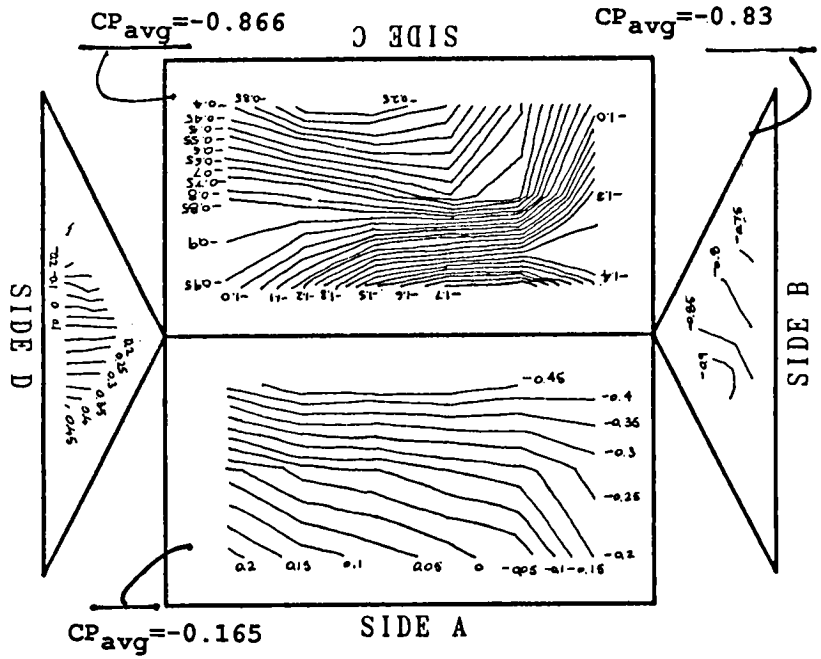

Surface pressure contours on atrium model surfaces.

A 7- **Pitched roof** (45° wind incidence)

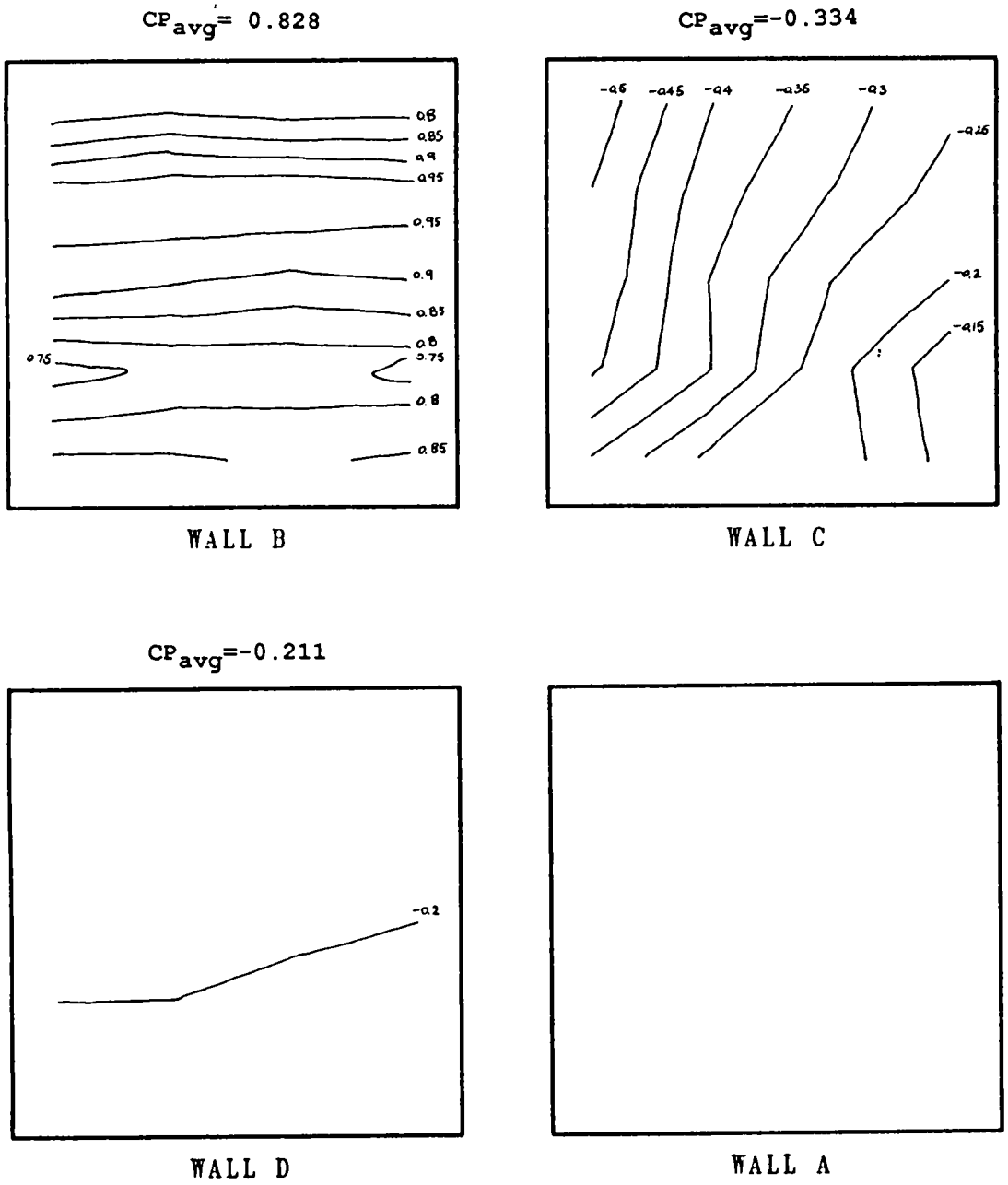

Surface pressure contours on atrium model surfaces.

A 8- **Pitched roof** (90° wind incidence)

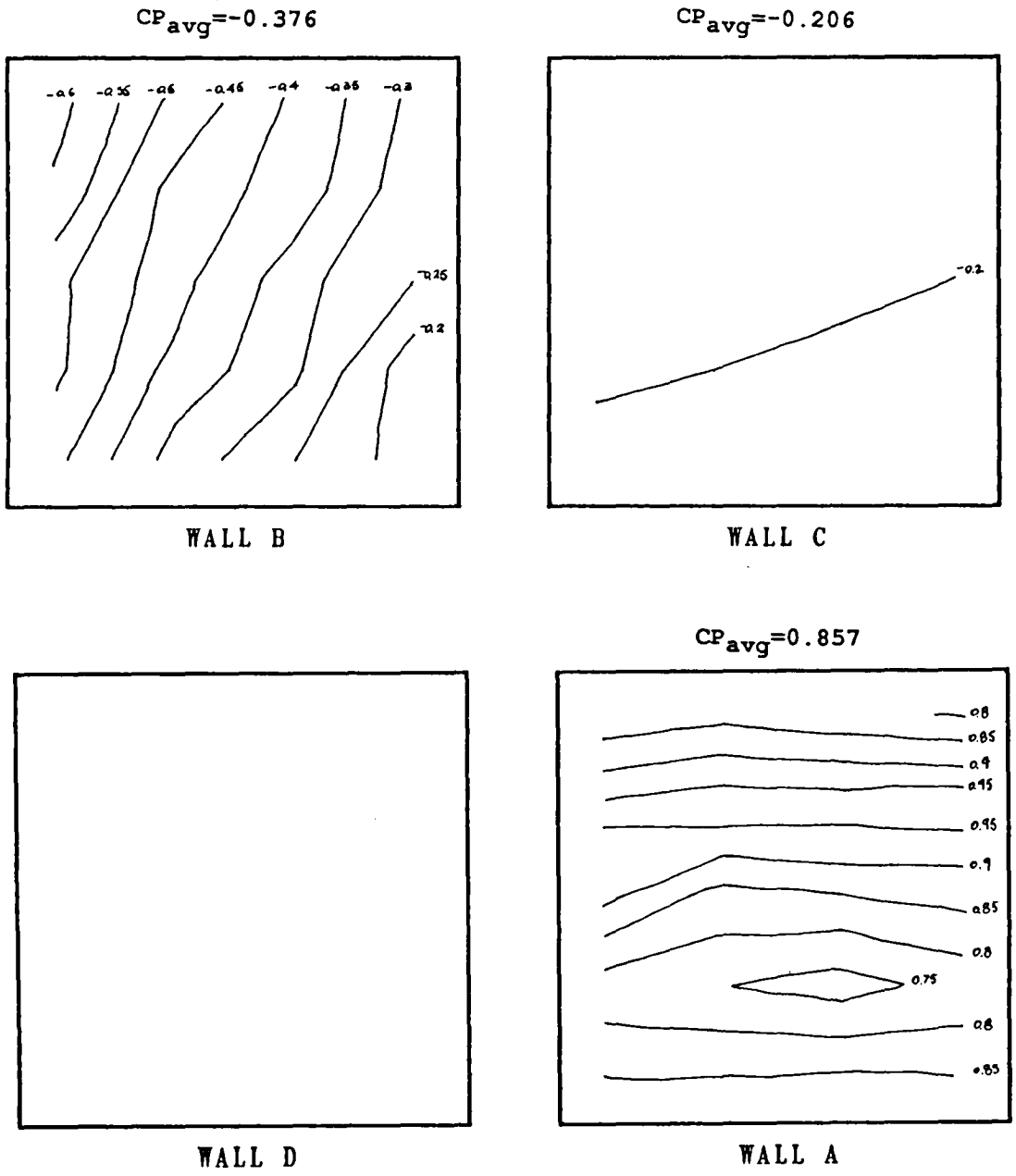

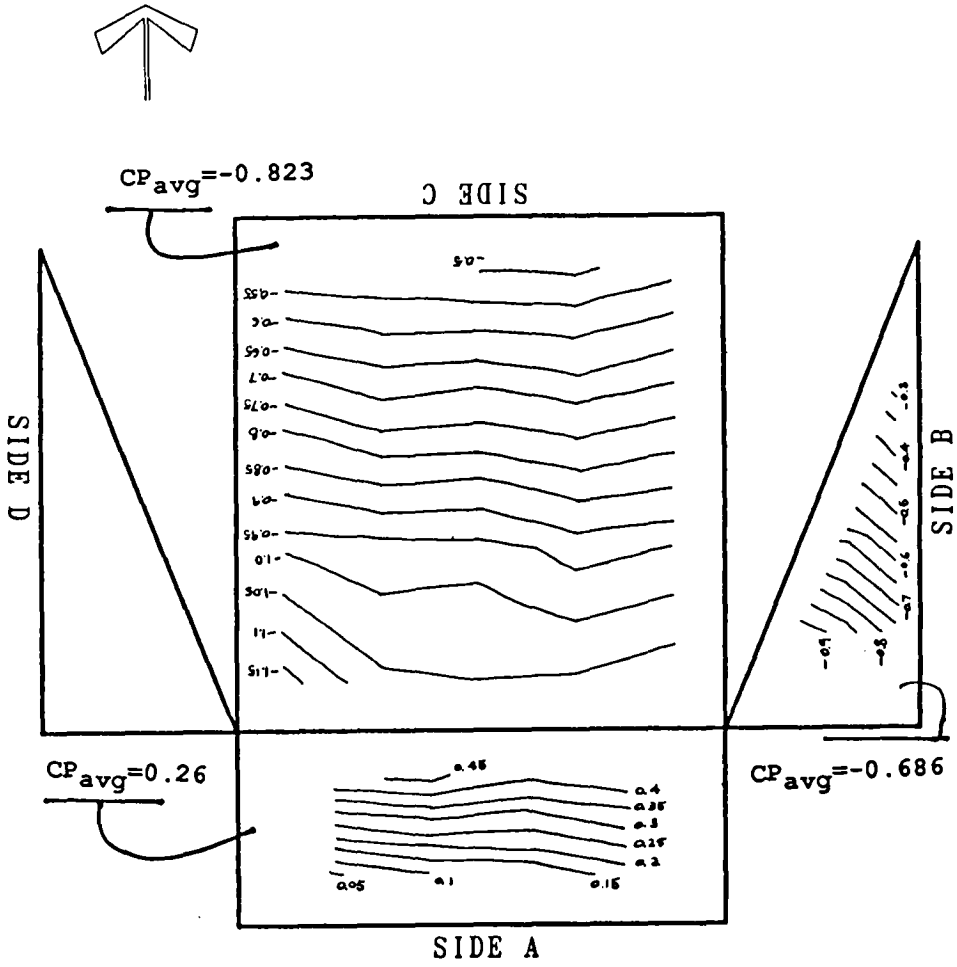

Surface pressure contours on atrium model surfaces.

A 9- **Monopitched roof** (0° wind incidence)

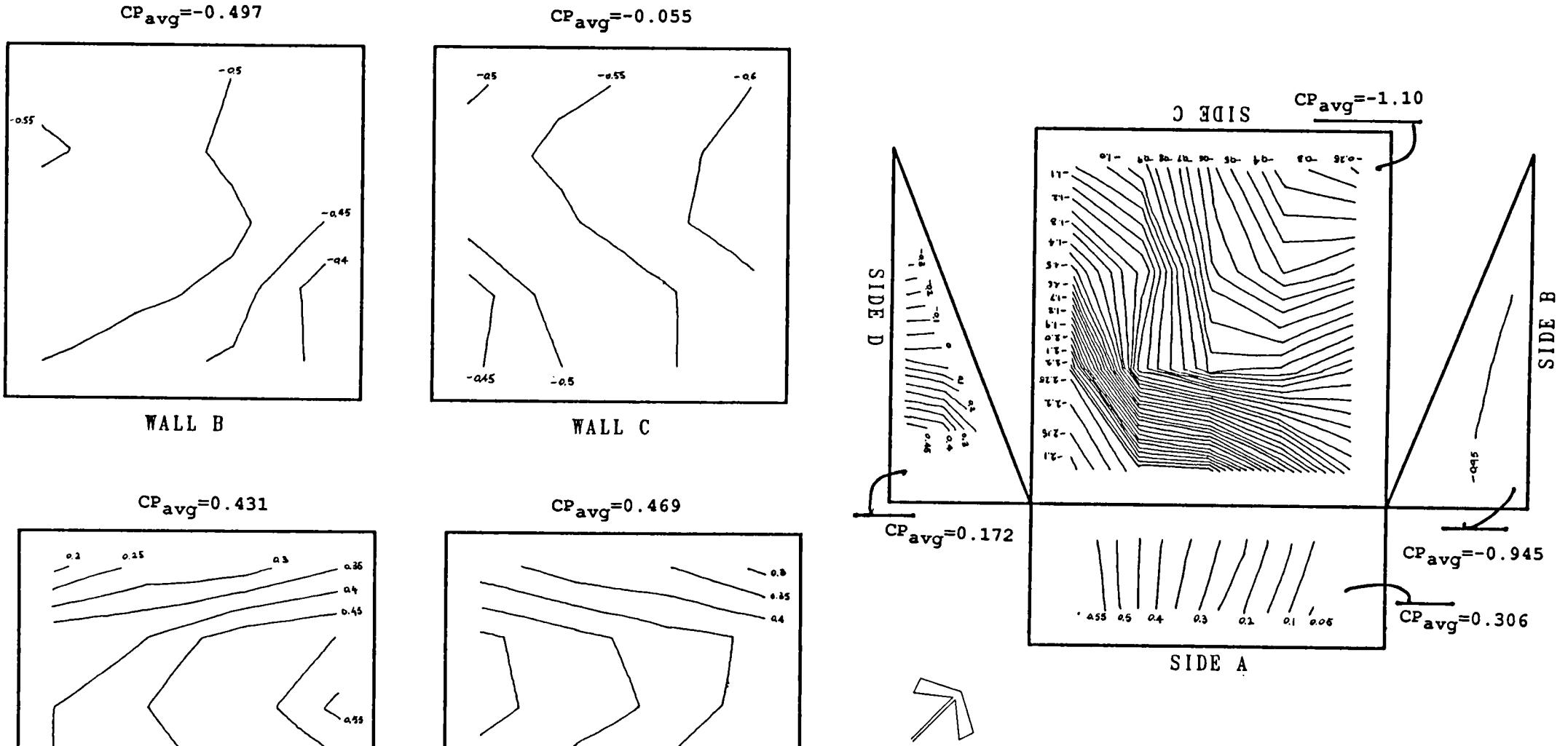

Surface pressure contours on atrium model surfaces.

A 10- **Monopitched roof** (45° wind incidence)

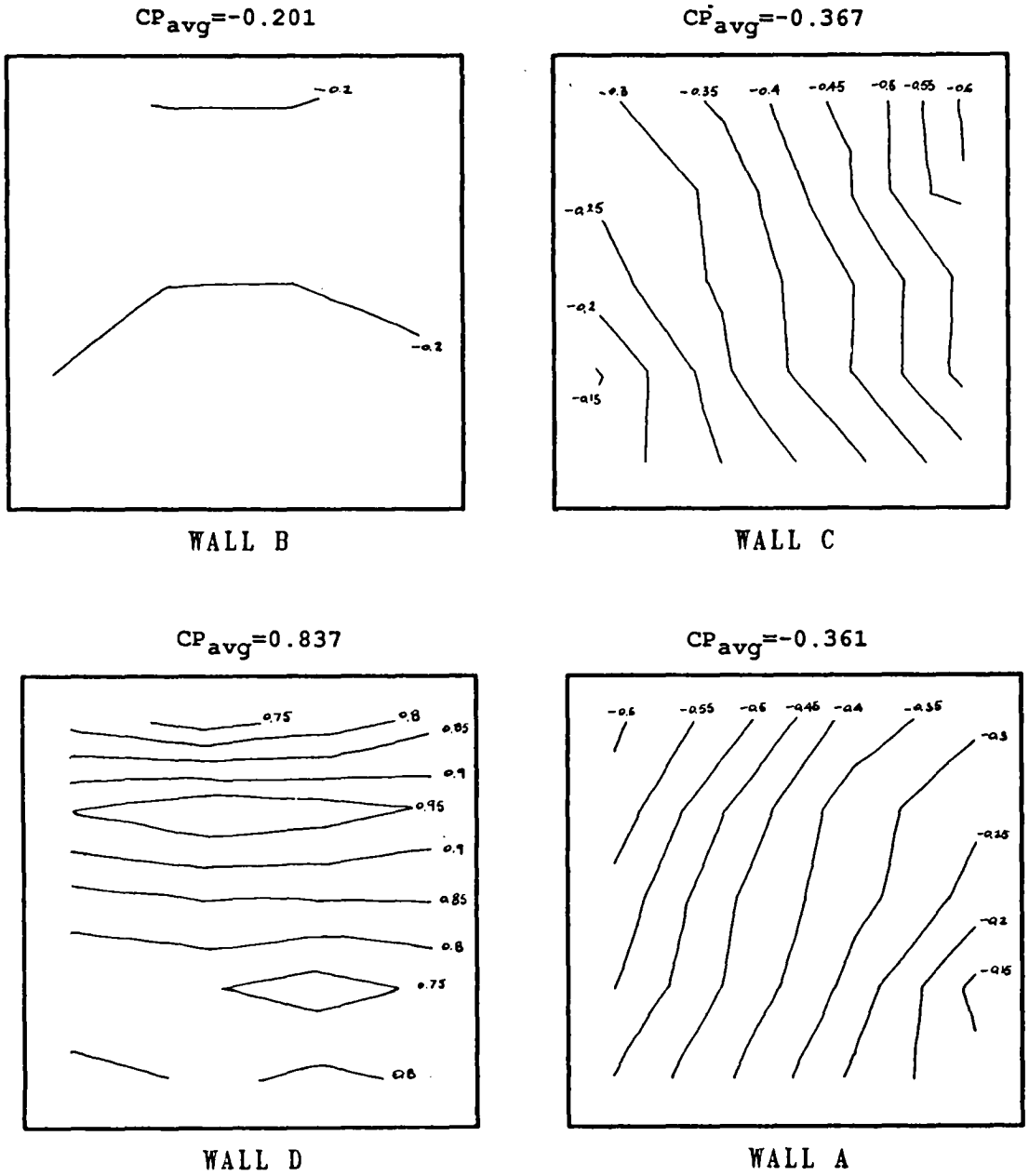

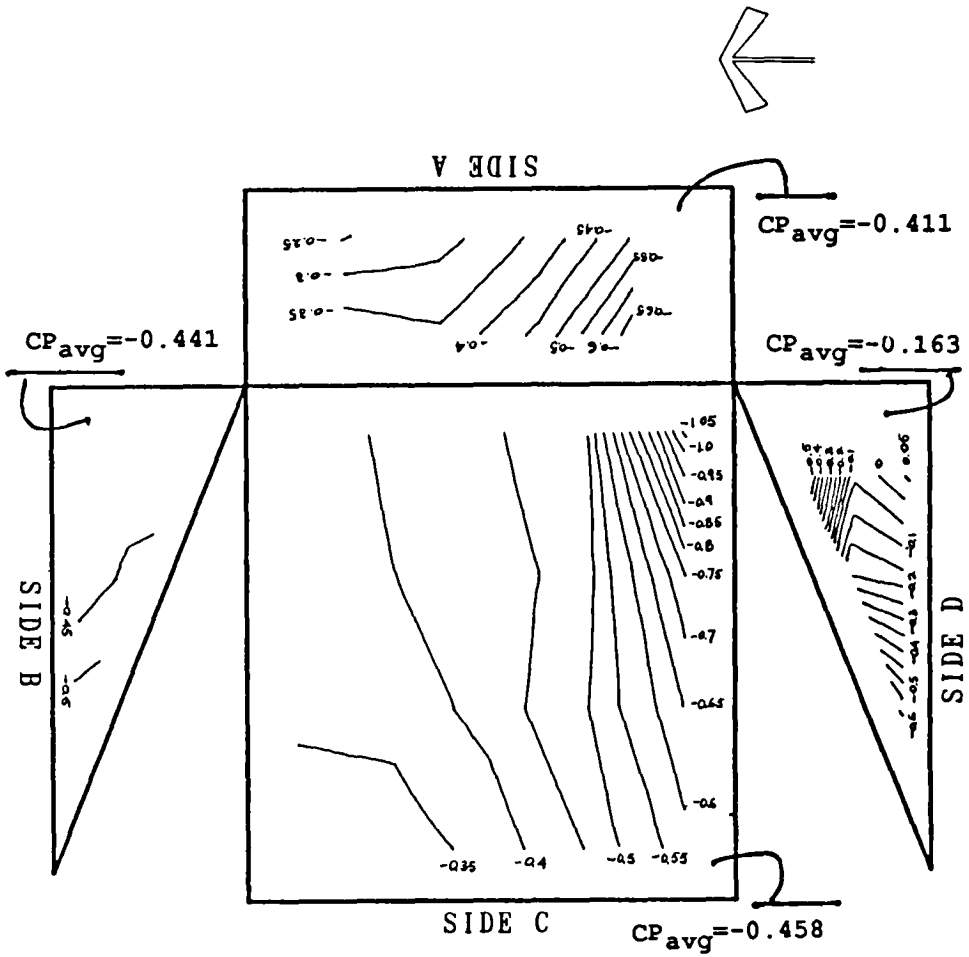

Surface pressure contours on atrium model surfaces.

A 11- **Monopitched roof** (90° wind incidence)

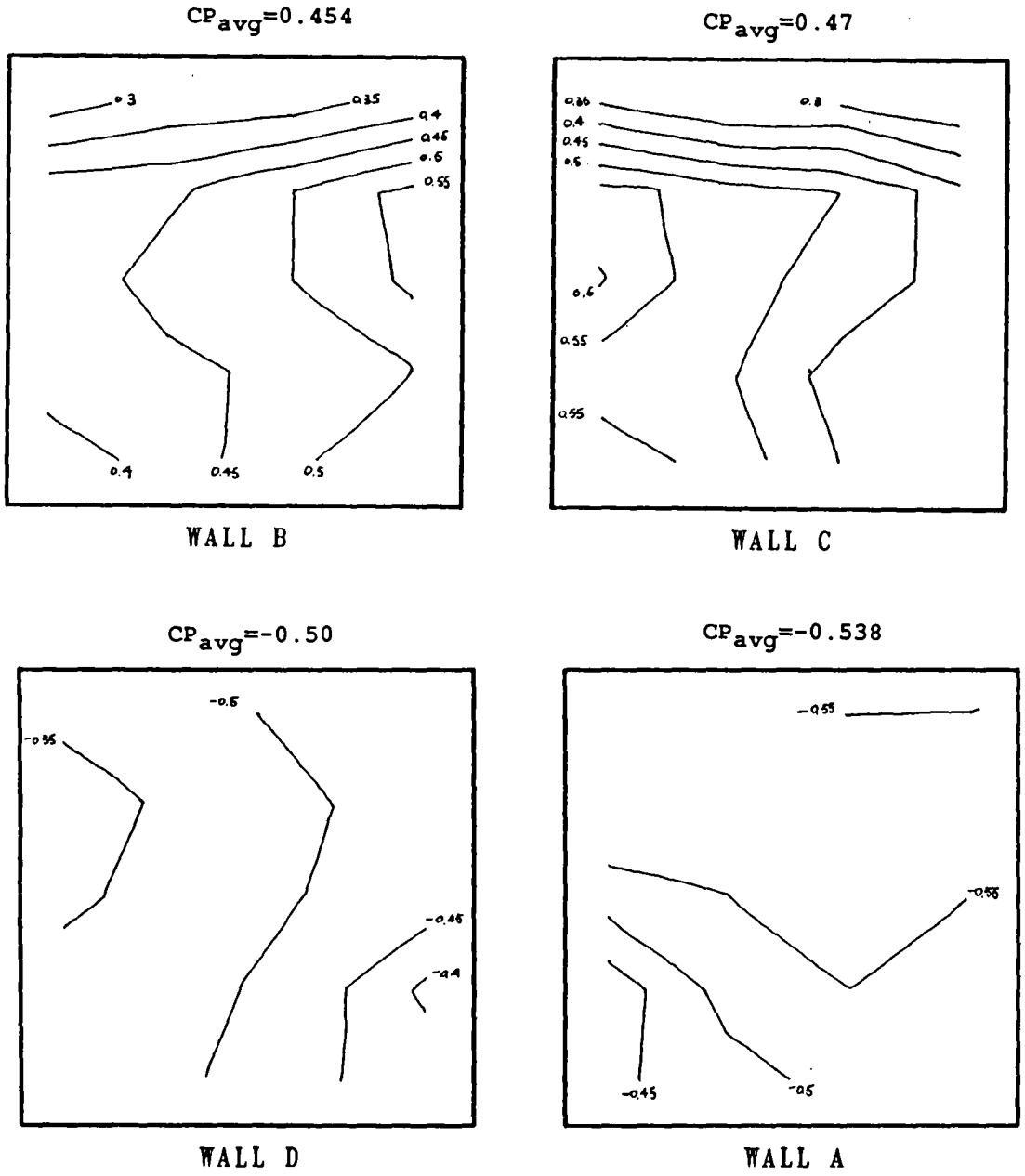

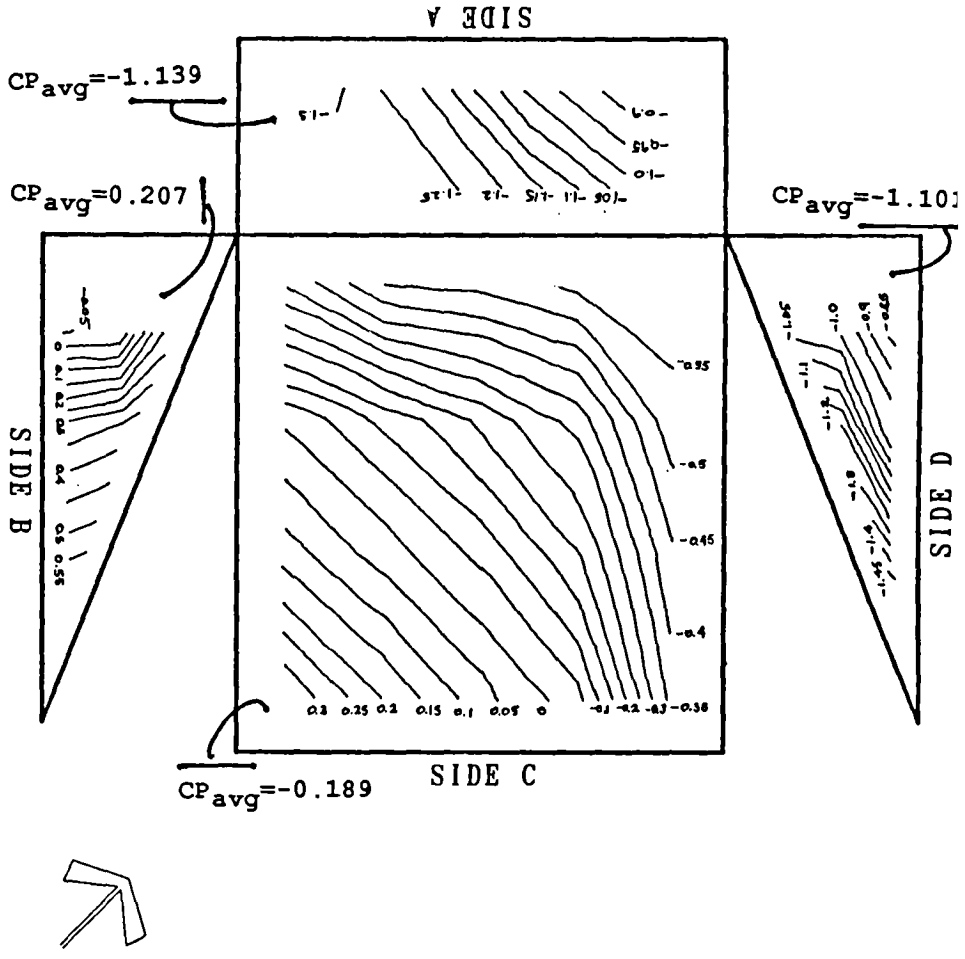

Surface pressure contours on atrium model surfaces.

A 12- **Monopitched roof** (135° wind incidence)

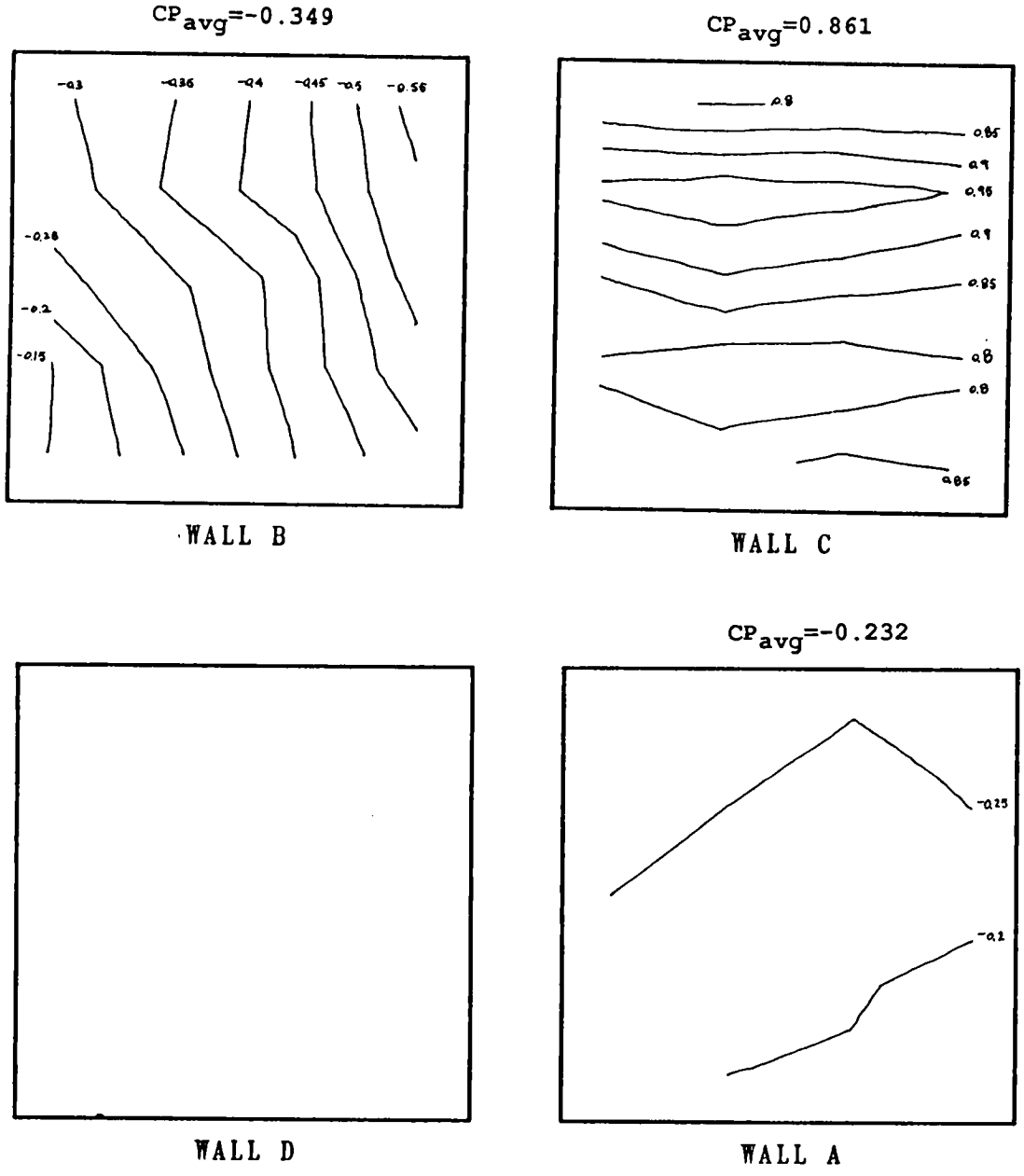

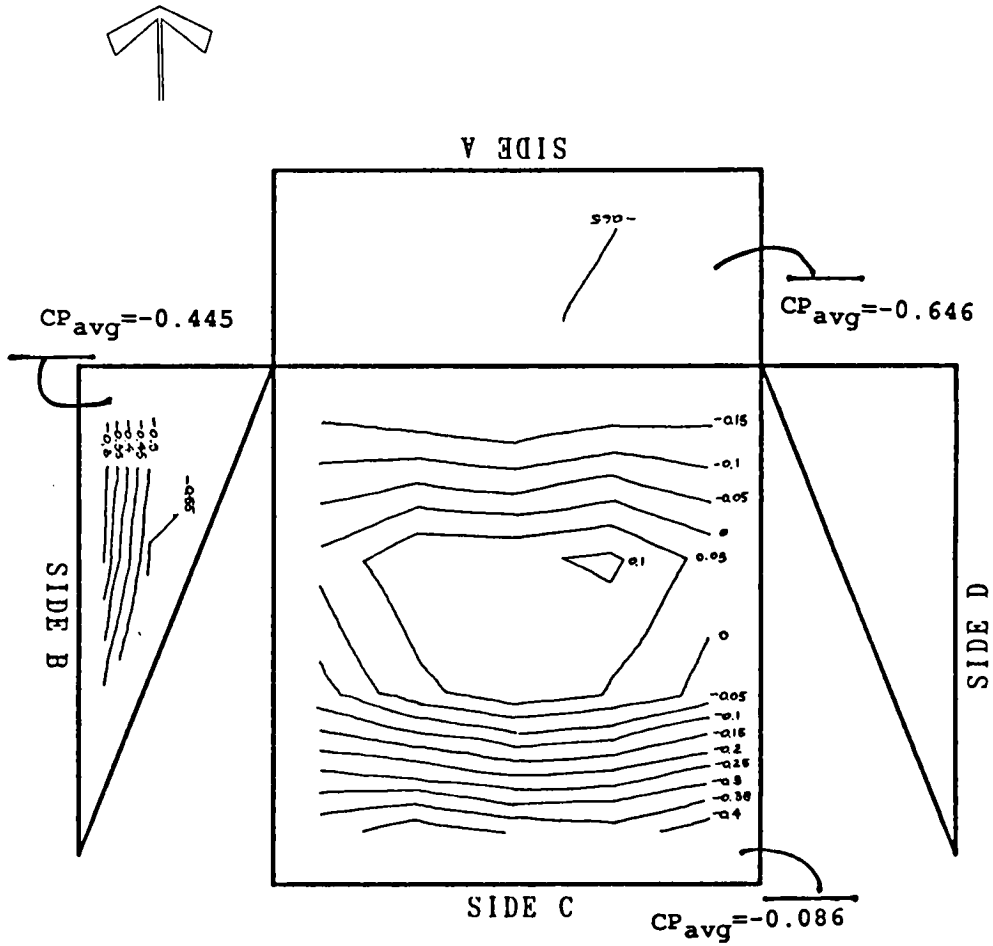

Surface pressure contours on atrium model surfaces.

A 13- **Monopitched roof** (180° wind incidence)

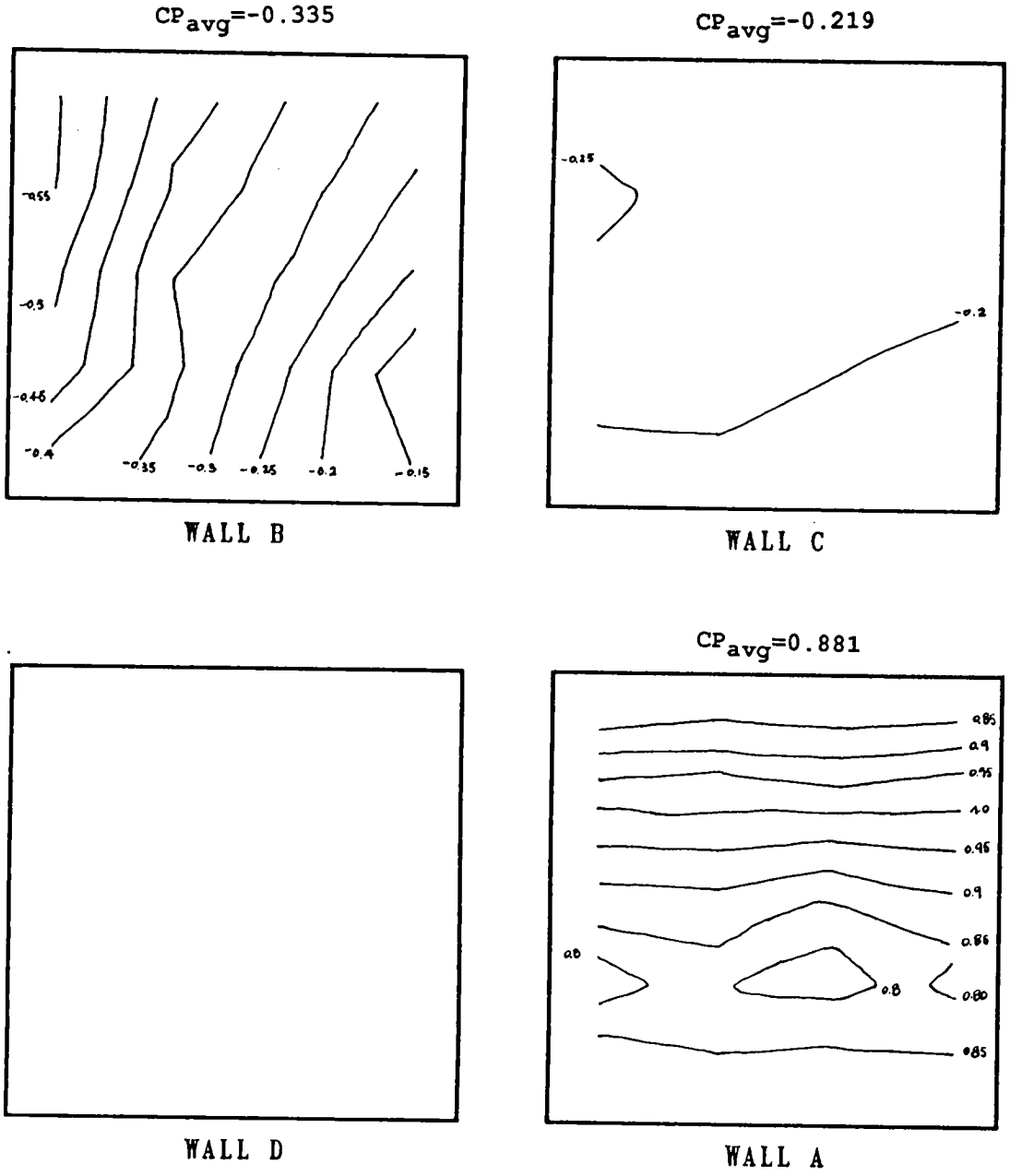

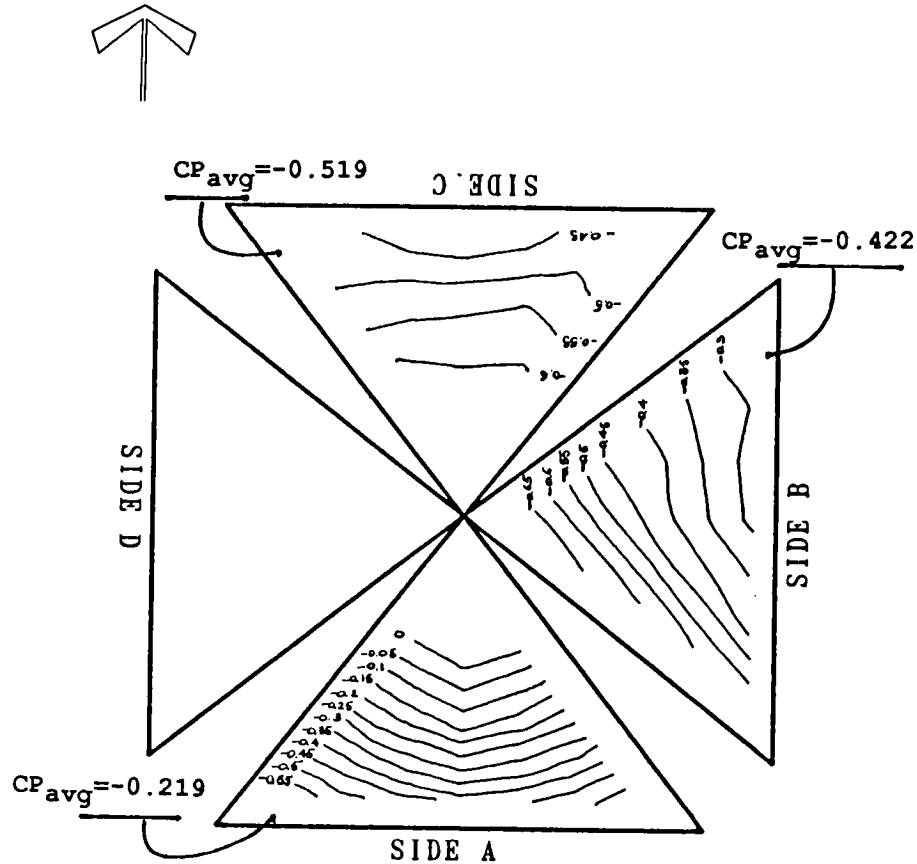

Surface pressure contours on atrium model surfaces.

A 14- **Pyramidal roof** (0° wind incidence)

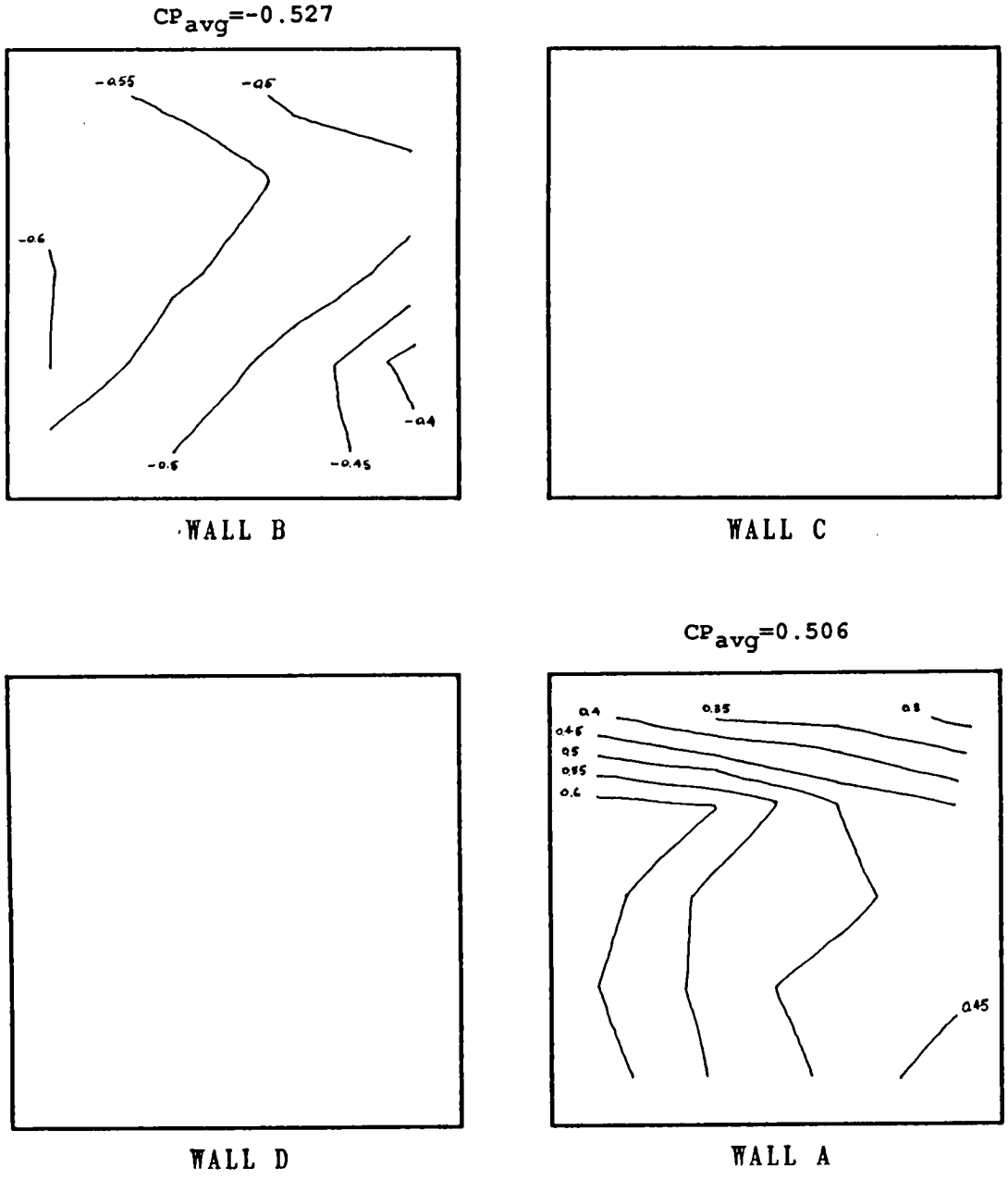

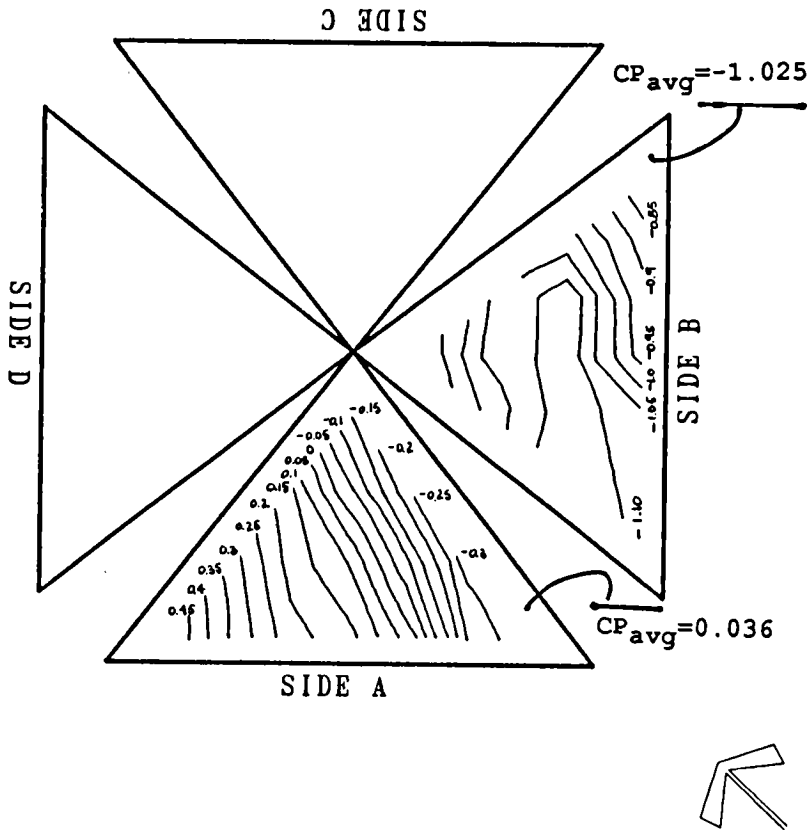

Surface pressure contours on atrium model surfaces.

A 15- Pyramidal roof (45° wind incidence)

		C05X05	C10X10		CO5X10		C05X15			C10X15		
	Floor leve	L1	L1	L2	L1	L2	L1	L2	L3	L1	L2	L3
FACADE A	1	0.28	0.27	0.27	0.28		0.26			0.27	0.27	
	2	0.27	0.27	0.27	0.26		0.27			0.27	0.27	
	3	0.32	0.32	0.32	0.30		0.31			0.31	0.31	
	4	0.30	0.30	0.30	0.28		0.28			0.28	0.28	
FACADE B	1	-0.10	-0.12	-0.07	-0.11	-0.05	-0.12	-0.04	0.00	-0.10	0.05	0.07
	2	-0.11	-0.10	-0.03	-0.10	-0.03	-0.10	-0.03	0.05	-0.10	0.06	0.06
	3	-0.10	-0.11	-0.05	-0.10	-0.01	-0.10	-0.03	0.07	-0.10	0.06	0.08
	4	-0.10	-0.09	-0.04	-0.10	-0.0.4	-0.10	-0.05	0.07	-0.10	0.05	0.06
FACADE C	1	0.00	0.06	0.06	-0.01		-0.07			-0.01	-0.01	
	2	0.02	0.10	0.10	-0.06		0.04			0.07	0.07	
	3	0.03	0.06	0.06	-0.08		-0.02			0.07	0.07	
	4	0.05	0.03	0.03	-0.07		-0.10			-0.08	-0.08	
FACADE D	1	-0.10	-0.07	-0.12	-0.05	-0.11	0.00	-0.04	-0.12	0.07	0.05	-0.10
	2	-0.11	-0.03	-0.10	-0.03	-0.10	0.05	-0.03	-0.10	0.06	0.06	-0.10
	3	-0.10	-0.05	-0.11	-0.01	-0.10	0.07	-0.03	-0.10	0.08	0.06	-0.10
	4	-0.10	-0.04	-0.09	-0.0.4	-0.10	0.07	-0.05	-0.10	0.06	0.05	-0.10
		C15X15			C10x05		C15x05			C15x10		
	Floor leve	L1	L2	L3	L1	L2	L1	L2	L3	L1	L2	L3
FACADE A	1	0.26	0.26	0.26	0.27	0.27	0.28	0.27	0.28	0.27	0.27	0.27
	2	0.25	0.27	0.25	0.27	0.27	0.27	0.27	0.27	0.26	0.27	0.26
	3	0.32	0.32	0.32	0.32	0.32	0.32	0.32	0.32	0.32	0.33	0.32
	4	0.29	0.30	0.29	0.29	0.29	0.30	0.30	0.30	0.29	0.30	0.29
FACADE B	1	-0.12	-0.01	0.05	-0.11		-0.12			-0.12	-0.03	
	2	-0.10	0.06	0.05	-0.13		-0.12			-0.10	-0.06	
	3	-0.10	0.06	0.09	-0.13		-0.11			-0.08	-0.03	
	4	-0.09	0.06	0.07	-0.10		-0.09			-0.10	-0.03	
FACADE C	1	-0.05	0.00	-0.05	0.06	0.06	0.00	0.09	0.00	0.09	0.09	0.09
	2	0.08	0.09	0.08	0.06	0.06	0.07	0.08	0.07	0.07	0.08	0.07
	3	0.08	0.09	0.08	0.08	0.08	0.05	0.06	0.05	0.08	0.09	0.08
	4	-0.05	-0.05	-0.05	0.06	0.06	0.08	0.08	0.08	0.02	0.06	0.02
FACADE D	1	0.05	-0.01	-0.12	-0.11		-0.12			-0.03	-0.12	
	2	0.05	0.06	-0.10	-0.13		-0.12			-0.06	-0.10	
	3	0.09	0.06	-0.10	-0.13		-0.11			-0.03	-0.08	
	4	0.07	0.06	-0.09	-0.10		-0.09			-0.03	-0.10	

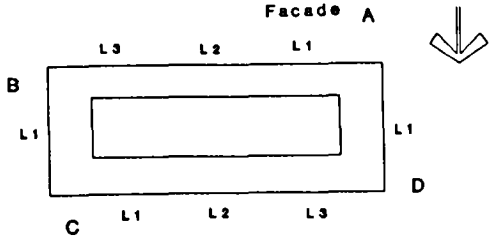

B 1- Internal flow coefficient, CQ1, for unsheltered courtyards, **(wind angle 0°).**

	Floor leve	C05X05 L1	C10X10 L1	L2	CO5X10 L1	L2	C05X15 L1	L2	L3	C10X15 L1	L2	L3
FACADE A	1	0.23	0.23	0.21	0.25		0.23			0.24	0.23	
	2	0.24	0.24	0.23	0.25		0.23			0.24	0.23	
	3	0.27	0.27	0.27	0.25		0.26			0.28	0.26	
	4	0.23	0.24	0.24	0.23		0.23			0.23	0.23	
FACADE B	1	-0.21	-0.20	-0.18	-0.20	-0.16	-0.21	-0.17	-0.15	-0.19	-0.15	-0.15
	2	-0.20	-0.18	-0.16	-0.19	-0.17	-0.20	-0.18	-0.15	-0.17	-0.15	-0.14
	3	-0.19	-0.17	-0.17	-0.19	-0.17	-0.19	-0.19	-0.16	-0.18	-0.16	-0.15
	4	-0.19	-0.17	-0.19	-0.19	-0.17	-0.17	-0.18	-0.17	-0.18	-0.17	-0.19
FACADE C	1	-0.14	-0.12	-0.13	-0.12		-0.14			-0.10	-0.16	
	2	-0.13	-0.08	-0.08	-0.15		-0.12			-0.08	-0.10	
	3	-0.13	-0.10	-0.10	-0.14		-0.12			-0.08	-0.10	
	4	-0.12	-0.12	-0.15	-0.13		-0.14			-0.11	-0.17	
FACADE D	1	0.14	0.15	0.16	0.14	0.15	0.13	0.16	0.15	0.14	0.16	0.17
	2	0.15	0.16	0.16	0.16	0.16	0.15	0.17	0.17	0.16	0.17	0.16
	3	0.16	0.17	0.17	0.17	0.17	0.17	0.18	0.18	0.19	0.18	0.18
	4	0.14	0.15	0.16	0.15	0.15	0.16	0.15	0.16	0.16	0.15	0.15
	Floor leve	C15X15 L1	L2	L3	C10x05 L1	L2	C15x05 L1	L2	L3	C15x10 L1	L2	L3
FACADE A	1	0.25	0.19	0.19	0.23	0.22	0.25	0.25	0.23	0.25	0.23	0.21
	2	0.23	0.23	0.17	0.25	0.23	0.27	0.25	0.23	0.25	0.24	0.22
	3	0.28	0.27	0.27	0.28	0.27	0.29	0.28	0.28	0.28	0.28	0.27
	4	0.24	0.24	0.25	0.23	0.24	0.25	0.25	0.27	0.24	0.25	0.24
FACADE B	1	-0.19	-0.17	-0.20	-0.17		-0.16			-0.19	-0.18	
	2	-0.16	-0.18	-0.18	-0.19		-0.15			-0.16	-0.15	
	3	-0.14	-0.14	-0.17	-0.19		-0.15			-0.14	-0.16	
	4	-0.15	-0.14	-0.19	-0.16		-0.13			-0.14	-0.17	
FACADE C	1	-0.10	-0.13	-0.17	-0.13	-0.11	-0.16	-0.13	-0.12	-0.10	-0.10	-0.11
	2	-0.10	-0.05	-0.12	-0.14	-0.12	-0.14	-0.12	-0.10	-0.08	-0.08	-0.08
	3	-0.06	-0.08	-0.12	-0.12	-0.10	-0.13	-0.12	-0.10	-0.09	-0.09	-0.06
	4	-0.14	-0.19	-0.16	-0.13	-0.12	-0.12	-0.11	-0.10	-0.14	-0.16	-0.11
FACADE D	1	0.16	0.16	0.17	0.14		0.15			0.17	0.17	
	2	0.13	0.17	0.15	0.14		0.15			0.16	0.17	
	3	0.18	0.19	0.18	0.15		0.17			0.18	0.19	
	4	0.16	0.17	0.15	0.14		0.16			0.15	0.16	

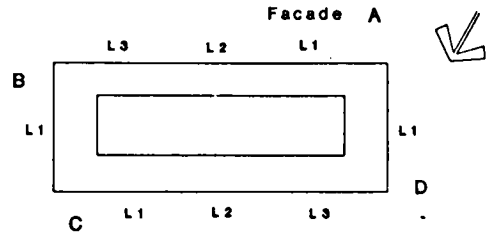

B 2- Internal flow coefficient, CQ1, for unsheltered courtyards, **(wind angle 30°).**

		C05X05	C10X10		CO5X10		C05X15			C10X15		
	Floor leve	L1	L1	L2	L1	L2	L1	L2	L3	L1	L2	L3
FACADE A	1	0.20	0.20	0.18	0.20		0.19			0.21	0.19	
	2	0.20	0.21	0.19	0.18		0.20			0.21	0.19	
	3	0.22	0.22	0.21	0.20		0.21			0.23	0.21	
	4	0.19	0.19	0.19	0.18		0.18			0.19	0.19	
FACADE B	1	-0.18	-0.18	-0.17	-0.19	-0.16	-0.20	-0.17	-0.150	-0.17	-0.16	-0.15
	2	-0.17	-0.16	-0.13	-0.19	-0.17	-0.19	-0.17	-0.140	-0.16	-0.16	-0.13
	3	-0.17	-0.16	-0.14	-0.19	-0.17	-0.19	-0.18	-0.160	-0.17	-0.15	-0.14
	4	-0.16	-0.16	-0.17	-0.19	-0.16	-0.18	-0.17	-0.140	-0.18	-0.18	-0.17
FACADE C	1	-0.18	-0.17	-0.18	-0.14		-0.14			-0.16	-0.16	
	2	-0.17	-0.13	-0.16	-0.17		-0.13			-0.14	-0.12	
	3	-0.17	-0.14	-0.16	-0.16		-0.12			-0.13	-0.14	
	4	-0.16	-0.17	-0.16	-0.14		-0.13			-0.12	-0.18	
FACADE D	1	0.20	0.18	0.20	0.18	0.21	0.17	0.21	0.210	0.17	0.19	0.22
	2	0.20	0.19	0.21	0.19	0.21	0.20	0.21	0.230	0.19	0.21	0.22
	3	0.22	0.21	0.22	0.22	0.23	0.23	0.23	0.240	0.22	0.23	0.23
	4	0.19	0.19	0.19	0.17	0.19	0.21	0.20	0.210	0.19	0.19	0.2
		C15X15			C10x05		C15x05			C15x10		
	Floor leve	L1	L2	L3	L1	L2	L1	L2	L3	L1	L2	L3
FACADE A	1	0.2	0.19	0.19	0.21	0.18	0.21	0.21	0.170	0.22	0.19	0.17
	2	0.19	0.21	0.16	0.21	0.19	0.23	0.21	0.200	0.22	0.21	0.19
	3	0.23	0.23	0.22	0.23	0.22	0.24	0.23	0.230	0.23	0.23	0.22
	4	0.19	0.2	0.19	0.19	0.17	0.21	0.20	0.210	0.2	0.19	0.19
FACADE B	1	-0.15	-0.17	-0.19	-0.14		-0.14			-0.16	-0.16	
	2	-0.15	-0.12	-0.16	-0.17		-0.13			-0.14	-0.12	
	3	-0.13	-0.13	-0.16	-0.16		-0.12			-0.13	-0.14	
	4	-0.16	-0.18	-0.19	-0.14		-0.13			-0.12	-0.18	
FACADE C	1	-0.19	-0.17	-0.15	-0.16	-0.19	-0.15	-0.17	-0.200	-0.15	-0.16	-0.17
	2	-0.16	-0.12	-0.15	-0.17	-0.19	-0.14	-0.17	-0.190	-0.13	-0.16	-0.16
	3	-0.16	-0.13	-0.13	-0.17	-0.19	-0.16	-0.18	-0.190	-0.14	-0.15	-0.17
	4	-0.19	-0.18	-0.16	-0.16	-0.19	-0.14	-0.17	-0.180	-0.17	-0.18	-0.18
FACADE D	1	0.19	0.19	0.2	0.20		0.19			0.19	0.21	
	2	0.16	0.21	0.19	0.18		0.20			0.19	0.21	
	3	0.22	0.23	0.23	0.20		0.21			0.21	0.23	
	4	0.19	0.2	0.19	0.18		0.18			0.19	0.19	

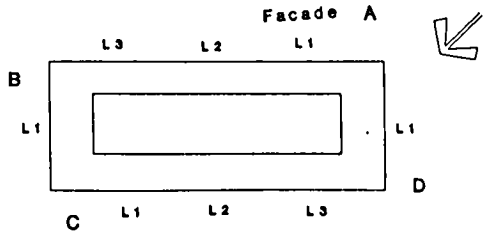

B 3- Internal flow coefficient, CQ1, for unsheltered courtyards, **(wind angle 45°).**

Atrium Index	Floor level	A		B		C		D		Internal Pressure CPI1
		L1	L2	L3	L4	L5	L6	L7	L8	
C10x10	1	0.27	as L1	-0.12	-0.07	0.06	as L5	as L4	as L3	
	2	0.26	- / -	-0.10	-0.03	0.10	- / -	- / -	- / -	
	3	0.32	- / -	-0.11	-0.05	0.07	- / -	- / -	- / -	
	4	0.30	- / -	-0.09	-0.04	0.03	- / -	- / -	- / -	
A1	1	0.25	- / -	-0.15	-0.11	-0.06	- / -	- / -	- / -	-0.065
	2	0.25	- / -	-0.14	-0.12	-0.06	- / -	- / -	- / -	
	3	0.30	- / -	-0.13	-0.10	-0.06	- / -	- / -	- / -	
	4	0.28	- / -	-0.16	-0.10	-0.06	- / -	- / -	- / -	
A2	1	0.26	- / -	-0.13	-0.09	0.06	- / -	- / -	- / -	-0.100
	2	0.26	- / -	-0.13	-0.10	0.04	- / -	- / -	- / -	
	3	0.30	- / -	-0.12	-0.10	0.01	- / -	- / -	- / -	
	4	0.29	- / -	-0.14	-0.09	-0.04	- / -	- / -	- / -	
A3	1	0.27	- / -	-0.12	-0.08	0.09	- / -	- / -	- / -	-0.110
	2	0.27	- / -	-0.12	-0.09	0.06	- / -	- / -	- / -	
	3	0.31	- / -	-0.11	-0.08	0.06	- / -	- / -	- / -	
	4	0.30	- / -	-0.13	-0.09	0.05	- / -	- / -	- / -	
A4	1	0.28	- / -	-0.11	-0.06	0.10	- / -	- / -	- / -	-0.125
	2	0.27	- / -	-0.11	-0.08	0.08	- / -	- / -	- / -	
	3	0.32	- / -	-0.11	-0.08	0.08	- / -	- / -	- / -	
	4	0.31	- / -	-0.11	-0.09	0.07	- / -	- / -	- / -	
A5	1	0.29	- / -	-0.04	0.08	0.14	- / -	- / -	- / -	-0.167
	2	0.28	- / -	-0.05	0.05	0.12	- / -	- / -	- / -	
	3	0.33	- / -	-0.06	0.05	0.12	- / -	- / -	- / -	
	4	0.31	- / -	-0.06	0.05	0.12	- / -	- / -	- / -	
A6	1	0.24	- / -	-0.18	-0.15	-0.11	- / -	- / -	- / -	-0.046
	2	0.24	- / -	-0.18	-0.15	-0.10	- / -	- / -	- / -	
	3	0.29	- / -	-0.18	-0.16	-0.10	- / -	- / -	- / -	
	4	0.27	- / -	-0.18	-0.17	-0.14	- / -	- / -	- / -	
A7	1	0.25	- / -	-0.16	-0.13	-0.10	- / -	- / -	- / -	-0.042
	2	0.24	- / -	-0.15	-0.14	-0.08	- / -	- / -	- / -	
	3	0.29	- / -	-0.15	-0.13	-0.09	- / -	- / -	- / -	
	4	0.27	- / -	-0.16	-0.14	-0.11	- / -	- / -	- / -	

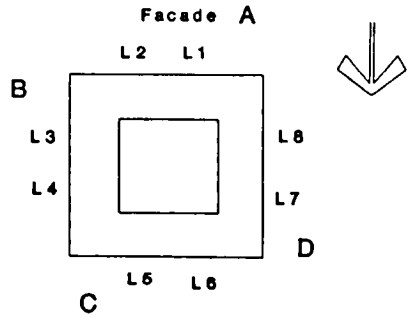

C 1- Internal flow coefficient, CQ1, for unsheltered atria, **(wind angle 0°).**

Atrium Index	Floor level	A		B		C		D		Internal Pressure CPI1
		L1	L2	L3	L4	L5	L6	L7	L8	
C10x10	1	0.23	0.21	-0.20	-0.18	-0.13	-0.13	0.15	0.15	
	2	0.24	0.23	-0.18	-0.15	-0.08	-0.08	0.16	0.16	
	3	0.27	0.26	-0.18	-0.17	-0.10	-0.10	0.17	0.17	
	4	0.24	0.24	-0.17	-0.20	-0.12	-0.15	0.15	0.25	
A1	1	0.23	0.23	-0.21	-0.20	-0.14	-0.15	0.15	0.15	
	2	0.25	0.21	-0.21	-0.19	-0.14	-0.14	0.16	0.12	-0.040
	3	0.27	0.25	-0.20	-0.18	-0.14	-0.13	0.17	0.14	
	4	0.22	0.23	-0.21	-0.20	-0.13	-0.14	0.13	0.14	
A2	1	0.25	0.25	-0.18	-0.17	-0.09	-0.10	0.17	0.18	
	2	0.27	0.23	-0.18	-0.16	-0.10	-0.09	0.19	0.15	-0.090
	3	0.29	0.26	-0.17	-0.17	-0.10	-0.09	0.20	0.17	
	4	0.24	0.26	-0.18	-0.17	-0.09	-0.09	0.16	0.17	
A3	1	0.26	0.26	-0.16	-0.15	-0.05	-0.07	0.19	0.19	
	2	0.28	0.24	-0.16	-0.15	-0.06	-0.06	0.21	0.16	-0.120
	3	0.30	0.27	-0.15	-0.14	-0.06	-0.06	0.21	0.18	
	4	0.26	0.27	-0.16	-0.15	-0.05	-0.07	0.17	0.18	
A4	1	0.27	0.27	-0.15	-0.14	0.05	-0.02	0.19	0.20	
	2	0.29	0.24	-0.15	-0.13	0.01	-0.03	0.21	0.17	-0.140
	3	0.31	0.28	-0.13	-0.13	0.00	-0.02	0.22	0.19	
	4	0.27	0.28	-0.14	-0.14	0.04	-0.03	0.18	0.19	
A5	1	0.28	0.28	-0.09	0.20	0.12	0.10	0.22	0.23	
	2	0.30	0.26	-0.10	0.17	0.11	0.10	0.24	0.19	-0.200
	3	0.32	0.30	-0.09	0.19	0.11	0.10	0.25	0.21	
	4	0.28	0.30	-0.08	0.19	0.13	0.10	0.21	0.22	
A6	1	0.21	0.21	-0.23	-0.22	-0.17	-0.17	0.12	0.11	
	2	0.24	0.19	-0.23	-0.21	-0.17	-0.16	0.13	0.10	0.000
	3	0.26	0.23	-0.22	-0.21	-0.17	-0.16	0.14	0.11	
	4	0.21	0.22	-0.23	-0.23	-0.18	-0.18	0.10	0.10	
A7	1	0.23	0.23	-0.21	-0.21	-0.14	-0.14	0.14	0.15	
	2	0.25	0.20	-0.20	-0.20	-0.13	-0.13	0.16	0.13	-0.050
	3	0.27	0.25	-0.20	-0.20	-0.14	-0.14	0.18	0.14	
	4	0.22	0.22	-0.21	-0.21	-0.14	-0.14	0.14	0.13	

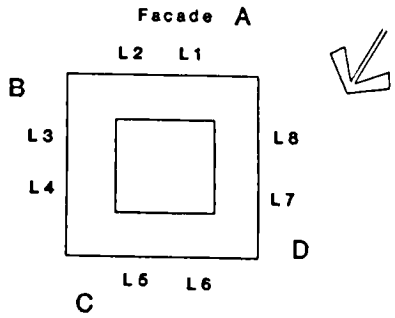

C 2- Internal flow coefficient, CQ1, for unsheltered atria, **(wind angle 30°).**

Atrium Index	Floor level	A		B		C		D		Internal Pressure CPI1
		L1	L2	L3	L4	L5	L6	L7	L8	
C10x10	1	0.20	0.18	-0.18	-0.16	as L4	as L3	as L2	as L1	
	2	0.21	0.19	-0.15	-0.13	-/-	-/-	-/-	-/-	
	3	0.22	0.21	-0.16	-0.14	-/-	-/-	-/-	-/-	
	4	0.19	0.19	-0.16	-0.18	-/-	-/-	-/-	-/-	
A1	1	0.21	0.20	-0.18	-0.19	-/-	-/-	-/-	-/-	-0.042
	2	0.22	0.17	-0.19	-0.16	-/-	-/-	-/-	-/-	
	3	0.23	0.20	-0.19	-0.16	-/-	-/-	-/-	-/-	
	4	0.19	0.19	-0.17	-0.17	-/-	-/-	-/-	-/-	
A2	1	0.22	0.22	-0.14	-0.14	-/-	-/-	-/-	-/-	-0.100
	2	0.24	0.20	-0.15	-0.13	-/-	-/-	-/-	-/-	
	3	0.25	0.22	-0.14	-0.13	-/-	-/-	-/-	-/-	
	4	0.21	0.22	-0.14	-0.13	-/-	-/-	-/-	-/-	
A3	1	0.24	0.24	-0.11	-0.11	-/-	-/-	-/-	-/-	-0.130
	2	0.26	0.21	-0.11	-0.10	-/-	-/-	-/-	-/-	
	3	0.27	0.24	-0.11	-0.10	-/-	-/-	-/-	-/-	
	4	0.22	0.23	-0.11	-0.11	-/-	-/-	-/-	-/-	
A4	1	0.24	0.25	-0.08	-0.09	-/-	-/-	-/-	-/-	-0.156
	2	0.26	0.22	-0.10	-0.08	-/-	-/-	-/-	-/-	
	3	0.28	0.24	-0.09	-0.09	-/-	-/-	-/-	-/-	
	4	0.23	0.24	-0.08	-0.10	-/-	-/-	-/-	-/-	
A5	1	0.26	0.27	0.07	0.05	-/-	-/-	-/-	-/-	-0.217
	2	0.28	0.23	0.03	0.06	-/-	-/-	-/-	-/-	
	3	0.30	0.26	0.04	0.05	-/-	-/-	-/-	-/-	
	4	0.25	0.27	0.08	0.04	-/-	-/-	-/-	-/-	
A6	1	0.17	0.16	-0.21	-0.20	-/-	-/-	-/-	-/-	0.019
	2	0.19	0.15	-0.22	-0.19	-/-	-/-	-/-	-/-	
	3	0.20	0.17	-0.21	-0.19	-/-	-/-	-/-	-/-	
	4	0.16	0.16	-0.21	-0.22	-/-	-/-	-/-	-/-	
A7	1	0.20	0.20	-0.18	-0.17	-/-	-/-	-/-	-/-	-0.046
	2	0.22	0.18	-0.17	-0.17	-/-	-/-	-/-	-/-	
	3	0.23	0.20	-0.17	-0.17	-/-	-/-	-/-	-/-	
	4	0.19	0.18	-0.17	-0.16	-/-	-/-	-/-	-/-	

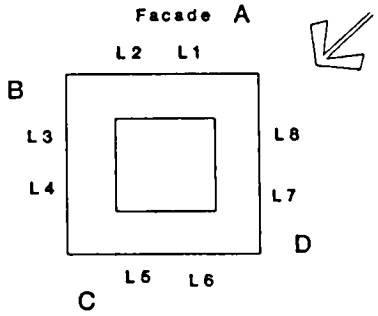

C 3- Internal flow coefficient, CQ1, for unsheltered atria, **(wind angle 45°).**

Atrium Index	Floor level	A		B		C		D		Internal Pressure CPI1
		L1	L2	L3	L4	L5	L6	L7	L8	
C10x10	1	0.16	as L1	-0.07	-0.02	-0.06	as L5	as L4	as L3	
	2	0.12	--/--	-0.03	0.03	-0.01	--/--	--/--	--/--	
	3	0.15	--/--	-0.05	0.00	-0.05	--/--	--/--	--/--	
	4	0.20	--/--	-0.06	-0.05	-0.12	--/--	--/--	--/--	
A1	1	0.17	--/--	-0.08	-0.07	-0.06	--/--	--/--	--/--	0.015
	2	0.12	--/--	-0.07	-0.06	-0.06	--/--	--/--	--/--	
	3	0.15	--/--	-0.08	-0.07	-0.07	--/--	--/--	--/--	
	4	0.19	--/--	-0.08	-0.07	-0.08	--/--	--/--	--/--	
A4	1	0.20	--/--	0.05	0.07	0.09	--/--	--/--	--/--	-0.033
	2	0.15	--/--	0.05	0.05	0.07	--/--	--/--	--/--	
	3	0.18	--/--	0.02	0.04	0.06	--/--	--/--	--/--	
	4	0.22	--/--	-0.04	0.03	0.06	--/--	--/--	--/--	
A5	1	0.23	--/--	0.10	0.12	0.13	--/--	--/--	--/--	-0.090
	2	0.18	--/--	0.11	0.10	0.12	--/--	--/--	--/--	
	3	0.20	--/--	0.10	0.10	0.11	--/--	--/--	--/--	
	4	0.25	--/--	0.08	0.10	0.11	--/--	--/--	--/--	
A6	1	0.16	--/--	-0.11	-0.09	-0.09	--/--	--/--	--/--	0.031
	2	0.12	--/--	-0.09	-0.13	-0.08	--/--	--/--	--/--	
	3	0.14	--/--	-0.10	-0.09	-0.09	--/--	--/--	--/--	
	4	0.19	--/--	-0.10	-0.10	-0.11	--/--	--/--	--/--	
A7	1	0.11	--/--	-0.15	-0.12	-0.13	--/--	--/--	--/--	0.027
	2	0.08	--/--	-0.11	-0.11	-0.11	--/--	--/--	--/--	
	3	0.11	--/--	-0..12	-0.11	-0.12	--/--	--/--	--/--	
	4	0.16	--/--	-0.14	-0.15	-0.16	--/--	--/--	--/--	

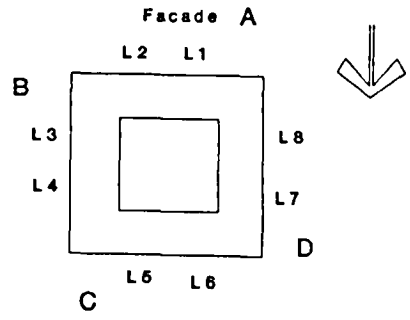

D 1- Internal flow coefficient, CQ1, for courtyards and atria in congested urban sites, **(Sc/ H = 2.3, normal pattern, wind angle 0°).**

Atrium Index	Floor level	A		B		C		D		Internal Pressure CPI1
		L1	L2	L3	L4	L5	L6	L7	L8	
C10x10	1	0.14	as L1	0.00	0.05	-0.07	as L5	as L4	as L3	
	2	0.12	--/--	0.05	0.05	-0.04	--/--	--/--	--/--	
	3	0.15	--/--	0.02	0.05	-0.06	--/--	--/--	--/--	
	4	0.18	--/--	-0.03	-0.03	-0.12	--/--	--/--	--/--	
A1	1	0.15	--/--	-0.05	-0.05	-0.07	--/--	--/--	--/--	0.017
	2	0.11	--/--	-0.05	-0.06	-0.08	--/--	--/--	--/--	
	3	0.13	--/--	-0.06	-0.06	-0.09	--/--	--/--	--/--	
	4	0.18	--/--	-0.07	-0.07	-0.09	--/--	--/--	--/--	
A4	1	0.18	--/--	0.07	0.09	0.06	--/--	--/--	--/--	-0.024
	2	0.14	--/--	0.07	0.07	0.05	--/--	--/--	--/--	
	3	0.17	--/--	0.07	0.0.7	0.03	--/--	--/--	--/--	
	4	0.21	--/--	0.04	0.06	0.04	--/--	--/--	--/--	
A5	1	0.20	--/--	0.12	0.14	0.10	--/--	--/--	--/--	-0.082
	2	0.16	--/--	0.13	0.12	0.11	--/--	--/--	--/--	
	3	0.20	--/--	0.12	0.11	0.10	--/--	--/--	--/--	
	4	0.23	--/--	0.10	0.11	0.10	--/--	--/--	--/--	
A6	1	0.09	--/--	-0.13	-0.12	-0.15	--/--	--/--	--/--	0.044
	2	0.07	--/--	-0.10	-0.11	-0.12	--/--	--/--	--/--	
	3	0.10	--/--	-0.10	-0.10	-0.12	--/--	--/--	--/--	
	4	0.14	--/--	-0.13	-0.14	-0.17	--/--	--/--	--/--	
A7	1	0.14	--/--	-0.08	-0.07	-0.10	--/--	--/--	--/--	0.026
	2	0.11	--/--	-0.07	-0.07	-0.09	--/--	--/--	--/--	
	3	0.14	--/--	-0.07	-0.08	-0.10	--/--	--/--	--/--	
	4	0.17	--/--	-0.09	-0.10	-0.12	--/--	--/--	--/--	

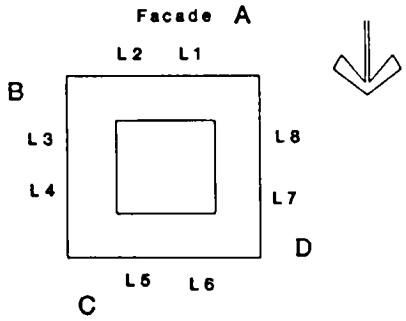

D 2- Internal flow coefficient, CQ1, for courtyards and atria in congested urban sites, **(Sc/ H = 2.3, staggered pattern, wind angle 0°).**

Atrium Index	Floor level	A		B		C		D		Internal Pressure CPI1
		L1	L2	L3	L4	L5	L6	L7	L8	
C10x10	1	0.12	as L1	-0.04	0.05	0.10	as L5	as L4	as L3	
	2	0.06	--/--	0.03	-0.03	0.00	--/--	--/--	--/--	
	3	0.06	--/--	0.04	0.03	-0.08	--/--	--/--	--/--	
	4	0.18	--/--	-0.07	-0.02	-0.12	--/--	--/--	--/--	
A1	1	0.14	--/--	-0.08	0.03	0.11	--/--	--/--	--/--	0.015
	2	0.06	--/--	-0.02	-0.09	-0.04	--/--	--/--	--/--	
	3	0.06	--/--	-0.04	-0.07	-0.10	--/--	--/--	--/--	
	4	0.19	--/--	-0.11	-0.06	-0.11	--/--	--/--	--/--	
A4	1	0.18	--/--	0.06	0.10	0.15	--/--	--/--	--/--	-0.034
	2	0.10	--/--	0.03	0.06	0.07	--/--	--/--	--/--	
	3	0.11	--/--	0.08	0.06	-0.02	--/--	--/--	--/--	
	4	0.21	--/--	-0.04	0.05	0.05	--/--	--/--	--/--	
A5	1	0.21	--/--	0.12	0.15	0.18	--/--	--/--	--/--	-0.100
	2	0.14	--/--	0.14	0.11	0.12	--/--	--/--	--/--	
	3	0.15	--/--	0.14	0.12	0.09	--/--	--/--	--/--	
	4	0.23	--/--	0.10	0.13	0.11	--/--	--/--	--/--	
A6	1	0.12	--/--	-0.10	-0.06	0.07	--/--	--/--	--/--	0.030
	2	0.03	--/--	-0.06	-0.09	-0.06	--/--	--/--	--/--	
	3	0.04	--/--	-0.06	-0.08	-0.10	--/--	--/--	--/--	
	4	0.17	--/--	-0.10	-0.10	-0.13	--/--	--/--	--/--	
A7	1	0.03	--/--	-0.14	-0.11	-0.10	--/--	--/--	--/--	0.032
	2	-0.05	--/--	-0.09	-0.12	-0.10	--/--	--/--	--/--	
	3	-0.04	--/--	-0.09	-0.09	-0.12	--/--	--/--	--/--	
	4	0.13	--/--	-0.14	-0.15	-0.18	--/--	--/--	--/--	

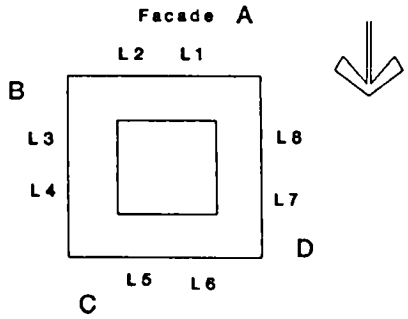

D 3- Internal flow coefficient, CQ1, for courtyards and atria in congested urban sites, **(Sc/ H = 1.5, normal pattern, wind angle 0°).**

Atrium Index	Floor level	A		B		C		D		Internal Pressure CPI1
		L1	L2	L3	L4	L5	L6	L7	L8	
C10x10	1	0.10	as L1	0.02	0.03	0.09	as L5	as L4	as L3	
	2	0.05	- - / - -	0.03	0.05	0.03	- - / - -	- - / - -	- - / - -	
	3	0.06	- - / - -	0.04	0.06	-0.05	- - / - -	- - / - -	- - / - -	
	4	0.14	- - / - -	-0.04	-0.03	-0.10	- - / - -	- - / - -	- - / - -	
A1	1	0.12	- - / - -	-0.03	0.00	0.09	- - / - -	- - / - -	- - / - -	0.010
	2	0.04	- - / - -	-0.05	-0.05	-0.04	- - / - -	- - / - -	- - / - -	
	3	0.05	- - / - -	-0.05	-0.04	-0.09	- - / - -	- - / - -	- - / - -	
	4	0.14	- - / - -	-0.06	-0.07	-0.08	- - / - -	- - / - -	- - / - -	
A4	1	0.15	- - / - -	0.07	0.09	0.13	- - / - -	- - / - -	- - / - -	-0.031
	2	0.09	- - / - -	0.07	0.07	0.07	- - / - -	- - / - -	- - / - -	
	3	0.10	- - / - -	0.07	0.07	0.00	- - / - -	- - / - -	- - / - -	
	4	0.17	- - / - -	0.06	0.06	0.06	- - / - -	- - / - -	- - / - -	
A5	1	0.18	- - / - -	0.12	0.14	0.16	- - / - -	- - / - -	- - / - -	-0.089
	2	0.12	- - / - -	0.13	0.11	0.11	- - / - -	- - / - -	- - / - -	
	3	0.14	- - / - -	0.13	0.12	0.09	- - / - -	- - / - -	- - / - -	
	4	0.20	- - / - -	0.11	0.12	0.11	- - / - -	- - / - -	- - / - -	
A6	1	-0.08	- - / - -	-0.12	-0.12	-0.11	- - / - -	- - / - -	- - / - -	0.033
	2	-0.05	- - / - -	-0.08	-0.10	-0.09	- - / - -	- - / - -	- - / - -	
	3	-0.05	- - / - -	-0.08	-0.08	-0.11	- - / - -	- - / - -	- - / - -	
	4	0.09	- - / - -	-0.11	-0.13	-0.16	- - / - -	- - / - -	- - / - -	
A7	1	0.09	- - / - -	-0.07	-0.07	0.05	- - / - -	- - / - -	- - / - -	0.013
	2	0.00	- - / - -	-0.06	-0.06	-0.06	- - / - -	- - / - -	- - / - -	
	3	0.03	- - / - -	-0.06	-0.06	-0.09	- - / - -	- - / - -	- - / - -	
	4	0.13	- - / - -	-0.08	-0.09	-0.11	- - / - -	- - / - -	- - / - -	

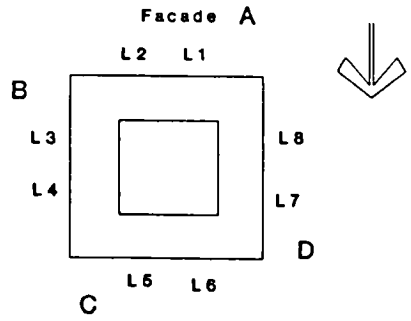

D 4- Internal flow coefficient, CQ1, for courtyards and atria in congested urban sites, **(Sc/ H = 1.5, staggered pattern, wind angle 0°).**

Atrium Index	Floor level	A		B		C		D		Internal Pressure CPI1
		L1	L2	L3	L4	L5	L6	L7	L8	
C10x10	1	0.20	0.20	-0.10	-0.04	as L4	as L3	as L2	as L1	
	2	0.22	0.18	-0.10	-0.07	- / -	- - / - -	- - / - -	- - / - -	
	3	0.21	0.18	-0.11	-0.11	- / -	- - / - -	- - / - -	- - / - -	
	4	0.18	0.19	-0.11	-0.12	- / -	- - / - -	- - / - -	- - / - -	
A1	1	0.17	0.17	-0.16	-0.13	- / -	- - / - -	- - / - -	- - / - -	0.013
	2	0.18	0.16	-0.15	-0.12	- / -	- - / - -	- - / - -	- - / - -	
	3	0.18	0.16	-0.15	-0.14	- / -	- - / - -	- - / - -	- - / - -	
	4	0.15	0.15	-0.16	-0.13	- / -	- - / - -	- - / - -	- - / - -	
A4	1	0.20	0.21	-0.11	-0.04	- / -	- - / - -	- - / - -	- - / - -	-0.053
	2	0.21	0.19	-0.10	-0.07	- / -	- - / - -	- - / - -	- - / - -	
	3	0.21	0.19	-0.11	-0.10	- / -	- - / - -	- - / - -	- - / - -	
	4	0.19	0.20	-0.11	-0.08	- / -	- - / - -	- - / - -	- - / - -	
A5	1	0.22	0.23	-0.06	0.08	- / -	- - / - -	- - / - -	- - / - -	-0.089
	2	0.23	0.20	-0.06	0.06	- / -	- - / - -	- - / - -	- - / - -	
	3	0.23	0.20	-0.08	-0.06	- / -	- - / - -	- - / - -	- - / - -	
	4	0.21	0.23	-0.05	0.00	- / -	- - / - -	- - / - -	- - / - -	
A6	1	0.17	0.17	-0.17	-0.14	- / -	- - / - -	- - / - -	- - / - -	0.022
	2	0.18	0.15	-0.16	-0.14	- / -	- - / - -	- - / - -	- - / - -	
	3	0.18	0.15	-0.16	-0.15	- / -	- - / - -	- - / - -	- - / - -	
	4	0.15	0.16	-0.17	-0.15	- / -	- - / - -	- - / - -	- - / - -	
A7	1	0.18	0.18	-0.14	-0.10	- / -	- - / - -	- - / - -	- - / - -	-0.008
	2	0.20	0.16	-0.13	-0.11	- / -	- - / - -	- - / - -	- - / - -	
	3	0.19	0.17	-0.14	-0.12	- / -	- - / - -	- - / - -	- - / - -	
	4	0.16	0.18	-0.14	-0.12	- / -	- - / - -	- - / - -	- - / - -	

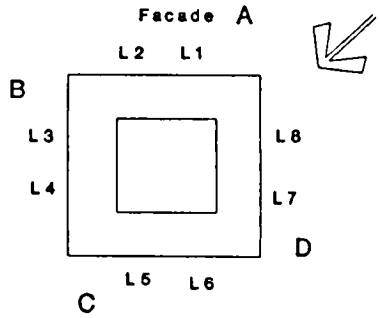

D 5- Internal flow coefficient, CQ1, for courtyards and atria in congested urban sites, **(Sc/ H = 2.3, normal pattern, wind angle 45°).**

Atrium Index	Floor level	A		B		C		D		Internal Pressure CPI1
		L1	L2	L3	L4	L5	L6	L7	L8	
C10x10	1	0.16	0.15	-0.10	-0.08	-0.06	-0.09	0.13	0.12	
	2	0.15	0.15	-0.10	-0.07	-0.06	-0.09	0.15	0.11	
	3	0.16	0.16	-0.09	-0.08	-0.08	-0.10	0.15	0.12	
	4	0.16	0.17	-0.11	-0.11	-0.12	-0.10	0.15	0.13	
A1	1	0.14	0.14	-0.13	-0.11	-0.11	-0.14	0.12	0.10	0.020
	2	0.13	0.13	-0.12	-0.11	-0.11	-0.14	0.12	0.09	
	3	0.15	0.14	-0.12	-0.10	-0.12	-0.13	0.13	0.10	
	4	0.15	0.15	-0.13	-0.12	-0.12	-0.13	0.13	0.12	
A4	1	0.19	0.17	-0.08	0.03	0.01	-0.08	0.17	0.15	-0.041
	2	0.16	0.17	-0.08	-0.04	-0.02	-0.07	0.16	0.13	
	3	0.18	0.18	-0.08	-0.06	-0.05	-0.08	0.17	0.14	
	4	0.20	0.19	-0.08	-0.03	-0.04	-0.08	0.18	0.17	
A5	1	0.21	0.19	0.04	0.10	0.10	0.05	0.19	0.17	-0.082
	2	0.19	0.19	0.04	0.08	0.08	0.04	0.18	0.16	
	3	0.20	0.20	0.04	0.07	0.07	-0.02	0.19	0.17	
	4	0.22	0.21	0.05	0.08	0.08	0.06	0.20	0.20	
A6	1	0.13	0.12	-0.16	-0.14	-0.13	-0.15	0.10	0.08	0.048
	2	0.12	0.11	-0.14	-0.13	-0.12	-0.14	0.11	0.06	
	3	0.13	0.13	-0.14	-0.14	-0.13	-0.15	0.11	0.07	
	4	0.14	0.14	-0.17	-0.16	-0.15	-0.15	0.11	0.10	
A7	1	0.16	0.15	-0.12	-0.10	-0.12	-0.09	0.13	0.11	0.008
	2	0.15	0.14	-0.11	-0.10	-0.12	-0.10	0.14	0.11	
	3	0.16	0.16	-0.12	-0.11	-0.13	-0.11	0.14	0.11	
	4	0.17	0.16	-0.13	-0.11	-0.12	-0.11	0.13	0.13	

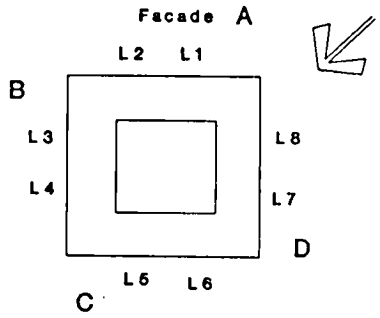

D 6- Internal flow coefficient, CQ1, for courtyards and atria in congested urban sites, **(Sc/ H = 2.3, staggered pattern, wind angle 45°).**

Atrium Index	Floor level	A		B		C		D		Internal Pressure CPI1
		L1	L2	L3	L4	L5	L6	L7	L8	
C10x10	1	0.15	0.17	0.10	0.14	as L4	as L3	as L2	as L1	
	2	0.17	0.16	-0.10	-0.08	- / -	- - / - -	- - / - -	- - / - -	
	3	0.21	0.15	-0.07	-0.10	- / -	- - / - -	- - / - -	- - / - -	
	4	0.14	0.17	0.07	-0.04	- / -	- - / - -	- - / - -	- - / - -	
A1	1	0.11	0.13	-0.08	0.08	- / -	- - / - -	- - / - -	- - / - -	0.048
	2	0.12	0.10	-0.13	-0.06	- / -	- - / - -	- - / - -	- - / - -	
	3	0.12	0.11	-0.16	-0.12	- / -	- - / - -	- - / - -	- - / - -	
	4	0.12	0.17	-0.16	-0.11	- / -	- - / - -	- - / - -	- - / - -	
A4	1	0.15	0.17	0.09	0.14	- / -	- - / - -	- - / - -	- - / - -	-0.012
	2	0.16	0.13	-0.06	0.06	- / -	- - / - -	- - / - -	- - / - -	
	3	0.17	0.15	-0.11	-0.08	- / -	- - / - -	- - / - -	- - / - -	
	4	0.16	0.20	-0.13	0.00	- / -	- - / - -	- - / - -	- - / - -	
A5	1	0.17	0.19	0.12	0.16	- / -	- - / - -	- - / - -	- - / - -	-0.069
	2	0.18	0.15	0.05	0.09	- / -	- - / - -	- - / - -	- - / - -	
	3	0.19	0.17	-0.05	-0.05	- / -	- - / - -	- - / - -	- - / - -	
	4	0.17	0.22	-0.09	0.07	- / -	- - / - -	- - / - -	- - / - -	
A6	1	0.12	0.12	-0.07	0.08	- / -	- - / - -	- - / - -	- - / - -	0.054
	2	0.12	0.09	-0.12	-0.08	- / -	- - / - -	- - / - -	- - / - -	
	3	0.12	0.10	-0.15	-0.12	- / -	- - / - -	- - / - -	- - / - -	
	4	0.12	0.16	-0.17	-0.12	- / -	- - / - -	- - / - -	- - / - -	
A7	1	0.14	0.16	0.06	0.12	- / -	- - / - -	- - / - -	- - / - -	-0.006
	2	0.15	0.12	-0.10	-0.02	- / -	- - / - -	- - / - -	- - / - -	
	3	0.15	0.14	-0.14	-0.10	- / -	- - / - -	- - / - -	- - / - -	
	4	0.14	0.19	-0.15	-0.09	- / -	- - / - -	- - / - -	- - / - -	

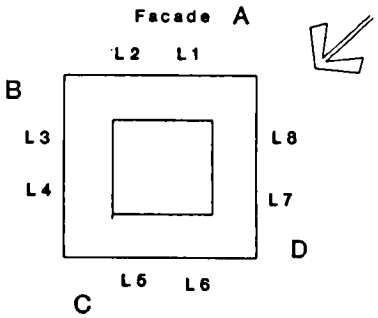

D 7- Internal flow coefficient, CQ1, for courtyards and atria in congested urban sites, **(Sc/ H = 1.5, normal pattern, wind angle 45°).**

Atrium Index	Floor level	A		B		C		D		Internal Pressure CPI1
		L1	L2	L3	L4	L5	L6	L7	L8	
C10x10	1	0.10	0.12	0.03	0.03	0.08	0.08	0.17	0.13	
	2	0.08	0.09	-0.02	0.09	0.00	0.04	0.13	0.11	
	3	0.11	0.11	-0.04	-0.02	-0.07	-0.08	0.09	0.10	
	4	0.16	0.17	-0.06	-0.08	-0.09	-0.08	0.07	0.09	
A1	1	0.10	0.10	-0.09	-0.07	-0.02	-0.07	0.16	0.12	0.027
	2	0.05	0.06	-0.10	-0.08	-0.07	-0.11	0.10	0.10	
	3	0.09	0.09	-0.11	-0.08	-0.10	-0.12	0.06	0.08	
	4	0.14	0.14	-0.11	-0.08	-0.10	-0.13	-0.03	0.07	
A4	1	0.14	0.14	0.05	0.07	0.10	0.08	0.18	0.16	-0.030
	2	0.10	0.10	0.02	0.10	0.05	-0.03	0.14	0.13	
	3	0.13	0.13	-0.04	0.05	-0.04	-0.07	0.11	0.13	
	4	0.18	0.17	-0.04	0.05	0.04	-0.07	0.11	0.13	
A5	1	0.17	0.17	0.10	0.11	0.14	0.12	0.20	0.18	-0.080
	2	0.13	0.13	0.08	0.10	0.09	0.08	0.16	0.15	
	3	0.16	0.15	0.08	0.10	0.06	0.02	0.14	0.15	
	4	0.20	0.20	0.07	0.11	0.07	0.05	0.14	0.16	
A6	1	0.07	0.06	-0.11	-0.10	-0.10	-0.11	0.15	0.10	0.044
	2	-0.04	0.03	-0.11	-0.09	-0.09	-0.12	0.09	0.08	
	3	0.07	0.05	-0.11	-0.10	-0.11	-0.10	0.04	0.07	
	4	0.13	0.13	-0.13	-0.12	-0.14	-0.15	-0.05	0.05	
A7	1	0.10	0.11	-0.06	-0.03	0.04	-0.05	0.17	0.13	0.013
	2	0.07	0.08	-0.08	-0.06	-0.06	-0.09	0.12	0.11	
	3	0.11	0.10	-0.09	-0.07	-0.09	-0.11	0.08	0.10	
	4	0.15	0.16	-0.10	-0.07	-0.10	-0.12	0.05	0.09	

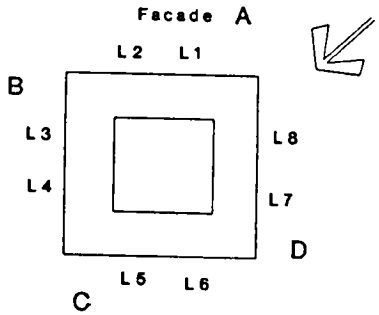

D 8- Internal flow coefficient, CQ1, for courtyards and atria in congested urban sites, **(Sc/ H = 1.5, staggered pattern, wind angle 45°).**

Appendix E:

Estimate of the change of flow rates with change of the room aperture area

The flow rate of air passing through an inlet and outlet aperture can be expressed as follow:

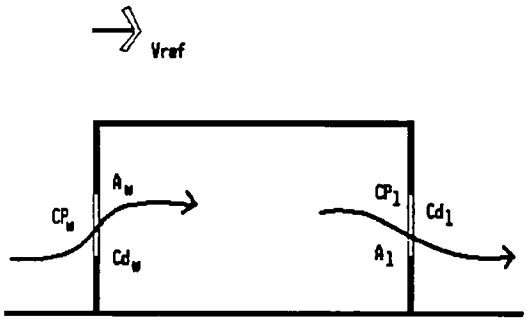

$$Q = V_{ref} \times \sqrt{\frac{CP_w - CP_l}{\frac{1}{Cd_w^2 A_w^2} + \frac{1}{Cd_l^2 A_l^2}}}$$

Where Cd is the discharge coefficient, A, the aperture area, CP, the external pressure coefficient, V_{ref}, a reference speed, and the indices w and l refer respectively to the windward and leeward.

The flow rate, $Q_{(1)}$, of air passing through a room having inlets with a total area $A_{w(1)}$, and outlets with a total area $A_{l(1)}$ can be expressed as follows;

$$Q_{(1)} = V_{ref} \times \sqrt{\frac{CP_w - CP_l}{\frac{1}{Cd_{w(1)}^2 A_{w(1)}^2} + \frac{1}{Cd_{l(1)}^2 A_{l(1)}^2}}}$$

If the opening areas are changed, the new volumetric flow, $Q_{(2)}$, can be written in the same way as $Q_{(1)}$, substituting $_{(1)}$ by $_{(2)}$. The change in the flow rate can be expressed as follows;

$$\frac{Q_{(1)}}{Q_{(2)}} = \left[\frac{\dfrac{1}{Cd_{w(1)}{}^2 A_{w(1)}{}^2} + \dfrac{1}{Cd_{l(1)}{}^2 A_{l(1)}{}^2}}{\dfrac{1}{Cd_{w(2)}{}^2 A_{w(2)}{}^2} + \dfrac{1}{Cd_{l(2)}{}^2 A_{l(2)}{}^2}} \right]^{0.5}$$

Assuming in the first case that A_w and A_l represent each 10% of the wall area, it can be found in Figure 10.1 that $Cd_w = 0.644$ and $Cd_l = 0.613$. If the aperture area is doubled, (increased to 20% of the wall surface), the new discharge coefficients are; $Cd_w = 0.684$ and $Cd_l = 0.622$. It follows that $Q_{(1)} / Q_{(2)} = 2.07$.

Now, if the aperture areas are increased from 10% to 60%, the new discharge coefficients are $Cd_w = 0.807$ and $Cd_l = 0.722$. It follows that $Q_{(1)} / Q_{(2)} = 7.3$. The new flow rate is seven times higher and not six times as it would have been estimated if the discharge coefficient was assumed constant.

How to use the design guide-lines

Conditions of use of the design guide-lines

Courtyard

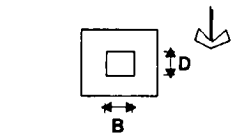

0.5H ≤ D/B ≤ 1.5H
Suburban boundary layer
Window area = 11% wall area

Atrium

Atrium depth= atrium height
Atrium breadth= atrium height

Criteria

● **Whole building relying on natural ventilation**

(best)	● ● ● ●	100% of building with	CQ1 => 0.15
	● ● ●	75(inclusive)-100%	CQ1 => 0.10
	● ●	50(inclusive)-75%	CQ1 => 0.10
	●	Less than 50%	CQ1 => 0.10
(worse)	X	same as above plus less than 75% with	CQ1 => 0.05

○ **Part of building relying on natural ventilation**

(best)	○ ○ ○ ○	12.5% or more of building with	CQ1 => 0.30
	○ ○ ○	3.12%	CQ1 => 0.30
	○ ○	3.12%	CQ1 => 0.25
(worse)	○	3.12%	CQ1 => 0.20

CQ1 is the ratio between the air velocity through the windows and that at the gradient height

CQF1 is an average value of CQ1 at one facade

CQT1 is an average value of CQ1 for the whole building

Appendix F: Design-guidelines for wind-driven natural ventilation in courtyard and atrium buildings.

Courtyard building in unsheleterd site

Courtyard depth and breadth

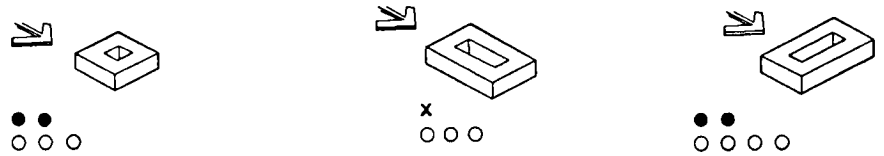

Courtyard area

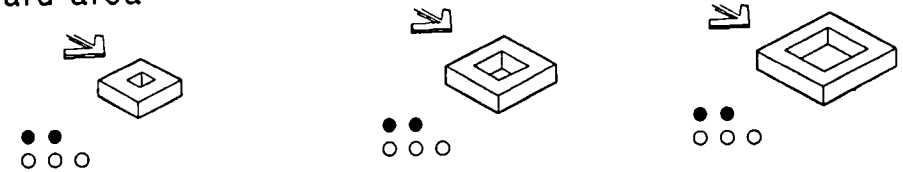

Orientation to wind

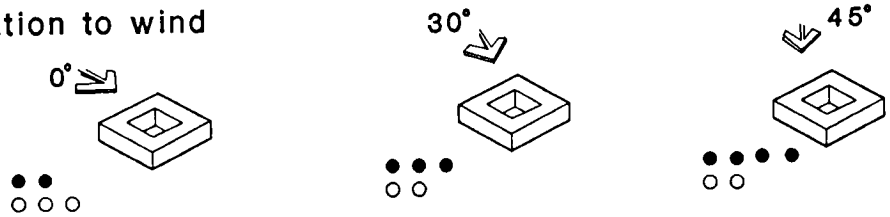

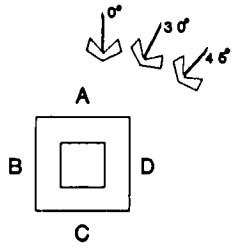

CQF1	A	B	C	D
0°	0.28-0.29 (0.28)	0.06-0.12 (0.08)	0.02-0.07 (0.06)	0.06-0.12 (0.08)
30°	0.23-0.26 (0.24)	0.15-0.19 (0.17)	0.11-0.14 (0.12)	0.14-0.17 (0.16)
45°	0.19-0.21 (0.2)	0.13-0.17 (0.16)	0.13-0.17 (0.16)	0.19-0.21 (0.2)

Atrium buildings in unsheltered site

Atrium with roof closed	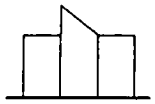	●●● ○○○	0°	CQT1=0.15	• Problems of migration of odours and contaminants must be addressed • Provide protuberant roof for collection of hot air and smoke
		●●● ○○	30°	CQT1=0.18	
		●●●● ○	45°	CQT1=0.19	
Atrium under suction mode	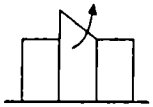	●● ○○○		CQT1=0.14	• Probably best suited for continuous venting • The matching strategy for smoke control is probably via the atrium
Weak suction		●●● ○○○		CQT1=0.17	
		●●● ○○		CQT1=0.17	
Strong suction	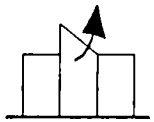	●● ○○○○		CQT1=0.13	
		●●● ○○○○		CQT1=0.17	
		●● ○○○		CQT1=0.16	
Atrium under positive pressure mode	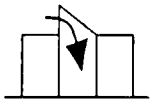	●●● ○○		CQT1=0.18	• Probably best suited for night-time-only venting or in sites where cool marine breezes prevail • The matching strategy for smoke control is probably away from the atrium
		●●● ○○		CQT1=0.18	
		●●●● ○		CQT1=0.19	
Atrium under near-atmospheric pressure mode	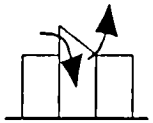	●●● ○○		CQT1=0.16	• This strategy is generally equivalent to one of the three others depending on whether the strongest roof air current is inwards, outwards or nil
		●●● ○○		CQT1=0.18	
		●●●● ○		CQT1=0.18	

Atrium and courtyard buildings in congested urban sites (0° wind incidence)

	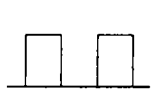	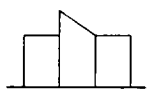	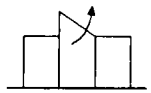	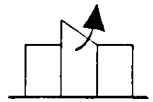	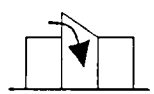	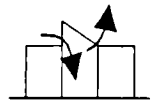
Group plan density ≅ 30%	X ○ CQT1-0.07	● X CQT1-0.09	● ○ CQT1-0.08	● ● ● ○ ○ CQT1-0.13	● ● X CQT1-0.10	● ● ● X CQT1-0.13
Group plan density ≅ 40%	X X CQT1-0.07	● X CQT1-0.08	● ○ CQT1-0.09	● ● ● ○ CQT1-0.14	● ● X CQT1-0.10	● ● X CQT1-0.10
Group plan density ≅ 50%	X X CQT1-0.06	X X CQT1-0.06	● X CQT1-0.08	● ● ● ○ CQT1-0.13	● ● X CQT1-0.10	● X CQT1-0.07
Comments			• The air intakes from shaded streets can be cooler than ambient • Noise and air pollution problems		• Air intake from roof may be cleaner than from streets	

Atrium and courtyard buildings in congested urban sites (45° wind incidence)

		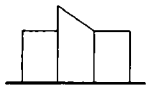	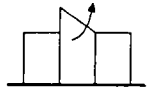	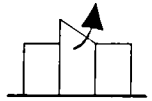	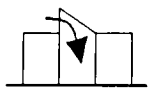	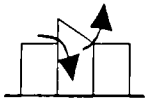
Group plan density ≃ 30%	● ● ● ○ CQT1-0.14	● ● ● X CQT1-0.15	● ● ● ○ CQT1-0.14	● ● ○ CQT1-0.14	● ● ● X CQT1-0.16	● ● ● ○ CQT1-0.13
Group plan density ≃ 40%	● ● ○ CQT1-0.12	● ● ● X CQT1-0.12	● ● ○ CQT1-0.11	● ● ○ CQT1-0.13	● ● ● X CQT1-0.12	● ● ● X CQT1-0.10
Group plan density ≃ 50%	● X CQT1-0.08	● ● X CQT1-0.09	● ● X CQT1-0.09	● ● ○ CQT1-0.12	● ● X CQT1-0.09	● X CQT1-0.07

Appendix G:

A stepwise method for estimating the natural ventilation cooling potential of courtyard and atrium buildings in a particular site.

Introduction

The step-by-step manual method presented here allows a rapid assessment of the cooling potential of natural ventilation in buildings in a specific site.

The procedure makes use of the flow coefficient data obtained from the wind tunnel tests in conjunction with the wind speed occurrence frequencies in the site considered[1].

The method will be applied here to a courtyard building, yet, it could be extended to any building type provided the velocity ratios are known. The format obtained at the end of the procedure is the **percentage of building for which thermal comfort is achieved** and the **percentage of time** for which these conditions are reached.

The method could be useful to assess at an early stage of the design whether natural ventilation can be successfully used in buildings to supplant mechanical cooling either wholly or partly. Partial use could be either seasonal, such as, extending the periods of the year in which mechanical cooling is not required, or spatial, such as, zoning the building where only parts that cannot be cooled naturally are mechanically conditioned. The method enables also the designer to tests several design alternatives and building orientations, and identify the most appropriate one.

Each step of the procedure is illustrated with an example. The prototype is chosen to be an office building type incorporating a courtyard with depth and breadth respectively 0.5 and 1 time the height. The building is to be located in a suburban terrain type but with no immediate surrounding obstacles. The wall porosity is around 10%. The climatic data chosen are that of the city of Algiers in Algeria. It is a sub-tropical Mediterranean marine climate, characterised by rainy and mild winters and by rainless and warm to hot summers. The relative humidity is large, (67% in annual average), and does not vary much with the seasons. Because of the great humidity, the conditions are generally oppressive during the summer.

---

[1] It must be stressed here that in order to judge the efficiency of natural ventilation with this method, it is imperative that **detailled** weather data are obtained.

Step 1: Determination of the thermal stress and conditions of comfort

Analysis of the annual cycle

The following method for the annual cycle analysis of the climate procedure is that devised by Givoni (1976).

Plot on a building bioclimatic chart the average hourly dry-bulb temperature month by month and hourly wet-bulb temperature (or humidity). The comfort zone and limits of the ambient conditions under which certain passive thermal control techniques can restore indoor thermal comfort can be read. Determine in particular the months for which natural ventilation can be effective.

For the example chosen, the building needs to be ventilated in the months of July and August during the hottest hours of the day, (i.e., from noon to 6 pm).

Figure 1:

Bioclimatic chart for the region of Algiers, Algeria.

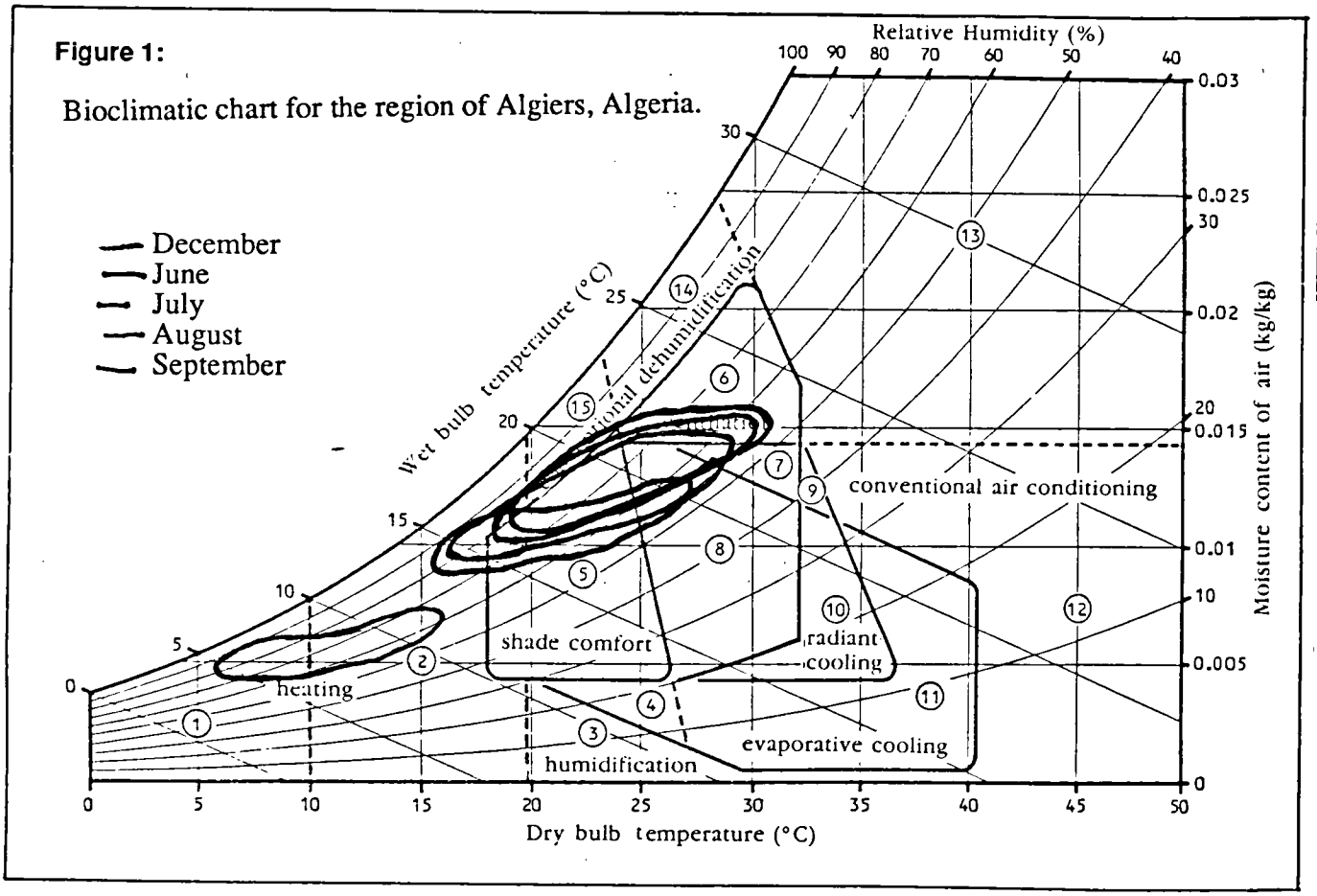

Table 1: Monthly average climatic data for Algiers. (Source: Office National de la Meteorologie, Dar-El-Beida, Algiers).

	Ambient temperatures (° C)		Relative humidity RH (%)		
	Max	Min	Max	Min	Avg
Jan	16.4	5.9	93.5	51.2	77.1
Feb	17.4	6.5	94.0	52.3	77.9
Mar	19.0	7.2	94.0	48.7	76.1
Apr	20.7	9.3	94.0	50.6	76.6
May	24.3	12.1	93.9	49.7	75.4
Jun	26.8	15.3	93.0	45.7	71.7
Jul	30.5	18.2	91.2	40.8	68.7
Aug	30.8	18.6	91.7	44.1	71.4
Sep	29.1	16.3	91.8	44.6	72.2
Oct	25.2	13.4	92.3	46.4	74.0
Nov	20.7	9.7	93.7	49.8	76.9
Dec	16.3	6.6	92.8	52.7	77.0

Determination of the air velocity to maintain thermal comfort during the hottest months

The following procedure which enables to determine the air velocity sufficient to restore thermal comfort can be found in Baker (1987).

a) Use one of the established indices such as the Corrected Effective Temperature (CET) that combines the effect of the environmental parameters, namely the mean radiant and air temperatures, humidities and air movement.

Choose a target value of this index, for example, the Neutral Temperature, Tn, to determine the benefit of different air velocities.

CET values can be obtained from nomograms, (like in Figure 2). The adequate chart must be used for appropriate activity level of the people and their clothing. In general the CET values are derived from the monthly averages for maximum day-time temperatures to account for worse cases[2].

The nomogram used for the example and shown in the Figure 2 was appropriate for people dressed in light clothing, (0.5 Clo units), and for a normal activity level (1 Met). Table 2 indicates the values of CET for different air velocities.

b) Determine the Neutral Temperature Tn at which most of the people are comfortable and which must be the target value of the CET. Humphrey's expression can be used, (Humphrey (1976).

$$Tn = 11.9 + 0.534 Tamb \mp 2.5\,^{\circ}C$$

where Tamb is the mean monthly outdoor temperature. The standard Tn is usually calculated for a person at rest and can be corrected for different clothing levels and activities, (see ASHRAE Handbook of Fundamentals (1989a)).

c) For each of the hottest months, establish the minimum required air velocity, Ucomf, for which the associated CET values fall within the upper and lower bands of Tn.

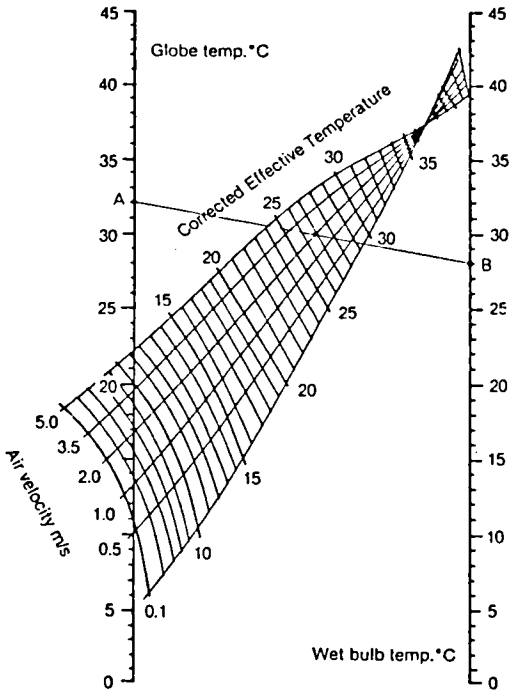

i) Locate the globe temperature (GT) (or ambient temperature in the case of well shaded building) on the left hand scale

ii) Locate the wet bulb temperature (WBT) on the right hand scale. If WBT is not available, it could be estimated from the psychometric chart from dry bulb temperatures (DBT) and relative humidities (RH)).

iii) Link the two points with a straight line.

iv) Mark the intersection of temperature line and a selected air velocity curve.

v) Read the value of CET on the inclined scale.

Figure 2: Corrected effective temperature nomogram (Source: Baker (1987)).

Table 2: Climatic/Comfort analysis for the hottest months (for day-time conditions), (CET0.1 is CET with 0.1 ms^{-1} air velocity).

	Tn+2.5° C	Tn	Tn-2.5° C	CET0.1	CET0.5	CET1	CET2
Jul	27.1	24.9	22.4	27.4	26.7	25.5	24.5
Aug	27.6	25.1	22.6	28	27.1	26	25

Table 2 indicates that 0.5 ms^{-1} is enough to restore human thermal comfort.

[2] For the night-time conditions CET is calculated from the 24-hour mean value temperatures together with 24-hours mean humidity values, (Baker (1987)).

Step 2: Ordering the wind data

a) Obtain the long term average hourly data of wind speed frequency of occurrence with the associated spatial distribution from the nearest meteorological station from the site.

b) Convert these wind speed data, (generally recorded at 10 m and in an open field terrain), into wind speeds at the gradient height, U_G, for the terrain under consideration. The power law profiles of the terrains allow to determine the conversion factors as follows, (see Gandemer (1976));

Open field terrain

$$U_{10meteo} = U_G \times \left[\frac{10}{270}\right]^{0.14}$$

Suburbs

$$U_{10meteo} = U_G \times \left[\frac{10}{330}\right]^{0.25}$$

City centre

$$U_{10meteo} = U_G \times \left[\frac{10}{400}\right]^{0.36}$$

For the example chosen,

$U_G = 1.59 \times U_{10meteo}$

Table 3: Long term average hourly data of wind speed frequency of occurrence. (Source: Office National de la Meteorologie, Dar-El-Beida, Algiers).

July					
$U_{10meteo}$ (ms^{-1})	1<=	2<=	3<=	5<=	10<=
U_G (ms^{-1})	1.6<=	3.2<=	4.8<=	8<=	16<=
CQ_{comf}	0.3<=	0.15<=	0.1<=	0.05<=	>0.05
N	18.7	17.3	14.3	8.4	0
NE	21.6	20	16.8	10.4	0.8
E	5.6	5.2	4.2	2.4	0
SE	0.81	0.7	0.4	0	0
S	2.6	2.4	1.8	0.7	0
SW	5.8	5.1	3.5	0.6	0
W	5.4	4.8	3.6	1.2	0
NW	5.2	4.8	4.0	2.4	0
August					
N	15.4	14.3	11.4	6.6	0
NE	19.8	18.4	14.7	8.5	0.6
E	6.8	6.3	5.0	3.0	0
SE	0.8	0.7	0.5	0	0
S	1.7	1.5	0.9	0	0
SW	8.3	7.3	4.9	0.8	0
W	6.2	5.6	3.9	1.2	0
NW	4.9	4.6	3.8	2.4	0

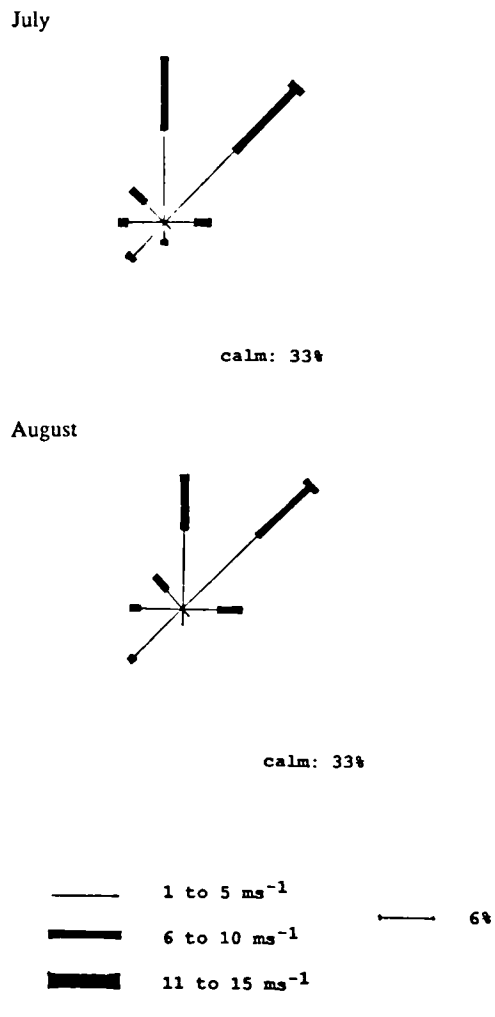

step 3: Conversion of wind speed data into flow coefficients required to maintained human thermal comfort.

a) Convert the tabulated wind speeds increments, (see Table 3), for which frequencies of occurrence are provided, into increments of velocity ratios, (or flow coefficients as it was called here), which are required to restore thermal comfort, CQ_{comf}, as follow:

$$CQ_{comf} = U_{comf} / U_G$$

b) Refer to the various sources of air velocity ratios, in particular the experimental data provided in Appendices B, C or D, to obtain the relevant values of velocity ratios for the prototype and for the wind angles of interest[3].

c) For each increment of CQ_{comf} which have been derived, determine the percentage of the building matching the increments CQ_{comf}, (see Table 4).

[3] The velocity ratios, CQ1, provided in the Appendices B, C or D correspond to the ratio of air speeds through the windows to that of the free stream. They represent thus maximum indoor air velocity ratios. If the occupants are located at a distance from the windows, than the average indoor air speeds at the middle of the room must be chosen. This can be obtained by multiplying the tabulated CQ1 values with the ratio of the windows area to that of the frontal room area as follows:

CQroom = CQ tabulated × (window areas) / (height of room × width of room).

Table 4: Percentage of the building above ranges of flow coefficients, CQ1, for two test orientations, (data from Appendix B1 and B3).

Building orientation: East				
	0.3<=	0.15<=	0.1<=	0.05<=
N	3%	12%	41%	69%
NE	0%	81%	100%	100%
E	19%	38%	56%	94%
SE	0%	81%	100%	100%
S	3%	12%	41%	69%
SW	0%	81%	100%	100%
W	19%	38%	56%	94%
NW	0%	81%	100%	100%
Building orientation: North East				
N	0%	81%	100%	100%
NE	19%	38%	56%	94%
E	0%	81%	100%	100%
SE	3%	12%	41%	69%
S	0%	81%	100%	100%
SW	19%	38%	56%	94%
W	0%	81%	100%	100%
NW	3%	12%	41%	69%

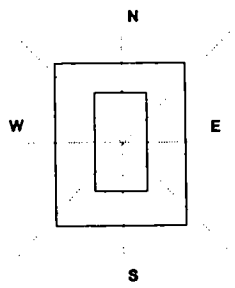

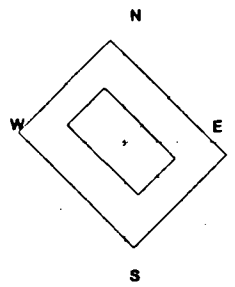

Step 4: Extent of the building under thermal comfort in conjunction with frequencies of occurrence.

Referring concurrently to the table of wind frequencies and the table of velocity ratios, total for ranges of percentage of building, (say, every 20% increment), the thermal comfort frequency of occurrence, (e.g., for 100% of the building, the occurrence of thermal comfort is the sum of the circled values in Table 3. The format obtained at the end of this procedure is the fraction of building under thermal comfort with the frequency of time for which these conditions are reached, (see Table 5).

estimated from the maximum day-time temperatures whereas the frequency of wind speeds and orientation available were that of monthly averages for 24 hours. In actual facts, the strongest breezes in the site coincide with the hottest hours of the day, and thus, it is likely the results would be better in reality.

The absence of hourly data of the wind orientation precludes any accurate estimate of the extent of the building under thermal comfort and the frequencies of occurrence. These data are imperative in order to estimate the real benefit of the ventilation in the hottest hours of the day.

Table 5: Estimate of the fraction of building under thermal comfort in conjunction with the frequencies of occurrence.

Building orientation: East					
	Percentage of building under thermal comfort				
	100%	80%<=	60%<=	40%<=	20%<=
Jul	25%	34%	44%	55%	57%
Aug	24%	35%	42%	52%	55%
Building orientation: North East					
Percentage of building under thermal comfort					
	100%	80%<=	60%<=	40%<=	20%<=
Jul	24%	41%	49%	60%	65%
Aug	21%	37%	40%	52%	58%

The results in Table 5 indicate, for example, that in August the thermal comfort may be maintained for 55% of the time for approximately 1/4 of the building, if the building is East oriented. It can also be noticed that, in general, the orientation NE is preferable.

However, they are reasons to believe that these results are underestimated. This is because the desirable air velocities were

With the present case the hourly data of wind speed were available but not the direction. As an hypothetical example it was assumed that the spatial distribution of the wind remains the same for each portion of hours. This assumption was made only to illustrate the method.

The same procedure was repeated for hours between noon and 18 pm, and the results are given in the table 7.

Table 6: Frequency of occurrence of 10 m wind speed with the associated direction during day time, (average from noon to 18 pm). The data are hypothetical.

July				
$U_{10meteo}$ (ms^{-1})	1<=	2<=	3<=	5<=
N	25.5	24.9	22.5	not av.
NE	27.5	26.8	24.2	-
E	7.8	7.7	6.9	-
SE	2.4	2.4	2.2	-
S	4.9	4.8	4.3	-
SW	12.7	12.5	11.2	-
W	10.4	10.2	9.2	-
NW	6.9	6.7	6.1	-
August				
N	20.1	19.7	17.8	not av.
NE	25.8	25.3	22.9	-
E	8.6	8.4	7.6	-
SE	1.9	1.9	1.7	-
S	3.8	3.7	3.4	-
SW	17.2	16.8	15.2	-
W	11.5	11.2	10.2	-
NW	5.7	5.6	5.1	-

Table 7: Estimate of the extent of building under thermal comfort in conjunction with the frequencies of occurrence[4].

Building orientation: East					
Percentage of building under thermal comfort	100%	80%<=	60%<=	40%<=	20%<=
Jul	44%	47%	-	91%	93%
Aug	45%	50%	-	89%	90%
Building orientation: North East					
Percentage of the building under thermal comfort	100%	80%<=	60%<=	40%<=	20%<=
Jul	43%	48%	-	91%	95%
Aug	39%	43%	-	88%	92%

[4] The abscence of data for wind frequencies in the range of 3 to 5 ms^{-1} could not allow estimates of time frequencies for percentage of building between 40% and 80%.

Step 5: Verdict on the effectiveness of natural ventilation

The last step is to decide whether the building could rely on natural ventilation fully, in part or not at all, on the basis of acceptable percentage of time where the thermal comfort can be maintained.

There is no standard acceptability criteria available at present, (Arens et al (1984)), so that the final judgement remains to the designer. Arens and Watanabe (1986) nevertheless, suggested that maybe 90% of the time, monthly, is an acceptable value. Yet, research is needed to define such criteria.

According to this Arens and Watanabe criterion, approximately 40% of the test building can rely on natural ventilation.

Following the present method, the designer can make an absolute judgement on whether the conditions are good enough or can compare the comfort conditions of several design options.